# Gérard Gouesbet Gérard Gréhan

# Generalized Lorenz-Mie Theories



### Generalized Lorenz-Mie Theories

#### Gérard Gouesbet and Gérard Gréhan

# Generalized Lorenz-Mie Theories



Prof. Gérard Gouesbet Université de Rouen CNRS UMR 6614 CORIA Site Universitaire du Madrillet BP 12 76801 ST.-ETIENNE DU ROUVRAY CX France

Prof. Gérard Gréhan Université de Rouen CNRS UMR 6614 CORIA Site Universitaire du Madrillet BP 12 76801 ST.-ETIENNE DU ROUVRAY CX France

E-mail: grehan@coria.fr

E-mail: gouesbet@coria.fr

"Additional material to this book can be downloaded from http://extra.springer.com"

ISBN 978-3-642-17193-2

e-ISBN 978-3-642-17194-9

DOI 10.1007/978-3-642-17194-9

© 2011 Springer-Verlag Berlin Heidelberg

This work is subject to copyright. All rights are reserved, whether the whole or part of the material is concerned, specifically the rights of translation, reprinting, reuse of illustrations, recitation, broadcasting, reproduction on microfilm or in any other way, and storage in data banks. Duplication of this publication or parts thereof is permitted only under the provisions of the German Copyright Law of September 9, 1965, in its current version, and permission for use must always be obtained from Springer. Violations are liable to prosecution under the German Copyright Law.

The use of general descriptive names, registered names, trademarks, etc. in this publication does not imply, even in the absence of a specific statement, that such names are exempt from the relevant protective laws and regulations and therefore free for general use.

Typesetting: Data supplied by the authors

Cover Design: Scientific Publishing Services Pvt. Ltd., Chennai, India

Printed on acid-free paper

 $9\; 8\; 7\; 6\; 5\; 4\; 3\; 2\; 1$ 

springer.com

## Contents

Ι	_		Maxwell's Electromagnetism and	
	Maxw	_	ations	
	I.1	General	Maxwell's Equations in Cartesian	
		Coordina	ates	
		I.1.1	Maxwell's Equations in Free Space	4
		I.1.2	Maxwell's Equations in Matter	
		I.1.3	Boundary Conditions	!
		I.1.4	Constitutive Relationships	(
		I.1.5	The Formulation in Fourier Space	8
		I.1.6	Time Harmonic Fields and Complex	
			Representatives	10
	I.2	Special N	Maxwell's Equations for l.l.h.i Media	1
		I.2.1	Special Maxwell's Equations in Cartesian	
			Coordinate Systems	1:
		I.2.2	Special Maxwell's Equations in Orthogonal	
			Curvilinear Coordinate Systems	1:
		I.2.3	Special Maxwell's Equations in Spherical	
			Coordinate Systems	1:
		I.2.4	Boundary Conditions	1
		I.2.5	Energy Propagation and Poynting	
			Theorem	1
		I.2.6	Momentum Propagation	1'
		I.2.7	Wave-Vector, Refractive Index and	
			Impedance	18
		1.2.8	Potentials	2

VI Contents

П	Resolu		pecial Maxwell's Equations	
	II.1		rthogonal Curvilinear Coordinate Systems	
			ability	
	II.2	Bromwich	Potentials	
		II.2.1	Generalities	
		II.2.2	Transverse Magnetic Wave	
		II.2.3	Transverse Electric Wave	
	II.3	Explicit T	Time Harmonic Dependence	
	II.4	Use of Sp	herical Coordinate Systems	
	II.5		tions	
		II.5.1	Reduction to Ordinary Differential	
			Equations	
		II.5.2	Harmonic Equation	
		II.5.3	Associated Legendre Equation	
		II.5.4	Spherical Bessel Equation	
		II.5.5	General Expressions for BSPs	
тт	Conon	alizad I an	enz-Mie Theory in the Strict Sense,	
11			Ts	
	III.1		ering Problem and Global Strategy	
	III.2	BSPs for the Incident Wave		
	III.3		res to Evaluate BSCs $g_n^m$	
		III.3.1	The First Method to Derive Quadrature	
		TII O O	Expressions	
		III.3.2	The Second Method to Derive Quadrature	
		TII O O	Expressions	
	TTT 4	III.3.3	Other Approaches	
	III.4		Scattered and Sphere Waves	
	III.5		ns of Field Components	
	III.6	Boundary Conditions and Generalized Scattering		
			ts	
	III.7		Field Components	
	III.8		Field Components in the Far Field Region	
	III.9		Intensities	
	III.10		gle	
	III.11		Energy Balance and Associated	
			tions	
		III.11.1	Generalities	
		III.11.2	Incident Field Balance	
		III.11.3	Scattering Cross-Section $C_{sca}$	
		III.11.4	Extinction Cross-Section $C_{ext}$	
	III.12	Momentu	m Balance and Radiation Pressure	
		III.12.1	Generalities	

Contents VII

		III.12.2 Longitudinal Radiation Pressure	
		(z -Direction)	67
		III.12.3 Transverse Radiation Pressure ( $x$ and $y$	
		Directions)	70
	III.13	Efficiency Factors	75
	III.14	Complement, Other GLMTs	76
IV	Gaussi	ian Beams and Other Beams	89
	IV.1	Gaussian Beam Description	90
		IV.1.1 The Solving Paradox	90
		IV.1.2 Elementary Description	92
		IV.1.3 Historical	93
		IV.1.4 Davis Formulation	94
		IV.1.5 The Order $L$ of Approximation	96
		IV.1.6 The Order $L^-$ of Approximation	96
		IV.1.7 Kogelnik's Model	98
		IV.1.8 Inaccuracies at Orders $L$ and $L^-$	99
	IV.2	GLMT at Orders $L$ and $L^-$	102
			102
			105
	IV.3	Numerical Computations of Beam Shape Coefficients	
			108
	IV.4	Other Beams	108
$\mathbf{V}$	T7::4-	C!	117
V			117
	V.1 V.2		117
	V . Z		120
			120
			124
		0 11, 1 111	130
	<b>1</b> 7.0	016,1 15	135
	V.3	Numerical Computations of BSCs by Using Finite	100
			136
			136
		V.3.2 Formulae Modifications for Programming	137
$\mathbf{VI}$	Specia	al Cases of Axisymmetric and Gaussian Beams	139
	VI.1	Axisymmetric Beams	139
	VI.2	The LSC-Decomposition and Gaussian-Like Beams	141
	VI.3		145
	VI.4	Lorenz-Mie Theory	150
	VI.5		153

VIII Contents

	VI.6	Numerical	Computations of Special BSCs by Using	
		Quadratur	es	155
		VI.6.1	Computer Programs	155
		VI.6.2	More on the Plane Wave Case	156
		VI.6.3	Numerical Behaviour of Quadratures	157
	VI.7	Computati	ions of Special BSCs by Using Finite Series	161
		VI.7.1	The Formulation	161
		VI.7.2	Routines	165
VII	The Le	ocalized A	approximation and Localized Beam	
				169
-	VII.1		es	169
	VII.2		Center Location Case	171
	V 11.2	VII.2.1	The Principle of Localization	171
		VII.2.1 VII.2.2	Special BSCs	171
		VII.2.2 VII.2.3	Numerical Evidence of Validity	172
		VII.2.3 VII.2.4	Physical Evidence of Validity	174
		VII.2.4 VII.2.5	Difference of Behaviour between Rigorous	114
		V 11.2.5	Methods and Localized Approximation	175
	VII.3	Arria I cost	tion Case	176
	VII.3 VII.4		Location	181
	V 11.4	VII.4.1	A Well Posed Problem	181
		VII.4.1 VII.4.2		
		VII.4.2 VII.4.3	BSCs $g_n^{+1}$ and $g_n^{-1}$ for Axis Location	182
		V11.4.3	BSCs $g_n^m$ for Arbitrary Location: First	105
		3711 4 4	Attempt	185
		VII.4.4	Final Generalization	189
		VII.4.5	Improved Formulation and Routines	190
	7.7TT =	VII.4.6	Examples of Results	191
	VII.5		ent on the Localized Approximation	191
	VII.6		ent on the Evaluation of Beam Shape	405
		Coefficient	s	195
VIII	Appli		nd Miscellaneous Issues	199
		VIII.0.1	Measurement Techniques	199
		VIII.0.2	Internal Fields and	
			Morphology-Dependent-Resonances	211
		VIII.0.3	Mechanical Effects	214
		VIII.0.4	Multiple Scattering	227
		VIII.0.5	Miscellaneous Topics	228

Contents

IX	Conclusion	231
A	Evaluation of Quadratures, Rels (III.130) and (III.131)	233
В	Evaluation of Quadradures, Rels (III.151) and (III.152)	235
$\mathbf{C}$	Evaluation of Quadratures, Rels (III.169) and (III.170)	237
D	To Reduce the Double Summations of Chapter IV to Single Summations	241
$\mathbf{E}$	Useful Relations to Derive the BSCs of Chapter IV	245
${f F}$	Computer Programs	247

# List of Figures

1.1	Spherical coordinate system. In these relations, $V_i$ designates the components of vector $\mathbf{V}$ ( $\mathbf{E}$ or $\mathbf{H}$ ) in the local Cartesian (orthogonal) system attached at point $x^k$	14
III.1	The geometry under study. $V$ means $E$ or $H$	38
IV.1 IV.2	The geometry	90 91
VI.1	Behaviour of $t_n(x)$ , Rel (VI.120), with $n$ as the	4 5 0
VI.2	parameter	158
VI.3	for $n = 1$	159
VI.4	(VI.122), for $n = 1$	160
VII.1	The localized interpretation of the BSCs $g_n$ . (a) for a plane wave, (b) for a Gaussian profile	173
VII.2	Integral VI.62 versus the limit of integration. The parameters are: description order $L$ , $2w_0 = 20\lambda$ , $\lambda = 0.5 \mu m$ , and the order $n$ of the coefficients (from 1 to 100).	175
VII.3	Sketch of a top-hat beam.	182
F.1	The interface to compute and display the Beam Shape Coefficient in the Localized Approximation. Example	- 1 -
F.2	of result for $g_{n,TM}^1$ for a plane wave	249
	location in a Gaussian beam	249

XII List of Figures

F.3	Example of a 3D diagram	250
F.4	Example of a 3D diagram	250
F.5	Example of input and output screens for 3D	
	computation	251
F.6	Example of a 2D diagram	251
F.7	Example of a 2D diagram	252
F.8	Examples of far field scattering diagrams computed for the same particle. The parameter is the beam waist	
	size	253
F.9	Interaction between a Gaussian beam and the light scattered in forward direction: linear scale, axis particle	
	location	254
F.10	Interaction between a Gaussian beam and the light scattered in forward direction: logarithmic scale, axis particle location.	254
F.11	Interaction between a Gaussian beam and the light scattered in forward direction: logarithmic scale, off	209
	axis particle location	255
F.12	Example of input and output for scattering	
	cross-section	255
F.13	Example of a screen when computing the pressure	
	versus the particle location	256
F.14	Example of a screen when computing the pressure	
	versus the particle diameter	256

Et Dieu dit: "Voici le signe de l'alliance que je mets entre moi et vous, et tous les êtres vivants qui sont avec vous, pour toutes les générations à venir. Je mets mon arc dans la nue, ce sera un signe d'alliance entre moi et la terre. Quand j'assemblerai des nuées au-dessus de la terre, l'arc apparaîtra dans la nue."

Gn, 9, 12-14. La Sainte Bible du Chanoine Crampon

Schwüles Gedünst schwebt in der Luft; lästig ist mir der trübe Druck: das bleiche Gewölk samml'ich zu blitzendem Wetter;

Weise der Brücke den Weg!

Richard Wagner. Das Rheingold Vierte Szene.

#### **Preface**

Examining the general subject of light scattering is like examining a gemstone having many facets. As a result, when people talk about light scattering they can mean any one of many things. Light can be scattered by individual particles of high symmetry (Lorenz-Mie theory or LMT) ranging in size from a small fraction of the wavelength of light (Rayleigh scattering) to many thousands of wavelengths (semiclassical scattering and ray theory), or by irregularly-shaped particles (e.g. Null-Field method). People can also mean scattering of light by crystalline or amorphous aggregates of such particles (Bragg scattering or pair-correlated scattering), or the repetitive scattering of light through a dense cloud of particles (multiple scattering and radiative transfer). People can mean scattering of light from sound waves in a gas (Rayleigh-Brillouin scattering), from thermally generated capillary waves on the surface of a liquid (surface scattering), or from long range density fluctuations in a system undergoing a phase transition (critical opalescence). They can mean the Doppler shift of the frequency of the light scattered by particles entrained in a flow (quasi-elastic light scattering), or the time dependent interference of light scattered by many particles undergoing Brownian motion (dynamic light scattering and diffusing wave spectroscopy). They can also mean the absorption of light by the molecules of a particle and re-radiation at a lower frequency (inelastic scattering). Since light scattering is such a large area of endeavor, one needs to clearly state which of the many facets one will be describing when explaining it to someone else. The particular facet that is the topic of this book is scattering by individual particles having a high degree of symmetry (LMT) by a transversely focused beam, which is today called generalized Lorenz-Mie theory, or GLMT for short.

There once was a time when the world of Lorenz-Mie scattering was relatively simple. LMT had been developed by a number of researchers during the time period extending from the last few decades of the 19th century to 1908. It provided an exact solution of the electromagnetic boundary value problem of scattering of an incident plane wave, such as sunlight, by a dielectric spherical particle, such as a small water droplet. The solution took the

XVI Preface

form of an infinite series of partial wave terms. This was the worst possible type of exact solution to have since the individual terms were cumbersome to calculate and the infinite series was frequently extremely slowly convergent. Unfortunately, in spite of these limitations, it was the only form of the exact solution to the light scattering problem that was known. Some researchers contented themselves by studying scattering from particles that were small compared with the wavelength of light, where the series contained only one term. Others devised clever analytical approximations such as Airy theory, asymptotic expansions, and stationary phase methods to describe scattering by a raindrop which was hundreds or thousands of times larger than the wavelength of light, and where the infinite series converged only after many hundreds or many thousands of terms. Yet others used motor-driven mechanical calculators until they overheated to calculate the ten or twenty terms in the series that were required for convergence when the water droplet was only a few times larger than the wavelength of light. By the early 1960's the computational difficulties had improved in the sense that those who had sufficient grant money to purchase run time on a mainframe computer could calculate Lorenz-Mie scattering for any size particle, and produce either long tables or large collections of graphs of the scattered intensity as a function of angle for various types of particles.

The invention of the gas laser in the early 1960's and the popularization of personal computers in the 1970's changed everything. Now anyone with a laser, a few lenses, a photodetector, and a PC could study light scattering and use it as a particle characterization tool. But, the nature of the laser beam itself caused everyone to realize that the trusted and time-tested Lorenz-Mie theory could no longer adequately describe what was now being observed in the laboratory. The width of the laser beam could easily be focused down to the diameter of the test particle or less, whereas Lorenz-Mie theory had assumed that both the beam amplitude and phase were constant over the particle diameter. In addition, people were very excited that all the things one could only dream of calculating back in the old days of mechanical calculators and mainframe computers could now be easily calculated if only one had the appropriate theory. If one had a PC, then run time was now free no matter how many hours or days the calculation took using the 2MHz clock speed and 64K of memory available in the first generation of machines.

And so the race was on to find a new extension of Lorenz-Mie theory appropriate to lasers. What theory of electromagnetic scattering by a tightly focused laser beam could be devised that was exact but also would be practical to use? After a number of initial theoretical attempts that ranged from somewhat unrealistic to somewhat successful, it began to become apparent that what today is known as GLMT might well be the best bet for a theory that was both mathematically exact and practical to implement. Practical is now defined differently than in the past due to both continuing improvements in memory and speed (but not price) of PCs, and their increased availability.

Preface XVII

Beginning in the late 1970's, the epicenter of the development of GLMT was located at the University of Rouen in the light scattering group of Prof. Gérard Gouesbet who headed the theory section and Dr. Gérard Gréhan who headed the experimental section. The continuous interplay between theory and experiment at Rouen kept the theory honest, maintaining the theoretician's dream of developing a theory that was mathematically exact while conforming to the experimenter's demand that the theory be practical to use. This book, written by the two Gérards who were centrally involved in the development of GLMT from the very beginning, tells the story of the theory both traveling down the main road of its development as well as down a number of side roads that discuss specific technical details. The development of GLMT was the product of many researchers both in Rouen and elsewhere working over a long period of time. A reasonably complete list of these participants is given immediately before the Introduction, and their contributions are amply referenced in Chapters 3 through 7. As one of these participants, I can say from personal experience that all the results that seem so obvious now, and the progressions of ideas that seem so straightforward, were not so obvious or straightforward then. Much soul searching, serious debate, and worry about how bold to be in print were required to develop GLMT from where it was in those years to where it is today.

The basic idea of GLMT is that a transversely localized beam that is a solution to Maxwell's equations can be written as an infinite series of spherical Bessel functions and spherical harmonics, each multiplied by a coefficient that is called a beam shape coefficient. There are then two separate parts to the derivation and application of the formulas of GLMT, (i) the way in which all the formulas of experimental interest depend on the beam shape coefficients, and (ii) how the beam shape coefficients are calculated for a particular beam of interest. The first part was understood from almost the very beginning. But, the second part turned out to be where all the complications were lurking, and it took many years to sort these complications out. The basic results from electromagnetic theory necessary to derive the main formulas of both LMT and GLMT are recounted in Chapters 1 and 2, and the GLMT formulas of experimental interest are written in terms of the beam shape coefficients in Chapter 3. This gives the overall essence of GLMT, except for the one nagging question that turned out to be a Pandora's box. Namely, how does one determine the beam shape coefficients for what people call a Gaussian laser beam, or some other type of beam? This question required a study, in much more detail and to a much greater depth than anyone could have realized beforehand, of exactly what a focused beam is and what it means for a beam to be an exact solution of Maxwell's equations. This was a great struggle because people knew that before one can decompose a beam into an infinite series of spherical Bessel functions and spherical harmonics, one has to know exactly what the beam is that one is attempting to decompose. It turned out that what people colloquially called a Gaussian beam was not in actuality a solution of Maxwell's equations. By the act of determining the XVIII Preface

beam shape coefficients of such a beam, one remodeled it from its original shape that was not quite a solution of Maxwell's equations to another beam that had not quite the original shape but that was a solution of the equations. It took a long time to understand this and to suitably control the beam remodeling procedure, even though in retrospect it is now all clear enough. This is why the various methods for obtaining the beam shape coefficients are spread out over Chapters 4-7. After all this effort over many years, I would not be surprised if the last word on obtaining and understanding the beam shape coefficients has yet to be written. But, the current state of the art is good. It is certainly able to be implemented in a practical and reliable way, and it agrees nicely with the results of experiments.

Perhaps a measure of GLMT's maturity today is the fact that although there are still new theoretical developments related to fundamental physics and mathematics, the subject is no longer dominated by them. GLMT has instead become a useful and valued tool for engineers who wish to characterize small solid or liquid particles and use these scattering measurements to assist in their design, testing, and calibration of a large variety of products, devices, and instruments. Many applications of GLMT are described in detail in Chapter 8 and are generously referenced there. As a similar measure of the maturity of the theory, although heroic individual efforts are still being made in code generation for various exotic extensions and uses of GLMT, both Mie and GLMT codes have become robust and highly developed. Standard libraries of them do exist, they have been published in books, and they are now available on the Internet. A highly developed and greatly tested library of computer programs is provided in the website connected to book.

I believe this book on GLMT has been written by the two Gérards to serve a large variety of audiences. On the one hand, with its computer programs it is useful as a practical tool for those who wish to apply GLMT to the interpretation of laboratory measurements. On the other hand, since the derivations in the book are rather complete with only a few steps left out here and there, the book serves as a useful archival reference for students seeking to learn the mathematics and physics of the subject. On yet a third hand, since most of the derivations begin in rather complete generality and many specific theoretical fine-points are discussed in detail, the book provides a good starting point for advanced researchers interested in either developing new insights into GLMT or extending it to particles having a more complicated response to external electric and magnetic fields. Since GLMT was developed largely by the Rouen group headed by Prof. Gérard Gouesbet and Dr. Gérard Gréhan, and since the two Gérards had leading roles in both the theoretical development and experimental testing of the theory from the very beginning, it is only natural that this book is authored by them.

Many hundreds of years ago it was believed that knowledge had reached its peak under the ancient Greeks. When one was studying a certain natural phenomena in those times, one would always ask what Aristotle, the greatest authority on all of Natural Philosophy, had to say on the subject. As I was Preface XIX

preparing to write this preface, I read the prefaces of a number of other specialized books on various facets of light scattering to see what other people had written. In doing so I came upon a quote I had never seen before. In the book "Light Scattering by Nonspherical Particles" edited by Michael Mishchenko, Joachim Hovenier, and Larry Travis (Academic Press, 2000) there is a Forward written by H. C. van de Hulst (pp.xxv-xxx). Near the end of the Forward, van de Hulst writes

"In more recent work on Mie theory two developments please me most:

- (a) The many papers, mostly by Gouesbet and his co-workers, on scattering of a focused (laser) beam that illuminates the sphere eccentrically
- (b) The glare points (in some papers wrongly called rainbows) showing under which angles the most intense radiation exits from a sphere fully illuminated by a distant source"

While I do not intend to place Henk van de Hulst on the same pedestal as Aristotle, this is a very nice tribute to GLMT nonetheless. In a similar vein, one might also parenthetically conjecture what the G might possibly otherwise be an abbreviation of in the acronym GLMT.

January 2010

James A. Lock Cleveland, Ohio, USA

#### **Preliminaries**

This book is written in English, or may be in American, or more likely in some kind of international language mixing miscellaneous influences from various countries. Whatever the used language is, it is not the natural language of the authors. Furthermore, because this book is written (that is to say not spoken), the reader will miss the delicious Frenchy Maurice Chevalier accent which is a part of our charm: nothing is perfect in this poor world!

Actually, most of our writing has been checked by our friend and colleague Alain Souillard, from the Rouen National Institute of Applied Sciences. However, such a checking is not enough to ensure correctness because:

- (i) several versions of each chapter have been written before approaching the final asymptotic version and it would not have been friendly to ask Alain Souillard to check again and again
- (ii) scientific terminology has not been checked just because Alain Souillard is not a scientist

At least, we believe that the reader will forgive us for the use of gallicisms and remaining language incorrectnesses. They should not be strong enough to prevent sufficient understanding.

We feel more concerned by the fact that misprints and incorrectnesses in formulae are likely to occur in such a book. Indeed, even a sign error may be a nightmare to theoreticians. As a relief, we may state that such problems are a manifestation of a physical reality, namely the creation of entropy along an information channel. Although this is however a very small relief indeed, the only remaining way to escape from the shame of making errors is to state that the blame for remaining imperfections rests on the shoulders of the other author, or on Nature which made us.

We are also looking forward to the readers who will kindly help us to improve the book by communicating to us regarding any incorrectness. Thanks to them in anticipation.

XXII Preliminaries

#### Acknowledgments

The development and completion of the generalized Lorenz-Mie theory (GLMT) stricto sensu and, more generally, of the generalized Lorenz-Mie theories (in the plural, as we shall explain later), and of applications, took place at the University of Rouen and at the National Institute of Applied Sciences of Rouen, first on the campus of Mont-Saint-Aignan and, thereafter, on the campus of Saint-Etienne du Rouvray. Very likely (as far as we remember), the first equations have been written in 1978 and the first article paper has been published in 1982 [1]. Therefore, more than thirty years have elapsed since the beginning of the story, and the third decade is over.

During this period of time, many students contributed to the topic, and it is here a right place and a right time to acknowledge all of them, namely (using a chronological order): B. Maheu (who helped taking care of the first chapter of this book), F. Corbin, F. Guilloteau, K.F. Ren, F. Onofri, D. Blondel, H. Mignon, T. Girasole, C. Rozé, N. Gauchet, H. Bultynck, H. Polaert, S. Meunier-Guttin-Cluzel, L. Méès and J. Ducastel. During such a long time, we also had many opportunities to enjoy local collaborations (using an alphabetic order): D. Allano, S. Belaid, M. Brunel, D. Lebrun, E. Lenglart, D. Lisiecki, C. Ozkül, F. Slimani, national collaborations: M.I. Angelova, D. Boulaud, P. Cetier, J.P. Chevaillier, J.B. Dementon, J. Fabre, K.I. Ichige, A. Kleitz, G. Martinot-Lagarde, B. Pouligny, F. Vannobel, J.P. Wolf, and international collaborations: G. Brenn, X. Cai, N. Damaschke, J. Domnick, F. Durst, L.X. Guo, Y.P. Han, P. Haugen, J.T. Hodges, R. Kleine, J.Y. Liu, J.A. Lock, J. Mroczka, A. Naqwi, Y. Ohtake, C. Presser, V. Renz, B. Rück, H.G. Semerjian, X. Shen, I. Shimizu, Y. Takahara, A.K.M.P. Taylor, C. Tropea, A. Ungut, Y. Wang, I. Wilhelmi, Z.S. Wu, D. Wysoczanski, F. Xu, T.H. Xu, S. Zhang, M. Ziema, and to make friends. We also acknowledge R. Petit from Aix-Marseille University who kindly accepted to check the first chapter and helped us to improve it.

From the first equations to what we consider as the "pivot" article in 1988 [2], ten years were required. Another five years has been necessary to reach the first genuine applications of the theory to a concrete problem in optical particle characterization, namely concerning the issue of trajectory ambiguity effects in phase Doppler anemometry [3], [4]. This was more than sufficient to pile up several thousands of pages of computations, including the ones spent in blind alleys, and the time spoiled by jumping cliffs or producing rubbish stuff. All this material has been preserved as a testimony of madness. As one can guess, some people wondered whether we were actually serious or not, crazy or not, what this theory was made for, whether it would be useful or not, worthwhile or not, or whether it was simply a game boosted by mind perversion. We therefore experienced some kind of negative social pressure which actually contributed to the expansion of the universe of GLMT. Anonymous acknowledgments are also required in this matter.

#### Introduction

For a physicist, and more generally for a scientist, one of the pleasures in everyday life is to detect exemplifying manifestations and avatars of the topic he is working on. Why do small tea leaves cluster to the center of the free surface of liquid in the cup, contrasting with the fact that centrifugal forces should drive them towards the wall? Why is liquid poured outside of a pot usually keen to follow the pot wall onto the table, in a persistent and irritating way, rather than flowing down, more or less vertically, to the cup? Why does a mirror change left to right but not top to bottom?

These three examples clearly concern tiny facts but should not be looked down upon when thinking about more challenging questions of physics and metaphysics, for small lanes may lead to large and unknown avenues. Actually a fascinating aspect of science is that it permits the study of familiar phenomena which are universal to some extent in so far as every human being may experience them, even if one stays away from modern cathedrals, we mean laboratories. Furthermore, behind these familiar phenomena are hidden deep arcana to decipher and reveal. Behind the simple action of shaking an ink-pen to supply ink to the pen, there is inertia and classical mechanics, while quantum theory is written on the sky by lasers piercing the night in some contemporary shows.

In optics, and to stick more closely to the topic of this book, in light scattering by particles, everyday surprises and observations may be specially appealing because they concern what could be the most privileged sense of humankind, namely vision. This metamorphoses photons to an enchanting world of shapes and colours that nearly everyone may enjoy, very often with a feeling of infinity and eternity, for instance when the sun rises on the Mississipi river or falls gently to sleep on Fuji-San.

The most striking example might be the rainbow, so marvelous that it has become a signature at the bottom of a contract between God and humanity in Jewish and Christian religions, or the scarf of Goddess Iris delivering messages from heaven to earth in the Greek mythology, or a bridge to Walhalla in 'Der Ring des Nibelungen' by Richard Wagner, inspired by old germanic and

XXIV Introduction

nordic legends. Even questions as naïve as: "Why is the sky blue at day while it displays all shares of reds in some dawns and twilights?", and "Why is it not as bright as the sun at night?", may lead to significant research and conclusions.

To give some qualitative clues for answering the first question, we mention that aforementioned blue and reds are due to the scattering of solar light by molecules and particles of terrestrial atmosphere. Moreover, scattering plays an essential role in cloudy days (a rather common feature in our Normandy), and also in foggy days (not so common, but still far from being exceptional). During these days it is possible to walk and drive without any infra-red assisting device thanks to a significant amount of solar and/or headlights photons which are scattered by droplets and crystals and somehow succeed to reach landscape details where they are scattered again to eventually reach the eyes. More generally, scattering is essential to our vision of the world since things are only visible thanks to the light they scatter from natural or artificial sources, changing the direction of travelling photons, modifying their amount, and generating colours through complex phenomena. As far as the above second question is concerned, it is deeply connected with the cosmological issue of the finiteness of Universe in space-time besides being may be a subtle coincidence allowing our eyes to get some rest!

In astronomy, the study of the light scattered by planetary atmospheres provides information on their composition ([5], [6]) but zodiacal light scattered outside of the ecliptic plane by dust particles of the solar planetary system limits the performances of spatial telescopes. In medicine, scattering of light by red cells of the blood enables to determine oxygen concentration ([7]), and the detection of tooth decay can be accomplished by studying the light scattered by tooth enamel ([8]). In surgery, there is interest in studying scattering interactions between light and biological tissues in order to master laser surgery as well as possible ([9]). In industry, applications of light scattering are manifold and potentially infinite in number. We would need a scientific and reckless Prévert to attempt to catalogue an endless inventory. Being scientists, but neither the reckless nor Prévert's type, we shall be content to mention some examples including the control of the transparency of drinking glasses, and of the luminous and mechanical properties of paints and sheets which depend strongly on the embedded scattering particles ([10], [11], [12], [13], old classical articles indeed). Other specific examples more relevant to the purpose of this book will be given later in a more restricted context.

This more restricted context is the electromagnetic scattering by particles. Concerning scattering, our framework is Quasi-Elastic Scattering (QES) which refers to the case when no change of frequency is involved in the light/matter interaction except that one due to the Doppler effect and the other singular one, from a finite frequency to a null frequency, when a photon is absorbed. Also, although it may be convenient to think of light in terms of photons and although scattering is a random quantum process at a more

Introduction XXV

fundamental level of description, assemblies of photons will be here modelled as electromagnetic waves.

Concerning particles, they *a priori* might be of arbitrary shape, arbitrary nature, arbitrary size, and embedded in media of arbitrary geometry with arbitrary distribution of particle concentrations.

The induced complexity is however still too big for us to handle in this book. The reader is invited to go to famous studies which should be present on any library shelf of a decent "scatterist" to get extensive information on the QES and underlying electromagnetism, such as those quoted as [14], [15], [16], [17], [18], [19], [20], [21] and [22]. As far as we are here concerned, attention will be focused on more restricted topics, not in an arbitrary way but because of the overwhelming difficulties involved in attempting to handle arbitrary situations with a single non arbitrary theory.

A first dichotomy to introduce might be between multiple and single scatterings. If it is temporarily accepted to describe light in terms of photons (whatever they are), then single scattering takes place when a photon entering a medium leaves it without having suffered more than one proper scattering event or when the first interaction between the photon and one particle leads to absorption. If more than one event (for instance two successive scatterings or one scattering followed by absorption) are involved during the life of the photon in the medium, then we are faced with multiple scattering. When the particle concentration is high in the medium, more complex phenomena may occur like dependent or coherent scattering (for instance, [23]). For multiple scattering, the interested reader may refer to the beautiful books by S. Chandrasekhar [24] and H.C. van de Hulst [18], and also by G. Kortüm [25] who introduces simple and efficient ideas in an appealing way. However, only single scattering will be here discussed (for most of the time) and it will be difficult enough to be enjoyable.

A second dichotomy is between direct and inverse problems. Assume that a particle is illuminated by a plane wave or by a laser beam and that you need know the properties of the scattered light. This is a direct problem. Conversely, assume that you know the properties of the scattered light but that you need the properties of the particle. This is an inverse problem. This dichotomy holds actually for both multiple and single scatterings. Rather clearly, an inverse problem is more difficult to solve that a direct problem. This increase of difficulty is vividly illustrated by Bohren and Huffman [22](pp. 9-11) who stated that a direct problem consists in describing the tracks of a given dragon while the inverse problem is to describe the dragon from its tracks. Most of this book will be devoted to direct problems, but optical particle sizing and, more generally, optical particle characterization, discussed in the last chapter, point out to genuine inverse problems.

Now, let us zoom again on a more restricted part of the landscape. Media containing a huge number of particles are essentially outside of the scope of this book. Suffice it to say that when particles are randomly distributed in space, it is usually enough to forget any phase relations and interference

XXVI Introduction

phenomena and simply to sum up scattered intensities to solve the direct problem. Therefore, we are here mostly concerned with the interaction between an electromagnetic wave and a single particle (or scatterers made out from a small number of particles, with coherent scattering).

As far as the particle is concerned, it can be of arbitrary size (not too small however to still own a bulk macroscopic character, and reasonably not too large since particles of infinite dimension do not exist) but its nature and shape are carefully chosen to make life easy, i.e. they are regular particles allowing one to use a method of separation of variables.

Most of the book is however devoted to the case when the scatterer is a homogeneous sphere defined by its diameter d and by its complex refractive index m. Then, when the incident wave is an usual ideal plane wave, the problem was actually solved about one century ago. The corresponding theory is usually granted to G. Mie [26]. However there is certainly some injustice in that. We must remember the work that Lorenz (often mis-written as Lorentz) accomplished about twenty years before ([27], [28]) although, admittedly, Lorenz is not likely to worry any more about it (but who knows actually?). The reader could refer to an article by N.A. Logan [29] to understand how Lorenz work has been unfairly overlooked, and also to historical articles from the 2nd International Congress on Optical Particle Sizing ([30] [31] and [32]). Even if an important Lorenz memoir has been lost, it still remains that he solved the problem of the scattering of waves by dielectric spheres though without explicitly referring to Maxwell's equations. Hence, it could be recommended to speak of the Lorenz-Mie Theory (LMT) instead of simply the Mie theory. One year after Mie, Debye ([33]) completed the theory by discussing the radiation pressure. Some people might then recommend to speak of Lorenz-Mie-Debye theory, but we feel that it is unnecessary. Debye being also very well known for other contributions to physics, he has already got his full share of fame.

Now, there is more to tell concerning the relationship between Mie and Lorenz. While Mie indeed relied on the macroscopic version of Maxwell's electromagnetism, Lorenz conversely relied on a mechanical theory of aether. Yet, both theories are empirically equivalent. The inquisitive reader might amazingly wonder how a "correct" theory (presumably the one based on Maxwell's equations) could agree with an "erroneous" theory (presumably the one based on mechanics). This is a very deep epistemological issue that cannot be extensively developed in this book. It is certainly an example of what is sometimes called the Duhem-Quine theorem telling that theories are under-determined by experiments [34], [35], [36], [37], [38].

One of the authors (Gouesbet Gérard) would now like to come to the original motivation which led to the theoretical developments described in this book. During his state thesis (a kind of thesis pertaining to a previous French university system), he studied diffusion and thermal diffusion phenomena of neutral species in a plasma of argon and helium [39]. This study required the measurements of plasma velocity by using laser Doppler velocimetry which,

Introduction XXVII

nowadays, is a well established technique for measuring flow velocities. In the most current optical set-up, a set of (more or less) parallel fringes is generated by making two laser beams (originating from the same source) interfering in a control volume. The flow under study is supposed to transport small inertia particles called tracers. When such a particle crosses the control volume, it generates a scattered light which is modulated at a certain frequency depending on the fringe spacing and on the velocity of the tracer, that is to say on the velocity of the flow (more properly, on the velocity component perpendicularly to the fringes). A photodetector is used to produce an electronic signal which is afterward processed by a processing device.

The plasma aforementioned above was a high frequency (laminar) plasma whose atom temperature was typically equal to 5 000 K (and the electron temperature to typically 10 000 K). It was seeded with alumina particles. The high temperatures involved led to a dilemma. If the injected alumina particles were too small, then they vaporized and could not produce any Doppler signal. If they were too big, then they would not be tracers any more, drifting behind the plasma flow. A compromise was necessary but there was no way at that time to control this compromise. The validity of the velocity measurements could only be indirectly checked (by verifying the conservation of mass), but there was no direct available way to do it. Furthermore, to make the situation a bit more confused, there was an erroneous dogma at that time (to become erroneous is common for a dogma) according to which decent Doppler signals could only be produced by particles smaller than the fringe spacing. However, it soon became obvious that having good Doppler signals did not imply that the particles were smaller than the fringe spacing, that is to say that they could be assumed to genuinely behave as tracers [40], [41]

The best direct way to solve the problem would have been to possess an instrument allowing one to measure simultaneously the size and the velocity of individual particles in flows, not only for small particles (tracers) but also for large particles. Similar needs and questions were put forward in different fields, like in plasma spraying or in the study of sprays in combustion systems. Several systems were proposed and studied, like relying on the use of the visibility or of the pedestal of Doppler signals [42], [43]. But, although satisfactory results were published in the archival literature or announced in conferences, there, however, were also many people becoming disappointed up to a situation where the topic of optical sizing received a rather poor reputation. In particular, the visibility and the pedestal techniques are no longer used nowadays. It became obvious that the topic was too much based on experiments, somewhat of a nearly pure empirical nature, without a sufficient theoretical effort to master the design and functioning of instruments.

What is likely to be the most important problem is that, in optically measuring the sizes of discrete particles in flows (possibly simultaneously with velocities, complex refractive indices, and concentrations), a laser source is usually required or, at least, very useful. Under some circumstances, the laser beam is expanded and/or the particles to be studied are small enough,

XXVIII Introduction

in such a way that the laser source can be safely considered as being a plane wave. An example is provided by the diffractometry technique. To design instruments and to interpret data, one can then rely more or less blindly on the basic theory for plane wave scattering, namely LMT. Indeed, for a long time, LMT has been the most powerful theoretical tool in that respect and, even nowadays, it remains famous and is being used. However, this theory is now a one-hundred-year-old lady, and although still very alive and waltz dancing, it is no wonder that it might become inappropriate in a large variety of situations, since the laser was still in the nimbus when Ludwig Lorenz and Gustav Mie write their equations.

Very often, the situation is not ideal enough to plaster an old theory on contemporary experiments. In LDA-based systems for instance, most data processing, design of instruments, and theoretical principles rely on the classical LMT, although the in going laser beams are usually focused. When the diameter of the discrete particles is not small with respect to the laser probe diameter (usually a Gaussian beam diameter or the width of the plateau in a top-hat beam), then we have to worry on the validity of the LMT which could be misleading. Also, in some cases, measurements directly rely on laser beam scattering properties ([44]). Consequently, we certainly need to rely on a more general theory, enabling us to compute the properties of the light scattered by an ideal sphere illuminated by a Gaussian beam or a top-hat beam, more generally by an arbitrary-shaped beam.

We shall call this theory the generalized Lorenz-Mie theory (GLMT), or sometimes the generalized Lorenz Mie theory in the strict sense (strictosensu) to which most of this book is devoted. Nevertheless, we shall also consider other cases, when the scatterer is not a homogeneous sphere defined by its diameter d and its complex refractive index m, but is another kind of scatterer whose properties allow one to solve the scattering problem by applying a method of separation of variables. The terminology "generalized Lorenz Mie theory" will be also used for these other cases, with the proviso that the kind of scatterer under study has to be specified. For instance, there will be a generalized Lorenz-Mie theory for infinite circular cylinders.

The existence of GLMTs is relevant to the understanding and to a better design of optical measurement techniques, such as for simultaneous measurements of velocities and sizes of particles embedded in flows, and therefore to the study of multiphase flows transporting discrete particles. Two-phase and multi-phase situations of this kind (suspensions, droplet and bubble flows) are indeed very common in industry, laboratories and environment. Examples involve the control, understanding and design of specific spray and particle combustion systems, of laden flows encountered by chemical and mechanical engineers in pipes and conduits, or also in standard chemical engineering processes such as fluidization, sedimentation and pneumatic transport. People may also be concerned with very small particles such as soots which are deeply inhaled into the lungs and can lead to the development of tumours, exemplifying that environmental care is one reason to develop optical particle

Introduction XXIX

sizing techniques (more generally optical particle characterization), in order to learn how to control the emission and the dispersion of such particles. Particularly relevant to this topic is the use of Diesel engines in individual cars, where we have to worry about the effects of exhaust particulate emission. In connection with energy supply and more precise control of energy conversion devices, we also have to perform characterization of droplets in spray flames and of solid particles in coal pulverized flames. Hydraulic engineers are concerned with sand and pollutant transport in rivers, lakes, and also in oceans where one must investigate spray droplets over the sea or deposition and dragging away of particulates in the sea and on the ground in connection with water motion. Industrial processes also include particulate clean-up devices such as electrostatic precipitators, oil mists from pumps, the influence of particle properties for cements and paints. These heteroclite examples are obviously very far from providing an exhaustive list, and only aim at giving a flavour of the richness of possible applications.

From a fundamental point of view, the knowledge of the size and the velocity distributions (or better of the size and velocity, particle by particle) of a dispersed phase is relevant to the understanding and to the prediction of heat and mass transfer, and of chemical reactions in many processes such as in combustion systems. It is also relevant to the understanding and to the prediction of the dispersion of particles by continuous motions in turbulent flows, a domain of research which is very active nowadays.

Therefore, the study of two-phase flows in which discrete particles are transported in and by turbulent structures are of interest both to the researcher, wishing to understand and describe the laws of nature, faced with difficult and challenging two-phase flow problems, and to the engineer who inevitably encounters them in a large variety of industrial situations, and has to design and control various plants and processes involving particle heat and mass transfer phenomena.

At first, the engineer may rely on correlations based on experimental results and adequate display of data using pertinent dimensionless groups. However, correlations are usually valid only for limited ranges of parameters, and extension of results beyond these ranges is always a risky affair. Then, the researcher must open the way for a second step, namely predictions through modelling and computer programming. This is also a risky affair which requires careful validations against well-designed experimental test-cases. For a background in such problems, see [45]) [46], [47], [48] [49] [50] and references therein.

Consequently, in any case, accurate and extensive measurements of sizes, velocities, and concentrations (and may be also shape and refractive index characterization) of the discrete particles in the flow under study are needed. The ideal aim would be to provide us with space- and time-dependent particle size spectra. Emphasis must be set on optical techniques which may be non intrusive (in principle they do not disturb the medium under study), and

XXX Introduction

supply us with local (in situ small control volumes), time-resolved data. A very relevant key-word for these techniques is: versatility.

Significant advances have indeed been accomplished for years thanks to the development of these optical techniques, combining laser at the input and computer at the output, two requisites of numerous modern experiments lying somewhere within light scattering theory.

The proceedings of a series of symposia, hold under the name: "Optical particle sizing: theory and practice" later on generalized to "Optical particle characterization", would allow the interested reader to follow the development of the field in a very comprehensive way. After the first symposium in Rouen, France, in 1987 organized by the authors of the book, subsequent conferences have been hold in Phoenix, Arizona, in 1990 (chaired by D. Hirleman), in Yokohama, Japan, in 1993 (chaired by M. Maeda), in Nüremberg, Germany, in 1995 (chaired by F. Durst), in Minneapolis, Minnesota, in 1998 (chaired by A. Naqwi), in Brighton, England, in 2001 (chaired by A. Jones), in Kyoto, Japan, in 2004 (chaired by M. Itoh) and in Gräz, Austria, in 2007 (chaired by O. Glätter). Beside proceedings stricto sensu e.g. ([51], [52], [53], [54]), selected articles have been published in "Applied Optics" and "Particle and Particle Systems Characterization".

Actually, although we had a specific motivation in mind when developing the GLMT, as discussed above, it is now clear that the range of applications has extended far more beyond what was originally expected and, let us tell it frankly, toward unexpected fields. An example concerns the interpretation of optical levitation experiments, see e.g. [55], [56], [57], [58], and references therein. However, many other applications have to be discussed, and they will indeed be discussed.

Discussions of scattering from shaped beams have previously been provided by several authors, with more or less extended degrees of generality. Indeed, the development of science takes place through a filiation where nothing emerges from nothing. We now briefly but fairly exhaustively discuss these works, limiting here ourselves to the ones prior to 1989. We start with Chew et al [59] [60] who discuss converging and diverging beams (respectively). To approach the case of laser beams, Morita et al [61] assume a beam with a Gaussian distribution of amplitude (which does not comply with Maxwell's equations however) and a scatter center smaller than the waist and located near it. Tsai and Pogorzelski [62] consider a  $TEM_{00}$  beam which is described by using an expansion of vectorial cylindrical functions in vectorial spherical functions. Then, the beam description complies with Maxwell's equations but exhibits two singularities where the electric fields are zero, located at  $\sqrt{2}$ times the waist radius from the beam axis. Their results concern small scatter centers centered at the beam waist. Tam [63] and Tam and Corriveau [64] generalize the method of Tsai and Pogorzelski to the beam mode  $TEM_{01}^*$  and to arbitrary location of the scatter center but do not present any numerical results. There is also a series of articles co-authored by Yeh ([65], [66], [67]) starting from a Rayleigh-Gans approximation up to the 1982-article in which Introduction XXXI

the  $TEM_{00}$  beam is described by its plane wave spectrum and the location of the scatter center is arbitrary. However, particles must be non absorbing and a practical limitation results from the time-consuming character of numerical computations (published results only concern particles with a size parameter smaller than about 5, i.e. diameters smaller than about twice the wavelength of the incoming electromagnetic wave). Kim and Lee [68] [69] describe the incoming  $TEM_{00}$  laser beam by using a complex point-source method and establish the corresponding theory for a spherical scatter center arbitrarily located in the beam. However, the complex point-source method introduces two singularities at which field amplitudes become infinite. Finally, we mention a more recent study by Barton et al [70]. Barton contribution will be given more discussion when appropriate in this book.

With the first GLMT-equations likely written in 1978, the first releases of the existence of a GLMT are testified (urbi) in the PhD thesis of G. Gréhan, in 1980 [71] or, the same year, in an internal report [72] and thereafter (orbi) in an AIAA conference in Palo Alto, California, in 1981 [73]. The first archival article, in which known precursors were acknowledged, was published in 1982, in the French language [1]. It dealt with a (special) GLMT concerning the case of an illuminating axisymmetric incident light beam interacting with a sphere defined by its properties (d, m), using the Bromwich formalism. The interaction is on-axis, that is to say the axis of propagation of the incident beam passes through the center of the scatterer (otherwise, the interaction is said to be off-axis). Algebraic expressions are established for scattered field amplitudes, and for scattered intensities, and specified in the far field. They introduced expansion coefficients associated with partial waves, denoted as  $g_n$ , and later on named beam shape coefficients. The obtained expressions are very close to the one of the Lorenz-Mie theory such as reported by Kerker [23] and can therefore easily be implemented in a classical Lorenz-Mie computer program, once the beam shape coefficients are calculated. The LMT itself is found to become a special case of the special GLMT.

The concept of axisymmetric light beam has been much later extensively discussed by Gouesbet [74]. An axisymmetric light beam is defined as a beam for which the component of the Poynting vector in the direction of propagation does not depend on the azimuthal angle in suitably chosen coordinates. In such coordinates, the partial wave representation of the beam is again found to be given by a special set  $\{g_n\}$  of beam shape coefficients. An example of such axisymmetric light beams is a laser beam, in the mode  $TEM_{00}$ , or Gaussian beam. By contrast, a laser sheet is not an axisymmetric light beam.

In 1985, the 1982-formalism is adapted to the case of a Gaussian beam modelled as a low-order Davis beam [75] called order L beam (L for lower) [76]. This adaptation could be viewed as a specification since a Gaussian beam has been said to be a special case of axisymmetric beams. However, the axisymmetric beams used in the 1982-article were too simple to match the description of an order L Davis beam. Actually, they could match a still

XXXII Introduction

simpler description of Gaussian beams called order  $L^-$  of description. Therefore, the specification to an order L Gaussian beam could also be viewed as a generalization. In the introduction of the article, we stated that we were providing a generalization of our previous contribution by modelling the Gaussian beam by field expressions more rigorous than the ones corresponding to an axisymmetric light profile. As we can see from the above discussion, this statement has now to be viewed as erroneous, due to the fact that, at that time, we did not possess a full mastering of the concept of axisymmetric light beam that became available only more than ten years later. We should have written that we were providing a generalization to axisymmetric light beams (order L Gaussian beams) more general than the axisymmetric light beams considered in 1982. Another (more significant) generalization is that further expressions are also provided for phase angles, cross-sections, efficiency factors, and radiation pressures. All these expressions involve again the special beam shape coefficients  $g_n$ .

Due to the difficulty (that we shall recurrently encounter) in providing a good enough description of Gaussian laser beams and, more generally, of any kind of shaped beams, and in providing descriptions exactly satisfying Maxwell's equations, in particular (this was not the case for the aforementionned order L and L<sup>-</sup> descriptions of Gaussian beams), we commented at that time that the theory was not yet rigorous. This was may be too severe. It would have been interesting and more relevant to separate in the results what was general, and what was specific to the illuminating beam under study, something that was done only later, in 1988. But, nevertheless, some emphasis on Gaussian beams has been useful for future developments. Furthermore, it was also worthwhile to carefully study the properties of and the degrees of approximations involved in the orders L and L<sup>-</sup> of description of Gaussian beams. This was done in 1985 [77].

In parallel to these developments, there was a real worry concerning the possibility of developing practical applications of the pregnant GLMT. Indeed, when we started trying to compute the beam shape coefficients  $q_n$ , it has been disappointingly discovered that these computations were too much time consuming, possibly two or three hours on the most powerful mainframe computer readily available in France at that time, for only one beam shape coefficient. Just consider now that for any realistic light scattering computation in the GLMT-framework, hundreds or thousands of such beam shape coefficients have to be calculated. The original expressions for evaluating the (special) beam shape coefficients relied on double quadratures. Eventually, another method, valid at that time for Gaussian beams, has been discovered. This method has been called the localized approximation, relying on a localized interpretation, inspired by the famous principle of localization of Van de Hulst [17]. The terminology "localized approximation" is however may be to be regretted and, certainly, is unfortunate. There is a sense in which the result obtained is an approximation because it is indeed an approximation to an ideal (unknown) Davis beam. However, there is a sense in which it Introduction XXXIII

is not an approximation, namely the fact that it provides field expressions which exactly satisfy Maxwell's equations. The examination of the literature demonstrated that the word "approximation" has often been interpreted in a negative manner, some authors then proposing other beam models supposed to be rigorous, not approximations. A better terminology would have been to say from the beginning that the localized interpretation provided a localized beam model, as will be later introduced. As far as we know, all beam descriptions are models, whether they do not satisfy or do satisfy Maxwell's equations. Such issues will have to be developed more extensively in the bulk of the book.

The first archival article on the localized approximation is dated 1986, by Gréhan et al [78]. In this article, the localized approximation is validated by comparing the GLMT (with the illuminating beam described with a localized beam model) and a Rayleigh-Gans approximation for Gaussian illumination. Other validations are discussed too, namely comparisons with theoretical results from Tsai and Pogorzelski [62] and from Yeh et al [67], and also with an experimental scattering diagram under laser beam illumination obtained from a sphere in optical levitation [57]. A validation is however not a rigorous justification which will become available only nearly ten years later [79], [80]. In 1987, the first computations of beam shape coefficients by quadratures (named "first exact values") became published, with computing times ranging from 30 s to 2 hr CPU, and favourably compared with the results of the localized approximation [81]. The same year, complementary computations of beam shape coefficients  $g_n$  were published, with comparisons between "exact" values at both orders L and  $L^-$ , and the localized approximation. Also, a discussion of the physical interpretation of the localized approximation is provided and the GLMT is again used to interpret, in a more extended way than previously, an optical levitation experiment. Furthermore, a comparison between GLMT and diffraction theory in the near forward direction is discussed [82]. A similar complementary discussion, in French, is available from Maheu et al [83], which is the first part of a two-part article. The second part [84] provides and discusses several GLMT-based scattering diagrams, phase angle computations, efficiency factors, and collected powers, that is to say the most extensive set of results hitherto obtained with the special GLMT. It has soon be also emphasized that such computations could be successfully carried out on a micro-computer, with a maximum of 64 Ko of variables accepted by micro-computers of the PC family running under DOS 3 [85]. Note that, nowadays, LMT-computations (not GLMT-computations however) are feasible on a mobile phone! [86]. Beside quadratures and localized approximation, a third technique to evaluate the beam shape coefficients, namely by using finite series, has also been introduced. We then possessed three methods which are compared in a 1988-article [87].

It was then clear that the special GLMT was mature and ready for applications. When approaching this result, it became obvious that it was the right time to build a final general version of the theory. A first version, for

XXXIV Introduction

arbitrary location of the scatterer, is discussed by Gouesbet et al in 1988 [88], with a strong emphasis, including in the title, on Gaussian beams. However, as stated in the conclusion, other beam descriptions could be used instead of a Gaussian beam, without changing the method used. In particular, this reference introduced new expressions and new beam shape coefficients which do not depend on the specific illuminated beam considered. These new beam shape coefficients, generalizing the special beam shape coefficients  $g_n$ , are denoted as  $g_{n,TM}^m$  and  $g_{n,TE}^m$ . Changing the beam description just implies to evaluate these general beam shape coefficients in a new way, adapted to the new description (or more generally to the new beam under study, e.g. laser sheets). A second more extended version, that we consider as the "pivot" article of GLMT, has also been published in 1988 [2]. Again, may be unfortunately, a strong emphasis is put on Gaussian beams, including in the title of the article, but the fact that GLMT works for arbitrary-shaped beams is made explicit in a companion article published in the same year [89], devoted to GLMT for arbitrary location of a scatterer in an arbitrary profile.

We may now pursue our brief history of GLMT by relying on a few review articles published on the topic, allowing one to follow subsequent developments in a concise way. The first review article was published in 1991 and, most essentially, presented the GLMT formalism under a single roof [90]. The next review article was published in 1994 [91]. The general formulation was required and it is once more pointed out that this formulation is insensitive to the nature of the incident beam. More important, genuine applications to optical particle characterization, in agreement with our original motivation, could be discussed, namely phase Doppler anemometry and trajectory ambiguity effects. Other miscellaneous applications concerned scattering responses and extinction cross sections, diffraction theory, optical levitation and radiation pressure. The third review article, in 2000 (with about 350 references) reported on new theoretical advances, in particular by discussing infinitely long cylinders and other shapes, and extended applications: radiation pressure, rainbows, imaging, morphology-dependent resonances, phase-Doppler instruments, etc. It also provided recommendations for future research [92]. See also Gouesbet [93] and Gouesbet et al [94].

Now, something special happened in 2008, namely that it was the hundredth anniversary of the famous Gustav Mie's article. This has been commemorated in several places (GAeF conference 2008 on "Light Scattering: Mie and More-commemorating 100 years Mie's 1908 publications", 3rd-4th July, Karlsruhe, Germany [95]; International Radiation Symposium IRS 2008, 3rd-8th August, Foz do Iguaçu, Brazil [96]; Eleventh Conference on Electromagnetic and Light Scattering, 7th-12th September 2008, Hatfield, UK [97]; Mie theory 1908-2008, Present Developments and Interdisciplinary Aspects of Light Scattering, 15th-17th September, Universität Halle-Wittenberg). It has been an opportunity for two more review articles [98], [99]. In particular, the second one (with again about 350 references) exhibited the fact that the use of generalized Lorenz-Mie theories and associated ingredients was more

Introduction XXXV

and more widespread, confirming the need for a book like the present one. Let us also mention a review of elastic light scattering theories, available from Wriedt [100], and the existence of a *scattering information portal* for the light scattering community discussed by Wriedt and Hellmers [101].

Furthermore, the series of published articles suffered from three main shortcomings. The first one is that, as usual in research, the development of our ideas did not follow a linear line. The reader wanting to fully exploit our study and check our derivations would then be condemned to the burden of reorganizing the published material. The second shortcoming is that many details have been omitted, the usual (unfortunately justified) prayer of referees and editors being to ask for drastic cuts. To go from relation n to relation (n+1), 20 intermediary pages of computations must sometimes be reproduced by the reader who is therefore left with a skeleton from which living flesh has been carefully removed to produce an article written in an objective, concise, modern scientific style. Finally, in practice, program sources are not being published in the archival literature. Scientists playing tennis usually ask to the authors to get the ball i.e. program sources, but the ones playing golf and wanting to move the ball alone must also reproduce non trivial computer programs.

These three shortcomings are essentially avoided in this book. The material is reorganized in a linear and comprehensive way. We take the reader by the hand and guide him in the forest, following a civilized track for berry pickers. People just wanting to get numerical results may have a bird's eye view on the formulation and may directly go to the computer programs to use them. Hopefully, this book might then be useful to and appreciated by both tennismen and golf players.

Although this book is dedicated to electromagnetism, there has been a few moves toward quantum mechanics, which are now briefly mentioned. The structure of quantum arbitrary shaped beams has been examined [102], [103]. Quantum cross-sections under quantum arbitrary shaped beam illumination are discussed for both elastic [104] and inelastic [105] scattering. Cross-sectional analogies between (vectorial) electromagnetic scattering and (scalar) quantum scattering have also been established, again both for elastic and inelastic cases, under plane wave and under quantum arbitrary shaped beam illuminations [106], [107], [108]. Also, a generalized optical theorem for non plane wave scattering in quantum mechanics has been established [109].

The book is organized as follows:

Chapter I provides a background in Maxwell's electromagnetism (in free space and in matter) and discusses Maxwell's equations. The content of this chapter is supposed to be sufficient to attack the rest of the book, but it is not meant to provide a detailed introduction to electromagnetism. Preferably, the reader should already possess some kind of basic knowledge to enter this book. Chapter I rather intends to recall what is necessary to proceed further and to introduce notations, as well as the basic language to be used.

XXXVI Introduction

Chapter II introduces the method of Bromwich scalar potentials which has been originally used to solve Maxwell's equations for the main case under study, that is to say to build the GLMT. Relationships between this method and other equivalent possible methods (such as the use of vector spherical wave functions) are also discussed.

Chapter III uses the material introduced in the first two chapters to describe the GLMT for arbitrary location of the scattering sphere in an arbitrary incident beam, that is to say without referring to any specific kind of illuminating beam. This theory introduces two sets of beam shape coefficients denoted as  $g_{n,TM}^m$  and  $g_{n,TE}^m$  which describe the illuminating beam and are recurrently used in GLMT-expressions. The expressions for the quadrature methods to evaluate these beam shape coefficients are discussed (although they are lengthy and costly to perform). Other formulations to deal with arbitrary shaped beam scattering are briefly considered. Other generalized Lorenz-Mie theories (i.e. for different shapes of the scatterer) are also introduced.

**Chapter IV** discusses specific beams, with a very strong emphasis on Gaussian beams.

**Chapter V** establishes that beam shape coefficients may also be computed by using a finite series method which is computationnally more efficient than quadratures. The introduction of these finite series provided a first significant step to speed-up GLMT-computations.

Chapter VI is devoted to the special case when the center of the scattering particle is located on-axis in an axisymmetric beam, such as a Gaussian beam (or a plane wave!), leading to dramatic simplifications. In particular, the double set  $\{g_{n,TM}^m, g_{n,TE}^m\}$  of beam shape coefficients reduces to a single set  $\{g_n\}$  of special beam shape coefficients. The similarity between LMT and GLMT in this case is striking, and we easily recover LMT from GLMT as another more special case. Also, a significant interest of this case is that the formulation becomes very similar to the one of the classical LMT, with the result that computer programs for LMT can readily be adapted to the special GLMT, once the beam shape coefficients are evaluated.

Chapter VII discusses a very beautiful method to evaluate beam shape coefficients  $(g_n, g_{n,TM}^m)$ , and  $g_{n,TE}^m$ , our favourite one indeed. It is actually the fastest one and provides many physical insights on the meaning of the beam shape coefficients. It has been called (may be unfortunately) the localized approximation, relying on a localized interpretation. It generates localized beam models which exactly satisfy Maxwell's equations.

Chapter VIII discusses concisely but fairly exhaustively the applications of GLMTs.

Introduction XXXVII

The bulks of the chapters provide basic knowledge, ordered in, we hope, a rather logical order. Most of these bulks are accompanied by complements. The aim of these complements is to address the reader to more technical or complementary matters, and to an exhaustive literature. Although they provide valuable information, allowing the reader to deepen the topic if required, their reading can be omitted at first without provoking any havoc in the understanding of the subsequent material dealt with. These complements are written in a concise way. Owing to this fact, they allow the reader to gain contact with all the material available at the present time (except for possible unfortunate omissions for which we apologize), without having to manage with an over-sized book. Chapter VIII is written in the same style than the complements.

To prepare the complements and Chapter VIII, we relied on ISIweb of knowledge, and made a list by extracting the articles citing the Rouen works on GLMTs. A significant number of them (but not all of them) are cited in this book. Some articles have been removed from the citing list when they are not enough relevant to the aim of this book (this should not be considered as a negative appraisal however). Conversely, some articles which do not pertain to the list have been used when they are found to be useful for a better understanding of the exposition and of the chronology of events. The corresponding cited articles may be arranged in three families. A first family corresponds to articles which explicitly use or rely on GLMTs. In a second family, GLMTs have not been used but could have been used. This is the family of GLMT-izable articles. A third family concerns citing articles which are not strictly relevant to GLMTs but are relevant to the more extended field of light scattering as a whole. They may give the reader a flavour of the environment in which GLMTs have to move. Furthermore, as a consequence of the above strategy for complement-like issues, the corresponding cited articles are not necessarily the first articles that were published in each individual topic. Rather, they may be articles pertaining to the citing list that may build on other earlier studies. These earlier studies may be reached from the reference lists of the cited articles. This discussion defines the sense in which the complements and Chapter VIII are exhaustive.

Appendices expose some technicalities of secondary significance. However, one of them should attract the particular attention of many readers, namely it contains a list of computer programs provided in a website connected to the book. This website also contains movies showing the interaction between some scatterers and ultra-short pulses.

This book being devoted to an up-to-date version of electromagnetic scattering theory, Maxwell's equations constitute the unescapable starting block. An usual attitude in textbooks dealing with scattering theory is to straight-away introduce special Maxwell's equations which are sufficient to develop the theory when only local, linear, homogeneous, isotropic and stationary media are considered. The reader wanting to adhere to such a point of view could immediately jump to section I.2. To build the house on firmer foundations, section I.1 is nevertheless devoted to a very general setting in order to emphasize assumptions underlying special Maxwell's equations that we shall have to cope with. It might appear strange to many people that writing Maxwell's equations in material arbitrary media is still an open problem, but such is the case indeed. Our account of this problem relies on Petit [110] and Dettwiller [111].

# I.1 General Maxwell's Equations in Cartesian Coordinates

The purpose of this section I.1 is to attempt to introduce a bit of generality and of rigor in the exposition, from Maxwell's equations in free space to the macroscopic Maxwell's equations to be used later in this book. This has however to be done in a rather concise way since this book is not intended to be a book on electromagnetism and, therefore, some readers, not yet familiar enough with electromagnetism, might find it discouraging. Then, let us advise that it is possible to jump directly to section I.2 and to consider Rels (I.56)-(I.59) as starting points, without too much havoc. Furthermore, these relations are commonly available from the literature and the reader might then, at least in a first step, trust them.

# I.1.1 Maxwell's Equations in Free Space

Electromagnetism is a major contribution of J.C. Maxwell who published in 1865 his celebrated set of equations. Elaborating on the knowledge accumulated in electricity and magnetism, and invoking a principle of conservation of electric charges to modify the equations known at that time, J. C. Maxwell achieved the unification of electricity and magnetism, presented a model of light as a special case of electromagnetic waves (to be later however completed by the development of quantum mechanics and concepts), and definitely introduced fields as physical entities on the foreground of the stage. Fields are now landmarks in the landscape of what may be called modern physics. Also this first unification is the starting point of a quest of a physical Holy Grail, namely the great unification of all forces acting in nature to move it towards an unknown destiny.

In vacuum, using Cartesian coordinates, the set of Maxwell's equations reads as:

$$(curl E_j)_i = -\frac{\partial B_i}{\partial t} \tag{I.1}$$

$$divB_i = 0 (I.2)$$

$$(curl B_j)_i = \mu_0 J_i + \mu_0 \epsilon_0 \frac{\partial E_i}{\partial t}$$
(I.3)

$$divE_i = \rho/\epsilon_0 \tag{I.4}$$

These equations introduce two vectorial fields  $E_i$  and  $B_i$ , two constants  $\epsilon_0$  and  $\mu_0$ , and two source terms  $\rho$  and  $J_i$ .  $E_i$  and  $B_i$  will be called electric field and magnetic induction field respectively. The constants  $\epsilon_0$  and  $\mu_0$  may be considered as properties of the vacuum in which the fields exist. They sometimes receive the generic name of inductive capacities of the vacuum. They may also be found to be called dielectric constant and magnetic permeability of the vacuum, respectively. In this book, following a French terminology, they will be called permittivity and permeability of the vacuum, respectively. Finally,  $\rho$  represents electric charges and  $J_i$  represents electric currents. Therefore, the set (I.1)–(I.4) governs the evolution of the fields, in relation with the existence of sources, in a vacuum characterized by two constants.

Although quantum physics definitely tells us that the vacuum is not empty, it may appear counter-intuitive that the vacuum has to be characterized by inductive capacities, particularly in the framework of a non-quantum theory as electromagnetism is. Indeed, the existence of inductive capacities definitely means that vacuum is not nothing! To avoid any conflict between the scientific and the non-scientific meanings of the word "vacuum", it might be preferable to speak of free space, as done by some authors.

Strictly speaking, free space means space without any source, i.e  $\rho = 0$ ,  $J_i = 0$ , leading to simplifications in the set (I.1)–(I.4). The absence of any source does not prevent the fields  $E_i$  and  $B_i$  from existing. For instance, the

propagation of light is perfectly well described by the no source version of the set (I.1)–(I.4).

It then appears that calling this set Maxwell's equations in free space is, *stricto sensu*, an improper denomination. The denomination is only acceptable because it is actually assumed that the geometric support of the sources is of lower dimensionality than the free space in which the fields evolve. For instance, electric charges are discrete charges like electrons of dimensionality zero, or electric currents flowing on wires of dimensionality one. Therefore, by tossing a point in the space, the probability of landing on the geometric support of the source is strictly zero. A mathematician would state that the Lebesgue measure of the geometric support is zero and that our free space is free almost everywhere.

The reader may have noted that it has not been attempted above to give precise names to  $\rho$  and  $J_i$ . The reason for the same can be made clear now. Because the geometric support of the sources is of lower dimensionality than the space,  $\rho$  and  $J_i$  cannot represent volumic densities. For a rigorous formulation,  $\rho$  and  $J_i$  should be represented using the theory of distributions. Examples are a discrete charge  $\rho$  located at a point P represented by a distribution  $\rho$   $\delta_P$  or a surface current located on a surface S represented by a distribution  $J_i$   $\delta_S$ , in which  $\delta_P$  and  $\delta_S$  denote Dirac distributions [112, [110]]. To avoid the use of the theory of distributions which is not compulsory in the bulk of this book, we shall be content with the loose formulation presented in the set (I.1)–(I.4).

# I.1.2 Maxwell's Equations in Matter

The set (I.1)–(I.4) in principle allows one to describe the electromagnetic theory at a microscopic level in matter. There is however no interest for us in such a description. Indeed, we are only interested in this book by macroscopic fields, the only ones to be measurable. In an electromagnetic macroscopic theory, fields  $E_i$  and  $B_i$  must be understood as being space and time averages of microscopic fields  $E_{i,m}$  and  $B_{i,m}$ , respectively, in which the subscript m stands for microscopic. However, for material media, we do not readily know how to average charges and currents to obtain a macroscopic charge density  $\rho$  and a current density  $J_i$ . Deriving macroscopic Maxwell's equations in matter from microscopic Maxwell's equations in vacuum therefore appears to be a commitment of tremendous difficulty.

One then deals with a phenomenological approach. This approach relies on the introduction of two new vectors  $P_i$  and  $M_i$ , called electric and magnetic polarizations, respectively. They characterize how the material reacts to external macroscopic electric and magnetic fields. Obviously there must be a microscopic interpretation behind these new vectors. For instance, let us consider the special case of a dielectric material. Although there is no net electric charges in such a material, the barycenter of positive charges in nuclei does not necessarily coincide with the barycenter of electronic negative charges (even in the absence of external fields). Therefore, the material may

be considered as an assembly of elementary electric dipoles. The electric polarization  $P_i$  then expresses the dipole moment of an infinitesimal volume, per unit volume. One then shows that the electric potential induced by the polarization of the dielectric material is equal to a potential created in free space by a fictitious distribution of charges. Comments would be fairly similar for the magnetic polarization  $M_i$ .

Therefore, once  $P_i$  and  $M_i$  are introduced, it is demanded to rewrite Maxwell's equations in matter in a way fairly similar to Maxwell's equations in free space. With such a requirement, the set (  $\square$  )–(  $\square$ 4 ) for free space case is rewritten in the presence of matter as:

$$(curl E_j)_i = -\frac{\partial B_i}{\partial t}$$
 (I.5)

$$div B_i = 0 (I.6)$$

$$(curl H_j)_i = J_i + \frac{\partial D_i}{\partial t}$$
 (I.7)

$$div D_i = \rho (I.8)$$

in which two new fields  $D_i$  (dielectric displacement) and  $H_i$  (magnetic field) have been introduced. A significant point is that the fields  $E_i$  and  $B_i$  in Rels (  $\blacksquare$  5)-(  $\blacksquare$  6) are macroscopic fields in matter and do not identify with microscopic fields described by the set (  $\blacksquare$  1)-(  $\blacksquare$  4). The newly introduced effective fields  $D_i$  and  $H_i$  are related to the macroscopic fields  $E_i$  and  $B_i$  by two relations:

$$D_i = \epsilon_0 E_i + P_i \tag{I.9}$$

$$H_i = B_i/\mu_0 - M_i \tag{I.10}$$

which, once that the set ([.5])–([.8]) is given, may be to some extent considered as definition relations for the polarizations  $P_i$  and  $M_i$  representing field modifications due to the presence of matter. In free space, when  $P_i$  and  $M_i$  are zero,  $D_i$  and  $H_i$  are proportional to  $E_i$  and  $B_i$  respectively, and the set ([.1])–([.4]) may be recovered from the set ([.5])–([.8]). Conversely, any attempt to formally obtain the set ([.1])–([.8]) by manipulating the sets ([.1])–([.4]) and ([.9])–([.10]) would fail due to our inability to formally express macroscopic fields  $E_i$  and  $B_i$  from the corresponding microscopic ones.

Rels (1.5)-(1.10) are sometimes found to be introduced as the starting point, for instance by Kerker 23. They form the basis of macroscopic electromagnetism in presence of matter assumed to form a continuous medium.

Following Stratton [15], let us summarize the assumptions of macroscopic electromagnetism as follows:

- (i) The theory is a macroscopic one.
- (ii) All fields  $E_i$ ,  $D_i$ ,  $B_i$ ,  $H_i$ , polarizations  $P_i$ ,  $M_i$  and source densities  $\rho$ ,  $J_i$ , are continuous functions of time with continuous time derivatives.

- (iii) These quantities are also continuous functions of space with continuous space derivatives in space domains having continuous physical properties.
- (iv) Discontinuities in the field vectors or in their derivatives are allowed to occur on separation surfaces between media when these surfaces exhibit discontinuities in physical properties.

# I.1.3 Boundary Conditions

The set ([1.5])-([1.8]) must be completed by boundary conditions and by the introduction of the Lorentz force.

In the broadest sense, boundary conditions comprehend limit conditions at the infinite (not discussed in this chapter) and jump conditions on separation surfaces between media (assumption (iv) in the previous subsection). Let us consider two media numbered 1 and 2 separated by a surface S equipped with a unit vector  $n_{12,i}$  normal to S and positively oriented towards the second medium. Jump conditions then read as:

$$(n_{12,i}) \wedge (E_{2,j} - E_{1,j}) = 0 \tag{I.11}$$

$$n_{12,i} (B_{2,i} - B_{1,i}) = 0$$
 (I.12)

$$[(n_{12,i}) \wedge (H_{2,j} - H_{1,j})]_k = J_{s,k}$$
(I.13)

$$n_{12,i} (D_{2,i} - D_{1,i}) = \rho_s$$
 (I.14)

in which  $F_i \wedge G_j$  designates a vectorial product,  $F_iG_i$  designates an inner product (Einstein summation rule being used) and  $J_{s,k}$ ,  $\rho_s$  are superficial current density and charge density on S, respectively.

On one hand, Rels (I.11) and (I.12) express the continuity of the tangential component of the electric field  $E_i$  and of the normal component of the magnetic induction field  $B_i$  when crossing the surface S, respectively.

On the other hand, Rels (I.13) and (I.14) mean that there is a discontinuity in the tangential component of the magnetic field  $H_i$  and in the normal component of the electric displacement  $D_i$ , respectively. Therefore, when the surface densities are zero, the tangential component of  $H_i$  and the normal component of  $D_i$  are also continuous.

It is of interest to remark that, if the mathematical theory of distributions is used to write Maxwell's equations (I.5)-(I.8), then the obtained set of equations (valid in the sense of distributions) contains both the differential equations (I.5)-(I.8) and the boundary conditions (I.11)-(I.14). Therefore, it is then no more compulsory to supplement the differential equations with boundary conditions III).

Because the electromagnetic fields depend on the source intensities and locations and because source motion may be induced by electromagnetic fields, it is also necessary to supplement the set of equations with another one expressing the elementary Lorentz force  $dF_i$  acting on an elementary volume dV.

This force reads as:

$$dF_i = [\rho E_i + (J_k \wedge B_l)_i]dV \tag{I.15}$$

Then, any electromagnetic problem complying with the general assumptions (i)–(iv) listed in subsection (I.1.2) is mathematically defined by the closed set of Rels (I.5)–(I.15). We are not done however because polarizations are still not explicitly expressed in terms of media properties. This requires the introduction of constitutive relationships.

## I.1.4 Constitutive Relationships

In many cases, only approximate expressions for polarizations  $P_i$  and  $M_i$  may reasonably be used because of the usual complex behaviour of real media. Indeed, a general approach to the constitutive relationships must introduce many complicated features such as field coupling, nonlinearity, spatial and temporal convolutions, nonisotropy and nonhomogeneity of the material ( $\boxed{110}$ ,  $\boxed{111}$ ). For instance, polarizations could be *a priori* expressed in terms of the fields  $E_i$  and  $H_i$  but the relevant expressions should involve:

- (i) not only  $E_i$  and  $H_i$ , but also coupled terms
- (ii) not only terms proportional to  $E_i$  and  $H_i$  but also constants (permanent polarizations) and higher order terms accounting for quadratic, cubic... effects
- (iii) not only  $E_i$  and  $H_i$  at a considered point but also in some neighborhood of it
- (iv) not only  $E_i$  and  $H_i$  at a considered date but also in some past neighborhood of it and
- (v) tensor expressions may appear on the stage to possibly account for nonisotropic electric and magnetic properties of the medium under study.

The study of the corresponding general constitutive relationships is still an open field of research. However, in this book, we shall be fortunate enough to be allowed to land on more comfortable media than the most general ones that the nature may have imagined. The landing process is illustrated by considering the electric polarization  $P_i$ . The discussion would be quite similar for the magnetic polarization  $M_i$ .

Discarding nonlinear effects and field coupling, the electric polarization  $P_i(r_i, t)$  at point  $r_i$  and at time t reads as:

$$P_{j}(r_{i},t) = \int_{V'} \int_{t'} E_{k}(r_{i}',t') R_{j}^{k}(r_{i},t;r_{i}',t') dV' dt'$$
 (I.16)

in which  $R_j^k$  is a Dirac response tensor characterizing electric properties of the medium versus space and time. The discrete sum over subscript k (Einstein rule) accounts for anisotropy. Quadratures over  $r_i'$  and t' express spatial and temporal convolutions required to describe nonlocal and nonperfect media, i.e media whose polarizations at location  $r_i$  and time t depend on a spatiotemporal neighborhood  $\left\{V^{'},t^{'}|r_i'\in V^{'},t^{\prime}\leq t,\text{ and }||r_i-r_i'||\leq v(t-t')\right\}$ , in which v is the speed of light in the considered medium.

Very usually, it may be safely assumed that the spatial variation of the electric field  $E_i$  is small enough to be accurately described by a low-order Taylor expansion, leading to:

$$P_{j}(r_{i},t) = \int_{t'} [E_{k}(r_{i},t')R_{j}^{k}(r_{i},t;t') + \frac{\partial E_{k}}{\partial r_{m}}(r_{i},t')S_{j}^{km}(r_{i},t;t')]dt'$$
 (I.17)

in which:

$$R_{j}^{k}(r_{i}, t; t') = \int_{V'} R_{j}^{k}(r_{i}, t; r_{i}', t') dV'$$
(I.18)

$$S_{j}^{km}(r_{i},t;t') = \int_{V'} R_{j}^{k}(r_{i},t;r_{i}',t')(r_{m}'-r_{m})dV'$$
 (I.19)

In local media when polarizations at point  $r_i$  do not depend on any space neighborhood, both Rels (L16) and (L17) reduce to:

$$P_{j}(r_{i},t) = \int_{t'} E_{k}(r_{i},t') R_{j}^{k}(r_{i},t;t') dt'$$
 (I.20)

In perfect media (which are local media with respect to time), instantaneously following the time variations of the fields, time convolutions also disappear leading to:

$$P_j(r_i, t) = E_k(r_i, t)R_j^k(r_i, t)$$
 (I.21)

If the medium is isotropic, then the Dirac response tensor is proportional to the Kronecker tensor  $(R_i^k \sim \delta_i^k)$  and Rel (I.21) may be written as:

$$P_j(r_i, t) = \epsilon_o \ \chi_e(r_i, t) \ E_j(r_i, t) \tag{I.22}$$

Under the same assumptions, the magnetic polarization takes a similar form which is however usually written as:

$$M_j(r_i, t) = \chi_m(r_i, t) \ H_j(r_i, t)$$
 (I.23)

The quantities  $\chi_e$  and  $\chi_m$  are called the electric and magnetic susceptibilities respectively.

Fields do not produce net electric charges as charges cannot be created nor destroyed in the framework of electromagnetism. However, electric fields may produce currents. Therefore, a last constitutive relationship relating the current density  $J_i$  in matter and the electric field  $E_i$  is required. For time-varying

electromagnetic fields in conducting media, a very general constitutive relationship then takes the form of a time convolution according to:

$$J_{j}(r_{i},t) = \int_{-\infty}^{t} E_{k}(r_{i},t') C_{j}^{k}(r_{i},t;t') dt'$$
 (I.24)

in which  $C_j^k$  is a tensor reducing to a scalar if current and electric field are colinear. For perfect media, the time convolution again disappears leading to the general assumption that the current density linearly, locally and isotropically depends on the electric field. For perfect insulating media, the current density is zero, a result which may be formally derived from the conductor case by setting the tensor  $C_j^k$  to zero.

## I.1.5 The Formulation in Fourier Space

Fourier transform changes the derivative operator  $(\frac{\partial}{\partial t})$  into an algebraic operator reading as  $(i\omega)$  with a proper definition of the transform,  $\omega$  being the angular frequency of a Fourier mode. Therefore, Maxwell's equations (I.5)–(I.8) become in Fourier space:

$$(curl \ \hat{E}_i)_i = -i\omega \hat{B}_i \tag{I.25}$$

$$div\hat{B}_i = 0 (I.26)$$

$$(curl\hat{H}_i)_i = \hat{J}_i + i\omega\hat{D}_i \tag{I.27}$$

$$div\hat{D}_i = \hat{\rho} \tag{I.28}$$

in which  $\hat{E}_j, ..., \hat{\rho}$  are the complex Fourier transforms of  $E_j, ..., \rho$ , respectively. Also, Fourier transform changes time convolutions (involved in constitutive relationships) to algebraic products. For instance, Rel (1.20) becomes:

$$\hat{P}_j(r_i,\omega) = \hat{E}_k(r_i,\omega)\hat{R}_j^k(r_i,\omega)$$
(I.29)

in which  $\hat{P}_j$  and  $\hat{R}_j^k$  are the complex Fourier transforms of  $P_j$  and  $R_j^k$ , respectively. Therefore, the constitutive relationship (I.20) for local, nonperfect media in Fourier space formally identifies with the relationship (I.21) for local and perfect media in physical space.

A 3 x 3 electric susceptibility Fourier tensor  $\chi_{e,j}^k$  may be introduced by the relation:

$$\epsilon_0 \chi_{e,j}^k(r_i,\omega) = \hat{R}_j^k(r_i,\omega) \tag{I.30}$$

in such a way that Rel (I.29) now reads as:

$$\hat{P}_{i}(r_{i},\omega) = \epsilon_{0} \chi_{e,i}^{k}(r_{i},\omega) \hat{E}_{k}(r_{i},\omega)$$
(I.31)

Similarly, the complex Fourier transform  $\hat{M}_j$  of the magnetic polarization  $M_j$  may be written as:

$$\hat{M}_j(r_i,\omega) = \chi_{m,j}^k(r_i,\omega) \, \hat{H}_k(r_i,\omega) \tag{I.32}$$

while the constitutive relationship (I.24) may be given the form:

$$\hat{J}_j(r_i, \omega) = \sigma_j^k(r_i, \omega) \ \hat{E}_k(r_i, \omega) \tag{I.33}$$

Physically, the imaginary parts of matrices  $\chi_{e,j}^k$ ,  $\chi_{m,j}^k$  and  $\sigma_j^k$  represent the energy dissipation (field damping) because of electric and magnetic polarizations and electric conduction respectively.

Gathering Rels (I.9), (I.10), (I.25) – (I.28) and the constitutive relationships (I.31) – (I.33), it is then found that Maxwell's equations in Fourier space for linear and local media read as:

$$(curl\hat{E}_j)_i = -i\omega \mu_i^k \hat{H}_k \tag{I.34}$$

$$div(\mu_i^k \hat{H}_k) = 0 (I.35)$$

$$(curl\hat{H}_j)_i = i\omega \epsilon_i^k \hat{E}_k \tag{I.36}$$

$$div\hat{D}_i = \hat{\rho} \tag{I.37}$$

in which:

$$\hat{D}_i = \epsilon_0(\delta_i^k + \chi_{e,i}^k) \hat{E}_k \tag{I.38}$$

$$\mu_i^k = \mu_0(\delta_i^k + \chi_{m,i}^k) \tag{I.39}$$

$$\epsilon_i^k = \epsilon_0(\delta_i^k + \chi_{e,i}^k) - \frac{i}{\omega}\sigma_i^k \tag{I.40}$$

If the medium is isotropic, then all the second-order tensors become proportional to the Kronecker tensor, and the whole set (I.34)–(I.40) may readily be rewritten in terms of scalar quantities, namely susceptibilities  $\chi_e, \chi_m$ , permeability  $\mu$ , permittivity  $\epsilon$  and conductivity  $\sigma$ , according to:

$$(curl\hat{E}_j)_i = -i\omega\mu\hat{H}_i \tag{I.41}$$

$$div\hat{H}_i = 0 \tag{I.42}$$

$$(curl\hat{H}_i)_i = i\omega\epsilon\hat{E}_i \tag{I.43}$$

$$div\hat{D}_i = \hat{\rho} \tag{I.44}$$

with:

$$\hat{D}_i = \epsilon_0 (1 + \chi_e) \hat{E}_i \tag{I.45}$$

$$\mu = \mu_0 (1 + \chi_m) \tag{I.46}$$

$$\epsilon = \epsilon_0 (1 + \chi_e) - \frac{i\sigma}{\omega} \tag{I.47}$$

It may be remarked that, for the special case of media without any charge density  $(\rho = 0)$ , the set (I.41)-(I.44) displays a complete equivalence between dielectrics and ohmic conductors. The same set may be used for both cases, with the expression for  $\epsilon$  containing the conductivity  $\sigma$  (Rel (I.47)).

Also, it may be mentioned that susceptibilities  $\chi_e$  and  $\chi_m$  satisfy the socalled Kramers-Kroning dispersion relationships. These relationships can be established from general symmetries and principles like assumptions of section I.1.2 [110]. If media are furthermore perfect, then susceptibilities  $\chi_e, \chi_m$ and conductivity  $\sigma$  become real quantities and identify with usual real static susceptibilities and conductivity.

# I.1.6 Time Harmonic Fields and Complex Representatives

The essence of any Fourier transform as previously discussed is that the formulation may be reduced to the study of normal modes. In this book, a normal mode is a time harmonic field with the time dependent term chosen to read as  $\exp(+i\omega t)$ . The alternative convention with  $\exp(-i\omega t)$  could have been chosen, but also with an alternative form for the Fourier transform used in Section (I.1.5).

However, once a convention is chosen, the whole formulation must remain consistent with it. Examples of errors induced by mistaking about the convention are discussed in [113]. It is nevertheless easy to switch from one convention to the other by taking complex conjugates.

Then, any real time harmonic quantity:

$$A(r_i, t) = a(r_i) \cos[\omega_0 t + \varphi(r_i)]$$
 (I.48)

may be described by a complex representative  $\tilde{A}$  defined by:

$$\tilde{A}(r_i) \exp(i\omega_0 t) = a(r_i) \exp[i \varphi(r_i)] \exp(i\omega_0 t)$$
 (I.49)

in which the tilde is used to denote complex representatives.

The Fourier transform of (I.48) then comes out to be:

$$\hat{A}(r_i, \omega) = \frac{1}{2} \left[ \tilde{A}(r_i) \ \delta(\omega - \omega_0) + \tilde{A}^*(r_i) \delta(\omega + \omega_0) \right]$$
 (I.50)

in which the star is used to denote complex conjugates.

Therefore, Maxwell's equations (I.25)–(I.28) in Fourier space will involve Dirac distributions. For instance, Rel (I.25) now reads as:

$$(curl\tilde{E}_{j})_{i} \delta(\omega - \omega_{0}) + (curl\tilde{E}_{j}^{*})_{i} \delta(\omega + \omega_{0}) =$$

$$-i\omega \left[\tilde{B}_{i} \delta(\omega - \omega_{0}) + \tilde{B}_{i}^{*} \delta(\omega + \omega_{0})\right]$$
(I.51)

But, we have:

$$\omega \ \delta(\omega - \omega_0) = \omega_0 \ \delta(\omega - \omega_0) \tag{I.52}$$

Therefore, identifying the coefficients of the Dirac distributions one obtains the following equation:

$$(curl\tilde{E}_j)_i = -i\omega_0 \ \tilde{B}_i \tag{I.53}$$

together with its complex conjugate.

The same arguments may be applied to all equations of the set (I.25)–(I.28). It then comes out that the complex representatives of harmonic fields exactly comply with the same set (I.25)–(I.28) as do the Fourier transforms. Accordingly, the complex representatives  $\tilde{E}_j$ ,  $\tilde{B}_j$ ,  $\tilde{D}_j$  and  $\tilde{\rho}$  also comply with the set (I.34)–(I.37) and also with (I.38), with notations defined by (I.39)–(I.40), to be supplemented by boundary conditions corresponding to (I.11)–(I.14).

It is of interest to remark that the same set can be formally obtained without any Fourier transforming by directly rewriting the initial set (1.5)—(1.8) with exp (i $\omega$ t)-harmonic complex representatives and, accordingly, with the derivative operator  $\frac{\partial}{\partial t}$  replaced by the algebraic operator ( $i\omega$ .).

However, such a procedure would not emphasize the physical meaning of the constitutive relationships summarized by Rels (I.38)–(I.40).

Another remark is that the permittivity and permeability tensors do not satisfy the same relationships with the electric and magnetic fields respectively, i.e. we have:

$$\tilde{B}_i = \mu_i^k \, \tilde{H}_k \tag{I.54}$$

whereas:

$$\tilde{D}_i \neq \epsilon_i^k \, \tilde{E}_k \tag{I.55}$$

This difference results from Rels (I.38)–(I.40) in which there is no magnetic counterpart to the electric conductivity tensor  $\sigma_i^k$ .

# I.2 Special Maxwell's Equations for l.l.h.i Media

This section is essentially devoted to special Maxwell's equations, i.e. to Maxwell's equations specified for the special case to be treated in this book, and to some consequences of them to be used later.

Media considered in this book are l.l.h.i. media: linear, local, homogeneous (with respect to space and also to time) and isotropic. There are no macroscopic sources, i.e. no macroscopic charge density and no macroscopic current

density. Because complex representatives are used in all the rest of this book, the tilde will be omitted from now on for convenience unless explicitly stated otherwise. We furthermore deal with  $\exp(i\omega t)$ -harmonic electromagnetic waves, i.e. the derivative operator  $(\frac{\partial}{\partial t})$  and the algebraic operator  $(i\omega)$  are equivalent.

# I.2.1 Special Maxwell's Equations in Cartesian Coordinate Systems

The complex representatives comply with the same set as the Fourier transforms (see section I.1.6), thus (I.45)–(I.47) gives the constitutive relationships for linear, local, homogeneous and isotropic media,  $\mu$  and  $\epsilon$  being furthermore constant quantities due to homogeneity with respect to space and time. Hence, the set (I.5)–(I.8) reduces to special Maxwell's equations reading as:

$$(curl E_j)_i = -\mu \frac{\partial H_i}{\partial t} \tag{I.56}$$

$$divH_i = 0 (I.57)$$

$$(curl H_j)_i = \epsilon \frac{\partial E_i}{\partial t} \tag{I.58}$$

$$divE_i = 0 (I.59)$$

The above equations involve only two fields  $E_i$  and  $H_i$  and two complex constants  $\mu$  and  $\epsilon$ , characterizing the medium, as defined by Rels (I.46)–(I.47).

# I.2.2 Special Maxwell's Equations in Orthogonal Curvilinear Coordinate Systems

By using the formulation of tensor calculus [II4] [II5], it is possible to efficiently transform Maxwell's equations (I.56)–(I.59) from Cartesian coordinate systems to any orthogonal curvilinear coordinate system. Orthogonal curvilinear coordinate systems are defined by a covariant metric tensor taking the form:

$$g_{km} = \begin{bmatrix} g_{11} & 0 & 0 \\ 0 & g_{22} & 0 \\ 0 & 0 & g_{33} \end{bmatrix} = \begin{bmatrix} (e_1)^2 & 0 & 0 \\ 0 & (e_2)^2 & 0 \\ 0 & 0 & (e_3)^2 \end{bmatrix}$$
(I.60)

i.e., the metric is defined by an infinitesimal length element ds given by:

$$ds^{2} = g_{km}dx^{k}dx^{m} = (e_{1}dx^{1})^{2} + (e_{2}dx^{2})^{2} + (e_{3}dx^{3})^{2}$$
(I.61)

in which  $x^k$  designates the coordinates (k = 1, 2, 3) and  $e_i$ 's may be called scale factors [116].

Maxwell's equations are now specified for such orthogonal curvilinear coordinate system, following for instance Poincelot [114].

Relation (I.56) becomes:

$$\frac{\partial}{\partial x^2} e_3 E_3 - \frac{\partial}{\partial x^3} e_2 E_2 = -\mu e_2 e_3 \frac{\partial}{\partial t} H_1 \tag{I.62}$$

$$\frac{\partial}{\partial x^3} e_1 E_1 - \frac{\partial}{\partial x^1} e_3 E_3 = -\mu e_3 e_1 \frac{\partial}{\partial t} H_2 \tag{I.63}$$

$$\frac{\partial}{\partial x^1} e_2 E_2 - \frac{\partial}{\partial x^2} e_1 E_1 = -\mu e_1 e_2 \frac{\partial}{\partial t} H_3 \tag{I.64}$$

Relation (I.57) becomes:

$$\frac{\partial}{\partial x^1} e_2 e_3 H_1 + \frac{\partial}{\partial x^2} e_3 e_1 H_2 + \frac{\partial}{\partial x^3} e_1 e_2 H_3 = 0 \tag{I.65}$$

Once these relations have been checked, it is just a rewriting exercise to find how equations (I.58)–(I.59) are modified, taking advantage of the similarity between (I.56)–(I.57), and (I.58)–(I.59).

Relation (I.58) becomes:

$$\frac{\partial}{\partial x^2} e_3 H_3 - \frac{\partial}{\partial x^3} e_2 H_2 = \epsilon \ e_2 e_3 \frac{\partial}{\partial t} E_1 \tag{I.66}$$

$$\frac{\partial}{\partial x^3} e_1 H_1 - \frac{\partial}{\partial x^1} e_3 H_3 = \epsilon \ e_3 e_1 \frac{\partial}{\partial t} E_2 \tag{I.67}$$

$$\frac{\partial}{\partial x^1} e_2 H_2 - \frac{\partial}{\partial x^2} e_1 H_1 = \epsilon \ e_1 e_2 \frac{\partial}{\partial t} E_3 \tag{I.68}$$

Finally, Rel (I.59) becomes:

$$\frac{\partial}{\partial x^1} e_2 e_3 E_1 + \frac{\partial}{\partial x^2} e_3 e_1 E_2 + \frac{\partial}{\partial x^3} e_1 e_2 E_3 = 0 \tag{I.69}$$

# I.2.3 Special Maxwell's Equations in Spherical Coordinate Systems

As an example relevant to the contents of this book, we may consider a spherical coordinate system defined by (Fig. I.1):

$$\begin{cases}
 x^1 = r \\
 x^2 = \theta \\
 x^3 = \varphi
 \end{cases}$$
(I.70)

From 3D-Pythagorus theorem:

$$ds^{2} = (dr)^{2} + (rd\theta)^{2} + (r \sin\theta \ d\varphi)^{2}$$
(I.71)

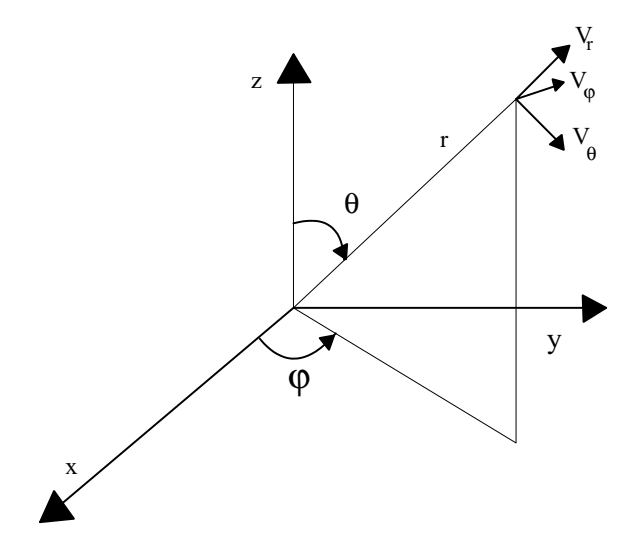


**Fig. I.1.** Spherical coordinate system. In these relations,  $V_i$  designates the components of vector  $\mathbf{V}(\mathbf{E} \text{ or } \mathbf{H})$  in the local Cartesian (orthogonal) system attached at point  $x^k$ .

Consequently the covariant metric tensor reads as:

$$g_{km} = \begin{bmatrix} 1 & 0 & 0 \\ 0 & r^2 & 0 \\ 0 & 0 & r^2 \sin^2 \theta \end{bmatrix}$$
 (I.72)

leading to:

$$\left. \begin{array}{l}
 e_1 = 1 \\
 e_2 = r \\
 e_3 = r \sin \theta
 \end{array} \right\} 
 \tag{I.73}$$

The set (I.62)–(I.69) can then be readily specified for this case by inserting (I.70)–(I.73) in it. The interest of spherical coordinates is due to the fact that most of this book is devoted to spherical particles. However, the set (I.62)–(I.69) is of interest for other shapes in so far as they can be properly described by orthogonal curvilinear coordinate systems, typical examples being circular cylinders, i.e. fibers (III) III III III IIII IIII.

# I.2.4 Boundary Conditions

Boundary conditions discussed in subsection (I.1.3) are here conveniently rewritten for l.l.h.i. media. Under the same assumptions as for Maxwell's equations (I.56)–(I.59), using again complex representatives, and remembering that there is no surface current density  $J_{s,k}$ , Rels (I.11) and (I.13) may be rewritten as:

$$(n_{12,i}) \wedge (E_{2,j} - E_{1,j}) = 0 \tag{I.74}$$

$$(n_{12,i}) \wedge (H_{2,i} - H_{1,i}) = 0 \tag{I.75}$$

expressing the continuity of the tangential components of both the electric and magnetic fields.

Limit conditions at infinity must also be added to the above boundary conditions. Assuming that the field sources remain in a bounded domain, the limit conditions express that all local Cartesian components of propagating time harmonic waves must (i) vanish at least as rapidly as  $r^{-1}$  and (ii) represent a divergent travelling wave, at infinity (15), pp 485-486).

The relations expressing the limit conditions depend on the choice of the coordinate system and will be written later when necessary.

# I.2.5 Energy Propagation and Poynting Theorem

The Poynting theorem discussed in this subsection concerns energy balance and propagation. Our starting point will be the definition of the Poynting vector  $S_i$  as the vectorial product of the electric and magnetic fields:

$$S_i = (E_i \wedge H_k)_i \tag{I.76}$$

in which complex representatives are not used.

The physical meaning of the Poynting vector may be investigated by first taking its divergence, leading to:

$$divS_k + E_i (curlH_k)_i - H_i (curlE_k)_i = 0 (I.77)$$

By using Maxwell's equations (I.7)–(I.10), Rel (I.77) becomes the Poynting identity:

$$\frac{\partial S_i}{\partial x_i} + J_i E_i + E_i \frac{\partial D_i}{\partial t} + H_i \frac{\partial B_i}{\partial t} = 0$$
 (I.78)

Integrating this identity over a volume  $\Omega$  bounded by a closed surface S equipped with a unit vector  $n_i$  pointing normally outward, the flux of the Poynting vector is found to satisfy:

$$\int \int_{S} S_{i} \ n_{i} \ dS = -\int \int \int_{\Omega} J_{i} E_{i} dV - \int \int \int_{\Omega} (E_{i} \frac{\partial D_{i}}{\partial t} + H_{i} \frac{\partial B_{i}}{\partial t}) dV \quad (I.79)$$

in which the volume integral of the divergence term has been converted to a surface integral.

Rel (I.79) may be interpreted as an energy balance over the volume  $\Omega$ . In vacuum in which electric and magnetic polarizations are zero and therefore in which  $B_i = \mu_0 H_i$  and  $D_i = \epsilon_0 E_i$  (Rels (I.9)-(I.10)), the interpretation of the energy balance is best carried out by rewriting Rel (I.79) under the form:

$$-\int \int \int_{\Omega} \frac{\partial w}{\partial t} dV = \int \int \int_{\Omega} J_i E_i dV + \int \int_{S} S_i n_i dS$$
 (I.80)

in which:

$$w = \frac{1}{2} \left( \epsilon_0 \ E_i^2 + \mu_0 H_i^2 \right) \tag{I.81}$$

The quantity w is interpreted as the electromagnetic energy per unit volume. Therefore, the left-hand-side of Rel (I.80) represents the decrease of electromagnetic energy contained in the volume  $\Omega$ . This decrease is provoked by two effects summed up in the right-hand-side, namely (i) the rate of change of the kinetic energy of the free charges inside  $\Omega$ , that is to say the power of the Lorentz forces acting on them and (ii) the energy loss inside  $\Omega$  due to electromagnetic waves propagating across the surface S.

As a special case relevant to the purpose of this book, let us consider inside the volume  $\Omega$  a scattering center surrounded by a non-absorbing medium. Because there is no free current density inside  $\Omega$ , the balance (I.80) reduces to:

$$-\int \int \int_{\Omega} \frac{\partial w}{\partial t} dV = \int \int_{S} S_{i} \ n_{i} \ dS \tag{I.82}$$

and it is seen that the flux of the Poynting vector contains all the information necessary to understand the energy balance. In particular, the decrease of electromagnetic energy density  $\boldsymbol{w}$  may have some extra-causes due to the presence of the scattering particle, namely absorption of energy in the scattering center material.

The above discussion in this subsection does not use complex representatives. Let us now consider  $\exp(+i\omega t)$ -harmonic fields and complex representatives. Then, the Poynting vector (I.76) must be redefined by considering time averages, say over one period, which are the quantities of interest. Furthermore, because the Poynting vector is not a linear function of the fields, some care must be taken in introducing its complex representative. In order to preserve the interpretation of the average energy propagation as the flux of the real part of the complex representative, the complex Poynting vector can be defined as:

$$\tilde{S}_i = \frac{1}{2} [\tilde{E}_j \wedge \tilde{H}_k^*]_i \tag{I.83}$$

in which the star designates a complex conjugate.

For completeness, it is of interest to discuss a bit the case of material dissipative media. In this context, the concept of electromagnetic energy density w does not come out as easily as in vacuum and it is no more obvious to interpret Rel (I.79) as an energy balance. However, for time harmonic fields in linear and local media, averaging over an integer number of periods (say one), it comes out that  $\square$ 

$$\int \int_{S} n_i \operatorname{Re}(\tilde{S}_i) dS = \int \int_{S} n_i \operatorname{Re}\left[\frac{1}{2}(\tilde{E}_j \wedge \tilde{H}_k^*)_i\right] dS \tag{I.84}$$

leading to:

$$\int \int_{S} n_{i} \operatorname{Re}(\tilde{S}_{i}) dS = \int \int \int_{\Omega} \operatorname{Re}\left\{\frac{i\omega}{2} \left[\tilde{E}_{i}(\epsilon_{i}^{k}\tilde{E}_{k})^{*} - \tilde{H}_{i}^{*}(\mu_{i}^{k}\tilde{H}_{k})\right]\right\} dV \quad (I.85)$$

The meaning of this relation is that the average energy flow through S expressed by the left-hand-side is minus the energy dissipation (Joule effect plus electric and magnetic losses) within  $\Omega$ .

In isotropic media where the tensors  $\epsilon_i^k$  and  $\mu_i^k$  reduce to scalars, it then comes out that:

$$\int \int_{S} n_i \operatorname{Re}(\tilde{S}_i) dS = \int \int \int_{Q} \frac{\omega}{2} \left[ I_m(\epsilon) | \tilde{E}_i |^2 + \operatorname{Im}(\mu) | \tilde{H}_i |^2 \right] dV \quad (I.86)$$

In vacuum, where  $\epsilon = \epsilon_0$  and  $\mu = \mu_0$  are real numbers, the right-hand-side of (I.86) is zero. Therefore, the meaning of this relation becomes that the absolute amount of energy flowing inside  $\Omega$  through S is equal to the absolute amount of energy flowing outside, a plain statement concerning the conservation of energy indeed.

As a last word, let us recall that the tilde will still be omitted in next chapters.

# I.2.6 Momentum Propagation

Similar to energy propagation, momentum propagation is involved by propagation of electromagnetic fields. The simplest relationship between energy E and momentum p can be written for a photon as:

$$E = p c (I.87)$$

which results from expressions of E and p in quantum mechanics in which c is the speed of light.

In classical electromagnetism, momentum can be defined from the Poynting vector by introducing a momentum field tensor.

For the restricted scope of this book, only momentum propagation in free space will be necessary ("free space" in the sense of section I.1.1). Then, it is possible to avoid defining the momentum field tensor and it comes out (110) p. 100-104) that the volumic density of the field momentum is proportional to the Poynting vector:

$$\frac{d p_i}{d V} = \epsilon_0 \left[ E_j \wedge B_k \right]_i = \epsilon_0 \mu_0 S_i \tag{I.88}$$

in which complex representatives are not used.

Considering a propagating electromagnetic wave for which the Poynting vector  $S_i$  is along the direction of propagation, we may write the flow of momentum through an infinitesimal surface dS with angle  $\theta$  between  $S_i$  and the

normal to dS. In free space, this momentum flow during dt is the momentum of the field contained inside an oblique cylinder with basis dS and length  $c dt = (\epsilon_0 \mu_0)^{\frac{-1}{2}} dt$ . Accordingly it can be written as:

$$dp_i = (\epsilon_0 \mu_0)^{\frac{1}{2}} S_i \cos \theta \, dS \, dt \tag{I.89}$$

which immediately results from (I.88) and is readily found to be coherent with the quantum mechanics interpretation of Rel (I.87) in the continuous limit.

If we only consider time harmonic fields, then the real part of the complex representatives will give the averages over an integer number n of periods T of the above quantities. Hence Rel (I.89) can also be written as:

$$\frac{1}{nT} \int_0^{nT} dp_i = (\epsilon_0 \mu_0)^{\frac{1}{2}} \operatorname{Re}(\tilde{S}_i) \cos \theta \, dS \tag{I.90}$$

Rel (I.90) is vectorial: it is the time-average flow of the momentum of the field per unit of time through the infinitesimal surface dS. This relation will be used later for computing pressure cross sections from momentum balance (chapter III).

## I.2.7 Wave-Vector, Refractive Index and Impedance

This section provides miscellaneous relations to be repeatedly used later. The underlying assumptions have been given at the beginning of section (I.2) and the relevant Maxwell's equations are the set (I.56)–(I.59). Again, the tilde to denote complex representatives is omitted. For  $exp(i\omega t)$ -harmonic fields when the operator  $(\frac{\partial}{\partial t})$  is replaced by the operator  $(i\omega.)$ , it is an exercise to show that the set (I.56)–(I.59) implies that both fields  $E_i$  and  $H_i$  satisfy the Helmholtz equation which, in Cartesian coordinates, reads as:

$$\frac{\partial^2 X_i}{\partial x_k^2} + \omega^2 \mu \epsilon X_i = 0 \tag{I.91}$$

in which  $X_i$  stands either for  $E_i$  or  $H_i$ .

The most celebrated solutions of the Helmholtz equation are the spherical wave (SW) and the plane wave (PW) reading as:

$$SW : \exp(-ik_ix_i)/(x_k^2)^{1/2}$$
 (I.92)

$$PW : \exp(-ik_ix_i) \tag{I.93}$$

in which irrelevant pre-factors are omitted. The wave-vector  $k_i$  depends on medium properties and is readily found to satisfy, for instance, using Rels (L91) and (L93):

$$k_i^2 = \omega^2 \mu \ \epsilon \tag{I.94}$$

A careful examination of the PW-solution [110] however shows that Rel (I.94) is the single relation the complex wave vector  $k_i$  is bound to comply with. The general solution is therefore what is called a dissociated plane wave in which  $Re(k_i)$  is not proportional to  $Im(k_i)$  and accordingly, isophase planes:

$$x_i \operatorname{Re}(k_i) = cst \tag{I.95}$$

do not identify with isoamplitude planes:

$$x_i \operatorname{Im}(k_i) = cst \tag{I.96}$$

Fortunately, many waves such as usual plane waves (or Gaussian laser beams) are not dissociated. From Rels (I.95)–(I.96), it is observed that isophases and isoamplitudes coincide if  $Re(k_i)$  is proportional to  $Im(k_i)$ . Under such an extra-assumption of colinearity between real and imaginary parts of the vector  $k_i$ , it is then possible to write:

$$k_i = k \ n_i \tag{I.97}$$

in which k is a complex wave-number and  $n_i$  a real unit vector. Then, from Rel (1.94) a wave-number k may indeed be defined according to:

$$k = \omega \sqrt{\mu \,\epsilon} \tag{I.98}$$

in which the square-root must be chosen to be consistent with the convention of an  $\exp(+i\omega t)$ -time dependence. This requires:

$$Re(k) > 0, Im(k) \le 0$$
 (I.99)

as it can be observed by inserting Rel (I.97) in (I.93) and requiring the PW amplitude to be damped during propagation.

A complex refractive index M may then be defined as the ratio of wavenumber for the considered material over wave-number in vacuum:

$$M = \sqrt{\frac{\mu \epsilon}{\mu_0 \epsilon_0}} = c\sqrt{\mu \epsilon} = \frac{kc}{\omega}$$
 (I.100)

in which we have used the fact that permeability and permittivity in vacuum comply with:

$$\epsilon_0 \ \mu_0 \ c^2 = 1$$
 (I.101)

Rel ( $\overline{1.100}$ ) implies that M may be written as:

$$M = N - iK \tag{I.102}$$

in which N>0,  $K \geq 0$  as a consequence of inequalities (1.99).

If a material defined by  $\mu_{sp}$ ,  $\epsilon_{sp}$  is surrounded by a nonabsorbing medium defined by  $\mu$ ,  $\epsilon$ , then a complex refractive index of the material relatively to the surrounding medium may be defined according to:

$$M = \sqrt{\frac{\mu_{sp} \epsilon_{sp}}{\mu \epsilon}} = \frac{k_{sp}}{k} \tag{I.103}$$

This will be the typical meaning of M in this book. If the alternative convention for the time dependence of the fields, i.e. fields evolving as  $\exp(-i\omega t)$ , is chosen, then k and M comply with the inequalities:

$$Re(k), Re(M) > 0; Im(k), Im(M) \ge 0$$
 (I.104)

instead of (I.99).

Finally, it is useful to comment on the relation between electric and magnetic fields, i.e. on the complex impedance of the medium. For plane waves defined by Rel (I.93), Maxwell's equation (I.56) leads to the general relation between complex representatives  $\tilde{E}_i$  and  $\tilde{H}_i$ :

$$\omega \ \mu \ \tilde{H}_i \ = \ \left[ k_j \ \wedge \ \tilde{E}_k \right]_i \tag{I.105}$$

expressing the fact that the complex vectors  $k_j$ ,  $\tilde{E}_j$ ,  $\tilde{H}_j$  form a complex direct orthogonal basis. For the special case of non dissociated plane waves whose wave-vector complies with Rel (I.94), it may be rewritten as:

$$\sqrt{\frac{\mu}{\epsilon}}\tilde{H}_i = [n_j \wedge \tilde{E}_k]_i \tag{I.106}$$

in which  $n_i$  is a real unit vector.

Although  $\tilde{E}_i$  and  $\tilde{H}_i$  are orthogonal in a plane wave, it must be noted that the real fields  $E_i$  and  $H_i$  in general do not possess the same property of orthogonality in contrast with a common naïve belief. This actually results from the fact that Rel (I.105) is not linear and only linear relationships can be automatically transferred from real quantities to their complex representatives.

Nevertheless, for a nonabsorbing medium in which  $\mu$  and  $\epsilon$  are real numbers, Rel (I.106) implies:

$$\sqrt{\frac{\mu}{\epsilon}} = \frac{\mid \tilde{E}_i \mid}{\mid \tilde{H}_i \mid} = \frac{\mid E_i \mid}{\mid H_i \mid} = \frac{E}{H}$$
 (I.107)

which defines the impedance of the nonabsorbing medium. (I.107) may also be rewritten as:

$$k = \omega \epsilon \frac{E}{H} = \omega \mu \frac{H}{E}$$
 (I.108)

A similar relation holds for some other special cases such as:

- (i) real fields on the front of a propagating wave inside a nonabsorbing medium (but not behind) (110, p89).
- (ii) real fields of a spherical wave propagating inside a nonabsorbing medium
- (iii) some complicated fields, at particular locations, for instance at the focus plane (waist plane) of a Gaussian laser beam where the wavefront is locally plane.

However, in general, the use of Rels ([1.105])—([1.108]) must be kept under careful control.

#### I.2.8 Potentials

From Maxwell's equation (I.6), using the fact that the divergence of a rotational is zero, it is possible to introduce a vector potential  $A_i$  according to:

$$B_i = (curl A_i)_i \tag{I.109}$$

For l.l.h.i. media considered in the present section, the magnetic field  $H_i$  may then be expressed in terms of the vector potential  $A_i$  according to:

$$H_i = B_i/\mu = (curl A_i)_i/\mu \tag{I.110}$$

However, it comes out that Rel (1.109) does not uniquely determine the vector potential  $A_i$  to which any gradient may be added because the rotational of a gradient is zero. The remaining indetermination may be cancelled out by demanding  $A_i$  to satisfy an extra-condition.

If this condition writes:

$$div A_i = 0 (I.111)$$

then the vector potential is stated to be defined within the Coulomb gauge. In this book however, we shall rather consider the Lorentz gauge [110] defined as follows.

Invoking (I.110), Maxwell's equation (I.56) may be rewritten as:

$$[curl(E_j + \frac{\partial A_j}{\partial t})]_i = 0 \tag{I.112}$$

Because the rotational of a gradient is zero, it is then also possible to introduce a scalar potential V such as:

$$E_j + \frac{\partial A_j}{\partial t} = -(gradV)_j \tag{I.113}$$

Fields are not modified by changing the potential doublet  $(A_i, V)$  to a new doublet  $(A'_i, V')$  such as:

$$A_{i}^{'} = A_{i} + (grad\varphi)_{i} \tag{I.114}$$

$$V^{'} = V - \frac{\partial \varphi}{\partial t} \tag{I.115}$$

Therefore, the potential doublet is not uniquely determined. In the Lorentz gauge, an extra-relation, the Lorentz condition, is specified reading as:

$$divA_i + \epsilon \ \mu \ \frac{\partial V}{\partial t} = 0 \tag{I.116}$$

Let us now start from Maxwell's equation (I.58) and insert in it the definitions (I.110) and (I.113) of the potentials  $A_i$  and V. Remembering that:

$$(curl\ curl\ \psi_j)_i = (grad\ div\ \psi_j)_i - \Delta\psi_i$$
 (I.117)

and invoking the Lorentz condition (L.116), it is readily found that:

$$\Delta A_i - \epsilon \mu \frac{\partial^2 A_i}{\partial t^2} = 0 \tag{I.118}$$

With the assumption of  $\exp(i\omega t)$ -harmonic fields, this becomes a Helmholtz relation for the potential vector which, in view of Rel (1.98), reads as:

$$\Delta A_i + k^2 A_i = 0 \tag{I.119}$$

Similarly, the scalar potential satisfies a Helmholtz equation.

Finally, the  $\exp(i\omega t)$ -harmonic electric field can be expressed as a function of only the vector potential. Invoking again the definition of the potential vector (I.110) and Maxwell's equation (I.58), the electric field  $E_i$  may be derived from the potential vector  $A_i$  as

$$E_i = \frac{1}{i\omega\epsilon\mu}(curl\ curl\ A_j)_i \tag{I.120}$$

Using again Rel (L117), the Helmholtz relation (L119) and Rels (L98) and (L100), it comes out that the electric field  $E_i$  reads as:

$$E_i = \frac{-i c}{kM} (grad \ div A_j)_i - i\omega A_i$$
 (I.121)

Therefore, instead of dealing with two fields  $E_i$  and  $H_i$ , it appears that we may deal with a single field  $A_i$  because, once  $A_i$  is determined, the fields  $E_i$  and  $H_i$  are determined within the Lorentz gauge by Rels (L121) and (L110).

# $\mathbf{II}$

# Resolution of Special Maxwell's Equations

In this chapter we present solutions of Maxwell's equations for time-harmonic waves in l.l.h.i. media. Hence, the starting point is section I.2. Again, one of our recurrent choice will be to introduce special cases as late as possible in the chain of the resolution of Maxwell's equations. Thus, the explicit time harmonic dependence of the waves only appears in section II.3 and the introduction of spherical coordinate systems (the one suitable for spherical scatterers) is postponed to section II.4.

# II.1 Special Orthogonal Curvilinear Coordinate Systems and Separability

It will be required to consider special Maxwell's equations and to solve them. The task is reasonably easy only if the coordinates are separable. Kerker (23, chapter I) and Morse and Fesbach (116, p 513) count eleven separable systems for the wave equation, including spherical coordinates , and discuss them. In this book, we shall use special orthogonal curvilinear systems (section I.2.2) in which the scale factors satisfy two-extra conditions reading as:

$$e_1 = 1 \tag{II.1}$$

$$\frac{\partial}{\partial x^1} \left( \frac{e_2}{e_3} \right) = 0 \tag{II.2}$$

This is in particular true for a spherical coordinate system (section I.2.3) in which indeed  $e_1 = 1$  and:

$$\frac{\partial}{\partial x^1} \left( \frac{e_2}{e_3} \right) = \frac{\partial}{\partial r} \left( \frac{1}{\sin \theta} \right) = 0 \tag{II.3}$$

More generally, within the set of eleven separable coordinate systems for the wave equation, there are only six coordinate systems satisfying the above

extra-conditions (III6), p 1765). Instead of dealing with the wave equation, however, we shall deal with the Bromwich scalar potential equation for which separability too will work. The relation between the wave equation and the Bromwich scalar potential equation is discussed in III as well as separability in spherical and cylindrical coordinate systems. In the most general case however, it must be pointed out that separability must be understood in terms of distributions (III2), III) rather than in terms of functions III.

Separability for the Bromwich scalar potential equation in spherical coordinates implies that these coordinates are suitable to develop GLMT for spheres such as considered in this book. Note that the difficulties in solving Maxwell's equations do not only depend on the shape of the scatterer but also on the material properties which must exhibit a spherical symmetry too. For instance, a sphere with randomly located inclusions, even spherical, would provide a scattering problem tremendously difficult to solve with no possibility of invoking global spherical symmetry. Conversely, spherical coordinate systems have been used for plane wave scattering by stratified spheres in which electromagnetic properties are stratified, i.e. the complex refractive index may vary radially. In such a case, the radial variation of the properties matches perfectly well the symmetry properties of the coordinate system and therefore does not kill separability, and a GLMT for multilayered spheres is feasible as will be discussed later.

More generally, all particle shapes which have been treated for plane wave scattering, like fibres or spheroids, can be investigated for shaped beams by invoking separability in the coordinate system tailored to the particle symmetry, as will also be discussed later.

#### II.2 Bromwich Potentials

#### II.2.1 Generalities

In the Anglo-saxon world, a favoured method to solve Maxwell's equations relies on the use of Hertz (or Hertz-Debye) potentials. This tradition is probably based on the success of the book by Stratton [15].

In any case, however, another method proposed by Bromwich [125], and extensively developed by Borgnis [126], may be used. Kerker [23] comments that Bromwich initially appears to be a late comer but that Bromwich solution actually could have been worked out as soon as 1899. In France, there is a strong tradition in using Bromwich method rather than that of Hertz one and, therefore, it is no wonder that our GLMT has been developed with it. Both methods are however, equivalent and, consequently, a GLMT based on Hertz potentials would be equivalent to our GLMT based on Bromwich scalar potentials (BSPs from now on). In particular, the formulation provided by Barton [70] has been shown to be equivalent to that of the authors by Lock [127]. Also, we expect that there would exist strong similarities between the

formulation of the authors and the one given by Kim and Lee [68], 69, although Kim and Lee's work was restricted to Gaussian beams, while we here consider arbitrary-shaped beams.

Furthermore, the Bromwich method, based on scalar potentials, will lead us to write field expressions in a scalar way. Such field expressions may equivalently be written in a vectorial way by using vector spherical wave functions. The vectorial formulation is more concise and may be found more elegant while some people may prefer to work with the more expanded scalar formulation. The situation is similar to the possibility of choice between dealing either with a vector or with its components. In some cases, like for the GLMT stricto sensu, it might be a matter of taste. However, let us consider the GLMT for the case of a sphere containing an eccentrically located spherical inclusion [128]. This GLMT requires the use of translational addition theorems which are better expressed in terms of vector spherical wave functions and, therefore, in this case, the use of a vectorial formalism may be in compulsory practice. As a result, the relationship between the scalar and vectorial formulations is discussed in [128]. It is just a matter of very easy translation. For similar reasons, another case where the vectorial presentation is superior to the scalar one concerns the case of a GLMT for assemblies of spheres and aggregates 129.

The Bromwich method enables us to find special solutions to Maxwell's equations for special orthogonal curvilinear coordinate systems introduced in Section II.1. More precisely, two special solutions are obtained which are linearly independent, namely Transverse Magnetic (TM) and Transverse Electric (TE) solutions. They can be expressed by two BSPs,  $U_{TM}$  and  $U_{TE}$ , respectively. After BSPs are known, they uniquely determine two special sets of field components ( $E_{i,TM}$ ,  $H_{i,TM}$ ) and ( $E_{i,TE}$ ,  $H_{i,TE}$ ), respectively. It can be established that BSPs comply with an unique linear differential equation. From this linearity and also from Maxwell's equations linearity, it follows that any linear combination of the two special solutions is a general solution. For a given problem, unknown coefficients in the general solution are fully determined by boundary conditions. Unicity of Maxwell's solutions for a completely specified problem then ensures us that the obtained general solution is the unique and general solution of the problem.

The sequel of this section is devoted to the introduction of BSPs and to the derivation of the relation between BSPs and field components. Our derivation closely follows Poincelot 114.

# II.2.2 Transverse Magnetic Wave

In the special orthogonal coordinate systems defined in section II.1, Maxwell's equations are given in section I.2.2. The first special solution is the Transverse Magnetic wave which is defined by demanding:

$$H_1 = 0 (II.4)$$

Rel (I.62) then simply reduces to:

$$\frac{\partial}{\partial x^2} e_3 E_3 = \frac{\partial}{\partial x^3} e_2 E_2 \tag{II.5}$$

A new function P which is a potential for the quantities  $e_2E_2$  and  $e_3E_3$  involved in (III.5) is introduced:

$$e_{2}E_{2} = \frac{\partial P}{\partial x^{2}}$$

$$e_{3}E_{3} = \frac{\partial P}{\partial x^{3}}$$
(II.6)

Then Rel ( $\overline{\text{II.5}}$ ) is automatically satisfied. A first BSP, U, is now introduced as a potential of the potential P through the relation:

$$P = \frac{\partial U}{\partial x^1} \tag{II.7}$$

From Rels (II.6) and (II.7), components  $E_2$  and  $E_3$  are then determined from U by:

$$E_2 = \frac{1}{e_2} \frac{\partial^2 U}{\partial x^1 \partial x^2} \tag{II.8}$$

$$E_3 = \frac{1}{e_3} \frac{\partial^2 U}{\partial x^1 \partial x^3} \tag{II.9}$$

The definition of P (II.6) is inserted in Maxwell's equations (I.67) and (I.68) specified for obtaining the TM-wave in terms of P:

$$- \frac{\partial}{\partial x^1} e_3 H_3 = \varepsilon \frac{e_3 e_1}{e_2} \frac{\partial^2 P}{\partial x^2 \partial t}$$
 (II.10)

$$\frac{\partial}{\partial x^1} e_2 H_2 = \varepsilon \frac{e_1 e_2}{e_3} \frac{\partial^2 P}{\partial x^3 \partial t}$$
 (II.11)

leading to, in terms of U:

$$- \frac{\partial}{\partial x^1} e_3 H_3 = \varepsilon \frac{e_3 e_1}{e_2} \frac{\partial^3 U}{\partial x^1 \partial x^2 \partial t}$$
 (II.12)

$$\frac{\partial}{\partial x^1} e_2 H_2 = \varepsilon \frac{e_1 e_2}{e_3} \frac{\partial^3 U}{\partial x^1 \partial x^3 \partial t}$$
 (II.13)

With conditions (II.1) and (II.2), Rels (II.12) and (III.13) then provide us with the way to determine components  $H_3$  and  $H_2$  from BSP U by using:

$$H_3 = -\frac{\varepsilon}{e_2} \frac{\partial^2 U}{\partial x^2 \partial t} \tag{II.14}$$

$$H_2 = \frac{\varepsilon}{e_3} \frac{\partial^2 U}{\partial x^3 \partial t} \tag{II.15}$$

We now consider Maxwell's equations (I.63) and (I.64). Using previously given relations, they readily become:

$$\frac{\partial E_1}{\partial x^3} = \frac{\partial^3 U}{(\partial x^1)^2 \partial x^3} - \mu \varepsilon \frac{\partial^3 U}{\partial x^3 (\partial t)^2}$$
 (II.16)

$$\frac{\partial E_1}{\partial x^2} = \frac{\partial^3 U}{(\partial x^1)^2 \partial x^2} - \mu \varepsilon \frac{\partial^3 U}{\partial x^2 (\partial t)^2}$$
 (II.17)

which are satisfied if a special solution  $E_1$  is expressed in terms of U by:

$$E_1 = \frac{\partial^2 U}{(\partial x^1)^2} - \mu \varepsilon \frac{\partial^2 U}{(\partial t)^2}$$
 (II.18)

Let us now discuss Maxwell's equation (I.66) which is rewritten as:

$$\frac{\partial E_1}{\partial t} = \frac{1}{\varepsilon e_2 e_3} \left( \frac{\partial}{\partial x^2} e_3 H_3 - \frac{\partial}{\partial x^3} e_2 H_2 \right) \tag{II.19}$$

Using (II.14) and (II.15), it becomes:

$$\frac{\partial E_1}{\partial t} = \frac{-1}{e_2 e_3} \left( \frac{\partial}{\partial x^2} \frac{e_3}{e_2} \frac{\partial^2 U}{\partial x^2 \partial t} + \frac{\partial}{\partial x^3} \frac{e_2}{e_3} \frac{\partial^2 U}{\partial x^3 \partial t} \right)$$
 (II.20)

which is satisfied with the following special solution for  $E_1$ :

$$E_1 = \frac{-1}{e_2 e_3} \left( \frac{\partial}{\partial x^2} \frac{e_3}{e_2} \frac{\partial U}{\partial x^2} + \frac{\partial}{\partial x^3} \frac{e_2}{e_3} \frac{\partial U}{\partial x^3} \right)$$
 (II.21)

A Comparison of (II.18) and (II.21) provides the differential equation for U:

$$\frac{\partial^2 U}{(\partial x^1)^2} - \mu \varepsilon \frac{\partial^2 U}{(\partial t)^2} + \frac{1}{e_2 e_3} \left( \frac{\partial}{\partial x^2} - \frac{e_3}{e_2} - \frac{\partial U}{\partial x^2} \right) + \frac{\partial}{\partial x^3} - \frac{e_2}{e_3} - \frac{\partial U}{\partial x^3} = 0 \quad (\text{II}.22)$$

The two Maxwell's equations involving divergences ((I.65) and (I.69)) have not been used. The reader might readily check that they add nothing more than what we have gained, being identically satisfied.

The relation div  $H_i = 0$  is identically satisfied due to  $H_1 = 0$ ,  $e_1 = 1$  and to Rels (II.14)-(II.15) while relation div  $E_i = 0$  is identically satisfied because div  $E_i$  is found to be equal to the derivative with respect to  $x^1$  of  $e_2$   $e_3$  times the left-hand-side of (II.22).

It is then found that the potential U is the key quantity of Bromwich formulation. The whole set of Maxwell's equations is fully equivalent to a

linear differential equation for U plus rules of derivation of field components to be used after U is determined. Only  $H_1$  is not expressed in terms of U, but this quantity is zero from the definition of the TM-wave.

For convenience, subscripts TM have been omitted in this section. They should be reintroduced to avoid any confusion with the TE-case: U becomes  $U_{TM}$  and the field components  $V_i$  become  $V_{i,TM}$ . These components are served again below to present them in a single dish:

$$H_{1.TM} = 0$$
 (TM-definition) (II.23)

$$H_{2,TM} = \frac{\varepsilon}{e_3} \frac{\partial^2 U_{TM}}{\partial x^3 \partial t}$$
 (II.24)

$$H_{3,TM} = -\frac{\varepsilon}{e_2} \frac{\partial^2 U_{TM}}{\partial x^2 \partial t}$$
 (II.25)

$$E_{1,TM} = \frac{\partial^2 U_{TM}}{(\partial x^1)^2} - \mu \varepsilon \frac{\partial^2 U_{TM}}{(\partial t)^2}$$
 (II.26)

$$E_{2,TM} = \frac{1}{e_2} \frac{\partial^2 U_{TM}}{\partial x^1 \partial x^2}$$
 (II.27)

$$E_{3,TM} = \frac{1}{e_3} \frac{\partial^2 U_{TM}}{\partial x^1 \partial x^3}$$
 (II.28)

### II.2.3 Transverse Electric Wave

The second special solution is the Transverse Electric wave which is defined by demanding:

$$E_1 = 0 (II.29)$$

Analysis of this case is fully similar to the previous one and is left as an exercise to the interested reader. It is then found that the Transverse Electric BSP  $U_{TE}$  complies with the same differential equation (II.22) as does  $U_{TM}$ . It is again to be emphasized here that this Bromwich scalar potential equation is not identical with the wave equation as an expert in light propagation theory might think and pray for from a superficial look (see discussion in [I2I]). Once  $U_{TE}$  is determined, all the corresponding field components can be derived according to a second dish in our menu:

$$E_{1,TE} = 0$$
 (TE-definition) (II.30)

$$E_{2,TE} = -\frac{\mu}{e_3} \frac{\partial^2 U_{TE}}{\partial x^3 \partial t}$$
 (II.31)

$$E_{3,TE} = \frac{\mu}{e_2} \frac{\partial^2 U_{TE}}{\partial x^2 \partial t}$$
 (II.32)

$$H_{1,TE} = \frac{\partial^2 U_{TE}}{(\partial x^1)^2} - \mu \varepsilon \frac{\partial^2 U_{TE}}{(\partial t)^2}$$
 (II.33)

$$H_{2,TE} = \frac{1}{e_2} \frac{\partial^2 U_{TE}}{\partial x^1 \partial x^2}$$
 (II.34)

$$H_{3,TE} = \frac{1}{e_3} \frac{\partial^2 U_{TE}}{\partial x^1 \partial x^3} \tag{II.35}$$

Clearly, instead of reproducing the analysis similar to the one in previous subsection, the reader if in a hurry could be content in simply checking that the TE-expressions do satisfy the whole set of Maxwell's equations.

## II.3 Explicit Time Harmonic Dependence

Invoking Fourier Transform, arbitrary waves may be expressed as sums or integrals of sinusoidal waves as discussed in Chapter I. Therefore, the rest of this book is devoted to sinusoidal waves without any significant loss of generality. It is recalled that the time dependence of the complex representative is assumed to be contained in an  $\exp(i\omega t)$  term, in which  $\omega$  is the angular frequency. Therefore, the derivative operator  $(\partial./\partial t)$  becomes a multiplicative operator  $(i\omega.)$ .

Invoking Rel (I.98), the differential equation for BSPs (II.22) then becomes:

$$\frac{\partial^2 U}{(\partial x^1)^2} + k^2 U + \frac{1}{e_2 e_3} \left[ \frac{\partial}{\partial x^2} \frac{e_3}{e_2} \frac{\partial U}{\partial x^2} + \frac{\partial}{\partial x^3} \frac{e_2}{e_3} \frac{\partial U}{\partial x^3} \right] = 0$$
 (II.36)

After  $U_{TM}$  and  $U_{TE}$  are determined, the expressions to derive the field components simplify to:

Transverse Magnetic Wave.

$$H_{1,TM} = 0 (II.37)$$

$$H_{2,TM} = \frac{i\omega\varepsilon}{e_3} \frac{\partial U_{TM}}{\partial x^3} \tag{II.38}$$

$$H_{3,TM} = -\frac{i\omega\varepsilon}{e_2} \frac{\partial U_{TM}}{\partial x^2}$$
 (II.39)

$$E_{1,TM} = \frac{\partial^2 U_{TM}}{(\partial x^1)^2} + k^2 U_{TM}$$
 (II.40)

$$E_{2,TM} = \frac{1}{e_2} \frac{\partial^2 U_{TM}}{\partial x^1 \partial x^2}$$
 (II.41)

$$E_{3,TM} = \frac{1}{e_3} \frac{\partial^2 U_{TM}}{\partial x^1 \partial x^3}$$
 (II.42)

#### Transverse Electric Wave.

$$E_{1,TE} = 0 \tag{II.43}$$

$$E_{2,TE} = -\frac{i\omega\mu}{e_3} \frac{\partial U_{TE}}{\partial x^3} \tag{II.44}$$

$$E_{3,TE} = \frac{i\omega\mu}{e_2} \frac{\partial U_{TE}}{\partial x^2} \tag{II.45}$$

$$H_{1,TE} = \frac{\partial^2 U_{TE}}{(\partial x^1)^2} + k^2 U_{TE} \tag{II.46}$$

$$H_{2,TE} = \frac{1}{e_2} \frac{\partial^2 U_{TE}}{\partial x^1 \partial x^2} \tag{II.47}$$

$$H_{3,TE} = \frac{1}{e_3} \frac{\partial^2 U_{TE}}{\partial x^1 \partial x^3} \tag{II.48}$$

In this section, and from now on, the time dependent term  $\exp(i\omega t)$  must be thought to be systematically omitted, as is the usual practice.

## II.4 Use of Spherical Coordinate Systems

By specifying the expressions for  $e_1, e_2, e_3$  of a spherical coordinate system (Rels (I.70), (I.73)) which comply with conditions (II.1)–(II.2) for using the Bromwich formulation, the differential equation (II.36) for BSPs becomes:

$$\frac{\partial^2 U}{\partial r^2} + k^2 U + \frac{1}{r^2 \sin \theta} \frac{\partial}{\partial \theta} \sin \theta \frac{\partial U}{\partial \theta} + \frac{1}{r^2 \sin^2 \theta} \frac{\partial^2 U}{\partial \varphi^2} = 0$$
 (II.49)

As stated in section II.2.3, it is readily checked that this equation differs from Helmholtz (wave) equation  $\Delta U + k^2 U = 0$  by a  $\frac{2}{r} \left( \frac{\partial U}{\partial r} \right)$  term.

After  $U_{TM}$  and  $U_{TE}$  are determined, the relations to derive the field components now become:

$$E_{r,TM} = \frac{\partial^2 U_{TM}}{\partial r^2} + k^2 U_{TM} \tag{II.50}$$

$$E_{\theta,TM} = \frac{1}{r} \frac{\partial^2 U_{TM}}{\partial r \partial \theta}$$
 (II.51)

$$E_{\varphi,TM} = \frac{1}{r\sin\theta} \frac{\partial^2 U_{TM}}{\partial r \partial \varphi}$$
 (II.52)

$$H_{r,TM} = 0 (II.53)$$

$$H_{\theta,TM} = \frac{i\omega\varepsilon}{r\sin\theta} \frac{\partial U_{TM}}{\partial\varphi} \tag{II.54}$$

II.5 BSP-Solutions 31

$$H_{\varphi,TM} = -\frac{i\omega\varepsilon}{r} \frac{\partial U_{TM}}{\partial \theta}$$
 (II.55)

$$E_{r,TE} = 0 (II.56)$$

$$E_{\theta,TE} = \frac{-i\omega\mu}{r\sin\theta} \frac{\partial U_{TE}}{\partial \varphi}$$
 (II.57)

$$E_{\varphi,TE} = \frac{i\omega\mu}{r} \frac{\partial U_{TE}}{\partial \theta} \tag{II.58}$$

$$H_{r,TE} = \frac{\partial^2 U_{TE}}{\partial r^2} + k^2 U_{TE} \tag{II.59}$$

$$H_{\theta,TE} = \frac{1}{r} \frac{\partial^2 U_{TE}}{\partial r \partial \theta}$$
 (II.60)

$$H_{\varphi,TE} = \frac{1}{r\sin\theta} \frac{\partial^2 U_{TE}}{\partial r \partial \varphi}$$
 (II.61)

We therefore now have to look for BSP-solutions.

### II.5 BSP-Solutions

## II.5.1 Reduction to Ordinary Differential Equations

Owing to coordinate separability in spherical coordinate systems, the partial derivative equation (PDE) for BSPs, (II.49), may be reduced to a set of three ordinary differential equations (ODE) by the method of variable separation, according to:

$$U(r, \theta, \varphi) = rR(kr) \; \Theta(\theta) \; \Phi(\varphi) \tag{II.62}$$

Indeed, inserting (II.62) into (II.49), and multiplying by:

$$\mathcal{M} = \frac{r}{R(kr) \Theta(\theta) \Phi(\varphi)}$$
 (II.63)

leads to

$$\frac{r}{R(kr)} \frac{d^2 r R(kr)}{dr^2} + k^2 r^2 = -\frac{1}{\sin \theta} \left( \frac{1}{\Theta(\theta)} \frac{d}{d\theta} \sin \theta \right) \frac{d\Theta(\theta)}{d\theta} + \frac{1}{\sin \theta} \frac{d^2 \Phi(\varphi)}{\Phi(\varphi)} \frac{d^2 \Phi(\varphi)}{d\varphi^2}$$
(II.64)

Because the members of (11.64) depend on independent variables, both of them must be equal to a (complex) constant which is conveniently written as a (a + 1).

Introducing:

$$x = kr, (II.65)$$

the LHS of (II.64) then becomes:

$$\frac{d}{dx} \left[ x^2 \frac{dR(x)}{dx} \right] + \left[ x^2 - a(a+1) \right] R(x) = 0 \tag{II.66}$$

which is called the spherical Bessel equation.

The RHS of (II.64) then produces the spherical harmonic equation. Multiplying by  $sin^2\theta$ , we obtain:

$$a(a+1)\sin^2\theta + \frac{\sin\theta}{\Theta(\theta)} \frac{d}{d\theta}\sin\theta \frac{d\Theta(\theta)}{d\theta} = -\frac{1}{\Phi(\varphi)} \frac{d^2\Phi(\varphi)}{d\varphi^2}$$
(II.67)

Again, both members must be equal to a (complex) constant taken as  $b^2$ , leading to the associated Legendre equation:

$$(1 - u^2) \frac{d^2 \Theta(\theta)}{du^2} - 2u \frac{d\Theta(\theta)}{du} + \left[ a(a+1) - \frac{b^2}{1 - u^2} \right] \Theta(\theta) = 0$$
 (II.68)

in which:

$$u = \cos \theta \tag{II.69}$$

and to the harmonic equation:

$$\frac{d^2\Phi}{d\varphi^2} + b^2\varphi = 0 \tag{II.70}$$

# II.5.2 Harmonic Equation

Continuity of function  $\Phi$  with respect to rotation around z-axis ( $2\pi$ -periodicity) requires the following boundary condition to be satisfied:

$$\varPhi(0) = \varPhi(2\pi) \tag{II.71}$$

Hence b in the harmonic equation (II.70) cannot be any complex number but must be an integer. If we choose m to be a positive integer, then the harmonic solutions of (II.70) simply take the form:

$$\Phi(\varphi) = \exp(\pm i \ m \ \varphi) \tag{II.72}$$

It is a pity that we have nothing more to say about these solutions in so far as this subsection is certainly somewhat too short when compared to the others. However, it may give us an opportunity to relax. II.5 BSP-Solutions 33

# II.5.3 Associated Legendre Equation

Although a and b in (II.68) are mathematically allowed to be complex constants, we have seen in section II.5.2 that b must be an integer m. Similarly a must be a non-negative integer.

Effectively, we are looking for solutions which are defined over the whole space. Therefore, our solution for the associated Legendre equation (II.68) must be defined for  $u=\pm 1$  all in cases when b=m integer. In particular, for b=0, Rel (II.68) reduces to the standard Legendre equation whose solutions remain finite at  $u=\pm 1$  only if constant a is a positive integer n (II.68), chap VII). The constants b and a being defined independently, the above restriction for a applies to the other solutions of (II.68) whatever the value of b. Consequently, function a is solution of the associated Legendre equation in the case when a0 is an integer and a1 in a positive integer.

Under such circumstances, the solutions of the associated Legendre equation are the associated Legendre functions  $P_n^m$ , often missnamed by physicists as associated Legendre polynomials, with n = (1, 2, ...) and m = (-n, ..., +n). In this book, they are defined according to the Bhagavad-Gita on Legendre functions, namely Robin  $\boxed{130}$ :

$$P_n^m(\cos\theta) = (-1)^m (\sin\theta)^m \frac{d^m P_n(\cos\theta)}{(d\cos\theta)^m}$$
 (II.73)

in which  $P_n$  are Legendre polynomials which may be defined by:

$$P_n(x) = P_n^0(x) = \frac{1}{2^n n!} \frac{d^n}{d x^n} (x^2 - 1)^n$$
 (II.74)

with the consequence that associated Legendre functions  $P_n^0$  identify with Legendre polynomials  $P_n$ . Definitions (II.73)–(II.74) follow Hobson's notation and can be collapsed into a single expression valid whatever be the value of m:

$$P_n^m(\cos\theta) = \frac{(-1)^m}{2^n \ n!} (\sin\theta)^m \frac{d^{n+m}}{(d \cos\theta)^{n+m}} (\cos^2\theta - 1)^n$$
 (II.75)

We advise that an alternative definition for  $P_n^m$ 's is also used by some authors (for instance Arfken) 131 as

$$P_n^m(\cos \theta) = (\sin \theta)^m \frac{d^m P_n(\cos \theta)}{(d \cos \theta)^m}$$
 (II.76)

Relations involving  $P_n^m$  's with the same parity for m (all odd, or all even) do not depend on the chosen definition. Otherwise, some care must be taken to avoid sign errors.

Legendre polynomials  $P_n$  and associated Legendre functions  $P_n^m$  comply with many relations from which it will rapidly prove useful to extract 132:

$$P_n^{-m}(\cos \theta) = (-1)^m \frac{(n-m)!}{(n+m)!} P_n^m(\cos \theta)$$
 (II.77)

# II.5.4 Spherical Bessel Equation

With the restriction that constant a is a positive integer (see previous section), basic solutions of the spherical Bessel equation (II.66) for n given are four spherical Bessel functions that we denote by  $\Psi_n^{(i)}$ , i = 1, 2, 3, 4 (II30), t3) as follows:

$$\Psi_n^{(1)}(x) = \sqrt{\frac{\pi}{2x}} J_{n+1/2}(x)$$
 (II.78)

$$\Psi_n^{(2)}(x) = \sqrt{\frac{\pi}{2x}} N_{n+1/2}(x)$$
 (II.79)

$$\Psi_n^{(3)}(x) = \sqrt{\frac{\pi}{2x}} H_{n+1/2}^{(1)}(x)$$
 (II.80)

$$\Psi_n^{(4)}(x) = \sqrt{\frac{\pi}{2x}} H_{n+1/2}^{(2)}(x)$$
 (II.81)

in which  $J, N, H^{(1)}$  and  $H^{(2)}$  are the ordinary Bessel functions, the Neumann function and Hankel functions of the first and second kind respectively (alternative denominations are ordinary Bessel function for J, Bessel functions of the first, second and third kind for  $N, H^{(1)}$  and  $H^{(2)}$  respectively).

For more details concerning these functions, the reader might refer to Stratton 15 and to Watson 133 which is our Bible for Bessel functions.

The spherical Bessel equation can be specified for a = n as follows:

$$\[ \frac{d^2}{dr^2} + k^2 \] \left( r \Psi_n^{(j)}(kr) \right) = \frac{n(n+1)}{r} \Psi_n^{(j)}(kr) \tag{II.82}$$

which is therefore the basic differential equation for these functions. The fact that the  $\Psi_n^{(i)}$ 's are here called basic does not however imply that they are linearly independent. Effectively, Hankel functions  $H^{(1)}$  and  $H^{(2)}$  comply with:

$$H_p^{(1)}(x) = J_p(x) + i N_p(x)$$
 (II.83)

$$H_p^{(2)}(x) = J_p(x) - i N_p(x)$$
 (II.84)

whatever be the value of p, implying:

$$\Psi_n^{(3)}(x) = \Psi_n^{(1)}(x) + i \Psi_n^{(2)}(x)$$
 (II.85)

$$\Psi_n^{(4)}(x) = \Psi_n^{(1)}(x) - i \Psi_n^{(2)}(x)$$
 (II.86)

In solving a given problem, not all of the  $\Psi_n^{(i)}$ 's are necessarily useful because choices may be imposed by physical constraints. More specifically, only

II.5 BSP-Solutions 35

 $x \Psi_n^{(1)}(x)$  is defined (no singularity) at coordinate center (x=0) and, for an  $\exp(i\omega t)$ -time dependence here chosen, only  $x \Psi_n^{(4)}(x)$  produces an outgoing spherical wave at infinity  $(x\to\infty)$ . With the alternative choice of an  $\exp(-i\omega t)$ -time dependence, the asymptotic spherical wave behaviour would be conversely produced by  $x \Psi_n^{(3)}(x)$ . The alternative  $\exp(+i\omega t)/\exp(-i\omega t)$  is reflected in Rels (II.85)—(II.86) by the alternative (-i)/(+i). It will later be made clear that we shall therefore only deal with  $\Psi_n^{(1)}$  and  $\Psi_n^{(4)}$ . Accordingly, it will be of interest to use Ricatti-Bessel functions  $\Psi_n(x)$  and  $\xi_n(x)$  defined by:

$$\Psi_n(x) = x\Psi_n^{(1)}(x) \tag{II.87}$$

$$\xi_n(x) = x\Psi_n^{(4)}(x) \tag{II.88}$$

In order to prevent any misconfusion, the reader should note that the spherical Bessel functions can be noted as  $\Psi_n^{(i)}$  as we do according to Robin (Meixner and Schäfke notation) or alternatively  $j_n$ ,  $y_n$ ,  $h_n^{(1)}$  and  $h_n^{(2)}$ . Our personal background and preferences in this book are more strongly oriented towards specific notations and indices than towards lower case letters that we feel more difficult to discriminate from upper case letters and from many common quantities designated by lower case latin characters.

## II.5.5 General Expressions for BSPs

Assembling results from previous subsections (II.5.2)–(II.5.4), it is found that any linear combination of functions of the kind:

$$r \begin{vmatrix} \Psi_n^{(1)}(kr) \\ \Psi_n^{(2)}(kr) \\ \Psi_n^{(3)}(kr) \\ \Psi_n^{(4)}(kr) \end{vmatrix} P_n^m(\cos\theta) \exp(\pm im\varphi)$$
 (II.89)

is a solution of the linear differential equation for BSPs (III.49).

In BSPs, which we shall deal with, physical constraints will reduce expression (II.89) to a simpler form: (i) as stated in section (II.5.4),  $\Psi_n^{(i)}$ 's are not allowed to appear together, only  $\Psi_n^{(1)}$  and  $\Psi_n^{(4)}$  will be allowed to perform on the stage, (ii)  $P_n^m$  and  $P_n^{-m}$  terms can be joined into a single  $P_n^{|m|}$  since Rel (II.77) shows that they are directly proportional to each other, (iii) the term with n=0 (and accordingly m=0) can be ignored because it is not the potential of any non trivial electromagnetic field: the associated BSP is independent from variables  $\theta$  and  $\varphi$  and complies with the spherical Bessel equation (II.82) specified for n=0. Accordingly, all the field components defined by Rels (II.50)-(II.61) vanish.

Therefore, BSPs will read as:

$$U(r,\theta,\varphi) = \sum_{n=1}^{\infty} \sum_{m=-n}^{+n} c_{nm} r \begin{pmatrix} \Psi_n^{(1)}(kr) \\ \Psi_n^{(4)}(kr) \end{pmatrix} P_n^{|m|}(\cos\theta) \exp(im\varphi)$$
(II.90)

i.e., in terms of Ricatti-Bessel functions (Rels (II.87)-(II.88)):

$$U(r,\theta,\varphi) = \sum_{n=1}^{\infty} \sum_{m=-n}^{+n} \frac{c_{nm}}{k} \begin{pmatrix} \Psi_n(kr) \\ \xi_n(kr) \end{pmatrix} P_n^{|m|}(\cos\theta) \exp(im\varphi) \text{ (II.91)}$$

An equivalent notation could be introduced by using the spherical surface harmonics  $Y_n^m(\theta, \varphi)$  defined by:

$$Y_n^m(\theta,\varphi) = \sqrt{\frac{(2n+1)(n-m)!}{4\pi(n+m)!}} P_n^m(\cos\theta) \exp(im\varphi)$$
 (II.92)

With definition (III.75) for  $P_n^m$ , spherical harmonics are here defined according to the Condon-Shortley phase convention (IIII), chap. 12).

These spherical harmonics form a landmark of quantum mechanics because they are eigenfunctions for the angular momentum. They express a natural separation between radial variable r appearing in  $\Psi_n^{(i)}(kr)$ , associated with an unique integer n, and angular variables  $(\varphi, \theta)$  associated with an unique extra integer m. They furthermore form a complete set of orthonormal functions over a spherical surface according to:

$$\int_{0}^{\pi} \int_{0}^{2\pi} Y_{n}^{m*}(\theta, \varphi) Y_{p}^{q}(\theta, \varphi) \sin \theta \ d\theta \ d\varphi = \delta_{nm} \delta_{pq}$$
 (II.93)

We however found more practical to write the U-expansion using Rel (II.90) or Rel (II.91) than by introducing both polynomials  $P_n^m$  and  $P_n^{-m}$ , or spherical surface harmonics in agreement with comments later given by Lock [127].

# III

# Generalized Lorenz-Mie Theory in the Strict Sense, and Other GLMTs

The general version of GLMT (in the strict sense, i.e. when the scaterer is a sphere defined by its diameter d and its complex refractive index M) has been exposed in 2 and 89. Ref 2 discusses the case of arbitrary location of the scatterer in a Gaussian beam. It mentions that the generalization from Gaussian beams to arbitrary shaped beams should be rather trivial. Indeed it is. The only thing to do was to separate the expressions valid independently of the illuminating beam from those specific of it. This was done in [89] explicitly discussing the case when the scatterer is arbitrarily located in an arbitrary shaped beam. A synthesis of these two articles is available from Gouesbet et al 90. This chapter is essentially an extended version of this synthesis and is therefore devoted to the generalized Lorenz-Mie theory (GLMT) for an arbitrary location of the scatterer in an arbitrary shaped beam. Some elements pertaining to this general framework are nevertheless postponed to next chapters for convenience, in particular concerning the evaluation of beam shape coefficients  $g_n^m$  by quadratures or finite series. Other GLMTs (for other scatterers) are discussed in a complement.

# III.1 The Scattering Problem and Global Strategy

The scatter center is a spherical particle completely defined by its diameter d and its complex refractive index M. This index is defined relatively to the surrounding medium assumed to be nonabsorbing. Usually in light scattering textbooks and pioneering articles, the particle medium is assumed to be non-magnetic. However, the case of magnetic media will be now discussed. As far as we understand, there is no special difficulty in accepting this extension.

The center of the scattering particle is located at the point  $O_P$  of a Cartesian coordinate system  $O_P xyz$ . The incident wave is described in another Cartesian coordinate system  $O_G uvw$  to be carefully chosen, depending on the nature of the wave. For instance, when the incident beam is a laser beam in its fundamental  $TEM_{00}$  mode (Gaussian beams, chapter IV),  $O_G$  should preferably be the waist center.

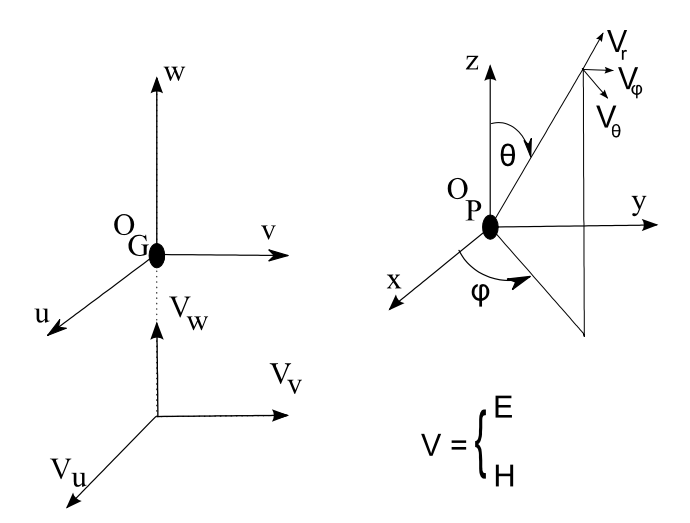


Fig. III.1. The geometry under study. V means E or H.

For convenience, it is assumed that axes  $O_G u$ ,  $O_G v$ ,  $O_G w$  are parallel to axes  $O_P x$ ,  $O_P y$ ,  $O_P z$  respectively. It is also assumed that the incident wave propagates from the negative w to the positive w and that we are able to describe it in terms of Cartesian field components  $E_u, E_v, E_w, H_u, H_v, H_w$  from which we may derive  $E_r, E_\theta, E_\varphi, H_r, H_\theta, H_\varphi$  in the spherical coordinate system  $(r, \theta, \varphi)$  associated with the particle frame of reference  $(O_P xyz)$ . The coordinates of  $O_G$  in the system  $(O_p xyz)$  are  $(x_0, y_0, z_0)$ .

Our aim is first to describe the properties of the scattered light observed at any point  $P(r, \theta, \varphi)$  in terms of field components and of associated quantities (phase angle, scattered intensities). We are also interested in integral quantities which do not depend on the point of observation P but on the scattering pattern as a whole (cross-sections, including radiation pressure cross-sections). We will be also concerned with the electromagnetic field inside the sphere. The global strategy to reach our objective may be decomposed in several steps that are outlined below in the framework of the Bromwich method.

i) The electromagnetic field in space is built up of three contributions. The first one is the incident wave which will be designated by a superscript i (possibly omitted when convenient). The second one is the scattered wave outside of the sphere. It will be designated by a superscript s when necessary. When there is no risk of any ambiguity, superscript s may also be omitted. In some of our previous studies, we also called this wave 'external wave' with superscript e. This practice is given up because, strictly speaking, the external wave should be the summation of the incident and scattered waves. The last and third contribution is the wave inside the sphere, which we call the internal wave or the sphere wave (superscript sp). Two BSPs are associated with each kind of waves (chapter II). We shall then be facing to six BSPs:  $U_{TM}^i$ ,  $U_{TE}^i$ ,  $U_{TM}^s$ ,  $U_{TE}^{sp}$ ,  $U_{TM}^{sp}$  and  $U_{TE}^{sp}$ .

- ii) Knowing the description of the incident wave, the incident BSPs  $U_{TM}^i$  and  $U_{TE}^i$  may be determined. They introduce two sets of coefficients  $g_{n,TM}^m$  and  $g_{n,TE}^m$  (n from 1 to  $\infty$  and m from -n to + n) which are equivalent to the description of the wave. They are therefore called beam shape coefficients (BSCs).
- iii) For particle sizing, we are more particularly interested in the scattered wave defined by BSPs  $U^s_{TM}$  and  $U^s_{TE}$ . These BSPs contain an infinite number of unknown coefficients which will be fully determined using boundary conditions at the surface of the sphere. These conditions will also allow us to fully determine the BSPs  $U^{sp}_{TM}$  and  $U^{sp}_{TE}$  for the internal wave.
- iv) When internal BSPs  $U_{TM}^{sp}$  and  $U_{TE}^{sp}$  are determined, the internal field components may be derived using the set of relations (II.50)–(II.61). The use of Poynting theorem afterward leads to expressions for internal intensities.
- v) When scattering BSPs  $U_{TM}^s$  and  $U_{TE}^s$  are determined, the scattered field components may be similarly derived using the set of relations (II.50)–(II.61). These components will simplify in the so-called far field zone as a consequence of the assumption  $r \gg \lambda$ .
- vi) The formulation is then completed by deriving expressions for the phase angle, scattered intensities (Poynting theorem), cross sections for absorption, scattering and extinction (energy balance) and radiation pressure force components or cross-sections (momentum balance).

#### III.2 BSPs for the Incident Wave

To write incident wave BSPs,  $U_{TM}^i$  and  $U_{TE}^i$ , Rel (II.90), or (II.91), is invoked. Among the four spherical Bessel functions  $\Psi_n^{(i)}$  introduced in section II.5.4, the relevant one is here  $\Psi_n^{(1)}(kr)$  because only  $r \Psi_n^{(1)}(kr)$  is defined at the coordinate center r=0. Then, relabelling coefficients  $c_{nm}$  for later convenience, we immediately obtain:

$$U_{TM}^{i} = E_{0} \sum_{n=1}^{\infty} \sum_{m=-n}^{+n} c_{n}^{pw} g_{n,TM}^{m} r \Psi_{n}^{(1)}(kr) P_{n}^{|m|}(\cos \theta) \exp(im\varphi) \text{ (III.1)}$$

$$U_{TE}^{i} = H_{0} \sum_{n=1}^{\infty} \sum_{m=-n}^{+n} c_{n}^{pw} g_{n,TE}^{m} r \Psi_{n}^{(1)}(kr) P_{n}^{|m|}(\cos \theta) \exp(im\varphi) \quad (III.2)$$

in which  $E_0$  and  $H_0$  are field amplitudes which may incorporate complex numbers. Coefficients  $c_n^{pw}$  (pw for plane wave) are isolated because they appear in the Bromwich formulation of the pure LMT  $\blacksquare$ . They are given by:

$$c_n^{pw} = \frac{1}{ik} (-i)^n \frac{2n+1}{n(n+1)}$$
 (III.3)

Clearly, the reader might imagine that coefficients  $c_n^{pw}$  are isolated just by fun or mischief but the development of the theory will show that it is an

adequate attitude. It allows us to disconnect the  $c_n^{pw}$ 's and the  $g_n^m$ 's. With the former ones being specific of the plane wave case, we must think of the latter ones as specific of the non-plane character of the wave, and hence their name of beam shape coefficients.

Rel (III.1) and (III.2) may also be rewritten in terms of Ricatti-Bessel functions (sections II.5.4 and II.5.5), leading to:

$$U_{TM}^{i} = \frac{E_{0}}{k} \sum_{n=1}^{\infty} \sum_{m=-n}^{+n} c_{n}^{pw} g_{n,TM}^{m} \Psi_{n}(kr) P_{n}^{|m|}(\cos \theta) exp(im\varphi) \quad (III.4)$$

$$U_{TE}^{i} = \frac{H_0}{k} \sum_{n=1}^{\infty} \sum_{m=-n}^{+n} c_n^{pw} g_{n,TE}^{m} \Psi_n(kr) P_n^{|m|}(\cos\theta) exp(im\varphi) \quad (III.5)$$

A complete description of the incident wave in terms of BSPs now requires the knowledge of BSCs  $g_n^m$  which clearly must be determined from the description of the incident wave.

# III.3 Quadratures to Evaluate BSCs $g_n^m$

## III.3.1 The First Method to Derive Quadrature Expressions

From the knowledge of the incident Cartesian field components  $E_u$ ,  $E_v$ ,  $E_w$ ,  $H_u$ ,  $H_v$ ,  $H_w$  in coordinate system  $O_Guvw$ , the field components  $E_r$ ,  $E_\theta$ ,  $E_\varphi$ ,  $H_r$ ,  $H_\theta$ ,  $H_\varphi$  in the spherical coordinate system  $(r, \theta, \varphi)$  may be readily derived. Among these six components, the radial fields  $E_r$  and  $H_r$  play a special role because of the definition of the TM- and TE-waves (sections II.2–II.4). Recalling that any field component is the summation of the corresponding special TM- and TE-wave components and that, by definition,  $E_{r,TE} = H_{r,TM} = 0$ , this effectively leads to:

$$E_r = E_{r,TM} + E_{r,TE} = E_{r,TM} \tag{III.6}$$

$$H_r = H_{r,TM} + H_{r,TE} = H_{r,TE}$$
 (III.7)

i.e. the radial electric field  $E_r$  is equal to the special radial electric field of the TM-wave and the radial magnetic field  $H_r$  is equal to the special radial magnetic field of the TE-wave. The knowledge of these fields  $E_r$  and  $H_r$  is sufficient to fully determine the BSPs  $U_{TM}^i$  and  $U_{TE}^i$ . The procedure for the TM-case is examined with some details hereafter and similarity will permit to shorten the discussion of the TE-case.

From Rels (III.6) and (II.50) we obtain for the incident wave:

$$E_r = E_{r,TM} = \frac{\partial^2 U_{TM}^i}{\partial r^2} + k^2 U_{TM}^i$$
 (III.8)

The left-hand-side  $E_r$  is assumed to be known. Then, inserting Rel (III.1) for  $U_{TM}^i$  in (III.8) leads to the following relation to determine the infinite set of coefficients  $g_{n,TM}^m$ :

$$E_{r} = E_{0} \sum_{n=1}^{\infty} \sum_{m=-n}^{+n} c_{n}^{pw} g_{n,TM}^{m} \left( \frac{d^{2}r\Psi_{n}^{(1)}(kr)}{dr^{2}} + k^{2}r\Psi_{n}^{(1)}(kr) \right)$$

$$P_{n}^{|m|}(\cos\theta) \exp(im\varphi)$$
(III.9)

However,  $\Psi_n^{(1)}$  complies with the spherical Bessel equation (II.82) which leads to:

$$E_r = E_0 \sum_{n=1}^{\infty} \sum_{m=-n}^{+n} c_n^{pw} g_{n,TM}^m \frac{n(n+1)}{r} \Psi_n^{(1)}(kr) P_n^{|m|}(\cos \theta) \exp(im\varphi)$$
(III.10)

To isolate BSCs  $g_{n,TM}^m$ , the orthogonality relation for exponentials is invoked to get rid of angle  $\varphi$ :

$$\int_0^{2\pi} exp(i(m-m')\varphi)d\varphi = 2\pi \delta_{mm'}$$
 (III.11)

Afterward the orthogonality relation for  $P_n^{m'}$  s 130 is used to get rid of angle  $\theta$ :

$$\int_{0}^{\pi} P_{n}^{m}(\cos \theta) P_{l}^{m}(\cos \theta) \sin \theta \ d\theta = \frac{2}{2n+1} \frac{(n+m)!}{(n-m)!} \ \delta_{nl}$$
 (III.12)

To take advantage of (III.11) and (III.12), Rel (III.10) is successively multiplied by integral operators  $\int_0^{2\pi}$ .  $exp(-im'\varphi)\ d\varphi$  and  $\int_0^{\pi}$ .  $P_{n'}^{m'}(cos\theta)\ sin\theta\ d\theta$  to obtain:

$$g_{n,TM}^{m} = \frac{1}{E_{0}c_{n}^{pw}} \frac{2n+1}{4\pi n(n+1)} \frac{(n-|m|)!}{(n+|m|)!} \frac{r}{\Psi_{n}^{(1)}(kr)}$$

$$\int_{0}^{\pi} \int_{0}^{2\pi} E_{r} P_{n}^{|m|}(\cos\theta) exp(-im\varphi) \sin\theta d\theta d\varphi$$
(III.13)

The left-hand-side of (III.13) must be a constant as shown by Rels (II.90)—(II.91) or (III.11)—(III.2) while, conversely, the right-hand-side still depends on radial variable r, through  $\frac{r}{\psi_n^{(1)}}$  and  $E_r$ . Therefore the remaining r-dependence must be apparent and must vanish once the incident component  $E_r$  has been developed as a function of r, at least if the beam description perfectly satisfies Maxwell's equations (see [79], [80] discussing this issue in the case of Gaussian beams). In other words, any assigned value a of r should ideally work, leading to:

$$g_{n,TM}^{m} = \frac{1}{E_{0}c_{n}^{pw}} \frac{2n+1}{4\pi n(n+1)} \frac{(n-|m|)!}{(n+|m|)!} \frac{a}{\psi_{n}^{(1)}(ka)}$$

$$\int_{0}^{\pi} \int_{0}^{2\pi} E_{r}(r=a) P_{n}^{|m|}(\cos\theta) exp(-im\varphi) \sin\theta d\theta d\varphi$$
(III.14)

For numerical efficiency however, the value of a should not be arbitrarily chosen (see discussion in sections IV.3 and VI.6.3). Furthermore, when the beam description does not perfectly satisfy Maxwell's equations, Rel (III.14) generates artifacts which still depend on r, possibly leading to significant errors if the value r = a is poorly chosen [79, 80].

Another way to get rid of variable r is to invoke the following relation for spherical Bessel functions  $\Psi_n^{(1)}$  (131, p. 412):

$$\int_{0}^{\infty} \Psi_{n}^{(1)}(kr) \, \Psi_{n'}^{(1)}(kr) \, d(kr) = \frac{\sin\left[(n-n') \, \pi/2\right]}{n \, (n+1) - n' \, (n'+1)} \, for \, n \neq n'$$

$$\int_{0}^{\infty} \Psi_{n}^{(1)}(kr) \, \Psi_{n'}^{(1)}(kr) \, d(kr) = \frac{\pi}{2 \, (2n+1)} \, for \, n = n'$$
(III.15)

As pointed out by Lock [127], we previously used an incorrect relation (for instance in [2]):

$$\int_0^\infty \Psi_n^{(1)}(kr)\Psi_{n'}^{(1)}(kr)d(kr) = \frac{\pi}{2(2n+1)}\delta_{nn'}$$
 (III.16)

However, this incorrection does not introduce any further error because, we actually only need to use the case n=n' and, in this special case, the incorrect relation (III.16) turns out to be an exact relation. Then, from (III.13), isolating  $\Psi_n^{(1)}$  and multiplying by the integral operator  $\int_0^\infty$ .  $\Psi_{n'}^{(1)}(kr) \ d(kr)$ , we obtain:

$$g_{n,TM}^{m} = \frac{(2n+1)^{2}}{2\pi^{2}n(n+1)c_{n}^{pw}} \frac{(n-|m|)!}{(n+|m|)!} \int_{0}^{\pi} \int_{0}^{2\pi} \int_{0}^{\infty} \frac{E_{r}(r,\theta,\varphi)}{E_{0}}$$

$$r \Psi_{n}^{(1)}(kr) P_{n}^{|m|}(\cos\theta) \exp(-im\varphi) \sin\theta \ d\theta \ d\varphi \ d(kr)$$
(III.17)

Let us emphasize that, in principle, (III.13), (III.14) and (III.17) are strictly equivalent relations. In practice, such is not the case when the beam description does not perfectly satisfy Maxwell's equations, as usual for shaped beams. This issue is extensively discussed in the case of Gaussian beams by Gouesbet et al [134].

The procedure for TE-beam shape coefficients is strictly similar. We first use Rels (III.7) and (II.59) to obtain:

$$H_r = H_{r,TE} = \frac{\partial^2 U_{TE}^i}{\partial r^2} + k^2 U_{TE}^i$$
 (III.18)

The left-hand-side  $H_r$  being assumed to be known, and using again (II.82), the relation to determine coefficients  $g_{n,TE}^m$ , similar to (III.10), reads as:

$$H_r = H_0 \sum_{n=1}^{\infty} \sum_{m=-n}^{+n} c_n^{pw} g_{n,TE}^m \frac{n(n+1)}{r} \Psi_n^{(1)}(kr) P_n^{|m|}(\cos \theta) exp(im\varphi)$$
(III.19)

Invoking again (III.11) and (III.12) leads to:

$$g_{n,TE}^{m} = \frac{1}{H_0 c_n^{pw}} \frac{2n+1}{4\pi n(n+1)} \frac{(n-|m|)!}{(n+|m|)!} \frac{r}{\Psi_n^{(1)}(kr)}.$$
$$\int_0^{\pi} \int_0^{2\pi} H_r P_n^{|m|}(\cos\theta) exp(-im\varphi) \sin\theta \ d\theta \ d\varphi \quad \text{(III.20)}$$

allowing us to suppress the apparent r-dependence of these BSCs either by specifying r = a:

$$g_{n,TE}^{m} = \frac{1}{H_{0}c_{n}^{pw}} \frac{2n+1}{4\pi n(n+1)} \frac{(n-|m|)!}{(n+|m|)!} \frac{a}{\varPsi_{n}^{(1)}(ka)}.$$

$$(\text{III.21})$$

$$\int_{0}^{\pi} \int_{0}^{2\pi} H_{r} (r=a) P_{n}^{|m|}(\cos\theta) exp(-im \varphi) \sin\theta \ d\theta \ d\varphi$$

or by invoking (III.15):

$$g_{n,TE}^{m} = \frac{(2n+1)^{2}}{2\pi^{2}n(n+1)c_{n}^{pw}} \frac{(n-|m|)!}{(n+|m|)!} \int_{0}^{\pi} \int_{0}^{2\pi} \int_{0}^{\infty} \frac{H_{r}(r,\theta,\varphi)}{H_{0}}$$

$$r\Psi_{n}^{(1)}(kr)P_{n}^{|m|}(\cos\theta)exp(-im\varphi)\sin\theta \ d\theta \ d\varphi \ d(kr)$$
(III.22)

Quadrature relations (III.14), (III.21) and (III.22) might also be rewritten by using Ricatti-Bessel functions  $\Psi_n$  (Rel II.87) or by using spherical surface harmonics  $Y_n^m$  (section II.5.5). Owing to this last fact, it is stated that the BSCs have been expressed by using a spherical harmonic expansion technique. Later on, in chapter V, it will be established that BSCs may also be expressed by finite series rather than by quadratures, with the aid of a Neumann expansion technique. At the present stage however, we possess two different quadrature formulations to evaluate the BSCs, by using either double quadratures (III.14), (III.21), or triple quadratures (III.17), (III.22). Clearly, both techniques exhibit distinct advantages and disadvantages. The double quadrature technique is the fastest but the value of a may have to be chosen carefully. Conversely, the triple quadrature technique does not have to

concern with any special value of r, but it leads to much more time-consuming runs. These problems will be discussed in sections (IV.3) and (VI.6.3). Also, by examining the convergence of the results in the triple quadrature technique when integration over r takes place on a finite domain  $[0, r_{max}]$ , it will be possible to provide direct physical insights on the so-called localized approximation (section VII.2.4). Furthermore, in many cases, even for Gaussian beams indeed, we do not possess expressions of the field components perfectly satisfying Maxwell's equations. Therefore, notwithstanding numerical problems associated with the value of a, the  $g_n^m$ -values practically evaluated by the double quadrature technique may become a-dependent. Such a dependence should be small indeed when the departure of field components from Maxwell's equations is small, but it is expected that, in some cases, the dependence might become significant. Conversely, the r-integration involved in the triple quadrature technique may provide some optimization and smoothing of inaccuracies involved in the beam description. For details concerning these issues, again see [79], [80] and [134].

It then appears that the beam shape coefficients  $g_{n,X}^m$  (X = TM, TE) may be evaluated by using two kinds of quadratures, either by using twodimensional angular quadratures or by using three-dimensional quadratures on the whole space. To better understand the relationship between both formulations, Gouesbet *et al* [134] specify them to the case of a special GLMT with special beam shape coefficients  $g_n$  which, by using a Davis description of Gaussian beams, can be analytically evaluated. It is shown that both formulations may actually lead to artifacts when the beam description does not exactly satisfy Maxwell's equations. Recommendations for detection and removal of these artifacts are given.

There also exist a hybrid technique, called the integral localized approximation, which simultaneously uses a quadrature and prescriptions from the localized approximation. In the article in which this technique is introduced 135, two preferred properties for discussing methods to evaluate beam shape coefficients, namely speed and flexibility, are discussed. The speed property refers to the amount of work left to the computer and is satisfied when numerical computations are not time consuming in terms of CPU. The flexibility property refers to the amount of work left to the brain and is satisfied when a change in the description of the illuminating beam does not require a heavy extra-analytical work. Both properties are satisfied by the integral localized approximation. This technique is applied to Gaussian beams, laser sheets, and laser beams in the mode  $TEM_{01}^*$ . Furthermore, the case of laser sheets allows one to demonstrate that the integral localized approximation enjoys another property (called stability) which is not necessarily enjoyed by the localized approximation. Also, in certain cases (e.g. laser sheets), the integral localized approximation may even be faster than the localized approximation.

# III.3.2 The Second Method to Derive Quadrature Expressions

This section is devoted to the second method to obtain quadrature expressions for the BSCs  $g_n^m$ . It is again assumed that we know  $E_r(r, \theta, \varphi)$  and  $H_r(r, \theta, \varphi)$ . For a given value of r, they only depend on  $\theta$  and  $\varphi$  and take the form  $g(\theta, \varphi)$ . It is furthermore assumed that g is continuous as well as its first and second derivatives i.e. g is  $C^2$ . This condition is generic for electric and magnetic fields. Then  $g(\theta, \varphi)$  may be expanded in spherical surface harmonics  $Y_n^m(\theta, \varphi)$ . This theorem is quoted by Stratton [15] and a demonstration can be found in Courant and Hilbert [136]. Following these authors and slightly modifying the presentation of the theorem to express it with  $\exp(\mathrm{im}\varphi)$  functions, it is found that the fields  $E_r$  and  $H_r$  may be expanded as:

$$E_r = E_0 \sum_{n=0}^{\infty} \sum_{m=-n}^{+n} c_{n,TM}^m (r) P_n^{|m|} (\cos \theta) exp(im\varphi)$$
 (III.23)

$$H_r = H_0 \sum_{n=0}^{\infty} \sum_{m=-n}^{+n} c_{n,TE}^m(r) P_n^{|m|}(\cos \theta) exp(im\varphi)$$
 (III.24)

in which:

$$c_{n,TM}^{m}(r) = \frac{2n+1}{4\pi} \frac{(n-|m|)!}{(n+|m|)!} \int_{0}^{\pi} \int_{0}^{2\pi} \frac{E_{r}(r,\theta,\varphi)}{E_{0}} P_{n}^{|m|}(\cos\theta)$$
(III.25)

$$exp(-im\varphi) \sin\theta \ d\theta \ d\varphi$$

$$c_{n,TE}^{m}(r) = \frac{2n+1}{4\pi} \frac{(n-|m|)!}{(n+|m|)!} \int_{0}^{\pi} \int_{0}^{2\pi} \frac{H_{r}(r,\theta,\varphi)}{H_{0}} P_{n}^{|m|}(\cos\theta)$$
(III.26)

$$exp(-im\varphi) \sin\theta \ d\theta \ d\varphi$$

However, the electric field  $E_r$  expanded in (III.23) has also been previously expanded by using the Bromwich method in (III.10). With spherical surface harmonics forming a complete set of orthogonal functions (section II.5.5), corresponding terms in (III.23) and (III.10) may be identified leading to:

$$c_{n,TM}^{m}(r) = c_{n}^{pw} g_{n,TM}^{m} \frac{n(n+1)}{r} \Psi_{n}^{(1)}(kr) \quad n \neq 0$$

$$c_{0,TM}^{0} = 0$$
(III.27)

 $g_{n,TM}^m$ 's may then be obtained as in Rel (III.13) by combining (III.27) and (III.25), leading to double finite integrals over  $\theta$  and  $\varphi$ . Obviously Rels (III.14) and (III.17) of the BSCs can then be recovered.

Proceeding similarly with the magnetic field component  $H_r$ , Rels (III.20)(III.22) are also recovered.

The fact that  $c_{0,TM}^0 = c_{0,TE}^0 = 0$  possesses an obvious physical meaning. Let us consider the coefficient  $c_{0,TM}^0$ . From (III.25), it reads as:

$$c_{0,TM}^{0}(r) = \frac{1}{4\pi E_0} \int_0^{\pi} \int_0^{2\pi} E_r \sin\theta \ d\theta \ d\varphi$$
 (III.28)

The surface integral represents the flux of the electric field component  $E_r$  through a sphere of radius unity. It may be converted to a volume integral by using the Ostrogradsky theorem leading to:

$$c_{0,TM}^{0}(r) = \frac{1}{4\pi E_0} \int \int \int_{v} div \ E_i \ dv$$
 (III.29)

Nullity of  $c_{0,TM}^0(r)$  then follows from the nullity of  $div E_i$  because of the absence of any charge inside the sphere (I.59). Similarly, nullity of  $c_{0,TE}^0(r)$  follows from the nullity of  $div H_i$  (I.57).

## III.3.3 Other Approaches

#### On Barton et al. (1988) formulation

It has been stated in section (II.2.1) that our formulation of the GLMT and the one by Barton et al [70] are equivalent. The discussion of mechanical effects, absent from [70], has later been exposed in [137], with numerical results provided. This section is the right place to provide a direct check and also some translation formulae between both formulations. It is first remarked that Rel (7) in [89], here Rel (III.10), concerning the expansion of the electric field component  $E_r$ , is identical with Rel (15) in [70]. It is therefore enough for a direct check of equivalence to provide translation formulae between  $g_n^m$ -coefficients introduced by us and  $A_{nm}$ -coefficients introduced by Barton et al. One "pierre de Rosette" will be the double quadrature expressions. Indeed, Barton's team only used such expressions in practice because they are faster than triple quadratures. In the framework of their 1988 study devoted to Gaussian beams, they could have also used finite series (chapter V) or localized approximation (chapter VII) which are still faster. However, these two last techniques require an extra-analytical work when the beam shape is modified. Therefore, in later studies devoted to interacting particles in which incident fields on one particle result from fields scattered by another particle (138 139), the use of double quadratures was certainly the most useful.

The double quadrature expression for the  $g_n^m$ 's, i.e. Rel (III.14), is written by Barton *et al* [70], using coefficients  $A_{nm}$ 's, as:

$$A_{nm} = \frac{a^2}{n(n+1)\Psi_n(ka)} \int_0^{\pi} \int_0^{2\pi} E_r(r=a) Y_n^{m*}(\theta, \varphi) \sin \theta \ d\theta \ d\varphi \quad \text{(III.30)}$$

in which the spherical surface harmonics  $Y_n^m$  ( $\theta$ ,  $\varphi$ ) are given by Rel (II.92). Because the  $P_n^m$  's are real functions, this becomes:

$$A_{nm} = \frac{a^2}{n(n+1)\Psi_n(ka)} \sqrt{\frac{(2n+1)(n-m)!}{4\pi(n+m)!}} \int_0^{\pi} \int_0^{2\pi} E_r(r=a) .$$
(III.31)
$$P_n^m(\cos\theta) \exp(-im\varphi) \sin\theta \ d\theta \ d\varphi$$

Comparing (III.31) and (III.14) and using (III.3), it is then found that:

$$g_{n,TM}^{m} = \frac{k^2 n(n+1)}{E_0 i^{n-1} (-1)^n} \sqrt{\frac{(n-m)!}{4\pi (2n+1)(n+m)!}} A_{nm} , m \ge 0$$
 (III.32)

For  $m \le 0$ , we first use (II.77) to rewrite (III.31) as:

$$A_{nm} = \frac{(-1)^m a^2}{n(n+1)\Psi_n(ka)} \sqrt{\frac{(2n+1)(n+m)!}{4\pi(n-m)!}} \int_0^{\pi} \int_0^{2\pi} E_r(r=a) .$$
(III.33)
$$.P_r^{|m|}(\cos\theta) \exp(-im\varphi) \sin\theta \ d\theta \ d\varphi$$

leading to:

$$g_{n,TM}^m = \frac{k^2 \ n(n+1)}{E_0 i^{n-1} (-1)^{n+m}} \ \sqrt{\frac{(n+m)!}{4\pi (2n+1)(n-m)!}} \ A_{nm} \ , \ m \le 0 \quad \text{(III.34)}$$

Similarly, to the  $g_{n,TE}^m$ 's in our formulation correspond the coefficients  $B_{nm}$ 's in Barton *et al* formulation. The translation formulae are found to be identical with H and TE instead of E and TM. Again, see Lock [127] for comments on the relationship between both formulations.

We take the opportunity of this discussion to correct an erroneous statement, recurrently found in the literature, according to which GLMT is restricted to the case of illuminating Gaussian beams, or even to the case of weakened focused Gaussian beams (no reference for the sake of charity). This erroneous statement may have been inspired by the specification of Gaussian beams during the early developments of GLMT, from 1982 to 1988, and also by the fact that the "pivot" article [2] heavily exemplifies, including in the title, the case of Gaussian beams. More credence has certainly been given to the erroneous statement by the fact that Barton and collaborators called their version the "arbitrary beam theory" (ABT), e.g. in [70], [137], [140]. However, the GLMT is a genuine ABT too as illustrated, already in 1988, by [89] and also in the first review article on GLMT [90].

#### Plane wave spectrum approach

Actually, there are essentially two ways to deal with arbitrary shaped beam scattering. In the first way, the illuminating beam is described by using infinite series of partial waves (partial-wave sum of spherical multipole waves). This is the choice implemented in the GLMT, including Barton's version. In the second way, it is described by using an angular spectrum of plane waves. Each plane wave is afterward expanded into partial waves, e.g. using vector spherical harmonics. The connection between the two approaches is discussed by Lock [141].

For a background on plane wave spectra, the reader may refer to Goodman 142. The use of a plane wave spectrum was the technique already used in 1979 by Colak et al 66 and in 1982 by Yeh et al 67 to discuss focused beam scattering. Later on, it is used also by Khaled et al 143, 144 to discuss the scattered and internal intensity of a sphere illuminated with a Gaussian beam, and the internal electric energy in a spherical particle illuminated with a plane wave or an off-axis Gaussian beam, in connection with the discussion of resonances 145. The plane wave spectrum approach is also used by Ratowsky et al [146], [147] to study ball lens reflections, and the coupling efficiency between a laser diode and an optical fiber through a ball lens. A discussion of the plane wave spectrum approach to electromagnetic beams is provided by Doicu and Wriedt [148] in 1997. It relies on the Davis' method for the description of Gaussian beams. Incidentally, but significantly, as a by-product, those authors provided a justification of the localized approximation for on-axis and off-axis beams. In 2005, Peng Li et al [149] used an angular spectrum analysis to investigate optical scattering spectroscopy of a single spherical scatterer illuminated with a tightly focused supercontinuum (obtained from short laser pulses). They mention that GLMT was applied to investigate scattering of Gaussian beams. However, they add, a paraxial Gaussian beam is not suitable for modelling tightly focused field produced by high numerical aperture objective lens. Although, strictly speaking, these two sentences are correct, the next sentence in the article, telling us that an angular spectrum representation, on the other hand (!), can be used to describe strongly focused beam, suggested that GLMT would not be able to do it. This would however be an erroneous statement. In 2008, Lermé et al 150 also used an angular spectrum to deal with tightly focused beams, justifying this choice by using arguments similar to the ones of Peng Li et al above, deserving similar comments. We take the opportunity of this paragraph to mention that GLMT can efficiently deal with the case of beams focused by a high numerical aperture objective as achieved by Lock and experimentally tested, see section on mechanical effects in Chapter VIII.

The use of plane wave spectra has also been reintroduced by Albrecht *et al* [151] under the name of FLMT (Fourier Lorenz-Mie theory). GLMT then provides benchmark data to assess the validity of FLMT. Under the explicit name of FLMT, plane wave spectra have been used by Albrecht *et al* [152] to discuss the signals generated in the phase Doppler technique, and particularly the

trajectory ambiguity effect, by Bech and Leder [153] to discuss particle sizing using ultra-short laser pulses, and also by Bakic et al [154] dealing with time integrated detection of femtosecond laser pulses scattered by small droplets. FLMT is also used by Borys et al [155] in discussing light scattering analysis, and comparing an extended geometrical optics technique (EGO) with the FLMT variant of GLMT, and by Damaschke et al [156] in dealing with optical particle sizing in backscatter. The FLMT approach is comprehensively summarized in a book by Albrecht et al on laser Doppler and phase Doppler measurements, see section on measurement techniques in Chapter VIII.

In 1995, Lock, discussing the relationship between an expansion in an infinite series of partial waves or in an angular spectrum of plane waves, mentioned that no consensus has been reached as to which computational method for beam scattering is superior to the other or on whether one method possesses a richness of physical interpretation that is not manifest in the other [157]. This might still be true nowadays, and might remain true for a long time. Also, very likely, any researcher mastering one method (whatever the reason, possibly contingent) might be reluctant to attempt mastering the other. However, there are a few remarks to be made which make us preferring using an expansion in an infinite series.

The first remark concerns a problem of esthetic attractiveness. The plane wave spectrum approach is a two-step, or say, hybrid approach. The first step makes an expansion over a spectrum of plane waves, and the second step makes a Lorenz-Mie expansion over partial waves. Conversely, GLMT is an one-step approach, directly making an expansion into partial waves. Obviously, the richness of partial waves enjoyed by GLMT is far more important than the one by LMT. In LMT, we have an index n ranging from 1 to infinity while, in GLMT, we have another subscript m ranging from -n to = +n. Although the notion of beauty is a bit suggestive, we are more attracted to the more unified one-step approach than to the hybrid two-step approach.

Next, the use of a plane wave expansion is computationally much less efficient than GLMT, particularly when the localized approximation is implemented, a fact which may not be independent of the previous remark. Lock made timing comparisons between different ways of achieving GLMT computations, using a Compaq 386-33 MHz personal computer equipped with a Weitek numerical processor 157. For certain typical parameters, and 361 values of the scattering angle  $\theta$ , GLMT-computations for Gaussian beams with the localized approximation required 195 s. A corresponding classical Lorenz-Mie calculation required only 3 s, that is to say the Gaussian beam program runs almost 70 times slower than Mie theory (at least for the studied parameters). For this, we might already infer that a plane wave spectrum approach requiring more than 70 plane waves will run slower than GLMT. A GLMT program in which beam shape coefficients were evaluated by using quadratures required 4.5 h which is a factor of 83 slower than for the GLMT-program with localized calculations of the beam shape coefficients. Using a plane wave spectrum approach, the time required to evaluate beam shape coefficients (which is not the total time required) was 14 h. The total run time might have been about twice the time required to deal with the beam shape coefficients (J.A. Lock, personal communication). Therefore, in the case under study, the use of the plane wave spectrum approach would have been about 500 times slower than the GLMT with the localized approximation. The computational intensiveness of the use of a plane wave spectrum approach is also mentioned by Moore and Alonso [158]. Let us note that these timing studies have been published in 1995. Run times would be much shorter nowadays since computation speed has changed very fast as a function of time is also mentioned by Moore and Alonso [158].

Finally, there is a theoretical problem which, as far as we know, will deserve a specific study. Consider a beam description which does not exactly satisfy Maxwell's equations and build a plane wave spectrum out of it. Because each plane wave exactly satisfies Maxwell's equations, the result will exactly satisfy Maxwell's equations. Some authors are possibly proud in saying that they have obtained an exact solution. It might be better to say that, in such a case, the plane wave spectrum approach provides a kind of uncontrolled remodelling of the beam, from a non-Maxwellian description to a Maxwellian description. In other words, a plane wave representation indeed exactly satisfies Maxwell's equations, but the shape of the beam obtained may be different from the intended one. To be even-handed, such beam remodeling is also used in GLMT but there are many papers dealing with this remodeling and consequences. In contrast, this issue has not been discussed for the plane wave spectrum approach. We are not able, at the present time, to tell much more concerning this important issue.

# III.4 BSPs for Scattered and Sphere Waves

The BSPs for scattered waves are now needed. Similarly, as in the case of (III.4)-(III.5), they can be expressed from (II.90)-(II.91) as:

$$U_{TM}^{s} = \frac{-E_0}{k} \sum_{n=1}^{\infty} \sum_{m=-n}^{+n} c_n^{pw} A_n^m \xi_n(kr) P_n^{|m|}(\cos \theta) \exp(im\varphi)$$
 (III.35)

$$U_{TE}^{s} = \frac{-H_{0}}{k} \sum_{n=1}^{\infty} \sum_{m=-n}^{+n} c_{n}^{pw} B_{n}^{m} \xi_{n}(kr) P_{n}^{|m|}(\cos \theta) \exp(im\varphi)$$
 (III.36)

Clearly, the choice for the sign minus has no physical significance but only aims to produce better looking expressions for the coefficients  $A_n^m$  and  $B_n^m$  (section III.6). Conversely, the choice of  $\xi_n(kr)$  instead of  $\Psi_n(kr)$  possesses the physical meaning of producing an outgoing spherical wave with proper form in the limit  $kr \to \infty$  (section II.5.4). Such a required behaviour will be later evidenced when considering scattered field components in the far-field region (section III.8).

For the sphere wave BSPs, we similarly write:

$$U_{TM}^{sp} = \frac{kE_0}{k_{sp}^2} \sum_{n=1}^{\infty} \sum_{m=-n}^{+n} c_n^{pw} C_n^m \Psi_n(k_{sp}r) P_n^{|m|}(\cos \theta) \exp(im\varphi) \quad \text{(III.37)}$$

$$U_{TE}^{sp} = \frac{kH_0}{k_{sp}^2} \sum_{n=1}^{\infty} \sum_{m=-n}^{+n} c_n^{pw} D_n^m \Psi_n(k_{sp}r) P_n^{|m|}(\cos\theta) \exp(im\varphi) \quad \text{(III.38)}$$

in which  $k_{sp}$  is the wave number in the sphere material.

Prefactors in (III.37) and (III.38) again do not possess a deep physical meaning but only aim at producing better looking expressions when the formulation is further developed. However, the choice of  $\Psi_n$ 's is demanded by the fact that field components of the sphere wave must be defined at r=0 (section II.5.4).

BSPs  $U_{TM}^s$ ,  $U_{TE}^s$ ,  $U_{TM}^{sp}$ ,  $U_{TE}^{sp}$  and corresponding field components are completely determined once the coefficients  $A_n^m$ ,  $B_n^m$ ,  $C_n^m$ ,  $D_n^m$  in Rels (III.35) are known. These coefficients are determined by boundary conditions at the surface of the sphere.

### III.5 Expansions of Field Components

Before invoking the boundary conditions at the surface of the sphere, it is convenient to explicitly display the expressions for field components. The special TM- and TE-field components of the incident wave are deduced from BSPs (III.4)-(III.5) by using rules of derivation (II.50)-(II.61):

$$E_{r,TM}^{i} = kE_{0} \sum_{n=1}^{\infty} \sum_{m=-n}^{+n} c_{n}^{pw} g_{n,TM}^{m} \left[ \Psi_{n}^{"}(kr) + \Psi_{n}(kr) \right] P_{n}^{|m|}(\cos \theta) \exp(im\varphi)$$
(III.39)

$$E_{\theta,TM}^{i} = \frac{E_{0}}{r} \sum_{n=1}^{\infty} \sum_{m=-n}^{+n} c_{n}^{pw} g_{n,TM}^{m} \Psi_{n}^{'}(kr) \tau_{n}^{|m|}(\cos\theta) \exp(im\varphi) \quad (\text{III}.40)$$

$$E_{\varphi,TM}^{i} = i \frac{E_{0}}{r} \sum_{n=1}^{\infty} \sum_{m=-n}^{+n} m c_{n}^{pw} g_{n,TM}^{m} \Psi_{n}^{'}(kr) \pi_{n}^{|m|}(\cos \theta) \exp(im\varphi)$$
(III.41)

$$H_{rTM}^i = 0 (III.42)$$

$$H_{\theta,TM}^{i} = \frac{-H_{0}}{r} \sum_{n=1}^{\infty} \sum_{m=-n}^{+n} m c_{n}^{pw} g_{n,TM}^{m} \Psi_{n} (kr) \pi_{n}^{|m|} (\cos \theta) \exp(im\varphi)$$
(III.43)

$$H_{\varphi,TM}^{i} = \frac{-i H_0}{r} \sum_{n=1}^{\infty} \sum_{n=1}^{+n} c_n^{pw} g_{n,TM}^{m} \Psi_n (kr) \tau_n^{|m|} (\cos \theta) \exp(im\varphi)$$
(III.44)

$$E_{r,TE}^i = 0 (III.45)$$

$$E_{\theta,TE}^{i} = \frac{E_0}{r} \sum_{n=1}^{\infty} \sum_{m=-n}^{+n} m c_n^{pw} g_{n,TE}^{m} \Psi_n (kr) \pi_n^{|m|} (\cos \theta) \exp(im\varphi) \quad (\text{III.46})$$

$$E_{\varphi,TE}^{i} = \frac{i E_{0}}{r} \sum_{n=1}^{\infty} \sum_{m=-n}^{+n} c_{n}^{pw} g_{n,TE}^{m} \Psi_{n} (kr) \tau_{n}^{|m|} (\cos \theta) \exp(im\varphi) \quad (\text{III.47})$$

$$H_{r,TE}^{i} = k H_{0} \sum_{n=1}^{\infty} \sum_{m=-n}^{+n} c_{n}^{pw} g_{n,TE}^{m} \left[ \Psi_{n}^{"}(kr) + \Psi_{n}(kr) \right] P_{n}^{|m|}(\cos \theta) \exp(im\varphi)$$
(III.48)

$$H_{\theta,TE}^{i} = \frac{H_{0}}{r} \sum_{n=1}^{\infty} \sum_{m=-n}^{+n} c_{n}^{pw} g_{n,TE}^{m} \Psi_{n}^{'}(kr) \tau_{n}^{|m|}(\cos \theta) \exp(im\varphi) \quad \text{(III.49)}$$

$$H_{\varphi,TE}^{i} = \frac{i H_{0}}{r} \sum_{n=1}^{\infty} \sum_{n=1}^{+n} m c_{n}^{pw} g_{n,TE}^{m} \Psi_{n}^{'}(kr) \pi_{n}^{|m|}(\cos \theta) \exp(im\varphi) \text{ (III.50)}$$

in which we have used Rel (I.108) and introduced generalized Legendre functions:

$$\tau_n^k(\cos\theta) = \frac{d}{d\theta} P_n^k(\cos\theta)$$
 (III.51)

$$\pi_n^k(\cos\theta) = \frac{P_n^k(\cos\theta)}{\sin\theta}$$
 (III.52)

Generalized Legendre functions  $\tau_n^1$  and  $\pi_n^1$  identify with usual Legendre functions of the LMT, namely  $\tau_n$  and  $\pi_n$  respectively. Mind however that, for Legendre polynomials, the correspondence between GLMT and LMT does not read as  $P_n^1 = P_n$  but as  $P_n^0 = P_n$ .

The use of Rel (I.108) implies that  $E_0$  and  $H_0$  must be defined in agreement with conditions of validity previously defined (see section I.2.7). For the sake of coherence with the LMT-expressions, it has been chosen to write  $E_0$  and  $H_0$  explicitly outside of the summations. Thus,  $E_0$  and  $H_0$  play the role of

reference amplitudes. What is therefore needed is that  $E_0$  and  $H_0$  must be defined at a particular location where Rel (I.108) holds and accordingly is considered as a reference location. In the case of plane waves, any location is a reference location. In the case of Gaussian beams (chapter IV), the reference location may be conveniently taken to be the waist center, in correspondence with the fact that a Gaussian beam is locally a plane wave in the waist region.

Similarly, for the scattered wave, the special field components are obtained from BSPs (III.35) and (III.36) with derivation rules (II.50)-(II.61):

$$E_{r,TM}^{s} = -kE_{0} \sum_{n=1}^{\infty} \sum_{m=-n}^{+n} c_{n}^{pw} A_{n}^{m} \left[ \xi_{n}^{"}(kr) + \xi_{n}(kr) \right] P_{n}^{|m|}(\cos \theta) exp(im\varphi)$$
(III.53)

$$E_{\theta,TM}^{s} = -\frac{E_0}{r} \sum_{n=1}^{\infty} \sum_{m=-n}^{+n} c_n^{pw} A_n^m \xi_n^{'}(kr) \tau_n^{|m|}(\cos \theta) \exp(im\varphi) \quad \text{(III.54)}$$

$$E_{\varphi,TM}^{s} = -\frac{i E_{0}}{r} \sum_{n=1}^{\infty} \sum_{m=-n}^{+n} m c_{n}^{pw} A_{n}^{m} \xi_{n}^{'}(kr) \pi_{n}^{|m|}(\cos \theta) \exp(im\varphi)$$
(III.55)

$$H_{r,TM}^s = 0 (III.56)$$

$$H_{\theta,TM}^{s} = \frac{H_0}{r} \sum_{n=1}^{\infty} \sum_{m=-n}^{+n} m c_n^{pw} A_n^m \xi_n(kr) \pi_n^{|m|}(\cos \theta) \exp(im\varphi) \text{ (III.57)}$$

$$H_{\varphi,TM}^s = \frac{iH_0}{r} \sum_{n=1}^{\infty} \sum_{m=-\infty}^{+n} c_n^{pw} A_n^m \xi_n(kr) \tau_n^{|m|}(\cos\theta) \exp(im\varphi) \quad (\text{III.58})$$

$$E_{r,TE}^s = 0 (III.59)$$

$$E_{\theta,TE}^{s} = \frac{-E_0}{r} \sum_{n=1}^{\infty} \sum_{m=-n}^{+n} m c_n^{pw} B_n^m \xi_n(kr) \pi_n^{|m|}(\cos \theta) \exp(im\varphi)$$
(III.60)

$$E_{\varphi,TE}^{s} = -\frac{iE_{0}}{r} \sum_{n=1}^{\infty} \sum_{m=-n}^{+n} c_{n}^{pw} B_{n}^{m} \xi_{n}(kr) \tau_{n}^{|m|}(\cos\theta) \exp(im\varphi) \quad \text{(III.61)}$$

$$H_{r,TE}^{s} = -kH_{0} \sum_{n=1}^{\infty} \sum_{m=-n}^{+n} c_{n}^{pw} B_{n}^{m} \left[ \xi_{n}^{"}(kr) + \xi_{n}(kr) \right] P_{n}^{|m|}(\cos\theta) exp(im\varphi)$$
(III.62)

$$H_{\theta,TE}^{s} = -\frac{H_{0}}{r} \sum_{n=1}^{\infty} \sum_{m=-n}^{+n} c_{n}^{pw} B_{n}^{m} \xi_{n}^{'}(kr) \tau_{n}^{|m|}(\cos \theta) \exp(im\varphi) \quad \text{(III.63)}$$

$$H_{\varphi,TE}^{s} = -\frac{i H_{0}}{r} \sum_{n=1}^{\infty} \sum_{m=-n}^{+n} m c_{n}^{pw} B_{n}^{m} \xi_{n}^{'}(kr) \pi_{n}^{|m|}(\cos \theta) \exp(im\varphi)$$
(III.64)

Finally, from (III.37), (III.38), the field components for the sphere wave are found to read as:

$$E_{r,TM}^{sp} = kE_0 \sum_{n=1}^{\infty} \sum_{m=-n}^{+n} c_n^{pw} C_n^m \left[ \Psi_n^{"}(k_{sp}r) + \Psi_n(k_{sp}r) \right] P_n^{|m|}(\cos\theta) exp(im\varphi)$$
(III.65)

$$E_{\theta,TM}^{sp} = \frac{E_0}{r} \frac{k}{k_{sp}} \sum_{n=1}^{\infty} \sum_{m=-n}^{+n} c_n^{pw} C_n^m \Psi_n'(k_{sp}r) \tau_n^{|m|}(\cos \theta) \exp(im\varphi)$$
(III.66)

$$E_{\varphi,TM}^{sp} = \frac{i E_0}{r} \frac{k}{k_{sp}} \sum_{n=1}^{\infty} \sum_{m=-n}^{+n} m c_n^{pw} C_n^m \Psi_n'(k_{sp}r) \pi_n^{|m|}(\cos \theta) \exp(im\varphi)$$
(III.67)

$$H_{r,TM}^{sp} = 0 (III.68)$$

$$H_{\theta,TM}^{sp} = \frac{-H_0}{r} \frac{\mu}{\mu_{sp}} \sum_{n=1}^{\infty} \sum_{m=-n}^{+n} m c_n^{pw} C_n^m \Psi_n(k_{sp}r) \pi_n^{|m|}(\cos \theta) \exp(im\varphi)$$
(III.69)

$$H_{\varphi,TM}^{sp} = -\frac{iH_0}{r} \frac{\mu}{\mu_{sp}} \sum_{n=1}^{\infty} \sum_{m=-n}^{+n} c_n^{pw} C_n^m \Psi_n(k_{sp}r) \tau_n^{|m|}(\cos \theta) \exp(im\varphi)$$
(III.70)

$$E_{r,TE}^{sp} = 0 (III.71)$$

$$E_{\theta,TE}^{sp} = \frac{E_0}{r} \frac{\mu_{sp}}{\mu} \frac{k^2}{k_{sp}^2} \sum_{n=1}^{\infty} \sum_{m=-n}^{+n} m c_n^{pw} D_n^m \Psi_n(k_{sp}r) \pi_n^{|m|}(\cos \theta) \exp(im\varphi)$$
(III.72)

$$E_{\varphi,TE}^{sp} = \frac{iE_0}{r} \frac{\mu_{sp}}{\mu} \frac{k^2}{k_{sp}^2} \sum_{n=1}^{\infty} \sum_{m=-n}^{+n} c_n^{pw} D_n^m \Psi_n(k_{sp}r) \tau_n^{|m|}(\cos\theta) \exp(im\varphi)$$
(III.73)

$$H_{r,TE}^{sp} = kH_0 \sum_{n=1}^{\infty} \sum_{m=-n}^{+n} c_n^{pw} D_n^m \left[ \Psi_n^{"}(k_{sp}r) + \Psi_n(k_{sp}r) \right] P_n^{|m|}(\cos\theta) exp(im\varphi)$$
(III.74)

$$H_{\theta,TE}^{sp} = \frac{H_0}{r} \frac{k}{k_{sp}} \sum_{n=1}^{\infty} \sum_{m=-n}^{+n} c_n^{pw} D_n^m \Psi_n'(k_{sp}r) \tau_n^{|m|}(\cos \theta) \exp(im\varphi)$$
(III.75)

$$H_{\varphi,TE}^{sp} = \frac{i H_0}{r} \frac{k}{k_{sp}} \sum_{n=1}^{\infty} \sum_{m=-n}^{+n} m c_n^{pw} D_n^m \Psi_n'(k_{sp}r) \pi_n^{|m|}(\cos \theta) \exp(im\varphi)$$
(III.76)

in which we have again used (I.108), and also (I.103).

The set (III.65)—(III.76) could also be rewritten by introducing the relative complex refractive index M of the sphere material relatively to the surrounding medium, as given by (I.103). In the whole set giving special field components, the "prime" and "double prime" indicate the first and second derivatives with respect to the argument respectively. It is furthermore recalled that field components are obtained by adding the corresponding special TM- and TE-field components.

## III.6 Boundary Conditions and Generalized Scattering Coefficients

Coefficients  $A_n^m$ ,  $B_n^m$ ,  $C_n^m$  and  $D_n^m$  are called generalized scattering coefficients. They are determined from the boundary conditions at the surface of the sphere (r=d/2) which state that electric and magnetic fields are tangentially continuous on this surface (section I.2.4). It is actually an exercise to check that the same results are obtained if these conditions are applied either to  $\theta$ - or to  $\varphi$ -field components. Indeed, working with  $\theta$ -fields (for example), it is found that the boundary conditions fully determine all the generalized scattering coefficients. Therefore, the conditions for  $\varphi$ -fields cannot contain any more information and must identify with the conditions for the  $\theta$ -fields. We then write:

$$V_{\theta,X}^i + V_{\theta,X}^s = V_{\theta,X}^{sp} \tag{III.77}$$

in which V stands for E or H, and X for TM or TE, providing four conditions for four sets of coefficients. Picking up formulae from section (III.5) specified for r = d/2, the boundary conditions reduce to:

$$M[g_{n,TM}^{m}\Psi_{n}^{'}(\alpha) - A_{n}^{m}\xi_{n}^{'}(\alpha)] = C_{n}^{m}\Psi_{n}^{'}(\beta)$$
 (III.78)

$$M^{2}[g_{n,TE}^{m}\Psi_{n}(\alpha) - B_{n}^{m}\xi_{n}(\alpha)] = \frac{\mu_{sp}}{\mu}D_{n}^{m}\Psi_{n}(\beta)$$
 (III.79)

$$[g_{n,TM}^m \Psi_n(\alpha) - A_n^m \xi_n(\alpha)] = \frac{\mu}{\mu_{sp}} C_n^m \Psi_n(\beta)$$
 (III.80)

$$M[g_{n,TE}^{m}\Psi_{n}^{'}(\alpha) - B_{n}^{m}\xi_{n}^{'}(\alpha)] = D_{n}^{m}\Psi_{n}^{'}(\beta)$$
 (III.81)

in which we introduced the size parameter  $\alpha$  and the optical size parameter  $\beta$  given by:

$$\alpha = \frac{\pi d}{\lambda} \tag{III.82}$$

$$\beta = M\alpha \tag{III.83}$$

in which  $\lambda$  is the wavelength in the surrounding medium. Solving the set (III.78)-(III.81) leads to:

$$A_n^m = a_n \ g_{n,TM}^m \tag{III.84}$$

$$B_n^m = b_n \ g_{n.TE}^m \tag{III.85}$$

$$C_n^m = c_n \ g_{n,TM}^m \tag{III.86}$$

$$D_n^m = d_n \ g_{n,TE}^m \tag{III.87}$$

in which:

$$a_n = \frac{\mu_{sp}\Psi_n(\alpha)\Psi'_n(\beta) - \mu M\Psi'_n(\alpha)\Psi_n(\beta)}{\mu_{sp}\xi_n(\alpha)\Psi'_n(\beta) - \mu M\xi'_n(\alpha)\Psi_n(\beta)}$$
(III.88)

$$b_n = \frac{\mu M \Psi_n(\alpha) \Psi'_n(\beta) - \mu_{sp} \Psi'_n(\alpha) \Psi_n(\beta)}{\mu M \xi_n(\alpha) \Psi'_n(\beta) - \mu_{sp} \xi'_n(\alpha) \Psi_n(\beta)}$$
(III.89)

$$c_{n} = \frac{M\mu_{sp}[\xi_{n}(\alpha)\Psi_{n}^{'}(\alpha) - \xi_{n}^{'}(\alpha)\Psi_{n}(\alpha)]}{\mu_{sp}\xi_{n}(\alpha)\Psi_{n}^{'}(\beta) - \mu M\xi_{n}^{'}(\alpha)\Psi_{n}(\beta)}$$
(III.90)

$$d_{n} = \frac{\mu M^{2} [\xi_{n} (\alpha) \Psi'_{n}(\alpha) - \xi'_{n}(\alpha) \Psi_{n}(\alpha)]}{\mu M \xi_{n}(\alpha) \Psi'_{n}(\beta) - \mu_{sn} \xi'_{n}(\alpha) \Psi_{n}(\beta)}$$
(III.91)

The coefficients  $a_n$ ,  $b_n$ ,  $c_n$ ,  $d_n$  are the classical scattering coefficients of the LMT. Therefore, the generalized scattering coefficients are the products of LMT-scattering coefficients by BSCs. Furthermore, the bracketed term in III.90 and III.91 can be shown to be equal to +i, by using a Wronskian relation.

If the particle is non-magnetic, then  $\mu_{sp} = \mu$  and Rels (III.88)-(III.91) simplify. This is an usual assumption indeed in light scattering theory but it has been relaxed for the sake of more generality. Also, at the time when the GLMT was built, people dealing with optical particle sizing were usually not interested in the sphere wave, with coefficients  $C_n^m$  and  $D_n^m$ . This is the

reason why we did not gave them in our articles. A counter-example however concerns the study of explosive interactions between laser beams and droplets [159] [160]. Nowadays, as we shall see in Chapter VIII, internal fields became important for many reasons.

## III.7 Scattered Field Components

Summing scattered TM- and TE-waves (Rels (III.53)-(III.64) supplemented with Rels (III.84)-(III.85)), the whole set of scattered field components is given by (omitting the superscript s):

$$E_r = -kE_0 \sum_{n=1}^{\infty} \sum_{m=-n}^{+n} c_n^{pw} a_n g_{n,TM}^m [\xi_n^"(kr) + \xi_n(kr)]$$

$$P_n^{|m|}(\cos\theta) \exp(im\varphi)$$
(III.92)

$$E_{\theta} = \frac{-E_0}{r} \sum_{n=1}^{\infty} \sum_{m=-n}^{+n} c_n^{pw}$$
(III.93)

$$[a_{n} \ g_{n,TM}^{m} \ \xi_{n}^{'}(kr) \ \tau_{n}^{|m|}(\cos\theta) + mb_{n} \ g_{n,TE}^{m} \ \xi_{n}(kr) \ \pi_{n}^{|m|}(\cos\theta)] \ exp(im\varphi)$$

$$E_{\varphi} = -\frac{iE_0}{r} \sum_{n=1}^{\infty} \sum_{m=-n}^{+n} c_n^{pw}$$
 (III.94)

$$[ma_n \ g_{n,TM}^{m} \ \xi_n^{'}(kr) \ \pi_n^{|m|}(\cos\theta) + b_n \ g_{n,TE}^{m} \ \xi_n(kr) \ \tau_n^{|m|}(\cos\theta)] \ exp(im\varphi)$$

$$H_{r} = -kH_{0} \sum_{n=1}^{\infty} \sum_{m=-n}^{+n} c_{n}^{pw} b_{n} g_{n,TE}^{m} [\xi_{n}^{"}(kr) + \xi_{n}(kr)] P_{n}^{|m|}(\cos \theta) \exp(im\varphi)$$
(III.95)

$$H_{\theta} = \frac{H_0}{r} \sum_{n=1}^{\infty} \sum_{m=-n}^{+n} c_n^{pw}$$
(III.96)

$$[ma_n \ g_{n,TM}^m \ \xi_n(kr) \ \pi_n^{|m|}(\cos\theta) - b_n \ g_{n,TE}^m \ \xi_n^{'} \ (kr) \ \tau_n^{|m|}(\cos\theta)] \ exp(im\varphi)$$

$$H_{\varphi} = \frac{iH_{0}}{r} \sum_{n=1}^{\infty} \sum_{m=-n}^{+n} c_{n}^{pw}$$

$$[a_{n} \ g_{n\,TM}^{m} \ \xi_{n}(kr) \ \tau_{n}^{|m|}(\cos\theta) - mb_{n} \ g_{n\,TE}^{m} \ \xi_{n}^{'} \ (kr) \ \pi_{n}^{|m|}(\cos\theta)] \ exp(im\varphi)$$

# III.8 Scattered Field Components in the Far Field Region

It is fairly exceptional that people are interested in the expressions (III.92)-(III.97) for arbitrary values of r. A counter-example is however provided by Slimani et~al [I61] who discussed Gabor microholography, in the case of pure LMT. In most cases, only the so-called far field case is classically considered, i.e. when  $r \gg \lambda$ . Whether the condition  $r \gg \lambda$  is sufficient or whether it should be  $r \gg \lambda$  or  $r \gg \infty$   $\lambda$  is not a trivial matter. Slimani et~al [I61] show that the fields relax rather fastly to produce transverse waves (see later) but that, even when waves are transverse, they need propagate much more to reach an asymptotic far field behaviour. In forward direction, it has been found that the far field condition is rather severe, namely  $r > 20~000~\lambda$ . A systematic study of the actual condition for arbitrary  $\theta$ 's and  $\varphi$ 's would be welcome.

Mathematically, when  $r \gg \lambda$ , there exists an asymptotic expression for functions  $\xi_n$ 's (see for instance Kerker 23):

$$\xi_n(kr) \to i^{n+1} \exp(-ikr)$$
 (III.98)

Then, in this limit:

$$\xi_n^{"}(kr) + \xi_n(kr) = 0 \tag{III.99}$$

and (III.92), (III.95) become:

$$E_r = H_r = 0 (III.100)$$

Non-zero field components are also readily found to be:

$$E_{\theta} = \frac{iE_0}{kr} \exp(-ikr) \sum_{n=1}^{\infty} \sum_{m=-n}^{n} \frac{2n+1}{n(n+1)} \left[ a_n g_{n,TM}^m \tau_n^{|m|} (\cos \theta) + imb_n g_{n,TE}^m \tau_n^{|m|} (\cos \theta) \right] \exp(im\varphi)$$
(III.101)

$$E_{\varphi} = \frac{-E_0}{kr} \exp(-ikr) \sum_{n=1}^{\infty} \sum_{m=-n}^{n} \frac{2n+1}{n(n+1)} \left[ ma_n g_{n,TM}^m \pi_n^{|m|} (\cos \theta) + ib_n g_{n,TE}^m \tau_n^{|m|} (\cos \theta) \right] \exp(im\varphi)$$
(III.102)

$$H_{\varphi} = \frac{H_0}{E_0} E_{\theta} \tag{III.103}$$

$$H_{\theta} = -\frac{H_0}{E_0} E_{\varphi} \tag{III.104}$$

As expected, the scattered wave has become a transverse wave  $\blacksquare$ . This fact is also a posteriori justification of the choice of functions  $\xi_n$ 's for BSPs,  $U^s_{TM}$  and  $U^s_{TE}$  (III.35), (III.36).

From now on, unless specified, we only deal with far field expressions.

#### III.9 Scattered Intensities

According to Poynting theorem (section I.2.5), the scattered intensity is the real part of the Poynting vector associated with the scattered wave. Specifying Rel (I.83) for the transverse wave of the far field, the unique non zero component is:

$$S = \frac{1}{2} R_e [E_{\theta} H_{\varphi}^* - E_{\varphi} H_{\theta}^*]$$
 (III.105)

Furthermore, from now on, we introduce a normalizing condition:

$$\frac{E_0 H_0^*}{2} = \frac{1}{2} \sqrt{\frac{\epsilon}{\mu}} |E_0|^2 = 1$$
 (III.106)

for which the reader could refer to (I.107) with the proviso that the medium is non absorbing.

With such a condition, the scattered intensity S becomes a dimensionless scattered intensity  $S^+$ . In the plane wave case, the normalizing condition means that incident intensity is unity. For Gaussian beams (next sections), it means that the incident intensity is unity at the waist center of the laser beam.

Scattered field components (III.101)-(III.104) are then introduced in Rel (III.105) with condition (III.106). Scattered intensity  $S^+$  then naturally splits into the sum of two contributions  $I_{\theta}^+$  and  $I_{\varphi}^+$ , associated with  $\theta$ - and  $\varphi$ -field components respectively, reading as:

$$\begin{vmatrix} I_{\theta}^{+} \\ I_{\varphi}^{+} \end{vmatrix} = \frac{\lambda^{2}}{4\pi^{2}r^{2}} \begin{vmatrix} |\mathcal{S}_{2}|^{2} \\ |\mathcal{S}_{1}|^{2} \end{vmatrix}$$
(III.107)

Asymptotic expressions of the  $\xi_n$ 's are useful to simplify computations but they are not compulsory to establish that the wave tends to a transverse wave at infinity. Actually, components  $E_r$  and  $H_r$  behave like  $(\xi_n'' + \xi_n)$  and it can be deduced from spherical Bessel equation (II.82) that  $\xi_n''(x) + \xi_n(x) = \frac{n(n+1)}{x^2} \xi_n(x)$ . Hence  $E_r$  and  $H_r$  decrease like  $(r)^{-2}$  whereas  $E_\theta$ ,  $E_\varphi$ ,  $H_\theta$ ,  $H_\varphi$  decrease like  $(r)^{-1}$ . Accordingly the wave becomes transverse.

in which  $S_1$  and  $S_2$  are generalized amplitude functions defined by:

$$E_{\theta} = \frac{iE_0}{kr} exp(-ikr) \mathcal{S}_2 \tag{III.108}$$

$$E_{\varphi} = -\frac{E_0}{kr} exp(-ikr) \,\mathcal{S}_1 \tag{III.109}$$

leading to:

$$S_1 = \sum_{n=1}^{\infty} \sum_{m=-n}^{n} \frac{2n+1}{n(n+1)} \left[ ma_n g_{n,TM}^m \pi_n^{|m|} (\cos \theta) + ib_n g_{n,TE}^m \tau_n^{|m|} (\cos \theta) \right] \exp(im\varphi)$$
(III.110)

$$S_2 = \sum_{n=1}^{\infty} \sum_{m=-n}^{n} \frac{2n+1}{n(n+1)} \left[ a_n g_{n,TM}^m \tau_n^{|m|} (\cos \theta) + imb_n g_{n,TE}^m \pi_n^{|m|} (\cos \theta) \right] \exp(im\varphi)$$
(III.111)

### III.10 Phase Angle

Even when the incident beam is perfectly linearly polarized, the scattered light is in general elliptically polarized. The state of polarization is characterized by a phase angle  $\delta$  between components  $E_{\theta}$  and  $E_{\omega}$ .

Phase angle  $\delta$  between  $E_{\theta}$  and  $E_{\varphi}$  is the same as the one between  $\mathcal{E}_{\theta}$  and  $\mathcal{E}_{\varphi}$  given by (see Rels (III.108), (III.109)):

$$\mathcal{E}_{\theta} = i\mathcal{S}_2 = A_{\theta}e^{i\varphi_2} \tag{III.112}$$

$$\mathcal{E}_{\varphi} = -\mathcal{S}_1 = A_{\varphi} e^{i\varphi_1} \tag{III.113}$$

in which we defined real amplitudes  $A_{\theta}$  and  $A_{\varphi}$ , and phase angles  $\varphi_2$  and  $\varphi_1$  of the waves  $\mathcal{E}_{\theta}$  and  $\mathcal{E}_{\varphi}$ .

It is then an exercise to establish:

$$tan\delta = tan(\varphi_2 - \varphi_1) = \frac{Re(\mathcal{S}_1)Re(\mathcal{S}_2) + Im(\mathcal{S}_1)Im(\mathcal{S}_2)}{Im(\mathcal{S}_1)Re(\mathcal{S}_2) - Re(\mathcal{S}_1)Im(\mathcal{S}_2)}$$
(III.114)

Later on, it will be convenient to present another formulation of GLMT to examine some special cases in chapter VI, sections VI.1 and VI.2. This will provide an opportunity to add some extra discussion on Rel (III.114).

## III.11 Radiative Energy Balance and Associated Cross-Sections

#### III.11.1 Generalities

A radiative energy balance may be carried out in a sphere of radius r and center  $O_P$  surrounding the scatter center. For the sake of clarity, some subscripts, previously omitted for convenience, have to be reintroduced.

The radiative balance relies on total fields equal to incident fields plus scattered fields. Therefore, the different terms of the radiative balance equation will involve:

- (i) incident field components which will be written in expanded forms by summing TM- and TE-contributions (Rels (III.39)-(III.50)).
- (ii) scattered field components: taking  $r \gg \lambda$ , these components may be written by using their far-field expressions (section III.8).
- (iii) total field components (superscript t) arising from summing incident and scattered components at a point of the surface of the sphere:

$$\left\{ \begin{array}{ll}
 E_j^t = E_j^i + E_j^s \\
 H_j^t = H_j^i + H_j^s
 \end{array} \right\} 
 (III.115)$$

The dimensionless radial component  $S_r^+$  of the total Poynting vector is perpendicular to the surface of the sphere and gives the energy flux per unit area and unit of time as:

$$S_r^+ = \frac{1}{2} Re(E_\theta^t H_\varphi^{t*} - E_\varphi^t H_\theta^{t*})$$
 (III.116)

Integrating  $S_r^+$  on the surface of the sphere provides a measure of the amount of energy which is lost inside the sphere, i.e. which is absorbed by the scatter center. This measure is given by the absorption cross-section  $C_{sca}$  (homogeneous to an area) defined by:

$$-C_{abs} = + \int_{(S)} S_r^+ dS \tag{III.117}$$

From (III.115) and (III.116), the right-hand-side of (III.117) is found to be formed of three contributions, each one corresponding to a partial balance:

$$-C_{abs} = \mathcal{J}^i + \mathcal{J}^s + \mathcal{J}^{is} \tag{III.118}$$

in which:

$$\mathcal{J}^{i} = \int_{0}^{\pi} \int_{0}^{2\pi} \frac{1}{2} Re(E_{\theta}^{i} H_{\varphi}^{i*} - E_{\varphi}^{i} H_{\theta}^{i*}) r^{2} \sin \theta \ d\theta \ d\varphi \tag{III.119}$$

$$\mathcal{J}^{s} = \int_{0}^{\pi} \int_{0}^{2\pi} \frac{1}{2} Re(E_{\theta}^{s} H_{\varphi}^{s*} - E_{\varphi}^{s} H_{\theta}^{s*}) \ r^{2} \sin \theta \ d\theta \ d\varphi \tag{III.120}$$

$$\mathcal{J}^{is} = \int_0^{\pi} \int_0^{2\pi} \frac{1}{2} Re(E_{\theta}^i H_{\varphi}^{s*} + E_{\theta}^s H_{\varphi}^{i*} - E_{\varphi}^i H_{\theta}^{s*} - E_{\varphi}^s H_{\theta}^{i*}) r^2 \sin\theta \ d\theta \ d\varphi \tag{III.121}$$

The first integral  $\mathcal{J}^i$  represents an energy balance over the non-perturbed incident wave. Having assumed that the medium surrounding the particle is non-absorbing, there is no loss of energy associated with the incident wave only. Physically, we consequently must have:

$$\mathcal{J}^i = 0 \tag{III.122}$$

as will be mathematically checked in next subsection.

The second integral  $\mathcal{J}^s$  represents an energy balance over the scattered wave only. Since there is no scattered energy flowing inward the sphere,  $\mathcal{J}^s$  measures the amount of scattered energy flowing outward. By definition, this amount is the scattering cross-section  $C_{sca}$ :

$$\mathcal{J}^s = C_{sca} \tag{III.123}$$

From (III.118), (III.122) and (III.123), it follows that:

$$\mathcal{J}^{is} = -C_{abs} - C_{sca} = -C_{ext} \tag{III.124}$$

defining the extinction cross-section  $C_{ext}$ , i.e. the amount of energy lost by the incident wave by absorption plus scattering.

#### III.11.2 Incident Field Balance

This subsection mathematically checks that the physical condition (III.122) is satisfied.

Summing TM- and TE-fields in Rels (III.39)–(III.50), the  $\theta$ - and  $\varphi$ -components of the incident wave are found to be:

$$E_{\theta}^{i} = \frac{E_{0}}{r} \sum_{n=1}^{\infty} \sum_{m=-n}^{+n} c_{n}^{pw} [g_{n,TM}^{m} \Psi_{n}^{'} \tau_{n}^{|m|} + m g_{n,TE}^{m} \Psi_{n} \pi_{n}^{|m|}] \exp(im\varphi) \quad (\text{III}.125)$$

$$E_{\varphi}^{i} = \frac{E_{0}}{r} \sum_{n=1}^{\infty} \sum_{m=-n}^{+n} c_{n}^{pw} [img_{n,TM}^{m} \Psi_{n}^{'} \pi_{n}^{|m|} + ig_{n,TE}^{m} \Psi_{n} \tau_{n}^{|m|}] \exp(im\varphi) \quad (\text{III}.126)$$

$$H_{\theta}^{i} = \frac{H_{0}}{r} \sum_{n=1}^{\infty} \sum_{m=-n}^{+n} c_{n}^{pw} \left[ -m g_{n,TM}^{m} \Psi_{n} \ \pi_{n}^{|m|} + g_{n,TE}^{m} \Psi_{n}' \tau_{n}^{|m|} \right] \exp(im\varphi)$$
(III.127)

$$H_{\varphi}^{i} = \frac{H_{0}}{r} \sum_{n=1}^{\infty} \sum_{m=-n}^{+n} c_{n}^{pw} \left[-ig_{n,TM}^{m} \Psi_{n} \tau_{n}^{|m|} + img_{n,TE}^{m} \Psi_{n}' \pi_{n}^{|m|}\right] \exp(im\varphi)$$
(III.128)

in which the arguments (kr) and  $(\cos\theta)$  are omitted for convenience.

These relations are inserted in Rel (III.119) for  $\mathcal{J}^i$  and the integration over  $\varphi$  is readily performed using Rel (III.11) for the orthogonality of exponentials, leading to:

$$\mathcal{J}^{i} = 2\pi \operatorname{Re} \left\{ i \sum_{p=-\infty}^{+\infty} \sum_{n=|p|\neq 0}^{\infty} \sum_{m=|p|\neq 0}^{\infty} c_{n}^{pw} c_{m}^{pw*} \right.$$

$$\left[ I_{1} \left( g_{n,TM}^{p} g_{m,TM}^{p*} \Psi'_{n} \Psi_{m} - g_{n,TE}^{p} g_{m,TE}^{p*} \Psi'_{m} \Psi_{n} \right) \right.$$

$$\left. + p I_{2} \left( g_{n,TE}^{p} g_{m,TM}^{p*} \Psi_{n} \Psi_{n} - g_{n,TM}^{p} g_{m,TE}^{p*} \Psi'_{m} \Psi'_{n} \right) \right] \right\}$$

in which  $I_1$  and  $I_2$  are two integrals over  $\theta$  given by:

$$I_1 = \int_0^{\pi} (\tau_n^{|p|} \tau_m^{|p|} + p^2 \pi_n^{|p|} \pi_m^{|p|}) \sin \theta \ d\theta$$
 (III.130)

$$I_2 = \int_0^{\pi} (\pi_n^{|p|} \tau_m^{|p|} + \pi_m^{|p|} \tau_n^{|p|}) \sin \theta \ d\theta \tag{III.131}$$

These integrals are evaluated in Appendix A:

$$I_{1} = \frac{2n(n+1)}{2n+1} \frac{(n+|p|)!}{(n-|p|)!} \delta_{nm}$$
 (III.132)

$$I_2 = 0, p \neq 0 (III.133)$$

Consequently, (III.129) takes the form:

$$\mathcal{J}^{i} = Re \left( i \sum_{p=-\infty}^{+\infty} \sum_{n=|p|\neq 0}^{\infty} A_{np} |c_{n}^{pw}|^{2} [|g_{n,TM}^{p}|^{2} - |g_{n,TE}^{p}|^{2}] \Psi_{n} \Psi_{n}^{'} \right)$$
(III.134)

in which  $A_{np}$  are real numbers. It follows that  $\mathcal{J}^i$  is zero as expected.

# III.11.3 Scattering Cross-Section $C_{sca}$

The scattering cross-section  $C_{sca}$  may be evaluated from its definition ((III.123), (III.120)). Alternatively, comparing (III.120) and (III.105), it may also be written as:

$$C_{sca} = \int_0^{\pi} \int_0^{2\pi} (I_{\theta}^+ + I_{\varphi}^+) r^2 \sin \theta \ d\theta d\varphi$$
 (III.135)

which emphasizes more clearly the meaning of  $C_{sca}$  besides being more efficient for computations.

Scattered intensities  $I_{\theta}^{+}$  and  $I_{\varphi}^{+}$  are given by (III.107) supplemented with (III.110) and (III.111). Integration over  $\varphi$  is readily carried out by using again the orthogonality relation (III.111), leading to:

$$C_{sca} = \frac{\lambda^2}{2\pi} \sum_{p=-\infty}^{\infty} \sum_{n=|p|\neq 0}^{\infty} \sum_{m=|p|\neq 0}^{\infty} \frac{2n+1}{n(n+1)} \frac{2m+1}{m(m+1)}$$
(III.136)
$$\left[ I_1 \left( a_n a_m^* g_{n,TM}^p g_{m,TM}^{p*} + b_n b_m^* g_{n,TE}^p g_{m,TE}^{p*} \right) + ip I_2 \left( b_n a_m^* g_{n,TE}^p g_{m,TM}^{p*} - a_n b_m^* g_{n,TM}^p g_{m,TE}^{p*} \right) \right]$$

in which integrals over  $\theta$  are again  $I_1$  and  $I_2$  ((III.130) and (III.131)).

Using (III.132) and (III.133) for these integrals, and taking advantage of a permutation over subscripts p and m, the expression for  $C_{sca}$  becomes:

$$C_{sca} = \frac{\lambda^2}{\pi} \sum_{n=1}^{\infty} \sum_{m=-n}^{+n} \frac{2n+1}{n(n+1)} \frac{(n+|m|)!}{(n-|m|)!}$$

$$\{|a_n|^2 |g_{n,TM}^m|^2 + |b_n|^2 |g_{n,TE}^m|^2\}$$
(III.137)

# III.11.4 Extinction Cross-Section $C_{ext}$

From Rels (III.121) and (III.124), the extinction cross-section may be evaluated from a double integral involving both incident and scattered field components:

$$C_{ext} = \int_0^{\pi} \int_0^{2\pi} \frac{1}{2} Re(E_{\varphi}^i H_{\theta}^{s*} + E_{\varphi}^s H_{\theta}^{i*} - E_{\theta}^i H_{\varphi}^{s*} - E_{\theta}^s H_{\varphi}^{i*}) r^2 \sin\theta \ d\theta d\varphi$$
(III.138)

Incident field components are given by Rels (III.125)–(III.128) and scattered field components are given in the far-field in section III.8. Using non far-field expressions would obviously lead to the same results but with much computational penalty. The integration over  $\varphi$  is again easily performed by using (III.11), leading to:

$$C_{ext} = 2\pi \operatorname{Re} \left[ \sum_{p=-\infty}^{+\infty} \sum_{n=|p|\neq 0}^{+\infty} \sum_{m=|p|\neq 0}^{+\infty} c_n^{pw} c_m^{pw*} \right]$$

$$\left\{ I_1 \left[ (-i)^m \exp(ikr) \left( a_n^* g_{n,TM}^p g_{m,TM}^{p*} \Psi_n' - i b_n^* g_{n,TE}^p g_{m,TE}^{p*} \Psi_n \right) \right]$$

$$\left[ +i^n \exp(-ikr) \left( i a_n g_{n,TM}^p g_{m,TM}^{p*} \Psi_m + b_n g_{n,TE}^p g_{m,TE}^{p*} \Psi_m' \right) \right]$$

$$+pI_2 \left[ (-i)^m \exp(ikr) \left( a_m^* g_{n,TE}^p g_{m,TM}^{p*} \Psi_n - i b_m^* g_{n,TM}^p g_{m,TE}^{p*} \Psi_n' \right)$$

$$-i^n \exp(-ikr) \left( i a_n g_{n,TM}^p g_{m,TE}^{p*} \Psi_m' + b_n g_{n,TE}^p g_{m,TM}^{p*} \Psi_m \right) \right]$$

Integrals over  $\theta$  are again  $I_1$  and  $I_2$  given by (III.132), (III.133), leading to:

$$C_{ext} = \frac{4\pi}{k^2} \operatorname{Re} \left[ \sum_{n=1}^{\infty} \sum_{m=-n}^{+n} \frac{2n+1}{n(n+1)} \frac{(n+|m|)!}{(n-|m|)!} \right]$$

$$\{ (-i)^n exp(ikr) (a_n^* \Psi_n' |g_{n,TM}^m|^2 - ib_n^* \Psi_n |g_{n,TE}^m|^2)$$

$$+ i^n exp(-ikr) (ia_n \Psi_n |g_{n,TM}^m|^2 + b_n \Psi_n' |g_{n,TE}^m|^2) \}$$

$$\left[ (-i)^n exp(-ikr) (ia_n \Psi_n |g_{n,TM}^m|^2 + b_n \Psi_n' |g_{n,TE}^m|^2) \right]$$

This expression may be further simplified. Effectively, apart from the condition  $r \gg \lambda$  that we used to simplify the computations (although it is not compulsory), the radius r of the spherical surface is arbitrary. In the limit  $r \to \infty$ , we may take further advantage of asymptotic expressions for Ricatti-Bessel functions [162]:

$$\Psi_n(kr) \to \frac{1}{2} \left[ (-i)^{n+1} exp(ikr) + i^{n+1} \exp(-ikr) \right]$$
 (III.141)

leading to a final expression of  $C_{ext}$  which does not depend any more on r as it should:

$$C_{ext} = \frac{\lambda^2}{\pi} \operatorname{Re} \left[ \sum_{n=1}^{\infty} \sum_{m=-n}^{+n} \frac{2n+1}{n(n+1)} \frac{(n+|m|)!}{(n-|m|)!} (a_n |g_{n,TM}^m|^2 + b_n |g_{n,TE}^m|^2) \right]$$
(III.142)

In the case of plane waves, the extinction cross-section may also be obtained by relying on the so-called optical or extinction theorem [17]. However, applying this optical theorem to obtain the expression of  $C_{ext}$  in the case of shaped beams would lead to an erroneous result, just because the usual plane wave formulation of the optical theorem is not valid for shaped beams. The failure of the optical theorem for Gaussian-beam scattering by a spherical particle is discussed by Lock et al [163]. It is shown that the extinction cross section may be written as an infinite series in powers of the reciprocal of the beam width. The imaginary part of the forward scattering amplitude (the one associated with the plane wave optical theorem) is shown to be the first term in this series. Furthermore, two approximations to the extinction

cross section are presented for the special case of Gaussian-beam scattering, one which is accurate when the transverse width of the beam is larger than the target particle, and the other when the transverse width of the beam is smaller than the particle. A generalized optical theorem for on-axis Gaussian beams is furthermore available from Gouesbet et al [164]. We also recall that a similar issue has been recently investigated in a quantum mechanical framework [109]. Related to this issue, we also have the studies of Berg et al [165], [166] who studied, in the first part, the extinction caused by a single particle and presented a conceptual phase-based explanation for the optical theorem and, in the second part, dealt with the case of multiple particles.

Following Rel (III.124), the absorption cross-section can then be readily obtained as the substraction between  $C_{ext}$  (III.142) and  $C_{sca}$  (III.137).

### III.12 Momentum Balance and Radiation Pressure

#### III.12.1 Generalities

The approach used in this section to evaluate radiation pressure forces would be qualified as being heuristic by Bohren and Huffman ([22], p 120). A more rigorous approach would rely on the use of the energy-momentum tensor. Such an approach has been developed by Barton et al [137]. After a bit of algebra, it can be checked that both approaches lead to equivalent results, within irrelevant normation prefactors.

For a propagative, transverse wave, the reduced momentum  $P_i^+$  of the light is equal to the ratio of the reduced Poynting vector  $S_i^+$  over the speed c of the light (section I.2.6). This statement may be considered as the electromagnetic formulation of a quantum mechanical formulation associating momentum hv/c with energy hv of a photon (in which h is the Planck constant and v the frequency of the wave). Then, we have:

$$P_i^+ = S_i^+/c \tag{III.143}$$

When light is absorbed by the particle, a momentum transfer is therefore associated with energy transfer producing a radiation pressure force. The averaged reduced radiation pressure force  $F_i^+$  (i = x, y, z) exerted by the beam on the scatterer is given by the averaged net momentum removed from the incident beam (per unit of time), i.e. to the momentum given to the scatterer due to absorption minus the momentum lost by the scatterer due to reemitted (scattered) light. Rather than using force components, it is preferred to define the radiation pressure by a vector  $C_{pr,i}$  of radiation pressure cross-sections given by:

$$C_{pr,i} = cF_i^+ \tag{III.144}$$

It is an exercise to check that components  $C_{pr,i}$  are indeed physically homogeneous to areas. The total fields sum up incident and scattered components

(III.115). In the far field region, both incident and scattered fields are transverse waves  $\[ \]$ . Hence, the total field is a transverse wave and its Poynting vector is radial, along the direction of propagation of the wave. Then the momentum through any closed surface (S) only involves  $\int_{(S)} \frac{1}{2} Re \left[ E_j^t \wedge H_n^{t*} \right] e_{r,i} dS$  in which  $e_{r,i} = (\sin\theta\cos\varphi, \sin\theta\sin\varphi, \cos\theta)$  is the (local) radial unit vector. Expanding the total fields into incident plus scattered waves, (III.115) reveals three contributions to the momentum balance associated with incident fields, scattered fields and crossed terms. From its definition, the contribution of the incident (unperturbed) field is zero since it goes through any closed surface without leaving any momentum. We then have to discuss three components  $C_{pr,i}$  which are examined separately.

# III.12.2 Longitudinal Radiation Pressure $(z ext{-}Direction)$

Along the longitudinal direction  $(O_p z)$ , the radiation pressure cross-sectional component  $C_{pr,z}$  is then expressed by the relation:

$$C_{pr,z} = cF_z^+ = -\int_{(S)}^+ \frac{1}{2} Re[E_j^i \wedge H_n^{s*} + E_j^s \wedge H_n^{i*}]_r \, dS \cos \theta$$
$$-\int_{(S)}^+ \frac{1}{2} Re[E_j^s \wedge H_n^{s*}]_r \, dS \cos \theta \qquad (III.145)$$

in which the symbol + on the integral reminds us of using the normalizing condition (III.106). S is a large spherical surface surrounding the scatter center and dS its surface element.

The first term is the forward momentum removed from the beam and the second one is minus the forward momentum given by the scatterer to the scattered wave. We again choose for S a sphere of radius  $r \gg \lambda$  surrounding the scatter center. In this case, the two terms of the right-hand-side of (III.145) identify with Rels (III.121) and (III.120), with the only difference being that integrands are multiplied by (-  $\cos \theta$ ). There is no radiation pressure associated with the integral  $\mathcal{J}^i$  (III.119) since the unperturbed field does not leave any momentum to the scatterer. This relationship between (III.145) and  $\mathcal{J}^i$ ,  $\mathcal{J}^s$ ,  $\mathcal{J}^{is}$  indeed emphasizes the physical meaning of (III.145), associating the forward momentum removed from the beam with  $\mathcal{J}^{is}$ , i.e. with  $C_{ext}$ , and the forward momentum given to the wave with  $\mathcal{J}^s$ , i.e. with  $C_{sca}$ .

<sup>&</sup>lt;sup>2</sup> Scattered fields have been discussed in section III.8. Using component expressions (III.39)–(III.50) and the same argument as presented in footnote at the end of section III.8, it can be shown that incident fields too reduce to transverse waves.

(III.145) then becomes:

$$C_{pr,z} = \int_0^{\pi} \int_0^{2\pi} \frac{1}{2} Re(E_{\varphi}^i H_{\theta}^{s*} + E_{\varphi}^s H_{\theta}^{i*} - E_{\theta}^i H_{\varphi}^{s*})$$
(III.146)
$$-E_{\theta}^s H_{\varphi}^{i*}) r^2 \cos \theta \sin \theta \, d\theta d\varphi - \int_0^{\pi} \int_0^{2\pi} (I_{\theta}^+ + I_{\varphi}^+) r^2 \cos \theta \sin \theta \, d\theta d\varphi$$

in which the second integral has been rewritten using scattered intensities rather than scattered field components (similarly as for III.135).

With a short-hand notation, (III.146) may also be written as:

$$C_{pr,z} = \overline{\cos \theta} \ C_{ext} - \overline{\cos \theta} \ C_{sca} \tag{III.147}$$

in which  $\overline{\cos\theta}$  indicates integrations weighted by  $\cos\theta$ .

In one of our previous articles [76] devoted to Gaussian beams, the first term in the right-hand-side of (III.147) has been simply set equal to  $C_{ext}$ , leading to the approximate relation:

$$C_{pr,z} = C_{ext} - \overline{\cos \theta} \ C_{sca} \tag{III.148}$$

an expression given by van de Hulst [17] for the plane wave case.

This is certainly a good approximation when only a waist location of the particle is considered. It means that we assume that the wave-front on the scatterer is (nearly) a plane, permitting us to use the same formulation as van de Hulst. In the general case of arbitrary location of the particle in an arbitrary beam, this approximation is no longer valid.

We now evaluate successively the two terms of the right-hand-side of (III.147), starting with the second one:

$$\overline{\cos \theta} C_{sca} = \int_0^{\pi} \int_0^{2\pi} (I_{\theta}^+ + I_{\varphi}^+) r^2 \cos \theta \sin \theta \ d\theta d\varphi \tag{III.149}$$

Integration over  $\varphi$  again uses (III.11), and afterwards, in a similar manner as we have done for (III.136), we readily obtain:

$$\overline{\cos \theta} C_{sca} = \frac{\lambda^2}{2\pi} \sum_{p=-\infty}^{+\infty} \sum_{n=|p|\neq 0}^{+\infty} \sum_{m=|p|\neq 0}^{+\infty} \frac{2n+1}{n(n+1)} \frac{2m+1}{m(m+1)}$$

$$\left[ I_3(a_n a_m^* g_{n,TM}^p g_{m,TM}^{p*} + b_n b_m^* g_{n,TE}^p g_{m,TE}^{p*}) + ipI_4 \left( b_n a_m^* g_{n,TE}^p g_{m,TM}^{p*} - a_n b_m^* g_{n,TM}^p g_{m,TE}^{p*} \right) \right]$$

in which  $I_3$  and  $I_4$  are new integrals over  $\theta$  given by:

$$I_{3} = \int_{0}^{\pi} (\tau_{n}^{|p|} \tau_{m}^{|p|} + p^{2} \pi_{n}^{|p|} \pi_{m}^{|p|}) \cos \theta \sin \theta d\theta$$
 (III.151)

$$I_{4} = \int_{0}^{\pi} (\tau_{n}^{|p|} \ \pi_{m}^{|p|} + \tau_{m}^{|p|} \ \pi_{n}^{|p|}) \cos \theta \ \sin \theta d\theta \tag{III.152}$$

These integrals are evaluated in Appendix B:

$$I_{3} = \frac{2(n-1)(n+1)}{(2n-1)(2n+1)} \cdot \frac{(n+|p|)!}{(n-1-|p|)!} \quad \delta_{m,n-1}$$

$$+ \frac{2(m-1)(m+1)}{(2m-1)(2m+1)} \cdot \frac{(m+|p|)!}{(m-1-|p|)!} \quad \delta_{n,m-1}$$

$$I_{4} = \frac{2}{2n+1} \cdot \frac{(n+|p|)!}{(n-|p|)!} \quad \delta_{nm}$$
(III.154)

Inserting expressions (III.153), (III.154) for  $I_3$  and  $I_4$  in (III.150) leads to:

$$\overline{\cos \theta} C_{sca} = -\frac{2\lambda^2}{\pi} \sum_{n=1}^{\infty} \sum_{p=-n}^{+n} p \frac{2n+1}{n^2(n+1)^2} \frac{(n+|p|)!}{(n-|p|)!}$$
(III.155)
$$\operatorname{Re}(i \ a_n b_n^* \ g_{n,TM}^p \ g_{n,TE}^{p*}) - \frac{1}{(n+1)^2} \frac{(n+1+|p|)!}{(n-|p|)!}$$

$$\operatorname{Re}(a_n \ a_{n+1}^* \ g_{n,TM}^p \ g_{n+1,TM}^{p*} + b_n \ b_{n+1}^* \ g_{n,TE}^p \ g_{n+1,TE}^{p*})$$

We now consider the first term in the r.h.s. of (III.147):

$$\overline{\cos \theta} C_{ext} = \int_0^{\pi} \int_0^{2\pi} \frac{1}{2} \operatorname{Re}(E_{\varphi}^i H_{\theta}^{s*} + E_{\varphi}^s H_{\theta}^{i*} - E_{\theta}^i H_{\varphi}^{s*} - E_{\theta}^s H_{\varphi}^{i*})$$

$$r^2 \sin \theta \cos \theta \ d\theta \ d\varphi \tag{III.156}$$

Rel (III.156) is exactly the same as (III.138) except for the presence of  $\cos \theta$ . Following the same procedure as used in section III.11.4, we thus obtain the analogous one to Rel (III.139) where the  $\theta$ -integrals  $I_1$  and  $I_2$  are replaced by  $I_3$  and  $I_4$  respectively.

We then perform the  $\theta$ -integrations (III.151) and (III.152) and rearrange the subscripts to obtain:

$$\overline{\cos \theta} C_{ext} = 2\pi \sum_{p=-\infty}^{+\infty} \sum_{n=|p|\neq 0}^{\infty} \operatorname{Re} \left\{ \frac{2n(n+2)}{(2n+1)(2n+3)} \frac{(n+1+|p|)!}{(n-|p|)!} \right. (III.157)$$

$$c_n^{pw} c_{n+1}^{pw*} \{ (-i)^{n+1} \exp(ikr) [\Psi'_n - i\Psi_n] [a_{n+1}^* g_{n,TM}^p g_{n+1,TM}^{p*} + b_{n+1}^* g_{n,TE}^p g_{n+1,TE}^{p*}] + i^n \exp(-ikr) [\Psi'_{n+1} + i\Psi_{n+1}] [a_n g_{n,TM}^p g_{n+1,TM}^{p*} + b_n g_{n,TE}^p g_{n+1,TE}^{p*}] \}$$

$$+ \frac{2p}{2n+1} \frac{(n+|p|)!}{(n-|p|)!} |c_n^{pw}|^2 i^n \exp(-ikr) \left[ \Psi_n - i \Psi'_n \right]$$

$$(a_n g_{n,TM}^p g_{n,TE}^{p*} - b_n g_{n,TE}^p g_{n,TM}^{p*}) \right\}$$

Then, assuming a very large radius of the spherical surface used for integration, we can replace the Ricatti-Bessel functions by their asymptotic expression (III.141). Using also (III.3) and rearranging the summations, we obtain:

$$\overline{\cos \theta} C_{ext} = \frac{\lambda^2}{\pi} \sum_{n=1}^{\infty} \sum_{p=-n}^{+n} \left\{ \frac{1}{(n+1)^2} \frac{(n+1+|p|)!}{(n-|p|)!} \right\}$$

$$\operatorname{Re}[(a_n + a_{n+1}^*) g_{n,TM}^p g_{n+1,TM}^{p*} + (b_n + b_{n+1}^*) g_{n,TE}^p g_{n+1,TE}^{p*}]$$

$$-p \frac{2n+1}{n^2 (n+1)^2} \frac{(n+|p|)!}{(n-|p|)!} \operatorname{Re}[i(a_n + b_n^*) g_{n,TM}^p g_{n,TE}^{p*}]$$

Substracting (III.155) from (III.158) gives the final expression of the pressure cross-section  $C_{pr,z}$ :

$$C_{pr,z} = \frac{\lambda^2}{\pi} \sum_{n=1}^{\infty} \sum_{p=-n}^{+n} \left\{ \frac{1}{(n+1)^2} \frac{(n+1+|p|)!}{(n-|p|)!} \right\}$$

$$\operatorname{Re}[(a_n + a_{n+1}^* - 2a_n a_{n+1}^*) g_{n,TM}^p g_{n+1,TM}^{p*} + (b_n + b_{n+1}^* - 2b_n b_{n+1}^*) g_{n,TE}^p g_{n+1,TE}^{p*}]$$

$$+ p \frac{2n+1}{n^2(n+1)^2} \frac{(n+|p|)!}{(n-|p|)!} \operatorname{Re}[i(2a_n b_n^* - a_n - b_n^*) g_{n,TM}^p g_{n,TE}^{p*}]$$

# III.12.3 Transverse Radiation Pressure (x and y Directions)

Similar to the case of Rel (III.145), the tranverse radiation pressure cross-sectional components  $C_{pr,x}$  and  $C_{pr,y}$  are given by:

$$C_{pr,x} = cF_x^+ = -\int_{(S)}^+ \frac{1}{2} \operatorname{Re}[E_j^i \wedge H_n^{s*} + E_j^s \wedge H_n^{i*}]_r dS \sin \theta \cos \varphi$$
$$-\int_{(S)}^+ \frac{1}{2} \operatorname{Re}[E_j^s \wedge H_n^{s*}]_r dS \sin \theta \cos \varphi \qquad (III.160)$$

$$C_{pr,y} = cF_y^+ = -\int_{(S)}^+ \frac{1}{2} \operatorname{Re}[E_j^i \wedge H_n^{s*} + E_j^s \wedge H_n^{i*}]_r dS \sin \theta \sin \varphi$$
$$-\int_{(S)}^+ \frac{1}{2} \operatorname{Re}[E_j^s \wedge H_n^{s*}]_r dS \sin \theta \sin \varphi \qquad (III.161)$$

in which weighting factors are  $\sin\theta \cos\varphi$  and  $\sin\theta \sin\varphi$  respectively, instead of  $\cos\theta$ .

These relations may be rewritten, with the shorthand notation of Rel (III.147):

$$C_{pr,x} = \overline{\sin \theta} \cos \varphi \ C_{ext} - \overline{\sin \theta} \cos \varphi \ C_{sca}$$
 (III.162)

$$C_{pr,y} = \overline{\sin \theta} \ \overline{\sin \varphi} C_{ext} - \overline{\sin \theta} \ \overline{\sin \varphi} C_{sca}$$
 (III.163)

We now evaluate  $C_{pr,x}$ , starting again with the second term in the r.h.s. of (III.162). This term may be expressed by:

$$\overline{\sin\theta} \cos\varphi C_{sca} = \int_0^{\pi} \int_0^{2\pi} (I_{\theta}^+ + I_{\varphi}^+) r^2 \sin^2\theta \cos\varphi \ d\theta d\varphi \qquad (III.164)$$

After replacing  $I_{\theta}^{+}$  and  $I_{\varphi}^{+}$  by their expressions from (III.107), (III.110) and (III.1111), we perform the integration over  $\varphi$ . This integration requires the evaluation of a new integral which is:

$$\int_{0}^{2\pi} \cos \varphi \, \exp(ik\varphi) \, \exp(-ik'\varphi) \, d\varphi = \pi(\delta_{k',k+1} + \delta_{k,k'+1}) \qquad \text{(III.165)}$$

leading then to:

$$\overline{\sin \theta \cos \varphi} C_{sca} = \frac{\lambda^2}{4\pi} \sum_{p=-\infty}^{+\infty} \sum_{n=|p|\neq 0}^{+\infty} \sum_{m=|p+1|\neq 0}^{+\infty} \frac{2n+1}{n(n+1)} \frac{2m+1}{m(m+1)}$$

$$[I_5 \operatorname{Re}(U_{nm}^p) + I_6 \operatorname{Re}(V_{nm}^p)] \tag{III.166}$$

in which:

$$U_{nm}^{p} = a_{n} a_{m}^{*} g_{n,TM}^{p} g_{m,TM}^{p+1*} + b_{n} b_{m}^{*} g_{n,TE}^{p} g_{m,TE}^{p+1*}$$
(III.167)

$$V_{nm}^{p} = ib_{n}a_{m}^{*}g_{n,TE}^{p}g_{m,TM}^{p+1*} - ia_{n}b_{m}^{*}g_{n,TM}^{p}g_{m,TE}^{p+1*}$$
(III.168)

in which  $I_5$  and  $I_6$  are new integrals over  $\theta$ :

$$I_5 = \int_0^{\pi} (\tau_n^{|p|} \tau_m^{|p+1|} + p(p+1) \pi_n^{|p|} \pi_m^{|p+1|}) \sin^2 \theta \ d\theta$$
 (III.169)

$$I_6 = \int_0^{\pi} (p\pi_n^{|p|} \tau_m^{|p+1|} + (p+1) \pi_m^{|p+1|} \tau_n^{|p|}) \sin^2 \theta \ d\theta$$
 (III.170)

 $I_5$  and  $I_6$  are evaluated in Appendix C:

$$I_{5} = \begin{cases} \frac{2}{(2n+1)(2m+1)} \frac{(m+p+1)!}{(m-p-1)!} [(n-1)(n+1)\delta_{n,m+1} - (m-1)(m+1)\delta_{m,n+1}], p \geq 0\\ \frac{2}{(2n+1)(2m+1)} \frac{(n-p)!}{(n+p)!} [(m-1)(m+1)\delta_{m,n+1} - (n-1)(n+1)\delta_{n,m+1}], p < 0 \end{cases}$$
(III.171)

$$I_{6} = \begin{cases} \frac{2}{2n+1} \frac{(n+p+1)!}{(n-p-1)!} \delta_{nm}, & p \ge 0\\ \frac{-2}{2n+1} \frac{(n-p)!}{(n+p)!} \delta_{nm}, & p < 0 \end{cases}$$
(III.172)

Inserting (III.171) and (III.172) into (III.166), we first obtain:

$$\overline{\sin \theta} \cos \varphi C_{sca} = \frac{\lambda^2}{\pi} \left[ \sum_{p=0}^{\infty} \sum_{n=|p|\neq 0}^{\infty} \sum_{m=|p+1|\neq 0}^{\infty} \frac{(m+p+1)!}{(m-p-1)!} \right] (III.173)$$

$$\left\{ \operatorname{Re}(U_{nm}^p) \left[ \frac{1}{n^2} \delta_{n,m+1} - \frac{1}{m^2} \delta_{m,n+1} \right] \right.$$

$$+ \operatorname{Re}(V_{nm}^p) \frac{2n+1}{n^2(n+1)^2} \delta_{nm} \right\}$$

$$+ \sum_{p=-1}^{-\infty} \sum_{n=|p|\neq 0}^{\infty} \sum_{m=|p+1|\neq 0}^{\infty} \frac{(n-p)!}{(n+p)!}$$

$$\left\{ \operatorname{Re}(U_{nm}^p) \left[ \frac{1}{m^2} \delta_{m,n+1} - \frac{1}{n^2} \delta_{n,m+1} \right] \right.$$

$$- \operatorname{Re}(V_{nm}^p) \frac{2n+1}{n^2(n+1)^2} \delta_{nm} \right\}$$

in which the negative values of p are separated from the positive ones. Rearranging by playing with subscripts, (III.173) can be more concisely rewritten as follows:

$$\overline{\sin\theta}\cos\varphi C_{sca} = \frac{\lambda^2}{\pi} \sum_{p=1}^{\infty} \sum_{n=p}^{\infty} \sum_{m=p-1\neq 0}^{\infty} \frac{(n+p)!}{(n-p)!}$$

$$\{ [\operatorname{Re}(U_{mn}^{p-1} + U_{nm}^{-p})] [\frac{1}{m^2} \delta_{m,n+1} - \frac{1}{n^2} \delta_{n,m+1}]$$

$$+ \frac{2n+1}{n^2(n+1)^2} \delta_{nm} [\operatorname{Re}(V_{mn}^{p-1} - V_{nm}^{-p})] \}$$

in which summation over p now only involves  $p \geq 1$ .

The first term of the r.h.s. in (III.162) is (III.156) with  $\cos\theta$  replaced by  $\sin\theta \cos\varphi$ :

$$\overline{\sin\theta\cos\varphi}C_{ext} = \int_0^\pi \int_0^{2\pi} \frac{1}{2}\operatorname{Re}(E_\varphi^i H_\theta^{s*} + E_\varphi^s H_\theta^{i*} - E_\theta^i H_\varphi^{s*} - E_\theta^s H_\varphi^{i*})$$

$$r^2 \sin^2\theta \cos\varphi \, d\theta d\varphi \tag{III.175}$$

The  $\varphi$ -integration is carried out again using (III.165) and the  $\theta$ -integration with (III.169)-(III.170). The resulting expression can be rearranged as:

$$\overline{\sin\theta\cos\varphi}C_{ext} = \frac{\lambda^{2}}{4\pi}\operatorname{Re}\sum_{p=-\infty}^{+\infty}\sum_{n=|p|\neq 0}^{\infty}\sum_{m=|p+1|\neq 0}^{\infty}\frac{2n+1}{n(n+1)}\frac{2m+1}{m(m+1)} \qquad (III.176)$$

$$\left[I_{5}\left\{i^{n}\exp\left(-ikr\right)\left[\Psi'_{n}+i\Psi_{n}\right]\left[a_{m}g_{m,TM}^{p+1}g_{n,TM}^{p*}+b_{n}g_{m,TE}^{p+1}g_{n,TE}^{p*}\right]\right.$$

$$+i^{n}\exp\left(-ikr\right)\left[\Psi'_{m}+i\Psi_{m}\right]\left[a_{n}g_{n,TM}^{p}g_{m,TM}^{p+1*}+b_{n}g_{n,TE}^{p+1*}g_{m,TE}^{p+1*}\right]\right\}$$

$$+I_{6}\left\{i^{m-1}\exp\left(-ikr\right)\left[\Psi'_{m}+i\Psi_{m}\right]\left[a_{n}g_{n,TM}^{p}g_{m,TE}^{p+1*}-b_{n}g_{n,TE}^{p}g_{m,TM}^{p+1*}\right]\right.$$

$$+i^{n-1}\exp\left(-ikr\right)\left[\Psi'_{n}+i\Psi_{n}\right]\left[a_{m}g_{m,TM}^{p+1}g_{n,TE}^{p*}-b_{m}g_{m,TE}^{p+1*}g_{n,TM}^{p*}\right]\right\}$$

Again, we replace the Ricatti-Bessel functions by their asymptotic expression (III.141), assuming a very large radius of the spherical surface on which integration is carried out. We also introduce the following notations:

$$S_{nm}^{p} = (a_n + a_m^*) g_{n,TM}^{p} g_{m,TM}^{p+1*} + (b_n + b_m^*) g_{n,TE}^{p} g_{m,TE}^{p+1*}$$
(III.177)

$$T_{nm}^{p} = -i(a_n + b_m^*)g_{n,TM}^{p}g_{m,TE}^{p+1*} + i(b_n + a_m^*)g_{n,TE}^{p}g_{m,TE}^{p+1*}$$
(III.178)

Then, Rel (III.176) becomes:

$$\overline{\sin \theta} \cos \varphi C_{ext} = \frac{\lambda^2}{4\pi} \left[ \sum_{p=0}^{\infty} \sum_{n=|p|\neq 0}^{\infty} \sum_{m=|p+1|\neq 0}^{\infty} \frac{(m+p+1)!}{(m-p-1)!} \right] (III.179)$$

$$\left\{ \operatorname{Re} \left( S_{nm}^p \right) \left[ \frac{1}{n^2} \delta_{n,m+1} - \frac{1}{m^2} \delta_{m,n+1} \right] \right.$$

$$+ \operatorname{Re} \left( T_{nm}^p \right) \frac{2m+1}{m^2(m+1)^2} \delta_{nm} \right\}$$

$$+ \sum_{p=-1}^{\infty} \sum_{n=|p|\neq 0}^{\infty} \sum_{m=|p+1|\neq 0}^{\infty} \frac{(n-p)!}{(n+p)!}$$

$$\left\{ \operatorname{Re} \left( S_{nm}^p \right) \left[ \frac{1}{m^2} \delta_{m,n+1} - \frac{1}{n^2} \delta_{n,m+1} \right] \right.$$

$$- \operatorname{Re} \left( T_{nm}^p \right) \frac{2n+1}{n^2(n+1)^2} \delta_{nm} \right\} \right]$$

which can again be more concisely rewritten by rearranging subscripts and superscripts as follows:

$$\overline{\sin \theta} \cos \varphi C_{ext} = \frac{\lambda^2}{2\pi} \sum_{p=1}^{\infty} \sum_{n=p}^{\infty} \sum_{m=p-1}^{\infty} \frac{(n+p)!}{(n-p)!}$$

$$\left\{ \operatorname{Re}(S_{mn}^{p-1} + S_{nm}^{-p}) \left[ \frac{1}{m^2} \delta_{m,n+1} - \frac{1}{n^2} \delta_{n,m+1} \right] 
+ \frac{2n+1}{n^2(n+1)^2} \delta_{nm} \operatorname{Re}(T_{mn}^{p-1} - T_{nm}^{-p}) \right\}$$

Then, substracting (III.174) from (III.180), we obtain:

$$C_{pr,x} = cF_x^+ = \frac{\lambda^2}{2\pi} \sum_{p=1}^{\infty} \sum_{n=p}^{\infty} \sum_{m=p-1\neq 0}^{\infty} \frac{(n+p)!}{(n-p)!}$$

$$\left\{ \left[ \operatorname{Re} \left( S_{mn}^{p-1} + S_{nm}^{-p} - 2U_{mn}^{p-1} - 2U_{nm}^{-p} \right) \right] \left[ \frac{1}{m^2} \delta_{m,n+1} - \frac{1}{n^2} \delta_{n,m+1} \right] + \frac{2n+1}{n^2(n+1)^2} \delta_{nm} \left[ \operatorname{Re} \left( T_{mn}^{p-1} - T_{nm}^{-p} - 2V_{mn}^{p-1} + 2V_{nm}^{-p} \right) \right] \right\}$$

The triple summation can be reduced by expressing the Kronecker deltas and switching indices to give summations over  $n \in [1, \infty[$  and  $p \in [1, n]$ . After rearranging, an alternative to (III.181) is then:

$$C_{pr,x} = \frac{\lambda^2}{2\pi} \sum_{n=1}^{\infty} \frac{1}{n+1} \left\{ (n+2) \operatorname{Re} \left( 2U_{n,n+1}^0 + 2U_{n+1,n}^{-1} - S_{n,n+1}^0 - S_{n+1,n}^{-1} \right) \right.$$

$$\left. + \frac{1}{n+1} \sum_{p=1}^{n} \frac{(n+p)!}{(n-p)!} \left[ \operatorname{Re} \left( S_{n+1,n}^{p-1} + S_{n,n+1}^{-p} - 2U_{n+1,n}^{p-1} - 2U_{n,n+1}^{-p} \right) \right.$$

$$\left. - \frac{2n+1}{n^2} \operatorname{Re} \left( T_{nn}^{p-1} - T_{nn}^{-p} - 2V_{nn}^{p-1} + 2V_{nn}^{-p} \right) \right.$$

$$\left. - (n+p+1) \left( n+p+2 \right) \operatorname{Re} \left( S_{n,n+1}^p + S_{n+1,n}^{-p-1} - 2U_{n,n+1}^p - 2U_{n+1,n}^{-p-1} \right) \right] \right\}$$

Establishing the expression for  $C_{pr,y}$  is fully similar. The evaluation of the second term in the r.h.s. of (III.163), i.e.:

$$\overline{\sin\theta} \sin\varphi C_{sca} = \int_0^\pi \int_0^{2\pi} (I_\theta^+ + I_\varphi^+) r^2 \sin^2\theta \sin\varphi d\theta d\varphi \qquad (III.183)$$

starts by integrating over  $\varphi$  using:

$$\int_{0}^{2\pi} \sin\varphi \, \exp(ik\varphi) \exp(-ik'\varphi) d\varphi = i\pi(\delta_{k,k'+1} - \delta_{k',k+1})$$
 (III.184)

The rest of the procedure is left as an exercise to the reader. We find that  $\sin \theta \sin \varphi C_{sca}$  and  $\sin \theta \sin \varphi C_{ext}$  are deduced from  $\sin \theta \cos \varphi C_{sca}$  and

 $\overline{\sin \theta} \cos \varphi$   $C_{ext}$  respectively, by changing Re to Im. The final expression for  $C_{pr,y}$  is therefore identical to (III.181) but with Re replaced by Im:

$$C_{pr,y} = cF_y^+ = \frac{\lambda^2}{2\pi} \sum_{p=1}^{\infty} \sum_{n=p}^{\infty} \sum_{m=p-1\neq 0}^{\infty} \frac{(n+p)!}{(n-p)!}$$

$$\left\{ \left[ \operatorname{Im} \left( S_{mn}^{p-1} + S_{nm}^{-p} - 2U_{mn}^{p-1} - 2U_{nm}^{-p} \right) \right] \left[ \frac{1}{m^2} \delta_{m,n+1} - \frac{1}{n^2} \delta_{n,m+1} \right] + \frac{2n+1}{n^2(n+1)^2} \delta_{nm} \left[ \operatorname{Im} \left( T_{mn}^{p-1} - T_{nm}^{-p} - 2V_{mn}^{p-1} + 2V_{nm}^{-p} \right) \right] \right\}$$
(III.185)

Also, an alternative expression is (III.182) with Re replaced by Im.

Finally, from  $F_x^+, F_y^+, F_z^+$  we may readily derive the force components in spherical coordinate systems  $(F_r^+, F_\theta^+, F_\varphi^+)$  or in cylindrical coordinate systems  $(F_\rho^+, F_\varphi^+, F_z^+)$  if required. In cylindrical coordinate systems, the force components would play a special role in designing and interpreting optical levitation experiments e.g ([167], [168], [169], [56], [170], [58], [171], and references therein). For vertically travelling beams,  $F_z^+$  would be involved in the force balance between the upward radiation pressure force component and the downward weight of the particle.  $F_\rho^+$  (in which  $\rho$  designates a direction transverse to the beam) would determine whether the particle would be trapped in the beam or expelled away.

# III.13 Efficiency Factors

We call  $\mathcal{E}^+$  the reduced power geometrically incident on the particle. We may then define efficiency factors by the relation:

$$Q_i = \frac{C_i}{\mathcal{E}^+} \tag{III.186}$$

in which i stands for sca, abs, ext or pr,  $Q_i$  are dimensionless factors.

For a plane wave,  $\mathcal{E}^+$  is simply  $\pi d^2/4$  in which d is the particle diameter since the reduced incident intensity per unit of area is set to 1 using the normalizing condition (III.106). Then, (III.186) simply becomes:

$$Q_i = \frac{C_i}{\pi d^2/4} \tag{III.187}$$

The more useful efficiency factors are then:

 $egin{array}{ll} Q_{sca} & : ext{scattering efficiency factor} \\ Q_{abs} & : ext{absorption efficiency factor} \\ Q_{ext} & : ext{extinction efficiency factor} \\ \end{array}$ 

The above factors represent the relative amounts of geometrically incident energy which is scattered, absorbed and extinguished, respectively. It follows that efficiency factors are often more praised than cross-sections because they possess a very clear physical meaning.

In non-plane wave cases, (III.187) may be generalized to (III.186). However,  $\mathcal{E}^+$  is now a quantity more complex to evaluate although it can be done using the Poynting theorem. It depends on the nature of the incident beam and on the location of the scatter center in the beam. Its evaluation now requires integrations of incident intensities. As an example, see Hodges *et al* (172, 163) in the case of Gaussian beams.

# III.14 Complement, Other GLMTs

In this chapter, we have examined the GLMT *stricto sensu*. By extension, we propose to call GLMT any theory which solves a scattering problem by using a method of separation of variables. Essentially, the different GLMTs are distinguished by the kind of scatterer considered. This complement is devoted to a concise exposition of studies associated with GLMTs other than GLMT in a strict sense.

### Multilayered spheres

The case of an electromagnetic scattering from a multilayered sphere located in an arbitrary shaped beam has been solved by Onofri  $et\ al$ , by using the Bromwich potential method [173]. Two extreme particular cases pertain to this framework (i) the case of coated spheres, i.e. with only two layers and (ii) the case of a continuous radial gradient of refractive index which can be efficiently modelled using a large enough number of layers. As a specific result, the scattering coefficients for the present case are formally identical with the ones of the GLMT and, in particular, involve again the beam shape coefficients  $g_{n,TM}^m$  and  $g_{n,TE}^m$ . One consequence is that all the GLMT expressions that concern external waves, i.e. scattered intensities and cross sections, including radiation pressure cross sections, remain valid in the GLMT for multilayered spheres. This makes rather easy the adaptation of a computer code for GLMT to a computer code implementing the GLMT for multilayered spheres. Numerical results are provided for scattering diagrams and radiation pressure.

The above implementations used a technique according to Wu and Wang [174] for the evaluations of coefficients  $a_n$  and  $b_n$  involved in the formulation. Subsequently, improved algorithms for electromagnetic scattering of plane waves and shaped beams by multilayered spheres have been published by Wu et al [175]. The stability of the numerical scheme used allows one to extend the feasible range of computations, both in size parameter and in number of layers for a given size, by several orders of magnitude. This algorithm therefore produces an efficient opportunity to deal with spherical particles with a radial gradient of refractive index. In the article, accounting for some

hardware limiting features (available memory limitations), the number of layers used was as great as 15 000 with an outer size parameter as large as approximately 150 000. Some results are provided and discussed, in particular concerning the rainbow for a nonlinear profile of the refractive index.

Next, we provide a list of citing articles. Some of them are relevant indeed to the GLMT for multilayered spheres, but others are more restrictively and specifically relevant to the Wu et al algorithm [175]. Wu et al [176] dealt with the computation of Gaussian beam scattering for larger particles, in a GLMT-framework, with computational methods claimed to be improved. The case of coated spheres is also investigated. Rysakov and Ston 177, 178 investigated light scattering by a "soft" layered sphere. Sakurai and Kozaki 179, 180 and Sakurai et al 181 dealt with shaped beam scattering by a Luneberg lens (a spherically symmetric lens, with a variable-index refracting structure). Experimental results obtained from microwave scattering by a six-layer spherical lens are in good agreement with theoretical values. An extensive study of Luneberg lenses, however, under plane wave illumination, is available from Lock [182], [183], [184]. Smith and Fuller [185] dealt with photonic bandgaps in Mie scattering by concentrically stratified spheres. Deumié et al 186 were concerned with the production of overcoated microspheres for specific optical powders, and with their characterization. They remarked that a complete theory (like GLMT) would be required to predict the optical properties of the produced microspheres. Stout et al [187] discussed the absorption in multiple-scattering systems of coated spheres. Wen Yang [188] proposed an improved recursive algorithm for light scattering by a multilayered sphere. The algorithmic issue is also discussed by Hong Du 189. Voarino et al 190 dealt with optical properties calculated for multielectric quarter-wave coatings on microspheres, to be complemented by Voarino et al 191. Chen et al 192 were concerned with Gaussian beam scattering from arbitrarily shaped objects with rough surfaces. Wei Liang et al 193 dealt with a Mie scattering analysis of spherical Bragg "onion" resonators for the simplest case when the center of the onion resonator coincides with the center of the waist plane of a fundamental Gaussian beam, a case where the beam shape coefficients  $g_{n,X}^m$  reduce to the beam shape coefficients  $g_n$ . Wu et al 176 computed the scattering field of homogeneous and coated spheres under Gaussian beams and plane wave illumination. Combis and Robiche 194 discussed a computational method for the scattering of an axisymmetric laser beam by an inhomogeneous body of revolution, with a method which relies on a domain decomposition of the scattering zone into concentric spherical radially homogeneous subdomains. Voshchinnikov et al 195 modelled the optical properties of composite and porous interstellar grains, using in particular a model of layered particles, and the description of the behavior of particles with inclusions. Lock 196 was concerned with Debye series analysis of scattering of a plane wave by a spherical Bragg grating. Renxian Li et al 197 dealt with Debye series of normally incident plane-wave scattering by an infinite multilayered cylinder. Burlak and Grimalsky [198] studied high quality electromagnetic oscillations in inhomogeneous coated microspheres. Dartois [199] managed with the spectroscopic evidence of grain ice growth. Renxian Li et al again [200] discussed Debye series for light scattering by a multilayered sphere, or [201] Debye series for Gaussian beam scattering by a multilayered sphere. Sun et al [202] dealt with near-infrared light scattering by ice-water mixed clouds. Sun et al [203] dealt with Monte-Carlo simulation of backscattering by a melting layer of precipitation, to be completed by Sun et al [204] providing a new melting particle model and its application to scattering of radiowaves by a melting layer of precipitation (composed of melting snow particles, modelled by three-layered spherical particles, made out from air for the innermost layer, ice, and water for the outermost layer). Hai-Ying Li and Zhen-Sen Wu [205] discussed electromagnetic scattering by multilayered spheres in a Gaussian beam.

Rather than a GLMT, numerical methods can be used (whatever the kind of GLMT considered) but, even so, GLMT-results can be taken as a benchmark or as an independent means to check numerical results. Furthermore, conversely, problems attacked with numerical methods potentially provide possible applications of GLMTs. These remarks being made (and not to be repeated any more), an example of numerical methods applied to multilayered spheres is by Burlak and Grimalsky [198] who examined high quality electromagnetic oscillations in inhomogeneous coated microspheres. Also, Dartois [199] used a Discrete Dipole Approximation (DDA) to the study of scattering and absorption of light by spherical (and ellipsoidal) coated grains (motivated by "astronomy and astrophysics").

### Circular cylinders

Next, we consider the GLMT for the case of an arbitrary beam illuminating infinite circular cylinders (that is to say infinite cylinders with a circular section). Let us remark that the requirement of "infinity" is much less stringent for this case than for a plane wave illumination since a finite cylinder illuminated by a focused beam will essentially behave as an infinite cylinder. Hence, here we have a GLMT for infinite cylinders which, under rather easy circumstances, can be used for finite cylinders too.

The development of the GLMT for infinite circular cylinders was faster (only five years) than for the GLMT stricto sensu. This relatively short time was allowed thanks to the experience gained in the topic. Nevertheless, a full understanding of the situation and of different aspects of the situation required the use of mathematical techniques not commonly used in light scattering, namely the theory of distributions of Laurent Schwartz. The first article of the series of articles devoted to the problem was published in 1994 [HT]. The structure of this GLMT is at first sight very similar to the one of the GLMT stricto sensu. Cylindrical coordinates matching the geometry of the scatterer allow one to use again the Bromwich potential method. One important issue is that, as for the case of the sphere, the Bromwich potentials are assumed to be expressed by using coordinate separability according

to the form  $Z(z)R(\rho)\Phi(\varphi)$  in which  $(z,\rho,\varphi)$  are cylindrical coordinates. The theory can then be developed under this assumption, with expansions expressed in terms of beam shape coefficients and basic functions. Expressions are obtained for amplitudes and intensities of the internal and of the scattered waves, and specifications are made for the case of the far field. The special case of the plane wave is examined, and it is checked that the classical results for plane wave illumination are recovered from the more general GLMT described in the article. In the last section of the article, however, the case of Gaussian beams, modelled by retaining only the Maxwellian contribution of the Taylor expansion of first-order Davis beams [75], is examined and, most surprisingly, it is found that this case cannot be solved in the framework of the GLMT briefly described above. These features pointed out to an unexpected theoretical problem, namely that the principle of separation of variables did not allow one to build a proper GLMT, i.e. a GLMT valid whatever the structure of the illuminating beam. Conversely, it was found that we could build satisfactory Bromwich potentials, but that these potentials did not satisfy the principle of separation of variables. Hence, this first article from 1994 ended with two problems (i) can we build a correct GLMT by using potentials which do not satisfy the principle of separation of variables? and (ii) why did this principle failed?

A discussion of the first question was actually published the same year [II8]. In this article, a theory of interaction between a Gaussian beam described by a first-order Davis approximation and an infinite cylinder, introducing Bromwich scalar potentials that are not linear combination of separable potentials, was discussed. We found that the theory exhibited unexpected difficulties, failed to construct it and, the problem being well defined, believed that it would form a challenge that could attract the attention of other researchers. To tell the truth, we believed that we would not be able to solve this problem by ourselves. Actually, no GLMT giving up the principle of separation of variables has never been produced, and the answer to the first question is most likely negative, that is to say, we did not solve the aforementioned problem, and no one did it. However, we indeed find a way to build a satisfactory GLMT by examining the second question, that is to say by revisiting the principle of separation of variables.

The method of separation of variables, rather than being expressed by a principle, is actually better expressed by a theorem, called the separability theorem. This theorem states that, given a linear partial differential equation and special coordinates allowing one to find a family of separated solutions, all solutions of the equation can be obtained from linear combinations of the separated solutions. According to the above articles [117], [118], we would have to conclude that the theorem fails. Gouesbet [121], revisiting the theorem, provided a systematic constructive approach to find solutions which do not satisfy the separability theorem. Nevertheless, all that has been said above concerned usual functions. However, it has been afterwards established that the separability theorem may be recovered if the class of admissible solutions

is extended from functions to distributions [124]. The theory of distributions with its application to beam parametrization in light scattering, supposed to be easy-reading for a newcomer, is exposed by Gouesbet [206].

The use of distributions allowed one to solve the problem of interaction between shaped beams and infinite circular cylinders in a formal satisfactory way. First, a simple case is considered, namely that the Gaussian beam illuminates the infinite cylinder perpendicularly to its axis and the beam waist center of the beam is located on this axis [119]. Next, the case of a first-order Gaussian beam by an infinite cylinder with arbitrary location and arbitrary orientation has been considered [120]. The scattering of higher-order Gaussian beams, still with truncated Taylor expansions, is discussed in [207]. In particular, in these solutions, beam shape coefficients are generalized to beam shape distributions. Although distributions are used to build these theories, final results are expressed in terms of usual functions, therefore allowing the implementation of these results in computer programs.

The interaction between the infinite cylinder and an arbitrary shaped beam (Arbitrary Beam Theory) is discussed in [208]. It is expressed by using again the theory of distributions, providing the most general framework, allowing one in particular to deal again with truncated Taylor series from Davis beams. It is obviously not meant that the interaction between light and cylinders must always be expressed in terms of distributions. The set of usual functions is actually a subset of the set of distributions (which may be viewed as generalized functions) and, for some special incident beams (like for a plane wave) or special descriptions of arbitrary shaped beams (like for a Gaussian beam described by a plane wave spectrum), the theory in terms of distributions may be simplified to a theory in terms of usual functions. Conversely, any theory in terms of functions may be translated to a theory in terms of distributions.

In 1997 [209], three years only after the initial surprise concerning the status of the separability theorem [117], and the compulsory requirement to understand what was going on before proceeding further, practical numerical results became available. The cited article [209] concerned the restricted case of an illuminating Gaussian beam, normally incident on the cylinder, with the beam waist center located on the cylinder axis, and a convenient orientation of the leading electric field. Three different beam descriptions are essentially used (i) Maxwellian beams at limited order extracted from the Davis formulation (ii) a plane wave spectrum and (iii) a localized approximation in cylindrical coordinates, similar to the one already introduced in spherical coordinates. Let us note that our previous discussion in spherical coordinates, comparing GLMT with multipole expansions and variants with plane wave spectra, does not apply here to the case of cylindrical coordinates. Indeed, due to the continuous nature of one separation constant in cylindrical coordinates, the use of plane wave spectra is much more natural for cylinders than for spheres, as can be seen by inspecting the reference under discussion. Also, the localized approximation in cylindrical coordinates (or cylindrical localized approximation) was introduced in an empirical way, by analogy with the procedure used for the localized approximation in spherical coordinates, and justified by its consequences. It is only valid for the geometry under study in the article under discussion. Numerical results compared the three different beam descriptions mentioned above, with enlightening comments, and displayed scattering diagrams. The localized approximation empirically introduced in the above article has been afterwards rigorously justified, heavily relying on the theory of distributions [210]. Furthermore, the relationship between the theory in terms of distributions and the plane wave spectrum approach is discussed.

There is an interesting comment, concerning contingency in the development of science, which needs to be made now. When starting to develop the GLMT for cylinders, it could have been decided to deal straight away with a plane wave spectrum approach, and not to worry with the behavior of truncated Taylor series which revealed an apparent flaw concerning the separability theorem. Had this happened, then mastering the theory of distributions, or even using it, would have been unnecessary. However, this did not happen and there was then a problem with the separability theorem which had to be solved. As a result, thanks to the knowledge gained, the GLMT for cylinders could receive its most general formulation in terms of distributions [208] and the relationship between this general framework and easier frameworks in terms of functions could be understood.

However, may be more important, it is likely that, without the theory of distributions, the rigorous justification of the cylindrical localized approximation would have been impossible or, at least, more difficult. Furthermore, the cylindrical localized approximation has afterwards been generalized to the case of arbitrary location and orientation of the scatterer, and the rigorous justification heavily relied on the use of distributions too, although the final result no longer requires the use of distributions [211].

More numerical results are provided by Méès et al [212], in the general case of arbitrary location and arbitrary orientation of the scatterer, with a localized approximation (therefore avoiding the use of distributions) to describe the illuminating Gaussian beam in cylindrical coordinates, and the use of a plane wave spectrum approach to evaluate the beam shape coefficients. Comparisons between GLMT and geometrical optics, GLMT and plane wave scattering, are provided. A particular emphasis concerned a wave-guiding effect and the shift of the rainbow generated by the nature of the shaped beam.

Precursors might be Yokota et al [213] dealing with the scattering of a Hermite-Gaussian beam mode by parallel dielectric cylinders. Erez and Leviatan [214] considered the problem of wave scattering by a large 2D circular cylinder excited by a beam whose axis does not intersect the cylinder axis, with a theoretical analysis which is likely not akin to a GLMT. A GLMT for cylinders however, in which an illuminating Gaussian beam is parameterized

by using an angular spectrum of plane waves, is also discussed by Lock [215], and is applied to the study of morphology-dependent resonances of an infinitely long circular cylinder illuminated by a diagonally incident plane wave or a focused Gaussian beam [216]. Later on, internal and near-surface electromagnetic fields for an infinite cylinder illuminated by an arbitrary focused beam are discussed by Barton 217. Exterior caustics produced in such a situation (but for plane wave illumination) are studied by Lock et al [218]. The caustic theme is also discussed by Marston et al [219] in connection with the observation of enhanced backscattering by a tilted cylinder. Plane wave and Gaussian beam scattering by an infinite cylinder perpendicularly illuminated are compared by Mroczka and Wysoczanski, relying on the GLMT for cylinders [220]. Venkatapathi et al [221] dealt with measurement and analysis of angle-resolved scattering from small particles in a cylindrical microchannel, using a GLMT-approach. The channel is represented as a homogeneous dielectric cylinder perpendicularly illuminated. Beam shape coefficients are determined by using an angular spectrum of plane waves. In a subsequent article, Venkatapathi and Hirleman [222] dealt with the effect of beam size parameters on internal fields in an infinite cylinder irradiated by an elliptical Gaussian beam (or laser sheet). Plane wave and Gaussian beam scattering by long dielectric cylinders are available from Van den Bulcke et al who used an extended scattering simulator, with experiments comparing favorably with simulations, excepted when deviations occurred because of the finiteness of the cylinder and of the incident field in the experiment [223]. Scattering of shaped beam by an infinite cylinder of arbitrary orientation is discussed by Zhang and Han [224]. By relying on the use of an addition theorem for spherical vector wave functions under coordinate rotations, and relations between the spherical and cylindrical vector wave functions, cylindrical beam shape coefficients are expressed in terms of spherical beam shape coefficients. Resnick and Hopfer [225] are concerned with the mechanical simulation of primary cilia. A cilium can be modelled as a cylindrical rod capped by a hemisphere, and therefore offers some relevance to GLMT-computations or GLMT-ingredients such as the issue of beam description for laser trapping.

We now provide more but concerning non-homogeneous cylinders. Rainbow scattering by an inhomogeneous cylinder with an off-axis Gaussian beam at normal incidence is discussed by Guo and Wu [226]. Adler et al [227] dealt with the experimental observation of rainbow scattering by a coated cylinder. They mentioned that the theory of rainbow scattering for a coated cylinder has not been worked out in wave theory. Starting from the GLMT for cylinders, this could be done by using a generalization to the case of multilayered cylinders, including the case of arbitrary shaped beam illumination. The case when the cross-section of the cylinder is not exactly circular is mentioned. This points out to another GLMT soon to be discussed, the one for infinite elliptical cylinders. It is then obvious that GLMTs for cylinders, including for multilayered cylinders, pave the way to further studies concerning rainbow scattering in wave theory. An improved algorithm for electromagnetic

scattering (of plane wave however) by a radially stratified cylinder is discussed by Jiang et al [228]. Light scattering by bianisotropic particles is discussed by Novitsky, with also a section on light scattering by multilayered cylinders [229]. Finally, Wu and Li introduced Debye series for the scattering by a multilayered cylinder in an off-axis Gaussian beam [230]. Results with Debye series reach an agreement with those of GLMT. Some emphasis on the rainbow is pointed out.

### Elliptical cylinders

Next, we consider the GLMT for infinite elliptical cylinders (that is to say with an elliptical section rather than with a circular section). This GLMT is more technical than the previous one because the loss of symmetry when deforming a circular section to an elliptical section implies specific new difficulties. Also, Mathieu functions appearing on the stage are not specially simple to manage with. Nevertheless, the experience gained when dealing with circular cylinders has been much helpful before dealing with elliptical cylinders. In particular, the use of the theory of distributions is again an invaluable tool.

A general framework, in terms of distributions, for describing an arbitrary electromagnetic shaped beam in elliptical-cylinder coordinates, is described by Gouesbet et al [231]. This framework is illustrated by investigating the case of a first-order Davis Gaussian beam, more precisely the case of the Maxwellian contribution to a first-order Davis beam. More generally, higherorder Gaussian beams (more precisely Maxwellian contributions to higherorder Gaussian beams) are considered in [232]. The conclusion of the article stated that these studies on partial waves formed a required ingredient to the design of an elliptical localized approximation. Next, Gouesbet et al [233] provided a description of arbitrary shaped beams in elliptical cylinder coordinates, first in terms of distributions, and afterwards using an equivalent plane wave spectrum approach. However, the plane wave spectrum approach used is an extended one, in which some meaningless integrals must be thought of as being the expressions of a symbolic calculus whose rigorous justification is to be found in the theory of distributions. The lack of mathematical rigor (but not of exactness) associated with this calculus is compensated by the fact that, at the present time, most physicists will find it intuitively more appealing than a complete rigorous formulation. This way of viewing the plane wave spectrum approach in elliptical-cylinder coordinates is a bit rather different than the one used in circular-cylinder coordinates where it was restricted to the use of usual functions. The GLMT for infinitely long elliptical cylinders illuminated by arbitrary shaped beams is afterwards presented by Gouesbet and Méès 234. This GLMT may most conveniently be used when it is accompanied by a speeding-up localized approximation. Such a localized approximation is introduced and rigorously justified by Gouesbet et al [235] for the case of illuminating Gaussian beams, relying on the partial wave description of Maxwellian contributions to Davis beams, and on the theory of distributions, with however the configuration restriction that the cylinder is perpendicularly illuminated by the Gaussian beam. Nevertheless, the validity of the elliptical cylinder localized approximation for arbitrary shaped beams in GLMT for elliptical cylinders has been demonstrated too 236. The structure of GLMT for elliptical infinite cylinders is discussed by Gouesbet et al [237]. Rather than insisting on technicalities, this cited article provided a guide allowing one to gain a bird's eye view over the structure of the theory. As a by-product, the structure of the GLMT for circular cylinders is revisited. In particular, for circular cylinders, it was not immediately recognized that the use of distributions was compulsory in the most general case so that the historical development of the GLMT for circular cylinders did not evolve as easily as for elliptical cylinders. It was therefore useful to provide also a renewed bird's eye view of the story of the GLMT for circular cylinders. An introduction to the use of distributions for light scattering in elliptical cylinder coordinates is provided by Gouesbet et al [238], and a list of errata is provided by Gouesbet and Méès [239].

The GLMT for elliptical cylinders should have many applications. For instance, it could allow one to study the sensitivity of some measurement techniques, or of some phenomena, with respect to the deformation of a circular cylinder, or to investigate rainbow and morphology-dependent resonances in an elliptical cylinder within the framework of a rigorous electromagnetic approach. As a matter of fact, it could be relevant to the issue of rainbow scattering by a cylinder with an elliptical cross section, if not of a nearly elliptical cross section [240], or to the study of caustics [218]. Also, an investigation of the torque exerted on dielectric elliptical cylinders by highly focused laser beams has been performed by means of a diffraction theory [241]. Such a study could be revisited in a GLMT-framework, with the condition that this GLMT (for elliptical cylinders) should have to be extended to become able to deal with mechanical effects of light (which is not the case at the present time).

Applications of the GLMT for elliptical cylinders require efficient computer programs. Such programs do exist and numerical results have been obtained, but they have not been released in the archival literature, waiting for independent confirmations. Therefore, although the situation for the present GLMT is satisfactory from the theoretical point of view, it is fair to say that the state of the art concerning the GLMT for elliptical cylinders is severely under-developed.

### Sphere with an eccentrically located spherical inclusion

Another GLMT is the one concerning the case of a sphere with an eccentrically located spherical inclusion, which has been published in [128]. Its study would provide a step towards the study of a class of non-homogeneous particles but the associated configuration also presents a particular fundamental

interest because, to the electromagnetic problem which received a rigorous GLMT-solution, may be associated a Hamiltonian mechanical problem, in terms of trajectories, which is not integrable, as already discussed in a review article, in 2000 [92]. This non-integrability generates Hamiltonian chaos (in terms of trajectories) or equivalently optical chaos (in terms of rays). The sphere with an eccentrically located spherical inclusion then represents a particularly interesting topic for one of the authors of the book who devoted much time to the study of dissipative chaos, both experimentally and theoretically [242], [243]. For a recent numerical implementation concerning far-field scattering, see Han et al [244].

The 2D-Hamiltonian-optical configuration associated with the 3D-electromagnetic problem is known under the name of "annular billiard", extensively studied by Gouesbet et al [245], [246], [247]. An interesting feature of the annular billiard is that the terminologies "morphology-dependent resonances" and "whispering-gallery modes" cannot any more be considered as equivalent: there are morphology-dependent resonances which are no more whispering-gallery modes.

The annular billiard may also be investigated for its own interest or due to its connection with various other topics. Hentschel and Richter 248 used the annular billiard as a way to study quantum chaos in optical systems, a topic which may be of interest for future optical communication devices, or for the construction of microlasers with designed properties. They evidence that the simple ray picture provides a good qualitative description of certain system classes, but that only the wave description reveals the quantitative details. Or, in other words, they made computations showing the predictive power of the simple ray model when only the qualitative character of resonances is of interest. However, it proves to be essential to consult wave methods when one is interested in details. It has been argued (private communications) that the chaotic phenomena exhibited by the annular billiard are artefacts produced by the involved trajectory/ray approximation, and that nothing of that sort would appear in the complete electromagnetic problem. This is to be strongly disagreed, as certainly supported by the results of Hentschel and Richter showing that the trajectory/ray approach provides a kind of skeleton, to which flesh is attached by the wave approach.

The annular billiard is also discussed by Egydio de Carvalho et al [249] under two different situations (i) static boundaries and (ii) periodic time-dependent boundaries. In the second case, particles may exhibit a phenomenon called Fermi acceleration, associated with an unlimited energy growth. Chattaraj et al [250], [251] were also concerned with quantum chaos. However, they discussed the topic in the framework of what is called the quantum theory of motion, as developed by Louis de Broglie and David Bohm. In this theory, or better said in this interpretation, of quantum mechanics, there exists an underlying level of deterministic pseudo-classical trajectories. Determinism in quantum mechanics is then restored, the price to be paid

being the existence of hidden variables. A rather extensive discussion of hidden variables theories in quantum mechanics is available from Gouesbet [252].

### Assemblies of spheres and aggregates

The case of assemblies of spheres and aggregates is connected, as in the previous case, with chaotic phenomena, more specifically with what is called irregular or chaotic scattering, as summarized by Gouesbet and Gréhan [92]. The associated GLMT has been published by Gouesbet and Gréhan 129 but has not yet been implemented in its general form. It is again the case of a severely under-developed GLMT. Nevertheless, the case of electromagnetic field for a beam incident on two adjacent spherical particles is discussed by Barton et al [253]. A discussion of on-axis cluster spheres, rather uninteresting from the point of view of chaotic scattering, but relevant to the electromagnetic topic, is discussed by Bai et al [254], [255]. Also, Lecler et al 256 considered light scattering by a bisphere (a pair of spherical particles) in the far field. The basic algorithm relies on the generalization of the Lorenz-Mie theory to an aggregate of spheres. The method of separation of variables is used, in conjunction with translational addition theorems for spherical vector wave functions. In both cases (the host sphere with an eccentrically located spherical inclusion, and the assemblies of spheres and aggregates), the trajectory/ray approximations provide chaotic features which should form skeletons for more complex chaotic electromagnetic phenomena, worth to be examined.

Also, Xu and Gustafson [257], [258] compared light scattering calculations (by using a rigorous solution, and the discrete-dipole approximation, DDA) and experimental results, for two-spheres aggregates. It is found that the DDA solution, under certain circumstances, deviates significantly from the rigorous solution and from experimental results. Khlebtsov et al [259] dealt with clusters of colloidal gold and silver particles formed during slow and fast aggregation and, for calculating the optical properties of aggregates, also used a coupled dipole method (CDM or DDA) as well as an exact method of multipole expansion.

### Spheroids

We now deal with the GLMT for spheroids initiated by Barton [260], a case when the Bromwich method cannot be applied because the necessary conditions for scale factors are not satisfied. Later on, Barton also dealt with the case of a layered spheroid with arbitrary illumination [261]. The GLMT for spheroids has also been vigorously developed by Chinese people (and collaborators) originating from Xidian and Shanghai universities.

Regarding Xidian university, the expansion coefficients of a spheroidal particle illuminated by a Gaussian beam are discussed by Han and Wu [262] who also dealt with the scattering of a spheroidal particle illuminated by a Gaussian beam [263]. An important focus concerned the evaluation of spheroidal

beam shape coefficients for on-axis Gaussian beams. It is found that they can be expressed in terms of the spherical beam shape coefficients. An emphasis on the far field case is available from Han et al [264]. In this article, the size of the spheroid is large enough (up to 40  $\mu$ m, size parameter equal to about 200) to be of practical interest for various applications. The article also provides a discussion on the sensitivity of the rainbow to the particle shape and the validity of a formula, named the Möbius formula, is examined. Absorption and scattering by an oblate particle is discussed by Han and Wu [265]. A subsequent study by Han et al [266] is devoted to the description of off-axis arbitrary shaped beam in spheroidal coordinates. In this general off-axis case, spheroidal beam shape coefficients are expressed in terms of spherical beam shape coefficients. Numerical results are provided for Gaussian beam scattering properties, such as angular distributions of the intensity for various radii of the illuminating beam, locations of the beam focal point, eccentricities and complex refractive indices. Computations of scattered fields can be achieved for large size parameters, exceeding 700. Thereafter, the case of ultra-short pulse illumination is discussed by Han et al [267]. Time-dependent scattering intensities are presented as intensities versus time, at different scattering angles, and results are compared with the case of a perfect sphere with the aspect ratio as the main parameter. Zhang and Han presented a GLMT for the scattering by a confocal multilayered spheroidal particle illuminated by an axial Gaussian beam [268]. Resonant spectra of a deformed spherical microcavity (under plane wave illumination however) are discussed by Han et al [269]. The scattering of shaped beam by an arbitrarily oriented spheroid having layers with non-confocal boundaries is discussed by Han et al  $\boxed{270}$ .

Leaving Xidian, we now fly to Shanghai. On-axis Gaussian beam scattering, in a geometrical optics approximation, for spherical and spheroidal particles, is examined by Xu et al [271], [272], something which does not yet provide a GLMT. A genuine GLMT for spheroids, devoted to the case of an arbitrarily oriented, and located spheroid, illuminated by an arbitrary shaped beam, is however thereafter available from Xu et al [273], following a previous discussion of the expansions with beam shape coefficients for this problem 274. As for Han et al 266, spheroidal beam shape coefficients are expressed versus spherical beam shape coefficients. Expressions are also given for the extinction and scattering cross sections. Special cases (plane wave scattering by a spheroid, and shaped beam scattering by a sphere) can be recovered from the general case, as they should. Numerous numerical results are displayed, including scattering by laser sheets. In a fully completed GLMT, mechanical effects have to be studied. Accordingly, theoretical predictions of radiation pressure forces exerted on a spheroid by an arbitrary shaped beam are carried out by Xu et al [275]. One application concerns the behavior of an optical stretcher used for red blood cell deformation. An analytical solution for the radiation torque exerted on a spheroid, accompanied by many numerical results and physical discussions, are furthermore available from Xu et al [276].

### Miscellaneous shapes

We now consider other interesting scatterer shapes and configurations (although they are not all of them GLMT-izable). Barton considered electromagnetic field calculations for irregularly shaped, axisymmetric layered particles with focused illumination [277]. Kushta et al [278] dealt with extinction and scattering of a guided beam in a hollow dielectric waveguide or, in other words, with mode scattering by a spherical object that is placed inside a circular dielectric waveguide. The solution to the theoretical problem relies on the fact that each sub-system (the spherical inclusion, and the circular dielectric waveguide) can be treated using the method of separation of variables (they would correspond to the GLMT stricto sensu and to a GLMT for cylinders respectively). Neukammer et al [279] reported on 2D angular-resolved light scattering of various kinds of single blood cells, namely sphered red blood cells (erythrocytes), native erythrocytes elongated by hydrodynamic forces, and on white blood cells (lymphocytes), and also of oriented agglomerates consisting of two identical polystyrene microspheres. A theoretical approach used to deal with these particles was the discrete dipole approximation, but the generalized Lorenz-Mie theory has been used too to evaluate some matrix elements and some differential cross sections. Linear chains of as many as six identical polystyrene spheres in water were also considered. Kant [280] dealt with a generalized Lorenz-Mie theory for focused radiation interacting with finite solids of revolution, more specifically with spherical and finite cylindrical homogeneous particles. Thin, long cylinders may be approximated by prolate spheroids. Wang et al [281] dealt with the electromagnetic scattering from two parallel 2D targets arbitrarily located in a Gaussian beam, producing an approximate solution employing the reciprocity theorem and an equivalence principle. An application is done for the case of two parallel adjacent plasma-coated conducting cylinders. The same topic is considered again in an extended way by Wang et al [282]. Electromagnetic scattering of plane wave and Gaussian beams by parallel cylinders are discussed by Wang et al [283]. Guo et al [284] also used the reciprocity theorem and an equivalence principle to deal with electromagnetic scattering from two adjacent spherical objects. Clusters of spheres with a point source which can be located anywhere are examined by Moneda and Chrissoulidis [285]. The angular distribution of non-linear optical emission from spheroidal microparticles is discussed by Kasparian et al [286]. They used a geometrical optics technique but it is worth noting that GLMT (in the present case for spheroids) allows one to evaluate internal fields viewed as excitation fields, for instance to initiate fluorescence or other phenomena.

# Gaussian Beams and Other Beams

The GLMT-framework previously introduced concerns arbitrary shaped beams. In practice however, one is often concerned with well defined special kinds of beams and, when the nature of the beam is known, much more can be said about GLMT. In this chapter, we discuss the special case of Gaussian beams, with a complement providing more information on Gaussian beams and discussing other beams as well. Gaussian beams (laser beams in their fundamental mode TEM<sub>00</sub>) are widely employed in the field of optical particle sizing, corresponding to our original motivation in developing the GLMT (51, 52, 53, 54 for gaining a fairly complete background). Examples of applications of GLMT to the technique of phase-Doppler for simultaneous measurements of sizes and velocities of particles in flows may be found in [287], [288], [289], [290], among others. Another kind of special beams which is becoming more and more important for optical particle sizing is laser sheets also called cylindrical waves (see for instance [291], [292], 294, 295). It is of interest to remark that the description of a Gaussian beam is a limit case of the description of a cylindrical wave. See also discussions of top-hat beams in [296], [297]. Laser sheets and top-hat beams will be more extensively discussed in the complement. For phase-Doppler techniques, see chapter VIII.

Once the kind of beam to study is defined, the central problem to solve concerns the mathematical description of the beam, in particular, in the case of the GLMT  $stricto\ sensu$ , the knowledge of expressions for the field components  $E_r$  and  $H_r$  which are required to compute the BSCs. Several descriptions of Gaussian beams which are not necessarily equivalent are available from the literature. The GLMT-framework is obviously not dependent on any particular choice but result accuracy may be. We would like to possess a description which does not produce any singularity, contrary to what happens in Kim and Lee [69], and also which would provide a systematic procedure to possibly make the description arbitrarily close to perfection. The best candidate we found is Davis formulation [75] which is therefore now going to be discussed. The special case of arbitrary location of the scatterer in Gaussian

beams described according to Davis formulation has been discussed in Gouesbet  $et\ al\ (298)$  and (298), among others.

# IV.1 Gaussian Beam Description

# IV.1.1 The Solving Paradox

We consider a Gaussian beam propagating in a linear, isotropic, non absorbing medium defined by real permittivity  $\epsilon$  and permeability  $\mu$ . The discussion is carried out by referring to Fig. IV.1 which isolates a part of Fig. III.1.

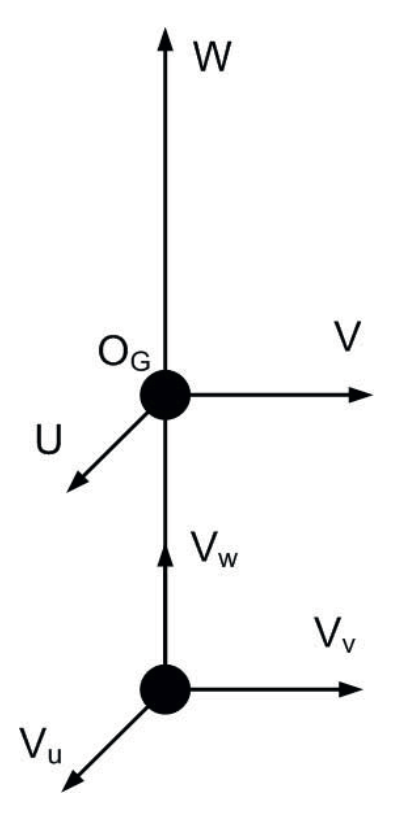
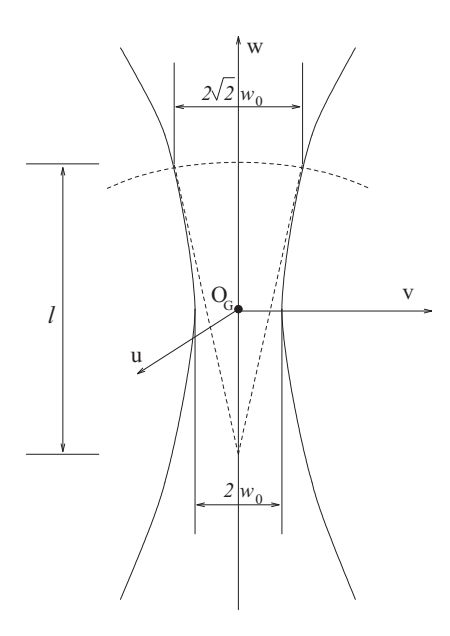


Fig. IV.1. The geometry

 $O_G w$  is the beam axis, with  $O_G$  located at the beam waist center. The beam propagates towards positive w and the electric field component is essentially vibrating in the plane  $(uO_G w)$ . The exact meaning of the word "essentially" will be clarified later. Let us however straight away state that it means that the electric field is exactly polarized along the direction u at the beam waist center (see Rels (IV.24)-(IV.25)).



**Fig. IV.2.** The geometrical meaning of  $w_0$  and l.

To describe a Gaussian beam, the simplest model we may imagine is to consider a linearly polarized plane wave propagating along w towards positive w and to introduce a spatial dependence of the field components. For instance, the electric field components for the plane wave  $(E_u, 0, 0)$ , in which  $E_u$  is a constant, then become  $(E_u(u, v, w), 0, 0)$  in which  $E_u$  is now space dependent. Maxwell's equation (I.59) then implies:

$$\frac{\partial E_u}{\partial u} = 0 \tag{IV.1}$$

which is not compatible with electric field components of the form -  $(E_u(u, v, w), 0, 0)$ . Because  $E_u$  should not depend on u, it cannot characterize a Gaussian beam.

Furthermore, for a plane wave with electric field components  $(E_u = cst, 0, 0)$ , magnetic field components should write  $(0, H_v = cst, 0)$  which would be extended for a Gaussian beam to  $(0, H_v(u, v, w), 0)$ . Maxwell's equation (I.57) then implies:

$$\frac{\partial H_v}{\partial v} = 0 \tag{IV.2}$$

which similarly again shows that our simple model is basically flawed.

Lax et al [299] remarked that such facts are the source of a paradox, known as the solving paradox. This paradox arises when, studying Gaussian beams, people assume electric field components of the form  $(E_u, 0, 0)$ , who

then forget that Rel (IV.1) must be satisfied and, nevertheless, at the end of the work succeed in obtaining a  $E_u$ -Gaussian wave solution both in u and v at the lowest order, in strong contradiction with Maxwell's equations.

We shall then have to develop a different approach which leads to somewhat unavoidable ironical result. Namely, a Gaussian beam,  $stricto\ sensu$ , i.e., exhibiting exact Gaussian profiles for  $E_u$  and  $H_u$  is not Maxwellian, i.e., does not exactly satisfy Maxwell's equations. Conversely, if we want our Gaussian beam to be Maxwellian, it will not exhibit perfect Gaussian profiles, i.e., a Gaussian beam (in one sense) is not Gaussian (in another sense). See figures in [79] exemplifying this statement.

### IV.1.2 Elementary Description

The paradox is solved by Lax et al [299] who examined a paraxial approximation and provided a perturbation procedure to systematically introduce higher order corrections.

Solutions of Maxwell's equations describing Gaussian beams are then expressed using expansions over successive powers of a small dimensionless parameter s defined by:

$$s = w_0/l = 1/(kw_0) = 1/b_0$$
 (IV.3)

in which  $w_0$  is the waist radius at amplitude equal to (1/e), l is known as the diffraction length, and k is the wave-number. By definition, the waist is the plane  $(uO_Gv)$ , i.e., the plane at which the width of the laser beam is the smallest. The waist radius  $w_0$  is, therefore, a characteristic length scale defining the radial extension of the beam. Before and after the waist, the beam converges and diverges, respectively. The rate of convergence (divergence) is measured by the diffraction length l which, therefore, is also called the divergence length or the spreading length. It is equal to twice the distance from the waist plane along the propagating axis  $O_Gw$  at which the beam expands by a factor  $\sqrt{2}$  (Fig. IV.2). The diffraction length l is, therefore, a characteristic length scale defining the beam in the longitudinal direction.

Radial and longitudinal length scales are related by (see Rel IV.3):

$$l = kw_0^2 (IV.4)$$

and, therefore, are not independent. When  $w_0$  decreases, i.e., the more the beam is efficiently focused at the waist, the more the spreading length decreases, meaning that the beam (converges) diverges more strongly.

Because the dimensionless parameter s appears as the ratio of two characteristic length scales defining the overall aspect of the beam, it is suggested to name it the beam aspect ratio or the beam shape factor. It has also been given the name of beam confinement factor and, furthermore, the word factor is sometimes replaced by the word parameter. For a plane wave  $(w_0 \to \infty)$ ,

the beam shape factor is 0, and it is therefore no surprise that plane waves may be exactly described without using any s-expansions. Because a Gaussian beam is much longer than large, i.e., it slowly converges (or diverges), the beam shape factor is different from 0 but still exhibits small values. A typical figure is  $s \approx 10^{-3}$  for  $\lambda = 0.5 \ \mu \text{m}$  and  $w_0 = 50 \ \mu \text{m}$ . Even for  $w_0 = 10 \ \mu \text{m}$ , that is in practice a very focused beam, s is about  $10^{-2}$ . The theoretical largest bound is for  $w_0 \approx \lambda$ , i.e.  $s \approx 1/(2\pi) \approx 0.16$ . It may be convenient to round this value to 0.25. For discussions concerning the behaviour of Gaussian beams which approach this limit, see [79], [80].

The inverse of s, i.e.,  $b_o$  (Rel IV.3) is equal to  $2 \pi w_0/\lambda$ . By analogy with the size parameter  $\alpha = \pi d/\lambda$ ,  $b_0$  can be named the beam waist parameter.

### IV.1.3 Historical

Following [299], expansions of solutions in terms of successive powers of s lead to arbitrarily refined descriptions of the beam. Because s is small, only a few terms are sufficient in practice in most situations. In the lowest-order, the structure of the field corresponds to electric field components of the form  $(E_u, 0, 0)$  in which  $E_u$  is not a constant. Field components then do not satisfy Maxwell's equations but only comply with their paraxial approximation. The next approximation of the field solutions is obtained by adding some components  $E_w$  and  $H_w$ . Maxwell's equations are still not satisfied but introduced inconsistencies are small, if the beam shape factor is small.

Other studies on the same topic agreed with the general method proposed by [299] in particular with the expressions of the paraxial approximation. The beam can then be described by Gauss, Gauss-Hermite or Gauss-Laguerre functions ([300], [301], [302], [303]). Because the description provided by Kogelnik is very famous and widespread, later we have to discuss the relation between Kogelnik formulation and the one used in this book (section IV.1.7).

After Lax et al [299], Davis [75] also presented a general procedure in terms of s-expansions. Although formulations by Lax et al and by Davis are equivalent, we shall rather favour Davis study because the introduction of a transversely polarized vector potential allowed him to present the theory in a simpler and more appealing way.

To mention later studies, Agrawal and Pattanayak 304 describe the electric field in terms of a plane wave spectrum and obtain the first-order correction to the Gaussian paraxial approximation, in agreement with Davis results. The similar use of a plane wave spectrum in the case of laser sheets is available from Ren et al 294. Couture and Belanger 305 then show that the whole set of corrections at all orders of the paraxial approximation may be understood as representing a spherical wave from a complex point source. However, Agrawal and Lax 306 emphasize the fact that introduced boundary conditions are different in Agrawal and Pattanayak 304, where corrections to the paraxial approximation are zero in the plane w = 0, and in Couture and Belanger 305, where corrections are zero on the axis u = v = 0,

leading to results which do not agree together. Finally a more recent article by Takenaka and Fukumitsu 307 provides corrections at all orders for Gauss-Hermite and Gauss-Laguerre paraxial approximations with the same boundary conditions as in Agrawal and Pattanayak 304.

### IV.1.4 Davis Formulation

This formulation has been explicitly used by the authors group for the first time (in a GLMT-framework) in Gouesbet *et al* [308]. It, however, appears that Gaussian beam descriptions we used in previous studies still pertain to Davis framework.

The laser beam is described by a transversely polarized vector potential  $A_i$  (section I.2.8) which is written similarly as for a plane wave:

$$A_i = (A_u, 0, 0) \tag{IV.5}$$

in which the component  $A_u$  reads as:

$$A_u = \Psi(u, v, w) \ exp(-ikw) \tag{IV.6}$$

in which the  $\exp(\mathrm{i}\omega t)$ -time dependent term is again omitted, as usual.  $\Psi$  (u, v, w) is a slowly varying unknown function and must be determined. Such a determination will involve spatial derivatives. However, both u and v scale with the (small) radial characteristic length  $w_0$  while conversely w scales with the (large) longitudinal characteristic length l. Rescaled dimensionless coordinates  $(\xi, \eta, \zeta)$  are therefore introduced according to:

$$\xi = \frac{u}{w_0}, \ \eta = \frac{v}{w_0}, \ \zeta = \frac{w}{l} \tag{IV.7}$$

in such a way that rescaled spatial derivatives  $\partial \Psi/\partial \xi$ ,  $\partial \Psi/\partial \eta$  and  $\partial \Psi/\partial \zeta$  now exhibit the same order of magnitude and are assumed to remain small with respect to  $\Psi$  since  $\Psi$  is a slowly varying function.

Within Lorentz gauge, vector potential  $A_u$  must satisfy the Helmholtz equation (Rel (I.119)):

$$\Delta A_u + k^2 A_u = 0 (IV.8)$$

which, by using (IV.6) and (IV.7), provides a partial derivative equation for  $\Psi$ :

$$\left(\frac{\partial^2}{\partial \xi^2} + \frac{\partial^2}{\partial \eta^2}\right) \Psi - 2i \frac{\partial \Psi}{\partial \zeta} + s^2 \frac{\partial^2 \Psi}{\partial \zeta^2} = 0$$
 (IV.9)

The solution for  $\Psi$  is searched by a perturbation procedure in which  $\Psi$  is expressed through a series expansion in terms of powers of  $s^2$ :

$$\Psi = \Psi_0 + s^2 \Psi_2 + s^4 \Psi_4 + \dots$$
 (IV.10)

Note that powers of  $s^2$ , not powers of s, are involved in (IV.10), this being a direct consequence of the structure of Rel (IV.9) which exhibits  $s^0$ - and  $s^2$ -terms.

The lowest-order term  $\Psi_0$  represents the fundamental mode of a Gaussian beam. Using Rel (IV.9), the reader may directly check that it is given by:

$$\Psi_0 = iQ \exp(-iQh_+^2) \tag{IV.11}$$

in which:

$$Q = \frac{1}{i + 2C} \tag{IV.12}$$

$$h_{+}^{2} = \xi^{2} + \eta^{2} \tag{IV.13}$$

in which  $h_{+}$  is therefore the rescaled distance to the beam axis.

Once  $\Psi_0$  is known, Rel (IV.9) shows that higher order functions  $\Psi_{2n}$  ( $n \ge 1$ ), i.e., corrections to the fundamental mode, may be recursively deduced from:

$$\left(\frac{\partial^2}{\partial \xi^2} + \frac{\partial^2}{\partial \eta^2} - 2i\frac{\partial}{\partial \zeta}\right)\Psi_{2n+2} = -\frac{\partial^2}{\partial \zeta^2}\Psi_{2n}, \qquad n \ge 0$$
 (IV.14)

Therefore the fundamental mode  $\Psi_0$  completely determines the vector potential  $A_i$  from which electric and magnetic fields are derived using Rels (I.121), (I.110):

$$E_{i} = -\frac{ic}{k} (grad \ div A_{j})_{i} - i \ \omega \ A_{i}$$

$$H_{i} = (curl A_{j})_{i} / \mu$$
(IV.15)

Rel (IV.15) has been written with the refractive index of vacuum (M=1) because the fields inside the scatterer are written using the refractive index of the scatter center relatively to the surrounding medium (see Rel (I.103) and section III.5).

The field components are then found to be:

$$E_u = E_0 \left[ \Psi_0 + s^2 \left( \Psi_2 + \frac{\partial^2 \Psi_0}{\partial \xi^2} \right) + \dots \right] \quad exp(-ikw)$$
 (IV.16)

$$E_v = E_0 \left[ s^2 \frac{\partial^2 \Psi_0}{\partial \xi \partial \eta} + s^4 \frac{\partial^2 \Psi_2}{\partial \xi \partial \eta} + \dots \right] \quad exp(-ikw)$$
 (IV.17)

$$E_w = E_0 \left[ -is \frac{\partial \Psi_0}{\partial \xi} - is^3 \left( \frac{\partial \Psi_2}{\partial \xi} + i \frac{\partial^2 \Psi_0}{\partial \xi \partial \zeta} \right) + \dots \right] exp(-ikw) \quad \text{(IV.18)}$$

$$H_u = 0 (IV.19)$$

$$H_v = H_0 \left[ \Psi_0 + s^2 \left( \Psi_2 + i \frac{\partial \Psi_0}{\partial \zeta} \right) + \dots \right] \quad exp(-ikw)$$
 (IV.20)

$$H_w = H_0 \left[ -is \frac{\partial \Psi_0}{\partial \eta} - is^3 \frac{\partial \Psi_2}{\partial \eta} + \dots \right] \quad exp(-ikw)$$
 (IV.21)

Let us consider the special case of a plane wave for which  $s \to 0$ . Then, Rels (IV.16), (IV.20), and (I.107) show that we must have:

$$E_0/H_0 = E_{u, \text{ plane wave}}/H_{v, \text{ plane wave}} = \sqrt{\mu/\epsilon}$$
 (IV.22)

# IV.1.5 The Order L of Approximation

Relations (IV.16)–(IV.21) offer the possibility of obtaining a Gaussian beam description with arbitrary increasing accuracy. Since the beam shape factor s is small, and even usually very small, it is in practice sufficient in most cases to retain only a few terms in the expansions. In particular, neglecting all terms with powers greater than 1, Rels (IV.16)–(IV.21) supplemented with Rels (IV.11)–(IV.13) become:

$$E_v = H_u = 0 (IV.23)$$

$$E_u = E_0 \, \Psi_0 \, \exp(-ikw) \tag{IV.24}$$

$$E_w = -\frac{2Qu}{l}E_u \tag{IV.25}$$

$$H_v = H_0 \ \Psi_0 \ exp(-ikw) \tag{IV.26}$$

$$H_w = -\frac{2Qv}{l}H_v \tag{IV.27}$$

These relations define what we have called the order L of approximation to the Gaussian beam description in which L stands for the lowest-order of approximation (see also the alternative form of Rels (IV.32)–(IV.36)). Strictly speaking, however, the order L is not the lowest-order but it does provide the lowest-order which remains valid with the same relative degree of accuracy in the whole space in a sense to be precised in section IV.1.8. Conversely, it may still be useful to consider the case when the beam shape factor is not small enough to allow the use of the lowest-order description. Discussions of higher-order Gaussian beams are then available from Barton and Alexander [309], Schaub et al, [310], Lock and Gouesbet [79], [80], Gouesbet et al [297], Gouesbet [311].

# IV.1.6 The Order $L^-$ of Approximation

At the order L of approximation, the non-zero field components are the transverse components  $E_u$  and  $H_v$  as for a plane wave, plus extra longitudinal components  $E_w$  and  $H_w$ . To determine whether the influence of the extra

components is significant, we may consider the ratios of longitudinal and transverse components reading as:

$$(E_w/E_u, H_w/H_v) = -2 Q s (\xi, \eta)$$
 (IV.28)

The modulus of Q depends only on  $\zeta$  (see IV.12), but is always smaller than 1 except at the waist plane ( $\zeta = 0$ ) where it is just equal to one. Furthermore s is a small parameter. It follows that longitudinal components may be neglected with respect to transverse ones as long as  $\xi$  and  $\eta$  are not too high, i.e., in a domain of space around the beam axis. Even when the longitudinal components may not be neglected relatively to transverse components, they may, however, become absolutely neglected due to the exponential decrease involved in the fundamental function  $\Psi_0$ , i.e., the amount of incident energy associated with both transverse and longitudinal components tend to vanish very fast when we depart from the beam axis.

Let us for instance consider the ratio  $|E_w/E_u|$  for a point located in the waist plane  $\zeta=0$  at which Q=1/i. This ratio is then equal to  $2s|\xi|$ . The relative significance of  $E_w$ , therefore, increases linearly with  $|\xi|$ . With a typical value  $s\approx 10^{-3}$ , the ratio, however, becomes equal to 1 % only for  $|\xi|=5$ , i.e., for planes cutting the u-axis at values of |u| equal to five times the beam radius. However, in the considered waist plane, the ratio  $|E_u/E_0|$  simply reads as:

$$|E_u/E_0| = exp\{-(\xi^2 + \eta^2)\}\$$
 (IV.29)

which takes over its largest values  $\exp(-\xi^2)$  for  $\eta = 0$ . This quantity is equal to  $e^{-25} \approx 10^{-11}$  in planes  $|\xi| = 5$  while the ratio  $|E_w/E_0|$  is then  $\approx 10^{-13}$ , corresponding to very small fields which are not expected to significantly affect scattering phenomena.

It is then concluded that an approximation lower than the lowest-order L, designated by  $L^-$  (a fairly pejorative terminology indeed), in which longitudinal field components are neglected, may be safely introduced. Therefore, field components at order  $L^-$  read as:

$$E_v = H_u = E_w = H_w = 0$$
 (IV.30)

$$\begin{pmatrix} E_u \\ H_v \end{pmatrix} = \begin{pmatrix} E_0 \\ H_0 \end{pmatrix} \Psi_0 \ exp(-ikw) \tag{IV.31}$$

In the framework of Davis formulation, the order  $L^-$  is obtained by neglecting all terms with powers higher than 0, i.e. the small parameter s does not appear any more at that order. This approximation has been used by  $\blacksquare$  in which the corresponding modelled laser beam was called an axisymmetric profile beam. Such a name has been afterwards given up because it is confusing (but see section VI.1).

Formulae at order L are clearly obtained from formulae at order  $L^-$  by adding extra-terms which are specific of the order L. To identify them

precisely, we shall use a double-valued symbol  $\epsilon_L$  which is equal to 0 or 1 depending on whether the beam is modelled at order  $L^-$  or L, respectively. With this notation (particularly convenient in Fortran programs to determine the influence of the quality of the beam model), field components at both orders may be rewritten as:

$$E_v = H_u = 0 (IV.32)$$

$$E_u = E_0 \, \Psi_0 \, \exp(-ikw) \tag{IV.33}$$

$$E_w = -\epsilon_L \, \frac{2Qu}{l} \, E_u \tag{IV.34}$$

$$H_v = H_0 \, \Psi_0 \, \exp(-ikw) \tag{IV.35}$$

$$H_w = -\epsilon_L \, \frac{2Qv}{l} \, H_v \tag{IV.36}$$

### IV.1.7 Kogelnik's Model

In this subsection, the relationship between the celebrated Kogelnik's formulation ([300], [301], [302], [303]) and the Davis formulation is investigated. Such a subsection is certainly compulsory due to the widespread use of Kogelnik's formulae. Our discussion focuses on the examination of electric field components. A discussion of magnetic field components would be fully similar and would not modify the conclusions of this subsection.

The expression for the  $E_u$ -component is the same at both orders L and  $L^-$  (Rel (IV.33) in which the symbol  $\epsilon_L$  does not appear). We start by modifying this expression, introducing the dimensional distance h to the beam axis, and two special lengths W and R according to:

$$h^2 = u^2 + v^2 = w_0^2 h_+^2$$
 (IV.37)

$$W = w_0 (1 + 4\zeta^2)^{1/2} = w_0 \left[ 1 + 4 \frac{w^2}{k^2 w_0^4} \right]^{1/2}$$
 (IV.38)

$$R = w \left( 1 + \frac{1}{4\zeta^2} \right) = w \left[ 1 + \frac{k^2 w_0^4}{4w^2} \right]$$
 (IV.39)

Then  $(i \ Q)$  can be re-expressed from (IV.12), (IV.7) and (IV.4) as:

$$iQ = w_0^2 \left[ \frac{1}{W^2} + \frac{ik}{2R} \right] \tag{IV.40}$$

Inserting these expressions into (IV.11) for  $\Psi_0$ , component  $E_u$  (IV.33) becomes:

$$E_u = E_0 \ w_0^2 \left[ \frac{1}{W^2} + \frac{ik}{2R} \right] \ exp \left[ -h^2 \left( \frac{1}{W^2} + \frac{ik}{2R} \right) \right] \ exp(-ikw)$$
 (IV.41)

This expression shows that W is the beam radius (or spot-size parameter) at longitudinal location w at amplitude 1/e. R is the radius of curvature of the wavefront at location w. It is of interest to remark from (IV.38)–(IV.39) that at the waist location (w = 0), we have  $W = w_0$  and the wavefront is plane ( $R \to \infty$ ), agreeing with previous statements, in particular in section (IV.1.2).

After some algebra, (IV.41) may be rewritten as:

$$\frac{E_u}{E_0} = \frac{w_0}{W} \exp\left[-h^2\left(\frac{1}{W^2} + \frac{ik}{2R}\right)\right] \exp(i\Lambda) \exp(-ikw) \tag{IV.42}$$

in which we introduced a phase term  $\Lambda$  given by:

$$\Lambda = \tan^{-1} \frac{w \lambda}{\pi w_0^2} = \tan^{-1} \frac{2w}{kw_0^2}$$
 (IV.43)

This agrees with classical Kogelnik's expressions except for the fact that the term  $(i \ \Lambda)$  in (IV.42) is written as  $(-i \ \Lambda)$  in [303]. This is likely to be a misprint. Furthermore, in Kogelnik's study,  $E_0$  is explicitly assigned the value (-ik). However, no value is assigned to  $E_0$  in Davis formulation and, in any case, it actually disappears from the GLMT-formulation due to the introduction of the normalizing condition (III.106). The conclusion is, therefore, that Kogelnik formulation is equivalent to the description of the beam in Davis framework at order  $L^-$ . The order L may then been afterwards obtained by adding longitudinal components  $E_w$  and  $H_w$ .

### IV.1.8 Inaccuracies at Orders L and $L^-$

Maxwell's equations can only be perfectly satisfied by the field components in the limit of an infinite expansion of function  $\Psi$  in Rel (IV.10) when we strictly work in the framework of Davis formulation (see [311], showing how we may both rely on and escape from this formulation). Therefore, at orders L and  $L^-$ , inconsistencies are inevitably introduced in the theory because Rels (IV.32)–(IV.36) do not satisfy Maxwell's equations. It may then be of interest to examine by a direct checking the amount of relative errors which is anchored in the theory due to this fact. This problem has been discussed by Gouesbet et al [308] in the framework of GLMT. Computations in this reference are difficult, lengthy and very involved, and therefore not reproduced in this book. In this subsection, we shall serve a simpler version which is sufficient to meet our purpose. The description of the beam is carried

out in the beam coordinate system  $(O_G uvw)$ . The beam existing, however, in Newtonian space independently of the chosen space parametrization, our conclusions will still remain valid for any other parametrization, in particular, in the particle coordinate system  $(O_P xyz)$ . The discussion starts by considering the order L of approximation  $(\epsilon_L = 1)$ .

The first Maxwell's equation (I.56) for exp ( $i\omega t$ )-sinusoidal waves, i.e.:

$$(curl E_i)_i = -i \ \mu \ \omega \ H_i \tag{IV.44}$$

reads as:

$$H_{i} = \begin{vmatrix} H_{u} \\ H_{v} \\ H_{w} \end{vmatrix} = -\frac{1}{i\mu\omega} \begin{vmatrix} \frac{\partial E_{w}}{\partial v} - \frac{\partial E_{v}}{\partial w} \\ \frac{\partial E_{w}}{\partial v} - \frac{\partial E_{w}}{\partial u} \\ \frac{\partial E_{w}}{\partial v} - \frac{\partial E_{u}}{\partial v} \end{vmatrix}$$
(IV.45)

From Rels (IV.33) and (IV.34), the first component  $H_u$  of  $H_i$  is then found to be:

$$H_u = -\frac{1}{i\mu\omega} \frac{\partial E_w}{\partial v} \tag{IV.46}$$

which becomes:

$$H_u = \frac{E_0}{i\mu\omega} \frac{2Qu}{l} \frac{\partial \Psi_0}{\partial v} \exp(-ikw)$$
 (IV.47)

In terms of dimensionless quantities, (IV.47) is found to be:

$$H_u = -4 H_0 s^2 Q^2 \eta \xi \Psi_0 \exp(-ikw)$$
 (IV.48)

while it should be zero according to Rel (IV.32), i.e. the error is:

$$\epsilon_u = H_u = -4 H_0 s^2 Q^2 \eta \xi \Psi_0 \exp(-ikw)$$
 (IV.49)

Similarly, from (IV.45), the second component  $H_v$  is found to be:

$$H_v = \frac{E_0}{i\mu\omega} \left[ ik\Psi_0 - \frac{\partial\Psi_0}{\partial w} - \frac{2Q}{l} \left( \Psi_0 + u \frac{\partial\Psi_0}{\partial u} \right) \right] \exp(-ikw)$$
 (IV.50)

instead of (IV.35). The error is:

$$\epsilon_v = \frac{E_0}{i\mu\omega} \left[ \frac{\partial \Psi_0}{\partial w} + \frac{2Q}{l} \left( \Psi_0 + u \frac{\partial \Psi_0}{\partial u} \right) \right] \exp(-ikw)$$
 (IV.51)

which becomes, with dimensionless variables:

$$\epsilon_v = 2 \ H_0 \ s^2 \ Q^2 \ \Psi_0 \ [-2\xi^2 + h_+^2] exp(-ikw)$$
 (IV.52)

For the third component  $H_w$ , we find from (IV.45), (IV.32) and (IV.33):

$$H_w = -\frac{2Qv}{l} H_v \tag{IV.53}$$

which is identical to (IV.36), leading to an error:

$$\epsilon_w = 0 \tag{IV.54}$$

In summary, the error implied using the order L of approximation is zero for the third component of (IV.45). For the second component, it is  $\epsilon_v \approx O(s^2)$ . Using the expression (IV.35) for  $H_v$ , it is possible to define a relative error:

$$\delta_v = \frac{\epsilon_v}{H_v} = 2 \ s^2 \ Q^2 \ (2\xi^2 - h_+^2) \tag{IV.55}$$

which is also  $O(s^2)$ . For  $\epsilon_u$ , we again find  $O(s^2)$ . It is, however, not possible to define a relative error  $\delta_u = \epsilon_u/H_u$  because  $H_u = 0$  according to Rel (IV.32). Nevertheless, using the leading component  $H_v$ , we may consider:

$$\delta_u = \frac{\epsilon_u}{H_v} = 4 \ s^2 \ Q^2 \ \eta \ \xi \tag{IV.56}$$

which is again  $O(s^2)$ . As a whole, the most significant relative errors are, therefore,  $O(s^2)$ . Similar conclusions are obtained when discussing the three other Maxwell's equations (I.57)–(I.59). Working out details is left as an exercise to the reader. It is found that Rel (I.58) is similarly satisfied with maximal relative errors which are  $O(s^2)$ . For Rels (I.57) and (I.59) involving divergences, absolute errors are  $O(s^3)$ , that is to say they are still smaller. Relative errors may be defined with respect to  $H_v$  and  $E_u$  respectively. They are also found to be  $O(s^3)$ .

In the limit  $s \to 0$ , it is, therefore, directly checked that field components satisfy all Maxwell's equations at order L (actually also at all higher orders). In the theoretical limit  $s \approx 0.25$  (section IV.1.2),  $s^2$  is  $\approx 5.10^{-2}$ . Therefore, the order L of approximation provides a very good description of the incident beam with uniform relative errors in the whole space which are at worst  $O(s^2)$ . With a typical value  $s \approx 10^{-3}$ , relative errors concerning divergence terms even go down to  $\approx 10^{-9}$ . These remarks justify that we are content in the most of this book to insist on the GLMT for Gaussian beams at the order L of approximation (and at the order  $L^-$  as a special case of the order L). Let us remark however that, when we depart from the beam waist center location, errors grow due to the existence of prefactors depending on rescaled coordinates. It is also recalled that, by adding further terms to Davis expansions, the description may be arbitrarily refined. We, however, insist again on the fact that this would not modify the GLMT-framework.

For more information concerning inaccuracies at order L, the reader could refer to Gouesbet et~al~[308] in which the discussion relies on a somewhat different principle. More specifically, Gouesbet et~al~[308] consider the special case when the beam and the particle coordinate systems coincide  $(O_p \equiv O_G)$ . There is no loss of generality in choosing such a special case to discuss inaccuracies but there is a formal interest because the GLMT-formulation then dramatically simplifies (see chapter VI). Contrary to what has been

done in this subsection, errors involved in the theory were also discussed by examining field components  $E_r$ ,  $E_\theta$ ,  $E_\varphi$ ,  $H_r$ ,  $H_\theta$ ,  $H_\varphi$  in a spherical coordinate system. For each field component  $\phi_i$ , a comparison was carried out between a value  $\phi_i^1$  obtained from projections using the original set (IV.32)–(IV.36) and another one  $\phi_i^2$  obtained in the GLMT-framework from BSPs. Because the set (IV.32)–(IV.36) does not perfectly satisfy Maxwell's equations, it is expected that, in general,  $\phi_i^1 \neq \phi_i^2$ . For radial components  $E_r$  and  $H_r$  however, the errors are found to be exactly zero. This is a direct consequence of the fact that these field components play a special role in the GLMT because they are the only ones to be used to evaluate the BSCs (section III.3). For  $\theta$ - and  $\varphi$ -components, relative errors are again found to be  $O(s^2)$  uniformly in space, confirming that introduced inconsistencies have no practical significance in most cases.

The case of order  $L^-$  is also discussed in 308. The conclusion is that the order  $L^-$  is also very good. This fact is emphasized in our discussion of section (IV.1.6). As done above at order L, it may also be examined as to how Maxwell's equations behave with respect to the order  $L^-$ . This is left as another exercise to the reader. For Maxwell's equations involving divergences, it is found that relative errors are O(s) instead of  $O(s^3)$  at order L. For the two other Maxwell's equations, the worst relative errors are also found to be O(s) instead of  $O(s^2)$  at order L. As numerical computations will later show differences between orders L and  $L^-$  are usually not significant. Even when the order L provides a refinement, this confirms that working with higher orders than L is very often (but not always) unnecessary. For higher order descriptions of Gaussian beams, see again, however, the previously quoted references, and section IV.4.

#### IV.2 GLMT at Orders L and $L^-$

# IV.2.1 Radial Field Components $E_r$ and $H_r$

To specify the GLMT to the case of Gaussian beams at orders L and  $L^-$ , it is only needed to specify the values of the BSCs  $g_{n,TM}^m$  and  $g_{n,TE}^m$  for this case. This in turn only requires to know the expressions for the radial field components  $E_r$  and  $H_r$  (Rels (III.14), (III.17), (III.21), (III.22)) which must, however, be expressed in a spherical coordinate system attached to the particle Cartesian coordinate system  $(O_p xyz)$ . The aim of this subsection is to derive the required expressions for  $E_r$  and  $H_r$ .

Starting from Cartesian field components (IV.32)–(IV.36) in the Cartesian coordinate system  $(O_G uvw)$  attached to the beam, Cartesian field components in the particle system  $(O_p xyz)$  are found to be:

$$E_y = H_x = 0 (IV.57)$$

$$E_x = E_0 \Psi_0 \exp[-ik(z - z_0)]$$
 (IV.58)

$$E_z = -\epsilon_L \frac{2Q}{l} (x - x_0) E_x \qquad (IV.59)$$

$$H_y = H_0 \Psi_0 \exp[-ik(z - z_0)]$$
 (IV.60)

$$H_z = -\epsilon_L \, \frac{2Q}{l} (y - y_0) H_y \tag{IV.61}$$

in which  $\Psi_0$  is again given by Rel (IV.11), but now:

$$h_{+}^{2} = \frac{1}{w_{0}^{2}} [(x - x_{0})^{2} + (y - y_{0})^{2}]$$
 (IV.62)

$$Q = \frac{1}{i + 2(\zeta - \zeta_0)} \tag{IV.63}$$

$$\zeta = \frac{z}{l}, \zeta_0 = \frac{z_0}{l} \tag{IV.64}$$

The relations between Cartesian and spherical components of the electric and magnetic fields read as:

$$E_r = E_x \cos\varphi \sin\theta + E_z \cos\theta \tag{IV.65}$$

$$E_{\theta} = E_x \cos \varphi \cos \theta - E_z \sin \theta \tag{IV.66}$$

$$E_{\varphi} = -E_x \sin \varphi \tag{IV.67}$$

$$H_r = H_u \sin\varphi \sin\theta + H_z \cos\theta \tag{IV.68}$$

$$H_{\theta} = H_y \sin\varphi \cos\theta - H_z \sin\theta \tag{IV.69}$$

$$H_{\varphi} = H_{u} cos \varphi \tag{IV.70}$$

leading to:

$$E_r = E_0 \Psi_0 \left[ \cos\varphi \sin\theta \left( 1 - \epsilon_L \frac{2Q}{l} r \cos\theta \right) + \epsilon_L \frac{2Q}{l} x_0 \cos\theta \right] \exp(K)$$
(IV.71)

$$E_{\theta} = E_{0}\Psi_{0} \left[ \cos\varphi \left( \cos\theta + \epsilon_{L} \frac{2Q}{l} r \sin^{2}\theta \right) - \epsilon_{L} \frac{2Q}{l} x_{0} \sin\theta \right] \exp(K)$$
(IV.72)

$$E_{\varphi} = -E_0 \, \Psi_0 \, \sin\varphi \, \exp(K) \tag{IV.73}$$

$$H_r = H_0 \Psi_0 \left[ \sin\varphi \, \sin\theta \left( 1 - \epsilon_L \frac{2Q}{l} \, r \, \cos\theta \right) + \epsilon_L \frac{2Q}{l} \, y_0 \, \cos\theta \right] \exp(K)$$
(IV.74)

$$H_{\theta} = H_{0}\Psi_{0} \left[ sin\varphi \left( cos\theta + \epsilon_{L} \frac{2Q}{l} r sin^{2}\theta \right) - \epsilon_{L} \frac{2Q}{l} y_{0} sin\theta \right] exp(K)$$
(IV.75)

$$H_{\varphi} = H_0 \, \Psi_0 \, \cos\varphi \, \exp(K) \tag{IV.76}$$

in which:

$$K = -ik(r\cos\theta - z_0) \tag{IV.77}$$

The  $E_r$  and  $H_r$  expressions (IV.71) and (IV.74) could then be inserted in Rels (III.14), (III.17), (III.21), and (III.22). However, it is in practice useful to elaborate a bit more on Rels (IV.71), (IV.74), in particular because variable  $\varphi$  may be easily isolated, and, therefore,  $\varphi$ -integrations may be readily carried out analytically.

In Rels (IV.71), (IV.74), variable  $\varphi$  explicitly appears in  $\cos\varphi$  and  $\sin\varphi$ , but it is also involved in function  $\Psi_0$  which may be rewritten as:

$$\Psi_0 = \Psi_0^0 \Psi_0^{\varphi} \tag{IV.78}$$

$$\Psi_0^0 = iQexp(-iQ\frac{r^2sin^2\theta}{w_0^2})exp(-iQ\frac{x_0^2 + y_0^2}{w_0^2})$$
 (IV.79)

$$\Psi_0^{\varphi} = exp\left[\frac{2iQ}{w_0^2}rsin\theta(x_0cos\varphi + y_0sin\varphi)\right]$$
 (IV.80)

in which  $\Psi_0^0$  does not depend on  $\varphi$ . The  $\varphi$ -dependent term  $\Psi_0^{\varphi}$  is then modified by replacing the functions sin and cos by exponentials of imaginary arguments, expanding the resulting exponentials, and finally expanding again terms of the form  $(a+b)^j$  to directly obtain a Fourier expansion:

$$\Psi_0^{\varphi} = \sum_{jp} \Psi_{jp} exp[i\varphi(j-2p)]$$
 (IV.81)

with the notations:

$$\sum_{j=0}^{jp} = \sum_{n=0}^{\infty} \sum_{p=0}^{j}$$
 (IV.82)

$$\Psi_{jp} = \left(\frac{iQrsin\theta}{w_0^2}\right)^j \frac{(x_0 - iy_0)^{j-p}(x_0 + iy_0)^p}{(j-p)! \ p!}$$
(IV.83)

In Gouesbet et~al [298], another procedure was used to expand  $\Psi_0^{\varphi}$ , leading to the appearance of quadruple summations  $\sum^{jplt}$  instead of double summations  $\sum^{jp}$  in (IV.81). Both formulations are actually equivalent but the one in Gouesbet et~al [298] is more complicated than necessary. As a matter of fact, the reader may also consult [298] to find a pedagogic method for expressing BSPs  $U_{TM}^i$  and  $U_{TE}^i$ . This method has not been repeated in this book.

From Rels (IV.71), (IV.74), and (IV.78)–(IV.83), the radial components  $E_r$  and  $H_r$  may be rewritten as:

$$E_{r} = E_{0} \frac{F}{2} \left[ \sum_{jp} \Psi_{jp} exp(ij_{+}\varphi) + \sum_{jp} \Psi_{jp} exp(ij_{-}\varphi) \right] + E_{0}x_{0}G \sum_{jp} \Psi_{jp} exp(ij_{0}\varphi)$$
(IV.84)

$$H_r = H_0 \frac{F}{2i} \left[ \sum_{jp} \Psi_{jp} exp(ij_+\varphi) - \sum_{jp} \Psi_{jp} exp(ij_-\varphi) \right] + H_0 y_0 G \sum_{jp} \Psi_{jp} exp(ij_0\varphi)$$
(IV.85)

in which:

$$F = \Psi_0^0 \sin\theta (1 - \epsilon_L \frac{2Q}{l} r \cos\theta) \exp(K)$$
 (IV.86)

$$G = \epsilon_L \Psi_0^0 \frac{2Q}{l} cos\theta exp(K)$$
 (IV.87)

$$j_{+} = j + 1 - 2p = j_0 + 1$$
 (IV.88)

$$j_{-} = j - 1 - 2p = j_0 - 1$$
 (IV.89)

# IV.2.2 Beam Shape Coefficients

# Gaussian Beam Shape Coefficients

Insertion of (IV.84) and (IV.85) into double quadrature expressions (III.14) and (III.21), and integration over  $\varphi$ , simplify the expressions of the BSCs to single quadratures over  $\theta$  according to:

$$g_{n,TM}^{m} = \frac{1}{c_{n}^{pw}} \frac{(2n+1)}{2n(n+1)} \frac{(n-|m|)!}{(n+|m|)!} \frac{a}{\Psi_{n}^{(1)}(ka)}$$

$$\int_{0}^{\pi} \left\{ \frac{F(r=a)}{2} \left( \sum_{j_{+}=m}^{jp} \Psi_{jp}(r=a) + \sum_{j_{-}=m}^{jp} \Psi_{jp}(r=a) \right) + x_{0}G(r=a) \sum_{j_{0}=m}^{jp} \Psi_{jp}(r=a) \right\} P_{n}^{|m|}(\cos\theta) \sin\theta d\theta$$
(IV.90)

$$g_{n,TE}^{m} = \frac{1}{c_{n}^{pw}} \frac{(2n+1)}{2n(n+1)} \frac{(n-|m|)!}{(n+|m|)!} \frac{a}{\Psi_{n}^{(1)}(ka)}$$

$$\int_{0}^{\pi} \left\{ \frac{iF(r=a)}{2} \left( -\sum_{j_{+}=m}^{jp} \Psi_{jp}(r=a) + \sum_{j_{-}=m}^{jp} \Psi_{jp}(r=a) \right) + y_{0}G(r=a) \sum_{j_{0}=m}^{jp} \Psi_{jp}(r=a) \right\} P_{n}^{|m|}(\cos\theta) \sin\theta d\theta$$
(IV.91)

Similarly, BSCs may be evaluated by double quadratures over  $\theta$  and r by inserting (IV.84) and (IV.85) into triple quadrature expressions (III.17), (III.22) and integrating over  $\varphi$ :

$$g_{n,TM}^{m} = \frac{1}{c_{n}^{pw}} \frac{(2n+1)^{2}}{\pi n(n+1)} \frac{(n-|m|)!}{(n+|m|)!} \int_{0}^{\pi} \int_{0}^{\infty} \left\{ \frac{F}{2} \left( \sum_{j+=m}^{jp} \Psi_{jp} + \sum_{j-=m}^{jp} \Psi_{jp} \right) + x_{0} G \sum_{j_{0}=m}^{jp} \Psi_{jp} \right\} r \Psi_{n}^{(1)}(kr) P_{n}^{|m|}(\cos\theta) \sin\theta \, d\theta \, d(kr) \quad (IV.92)$$

$$g_{n,TE}^{m} = \frac{1}{c_{n}^{pw}} \frac{(2n+1)^{2}}{\pi n(n+1)} \frac{(n-|m|)!}{(n+|m|)!} \int_{0}^{\pi} \int_{0}^{\infty} \left\{ \frac{iF}{2} \left( -\sum_{j_{+}=m}^{jp} \Psi_{jp} + \sum_{j_{-}=m}^{jp} \Psi_{jp} \right) + y_{0}G \sum_{j_{0}=m}^{jp} \Psi_{jp} \right\} r \Psi_{n}^{(1)}(kr) P_{n}^{|m|}(\cos\theta) \sin\theta \ d\theta \ d(kr)$$
 (IV.93)

In the whole set (IV.90)–(IV.93), the symbol  $\sum_{c}^{jp}$  designates sum  $\sum_{c}^{jp}$  restricted to condition c. Such double summations  $\sum_{c}^{jp}$  may be reduced to single summations (see chapter V).

In Gouesbet and Gréhan  $\square$  devoted to a special case, special BSCs  $g_n$  were introduced (with only one subscript, see chapter VI). These coefficients were expressed in terms of a matrix  $K_{nm}$  (Rel (34), in  $\square$ ) which, in the limit

of the classical Lorenz-Mie theory, identifies with the Kronecker matrix  $\delta_{nm}$ . Such a smart correspondence between GLMT and LMT is also likely to exist for the BSCs  $g_n^m$ . After having read chapter VI, the interested reader might try to design it. We never did.

### Remodelling of Gaussian beams

At both orders L and  $L^-$ , Gaussian beams may be described by the set (IV.57)–(IV.61) in Cartesian coordinates or by the set (IV.71)–(IV.76) in spherical coordinates. As we know (section IV.1.8), these sets of field components do not satisfy Maxwell's equations.

BSCs may afterward be evaluated, producing non-constant contributions due to the inaccuracy of the original description. The origin of these non-constant artefacts being well understood, they may safely be dismissed to generate BSCs which are constants, as they should. Then, once these constant BSCs and therefore the BSPs  $U_{TM}^i$  and  $U_{TE}^i$  are determined, the GLMT-framework provides a new set of field components in spherical coordinates by adding TM- and TE-contributions ([see Rels (III.39)–(III.50)]) from which we may readily also derive a new set of field components in Cartesian coordinates. The beams so generated are shaped beams in their own right, however now exactly satisfying Maxwell's equations. Therefore, they are not equivalent to the original ones. Because they satisfy Maxwell's equations while the original fields do not, it is possible to claim that the GLMT framework produces a remodelling (or reshaping) of the beam description. See Lock and Gouesbet [79], Gouesbet and Lock [80] and Gouesbet et al [297] for more details on this issue.

#### Symmetries

Relying on the remodelled description of the beam, we now discuss some symmetries which appear in the GLMT for Gaussian beams. We consider two particle locations, symmetrical with respect to the beam axis (Fig. III.1). These two locations are connected by the following change in the  $(x_0, y_0, z_0)$ -values:

$$(x_0, y_0, z_0) \xrightarrow{T} (-x_0, -y_0, z_0)$$
 (IV.94)

From (IV.83), we find:

$$\Psi_{jp}(-x_0, -y_0, z_0) = (-1)^j \Psi_{jp}(x_0, y_0, z_0)$$
 (IV.95)

From (IV.92) and (IV.93), accounting for (IV.95), we then establish:

$$\begin{pmatrix} g_{n,TM}^m \\ g_{n,TE}^m \end{pmatrix} (-x_0, -y_0, z_0) = (-1)^{m-1} \begin{pmatrix} g_{n,TM}^m \\ g_{n,TE}^m \end{pmatrix} (x_0, y_0, z_0)$$
 (IV.96)

From (IV.96) and the expressions for the various cross sections established in section III, we finally show that:

$$\begin{pmatrix}
C_{sca} \\
C_{ext} \\
C_{abs} \\
C_{pr,z}
\end{pmatrix} (-x_0, -y_0, z_0) = \begin{pmatrix}
C_{sca} \\
C_{ext} \\
C_{abs} \\
C_{pr,z}
\end{pmatrix} (x_0, y_0, z_0)$$
(IV.97)

but:

$$\begin{pmatrix} C_{pr,x} \\ C_{pr,y} \end{pmatrix} (-x_0, -y_0, z_0) = -\begin{pmatrix} C_{pr,x} \\ C_{pr,y} \end{pmatrix} (x_0, y_0, z_0)$$
 (IV.98)

An extensive discussion of symmetry properties in GLMT is available from Ren  $et\ al\ 312$ .

# IV.3 Numerical Computations of Beam Shape Coefficients by Using Quadratures

To avoid to the GLMT of remaining an object of pure spiritual contemplation, computer programs are also provided in this book. Numerical computations of BSCs using quadratures are considered. Although the computer programs are specified for Gaussian beams, at orders L and  $L^-$ , they are actually written to easily handle arbitrary beams by modifying a subroutine devoted to the evaluation of quadrature kernels, and could, therefore, have been also included in chapter III (Nobody's perfect !).

We provide routines to evaluate the BSCs  $g_{n,TM}^m$  or  $g_{n,TE}^m$  using triple quadratures of Rel (III.17) or Rel (III.22). They may be used for arbitrary beams once the expressions for the radial electric or magnetic components  $E_r$  or  $H_r$  are known. The expressions for  $E_r$  or  $H_r$  are written in the function FUNC. It is here specified for the case of Gaussian beams, but it is a child game to change it to any other case.

We recall that quadrature techniques (F1- and F2- formulations) are discussed by Gouesbet  $et\ al\ 134$ .

#### IV.4 Other Beams

In the bulk of this chapter, we provided details on the orders L and  $L^-$  of approximations to the description of Gaussian beams, and also alluded to other descriptions and to other beams. In this complement, we provide more information concerning other beams, including higher-order Gaussian beams. This issue pertains to the problem concerning the description of illuminating beams. However, there are actually two issues to be considered concerning the beam description (i) the coordinate system in which the beam is described, associated with the kind of scatterer under study and (ii) the kind of beam illuminating the scatterer, independently of the kind of scatterer.

IV.4 Other Beams 109

In this complement, we rather focus on the second issue, but both issues are actually strongly coupled together. For instance, a Gaussian beam (independently of the scatterer) may have to be described in spherical, cylindrical or spheroidal... coordinates (depending on the scatterer).

### Higher-order Gaussian beams

The order L of approximation is explicitly described by Davis [75] and is now called a first-order description. Explicit higher-order descriptions (thirdand fifth-order descriptions), in the framework of the Davis scheme, have afterwards been explicitly developed by Barton and Alexander 309. These higher-order beams have been used by Lock and Gouesbet [79] to provide a rigorous justification of the localized approximation to the beam shape coefficients, in the case of on-axis Gaussian beams. A way to assess the accuracy of the various description orders is to examine to which order with respect to the beam shape factor s they are accurate i.e. to which order with respect to s they satisfy Maxwell's equations. This depends on the processes used to handle the higher-order Davis-Barton beams. Lock and Gouesbet introduced three variants (i) the mathematically conservative version (ii) the L-type, and (iii) the symmetrized variant, and examined the accuracy of the Davis-Barton description for each variant. Without giving here details which would be too technical for a complement, let us mention that (see Table 1, in [79]), in a precise sense, the symmetrized version is accurate up to  $O(s^2)$ ,  $O(s^6)$ , and  $O(s^{10})$  included for first-order, third-order, and fifth-order beams, respectively. The case of off-axis Gaussian beams is discussed in a companion article 80. As a sequel of these studies, standard representations of Gaussian beams (standard beams) are discussed by Gouesbet et al [297] in which it is claimed that standard beams should be taken as the ideal description of Gaussian beams. Higher-order descriptions of Gaussian beams are also discussed by Gouesbet [311]. In this article, it is recalled that the first-, third- and fifth-order beams of the standard description identify with the corresponding beams in the Davis framework, or more specifically with those contributions in the Davis framework that exactly satisfy Maxwell's equations. However, furthermore, the standard description is known at all s-orders. Converting this standard description from spherical coordinates to Cartesian coordinates provides a new way to describe higher-order Gaussian beams. Converting afterwards from Cartesian to cylindrical coordinates then provide higher-order descriptions which may be used to discuss the GLMT for cylinders. Also, in the process, field expressions which can be easily obtained up to any desired s-order using simple differential operators are provided. Next, an exact description of arbitrary shaped beams for use in light scattering theories is provided by Gouesbet [313], with, however, some emphasis on Gaussian beams, in particular on standard beams. An improved standard beam representation is available from Polaert et al [314], exhibiting an infinite radius of convergence in contrast with what has been eventually observed with standard beams [315]. Furthermore, Barton considered electromagnetic field calculations for a sphere illuminated by a higher-order Gaussian beam, namely Hermite-Gaussian beams and doughnut beams [316], [317]. A fifth-order beam (and the localized approximation) is invoked by Evers et al [318] to discuss the extension of a computer program.

#### Laser sheets

A laser sheet (or elliptical Gaussian beam) may be realized by focusing a Gaussian beam with a cylindrical lens. Loosely speaking, laser sheets are Gaussian in two orthogonal directions. Instead of possessing one single beam waist radius  $w_0$ , they possess two beam waist radii, say  $w_{0x}$  along  $O_x$  and  $w_{0y}$  along  $O_y$ . The simpler case of Gaussian beam is recovered from a laser sheet under the condition  $w_{0x} = w_{0y}$ . Laser sheets have been used in various configurations, in particular in the field of optical particle characterization, hence a motivation to study them.

Laser sheet scattering by spherical particles has, therefore, been studied by Ren et al, in a GLMT framework [292]. To evaluate the beam shape coefficients, the localized approximation procedure valid for Gaussian beams has been empirically transferred to the case of laser sheets, and the validity of this transfer has been checked against computations carried out using quadratures. Scattering diagrams are exhibited for the case of a particle at the beam waist center, and also for off-axis particle location. Scatterings by plane waves, Gaussian beams, and laser sheets are compared. Complementary results concerned extinction cross sections and radiation pressure forces. The evaluation of a particle sizing technique (dual-cylindrical wave system) based on laser sheets is thereafter carried out by Gréhan et al [293], following previous proposals for the use of laser sheets in optical particle sizing by Naqwi et al [291], and by Naqwi and Durst [319]. The evaluation of laser sheet beam shape coefficients by use of a localized approximation is discussed by Ren et al [294]. The order of approximation involved in the electromagnetic field expression of a laser sheet is examined [320], generalizing a previous similar study carried out for the case of Gaussian beams [77]. Symmetry relations in laser sheets are discussed by Ren et al [312]. Laser sheets have also been discussed with respect to the use of the integral localized approximation [135], and have been implemented in a GLMT-based imaging mathematical model 321, 322, 323. They are used by Zhang et al 324 to simulate the behavior of a particle passing in a laser gradient field. The interaction between laser sheets and spheroids is discussed by Xu et al in a GLMT-framework [273], while Venkatapathi and Hirleman [222] dealt with the interaction between laser sheets and infinite cylinders, in a GLMT-framework too.

#### Top-hat beams

A Gaussian beam can be corrected to a top-hat profile beam, called a top-hat beam. Top-hat beams have been studied and used for optical particle sizing

IV.4 Other Beams 111

[325], [326], [296], motivating an interest to examine how such beams could be handled by a GLMT. Of course, the problem is to know how to accurately enough describe a top-hat beam. Corbin et al [296] introduced a localized approximation for top-hat beams by analogy to the one used for Gaussian beams and provided numerical results such as concerning scattering diagrams. This approach is refined by Gouesbet et al [297] in which the validity of the localized approximation for top-hat beams is assessed.

#### Actual beams

Theoretical discussions and refinements concerning the description of laser beams, including higher-order laser beams, have been and still can be of interest, if only to examine theoretical issues. However, the more refined a theoretical discussion, the more likely it may become inappropriate to deal with actual beams in the laboratory. Indeed, an actual beam in the laboratory may depart significantly from any a priori ideal description. For instance, Hodges et al [172] (with a comment by Pogorzelski [327]) provided experimental results concerning the forward scattering of a Gaussian beam by electrodynamically levitated droplets. Experimental results could not be fitted by theoretical calculations with a GLMT relying on a single Gaussian beam. Actually, the measured intensity profile of the incident laser beam did not closely follow a Gaussian distribution over the entire dynamic range of the camera used. However, the measured profile could be compared with two theoretical Gaussian profiles, one for a waist radius equal to 18  $\mu$ m and the other for a waist radius equal to 24  $\mu$ m. The upper beam-waist radius (24  $\mu$ m) described the measured beam very well for the central part of the profile, while the lower beam-waist radius  $(18\mu m)$  was well adapted to describe the outer edges of the beam. Many other results are available from Hodges et al 172, but the one reported above is may be the most significant to understand the situation created when the intensity profile of an actual laser beam in the laboratory deviates from an ideal Gaussian shape.

These experiments from Hodges et al [172] are soon after revisited by Lock and Hodges [328] discussing the far-field scattering of an axisymmetric laser beam of arbitrary profile by an on-axis spherical particle. In their article, Lock and Hodges performed an approximate partial wave analysis of the experimental laser beam profile and thereafter used this analysis to compute the scattering of the beam by a spherical particle placed on the beam axis. A check of the method used is that, when it is applied to a beam with a Gaussian profile, the partial wave coefficients obtained are nearly identical to the localized model Gaussian beam shape coefficients. In the approximate approach used, the beam phase is separately modelled. In a companion article, the same topic is examined in the case of off-axis location of the particle [329].

With the same motivation in mind, namely, dealing with actual beams in the laboratory, Gouesbet introduced a reformulation of the GLMT [330], [331] with the aim to solve an inverse problem, namely, determining the

beam shape coefficients from field measurements, or more conveniently from intensity measurements (on the beam axis), and this to be done for modulus and for phase as well (!). Both on-axis and off-axis locations are considered. To be specific, let us consider, as an example, the component  $S_z$  of the Poynting vector which, for an arbitrary shaped beam, is expressed in terms of beam shape coefficients  $g_{n,X}^m$ , X = TM, TE. It is shown that actually the beam shape coefficients may be replaced by three 4D arrays called density matrices. It is afterwards demonstrated that measuring  $S_z(r)$  for angular variables fixed in principle allows one to evaluate the density matrix components by solving a linear inversion problem. Furthermore, when the beam is axisymmetric, the three 4D density matrices degenerate to twelve 2x2 sub-matrices which, with an extra trick, can degenerate further to a single density matrix. Interest in the use of density matrices is only warranted if a significant amount of the GLMT can be rewritten in terms of them, rather than in terms of beam shape coefficients. This issue is investigated in [331] with a positive answer, leading to what can be called the density-matrix approach to GLMT. The use of the terminology "density-matrix" is justified in an appendix.

Relying on the previous studies, in their two previous articles, Polaert et al 332 dealt with the measurements of beam shape coefficients in GLMT for the on-axis case. As demonstrated by Gouesbet [330], [331], the use of a linear analysis from intensity measurements on the beam axis, as mentioned above, could allow the evaluation of the density matrices depending on the beam shape coefficients, but not of the beam shape coefficients themselves. This also means that the information on the phases of the beam shape coefficients are lost in the process. Although phases are very often unimportant, as in the framework of the density-matrix approach to the GLMT, they may be important in some cases, typically when fields have to be combined, leading to interference phenomena. Such is for instance the case when dealing with phase Doppler instruments, in which the scatterer is illuminated by two laser beams instead of by only one. The situation is a bit similar to the one encountered in quantum mechanics, when global phase terms are irrelevant, while relative phases are essential. In this article under discussion, it is then shown that beam shape coefficients can be retrieved from intensity measurements, both in amplitude and phase, if the linear analysis is replaced by a nonlinear analysis. The use of numerical experiments allows one to have better flexibility, and more extensive investigations of the efficiency of the algorithms, than experiments, including tests of robustness with respect to added noise. These theoretical results are thereafter implemented with success in the laboratory by Polaert et al [333]. The case of off-axis beams has not been studied.

#### Miscellaneous beams

In this subsection, we discuss various kinds of beams which are or may be of interest for GLMTs, but whose studies in this framework, or in a related framework, are rather scarce. To begin with, lasers in the mode  $TEM_{01}^*$  (or

IV.4 Other Beams 113

doughnut beams) are discussed in connection with a study of the integral localized approximation [135]. Mathieu beams, which are non-diffracting solutions of the wave equation in elliptical cylinder coordinates, are experimentally demonstrated by Guttierez-Vega et al [334]. Non-diffracting beams are reviewed (theoretical, experimental, and applied aspects) by Bouchal 335. Beam properties in the neighborhood of a double-heterostructure laser source are discussed by Wu et al 336. Chen et al 337 designed a bottle beam for single beam trapping. Hollow (ring-shaped beams), optical bottles, Bessel beams, non-diffracting Bessel beams, Gaussian modes (Gaussian, Laguerre-Gaussian, Hermite-Gaussian, etc.) are discussed by Soifer et al [338] in connection with the topic of optical microparticle manipulation. See also Marston  $\boxed{339}$  who discussed the scattering of a Bessel beam by a sphere, while Yin et al 340 extensively discussed the generation of dark hollow beams and their applications. Tryka [341] dealt with a beam representing a paraxial approximate solution of the scalar Helmholtz wave equation to derive an analytical formula for calculating the flux of radiation from a Gaussian source irradiating a spherical object. Van de Nes and Torok discussed the scattering of Gauss-Laguerre beams [342]. They derived an expression for the field distribution of such beams, possibly focused, in terms of Mie modes and they studied the light scattered by an aluminium sphere, illuminated by such incident fields. Evanescent fields may also be viewed as a special class of beams. In particular, Quinten et al [343] discussed scattering and extinction of evanescent waves by small particles. They show that, owing to the inhomogeneity of the evanescent field, higher multipole contributions are strongly enhanced as compared to plane wave excitation. We shall have other opportunities to mention evanescent fields. Nonparaxial generalizations of Gaussian beams are discussed by Moore and Alonso 158.

#### Laser pulses

Up to now, we have been dealing with c.w. (continuous wave) lasers, but the use of laser pulses opens the way to new possibilities that are worthy to explore. Consider for instance a spherical particle of diameter equal to  $100~\mu m$  illuminated by a laser pulse having a duration equal to 50 femtoseconds, that is to say to  $50 \times 10^{-15}$  second. In vacuum (or air), the light propagates over 0.3  $\mu m$  during one femtosecond. Therefore, the length of the pulse is about 15  $\mu m$ , i.e., significantly smaller than the size of the particle. If the particle were illuminated by c.w. lasers, then all scattering modes (diffraction, reflection, different refracted rays, surface waves, etc.) would be continuously emitted, overlapping in time, and therefore producing many interference effects which actually generate the complicated structure of typical scattering diagrams. However, with ultra-short laser pulses as above, owing to the small length of the pulse compared with the size of the particle, the different scattering modes will produce different scattering pulses, each one probing different aspects of the particle. This only should allow one to propose refined optical

characterization. It is, therefore, expected that laser pulse scattering, and particularly ultra-short laser pulse scattering, should open the way to new opportunities.

A generic formulation of a GLMT for a particle illuminated by laser pulses has been published by Gouesbet and Gréhan 344 and further discussed by Gouesbet et al 345, in which precursors are acknowledged. The word "generic" refers to the fact that the scatter center may be arbitrary, with the proviso that we know how to evaluate its continuous wave response (Using a continuous wave GLMT, numerical techniques, or approximations). The formulation is illustrated by examining a Rayleigh dipole (under circumstances allowing one to provide analytical derivations). The basic idea is very simple, and simply relies on Fourier transforming. The first direct Fast Fourier Transform (FFT) is used to decompose the illuminating laser pulse into a decomposition of elementary continuous waves. A GLMT (or more generally any kind of light scattering theory) is used to compute the response for each elementary wave and, afterwards, summation of elementary responses followed by an inverse FFT provides the total response to the incident pulse.

Under adequate circumstances, it is then observed that, indeed, a single incident pulse may generate a response made out from a train of pulses. For example, time-resolved diagrams for a sphere (diameter equal to 100  $\mu$ m) illuminated by plane wave and focused short pulses (duration equal to 100 fs) are discussed by Méès et al [346]. Diagrams are compared for plane wave, on-axis, and off-axis illuminations. The sequence of events exhibits the light diffracted by the particle in forward directions, refracted light through the particle in forward directions, then refracted light with scattering angles increasingly departing from forward directions, and higher-order scattering modes such as for light having undergone one or several internal reflections before leaving the particle... Diagrams are smooth since they do not involve interferences between the scattering modes which are temporarily separated, excepted for the rainbow. Interferences at the rainbow location persist under pulsed illumination because they are due to rays with closed optical paths, at and near the minimum of deviation of the rainbow. If we limit ourselves with the scattering mode for two internal reflections, then the response of the scatterer to a 100 fs pulse extends over 15 times the incident pulse duration. Still higher-order modes would come later. The case of time-integrated detection is also discussed. A somewhat similar study concerning the scattering of laser pulses by spheres is available from Méès et al [347]. In the article cited, surface wave modes are evidenced, and the influence of the duration of the pulse is examined.

An emphasis on internal fields is stressed by Méès et al [348]. Time-resolved diagrams allow one to observe the refractive penetration of the pulse in the particle, the travelling of the pulse inside the particle, pulse deformation due to the limit angle of refraction, first internal reflection and the emergence of modes coupled by diffraction, ..., and so on. Eventually, we only observe wave packets orbiting below the surface of the sphere when lower order modes

IV.4 Other Beams 115

have vanished. These wave packets are trapped and also diffractively (but very slowly) leak. They would generate morphology-dependent resonances in the case of continuous illumination. To illustrate the weakness of the energy leakage, let us mention that, for a 70 fs pulse, the decrease of energy in the final wave packets is estimated to be by a factor 10 in 20 ps. The same topic is considered by Méès et al [349] with a particular attention paid to the residual wave packets, and an examination of the influence of the refractive index (differences between water and glass particles). Furthermore, when examining the internal fields developing versus time during the interaction between a large enough sphere and a small enough duration short pulse, the occurrence of a high intensity spot with a speed faster than the one of light has been observed. This suggested the possibility, under certain circumstances, of Cerenkov-based radiation from supra-luminic excitation in micro-droplets by ultra-short pulses [350].

Complementary studies concerned the interaction of ultra-short pulses with multilayered particles by Méès et al [351], or with spheroids by Han et al [267]. Movies showing the interaction between various kinds of scatterers (homogeneous and coated spheres) and femtosecond pulses are available from the website connected to this book. Non-linear effects may also be studied. For instance, Méès et al [352] provided numerical simulations for two-photon absorption and fluorescence in a spherical micro-cavity illuminated using two laser pulses.

Furthermore, Brevik and Kulge [353] reported on the oscillations of a water droplet illuminated by a linearly polarized laser pulse, a variant of the radiation pressure problem. Favre et al 354 reported the observation of whitelight emission from femtosecond laser-induced plasma in a water droplet, an observation which is not completely independent of the proposal for the observation of Cerenkov-based radiation previously mentioned. In both cases, we depart from quasi-elastic light scattering, in the first case due to quantum mechanical effects (e.g. multiphoton ionization), in the second case due to relativistic effects. Lindinger et al [355] provided a series of time-resolved images of the explosion dynamics of micrometer-sized water droplets after femtosecond laser-pulse irradiation, for different laser intensities. The results of Méès et al 348 are used for the interpretation of the features observed. Bech and Leder 356 carried out numerical simulations to discuss the possibilities of particle sizing by ultrashort laser pulses, and pointed out that the temporal sequence of the scattered light events opens new methods of optical particle characterization. A discussion of surface waves is available. In particular, the evaluation of time-resolved surface wave signals can be of special importance for size measurements of particles for which, because of reduced transparence or high optical absorption, no refracted light is detected. This article is later completed by Bech and Leder [153] providing complementary results. Méjean et al 357 dealt with the remote detection and identification of biological aerosols using a femtosecond terawatt lidar system, inducing in-situ two-photon-excited fluorescence, a process simulated by Méès et al 352. For complementary related studies, see Méjean 358, Kasparian and Wolf 359, and Courvoisier et al 360, the latter aiming to the identification of biological microparticles using ultrafast depletion spectroscopy. Optical scattering spectroscopy using tightly focused supercontinuum, generated from short laser pulses, is discussed by Li et al [149] in the framework of an angular spectrum decomposition. Some calculations on the scattering efficiencies of a sphere illuminated by an optical pulse are discussed by Jones 361, using a trigonometric (cosine) pulse envelope (allowing more analytical algebraic manipulations than Gaussian envelopes). Lee et al [362] considered the determination of particle sizes and density distributions using ultra-short pulses in strongly scattering media, with a simplified random walk, ray tracing approach. Bakic et al 154 made measurements, compared with predictions, concerning the scattering of femtosecond laser pulses by small droplets, confirming the interest of ultra-short pulse approaches for optical characterization. They used time integrated detection (not time-resolved detection). One seemingly interesting feature is that a fine structure, called the ripple structure, no longer appears in the region rainbow of scattering, something which is claimed as being an advantage simplifying rainbow refractometry significantly. Let us, however, note that the ripple structure in rainbow refractometry contains additional information which may be worth to be used. For instance, van Beeck and Riethmuller 363 performed a sphericity test in rainbow refractometry by comparing the Airy and the ripple droplet diameters. See also Saengkaew et al [364], [365]. Furthermore, let us remark that optical trapping with pulses are feasible [149], [366].

As previously discussed, evaluations of BSCs  $g_n^m$  may be carried out by using quadratures. Historically, the quadrature techniques have been the first to be developed in so far as they quite naturally arise in the development of the GLMT. Because they are flexible, i.e. only kernels in the quadratures have to be modified when the incident beam is changed, they are well adapted to some specific problems, such as the study of shaped beam scattering by adjacent spherical particles [138]. However, when the nature of the incident beam is well defined, quadratures constitute the worst methods because they are very time-consuming in terms of CPU. An effort has been therefore performed to develop other techniques to evaluate BSCs. In this chapter, a technique using <u>finite</u> series is presented. The technique is rigorous and indeed mathematically equivalent to quadrature techniques when the incident beam description exactly satisfies Maxwell's equations. However, it is much faster running. There is nevertheless a price to pay for such an advantage. Indeed, when using the quadrature techniques, only quadrature integrands have to be changed when the incident beam description is modified. Conversely, when using the finite series technique, an extra analytical work and significant program modifications are required when the beam description is modified. Performing by hand these modifications may typically take one month. Fortunately, the procedure is quite general and the whole process may be in principle carried out in an automatic way by using a formal computation procedure which would furthermore generate FORTRAN sources. For details about published work on finite series, the reader may refer to Gouesbet et al 87, 367 and references therein.

#### V.1 The General Procedure

The BSCs  $g_n^m$  are determined by Rels (III.10) and (III.19) which are here recalled as:

$$\begin{pmatrix} E_r \\ H_r \end{pmatrix} = \begin{pmatrix} E_0 \\ H_0 \end{pmatrix} \sum_{n=1}^{\infty} \sum_{m=-n}^{+n} c_n^{pw} \begin{pmatrix} g_{n,TM}^m \\ g_{n,TE}^m \end{pmatrix} \frac{n(n+1)}{r}$$

$$\Psi_n^{(1)}(kr) P_n^{|m|}(\cos\theta) \exp(im\varphi)$$
(V.1)

Any method to determine BSCs must deal with these basic relations. In the quadrature techniques, Rel (V.1) has been processed by using what has been called spherical harmonic expansions (section III.3.1). Finite series are conversely obtained by using so-called Neumann expansions (or Bessel function expansions). The method relies on a beautiful theorem which may be found in Watson (133), p. 524-525).

According to this theorem, let us consider an equation having the form:

$$x^{1/2}g(x) = \sum_{n=0}^{\infty} c_n J_{n+1/2}(x)$$
 (V.2)

in which  $J_{n+1/2}$ 's are classical half-order Bessel functions. The Maclaurin expansion of the function g(x) reads as:

$$g(x) = \sum_{n=0}^{\infty} b_n x^n \tag{V.3}$$

Then the theorem states that coefficients  $c_n$  are given by:

$$c_n = \left(n + \frac{1}{2}\right) \sum_{m=0}^{\leq n/2} 2^{\frac{1}{2} + n - 2m} \frac{\Gamma(\frac{1}{2} + n - m)}{m!} b_{n-2m}$$
 (V.4)

From now on, this theorem will be called the Neumann Expansion Theorem (NET). To take advantage of it, one starts from Rel (V.1) and first discards the  $\varphi$ -dependence by acting with the integral operator  $\int_0^{2\pi}$ .  $exp(-im'\varphi) \, d\varphi$  and by using the orthogonality relation (III.11) to obtain (not forgetting that  $P_n^{|m|} = 0$  if n < |m|):

$$\int_{0}^{2\pi} {E_r \choose H_r} exp(-im\varphi)d\varphi = 2\pi {E_0 \choose H_0} \sum_{n=|m|}^{\infty} c_n^{pw} {g_{n,TM} \choose g_{n,TE}^m}$$

$$\frac{n(n+1)}{r} \Psi_n^{(1)}(kr) P_n^{|m|}(cos\theta)$$
(V.5)

The next step is to also discard  $\theta$ -dependence. This may be done in two ways. The first way is just to specify  $\theta = \pi/2$  in Rel (V.5), to invoke the following relations for associated Legendre polynomials 130:

$$P_n^m(0) = (-1)^{\frac{n+m}{2}} \frac{(n+m-1)!!}{2^{\frac{n-m}{2}} (\frac{n-m}{2})!}$$
  $(n-m)$  even 
$$(V.6)$$

$$P_n^m(0) = 0 \qquad (n-m) \text{ odd}$$

in which:

$$n!! = 1.3.5...n (-1)!! = 1$$
 (V.7)

and also a relation expressing spherical Bessel functions in terms of half-order Bessel functions (see Rel (II.78)):

$$\Psi_n^{(1)}(kr) = \sqrt{\frac{\pi}{2kr}} J_{n+1/2}(kr)$$
 (V.8)

to obtain, after some algebra:

$$(kr)^{1/2} \int_0^{2\pi} r \left( \begin{array}{c} E_r(\theta = \pi/2) \\ H_r(\theta = \pi/2) \end{array} \right) exp(-im\varphi) d\varphi = \pi \sqrt{2\pi} \left( \begin{array}{c} E_0 \\ H_0 \end{array} \right) \sum_{n=|m|,(n-m)even}^{\infty} c_n^{pw} n(n+1)$$
 
$$\left( \begin{array}{c} g_{n,TM}^m \\ g_{n,TE}^m \end{array} \right) P_n^{|m|}(0) J_{n+1/2}(kr)$$
 
$$(V.9)$$

For convenience, the expression (V.6) for  $P_n^m(0)$  has not been fully introduced in Rel (V.9) but it nevertheless appears explicitly through the fact that the summation in the r.h.s is restricted to even values of (n-m). This shows that all BSCs cannot be determined by using Rel (V.9) alone. It is then required to use a second way to discard variable  $\theta$ . This is carried out by deriving Rel (V.5) with respect to  $(\cos\theta)$ , specifying again  $\theta = \pi/2$  in the obtained relation, invoking other relations for associated Legendre polynomials [130]:

$$\frac{dP_n^m(\cos\theta)}{d\cos\theta}\Big|_{\cos\theta=0} = 0 , (n-m) \text{ even}$$

$$\frac{dP_n^m(\cos\theta)}{d\cos\theta}\Big|_{\cos\theta=0} = (-1)^{\frac{n+m-1}{2}} \frac{(n+m)!!}{2^{\frac{n-m-1}{2}}(\frac{n-m-1}{2})!} , (n-m) \text{ odd}$$

and also again Rel (V.8) to obtain, after some algebra:

$$(kr)^{1/2} \int_{0}^{2\pi} r \frac{\partial}{\partial \cos\theta} \left( \frac{E_r}{H_r} \right) \Big|_{\cos\theta=0} \exp(-im\varphi) d\varphi = \pi \sqrt{2\pi} \left( \frac{E_0}{H_0} \right)$$

$$\sum_{n=|m|,(n-m)odd}^{\infty} c_n^{pw} n(n+1) \left( \frac{g_{n,TM}^m}{g_{n,TE}^m} \right) \frac{dP_n^m(\cos\theta)}{d\cos\theta} \Big|_{\cos\theta=0} J_{n+1/2}(kr)$$

in which the expression (V.10) has not been fully introduced in Rel (V.11) for convenience, but nevertheless appears through the fact that the summation in the r.h.s. is restricted to odd values of (n-m).

The set of Rels (V.9) for (n-m) even and (V.11) for (n-m) odd provides a new way to determine all BSCs. When the beam is specified, the radial field components  $E_r$  and  $H_r$  may be expanded in Fourier series over  $\varphi$ . Then, the integration over  $\varphi$  in the l.h.s. of Rels (V.9), (V.11) may be performed. Setting x = kr, we therefore obtain relations which have the proper form (V.2) to apply the NET, leading eventually to the evaluation of the BSCs, as now exemplified in the case of Gaussian beams.

#### V.2 The NET Procedure for Gaussian Beams

#### V.2.1 Basic Relations

In the case of Gaussian beams,  $E_r$  and  $H_r$  are given in Rels (IV.84)-(IV.85). Expressing explicitly the coefficients  $c_n^{pw}$  (Rel (III.3)), Rels (V.9) and (V.11) then become

$$kr\sqrt{\frac{2kr}{\pi}} \left\{ \frac{F}{2} \left[ \sum_{j_{+}=m}^{jp} \Psi_{jp} + \sum_{j_{-}=m}^{jp} \Psi_{jp} \right] + x_{0} G \sum_{j_{0}=m}^{jp} \Psi_{jp} \right\}_{\theta = \frac{\pi}{2}} =$$
 (V.12)

$$\sum_{n=|m|,(n-m)\text{ even}}^{\infty} i^{n-1} (-1)^n (2n+1) g_{n,TM}^m P_n^{|m|}(0) J_{n+\frac{1}{2}}(kr)$$

<sup>&</sup>lt;sup>1</sup> F and G are  $\epsilon_L$  dependent.

$$kr\sqrt{\frac{2kr}{\pi}} \left\{ \frac{F}{2i} \left[ \sum_{j_{+}=m}^{jp} \Psi_{jp} - \sum_{j_{-}=m}^{jp} \Psi_{jp} \right] + y_{0} G \sum_{j_{0}=m}^{jp} \Psi_{jp} \right\}_{\theta = \frac{\pi}{2}} =$$

$$\sum_{n=|m|,(n-m) \text{ even}}^{\infty} i^{n-1} (-1)^{n} (2n+1) g_{n,TE}^{m} P_{n}^{|m|}(0) J_{n+\frac{1}{2}}(kr)$$

$$kr\sqrt{\frac{2kr}{\pi}} \left. \left\{ \frac{1}{2} \frac{\partial}{\partial cos\theta} F \left[ \sum_{j_{+}=m}^{jp} \varPsi_{jp} + \sum_{j_{-}=m}^{jp} \varPsi_{jp} \right] + x_{0} \right. \frac{\partial}{\partial cos\theta} \left. G \sum_{j_{0}=m}^{jp} \varPsi_{jp} \right\}_{\theta=\frac{\pi}{2}} = \\ \qquad \qquad (\text{V}.14)$$

$$\sum_{n=|m|,(n-m) \text{ odd}}^{\infty} i^{n-1} \left. (-1)^{n} \left. (2n+1) \right. \left. g_{n,TM}^{m} \left. \frac{dP_{n}^{|m|}(cos\theta)}{dcos\theta} \right|_{\theta=\frac{\pi}{2}} J_{n+\frac{1}{2}}(kr) \right.$$

$$kr\sqrt{\frac{2kr}{\pi}} \left. \left\{ \frac{1}{2i} \frac{\partial}{\partial cos\theta} F \left[ \sum_{j_{+}=m}^{jp} \varPsi_{jp} - \sum_{j_{-}=m}^{jp} \varPsi_{jp} \right] + y_{0} \right. \frac{\partial}{\partial cos\theta} \left. G \sum_{j_{0}=m}^{jp} \varPsi_{jp} \right\}_{\theta = \frac{\pi}{2}} \right.$$

$$\left. \left. \left( V.15 \right) \right.$$

$$\left. \sum_{n=|m|,(n-m) \ odd}^{\infty} i^{n-1} \left. \left( -1 \right)^{n} \left. \left( 2n+1 \right) \right. g_{n,TE}^{m} \left. \left. \frac{dP_{n}^{|m|}(cos\theta)}{dcos\theta} \right|_{\theta = \frac{\pi}{2}} \right. \right.$$

$$\left. J_{n+\frac{1}{2}}(kr) \right.$$

From Rels (V.12) and (V.14), we obtain four relations to evaluate the BSCs  $g_{n,TM}^m$ :

# (i) n and m even:

$$kr\sqrt{\frac{2kr}{\pi}} \left\{ \frac{1}{2}F \left[ \sum_{j_{+}=2q}^{jp} \Psi_{jp} + \sum_{j_{-}=2q}^{jp} \Psi_{jp} \right] + x_{0} G \sum_{j_{0}=2q}^{jp} \Psi_{jp} \right\}_{\theta = \frac{\pi}{2}} =$$

$$\sum_{n=|2q|}^{\infty} e^{i^{n-1}} (-1)^{n} (2n+1) g_{n,TM}^{2q} P_{n}^{|2q|}(0) J_{n+1/2}(kr)$$

in which  $\sum_{n} e$  designates a summation restricted to even values of the integer n.

#### (ii) n and m odd:

$$kr\sqrt{\frac{2kr}{\pi}} \left\{ \frac{1}{2}F \left[ \sum_{j_{+}=2q+1}^{jp} \Psi_{jp} + \sum_{j_{-}=2q+1}^{jp} \Psi_{jp} \right] + x_{0}G \sum_{j_{0}=2q+1}^{jp} \Psi_{jp} \right\}_{\theta = \frac{\pi}{2}}$$

$$(V.17)$$

$$\sum_{n=|2q+1|}^{\infty} o \ i^{n-1} \ (-1)^{n} \ (2n+1) \ g_{n,TM}^{2q+1} \ P_{n}^{|2q+1|}(0) \ J_{n+1/2}(kr)$$

in which  $\sum_{n} o$  designates a summation restricted to odd values of the integer n.

#### (iii) n odd and m even:

$$kr\sqrt{\frac{2kr}{\pi}} \left\{ \frac{1}{2} \frac{\partial}{\partial cos\theta} F \left[ \sum_{j_{+}=2q}^{jp} \Psi_{jp} + \sum_{j_{-}=2q}^{jp} \Psi_{jp} \right] + x_{0} \frac{\partial}{\partial cos\theta} G \sum_{j_{0}=2q}^{jp} \Psi_{jp} \right\}_{\theta = \frac{\pi}{2}}$$

$$(V.18)$$

$$\sum_{n=|2q|}^{\infty} i^{n-1} (-1)^{n} (2n+1) g_{n,TM}^{2q} \frac{dP_{n}^{|2q|}(cos\theta)}{dcos\theta} \bigg|_{\theta = \frac{\Pi}{2}} J_{n+1/2}(kr)$$

# (iv) n even and m odd:

$$kr\sqrt{\frac{2kr}{\pi}} \qquad \left\{ \frac{1}{2} \frac{\partial}{\partial cos\theta} F \left[ \sum_{j_{+}=2q+1}^{jp} \Psi_{jp} + \sum_{j_{-}=2q+1}^{jp} \Psi_{jp} \right] + x_{0} \frac{\partial}{\partial cos\theta} G \sum_{j_{0}=2q+1}^{jp} \Psi_{jp} \right\}_{\theta = \frac{\pi}{2}} = \sum_{n=|2q+1|}^{\infty} e^{in-1} (-1)^{n} (2n+1) g_{n,TM}^{2q+1} \frac{dP_{n}^{|2q+1|}(cos\theta)}{dcos\theta} \bigg|_{\theta = \frac{\pi}{2}} J_{n+1/2}(kr)$$

$$(V.19)$$

Similarly, from Rels (V.13) and (V.15), we obtain four relations to evaluate the BSCs  $g_{n,TE}^m$ :

#### (i) n and m even:

$$kr\sqrt{\frac{2kr}{\pi}} \left\{ \frac{1}{2i} F \left[ \sum_{j_{+}=2q}^{jp} \Psi_{jp} - \sum_{j_{-}=2q}^{jp} \Psi_{jp} \right] + y_{0} G \sum_{j_{0}=2q}^{jp} \Psi_{jp} \right\}_{\theta = \frac{\pi}{2}} = \sum_{n=|2q|}^{\infty} e^{i^{n-1}} (-1)^{n} (2n+1) g_{n,TE}^{2q} P_{n}^{|2q|}(0) J_{n+1/2}(kr)$$
(V.20)

# (ii) n and m odd

$$kr\sqrt{\frac{2kr}{\pi}} \left\{ \frac{1}{2i} F \left[ \sum_{j_{+}=2q+1}^{jp} \Psi_{jp} - \sum_{j_{-}=2q+1}^{jp} \Psi_{jp} \right] + y_{0} G \sum_{j_{0}=2q+1}^{jp} \Psi_{jp} \right\}_{\theta = \frac{\pi}{2}}$$

$$(V.21)$$

$$\sum_{n=|2q+1|}^{\infty} o^{i^{n-1}} (-1)^{n} (2n+1) g_{n,TE}^{2q+1} P_{n}^{|2q+1|} (0) J_{n+1/2}(kr)$$

#### (iii) n odd and m even

$$kr\sqrt{\frac{2kr}{\pi}} \left\{ \frac{1}{2i} \frac{\partial}{\partial \cos\theta} F \left[ \sum_{j_{+}=2q}^{jp} \Psi_{jp} - \sum_{j_{-}=2q}^{jp} \Psi_{jp} \right] + y_{0} \frac{\partial}{\partial \cos\theta} G \sum_{j_{0}=2q}^{jp} \Psi_{jp} \right\}_{\theta=\frac{\pi}{2}}$$

$$(V.22)$$

$$\sum_{n=|2q|}^{\infty} o i^{n-1} (-1)^{n} (2n+1) g_{n,TE}^{2q} \frac{dP_{n}^{|2q|}(\cos\theta)}{d\cos\theta} \bigg|_{\theta=\frac{\pi}{2}} J_{n+1/2}(kr)$$

#### (iv) n even and m odd

$$kr\sqrt{\frac{2kr}{\pi}} \qquad \left\{ \frac{1}{2i} \frac{\partial}{\partial cos\theta} F \left[ \sum_{j_{+}=2q+1}^{jp} \Psi_{jp} - \sum_{j_{-}=2q+1}^{jp} \Psi_{jp} \right] + y_{0} \frac{\partial}{\partial cos\theta} G \sum_{j_{0}=2q+1}^{jp} \Psi_{jp} \right\}_{\theta = \frac{\pi}{2}} = \sum_{n=|2q+1|}^{\infty} i^{n-1} (-1)^{n} (2n+1) g_{n,TE}^{2q+1} \left. \frac{dP_{n}^{|2q+1|}(cos\theta)}{dcos\theta} \right|_{\theta = \frac{\pi}{2}} J_{n+1/2}(kr)$$

$$(V.23)$$

The NET is afterward successively applied to each of the relations (V.16)-(V.23). Although no fundamental difficulty is involved, the amount of algebra is however rather tedious to handle. Only the case of the BSCs  $g_{n,TM}^m$ , for n and m even, will be here worked out in a detailed way.

# V.2.2 BSCs $g_{n,TM}^m$ , n and m Even

Considering the basic relation (V.16), it is first established, by using Rels (IV.77), (IV.79), (IV.86) and (IV.87), that:

$$F(\theta = \pi/2) = 2 \mathcal{A} \exp[-Z_0 s^2 k^2 r^2]$$
 (V.24)

$$G(\theta = \pi/2) = 0 \tag{V.25}$$

in which:

$$\mathcal{A} = \frac{1}{2} Z_0 \exp[-Z_0 \frac{x_0^2 + y_0^2}{w_0^2}] \exp(ikz_0)$$
 (V.26)

$$Z_0 = i \ Q(\theta = \pi/2) = \frac{1}{1 + 2\frac{iz_0}{I}}$$
 (V.27)

Furthermore, from (IV.83), the following relation holds:

$$\Psi_{jp}(\theta = \pi/2) = (kr)^j \Delta(j, p) \tag{V.28}$$

in which:

$$\Delta(j,p) = \left(\frac{Z_0}{kw_0^2}\right)^j \frac{(x_0 - iy_0)^{j-p}(x_0 + iy_0)^p}{p!(j-p)!}$$
(V.29)

Setting x = kr, and invoking Rel (V.6), Rel (V.16) takes the standard form (V.2) of the NET , with:

$$g(x) = \mathcal{A} \left[ \sum_{j_{+}=2q}^{jp} + \sum_{j_{-}=2q}^{jp} \right] \Delta(j,p) \ x^{j+1} \ exp(-Z_0 s^2 x^2)$$
 (V.30)

$$c_n = 0, n \text{ odd} (V.31)$$

$$c_n = \epsilon(n;0) \frac{\sqrt{\pi}}{\sqrt{2}} i^{n-1} (-1)^n (2n+1) g_{n,TM}^{2q} (-1)^{\frac{n}{2}+|q|} \frac{(n+2|q|-1)!!}{2^{\frac{n}{2}-|q|}(\frac{n}{2}-|q|)!} n \text{ even}$$
(V.32)

in which:

$$\epsilon \ (n; \alpha_j) = 0 \text{ if } n \text{ is equal to one of the } \alpha'_j \mathbf{s}$$

$$\epsilon \ (n; \alpha_j) = 1 \text{ otherwise}$$
(V.33)

In Rel (V.32), there is only one  $\alpha_j = 0$ , but the notation introduced in Rel (V.33) is more general for further use.

Rel (V.32) expresses the BSCs  $g_{n,TM}^{2q}$  (n even) in terms of coefficients  $c_n$ . By using the NET, these coefficients  $c_n$  may also be obtained from the Maclaurin expansion of the function g(x) given by Rel (V.30). However, the function g(x) is not in right form for further processing because Rel (V.3) exhibits a single summation over  $x^n$ -expansions while, conversely, Rel (V.30) is expressed in terms of double summations over j and p. However, double summations may be reduced to single summations by using (Appendix D):

$$\sum_{j_{+}=2q}^{jp} A_{jp} = \sum_{j=q-1}^{\infty} A_{2j+1,j+1-q} \qquad q > 0$$
 (V.34)

$$\sum_{j+2q}^{jp} A_{jp} = \sum_{j=|q|}^{\infty} A_{2j+1,j+1-q} \qquad q \le 0$$
 (V.35)

$$\sum_{j=2q}^{jp} A_{jp} = \sum_{j=q}^{\infty} A_{2j+1,j-q} \qquad q \ge 0$$
 (V.36)

$$\sum_{j=2q}^{jp} A_{jp} = \sum_{j=|q|-1}^{\infty} A_{2j+1,j-q} \qquad q < 0$$
 (V.37)

showing that the cases  $q=0,\,q>0$  and q<0 must be separately investigated.

(i) 
$$g_{n,TM}^{2q}$$
,  $n$  even,  $q = 0$ 

By using Rels (V.30), (V.35), and (V.36), the function g(x) becomes:

$$g(x) = \mathcal{A} \exp(-Z_0 s^2 x^2) \sum_{j=0}^{\infty} \left[ \Delta(2j+1, j+1) + \Delta(2j+1, j) \right] x^{2j+2} \quad (V.38)$$

Expanding the exponential, Rel (V.38) may be rewritten as:

$$g(x) = \sum_{m=0}^{\infty} \sum_{n=2m+2}^{\infty} \mathcal{A} \frac{(-Z_0 s^2)^m}{m!} \left[ \Delta(n-1-2m, \frac{n}{2}-m) + \Delta(n-1-2m, \frac{n}{2}-1-m) \right] x^n$$
(V.39)

It may however be shown that (Appendix E):

$$\sum_{m=0}^{\infty} \sum_{n=2m+2}^{\infty} e = \sum_{n=0}^{\infty} e \sum_{m=0}^{\frac{n}{2}-1} \epsilon(n;0)$$
 (V.40)

leading to:

$$g(x) = \sum_{n=0}^{\infty} e^{\sum_{m=0}^{\frac{n}{2}-1}} \mathcal{A} \epsilon (n;0) \frac{(-Z_0 s^2)^m}{m!}$$

$$\left[ \Delta(n-1-2m, \frac{n}{2}-m) + \Delta(n-1-2m, \frac{n}{2}-1-m) \right] x^n$$
(V.41)

This exactly takes the form of the Maclaurin expansion (V.3) that we were looking for. The coefficients  $b_n$  are then readily obtained as:

$$b_n = 0, n \text{ odd} (V.42)$$

$$b_n = \sum_{t=0}^{\frac{n}{2}-1} \mathcal{A} \ \epsilon(n;0) \frac{(-Z_0 s^2)^t}{t!}$$

$$\left[ \Delta(n-1-2t, \frac{n}{2}-t) + \Delta(n-1-2t, \frac{n}{2}-1-t) \right], \ n \text{ even}$$
(V.43)

Coefficients  $c_n$  are now available either from Rel (V.32) or from the NET-result (Rel (V.4)) leading to the following equation for n even, q = 0:

$$c_{n} = \epsilon(n;0) \frac{\sqrt{\pi}}{\sqrt{2}} i^{n-1} (-1)^{n} (2n+1) g_{n,TM}^{0} (-1)^{\frac{n}{2}} \frac{(n-1)!!}{2^{\frac{n}{2}}(\frac{n}{2})!}$$

$$= (n+\frac{1}{2}) \sum_{m=0}^{\leq n/2} 2^{\frac{1}{2}+n-2m} \frac{\Gamma(\frac{1}{2}+n-m)}{m!} \sum_{t=0}^{\frac{n}{2}-m-1} \mathcal{A} \epsilon(n-2m;0) \frac{(-Z_{0}s^{2})^{t}}{t!}$$

$$\left[ \Delta(n-2m-2t-1, \frac{n}{2}-m-t) + \Delta(n-2m-2t-1, \frac{n}{2}-m-t-1) \right]$$

This relation is only an intermediary result which is provided to help the reader. Actually, a better-looking expression may be obtained by showing that:

$$n!! = \frac{2^{\frac{1}{2}(n+1)}}{\sqrt{\pi}} \Gamma(\frac{n}{2} + 1)$$
 (V.45)

in which the celebrated Gamma function complies with:

$$\Gamma(n) = (n-1)! \tag{V.46}$$

$$\Gamma(z+1) = z\Gamma(z) \tag{V.47}$$

Inserting Rel (V.45) in Rel (V.44), setting  $n=2p,\,p\neq 0$ , and rearranging then leads to:

$$g_{2p,TM}^{0} = i \mathcal{A} 2^{2p} \frac{p!}{\Gamma(p+1/2)} \sum_{m=0}^{p} \frac{\Gamma(2p-m+1/2)}{2^{2m}m!} \sum_{t=0}^{p-m-1} \frac{(-Z_0 s^2)^t}{t!}$$

$$\epsilon(p-m;0) \left[ \Delta(2p-2m-2t-1, p-m-t) + \Delta(2p-2m-2t-1, p-m-t-1) \right]$$
(V.48)

(ii) 
$$g_{n,TM}^{2q}$$
,  $n$  even,  $q > 0$ 

For this case, g(x) becomes:

$$g(x) = \mathcal{A} \exp(-Z_0 s^2 x^2) \left[ \sum_{j=q-1}^{\infty} \Delta(2j+1, j+1-q) x^{2j+2} + \sum_{j=q}^{\infty} \Delta(2j+1, j-q) x^{2j+2} \right]$$
(V.49)

Expanding the exponential leads to:

$$g(x) = \sum_{m=0}^{\infty} \sum_{n=2m+2q}^{\infty} \mathcal{A} \frac{(-Z_0 s^2)^m}{m!} \Delta(n-2m-1, \frac{n}{2}-m-q) x^n$$

$$+ \sum_{m=0}^{\infty} \sum_{n=2m+2q+2}^{\infty} \mathcal{A} \frac{(-Z_0 s^2)^m}{m!} \Delta(n-2m-1, \frac{n}{2}-m-q-1) x^n$$
(V.50)

But, generalizing Rel (V.40), we have (Appendix E):

$$\sum_{m=0}^{\infty} \sum_{n=2m+2q}^{\infty} e = \sum_{n=0}^{\infty} \sum_{m=0}^{\frac{1}{2}(n-2q)} \epsilon(n;0,2,...,2q-2)$$
 (V.51)

leading to the Maclaurin expansion of g(x):

$$g(x) = \sum_{n=0}^{\infty} e^{i\frac{1}{2}(n-2q)} A \frac{(-Z_0 s^2)^m}{m!} \left[ \epsilon(n;0,2,...,2q-2)\Delta(n-2m-1,\frac{n}{2}-m-q) + \epsilon(m;\frac{1}{2}(n-2q)) \epsilon(n;0,2,...,2q) \Delta(n-2m-1,\frac{n}{2}-m-q-1) \right] x^n$$

$$(V.52)$$

from which coefficients  $b_n$  are determined:

$$b_n = 0, n \text{ odd } (V.53)$$

$$b_{n} = \sum_{t=0}^{\frac{1}{2}(n-2q)} \mathcal{A} \frac{(-Z_{0}s^{2})^{t}}{t!} \left\{ \epsilon(n;0,2,...,2q-2) \ \Delta(n-2t-1,\frac{n}{2}-t-q) + \epsilon(t;\frac{1}{2}(n-2q)) \ \epsilon(n;0,2,...,2q) \Delta(n-2t-1,\frac{n}{2}-t-q-1) \right\}, n \text{ even}$$

Coefficients  $c_n$  are now again available from two different sources, either from Rel (V.32) or from the NET-result (Rel (V.4)). Proceeding as for the previous case finally leads to:

$$\begin{split} g_{2p,TM}^{2q}(q>0) &= \frac{i\mathcal{A}}{(-1)^q} \ 2^{2(p-q)} \ \frac{(p-q)!}{\Gamma(p+q+1/2)} \end{split} \tag{V.55} \\ &\sum_{m=0}^p \frac{\Gamma(2p-m+1/2)}{2^{2m}m!} \\ &\sum_{t=0}^{p-m-q} \frac{(-Z_0s^2)^t}{t!} \ \left[ \epsilon \ (p-m;0,1,...,q-1) \right. \\ &\left. \Delta \ (2p-2m-2t-1,p-m-t-q) + \epsilon \ (t;p-m-q) \right. \\ &\left. \epsilon(p-m;0,1,...,q) \Delta (2p-2m-2t-1,p-m-t-q-1) \right] \end{split}$$
 (iii)  $g_{n,TM}^{2q}, n \ \text{even}, \ q<0$ 

Proceeding as before, it is found that the function g(x) reads as:

$$g(x) = \mathcal{A} \exp(-Z_0 s^2 x^2) \left[ \sum_{j=|q|}^{\infty} \Delta(2j+1, j+1-q) x^{2j+2} + \sum_{j=|q|-1}^{\infty} \Delta(2j+1, j-q) x^{2j+2} \right]$$
(V.56)

and the corresponding BSCs are given by:

$$\begin{split} g_{2p,TM}^{2q}(q<0) &= \frac{i\mathcal{A}}{(-1)^{|q|}} \ 2^{2(p-|q|)} \ \frac{(p-|q|)!}{\Gamma(p+|q|+1/2)} \\ &\qquad \qquad \sum_{m=0}^{p} \frac{\Gamma(2p-m+1/2)}{2^{2m}m!} \ \sum_{t=0}^{p-m-|q|} \frac{(-Z_0s^2)^t}{t!} \\ &\qquad \qquad [\epsilon(p-m;0,1,...,|q|-1) \\ &\qquad \qquad \Delta(2p-2m-2t-1,p-m-t-q-1) \\ &\qquad \qquad + \epsilon(t;p-m-|q|) \ \epsilon(p-m;0,1,...,|q|) \\ &\qquad \qquad \Delta(2p-2m-2t-1,p-m-t-q)] \end{split} \label{eq:general_property}$$

In this finite series technique, angle  $\varphi$  disappears by using a quadrature and angle  $\theta$  by using special values. The variable r naturally disappears by using the NET theorem, without having to use quadratures nor special values. This is to be compared with the quadrature techniques in section III in which angles  $\theta$  and  $\varphi$  disappear by using quadratures and variable r disappears by using either a quadrature or a special value. Therefore, if the beam description does not exactly satisfy Maxwell's equations, the finite series give BSCs which are constant complex numbers, automatically providing a remodelling of the beam description, without any artifact, in contrast with the quadrature techniques (see again Gouesbet  $et\ al\ 134$ ). From that point of view,

the quadrature and the finite series techniques are not strictly equivalent when the beam description does not exactly satisfy Maxwell's equations. Under such circumstances, the relationship between the finite series technique, without any apparent artifact, and the quadrature techniques remains to be investigated.

# V.2.3 Other BSCs $g_{n,TM}^m$

The procedure for the other BSCs being similar, this section essentially provides general indications to help the reader with only a few intermediary results.

# (i) $g_{n,TM}^m$ , n and m odd.

In this case, the starting point is Rel (V.17). This relation is given the standard form (V.2) in which the function g(x) reads as:

$$g(x) = \mathcal{A} \exp(-Z_0 s^2 x^2) \left[ \sum_{j_+=2q+1}^{jp} + \sum_{j_-=2q+1}^{jp} \right] \Delta(j,p) \quad x^{j+1}$$
 (V.58)

and the coefficients  $c_n$  are found to be:

$$c_n = 0,$$
  $n \ even$  (V.59)

$$c_{n} = \frac{\sqrt{\pi}}{\sqrt{2}} i^{n-1} (-1)^{n} (2n+1) g_{n,TM}^{2q+1} (-1)^{\frac{n}{2} + \frac{|2q+1|}{2}} \frac{(n+|2q+1|-1)!!}{2^{\frac{n}{2} - \frac{|2q+1|}{2}} (\frac{n}{2} - \frac{|2q+1|}{2})!}, n \text{ odd}$$
(V.60)

Double summations in Rel (V.58) are reduced to single summations by using (Appendix D):

$$\sum_{j_{+}=2q+1}^{jp} A_{jp} = \sum_{j=|q|}^{\infty} A_{2j,j-q} , \forall q$$
 (V.61)

$$\sum_{j=2q+1}^{jp} A_{jp} = \sum_{j=q+1}^{\infty} A_{2j,j-q-1}, q \ge 0$$
 (V.62)

$$\sum_{j=2q+1}^{jp} A_{jp} = \sum_{j=|q|-1}^{\infty} A_{2j,j-q-1}, q < 0$$
 (V.63)

showing that only two cases are to be considered:  $q \ge 0$  and q < 0.

Using the same procedure as before and also invoking (Appendix E):

$$\sum_{m=0}^{\infty} \sum_{n=2q+2m+1}^{\infty} o = \sum_{n=1}^{\infty} \sum_{m=0}^{\frac{1}{2}(n-2q-1)} \epsilon(n; 1, 3, ..., 2q-1)$$
 (V.64)

the BSCs  $g_{n,TM}^m$ , n and m odd, are found to be:

$$g_{2p+1,TM}^{2q+1}(q \ge 0) = \frac{\mathcal{A}}{(-1)^q} 2^{2(p-q)} \frac{(p-q)!}{\Gamma(p+q+3/2)}$$

$$\sum_{m=0}^{p} \frac{\Gamma(2p-m+3/2)}{2^{2m}m!}$$

$$\sum_{t=0}^{p-m-q} \frac{(-Z_0s^2)^t}{t!} \left[ \epsilon(p-m;0,1,...,q-1) \right.$$

$$\mathcal{\Delta}(2p-2m-2t,p-m-t-q) + \epsilon(t;p-m-q)$$

$$\epsilon(p-m;0,1,...,q) \mathcal{\Delta}(2p-2m-2t,p-m-t-q-1) \right]$$

$$g_{2p+1,TM}^{2q+1}(q<0) = \frac{\mathcal{A}}{(-1)^{|q|+1}} 2^{2(p+1-|q|)} \frac{(p-|q|+1)!}{\Gamma(p+|q|+1/2)}$$

$$\sum_{m=0}^{p} \frac{\Gamma(2p-m+3/2)}{2^{2m}m!}$$

$$\sum_{t=0}^{p-m-|q|+1} \frac{(-Z_0s^2)^t}{t!} \left[ \epsilon(t;p-m-|q|+1) \right.$$

$$\epsilon(p-m;0,1,...,|q|-1) \Delta(2p-2m-2t,p-m-t-q) + \epsilon(p-m;0,1,...,|q|-2) \Delta(2p-2m-2t,p-m-t-q-1) \right]$$
(V.66)

# (ii) $g_{n,TM}^m$ , n odd and m even.

The starting point is now Rel (V.18). New notations must however be introduced for this case. It is first established, starting again from (IV.87), (IV.86), (IV.79) and (IV.77) that:

$$\left. \frac{\partial F}{\partial \cos \theta} \right|_{\theta = \pi/2} = \left[ \mathcal{B}x + \mathcal{C}x^3 \right] \quad exp(-Z_0 s^2 x^2) \tag{V.67}$$

in which:

$$\mathcal{B} = i \ exp(-Z_0 \ \frac{x_0^2 + y_0^2}{w_0^2}) \ exp(ikz_0) \ \left[ Z_0 Z_0^{"} \frac{x_0^2 + y_0^2}{w_0^2} + 2\epsilon_L s^2 Z_0^2 - Z_0 - Z_0^{"} \right]$$
(V.68)

$$C = i \ exp(-Z_0 \ \frac{x_0^2 + y_0^2}{w_0^2}) \ exp(ikz_0) \ Z_0 \ Z_0^" \ s^2$$
 (V.69)

$$Z_0'' = \frac{1}{kr} \left. \frac{\partial Q}{\partial \theta} \right|_{\theta = \pi/2} = \frac{2}{kl[i - \frac{2z_0}{l}]^2}$$
 (V.70)

We also need:

$$\frac{\partial \Psi_{jp}}{\partial \cos \theta} \bigg|_{\theta = \pi/2} = \Omega(j, p) \quad x^{j+1} \tag{V.71}$$

in which:

$$\Omega(j,p) = \frac{-ij}{k^j w_0^2} \frac{(x_0 - iy_0)^{j-p} (x_0 + iy_0)^p}{p!(j-p)!} \left(\frac{Z_0}{w_0^2}\right)^{j-1} Z_o^{"}$$
 (V.72)

It is also needed to evaluate the derivative  $\partial G/\partial \cos\theta$ . The expression is rather involved and not given here. However, in doing this exercise, the reader will set:

$$\mathcal{D} = \frac{2\epsilon_L}{il} Z_0^2 exp(-Z_0 \frac{x_0^2 + y_0^2}{w_0^2}) \ exp(ikz_0)$$
 (V.73)

Rel (V.18) is then given the standard form (V.2) with the function g(x) given by:

$$g(x) = exp(-Z_0 s^2 x^2) \left\{ \mathcal{A} \left[ \sum_{j_+=2q}^{jp} + \sum_{j_-=2q}^{jp} \right] \Omega(j,p) \quad x^{j+2} \right.$$

$$\left. + \frac{\mathcal{B}}{2} \left[ \sum_{j_+=2q}^{jp} + \sum_{j_-=2q}^{jp} \right] \Delta(j,p) \quad x^{j+2} + \frac{\mathcal{C}}{2} \left[ \sum_{j_+=2q}^{jp} + \sum_{j_-=2q}^{jp} \right] \Delta(j,p) x^{j+4} \right.$$

$$\left. + x_0 \mathcal{D} \sum_{j_0=2q}^{jp} \Delta(j,p) \quad x^{j+1} \right\}$$

and the coefficients  $c_n$  reading as:

$$c_{n} = 0, n \text{ even}$$

$$c_{n} = \frac{\sqrt{\pi}}{\sqrt{2}} i^{n-1} (-1)^{n} (2n+1) g_{n,TM}^{2q} (-1)^{\frac{n+|2q|-1}{2}} (V.75)$$

$$\frac{(n+|2q|)!!}{2^{\frac{1}{2}(n-|2q|-1)} \left(\frac{n-|2q|-1}{2}\right)!}, n \text{ odd}$$

After having reduced double summations in Rel (V.74) to single summations by using expressions given in the Appendix D, it is found that the cases q=0, q>0 and q<0 must be treated separately. Each of these cases is processed similarly as before, leading to:

$$\begin{split} g^0_{2p+1,TM} &= \frac{-p!}{\Gamma(p+3/2)} 2^{2p} \sum_{m=0}^p \frac{\Gamma(2p-m+3/2)}{2^{2m}m!} \sum_{t=0}^{p-m} \frac{(-Z_0 s^2)^t}{t!} \\ & \{ x_0 \mathcal{D} \Delta (2p-2m-2t, p-m-t) + \\ & + \epsilon (p-m;0) \epsilon(t;p-m) \frac{\mathcal{B}}{2} [\Delta (2p-2m-2t-1, p-m-t) + \\ & + \Delta (2p-2m-2t-1, p-m-t-1)] + \epsilon (p-m;0) \epsilon(t;p-m) \times (\text{V}.76) \\ & \times \mathcal{A} \left[ \Omega (2p-2m-2t-1, p-m-t) \right] + \\ & + \Omega (2p-2m-2t-1, p-m-t-1) \right] + \\ & + \epsilon (p-m;0,1) \epsilon(t;p-m,p-m-1) \\ & \frac{\mathcal{C}}{2} [\Delta (2p-2m-2t-3, p-m-t-1) + \\ & + \Delta (2p-2m-2t-3, p-m-t-2) \right] \} \end{split}$$

$$\begin{split} g_{2p+1,TM}^{2q}(q>0) &= \frac{-2^{2(p-q)}}{(-1)^q} \frac{(p-q)!}{\Gamma(p+q+3/2)} \sum_{m=0}^p \frac{\Gamma(2p-m+3/2)}{2^{2m}m!} \\ &\sum_{t=0}^{p-m-q} \frac{(-Z_0s^2)^t}{t!} \\ &\{ \epsilon(p-m;0,1,...,q-1) \\ [\mathcal{A} \quad \Omega(2p-2m-2t-1,p-m-t-q) + \\ &+ \frac{\mathcal{B}}{2} \ \Delta(2p-2m-2t-1,p-m-t-q) + \\ &+ \kappa_0 \mathcal{D} \quad \Delta(2p-2m-2t,p-m-t-q)] + \\ &+ \epsilon(t;p-m-q)\epsilon(p-m;0,1,...,q) \times \\ &\times [\mathcal{A} \quad \Omega(2p-2m-2t-1,p-m-t-q-1) + \\ &+ \frac{\mathcal{B}}{2} \quad \Delta(2p-2m-2t-1,p-m-t-q-1) + \\ &+ \frac{\mathcal{C}}{2} \ \Delta(2p-2m-2t-3,p-m-t-q-1)] + \\ &+ \epsilon(t;p-m-q,p-m-q-1)\epsilon(p-m;0,1,...,q+1) \times \\ &\times \frac{\mathcal{C}}{2} \quad \Delta(2p-2m-2t-3,p-m-t-q-2) \} \end{split}$$

$$\begin{split} g_{2p+1,TM}^{2q}(q<0) &= \frac{-2^{2(p-|q|)}}{(-1)^{|q|}} \frac{(p-|q|)!}{\Gamma(p+|q|+3/2)} \sum_{m=0}^{p} \frac{\Gamma(2p-m+3/2)}{2^{2m}m!} \\ & \sum_{t=0}^{p-m-|q|} \frac{(-Z_0s^2)^t}{t!} \\ & \{\epsilon(p-m;0,1,...,|q|-1) \\ & [\mathcal{A} \quad \Omega(2p-2m-2t-1,p-m-t-q-1) + \\ & + \frac{\mathcal{B}}{2} \quad \Delta(2p-2m-2t-1,p-m-t-q-1) + \\ & + \kappa_0 \mathcal{D} \quad \Delta(2p-2m-2t,p-m-t-q)] + \\ & + \epsilon(t;p-m-|q|)\epsilon(p-m;0,1,...,|q|) \times \\ & \times [\mathcal{A} \quad \Omega(2p-2m-2t-1,p-m-t-q) + \\ & + \frac{\mathcal{B}}{2} \quad \Delta(2p-2m-2t-1,p-m-t-q) + \\ & + \frac{\mathcal{C}}{2} \quad \Delta(2p-2m-2t-3,p-m-t-q-2)] + \\ & + \epsilon(t;p-m-|q|,p-m-|q|-1)\epsilon(p-m;0,1,...,|q|+1) \times \\ & \times \frac{\mathcal{C}}{2} \quad \Delta(2p-2m-2t-3,p-m-t-q-1) \} \end{split}$$

# (iii) $g_{n,TM}^m$ , n even and m odd.

Starting from Rel (V.19), the reader is now sufficiently well trained to readily establish:

$$\begin{split} g_{2p,TM}^{2q+1}(q \geq 0) &= \frac{i}{(-1)^q} 2^{2(p-q-1)} \frac{(p-q-1)!}{\Gamma(p+q+3/2)} \sum_{m=0}^p \frac{\Gamma(2p-m+1/2)}{2^{2m}m!} \\ &\sum_{t=0}^{p-m-q-1} \frac{(-Z_0 s^2)^t}{t!} \times \\ &\times \{\epsilon(p-m;0,1,...,q)[\frac{\mathcal{B}}{2} \varDelta(2p-2m-2t-2,p-m-t-q-1) + \\ &+ x_0 \mathcal{D} \quad \varDelta(2p-2m-2t-1,p-m-t-q-1) + \\ &+ \mathcal{A} \quad \varOmega(2p-2m-2t-2,p-m-t-q-1)] + \\ &+ \frac{1}{2} \epsilon(t;p-m-q-1) \epsilon(p-m;0,1,...,q+1) \times \\ &\times [\mathcal{B} \quad \varDelta(2p-2m-2t-2,p-m-t-q-2) + \\ &+ 2\mathcal{A} \quad \varOmega(2p-2m-2t-2,p-m-t-q-2) + \\ &+ \mathcal{C} \quad \varDelta(2p-2m-2t-4,p-m-t-q-2)] + \\ &+ \frac{\mathcal{C}}{2} \quad \epsilon(t;p-m-q-1,p-m-q-2) \epsilon(p-m;0,1,...,q+2) \times \\ &\times \varDelta(2p-2m-2t-4,p-m-t-q-3) \} \end{split}$$

$$\begin{split} g_{2p,TM}^{2q+1}(q<0) &= \frac{-i}{(-1)^{|q|}} 2^{2(p-|q|)} \frac{(p-|q|)!}{\Gamma(p+|q|+1/2)} \sum_{m=0}^{p} \frac{\Gamma(2p-m+1/2)}{2^{2m}m!} \\ &\sum_{t=0}^{p-m-|q|} \frac{(-Z_0s^2)^t}{t!} \times \\ &\times \{\epsilon(p-m;0,1,...,|q|-1) \times \\ &\times [x_0\mathcal{D} \quad \Delta(2p-2m-2t-1,p-m-t-q-1) + \\ &+ \frac{\mathcal{B}}{2} \quad \Delta(2p-2m-2t-2,p-m-t-q-2) + \\ &+ \mathcal{A} \quad \Omega(2p-2m-2t-2,p-m-t-q-2)] + \quad \text{(V.80)} \\ &+ \epsilon(t;p-m-|q|)\epsilon(p-m;0,1,...,|q|) \times \\ &\times [\frac{\mathcal{B}}{2} \quad \Delta(2p-2m-2t-2,p-m-t-q-1) + \\ &+ \mathcal{A} \quad \Omega(2p-2m-2t-2,p-m-t-q-1) + \\ &+ \mathcal{A} \quad \Omega(2p-2m-2t-2,p-m-t-q-1) + \\ &+ \frac{\mathcal{C}}{2} \quad \Delta(2p-2m-2t-4,p-m-t-q-3)] + \\ &+ \frac{\mathcal{C}}{2} \epsilon(t;p-m-|q|,p-m-|q|-1)\epsilon(p-m;0,1,...,|q|+1) \times \\ &\times \Delta(2p-2m-2t-4,p-m-t-q-2) \} \end{split}$$

# V.2.4 BSCs $g_{n,TE}^m$

BSCs  $g_{n,TE}^m$  may be similarly obtained from the set (V.20)-(V.23). However, notwithstanding the fact that deriving the required expressions by using again the NET -procedure would be an enjoyable task, it appears that detailed computations are no more necessary. Indeed, it is readily observed that the set (V.20)-(V.23) may be deduced from the set (V.16)-(V.19) by applying to the latter a transformation T defined as follows:

$$\sum_{j_{+}=} \rightarrow \frac{1}{i} \sum_{j_{+}=} \tag{V.81}$$

$$\sum_{j_{-}=} \rightarrow -\frac{1}{i} \sum_{j_{-}=} \tag{V.82}$$

$$x_0 \to y_0$$
 (V.83)

in which Rel (V.83) must be used only when  $x_0$  explicitly appears in the set (V.16)-(V.19), i.e. in terms associated with G. BSCs  $g_{n,TE}^m$  may therefore readily be obtained from BSCs  $g_{n,TM}^m$  by applying to them the transformation T, the unique difficulty being possibly to correctly identify the terms corresponding to  $\sum_{j_+=}^{\Sigma}$  or to  $\sum_{j_-=}^{\Sigma}$ . For the careful worker having kept the details of his computations for the BSCs  $g_{n,TM}^m$ , it would take only about one

hour to establish the corresponding expressions for the BSCs  $g_{n,TE}^m$ . It has not been found useful to serve them in this book. They are available from Gouesbet *et al* 368.

# V.3 Numerical Computations of BSCs by Using Finite Series

Twenty different expressions are required to compute all the BSCs  $g_n^m$ . These expressions look awkward but may actually be rather easily and efficiently programmed, leading to fast running routines. However, if expressions in section V.2 have been given to help the reader to make the connection with Gouesbet *et al* [368], they are not in the more appropriate form for numerical computations. Some rewriting is indeed necessary for the sake of efficiency.

#### V.3.1 Dimensionless Formulation

The dimensionless formulation is expressed in terms of dimensionless coordinates specifying the location of the beam waist center with respect to the particle center (see section III-1, and section IV.2.1):

$$x_0^+ = x_0/w_0, y_0^+ = y_0/w_0, z_0^+ = z_0/l (V.84)$$

and in terms of the beam shape factor s. The reader may need to recall Rels (IV.3) and (IV.4) to check our derivations. The eight quantities  $Z_0, Z_0^*, \mathcal{A}, \mathcal{B}, \mathcal{C}, \mathcal{D}, \Delta(j, p)$  and  $\Omega(j, p)$  from Rels (V.27), (V.70), (V.26), (V.68), (V.69), (V.73), (V.29) and (V.72) respectively may then be rewritten according to:

$$Z_0 = \frac{1}{1 + 2iz_0^+} \tag{V.85}$$

$$Z_0" = \frac{2s^2}{(i - 2z_0^+)^2} \tag{V.86}$$

$$\mathcal{A} = \frac{1}{2} Z_0 \exp[-Z_0(x_0^{+2} + y_0^{+2})] \exp(i\frac{z_0^+}{s^2})$$
 (V.87)

$$\mathcal{B} = i \ exp[-Z_0(x_0^{+2} + y_0^{+2})] \ exp(i\frac{z_0^+}{s^2})$$

$$\{Z_0 \ Z_0^" \ (x_0^{+2} + y_0^{+2}) + 2\epsilon_L s^2 Z_0^2 - Z_0 - Z_0^"\}$$
(V.88)

$$C = i \exp[-Z_0(x_0^{+2} + y_0^{+2})] \exp(i\frac{z_0^+}{s^2}) Z_0 Z_0^" s^2$$
 (V.89)

$$\begin{pmatrix} x_0 \\ y_0 \end{pmatrix} \mathcal{D} = \frac{2\epsilon_L}{i} \begin{pmatrix} x_0^+ \\ y_0^+ \end{pmatrix} s Z_0^2 \exp[-Z_0(x_0^{+2} + y_0^{+2})] \exp(i\frac{z_0^+}{s^2})$$
 (V.90)

$$\Delta(j,p) = (Z_0 s)^j \frac{(x_0^+ - iy_0^+)^{j-p} (x_0^+ + iy_0^+)^p}{p!(j-p)!}$$
(V.91)

$$\Omega(j,p) = -i \ j \ s \ (Z_0 s)^{j-1} \ Z_0^{"} \frac{(x_0^+ - i y_0^+)^{j-p} (x_0^+ + i y_0^+)^p}{p!(j-p)!}$$
(V.92)

showing that all introduced quantities were indeed dimensionless, excepted  $\mathcal{D}$ . However,  $\mathcal{D}$  never appears alone but in groups  $(x_0\mathcal{D})$  and  $(y_0\mathcal{D})$  for BSCs  $g_{n,TM}^m$  and  $g_{n,TE}^m$  respectively. Rel (V.90) shows that these groups are indeed dimensionless.

## V.3.2 Formulae Modifications for Programming

Finite series expressions for BSCs are modified by using the dimensionless formulation of section V.3.1 and invoking (Abramowitz and Stegun [369], pp 255):

$$\Gamma(n+\frac{1}{2}) = \frac{1.3.5...(2n-1)}{2^n}\Gamma(1/2)$$
 (V.93)

leading to, for n even and m = 0:

$$g_{2p,TM}^{0} = i \mathcal{A} \frac{8^{p}p!}{1.3...(2p-1)} \sum_{m=0}^{p} \frac{1.3....(2(2p-m))}{2^{2p-m}2^{2m}m!} \sum_{t=0}^{p-m-1} \frac{(-Z_{0}s^{2})^{t}}{t!} \epsilon(p-m;0)[\Delta(2p-2m-2t-1,p-m-t) + \Delta(2p-2m-2t-1,p-m-t-1)]$$
(V.94)

Such modifications being easy to carry out, it has not been felt useful to rewrite the full set of expressions in this book. Computer programs are available from the website connected to this book.

# Special Cases of Axisymmetric and Gaussian Beams

# VI.1 Axisymmetric Beams

We define an axisymmetric beam [74] to be a beam for which the z-component  $S_z$  of the Poynting vector, in which z is the direction of propagation of the beam, does not depend on the azimuthal angle  $\varphi$ , in suitably chosen coordinate systems.

In such a (spherical) coordinate system  $(r, \theta, \varphi)$ , when the beam is generic, i.e. when the energy flowing on the beam axis is not zero, the BSCs  $g_n^m$  are found to satisfy (after much algebra) [74]:

$$g_n^m = 0, |m| \neq 1 g_{n,TM}^1 = \frac{1}{K} g_{n,TM}^{-1} = -i\varepsilon g_{n,TE}^1 = \frac{i\varepsilon}{K} g_{n,TE}^{-1}$$
 (VI.1)

in which the parameter  $\varepsilon$  is  $\pm 1$  while the parameter K is a real number. The sign  $\varepsilon$  is not a property of the beam in the strict sense but depends on the coordinate system in which it is described. More specifically, we have  $\varepsilon = -1$  (+1) when the energy flux flows toward positive z's (negative z's). From now on, we consider beams propagating in the positive z-direction and therefore take  $\varepsilon = -1$ . As far as K is concerned, it defines the polarization state of the beam as a linear combination of a state for which the radial electric field component  $E_r$  is proportional to  $\cos \varphi$  and of another state for which  $E_r$  is proportional to  $\sin \varphi$ . Nonmixed states of polarization correspond to  $K = \pm 1$ .

Conversely, it can be demonstrated that, if the BSCs satisfy Rel (VI.1), with  $g_{n,TM}^1 \neq 0$ , then the beam is a generic axisymmetric beam.

It is then seen that, for a generic axisymmetric beam, the double set of BSCs  $\{g_{n,TM}^m, g_{n,TE}^m\}$  reduces to a single set of special BSCs  $\{g_n\}$  that we conveniently define as (with  $\varepsilon = -1$ ):

$$\frac{g_n}{2} \equiv g_{n,TM}^1 = \frac{1}{K} g_{n,TM}^{-1} = i g_{n,TE}^1 = \frac{-i}{K} g_{n,TE}^{-1} \neq 0 \tag{VI.2}$$

in which the prefactor 1/2 is actually not essential but later produces better looking expressions.

Let us select a nonmixed state of polarization for which K=+1, i.e. we now have:

$$\begin{array}{c|c} g_n^m = 0, & |m| \neq 1 \\ \frac{g_n}{2} \equiv g_{n,TM}^1 = g_{n,TM}^{-1} = ig_{n,TE}^1 = -ig_{n,TE}^{-1} \end{array} \right\} \tag{VI.3}$$

Chapters IV and V were mostly devoted to a special case of the GLMT when the incident beam is a laser beam in its fundamental (Gaussian) mode  $TEM_{00}$ , with however an arbitrary location of the particle. The axis  $O_Pz$  of the particle Cartesian coordinate system  $(O_Pxyz)$ , see Fig (III.1), then in general does not coincide with the axis  $O_Gw$  of the beam Cartesian coordinate system. This is called the off-axis case.

Let us now consider the case when the center of the scatter center is located on the beam axis, i.e. axis  $O_Pz$  coincides with axis  $O_Gw$ . This is called the on-axis case. Clearly, a Gaussian beam is a generic axisymmetric beam and, in the on-axis case, the coordinate system is suitably chosen. Therefore, the BSCs of an on-axis Gaussian beam reduce to Rel (VI.1), i.e. an on-axis Gaussian beam may be described by a single set  $\{g_n\}$  of special BSCs. We shall later check that such is indeed the case. More particularly, for an on-axis Gaussian beam flowing toward the positive z-direction, with the electric field polarized in the x-direction at its focal waist (as is assumed to be the case in chapter III), we shall find that Rel (VI.3) is valid. The validity of Rel (VI.3) alone however does not ensure that we are facing a Gaussian beam. Gaussianity requires specific behaviours of the functions  $g_n = g_n(n)$  on which Rel (VI.3) tells us nothing. Nevertheless, due to the strong relationship between Rel (VI.3) and Gaussianity, we shall say that a beam defined by Rel (VI.3) is (structurally) Gaussian-like.

A still more special case when the particle center is located at the beam waist center  $(O_P \equiv O_G)$  of a Gaussian beam will be considered too. Finally, starting from this last case and letting the Gaussian beam radius increase toward infinity, the Gaussian beam tends to a plane wave and the classical LMT will be recovered as a special case of GLMT, as it should. Clearly, LMT could also be recovered from infinitely many other cases such as from off-axis Gaussian beams or from laser sheets. But it is particularly convenient to use on-axis Gaussian beams, with beam waist center location, as the starting point to recover LMT.

Historically, the GLMT has been developed by starting with the special case of beam waist center location [I] before considering successively the axis location case [76], then arbitrary location and arbitrary beam [298], [2], [89]. In the present book, instead of proceeding from special cases toward generality, we proceed in the reverse way, from generality toward special cases. Starting from the general case, this section makes us landing on the restricted case of axisymmetric beams. However, due to the big amount of algebra required for this landing process, the reader is kindly invited to refer to Gouesbet [74] for details.

# VI.2 The LSC-Decomposition and Gaussian-Like Beams

We now consider Gaussian-like beams for which the set of BSCs satisfies Rel (VI.3). The incident BSPs (Rels (III.1)-(III.2)) then read as:

$$U_{TM}^{i} = E_{0}r\cos\varphi \sum_{n=1}^{\infty} c_{n}^{pw} g_{n} \Psi_{n}^{(1)}(kr) P_{n}^{1}(\cos\theta)$$
 (VI.4)

$$U_{TE}^{i} = H_{0}r \sin \varphi \sum_{n=1}^{\infty} c_{n}^{pw} g_{n} \Psi_{n}^{(1)}(kr) P_{n}^{1}(\cos \theta)$$
 (VI.5)

In view of Rels (II.50), (II.56), the electric field component  $E_r$  is therefore proportional to  $\cos \varphi$ , indeed corresponding to a nonmixed state of polarization as announced in section VI.1. We then see that the double summations over n and m reduce to single summations over n only. Therefore we straight away observe that GLMT for Gaussian-like beams (or also more generally for axisymmetric beams) will dramatically simplify.

In particular, let us consider the generalized amplitude functions  $S_2$  and  $S_1$  of Rels (III.111) and (III.110). For Gaussian-like beams, they reduce to:

$$S_2 = \cos \varphi S_2 \tag{VI.6}$$

$$S_1 = i \sin \varphi S_1 \tag{VI.7}$$

then defining two amplitude functions  $S_2$  and  $S_1$ , which do not depend on  $\varphi$ , and read as:

$$S_2 = \sum_{n=1}^{\infty} \frac{2n+1}{n(n+1)} g_n \left[ a_n \tau_n(\cos \theta) + b_n \pi_n(\cos \theta) \right]$$
 (VI.8)

$$S_1 = \sum_{n=1}^{\infty} \frac{2n+1}{n(n+1)} g_n \left[ a_n \pi_n(\cos \theta) + b_n \tau_n(\cos \theta) \right]$$
 (VI.9)

again only involving single summations.

The amplitude functions  $S_2$  and  $S_1$  are exactly the ones which appear in the classical LMT but for the appearance of the set  $\{g_n\}$  of special BSCs. They also are exactly the ones which were introduced in the case of Gaussian beams [I] [76], coherently with the fact that Gaussian beams are Gaussian-like.

Let us now consider a class of beams for which BSCs  $g_n^{\pm 1}$  are defined versus  $g_n$  as shown in Rel (VI.3), without however assuming the nullity of the BSCs  $g_n^m$ ,  $|m| \neq 1$ . Rels (VI.6)-(VI.7) then generalize to:

$$S_2 = \cos \varphi \ S_2 + S_2' \tag{VI.10}$$

$$S_1 = i \sin \varphi S_1 + S_1' \tag{VI.11}$$

in which the complementary generalized amplitude functions  $\mathcal{S}_2^{'}$  and  $\mathcal{S}_1^{'}$  incorporate the contributions of the BSCs  $g_n^m, |m| \neq 1$ . Rels (III.111), (III.110) for the generalized amplitude functions  $\mathcal{S}_2$  and  $\mathcal{S}_1$  and Rels (VI.8)-(VI.9) for the amplitude functions  $\mathcal{S}_2$  and  $\mathcal{S}_1$  then imply:

$$S_{2}' = \sum_{n=1}^{\infty} \sum_{\substack{m=-n \ |m|\neq 1}}^{+n} \frac{2n+1}{n(n+1)} \left[ a_{n} \ g_{n,TM}^{m} \ \tau_{n}^{|m|}(\cos\theta) + i \ m \ b_{n} \ g_{n,TE}^{m} \ \pi_{n}^{|m|}(\cos\theta) \right] \exp(im\varphi)$$

$$+ \sum_{n=1}^{\infty} \frac{2n+1}{n(n+1)} \left[ a_{n} \ \tau_{n}(\cos\theta)(\cos\varphi \ G_{n,TM}^{+} + i \ \sin\varphi \ G_{n,TM}^{-}) + b_{n} \ \pi_{n}(\cos\theta) \ (i \ \cos\varphi \ G_{n,TE}^{-} - \sin\varphi \ G_{n,TE}^{+}) \right]$$
(VI.12)

$$S_{1}^{'} = \sum_{n=1}^{\infty} \sum_{\substack{m=-n \\ |m| \neq 1}}^{+n} \frac{2n+1}{n(n+1)} \left[ m \ a_{n} \ g_{n,TM}^{m} \ \pi_{n}^{|m|}(\cos \theta) + i \ b_{n} \ g_{n,TE}^{m} \ \tau_{n}^{|m|}(\cos \theta) \right] \exp(im\varphi)$$

$$+\sum_{n=1}^{\infty} \frac{2n+1}{n(n+1)} \left[ a_n \, \pi_n(\cos\theta) \, \left( \cos\varphi \, G_{n,TM}^- + i \, \sin\varphi \, G_{n,TM}^+ \right) \right.$$

$$\left. + b_n \, \tau_n \left( \cos\theta \right) \left( i \, \cos\varphi \, G_{n,TE}^+ - \sin\varphi \, G_{n,TE}^- \right) \right]$$
(VI.13)

in which:

$$G_{n,TM}^{+} = g_{n,TM}^{+1} + g_{n,TM}^{-1} - g_n$$
 (VI.14)

$$G_{n,TE}^{+} = g_{n,TE}^{+1} + g_{n,TE}^{-1}$$
 (VI.15)

$$G_{n,TM}^{-} = g_{n,TM}^{+1} - g_{n,TM}^{-1}$$
 (VI.16)

$$G_{nTE}^{-} = g_{nTE}^{+1} - g_{nTE}^{-1} + i g_n$$
 (VI.17)

By using Rels (VI.10) and (VI.11), the Rel (III.107) for the scattered intensities becomes:

$$\begin{pmatrix} I_{\theta}^{+} \\ I_{\varphi}^{+} \end{pmatrix} = \begin{pmatrix} I_{\theta}^{+L} \\ I_{\varphi}^{+L} \end{pmatrix} + \begin{pmatrix} I_{\theta}^{+S} \\ I_{\varphi}^{+S} \end{pmatrix} + \begin{pmatrix} I_{\theta}^{+C} \\ I_{\varphi}^{+C} \end{pmatrix}$$
(VI.18)

in which:

$$\begin{pmatrix} I_{\theta}^{+L} \\ I_{\varphi}^{+L} \end{pmatrix} = \frac{\lambda^2}{4\pi^2 r^2} \begin{pmatrix} i_2 & \cos^2 \varphi \\ i_1 & \sin^2 \varphi \end{pmatrix}$$
(VI.19)

with intensity functions  $i_j$  (j = 1, 2) given by:

$$i_j = |S_j|^2 \tag{VI.20}$$

and:

$$\begin{pmatrix} I_{\theta}^{+S} \\ I_{\varphi}^{+S} \end{pmatrix} = \frac{\lambda^2}{4\pi^2 r^2} \; \begin{pmatrix} |\mathcal{S}_2^{\prime}|^2 \\ |\mathcal{S}_1^{\prime}|^2 \end{pmatrix} \tag{VI.21}$$

$$\begin{pmatrix} I_{\theta}^{+C} \\ I_{\varphi}^{+C} \end{pmatrix} = \frac{\lambda^2}{2\pi^2 r^2} \begin{pmatrix} \cos \varphi \operatorname{Re}(S_2 \mathcal{S}_2^{'*}) \\ \sin \varphi \operatorname{Re}(iS_1 \mathcal{S}_1^{'*}) \end{pmatrix}$$
(VI.22)

The first term (VI.19) with superscript L possesses exactly the same structure as in LMT. The only difference is that the amplitude functions  $S_1$  and  $S_2$  defining the intensity functions  $i_j$  contain special BSCs which do not appear in LMT. This term may be called Leader or LMT-term, justifying the use of a superscript L. The second term (VI.21) contains complementary amplitude functions  $S_2'$  and  $S_1'$  which must be added to LMT-terms ( $\cos \varphi S_2$ ) and  $(i \sin \varphi S_1)$  in Rels (VI.6), (VI.7) to produce generalized amplitude functions  $S_2$  and  $S_1$ . This second term is therefore called the secondary term (superscript S). Finally, the last term (VI.22) involves a coupling between leader and secondary terms and will therefore be named a Cross or Coupling term (superscript C). Hence, Rel (VI.18) tells us that the scattered intensities in GLMT are the summation of Leader-, Secondary- and Coupling-terms. This is called a LSC-decomposition.

Let us now consider the Rel (III.114) for the phase angle and introduce:

$$\tan \delta_0 = \frac{\text{Re}(S_1) \text{Im}(S_2) - \text{Re}(S_2) \text{Im}(S_1)}{\text{Re}(S_1) \text{Re}(S_2) + \text{Im}(S_1) \text{Im}(S_2)}$$
(VI.23)

which is formally identical to the expression in the LMT-framework but again for the appearance of special BSCs involved in the amplitude functions  $S_j$ . The angle  $\delta_0$  may then be thought as a leader angle. Inserting Rels (VI.6) and (VI.7) in (III.114), it is then found that the phase angle  $\delta$  and the leader angle  $\delta_0$  are linked by the relation:

$$\tan \delta = \tan (\delta_0 + \delta_1) + \tan \delta_2$$
 (VI.24)

in which:

$$\tan \delta_1 = \frac{-b \tan \delta_0}{1 + b + \tan^2 \delta_0} \tag{VI.25}$$

$$\tan \delta_2 = \frac{a}{1+b} \tag{VI.26}$$

in which:

$$a = \frac{\mathcal{N}'}{\mathcal{D}_0} \tag{VI.27}$$

$$b = \frac{\mathcal{D}'}{\mathcal{D}_0} \tag{VI.28}$$

in which:

$$\mathcal{D}_0 = \text{Re}(S_1) \ \text{Re}(S_2) + \text{Im}(S_1) \ \text{Im}(S_2)$$
 (VI.29)

$$\mathcal{N}' = \frac{1}{\cos \varphi} [\operatorname{Re}(S_1) \operatorname{Im}(S_2^{'}) - \operatorname{Im}(S_1) \operatorname{Re}(S_2^{'})]$$

$$+ \frac{1}{\sin \varphi} [\operatorname{Re}(S_2) \operatorname{Re}(S_1^{'}) + \operatorname{Im}(S_2) \operatorname{Im}(S_1^{'})]$$

$$+ \frac{1}{\sin \varphi \cos \varphi} [\operatorname{Re}(S_1^{'}) \operatorname{Re}(S_2^{'}) + \operatorname{Im}(S_1^{'}) \operatorname{Im}(S_2^{'})]$$
(VI.30)

$$\mathcal{D}' = \frac{1}{\cos \varphi} [\operatorname{Re}(S_1) \operatorname{Re}(S_2') + \operatorname{Im}(S_1) \operatorname{Im}(S_2')]$$

$$+ \frac{1}{\sin \varphi} [\operatorname{Re}(S_2) \operatorname{Im}(S_1') - \operatorname{Im}(S_2) \operatorname{Re}(S_1')]$$

$$+ \frac{1}{\sin \varphi \cos \varphi} [\operatorname{Im}(S_1') \operatorname{Re}(S_2') - \operatorname{Re}(S_1') \operatorname{Im}(S_2')]$$
(VI.31)

It is then observed that Rel (VI.24) involves complementary angles  $\delta_1$  and  $\delta_2$  which depend in a rather complex way on leader, secondary and cross terms, that is no nice LSC-decomposition appears in an obvious way for this quantity.

For the cross-sections (Rels (III.137), (III.142), (III.159), (III.182), (III.185)), the procedure consists first in isolating in the summations the terms containing BSCs  $g_n^m$ , |m| = 1, by using (from Rels (VI.14)–(VI.17)):

$$g_{n,TM}^{1} = \frac{1}{2} [G_{n,TM}^{+} + G_{n,TM}^{-} + g_{n}]$$
 (VI.32)

$$g_{n,TM}^{-1} = \frac{1}{2} [G_{n,TM}^{+} - G_{n,TM}^{-} + g_n]$$
 (VI.33)

$$g_{n,TE}^1 = \frac{1}{2} [G_{n,TE}^+ + G_{n,TE}^- - ig_n]$$
 (VI.34)

$$g_{n,TE}^{-1} = \frac{1}{2} [G_{n,TE}^{+} - G_{n,TE}^{-} + ig_n]$$
 (VI.35)

The cross-section expressions may afterward be split into three contributions (i) the leading term involving only special BSCs  $g_n$  (ii) the secondary term involving BSCs  $g_n^m$ ,  $|m| \neq 1$ , and quantities  $G_{n,TM}^+, G_{n,TM}^-, G_{n,TE}^+, G_{n,TE}^-$  and (iii) the cross-term involving multiplicative coupling of all these quantities, according to:

$$C_i = C_i^L + C_i^S + C_i^C (VI.36)$$

in which the subscript i designates any cross-section.

The leader terms are found to be:

$$C_{sca}^{L} = \frac{\lambda^{2}}{2\pi} \sum_{n=1}^{\infty} (2n+1) |g_{n}|^{2} [(a_{n})^{2} + (b_{n})^{2}]$$
 (VI.37)

$$C_{ext}^{L} = \frac{\lambda^2}{2\pi} \operatorname{Re} \sum_{n=1}^{\infty} (2n+1) |g_n|^2 (a_n + b_n)$$
 (VI.38)

$$C_{pr,x}^{L} = C_{pr,y}^{L} = 0$$
 (VI.39)

$$C_{pr,z}^{L} = \frac{\lambda^{2}}{2\pi} \sum_{n=1}^{\infty} \frac{2n+1}{n(n+1)} |g_{n}|^{2} \operatorname{Re}(a_{n} + b_{n}^{*} - 2a_{n}b_{n}^{*})$$
(VI.40)

$$+\frac{n(n+2)}{n+1}\operatorname{Re}\left[g_{n}g_{n+1}^{*}(a_{n}+b_{n}+a_{n+1}^{*}+b_{n+1}^{*}-2a_{n}a_{n+1}^{*}-2b_{n}b_{n+1}^{*})\right]$$

which again formally identify with the corresponding expressions in the LMT-framework but for the appearance of special BSCs. It is interesting to remark that the leading terms  $C_{pr,x}^L$  and  $C_{pr,y}^L$  of the transverse radiation pressure cross-sections are zero as it would be for a plane wave. The expressions for the secondary and cross terms are not given. They are indeed too awkward and unpleasant to contemplate. For further use however, it must be noted that they are zero when the coefficients  $g_n^m, |m| \neq 1$  and  $G_{n,TM}^+, G_{n,TM}^-, G_{n,TE}^+, G_{n,TE}^-$  are zero. Finally, we mention that LSC-decompositions were first introduced in Gouesbet  $et\ al\ [298]$ . The discussion of LSC-decompositions is here refined thanks to the prior introduction of axisymmetric beams.

#### VI.3 Axis Location in a Gaussian Beam

The above formulation is now specified to the case when the center of the scatterer is located on the axis of the Gaussian beam  $(O_P \text{ on axis } O_G w)$ :

$$x_0 = y_0 = 0 (VI.41)$$

Rel (IV.83) then implies:

$$\Psi_{ip}(x_0 = y_0 = 0) = \delta_i^0 \tag{VI.42}$$

i.e. all  $\Psi_{ip}$ 's are zero excepted:

$$\Psi_{00}(x_0 = y_0 = 0) = 1 \tag{VI.43}$$

This leads to a dramatic simplification of the GLMT because, inserting Rel (VI.42) in the expressions for the BSCs  $g_n^m$  (for instance Rels (IV.92), (IV.93)), it is found that all BSCs  $g_n^m$  become equal to 0, excepted for |m| = 1. Furthermore, the nonzero BSCs satisfy:

$$g_{n,TM}^{1} = g_{n,TM}^{-1} = \frac{k(2n+1)}{2i^{n-1}(-1)^{n}\pi n(n+1)} \int_{0}^{\pi} \int_{0}^{\infty} F(x_{0} = y_{0} = 0)$$

$$r\Psi_{n}^{(1)}(kr)P_{n}^{1}(\cos\theta) \sin\theta \ d\theta \ d(kr)$$
(VI.44)

$$g_{n,TE}^{1} = -g_{n,TE}^{-1} = \frac{k(2n+1)}{2i^{n-2}(-1)^{n-1}\pi n(n+1)} \int_{0}^{\pi} \int_{0}^{\infty} F(x_{0} = y_{0} = 0)$$

$$r\Psi_{n}^{(1)}(kr)P_{n}^{1}(\cos\theta)\sin\theta \ d\theta \ d(kr)$$
(VI.45)

Rels (VI.44) and (VI.45) together with Rels (VI.15) and (VI.16) show that:

$$G_{n,TE}^+ = G_{n,TM}^- = 0$$
 (VI.46)

Rels (VI.44) and (VI.45) also imply:

$$g_{n,TM}^1 = i \ g_{n,TE}^1$$
 (VI.47)

$$g_{n,TM}^{-1} = -i g_{n,TE}^{-1}$$
 (VI.48)

Therefore, the knowledge of one set of coefficients such as  $\{g_{n,TM}^1\}$  is sufficient to determine all the other sets  $\{g_{n,TM}^{-1}\}$ ,  $\{g_{n,TE}^1\}$ ,  $\{g_{n,TE}^{-1}\}$ . More specifically, BSCs for axis location in a Gaussian beam satisfy Rel (VI.3), i.e. as previously announced, Gaussian beams are Gaussian-like.

The definition of special BSCs  $g_n$ 's in Rel (VI.3) and Rels (VI.14), (VI.17) then also imply that:

$$G_{n,TM}^+ = G_{n,TE}^- = 0$$
 (VI.49)

The special BSCs  $g_n$  are then readily found to read as:

$$g_n = \frac{k(2n+1)}{i^{n-1} (-1)^n \pi n (n+1)} \int_0^{\pi} \int_0^{\infty} F(x_0 = y_0 = 0) r \Psi_n^{(1)}(kr)$$

$$(VI.50)$$

$$P_n^1(\cos \theta) \sin \theta \ d\theta \ d(kr)$$

which involves a double quadrature over  $\theta$  and r. If the BSCs  $g_n^m$  are expressed by using Rels (IV.90), (IV.91), (III.3), then the special BSCs may be expressed in terms of a single quadrature over  $\theta$ , according to:

$$g_n = \frac{k}{2 i^{n-1} (-1)^n n (n+1)} \frac{a}{\Psi_n^{(1)}(ka)} \int_0^{\pi} F(r=a, x_0 = y_0 = 0)$$

$$(VI.51)$$

$$P_n^1(\cos \theta) \sin \theta d\theta$$

The validity of the Gaussian-like Rel (VI.3) induces dramatic simplifications in the expressions for the BSPs (Rels (III.1), (III.2), (III.4), (III.5), (III.35), (III.36), (III.37), (III.38)), for the incident beam field components (Rels (III.39)–(III.50)), for the scattered wave field components (Rels (III.53)–(III.64)), for the sphere field components (Rels (III.65)–(III.76)) and also in Rels (III.92)–(III.97) and (III.101)–(III.104), which may now be expressed by using the set of special BSCs. In particular, the expressions (III.101)–(III.104) for the scattered field components in the far field now simplify to:

$$E_{\theta} = \frac{iE_0}{kr} \exp(-ikr) \cos \varphi \sum_{n=1}^{\infty} \frac{2n+1}{n(n+1)} g_n \left[ a_n \tau_n(\cos \theta) + b_n \pi_n(\cos \theta) \right]$$
(VI.52)

$$E_{\varphi} = \frac{-iE_0}{kr} \exp(-ikr) \sin \varphi \sum_{n=1}^{\infty} \frac{2n+1}{n(n+1)} g_n \left[ a_n \pi_n(\cos \theta) + b_n \tau_n(\cos \theta) \right]$$
(VI.53)

together with Rels (III.103)-(III.104) which remain unchanged.

Because the complementary amplitude functions  $S'_1$  and  $S'_2$  are zero (as a direct consequence of Rel (VI.3)), the secondary and cross terms in Rel (VI.18) become also identical to zero and the scattered intensities reduce to leader terms according to:

$$\begin{pmatrix}
I_{\theta}^{+}(x_{0}=y_{0}=0) \\
I_{\varphi}^{+}(x_{0}=y_{0}=0)
\end{pmatrix} = \frac{\lambda^{2}}{4\pi^{2}r^{2}} \begin{pmatrix}
i_{2}(x_{0}=y_{0}=0)\cos^{2}\varphi \\
i_{1}(x_{0}=y_{0}=0)\sin^{2}\varphi
\end{pmatrix}$$
(VI.54)

in which the intensity functions are defined by Rel (VI.20).

The complementary phase angles  $\delta_1$  and  $\delta_2$  are also readily found to be 0. Therefore the phase angle  $\delta$  becomes equal to the leader angle  $\delta_0$ :

$$\tan \delta = \tan \delta_0$$
 (VI.55)

leading to:

$$\tan \delta = \frac{\text{Re}(S_1) \text{Im}(S_2) - \text{Re}(S_2) \text{Im}(S_1)}{\text{Re}(S_1) \text{Re}(S_2) + \text{Im}(S_1) \text{Im}(S_2)}$$
(VI.56)

which is strictly identical with the expression in the LMT-framework, but again for the appearance of the  $g_n$ 's in the amplitude functions  $S_i$ .

Similarly, all secondary and cross-terms are zero in the expressions for the cross-sections as a result of the nullity of the  $g_n^{m}$ 's,  $|m| \neq 1$  and of Rels (VI.46), (VI.49).

The cross-section expressions then identify with the expressions for the leader terms:

$$C_{sca} = \frac{\lambda^2}{2\pi} \sum_{n=1}^{\infty} (2n+1) |g_n|^2 \left[ |a_n|^2 + |b_n|^2 \right]$$
 (VI.57)

$$C_{ext} = \frac{\lambda^2}{2\pi} \operatorname{Re} \sum_{n=1}^{\infty} (2n+1) |g_n|^2 (a_n + b_n)$$
 (VI.58)

$$C_{pr,x} = C_{pr,y} = 0$$
 (VI.59)

$$C_{pr,z} = \frac{\lambda^2}{2\pi} \sum_{n=1}^{\infty} \frac{2n+1}{n(n+1)} |g_n|^2 \operatorname{Re} \left[ (a_n + b_n^* - 2a_n b_n^*) \right] + \frac{n(n+2)}{n+1}$$
(VI.60)
$$\operatorname{Re} \left[ g_n g_{n+1}^* (a_n + b_n + a_{n+1}^* + b_{n+1}^* - 2a_n a_{n+1}^* - 2b_n b_{n+1}^*) \right]$$

In particular Rel (VI.59) shows that there is no transverse radiation pressure force when the scatter center is located on the axis of a Gaussian beam. Considering the way used to establish this result, it appears to be more generally valid for Gaussian-like beams.

The set of formulae obtained in the GLMT-framework for axis location in Gaussian beams is strikingly similar to the set of corresponding formulae in classical LMT. More precisely, the relations for field components, scattered intensities, phase angle, scattering and extinction cross-sections (and hence for absorption cross-section), and transverse radiation pressure cross-sections are formally identical in the present special case of GLMT and in the LMT, but for the appearance of special BSCs.

This may be understood as a consequence of the fact that all secondary and cross terms have disappeared from the formulation. A practical consequence is that any owner of computer programs handling LMT-formulae may readily adapt them by modifying a few statements, essentially incorporating multiplications by special BSCs, and implementing a subroutine to evaluate these coefficients.

Such a formal identification however does not hold for the longitudinal radiation pressure cross-section, a fact which is attributed to wave-front curvature. Indeed, for a plane wave, Rel (III.147) would read as [17]:

$$C_{pr,z} = C_{ext} - \overline{\cos \theta} \ C_{sca}$$
 (VI.61)

which is formally different of Rel (III.147). The expressions obtained in this section are in agreement with those given by Gouesbet *et al* [76] excepted for the cross-section  $C_{pr,z}$  which was derived by using Rel (VI.61) instead of Rel (III.147).

This section will be ended by elaborating a bit more on the expressions for the special BSCs  $g_n$ . For the case under study, Rel (IV.86) expressing the function F is specified for  $x_0 = y_0 = 0$ .

Rels (VI.50) and (VI.51) become:

$$g_{n} = \frac{k(2n+1)}{i^{n-1}(-1)^{n}\pi n(n+1)} \int_{0}^{\pi} \int_{0}^{\infty} iQ \exp\left[-iQ\frac{r^{2}\sin^{2}\theta}{w_{0}^{2}}\right] \left(1 - \epsilon_{L}\frac{2Q}{l}r\cos\theta\right)$$

$$(VI.62)$$

$$\exp[-ik(r\cos\theta - z_{0})] r \Psi_{n}^{(1)}(kr) P_{n}^{1}(\cos\theta) \sin^{2}\theta d\theta(kr)$$

$$g_{n} = \frac{k}{2i^{n-1}(-1)^{n}n(n+1)} \frac{a}{\Psi_{n}^{(1)}(ka)} \int_{0}^{\pi} iQ \exp\left[-iQ\frac{a^{2}\sin^{2}\theta}{w_{0}^{2}}\right]$$
(VI.63)
$$\left(1 - \epsilon_{L} \frac{2Q}{I} a \cos\theta\right) \exp\left[-ik(a \cos\theta - z_{0})\right] P_{n}^{1}(\cos\theta) \sin^{2}\theta d\theta$$

in which Q reads as:

$$Q = \frac{1}{i + \frac{2}{7}(r\cos\theta - z_0)}$$
 (VI.64)

in Rel (VI.62) with r = a in Rel (VI.63).

The next special case is to assume that the scatter center is located at the beam waist center, i.e. the condition  $z_0 = 0$  also holds. Rels (VI.62)-(VI.64) simplify accordingly. For instance, Rel (VI.62) becomes:

$$g_{n} = \frac{k(2n+1)}{i^{n-1}(-1)^{n}\pi n(n+1)} \int_{0}^{\pi} \int_{0}^{\infty} f \exp(-ikr\cos\theta) \ r \Psi_{n}^{(1)}(kr)$$

$$(VI.65)$$

$$P_{n}^{1}(\cos\theta) \sin^{2}\theta \ d\theta \ d(kr)$$

in which the function f reads as:

$$f = i \ Q(z_0 = 0) \ \exp\left[-iQ(z_0 = 0) \ \frac{r^2 \sin^2 \theta}{w_0^2}\right] \ (1 - \epsilon_L \frac{2Q(z_0 = 0)}{l} r \cos \theta)$$
(VI.66)

If the beam is described at the order  $L^-$ , the function f simplifies to:

$$f = i \ Q(z_0 = 0) \ \exp\left[-iQ(z_0 = 0) \ \frac{r^2 \sin^2 \theta}{w_0^2}\right]$$
 (VI.67)

This was essentially the case investigated in Gouesbet and Gréhan [1].

## VI.4 Lorenz-Mie Theory

The LMT must be a special case of the GLMT. Such a special case may be recovered from an arbitrary location in an arbitrary beam by letting the transverse characteristic length scales of the beam tending to the infinite. The simplest procedure available to us in this book is however to consider the case of axis location in a Gaussian beam. Letting the beam waist radius  $w_0$  going to infinity which means that the beam locally becomes a plane wave leads to (Rel (IV.4)):

$$l \to \infty$$
 (VI.68)

and therefore to (Rel (VI.64)):

$$Q \to 1/i$$
 (VI.69)

The expression (VI.62) for the special BSCs  $g_n$  becomes:

$$g_n = \frac{k(2n+1)e^{ikz_0}}{i^{n-1}(-1)^n \pi n(n+1)} \int_0^{\pi} \int_0^{\infty} \exp(-ikr\cos\theta) \ r \Psi_n^{(1)}(kr)$$

$$(VI.70)$$

$$P_n^1(\cos\theta) \sin^2\theta \ d\theta \ d(kr)$$

It now happens that the term  $\exp(-ikr\cos\theta)$  may be expanded in terms of spherical Bessel functions and of Legendre polynomials (130, t3, p313) according to:

$$\exp(-ikr\cos\theta) = \sum_{n=0}^{\infty} i^n (-1)^n (2n+1) \, \Psi_n^{(1)}(kr) \, P_n(\cos\theta)$$
 (VI.71)

Deriving Rel (VI.71) with respect to  $\cos \theta$  and recalling the definition of associated Legendre functions  $P_n^1(\cos \theta)$  in Rel (II.73) leads to:

$$\exp(-ikr\cos\theta) = \frac{1}{ikr} \sum_{n=1}^{\infty} i^n (-1)^n (2n+1) \Psi_n^{(1)}(kr) \frac{P_n^1(\cos\theta)}{\sin\theta}$$
 (VI.72)

which may be inserted in Rel (VI.70) to provide:

$$g_{n} = \exp(ikz_{0}) \sum_{m=1}^{\infty} \frac{2n+1}{\pi n(n+1)} \frac{(-1)^{m} i^{m} (2m+1)}{(-1)^{n} i^{n}}$$

$$\int_{0}^{\infty} \Psi_{m}^{(1)}(kr) \Psi_{n}^{(1)}(kr) d(kr) \int_{0}^{\pi} P_{m}^{1}(\cos\theta) P_{n}^{1}(\cos\theta) \sin\theta \ d\theta$$
(VI.73)

Invoking orthogonality properties for associated Legendre functions (Rel (III.12)), and the Rel (III.15) for the spherical Bessel functions, then readily leads to:

$$g_n = \exp(ikz_0), \quad \forall n$$
 (VI.74)

Therefore the special BSCs for a plane wave reduce to a phase term which is actually irrelevant. Such a phase term would appear in the expressions for the field components but would disappear in the expressions for the scattered intensities and cross-sections (Rels (VI.54), (VI.57)-(VI.60)) which involve  $|g_n|^2$  and  $g_n g_{n+1}^*$ . It also disappears in the expression (VI.56) for the phase angle. Without any loss of generality, it is then possible to set:

$$g_n = 1,$$
  $\forall n$  (VI.75)

which is just actually Rel (VI.74) in the case of a beam waist center location. Clearly, the same results must be obtained if arbitrary location is considered instead of an axis location. Indeed, in the limit  $w_0 \to \infty$ , Rel (IV.83) for the  $\Psi_{jp}$ 's and Rels (IV.90)-(IV.91) or (IV.92)-(IV.93) for the BSCs  $g_n^m$  imply:

$$\Psi_{ip} \to 0 \text{ but for } \Psi_{00} = 1$$
 (VI.76)

$$g_n^m \to 0, |m| \neq 1$$
 (VI.77)

which are exactly the relations which have been obtained in the axis location case, i.e. Rels (VI.76)-(VI.77) are valid both in the axis location case of a Gaussian beam and for a plane wave. This is not very surprising in so far as any line parallel to the direction of propagation of a plane wave may be considered as a degenerate axis of a Gaussian beam of infinite beam radius.

Following a procedure quite similar to the one used to establish Rel (VI.74), one then shows that the BSCs  $g_n^m$ , |m| = 1 satisfy:

$$g_{n,TM}^1 = g_{n,TM}^{-1} \rightarrow \frac{1}{2} \exp(ikz_0)$$
 (VI.78)

$$g_{n,TE}^{1} = -g_{n,TE}^{-1} \rightarrow -\frac{i}{2} \exp(ikz_0)$$
 (VI.79)

which, together with Rel (VI.3), implies again Rel (VI.74).

By using Rel (VI.74) or Rel (VI.75), it is then readily found that:

$$\begin{vmatrix} I_{\theta}^{+} \\ I_{\varphi}^{+} \end{vmatrix} = \frac{\lambda^{2}}{4\pi^{2}r^{2}} \begin{vmatrix} i_{2}\cos^{2}\varphi \\ i_{1}\sin^{2}\varphi \end{vmatrix}$$
(VI.80)

in which intensity functions  $i_j$  are

$$i_j = |S_j|^2 \tag{VI.81}$$

in which the amplitude functions  $S_j$  may be written as:

$$S_1 = \sum_{n=1}^{\infty} \frac{2n+1}{n(n+1)} \left[ a_n \pi_n(\cos \theta) + b_n \tau_n(\cos \theta) \right]$$
 (VI.82)

$$S_2 = \sum_{n=1}^{\infty} \frac{2n+1}{n(n+1)} \left[ a_n \tau_n(\cos \theta) + b_n \pi_n(\cos \theta) \right]$$
 (VI.83)

and also:

$$\tan \delta = \frac{\text{Re}(S_1) \text{Im}(S_2) - \text{Re}(S_2) \text{Im}(S_1)}{\text{Re}(S_1) \text{Re}(S_2) + \text{Im}(S_1) \text{Im}(S_2)}$$
(VI.84)

$$C_{sca} = \frac{\lambda^2}{2\pi} \sum_{n=1}^{\infty} (2n+1) \left[ |a_n|^2 + |b_n|^2 \right]$$
 (VI.85)

$$C_{ext} = \frac{\lambda^2}{2\pi} \operatorname{Re} \sum_{n=1}^{\infty} (2n+1) (a_n + b_n)$$
 (VI.86)

$$C_{pr,x} = C_{pr,y} = 0 (VI.87)$$

which are exactly the classical formulae of the LMT.

For the cross-section  $C_{pr,z}$ , the story is just a bit more complicated. Starting from Rel (VI.60), one first obtains:

$$C_{pr,z} = \frac{\lambda^2}{2\pi} \sum_{n=1}^{\infty} \frac{2n+1}{n(n+1)} \operatorname{Re} \left( a_n + b_n^* - 2a_n b_n^* \right) + \frac{n(n+2)}{n+1}$$

$$\operatorname{Re} \left( a_n + b_n + a_{n+1}^* + b_{n+1}^* - 2a_n a_{n+1}^* - 2b_n b_{n+1}^* \right)$$
(VI.88)

which is not the usual expression for LMT. However, one just remark that:

$$\sum_{n=1}^{\infty} \frac{n(n+2)}{n+1} \operatorname{Re} \left( a_{n+1}^* + b_{n+1}^* \right) = \sum_{n=1}^{\infty} \frac{(n-1)(n+1)}{n} \operatorname{Re} \left( a_n + b_n \right) \text{ (VI.89)}$$

which, inserted into (VI.88), readily leads to the usual expression for LMT:

$$C_{pr,z} = \frac{\lambda^2}{\pi} \operatorname{Re} \left[ \sum_{n=1}^{\infty} (2n+1) \frac{(a_n + b_n)}{2} - \frac{2n+1}{n(n+1)} a_n b_n^* \right]$$

$$-\frac{n(n+2)}{n+1} \left( a_n a_{n+1}^* + b_n b_{n+1}^* \right)$$
(VI.90)

It follows from this section that LMT is indeed a special case of GLMT, as it should.

## VI.5 A Theorem for the Special BSCs

The theorem states that the special BSCs are real numbers for the beam waist center location case. The result in Rel (VI.75) is just a special case of this theorem. Due to Rel (VI.3), the theorem carries over to the BSCS  $g_{n,TM}^m$ , |m| = 1 which are also real numbers and implies that the BSCs  $g_{n,TE}^m$ , |m| = 1 are pure imaginary numbers. These results provide easy tests for computer programming. The proof is as follows.

With  $z_0 = 0$ , Rel (VI.65) may be rewritten as:

$$g_{n} = \frac{k (2n+1)}{\pi n(n+1)(-1)^{n} i^{n-1}} \int_{0}^{\pi} \int_{0}^{\infty} i Q(z_{0} = 0) \exp \left[ -iQ(z_{0} = 0) \frac{r^{2} \sin^{2} \theta}{w_{0}^{2}} \right]$$

$$\left( 1 - \epsilon_{L} \frac{2Q(z_{0} = 0)}{l} r \cos \theta \right) \exp(-ikr \cos \theta)$$

$$\Psi_{n}(kr) P_{n}^{1}(\cos \theta) \sin^{2} \theta d\theta d(kr)$$
(VI.91)

in which  $Q(z_0 = 0)$  is, from Rel (VI.64):

$$Q(z_0 = 0) = \frac{1}{i + \frac{2}{7}r\cos\theta}$$
 (VI.92)

complying with the relation:

$$i \ Q(z_0 = 0) = 1 - 2 \frac{r \cos \theta}{l} \ Q(z_0 = 0)$$
 (VI.93)

Denoting a real prefactor by  $\alpha$ , Rel (VI.91) may be rewritten as:

$$g_n = \frac{\alpha}{i^{n+1}} \int_0^{\pi} \int_0^{\infty} K \Psi_n(kr) P_n^1(\cos \theta) \sin^2 \theta \ d\theta \ d(kr)$$
 (VI.94)

in which the partial kernel K reads as:

$$K = \left[\frac{1}{i + 2\frac{r\cos\theta}{l}}\right]^2 exp\left[-\frac{ir^2\sin^2\theta/w_0^2}{i + 2r\cos\theta/l}\right] \exp(-ikr\cos\theta)$$
 (VI.95)

For the case under study, coordinates  $(x,\ y,\ z)$  and  $(u,\ v,\ w)$  identify and, conveniently reintroducing the variables  $h^+$  and  $\zeta$  (Rels (IV.13) and (IV.7)), the partial kernel reads as:

$$K = \left(\frac{1}{i+2\zeta}\right)^2 \exp\left(-\frac{ih_+^2}{i+2\zeta}\right) \exp(-ik\zeta l)$$
 (VI.96)

which may be rewritten as:

$$K = \frac{4\zeta^2 - 1 - 4i\zeta}{(4\zeta^2 + 1)^2} \exp\left(-\frac{h_+^2}{4\zeta^2 + 1}\right) \exp\left[-i\zeta\left(\frac{2h_+^2}{4\zeta^2 + 1} + kl\right)\right] \quad (VI.97)$$

from which it is found that:

$$Re(K) = \frac{1}{(4\zeta^2 + 1)^2} \exp(-\frac{h_+^2}{4\zeta^2 + 1}) \left\{ \left( 4\zeta^2 - 1 \right) \cos \left[ \zeta \left( \frac{2h_+^2}{4\zeta^2 + 1} + kl \right) \right] - 4\zeta \sin \left[ \zeta \left( \frac{2h_+^2}{4\zeta^2 + 1} + kl \right) \right] \right\}$$
(VI.98)

$$\operatorname{Im}(K) = \frac{-1}{(4\zeta^2 + 1)^2} \exp\left(-\frac{h_+^2}{4\zeta^2 + 1}\right) \left\{ \left(4\zeta^2 - 1\right) \sin \left[\zeta \left(\frac{2h_+^2}{4\zeta^2 + 1} + kl\right)\right] + 4\zeta \cos \left[\zeta \left(\frac{2h_+^2}{4\zeta^2 + 1} + kl\right)\right] \right\}$$

$$(VI.99)$$

Integration over  $\theta$  in Rel (VI.94) may be arranged by splitting the interval  $(0, \pi)$  into two intervals  $(0, \pi/2)$  and  $(\pi/2, \pi)$  and by introducing the change of variables  $\theta \to \varphi = \pi - \theta$ :

$$\int_0^{\pi} .\sin^2 \theta d\theta = \int_0^{\pi/2} .\sin^2 \theta d\theta + \int_0^{\pi/2} .\sin^2 \varphi d\varphi$$
 (VI.100)

Furthermore, it is readily found that:

$$\zeta(\theta) = -\zeta(\varphi) \tag{VI.101}$$

$$h_{+}(\theta) = h_{+}(\varphi) \tag{VI.102}$$

leading to:

$$\operatorname{Re}(K)(\theta) = \operatorname{Re}(K)(\varphi)$$
 (VI.103)

$$Im(K)(\theta) = -Im(K)(\varphi)$$
 (VI.104)

Therefore, Rel (VI.94) becomes:

$$g_n = \frac{\alpha}{i^{n+1}} \int_0^{\pi/2} \int_0^{\infty} \left\{ \operatorname{Re}(K)(\theta) \left[ P_n^1(\cos \theta) + P_n^1 \left( -\cos \theta \right) \right] + i \operatorname{Im}(K)(\theta) \right.$$

$$\left. \left[ P_n^1(\cos \theta) - P_n^1 \left( -\cos \theta \right) \right] \right\} \Psi_n(kr) \sin^2 \theta \ d\theta \ d(kr)$$
(VI.105)

Associated Legendre functions however comply with the symmetry relation (130, t1):

$$P_n^m(\cos \theta) = (-1)^{n-m} P_n^m (-\cos \theta)$$
 (VI.106)

leading us to separately consider the cases n even and n odd. Still using the notation  $\alpha$  for any real prefactor, one finds:

$$g_{n=2k} = \alpha i^n \int_0^{\pi/2} \int_0^\infty \operatorname{Im}(K)(\theta) \, \Psi_n(kr) \, P_n^1(\cos \theta) \, \sin^2 \theta \, d\theta \, d(kr) \quad (\text{VI}.107)$$

$$g_{n=2k+1} = \alpha i^{n-1} \int_0^{\pi/2} \int_0^\infty \operatorname{Re}(K)(\theta) \, \Psi_n(kr) \, P_n^1(\cos \theta) \, \sin^2 \theta \, d\theta \, d(kr)$$
(VI.108)

We are done i.e. special BSCs for beam waist center location are indeed real numbers (at the order L of approximation). This result is a special case of BSCs symmetry relations such as discussed more extensively by Ren  $et\ al$  312.

## VI.6 Numerical Computations of Special BSCs by Using Quadratures

#### VI.6.1 Computer Programs

From Rel (VI.3) expressing the special BSCs  $g_n$  in terms of BSCs  $g_n^m$ , |m| = 1, in the axis location case, and from Rels (III.17) and (III.14) expressing the BSCs  $g_{n,TM}^m$  (BSCs  $g_{n,TE}^m$  could be similarly used) in the most general case in terms of triple and double quadratures respectively, it is found that special BSCs  $g_n$  may also be expressed in terms of triple and double quadratures respectively. These quadratures involve the expression of the radial electric field component  $E_r(r, \theta, \varphi)$ . In the case of Gaussian beams, with axis location, the component  $E_r(r, \theta, \varphi)$  reads as, from Rel (IV.71):

$$E_r = \left\{ E_0 \ iQ \ \exp\left[-iQ\frac{r^2\sin^2\theta}{w_0^2}\right] \sin\theta \left(1 - \epsilon_L \frac{2Q}{l}r\cos\theta\right) \exp\left[-ik(r\cos\theta - z_0)\right] \right\} \cos\varphi$$
(VI 109)

This relation is a special case of a more general relation, valid for Gaussian beams and also for a broader class of beams (see section VI.1), in which the component  $E_r(r, \theta, \varphi)$  takes the form:

$$E_r(r, \theta, \varphi) = E_r(r, \theta) \cos \varphi$$
 (VI.110)

Then the integration over  $\varphi$  may be readily carried out leading to two new expressions for the special BSCs:

$$g_n = \frac{2n+1}{\pi n(n+1)i^{n-1}(-1)^n} \int_0^\infty kr \Psi_n^{(1)}(kr) \int_0^\pi \frac{E_r(r,\theta)}{E_0} P_n^1(\cos\theta) \sin\theta \, d\theta \, d(kr)$$
(VI.111)

$$g_n = \frac{ka}{2n(n+1)i^{n-1}(-1)^n \Psi_n^{(1)}(ka)} \int_0^{\pi} \frac{E_r(a,\theta)}{E_0} P_n^1(\cos\theta) \sin\theta \ d\theta \ (\text{VI}.112)$$

in which triple and double quadratures have been reduced to double and single quadratures respectively.

Computer programs are available from the website connected to this book. This first routine evaluates the special BSCs according to Rel (VI.111). The field  $E_r(r,\theta)$  is specified for Gaussian beams. The second routine evaluates the special BSCs according to Rel (VI-112). The field  $E_r(r,\theta)$  is specified for Gaussian beams too.

#### VI.6.2 More on the Plane Wave Case

Rel (VI.112) provides a new opportunity to discuss the plane wave case for which it has been found that the special BSCs are just phase terms (section VI.4, Rel (VI.74)). The same dish is again served here accompanied however with a somewhat different kind of wine.

For a plane wave, the field  $E_r$   $(r, \theta)$  is readily found to read as:

$$E_r(r,\theta) = E_0 \sin\theta \exp[-ik(r\cos\theta - z_0)]$$
 (VI.113)

Omitting the constant phase term  $\exp(ikz_0)$  for convenience, Rel (VI.112) becomes:

$$g_n = \frac{ka}{2n(n+1)i^{n-1}(-1)^n \Psi_n^{(1)}(ka)} \int_0^{\pi} P_n^1(\cos\theta) \sin^2\theta \exp(-ika\cos\theta) d\theta$$
(VI.114)

By using a recurrence relation between associated Legendre functions  $P_n^1$  and Legendre polynomials  $P_n$  (132, p239):

$$(2n+1) \sin \theta \ P_n^1(\cos \theta) = n(n+1) \ [P_{n+1}(\cos \theta) - P_{n-1}(\cos \theta)] \ (VI.115)$$

and also the expansion relation (VI.71), and finally invoking the orthogonality relation of associated Legendre functions (Rel (III.12)), the integral in Rel (VI.114) is found to be:

$$I = -\frac{n(n+1)}{2n+1} (-i)^{n-1} \left[ \Psi_{n+1}^{(1)}(ka) + \Psi_{n-1}^{(1)}(ka) \right]$$
 (VI.116)

This relation may be modified by using a recurrence relation for the spherical Bessel functions (132, p377):

$$\Psi_n^{(1)}(x) + \Psi_{n-1}^{(1)}(x) = \frac{2n+1}{x} \, \Psi_n^{(1)}(x) \tag{VI.117} \label{eq:VI.117}$$

Rel (VI.75) stating that the special BSCs are unity for the beam waist center location is then readily recovered, as it should (phase term omitted).

#### VI.6.3 Numerical Behaviour of Quadratures

The evaluation of BSCs  $g_n^m$  (section IV.3) and  $g_n$  by quadratures exhibits particular difficulties because the spherical Bessel functions and associated Legendre functions involved in the integrands possess complex oscillatory behaviours. It consequently requires significant CPU-time and the accuracy of the results may be limited if numerical integration routines are not efficient enough. This problem is strongly connected with the choice of the value r = a in the methods where the value of r is specified. A poorly chosen value may lead to quite inaccurate results. It has been chosen in this book to discuss these issues in the simpler case of special BSCs  $g_n$ . Conclusions would be similar for BSCs  $g_n^m$ .

The expression  $E_r$   $(a, \theta)$  involved in Rel (VI.112) is given here for Gaussian beams by the bracket term of Rel (VI.109) as:

$$E_r(r=a) = E_0 iQ \exp\left[-iQ \frac{a^2 \sin^2 \theta}{w_0^2} - ika \cos \theta\right] \sin \theta \left(1 - \epsilon_L \frac{2Q}{l} a \cos \theta\right) \exp(ikz_0)$$

(VI.118)

Therefore, on the one hand, the integrand in Rel (VI.112) contains an exponential contribution depending on "a" reading as:

$$A = \exp\left[-iQ \frac{a^2 \sin^2 \theta}{w_0^2} - i k a \cos \theta\right]$$
 (VI.119)

On the other hand, the prefactor contains an a-dependent term  $1/t_n(ka)$  in which:

$$t_n(ka) = \frac{2n(n+1)\Psi_n^{(1)}(ka)}{ka}$$
 (VI.120)

If a big value of r=a is chosen, then A is very oscillatory, making the integration difficult. Conversely, let us choose a very small value of r=a such as  $ka \ll n$ . Then an asymptotic expression for the spherical Bessel functions when the argument is much smaller than the order [369] allows us to approximate Rel (VI.120) by:

$$t_n(ka) \approx 2^{n+1} n \frac{(n+1)!}{(2n+1)!} ka$$
 (VI.121)

Rel (VI.121) leads to very small values indeed, implying numerical difficulties. For example, for x = ka = 0.01, we have  $t_{16} \approx 10^{-47}$ ,  $t_{64} \approx 10^{-232}$ ,  $t_{128} = 10^{-251}$ . Therefore, the chosen value of r should not be neither too big, nor too small.

Let us now consider Fig (VI.1) which exhibits  $t_n(x)$  versus x for several values of n, evaluated using Rel (VI.120). The function displays a maximum for  $x \approx n$  and afterward an oscillatory behaviour. This fact suggests that a good choice should be to take  $x = ka \approx n$ . Of course, this particular choice

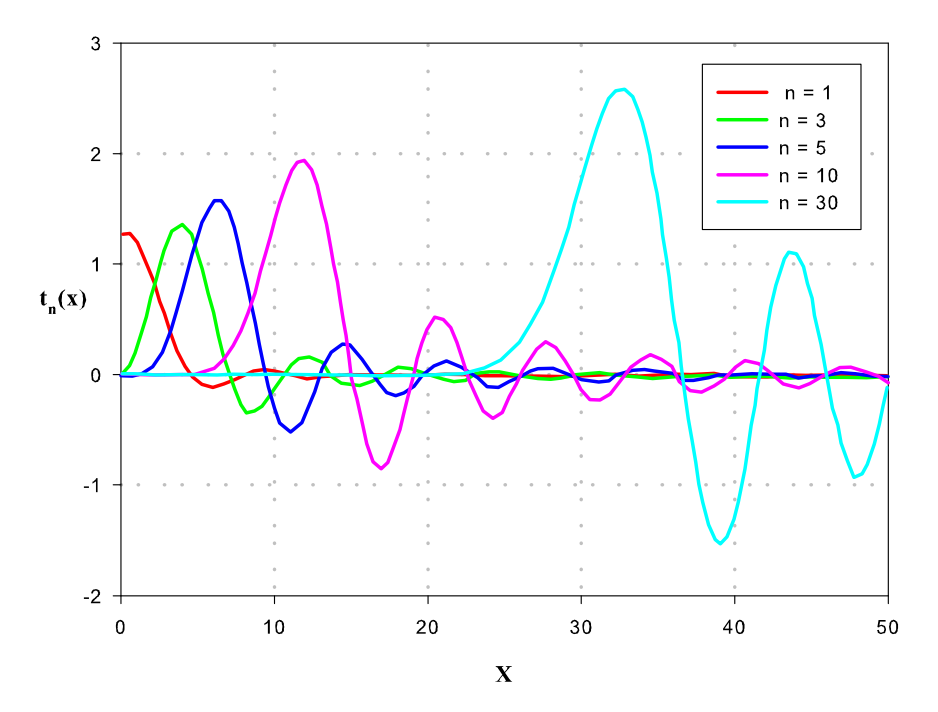


**Fig. VI.1.** Behaviour of  $t_n(x)$ , Rel (VI.120), with n as the parameter.

is not compulsory. It would still be reasonable to choose x at or near other extrema of the function without significantly influencing the accuracy of the results. However, it should definitely not be chosen near zeros of the function, nor too small or too large with respect to n.

Figs (VI.2) to (VI.4) display some examples of the behaviour of the integrand involved in Rel (VI.112), i.e.:

$$\mathcal{J}(x,n) = \frac{E_r(x/k,\theta)}{E_0} P_n^1(\cos\theta) \sin\theta \qquad (VI.122)$$

versus  $\theta$  for various values of x = ka, and n.

Fig (VI.2) shows  $Re(\mathcal{J}(x,1))$  for three values of x, with  $w_0=10\mu\mathrm{m}$ ,  $\lambda=0.5145~\mu\mathrm{m}$ ,  $z_0=0$  and  $\epsilon_L=1$ . The maximum of  $t_1(x)$  is at x=0, i.e. a=0. The integration becomes the greatest (in modulus) when this value a=0 is approached, compensating for the fact that the prefactor  $1/t_n(x)$  takes on its smallest value. If x is increased, the integrand exhibits oscillatory behaviours which are inconvenient for numerical integration. The proposed choice  $x\approx n$  would here lead to  $a\approx 0.08$  (x=0.08) which indeed appears also to be a good choice in Fig VI.2. In this case, it may be shown that the imaginary part of the integrand is an odd function and therefore

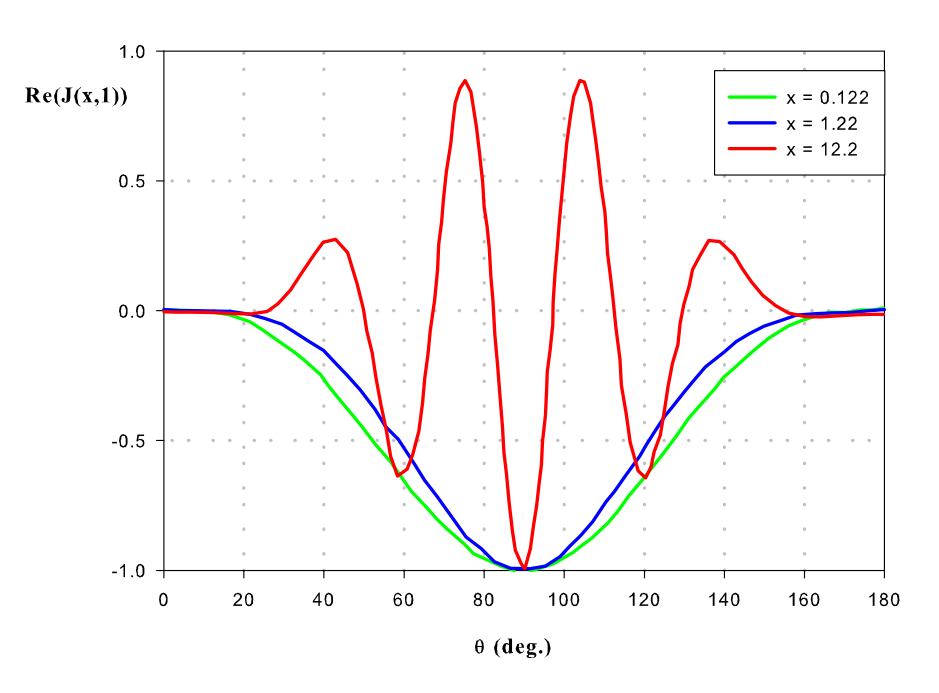


**Fig. VI.2.** Behaviour of real part  $\mathcal{J}(x,n)$ , Rel (VI.122), for n=1.

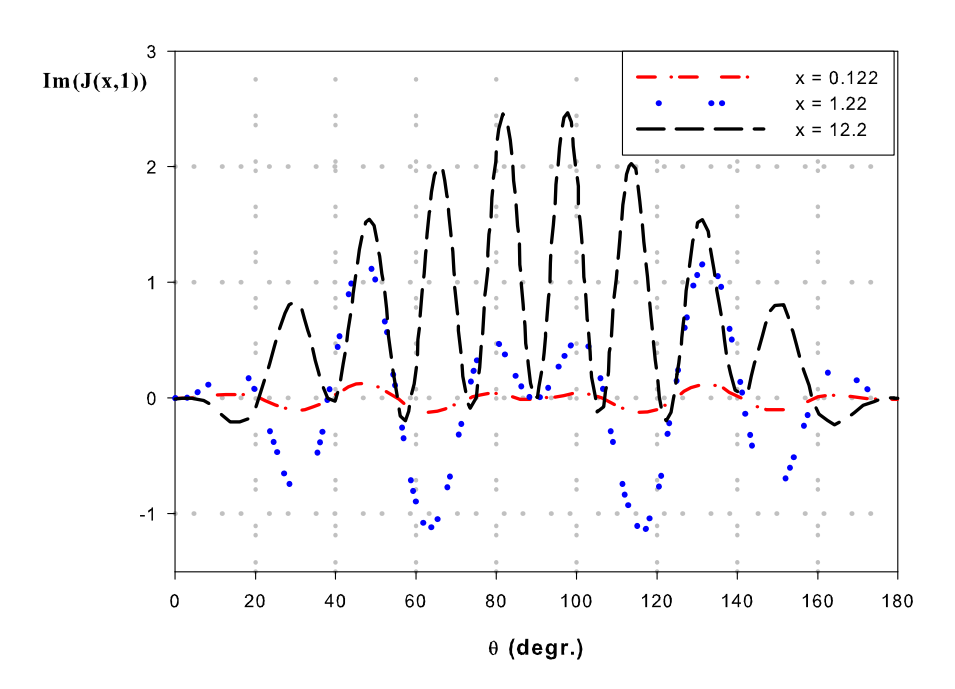
does not contribute to  $g_1$ . The result that  $g_1$  must be here a real number is therefore recovered.

Fig VI.3 similarly displays  $Im(\mathcal{J}(x,10))$ . The maximum of  $t_n(10)$  is here for  $n \approx 10$ . The criterion  $x \approx n$  here implies to take  $a \approx 0.8$ , say 1  $\mu$ m (x = 4.8849). For such a value, the imaginary part of the integrand is nearly always positive. Although oscillations are present, they will therefore not affect significantly the accuracy of the result. Conversely, for smaller values of x, oscillations develop between positive and negative values, spoiling the accuracy. Such spoiling oscillations also develop when x is increased above the criterion value as illustrated in Fig VI.4 for  $a = 10\mu$ m (x = 122).

Many observations of this kind and numerical experiments lead us to the conclusion that the value of a should indeed be chosen according to the criterion  $x \approx n$ , i.e.  $a \approx n/k$ . With such a criterion, it is simultaneously observed that both the function  $t_n(x)$  and the integral take on maximal values, and that the oscillations of the integrand do not significantly spoil the accuracy of the results.

No damage would be done if the criterion was rewritten as:

$$a \approx \frac{(n+1/2)\lambda}{2\pi}$$
 (VI.123)



**Fig. VI.3.** Behaviour of the imaginary part of  $\mathcal{J}(x,n)$ , Rel (VI.122), for n=1.

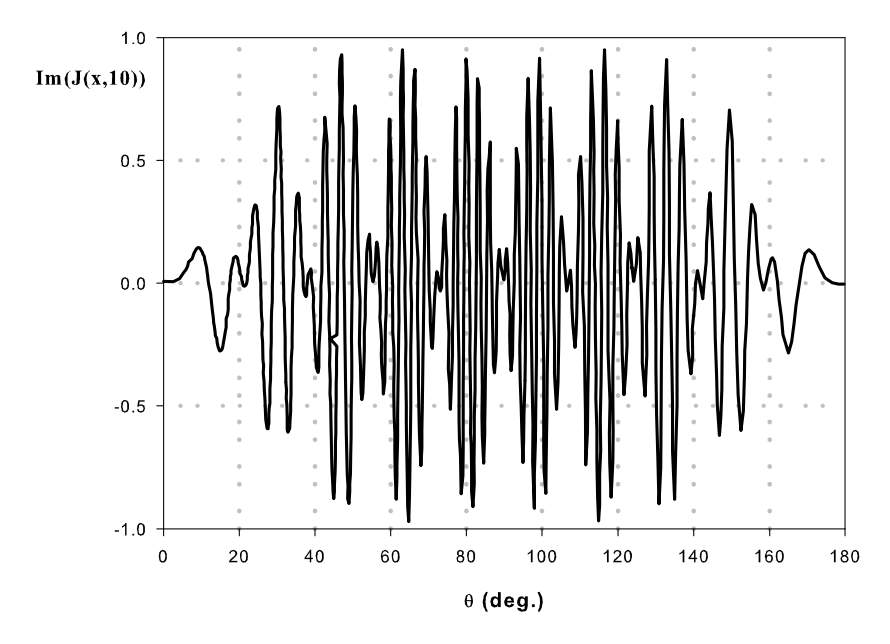


**Fig. VI.4.** Imaginary part of  $\mathcal{J}(x,n)$ , Rel (VI.122), for n=10 and a too large value of x.

Such an expression will reappear in the next chapter when developing the localized approximation to the BSCs. Therefore, the above discussion may be considered as a first introduction to the localized approximation technique which plays an important role for an efficient implementation of GLMT. The criterion of Rel (VI.123) also appears when studying quadratures to the BSCs by using a stationary point (or stationary phase) derivation (Appendix A of Lock, [127]), pointing out that it indeed possesses a deep signification to be revealed later.

When using Rel (VI.111) involving an extra integration over r, the inner integration is the same than for Rel (VI.112). Our previous discussion implies that the inner integration contributes most to the final result for values of r complying with the criterion  $kr \approx n$ . For example, when n=30, the integration between x=0 and x=25 provides a very small contribution. In practice therefore, the integration over r between 0 and  $\infty$  can be replaced by an integration between well chosen values  $r_{min}$  and  $r_{max}$ . This issue will be more extensively discussed in chapter VII to vividly illustrate localized properties of the BSCs. Also, the use of a  $r_{max}$ -value as an upper bound for this quadrature technique prevents us to observe divergence effects when the beam description does not exactly satisfy Maxwell's equations [134].

#### VI.7 Computations of Special BSCs by Using Finite Series

#### VI.7.1 The Formulation

The procedure of Neuman expansion to express BSCs  $g_n^m$  in terms of finite series (chapter V) may be similarly used to express the special BSCs. This actually corresponds to the historical development in which the finite series for  $g_n$ 's have been obtained (Gouesbet et al [87]) before generalizing to the  $g_n^m$ 's. In this book, it is more convenient to specify the formulae obtained in chapter V to the axis location case  $(x_0 = y_0 = 0)$ .

It is then known that all  $\Psi_{jp}$  's are zero but for  $\Psi_{00} = 1$  (Rels (VI.42)-(VI.43)). From Rel (V.28) linking  $\Psi_{jp}$  's and  $\Delta$  (j, p) 's, or directly from Rel (V.29), it is also found that:

$$\Delta(j,p) = \delta_0^j \ \delta_0^p \tag{VI.124}$$

Furthermore, Rel (V.71) implies that all  $\Omega$  (j, p)'s are zero, even for j = 0. These results lead to dramatic simplifications for the expressions giving the BSCs  $g_n^m$ .

As an example, let us consider Rel (V.80) for BSCs  $g_{2p,TM}^{2k+1}$  ( $k \geq 0$ ). All the terms involving  $\Omega(j,p)$  become equal to zero. The term containing  $\mathcal{D}$  is also zero due to  $x_0 = 0$ . Then Rel (V.80) reduces to:

$$\begin{split} g_{2p,TM}^{2k+1}(k \geq 0) &= \frac{i}{(-1)^k} \; 2^{2(p-k-1)} \; \frac{(p-k-1)!}{\Gamma(p+k+3/2)} \; \sum_{m=0}^p \frac{\Gamma(2p-m+1/2)}{2^{2m}m!} \\ & \sum_{t=0}^{p-m-k-1} \frac{(-Z_0 s^2)^t}{t!} \; \{ \epsilon(p-m;0,1,...,k) \\ & \frac{\mathcal{B}}{2} \Delta(2p-2m-2t-2,p-m-t-k-1) \\ & + \frac{1}{2} \epsilon(t;p-m-k-1) \epsilon(p-m;0,1,...,k+1). \\ & [\mathcal{B} \Delta(2p-2m-2t-2,p-m-t-k-2) \\ & + \mathcal{C} \Delta(2p-2m-2t-4,p-m-t-k-2)] + \\ & \frac{\mathcal{C}}{2} \epsilon(t;p-m-k-1,p-m-k-2). \\ & \epsilon(p-m;0,1,...,k+2) \; \Delta(2p-2m-2t-4,p-m-t-k-3) \} \end{split}$$

Subscript couples in  $\Delta$ -terms of Rel (VI.125) are now listed:

$$(2p-2m-2t-2, p-m-t-k-1)$$
 (VI.126)

$$(2p-2m-2t-2, p-m-t-k-2)$$
 (VI.127)

$$(2p-2m-2t-4, p-m-t-k-2)$$
 (VI.128)

$$(2p-2m-2t-4, p-m-t-k-3)$$
 (VI.129)

We now remember that only  $\Delta$  (0, 0) is not zero. Therefore,  $\Delta$ -terms with subscripts of Rel (VI.126) are not zero if there exist values of p, m, t and k such as:

$$2(p - m - t - 1) = (p - m - t - 1) - k = 0$$
 (VI.130)

which is possible only if k = 0, that is:

$$m = 2k + 1 = 1 (VI.131)$$

From Rel (VI.127), it is similarly found that nonzero  $\Delta$ -terms may only appear if:

$$2(p-m-t-1) = (p-m-t-1) - (k+1) = 0$$
 (VI.132)

which is possible only if k = -1, that is:

$$m = 2k + 1 = -1 (VI.133)$$

From Rels (VI.128) and (VI.129), it is similarly found that characteristic equations may only be satisfied if k = 0 (m = 1) and k = -1 (m = -1), respectively. It has therefore been demonstrated that:

$$g_{2p,TM}^m(m \text{ odd}, |m| \neq 1) = 0$$
 (VI.134)

Examining all finite series relations for BSCs  $g_n^m$  given in chapter V, it is more generally established that:

$$g_{2p,TM}^{2k} = g_{2p+1,TM}^{2k} = g_{2p}^m(m \text{ odd}, |m| \neq 1) = g_{2p+1}^m(m \text{ odd}, |m| \neq 1) = 0$$
 (VI.135)

and similarly for TE-BSCs.

Therefore, we recover a known result, namely that all BSCs  $g_n^m$  become zero, but for |m| = 1. Next step is to evaluate successively all coefficients  $g_n^m$  with |m| = 1. For instance, starting from Rel (VI.125) and specifying k = 0 (m = 1) yields:

$$g_{2p,TM}^{1} = \frac{i}{4} 2^{2p} \frac{(p-1)!}{\Gamma(p+3/2)} \sum_{m=0}^{p} \frac{\Gamma(2p-m+1/2)}{2^{2m}m!} \sum_{t=0}^{p-m-1} \frac{(-Z_{0}s^{2})^{t}}{t!}$$

$$\left\{ \epsilon(p-m;0) \frac{\mathcal{B}}{2} \Delta(2p-2m-2t-2,p-m-t-1) + \frac{1}{2} \epsilon(t;p-m-1) \epsilon(p-m;0,1) \mathcal{C} \Delta(2p-2m-2t-4,p-m-t-2) \right\}$$

Separating the r.h.s of Rel (VI.136) in two terms, taking advantage of the properties of the symbol  $\epsilon(n; \alpha_j)$  defined by Rel (V.32) and using  $\Delta(0, 0) = 1$ , it is then found that:

$$\begin{split} g_{2p,TM}^1 &= \frac{i}{4} \ 2^{2p} \ \frac{(p-1)!}{\Gamma(p+3/2)} \left\{ \sum_{m=0}^{p-1} \frac{\mathcal{B}}{2} \ \frac{\Gamma(2p-m+1/2)}{2^{2m}m!} \ \frac{(-Z_0 s^2)^{p-m-1}}{(p-m-1)!} \right. \\ &+ \left. \sum_{m=0}^{p-2} \frac{\mathcal{C}}{2} \ \frac{\Gamma(2p-m+1/2)}{2^{2m}m!} \ \frac{(-Z_0 s^2)^{p-m-2}}{(p-m-2)!} \right\} \end{split}$$

With j = (p - m - 1) in the first term of the r.h.s. and j = (p - m - 2) in the second term, and rearranging the obtained second term, Rel (VI.137) finally may take the form:

$$g_{2p+2,TM}^{1} = \sum_{j=0}^{p} \frac{i \ p!}{j!(p-j)!} \frac{\Gamma(p+j+5/2)}{\Gamma(p+5/2)} (-4Z_{0}s^{2})^{j} \left[ \frac{\mathcal{B}}{2} - j \ \epsilon(j;0) \frac{\mathcal{C}}{2Z_{0}s^{2}} \right]$$
(VI.138)

in which  $\mathcal{B}$  and  $\mathcal{C}$  must be specified for the case  $(x_0 = y_0 = 0)$  leading to (from Rels (V.67)-(V.68)):

$$\mathcal{B} = -i \exp(ikz_0) \left[ Z_0 + Z_0'' - 2\epsilon_L s^2 Z_0^2 \right]$$
 (VI.139)

$$C = i Z_0 Z_0^{"} s^2 \exp(ikz_0)$$
 (VI.140)

Having now understood the procedure of reduction of the BSCs  $g_{2p,TM}^1$ , the reader could undertake the task of evaluating similarly all other relevant coefficients, with |m| = 1, to find:

$$g_{2p+2,TM}^1 = g_{2p+2,TM}^{-1} = i \ g_{2p+2,TE}^1 = -i \ g_{2p+2,TE}^{-1}$$
 (VI.141)

which are therefore all given by Rel (VI.138) and:

$$g_{2p+1,TM}^1 = g_{2p+1,TM}^{-1} = i \ g_{2p+1,TE}^1 = -i \ g_{2p+1,TE}^{-1}$$
 (VI.142)

in which  $g_{2\nu+1,TM}^1$  is given by a relation rather similar to Rel (VI.138):

$$g_{2p+1,TM}^{1} = \frac{1}{2} Z_{0} \exp(ikz_{0}) \sum_{j=0}^{p} \frac{p!}{j!(p-j)!} \frac{\Gamma(p+j+3/2)}{\Gamma(p+3/2)} (-4Z_{0} s^{2})^{j}$$
(VI.143)

Both Rels (VI.141) and (VI.142) may be rewritten by replacing subscripts (2p+2) and (2p+1) by a single subscript n (odd or even). Comparing with Rel (VI.3) expressing special BSCs  $g_n$  in terms of  $g_{n,TM}^1, \ldots, g_{n,TE}^{-1}$ , it is therefore found that the  $g_n$ 's are given by two formulae, depending on the parity of n:

$$g_{2p+1} = Z_0 \exp(ikz_0) \sum_{j=0}^{p} \frac{p!}{j!(p-j)!} \frac{\Gamma(p+j+3/2)}{\Gamma(p+3/2)} (-4 Z_0 s^2)^j \text{ (VI.144)}$$

$$g_{2p+2} = \frac{1}{k} \exp(ikz_0) \sum_{j=0}^{p} \frac{p!}{j!(p-j)!} \frac{\Gamma(p+j+5/2)}{\Gamma(p+5/2)} \left[ A - \frac{j B}{Z_0} \right] (-4 Z_0 s^2)^j$$
(VI.145)

in which new notations have been introduced:

$$A = k(Z_0 + Z_0)^2 - \frac{2}{l}\epsilon_L Z_0^2$$
 (VI.146)

$$B = -kZ_0Z_0^{"} \tag{VI.147}$$

 $Z_0$  (Rel (V.27)) does not depend on  $\epsilon_L$ . Therefore the BSCs  $g_n$ 's (n odd, Rel (VI.144)) are insensitive to the order of approximation  $L^-$  or L of the description of the laser beam. BSCs  $g_n$  (n even, Rel (VI.145)) conversely are different for orders L and  $L^-$  due to  $\epsilon_L$  involved in Rel (VI.146).

Let us now consider the more special case of a beam waist center location. Then,  $Z_0$  and  $Z_0$ " (Rels (V.27), (V.70)) simplify to:

$$Z_0 = 1, \quad Z_0'' = \frac{-2}{kl} = -2 s^2$$
 (VI.148)

and Rels (VI.144)-(VI.145) reduce to:

$$g_{2p+1} = \sum_{j=0}^{p} \frac{p!}{j!(p-j)!} \frac{\Gamma(p+j+3/2)}{\Gamma(p+3/2)} (-4 s^2)^j$$
 (VI.149)

$$g_{2p+2} = \sum_{j=0}^{p} \frac{p!}{j!(p-j)!} \frac{\Gamma(p+j+5/2)}{\Gamma(p+5/2)} \left[ 1 - 2 \ s^2 \ (j+1+\epsilon_L) \right] \ (-4 \ s^2)^j$$
(VI.150)

The fact that the special BSCs  $g_n$  are real numbers for the beam waist center location case as demonstrated in section (VI.5) by using quadratures is here recovered by using finite series. The statement holds at both orders L and  $L^-$ .

At order  $L^-$ , Rel (VI.149) is unchanged and Rel (VI.150) simplifies a bit. If  $O(s^2)$  is furthermore neglected with respect to 1, one obtains:

$$g_{2p+1} = \sum_{i=0}^{p} \frac{p!}{j!(p-j)!} \frac{\Gamma(p+j+3/2)}{\Gamma(p+3/2)} (-4 s^2)^j$$
 (VI.151)

$$g_{2p+2} = \sum_{j=0}^{p} \frac{p!}{j!(p-j)!} \frac{\Gamma(p+j+5/2)}{\Gamma(p+5/2)} (-4 s^2)^j$$
 (VI.152)

These two last relations have been obtained for the first time by Ferguson and Currie [370]. The work by Ferguson and Currie actually made us aware of the existence of Neuman expansions.

Let us finally assume the LMT-limit, i.e.  $w_0 \to \infty$ ,  $s \to 0$ . Then only the first term j=0 is preserved in Rels (VI.151)-(VI.152) leading to  $g_n=1$ ,  $\forall n$ , as it should. The LMT-limit may similarly be studied in Rels (VI.144)-(VI.145) to recover  $g_n = exp(ikz_0)$ .

#### VI.7.2 Routines

One first considers the simplest relations (VI.151) and (VI.152). For programming efficiency, elementary modifications of the formulae are introduced, including the use of Rel (V.94). A single routine has been constructed for both n odd or even.

When n becomes big (n greater than about 4  $\pi$   $w_0/\lambda$ ), this routine produces  $|g_n|$ 's increasing steadily, creating two alternating series, one for n odd and the other for n even. Using the language of localized approximation (next chapter), this unpleasant behaviour appears when the order n of the coefficients corresponds to rays passing at a distance from the axis bigger than about twice the beam waist radius. The energy associated with such rays is very small and should be very insignificant in practical situations. It is however interesting to check whether this behaviour is a real one or results from numerical artefacts.

A first checking may be carried out by evaluating the special BSCs of Rels (VI.151)-(VI.152) by using recurrence formulae. For instance, Rel (VI.151) may be formulated as:

$$g_{2p+1} = \sum_{j=0}^{p} g_{2p+1,j}$$
 (VI.153)

$$g_{2p+1,j} = \frac{p!}{j!(p-j)!} \frac{\Gamma(p+j+3/2)}{\Gamma(p+3/2)} (-4 s^2)^j$$
 (VI.154)

One then introduces a ratio  $r_i$  given by:

$$r_{j} = \frac{g_{2p+1,j+1}}{g_{2p+1,j}} = \frac{j!(p-j)!}{(j+1)!(p-j-1)!} \frac{\Gamma(p+j+5/2)}{\Gamma(p+j+3/2)} (-4s^{2})$$
(VI.155)

which may be rewritten by using Rel (V.94) as:

$$r_j = \frac{(p-j)}{(j+1)}(p+j+3/2)(-4s^2)$$
 (VI.156)

One then readily establishes the following recurrence expression:

$$g_{2p+1} = 1 + \sum_{j=0}^{p-1} r_j \ g_{2p+1,j}$$
 (VI.157)

Similarly, one obtains:

$$g_{2p+2} = 1 + \sum_{j=0}^{p-1} r'_{j} g_{2p+2,j}$$
 (VI.158)

in which:

$$r'_{j} = \frac{(p-j)}{(j+1)}(p+j+5/2)(-4s^{2})$$
 (VI.159)

Rels (VI.149)-(VI.150) may be treated similarly as Rels (VI.151)-(VI.152). Because Rels (VI.149) and (VI.151) are identical, there is no modification for the BSCs  $g_{2p+1}$ . The recurrence expression for the BSCs  $g_{2p+2}$  however becomes:

$$g_{2p+2} = [1 - 2s^2(1 + \epsilon_L)] + \sum_{j=0}^{p-1} r_j'' \quad g_{2p+2,j}$$
 (VI.160)

in which:

$$r_{j}^{"} = \frac{(p-j)}{(p+j)}(p+j+5/2)\frac{[1-2s^{2}(1+\epsilon_{L})-2(j+1)s^{2}]}{[1-2s^{2}(1+\epsilon_{L})-2js^{2}]}(-4s^{2}) \quad (VI.161)$$

All these recurrence formulae have been implemented in a routine

Results obtained by using this last program (when specified for Rels (VI.151)-(VI.152)) are identical to the previous ones, confirming the increase of  $|g_n|$  when n increases. Because truncation errors might be suspected to be the cause of the observed behaviour, another checking may be carried out by programming the expressions with symbolic computations yielding infinite accuracy. The routines use the MAPLE software.

A first routine evaluates Rels (VI.151)–(VI.152) using recurrence expressions. A second routine similarly evaluates Rels (VI-149) and (VI-150) at the orders  $L^-$  or L.

Results obtained by symbolic computation agree with those obtained by FORTRAN routines. Whether the divergence effect of  $|g_n|$  is consistent with physics, requires examining.

One then examines the description of the incident electromagnetic field incorporating the special BSCs. The incident radial electric field component for the axis location case reads as, from Rel (IV.71):

$$E_r = E_0 iQ \exp\left[-iQ\frac{r^2\sin^2\theta}{w_0^2}\right] \cos\varphi \sin\theta \left[1 - \epsilon_L \frac{2Q}{l}r\cos\theta\right]$$

$$\exp(-ikr\cos\theta) \exp(ikz_0)$$
(VI.162)

But this field component may also be obtained from Rels (III.39), (III.45), which after specification for the case under study and using Rel (III.3) may be rewritten as:

$$E_r = \frac{E_0}{kr} \cos \varphi \sum_{n=1}^{\infty} i^{n-1} (-1)^n (2n+1) g_n \Psi_n^{(1)}(kr) P_n^1(\cos \theta)$$
 (VI.163)

leading to:

$$kr iQ \exp[-iQ\frac{r^2\sin^2\theta}{w_0^2}] \sin\theta[1-\epsilon_L\frac{2Q}{l}r\cos\theta] \exp(-ikr\cos\theta) \exp(ikz_0) =$$

$$\sum_{n=0}^{\infty} i^{n-1}(-1)^n (2n+1)g_n\Psi_n^{(1)}(kr)P_n^1(\cos\theta)$$

Let us now examine the more special case of beam waist center location  $(z_0 = 0, Q = 1/i)$  and specify  $\theta = 90^{\circ}$ . By using Rel (V.6) specified for m = 1, Rel (VI.164) becomes:

$$kr \exp(-\frac{r^2}{w_0^2}) = \sum_{n=1}^{\infty} i^{n-1} (-1)^n (2n+1) g_n \Psi_n^{(1)}(kr) (-1)^{\frac{n+1}{2}} \frac{n!!}{2^{\frac{n-1}{2}} (\frac{n-1}{2})!}$$
(VI.165)

<sup>&</sup>lt;sup>1</sup> The programs have been written in MAPLE V release 3.

For n odd:

$$i^{n-1}(-1)^n(-1)^{\frac{n+1}{2}} = 1$$
 (VI.166)

Furthermore, a direct evaluation shows that  $g_1 = 1$ . Therefore, Rel (VI.166) is rewritten as:

$$kr \exp(-\frac{r^2}{w_0^2}) = 3\Psi_n^{(1)}(kr) + \sum_{n=3}^{\infty} (2n+1)g_n\Psi_n^{(1)}(kr) \frac{n!!}{2^{\frac{n-1}{2}}(\frac{n-1}{2})!}$$
 (VI.167)

A MAPLE routine FIELD evaluates the r.h.s. of Rel (VI.167).

Results obtained from FIELD agree perfectly well with the l.h.s. of Rel (VI.167), even if the  $|g_n|$ 's become very great, alternating in sign when the order n of the coefficient increases. Such a behaviour, historically first observed by using finite series, is actually also observed by using quadratures, as it should have been expected in so far as finite series and quadratures are rigorous mathematically equivalent formulations (in the limit of a beam description exactly satisfying Maxwell's equations). Conversely, such a behaviour is not observed if the BSCs are computed using a localized interpretation to which the next chapter is devoted. Numerical results are available from Gouesbet et al [87].

#### VII

# The Localized Approximation and Localized Beam Models

#### VII.1 Generalities

Beside more or less classical mathematical functions, numerical computations for GLMT require accurate enough computations of BSCs  $g_n^m$  or  $g_n$  describing the incident beam. These BSCs may be in fact, at least in some cases, experimentally evaluated on an actual beam in a laboratory [328], [329], [330], [331], [332], [333] but, in this book, we mostly discuss the evaluation of BSCs from a priori, or better said assumed, known mathematical descriptions of the incident beam. Then, because a huge amount of BSCs must be evaluated before assembling GLMT-series, much effort has been devoted to the development of efficient schemes and algorithms. This chapter is devoted to the most efficient technique available up to now, namely the localized approximation relying on a localized interpretation of the BSCs, and leading to the construction of localized beam models exactly satisfying Maxwell's equations.

In previous chapters, two methods have been considered. The quadrature technique (with integration over variable r or not) historically appears as the first one. It is the most natural method in so far as, when developing the theory, it possesses an obvious character to the researcher. There is a strong interest in this method because it is the most flexible one. Indeed, only the kernel of the quadratures is to be modified when the nature of the incident beam is changed.

However, even when integration over variable r is not carried out, it is the most time-consuming technique in terms of CPU requirements, numerical difficulties being enhanced by the oscillatory behaviour of the integrands. In the early times of the GLMT, one hour CPU was a typical time required to evaluate only one special BSC  $g_n$  with enough accuracy by using available mainframe computers. There was thus a danger that GLMT could remain for a long time a pure subject of spiritual contemplation. A relief about this issue was obtained by the breakthrough of introducing the finite series technique.

Finite series are numerically much more efficient than quadratures and opened the way to fast GLMT-computations. There is however a price to pay

for this advantage. While quadrature expressions are immediately adaptable to any kind of incident beams as soon as the expressions for the incident radial electromagnetic field components  $E_r$  and  $H_r$  are available, extra algebra is required with finite series to derive new finite series expressions when the nature of the beam is changed. Nevertheless, because there exists a general procedure for finite series derivations as discussed in chapter V, it is very likely that a full automatic process might be designed by concatenating symbolic computation procedures and numerical routines. It is also recalled that both techniques, quadratures and finite series, are rigorous and strictly equivalent at least when beam descriptions exactly satisfy Maxwell's equations.

This chapter is devoted to a third method to compute the BSCs, namely the localized approximation relying on a localized interpretation. It is the fastest method leading to very simple formulae. In some cases, simple exponential evaluations which may be handled using pocket calculators are sufficient to compute BSCs. It is likely that there is no way to be more efficient. Indeed, because the evaluation of the BSCs then becomes an easy task, GLMT may be more routinely usable for various applications.

The formulation of the localized approximation (for Gaussian beams) has been discussed in a series of articles from the case of the special BSCs  $g_n$  [78] to the final generalization for all BSCs  $g_n^m$  [371]. The reader might expect that, as usually done in this book, we would proceed from the most general case to the more specific one. This would however be unreasonable because the method, as developed in the above articles, is neither physically nor mathematically firmly based. The most convincing and pedagogic way (in the bulk of this book) is then to proceed from special cases toward generalization as it has historically been carried out.

Indeed, the original method of derivation of the localized approximation formulae relies on a bit of physics, a tiny amount of mathematics and much intuition. It has often been like a guess game. It is hoped that the reader will forgive us if we state that we are fascinated by the success of this game which will eventually lead to simple, numerically efficient and accurate expressions with what is found to be a remarkable economy of physical and mathematical tools. We find that there is some kind of formal beauty in the game that we propose to the reader to play with us.

Later on, the localized approximation was the subject of more developments and, in particular, received a rigorous justification. These later works however involve many technicalities that we better have not to incorporate in this book excepted, at the end of this chapter, as a complement. Therefore, the body of this chapter is to be considered as an introduction to the topic of localization, wandering on an easy trail, starting from a fresh valley and climbing, step by step, up to the top of an easy hill. For climbing mountains rather than a hill, see articles quoted in the complement.

#### VII.2 The Waist Center Location Case

#### VII.2.1 The Principle of Localization

The localized approximation historically relies on a principle of localization stated by van de Hulst [17] in the case of the LMT devoted to plane wave scattering. One of the interests in starting with the waist center location case of a Gaussian beam is that, for such a location, the wave is indeed (locally) plane. Therefore the extension of the principle of localization from plane waves to Gaussian beams might a priori appear as a rather trivial exercise.

The principle of localization is a hybrid concept in which LMT series characterizing waves are interpreted in a local way in terms of geometrical optics rays. According to this principle, each term of order n in plane wave amplitude functions (Rels (VI.82)-(VI.83)) is associated with a ray (actually an annular bundle of rays) located at a distance  $\rho_n$  of the propagation axis passing through the center of the scatterer. The value of  $\rho_n$  is given by:

$$\rho_n = \frac{(n+1/2)\lambda}{2\pi} \tag{VII.1}$$

A formal justification of the principle of localization is deduced from the asymptotic behaviour of Bessel functions of order (n+1/2) which are involved in the expressions for the scattering coefficients  $a_n$  and  $b_n$  (see Rels (III.88)-(III.89) and (II.87), (II.88), (II.78), (II.81)). In particular, it is found that contributions of Bessel functions to series become negligible when (n+1/2) is larger than the size parameter  $\alpha = \pi d/\lambda$ . Conversely, significant contributions are produced by terms such as  $(n+1/2) < \alpha$ , associated with light rays passing in the neighborhood of the scatter center. Such behaviours have been briefly discussed in section (VI.6.3) and are echoed in Rel (VI.123) to compare with Rel (VII.1). A somewhat more formal justification may be found by using a method known as a stationary-phase technique on which we shall return in the complement. Soon, we shall also directly evidence the localized character of the special BSCs.

## VII.2.2 Special BSCs

It is recalled that, in the beam waist center location case under study, the special BSCs are given by Rel (VI.62) which also reads as:

$$g_n = \frac{2n+1}{i^{n-1}(-1)^n \pi n(n+1)} \int_0^{\pi} \int_0^{\infty} iQ \exp\left[-iQ \frac{r^2 \sin^2 \theta}{\omega_0^2}\right]$$

$$(VII.2)$$

$$(1 - \epsilon_L \frac{2Q}{l} r \cos \theta) \exp(-ikr \cos \theta) \Psi_n(kr) P_n^1(\cos \theta) \sin^2 \theta \ d\theta \ d(kr)$$

in which Q is  $Q(z_0 = 0)$ .

In Cartesian coordinate components, the description of the incident beam may be written from Rels (IV.57)-(IV.61) specified for the case under study  $(x_0 = y_0 = z_0 = 0)$  as:

$$E_y = H_x = 0 (VII.3)$$

$$E_z = H_z = 0 (VII.4)$$

$$E_x = \{E_0 \exp(-ikz)\} \exp(-\frac{x^2 + y^2}{w_0^2})$$
 (VII.5)

$$H_y = \{H_0 \exp(-ikz)\} \exp(-\frac{x^2 + y^2}{w_0^2})$$
 (VII.6)

in which the order  $L^-$  of approximation ( $\epsilon_L = 0$ ) has been assumed. The bracket  $\{ \}$ - terms are plane wave contributions multiplied by Gaussian contributions specific to the Gaussian beam under study.

Inspired by the principle of localization, it is conjectured that the special BSCs are also localized and that they actually correspond to the Gaussian contributions in Rels (VII.5)-(VII.6) at discrete distances  $\rho_n$  from the beam axis, leading to:

$$\tilde{g_n} = \exp\left[-\left(\frac{\rho_n}{w_0}\right)^2\right] = \exp\left[-\left(\frac{(n+1/2)\lambda}{2\pi w_0}\right)^2\right]$$
 (VII.7)

in which the symbol "tilde" designates the localized approximation. Rel (VII.7) is the localized formulation of Rel (VII.2), exhibiting indeed a dramatic simplification if we are lucky enough for our conjecture to work.

In the limit of a plane wave  $(w_0 \rightarrow \infty)$ , Rel (VII.7) becomes:

$$\tilde{g_n} \to 1$$
 (VII.8)

i.e. rigorous  $g_n$ 's and approximated  $\tilde{g_n}'s$  have the same limit in the plane wave case. The underlying idea may then be easily illustrated as in Fig VII.1.

## VII.2.3 Numerical Evidence of Validity

Numerical evidence of validity of Rel (VII.7) may best be obtained by comparing  $\tilde{g}_n$ -values from the localized approximation and  $g_n$ -values evaluated either by quadratures or finite series. Such comparisons appear in several places in the literature such as in Maheu *et al* [81] and Gouesbet *et al* [87]. It will be here sufficient to provide Table VII.1 extracted from Gouesbet *et al* [87].

For data in this table, the wavelength is  $\lambda = 0.5 \,\mu\text{m}$  and the beam waist radius is  $w_0 = 10\lambda$ , corresponding to a beam shape factor s = 0.015915, that is to say to a strongly focused beam. As known for a beam waist center

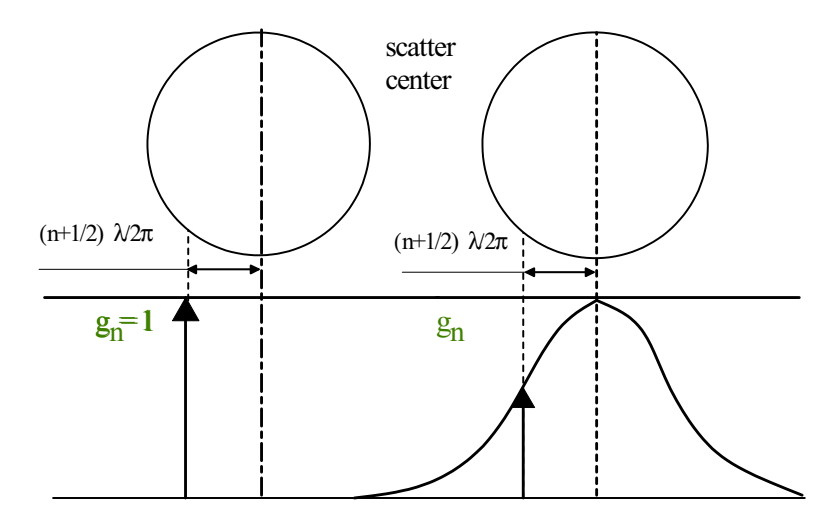


**Fig. VII.1.** The localized interpretation of the BSCs  $g_n$ . (a) for a plane wave, (b) for a Gaussian profile.

**Table VII.1.** Comparison of the values of special BSCs for a beam waist center location case.

	A	В	С	D	Е
$g_1$	0.995	0.995	1	1	0.99943
$g_2$	0.996	0.995	0.99898	0.99949	0.99841
$g_3$	-	1	0.99746	0.99746	0.99690
$g_4$	-	-	0.99544	0.99595	0.99488
$g_5$	0.993	0.992	0.99292	0.99292	0.99236
$g_6$	0.989	0.989	0.98991	0.99041	0.98935
$g_{30}$	0.788	0.787	0.79030	0.79070	0.79006
$g_{45}$	0.585	0.589	0.59191	0.59191	0.59191
$g_{60}$	0.394	0.394	0.39555	0.39575	0.39567
$g_{80}$	0.192	0.193	0.19358	0.19368	0.19369
$g_{100}$	0.077	0.077	0.07739	0.07743	0.07742

location, the special BSCs are real numbers (sections VI.5). They here have been evaluated by using quadratures at order L (column A) and at order  $L^-$  (column B), finite series at order L (column C) and at order  $L^-$  (column D), and localized approximation (column E), showing that the approximation is very good indeed.

<sup>&</sup>lt;sup>1</sup> Note that we still keep on with the word "approximation" as in the historical process, but this is a point of view to be later revised and refined.

coefficient	$kr^-$	kr+
$g_1$	0.6	2.5
$g_2$	1.5	4
$g_6$	6	9
$g_{30}$	30	50
$g_{45}$	45	75
$g_{60}$	60	90
$g_{80}$	80	120
$g_{100}$	100	150

**Table VII.2.** kr-localization domains

#### VII.2.4 Physical Evidence of Validity

This subsection complements section (VI.6.3) devoted to numerical behaviours of quadratures in which some clues for localization were observed, in particular Rel (VI.123). Numerical computations of special BSCs are carried out using the GNF2 code mentioned in section (VI.6.1). BSCs  $g_n$  are evaluated according to Rel (VI.62) at the order L, for a beam waist diameter  $2w_0 = 20\lambda$ , and  $\lambda = 0.5 \ \mu\text{m}$ . Results are plotted in Fig (VII.2) versus  $log_{10}(kr_{max})$ , the integral over (kr) in Rel (VI.62) being carried out from 0 up to  $(kr_{max})$ .

For each BSC  $g_n$  displayed in the figure, one observes that the contribution to the integral is located (localized) in a narrow interval of (kr). To quantify this statement, let us introduce fairly arbitrarily a localization domain  $(kr^-, kr^+)$  such as integrations from 0 to  $(kr^-)$ , and 0 to  $(kr^+)$ , contribute 2% and 50% respectively to the total value of the coefficient. Table (VII.2) clearly exhibits that the localization domain is strongly correlated with the order n of the coefficient. Localized values of (kr) are found to be such that  $(kr) \approx (n)$ , leading to  $r \approx (n+1/2)\lambda/(2\pi)$ . Of course, this discussion possesses a strong heuristic character but it physically illustrates in a very clear way why special BSCs may be locally interpreted.

Of course, because the principle of localization is expressed in terms of distances to the axis  $\rho_n$ , the presentation in Fig (VII.2) in terms of radial values (kr) is not the most appropriate. A better discussion would require  $g_n$ -integrations using cylindrical coordinates and studying contributions of shells  $(\rho, \rho + \Delta \rho)$ . Such a study is available from Maheu et al [372] from which Table VII.3 is extracted. For each  $g_n$ , there exists a cylindrical shell limited by two distances  $(k\rho^-)$  and  $(k\rho^+)$  to the beam axis such as integrations up to  $(k\rho^-)$  and  $(k\rho^+)$  in cylindrical coordinates contribute to 10 % and 90 % of the coefficient values respectively. The 50 %-contribution corresponds to a shell radius  $(k\rho_{50})$ . It is observed that values of (n+1/2) are always included in

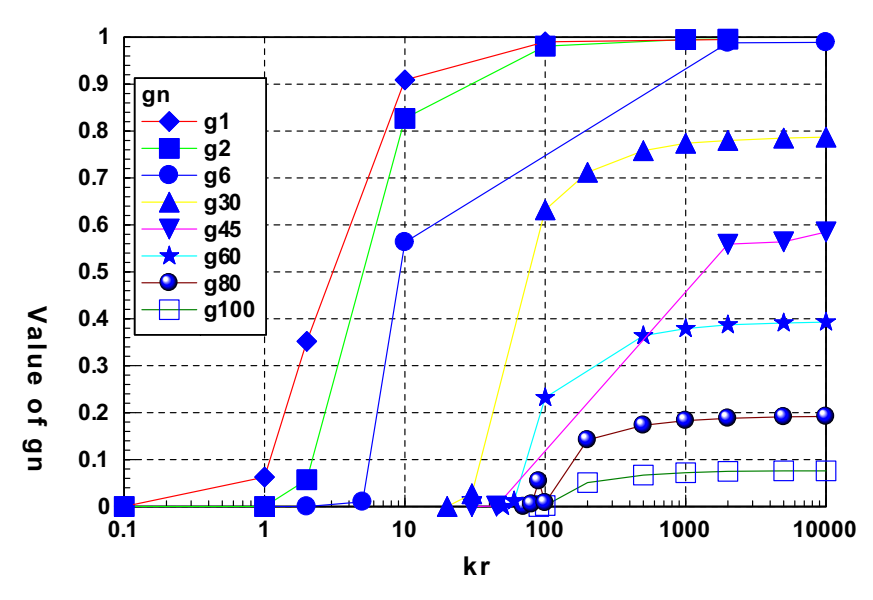


**Fig. VII.2.** Integral VI.62 versus the limit of integration. The parameters are: description order L,  $2w_0 = 20\lambda$ ,  $\lambda = 0.5 \,\mu m$ , and the order n of the coefficients (from 1 to 100).

coefficient	$k\rho^-$	$k\rho^+$	$k\rho_{50}$	(n+1/2)
$g_1$	1.0	5.5	2.6	1.5
$g_4$	3.2	9.2	5.7	4.5
$g_5$	4.2	10.5	6.8	5.5
$g_6$	4.8	12	8.0	6.5
$g_{60}$	53	70	60	60.5

**Table VII.3.**  $\rho$ -localization domains

the shell radii  $(k\rho^-, k\rho^+)$  and correlate well with  $(k\rho_{50})$  particularly when the order n increases.

## VII.2.5 Difference of Behaviour between Rigorous Methods and Localized Approximation

The quality of the localized approximation may be assessed by displaying comparisons such as in Table VII.1 (and others to come). Quality and validity may therefore be numerically checked leading to the conclusion that the approximation appears to be very good, with an insignificant loss of accuracy in most situations. Nevertheless, it has been observed and carefully checked in section VI.7.2 by using finite series that  $|g_n|$  becomes big, increasing steadily, when the order n increases beyond a value corresponding to rays passing at a

distance from the axis bigger than about twice the beam waist radius. Such a behaviour is not observed for localized values (Rel (VII.7)) which quickly decrease with the order. Such a decrease physically makes sense because the electromagnetic density of energy decreases very fast when departure from the beam axis is increased. In section (VI.7.2), it has also been shown that increase of  $|g_n|$  with rigorous methods is compatible with physics, due to the fact that the  $g_n$ 's actually create two alternating series, one for n odd and the other for n even. The difference of behaviour between rigorous methods and localized approximation appears only for big n's, i.e. far away from the beam axis where the electromagnetic density becomes very small indeed, and therefore is not expected to spoil results when the localized approximation is used rather than a rigorous technique.

Let us note that a word of caution is necessary here concerning the above heading. When using the terminology "rigorous methods", we referred to quadratures and finite series. But these methods are rigorous only if the beam description used exactly satisfies Maxwell's equations. Otherwise, they may introduce artifacts 134 and, even when they produce constant values, like when using finite series, we have to say that the beam has been "remodelled". Therefore, in most cases (when the beam description does not exactly satisfy Maxwell's equations), the so-called rigorous methods are not rigorous at all. Now, let us consider the localized approximation. It has indeed been introduced as an approximation (from Van de Hulst' principle of localization) but it produces beams which exactly satisfy Maxwell's equations, and well anticipate higher-order beams, up to the point where standard beams are introduced with the claim that they could provide a genuine definition of Gaussian beams [297], [311], [313], [314], washing out the limitations of the Davis scheme of description. At this stage, we may wonder to what the localized approximation is an approximation, since the so-called rigorous methods do not provide rigorous solutions. Independently of the historical justification of the word "approximation", we might conversely very well decide that localized beams, exactly satisfying Maxwell's equations, obtained by using a so-called localized approximation, are not approximations any more, but genuine beams in their own right.

#### VII.3 Axis Location Case

The beam waist center location case has been treated using a rather trivial generalization of the principle of localization as stated by van de Hulst (1957) [17], and therefore possesses a rather firm foundation based on the properties of mathematical functions involved in the formulation. The quality of the localized approximation at this stage, as exemplified by Table (VII.1) is however somewhat unexpected, surprising and even looks a bit magic.

Encouraged by these results, we are now going to proceed to a next generalization to the axis location case. Clearly, more difficulties become now

involved in the problem. For example, special BSCs become complex numbers and therefore do not fit any more the simple mental image depicted in Fig (VII.1). Also, the wave-front is no more plane. Another difficulty is that coordinate z now explicitly appears in the field component expressions but must disappear in the expressions for the localized  $\tilde{g}_n$ 's. The reader who would study chronologically our articles on localized approximation, all of them available from the bibliography, would remark that we had hesitations about the best way to proceed further, and that several equivalent procedures, more or less elegant, have been designed and discussed. In this book, we shall settle down to our favorite presentation (although this might be a point of subjective personal taste).

Indeed, a mere generalization of the principle of localization as stated by van de Hulst, successful for the beam waist center location case, is no more sufficient to solve the axis location case. It will be required to be more inventive and, even if we do not like it (but we actually like it), more audacious. The game is now to guess an extended procedure to design  $\tilde{g}_n$ -expressions for the axis location case with the proviso that the expression (VII.7) for the beam waist center location case must be recovered as a special case.

Cartesian field components as for Rels (VII.3)-(VII.6) are no more considered because they are not easily tractable if it is wanted to investigate not only the order  $L^-$  of approximation, but also the order L. In particular, using Cartesian field components, we do not exactly know how to manage with longitudinal field components  $E_z$ ,  $H_z$  which are not zero at order L. Actually, Cartesian components are certainly unessential when compared with radial field components  $E_r$  and  $H_r$ . Because only these radial field components are required to determine incident BSPs, they are without any doubt the essence and they deserve a due privilege. Furthermore, they incorporate relevant information from all Cartesian components. For the axis location case under study, they are found to read as, from Rels (IV-71), (IV-74):

$$\begin{pmatrix} E_r \\ H_r \end{pmatrix} = \left\{ \begin{array}{c} \left( \begin{array}{c} E_0 \cos \varphi \\ H_0 \sin \varphi \end{array} \right) \sin \theta \ exp(-ikz) \right\} \quad \left[ 1 - \epsilon_L \frac{2Q}{l} z \right] \ iQ \ \exp \ \left[ -iQ \frac{r^2 \sin^2 \theta}{w_0^2} \right] \exp(ikz_0) \\ (\text{VII}.9) \end{array}$$

in which it is recalled that according to Rel (IV.63):

$$Q = \frac{1}{i + 2\frac{z - z_0}{I}}$$
 (VII.10)

In Rel (VII.9), the brace term {} is the only one which would appear if the incident beam were a plane wave. The multiplicand factor in (VII.9) is then specific to the Gaussian beam under examination.

Although it is known (chapter VI) that we must not distinguish between a set of BSCs  $g_n$  associated with TM-waves and another set of BSCs  $g_n$  associated with TE-waves ( $g_{n,TM} = g_{n,TE} = g_n$ ), the distinction will be maintained for convenience at the beginning of the present procedure. Since the field component  $E_r$  must be related to BSCs  $g_{n,TM}$  and the field component  $H_r$ 

must be related to BSCs  $g_{n,TE}$ , a procedure starting from Rel (VII.9) will provide separate expressions for  $\tilde{g}_{n,TM}$  (starting from  $E_r$ ) and  $\tilde{g}_{n,TE}$  (starting from  $H_r$ ) with the necessary condition that the following expression must be recovered:

$$\tilde{g}_{n,TM} = \tilde{g}_{n,TE} = \tilde{g}_n \tag{VII.11}$$

Indeed, any attempt to design a localized approximation leading to  $\tilde{g}_{n,TM} \neq \tilde{g}_{n,TE}$  should be immediately given up. Let us call  $\mathcal{A}$  the Gaussian contribution in Rel (VII.9) and first consider the TM-BSCs  $\tilde{g}_{n,TM}$ . When the Gaussian contribution is 1, it is known (section VII.2.2) that  $g_{n,TM} = \tilde{g}_{n,TM} = 1$  (plane wave case). Since BSCs  $g_n$  contain all the information on the incident wave, our first obvious Ansatz must be:

$$\tilde{g}_{n,TM} = \hat{f}_{TM}(\mathcal{A})$$
 (VII.12)

in which  $\hat{f}_{TM}$  is an operator acting on  $\mathcal{A}$  to produce the  $\tilde{g}_{n,TM}$ 's. The BSCs  $g_{n,TM}$  being constant numbers, the operator  $\hat{f}_{TM}$  must comply with three simple properties (i) eliminate variable z in  $\mathcal{A}$ , (ii) eliminate variable r sin  $\theta$  in  $\mathcal{A}$ , (iii) introduce a subscript n. We are now going to guess the operator  $\hat{f}_{TM}$  in view of these properties. For this guess, two guides are invoked (i) use physics when convincing arguments may be found (ii) be as simple as possible, assuming that nature likes simplicity. The quality of the guess will be afterward checked by direct comparisons between guess results and so-called rigorous computations. Remarkably enough, our first trial in designing a localized approximation for special BSCs  $g_n$  in the axis location case has been immediately successful.

Our first guess concerns the way to eliminate the variable z. This could be produced by integrating over z, the range of integration being from  $(-\infty)$  to  $(+\infty)$  since no reason appears to choose any specific finite range. Then, the special case  $w_0 \to \infty$  should be considered, leading also to  $l \to \infty$  (Rel (IV.4)), namely to the plane wave case obtained as a limit of the Gaussian beam case. For the plane wave case,  $\mathcal{A}$  is a constant and the integration over z leads to the introduction of an infinite quantity in conflict with the finite character of the BSCs  $q_{n,TM}$ .

The simplest way to proceed is then alternatively to set z to a special value, namely z=0 since this value is the only one playing a special role (it defines the center of the coordinate system  $O_Pxyz$ ). We may also consider a small test scatter center located at point  $O_P$ . The interaction between the incident beam and the test particle possesses a local character via the boundary conditions to be written at the surface of the scatter center. The choice z=0 reflects this local character. This last argument is not fully convincing since actually we do not consider a scattering problem here, but only the description of the Gaussian beam irrespective of the presence of any scatter center. However, it gives some further intuitive support to our

choice. This guess may seem rather brutal, and it is indeed, but it will work efficiently.

To eliminate  $(r \sin \theta)$ , the principle of localization is again invoked. The quantity  $(r \sin \theta)$  must then be replaced by  $\rho_n$  (Rel (VII.1)), simultaneously eliminating  $(r \sin \theta)$  and introducing a subscript n as required.

To sum up, from such very simple considerations, it is tentatively assumed that the action of the operator  $\hat{f}_{TM}$  is (i) to replace z by 0 (ii) to replace  $(r \sin \theta)$  by (n+1/2)  $(\lambda/2\pi)$ . Consequently, a localized approximation to the BSCs  $g_{n,TM}$  is obtained according to:

$$\tilde{g}_{n,TM} = i \ \overline{Q} \exp \left[ -i \ \overline{Q} \ (\frac{\rho_n}{w_0})^2 \right] \ \exp(ikz_0)$$
 (VII.13)

in which:

$$\overline{Q} = Q(z=0) = \frac{1}{i - \frac{2z_0}{l}} \tag{VII.14}$$

Since the Gaussian contribution  $\mathcal{A}$  in Rel (VII.9) is the same for  $E_r$  and  $H_r$ , it is immediately concluded that:

$$\tilde{g}_{n,TE} = \hat{f}_{TE}(\mathcal{A})$$
 (VII.15)

in which:

$$\hat{f}_{TM} = \hat{f}_{TE} = \hat{f} \tag{VII.16}$$

to ensure:

$$\tilde{g}_{n,TM} = \tilde{g}_{n,TE} = \tilde{g}_n$$
 (VII.17)

a relation also satisfied by the exact special BSCs.

For the waist center location case, adding the assumption  $z_0 = 0$ , Rels (VII.13) and (VII.17) reduce to Rel (VII.7) as it should. Furthermore, when  $w_0 \to \infty$ ,  $\tilde{g}_n$ 's reduce to  $\exp(ikz_0)$ , a result which is known to be also true for the exact BSCs  $g_n$  (section VI.4).

It must be noted that the double-valued quantity  $\epsilon_L$  does not appear any more in the expression for the localized special BSCs (VII.13). This statement will remain true in the case of arbitrary location when we have to design a localized approximation to the BSCs  $g_n^m$ . Therefore, the results of the localized approximation are identical irrespectively of the order L or  $L^-$  of approximation to the description of the Gaussian beam. This is indeed an interesting remark because it is recurrently observed that BSCs are usually very close, whatever the order of approximation (L or  $L^-$ ) to the description of the beam. The mathematical reason why our localized approximation exhibits such a behaviour is that the variable z has been set equal to 0, therefore eliminating the  $\epsilon_L$ -term (2Qz/l) in Rel (VII.9). Because descriptions at orders L and  $L^-$  are usually very close, this discussion a posteriori justifies once more the action  $z \to 0$  of the operator  $\hat{f}$ .

	С	D	E
$g_1$	(0.908000,-0.289025)	(0.711599,-0.453018)	(0.866610,-0.260209)
$g_2$	(0.832928,-0.235844)	(0.696343,-0.420356)	(0.797050,-0.214093)
$g_3$	(0.720320,-0.156074)	(0.635318,-0.289705)	(0.701829,-0.155877)
$g_4$	$(0.598260, -0.869411 \ 10^{-1})$	(0.586754,-0.213104)	$(0.590465, -0.952384 \ 10^{-1})$
$g_5$	$(0.466748, -0.284455 \ 10^{-1})$	$(0.485435, -0.919815 \ 10^{-1})$	$(0.473422, -0.411516 \ 10^{-1})$
$g_6$	$(0.347808, -0.115944 \ 10^{-1})$	$(0.407329, -0.236618 \ 10^{-1})$	$(0.360594, 0.413758 \ 10^{-1})$
$g_7$	$(0.245946, 0.325540 \ 10^{-1})$	$(0.294773, 0.401488 \ 10^{-1})$	$(0.259920, 0.270357 \ 10^{-1})$
$g_8$	$(0.164718, 0.405967 10^{-1})$	$(0.216080, 0.673214 \ 10^{-1})$	$(0.176476, 0.396080 \ 10^{-1})$
$g_9$	$(0.104385, 0.389802 \ 10^{-1})$	$(0.133797, 0.756275 \ 10^{-1})$	$(0.112199, 0.412818 \ 10^{-1})$
$g_{10}$	$(0.623670 \ 10^{-1}, \ 0.324501 \ 10^{-1})$	$(0.827317 \ 10^{-1}, \ 0.702225 \ 10^{-1})$	$(0.662695 \ 10^{-1}, \ 0.361157 \ 10^{-1})$
$g_{11}$	$(0.366894 \ 10^{-1}, \ 0.236073 \ 10^{-1})$	$(0.405030 \ 10^{-1}, \ 0.562417 \ 10^{-1})$	$(0.359451 \ 10^{-1}, \ 0.278998 \ 10^{-1})$
<i>0</i> 12	$(0.202714 \ 10^{-1} \ 0.168525 \ 10^{-1})$	$(0.181172 \ 10^{-1} \ 0.419980 \ 10^{-1})$	$(0.175703 \ 10^{-1} \ 0.194352 \ 10^{-1})$

**Table VII.4.** Comparison of BSCs  $g_n$  for a location along the beam axis under severe values of the parameters

**Table VII.5.** Comparison of BCSs  $g_n$  for a location along the beam axis under reasonable values of the parameters

	C	D	Е
$g_1$	$(0.240798 \ 10^{-1}, -0.153297)$	$(0.240798 \ 10^{-1}, -0.153297)$	$(0.253834 \ 10^{-1}, -0.152871)$
$g_2$	$(0.264021 \ 10^{-1}, -0.152549)$	$(0.252410 \ 10^{-1}, -0.152923)$	$(0.276870 \ 10^{-1}, -0.152086)$
$g_3$	$(0.298856 \ 10^{-1}, -0.151427)$	$(0.298856 \ 10^{-1}, -0.151427)$	$(0.311085 \ 10^{-1}, -0.150847)$
$g_{18}$	$(0.128509, -0.101413 \ 10^{-1})$	$(0.128575, -0.111656 \ 10^{-1})$	$(0.125475, -0.108190 \ 10^{-1})$
$g_{19}$	$(0.125886, +0.908621 \ 10^{-2})$	$(0.125886, +0.908621 \ 10^{-2})$	$(0.122822, +0.756862 \ 10^{-2})$
$g_{20}$	$(0.120158, +0.281921 \ 10^{-1})$	$(0.120158, +0.272750 \ 10^{-1})$	$(0.117261, +0.258397 \ 10^{-1})$
$g_{21}$	$(0.111131, +0.466865 10^{-1})$	$(0.111131, +0.466865 10^{-1})$	$(0.108703, +0.434121 \ 10^{-1})$

Again, many validations of Rel (VII.13) are available from the literature, for instance in Gouesbet *et al* [367], the most convincing ones being obtained by comparing localized values  $\tilde{g}_n$  and so-called exact values  $g_n$ . Table (VII.4) below, extracted from Gouesbet *et al* [367], provides such comparisons.

For this table, the wavelength is  $0.5~\mu\mathrm{m}$ . The laser is strongly focused with  $w_0 = \lambda$  and the waist ordinate is  $z_0 = 1~\mu m$  very close to the waist, in a region of the beam where the curvature evolves very fastly ( $l = \pi~\mu\mathrm{m}$ ). Columns C, D, E possess the same meaning as in Table (VII.1), i.e. they correspond to finite series at orders L and  $L^-$ , and localized approximation respectively. As expected, the special BSCs are now complex numbers. The case under study is here a very difficult one because of the strong focus of the beam and of the chosen value of  $z_0$ . The beam shape factor s is  $1/2\pi$ , i.e. its theoretical largest bound (see section IV.1.2). It is indeed one of the worst situations which can be encountered. In particular, finite series at orders L and  $L^-$  provide significantly different results. Accounting for this remark, results of the localized approximation in column E compare very favourably with results in columns C and D.

A more reasonable case is exhibited in Table VII.5. The wavelength is still 0.5  $\mu$ m and we still have  $w_0 = \lambda$  as before. But the waist ordinate is now  $z_0 = 10 \ \mu$ m, i.e. a test particle would not be located in a (locally) strongly

focused beam. Column labels have the same meaning as previously. Finite series at orders L and  $L^-$  provide very similar results, both for the real and imaginary parts. The agreement with localized approximation is furthermore very satisfactory indeed. As the reader may now expect from such results, the agreement between localized approximation and rigorous techniques may indeed become very good, up to many digits (typically 1 part per  $10^5$ ), when easier cases (smaller values of the beam shape factor s) are considered. Indeed, in this section, it has been chosen to provide difficult examples in order to exemplify the capabilities of the localized approximation.

It is not useful to extensively discuss here the gain in CPU produced by using localized approximation formulae. Most clearly, evaluations by using Rel (VII.13) are nearly instantaneous and, from that point of view, cannot decently be compared with quadratures or even with finite series. It has been mentioned in section VI.3 that any owner of a LMT-routine could trivially adapt it for GLMT in the case of a Gaussian beam with axis location. The reader may now realize how much this is true when the localized approximation Rel (VII.13) is used to compute the special BSCs, adding a negligible amount of computational time.

Finally, an axis location case may be defined for any kind of beam exhibiting an axis of symmetry. If the expressions for the radial field components  $E_r$ and  $H_r$  are not known, the above procedure cannot be applied in a strict way to express a localized approximation to the BSCs  $g_n$ . However, the simple basic idea displayed in Fig VII.1 may still tentatively be used to approach a solution to this problem. An example is provided by the top-hat beams which may be used for optical particle sizing (326, 296, and references therein). The intensity repartition inside such a beam is illustrated in Fig VII.3. It is constant inside a circle of radius L on a plateau and falls down to 0 outside of it. In the axis location case, such a beam may be modelled by using the localized approximation, taking constant values of the  $\tilde{g}_n$  's, different from 0, for n up to a critical value  $n_c$  given by  $\rho_{n_c} < L < \rho_{n_c+1}$  (see Rel (VII.1)), and setting  $\tilde{g}_n = 0$  for  $n > n_c$ . Top-hat beam scattering with localized approximation according to the above idea has been discussed in Corbin et al 296 and fully analyzed in Gouesbet et al 297, this latter article vividly illustrating the validity of the localized interpretation behind the localized approximation in the case of on-axis beams.

## VII.4 Arbitrary Location

## VII.4.1 A Well Posed Problem

Having designed a localized approximation to the special BSCs  $g_n$ , the question now arises to know whether it is possible to design a generalization to localized BSCs  $\tilde{g}_n^m$ . The answer is necessarily positive meaning that we are faced to a well-posed problem. Effectively, both sets  $\{g_n\}$  and  $\{g_{n,TM}^m, g_{n,TE}^m\}$ 

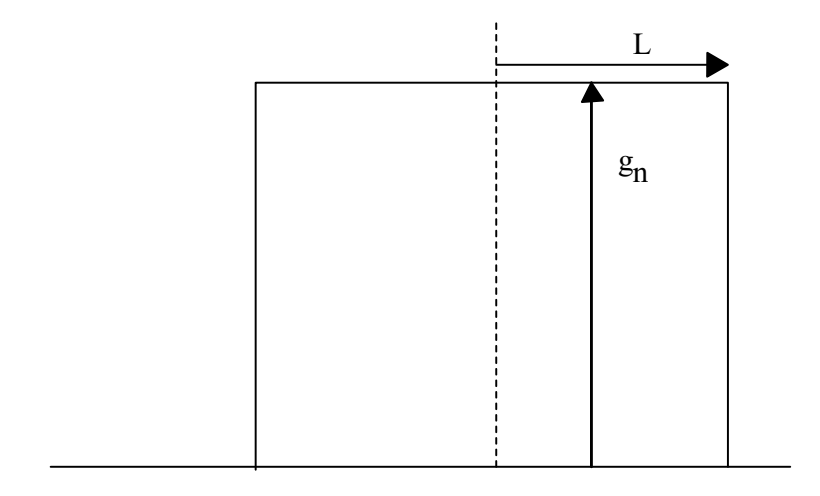


Fig. VII.3. Sketch of a top-hat beam.

fully describe the incident beam and are therefore equivalent, the only difference between these sets being due to the choice of the location of the particle coordinate system with respect to the beam coordinate system. Consequently, there must exist relations reading as:

$$g_{n,TM}^m = f_{n,TM}^m(g_n) \tag{VII.18}$$

$$g_{n,TE}^m = f_{n,TE}^m(g_n) \tag{VII.19}$$

and also:

$$g_n = h_n \left( g_{n,TM}^m, g_{n,TE}^m \right) \tag{VII.20}$$

In particular, these relations show that we potentially possess a new method to evaluate BSCs  $g_n^m$  once the special BSCs  $g_n$  are known (whatever the method used for these special BSCs). The key to solve the problem of finding the functions  $f_n^m$  is the use of translational theorems (famous in the context of quantum mechanics) for spherical Bessel functions and associated Legendre functions such as discussed by Danos and Maximon [373], Liang and Lo [374], Ronchi [375] or Dalmas and Deleuil [376]. Actually such a method has been designed by Doicu [377]. The existence of the functions  $f_{n,TM}^m$  and  $f_{n,TE}^m$  however ensures us anyway that we must be able to design a localized approximation to the BSCs  $g_n^m$ .

## VII.4.2 BSCs $g_n^{+1}$ and $g_n^{-1}$ for Axis Location

New difficulties however arise for BSCs  $g_n^m$  that have not been encountered for the special BSCs  $g_n$ . The first one is that we are now facing two sets of

BSCs, one for TM-waves and the other for TE-waves. A second difficulty is that we must now deal with a subscript n and a superscript m.

As far as the subscript n is concerned, it may be tentatively assumed that the reduction procedure previously used remains essentially valid. Through the localization principle, this procedure induces a discretization of space in the directions perpendicular to z ( $\rho$ -directions) conveyed by the introduction of discrete radial locations  $\rho_n$ . Due to this discretization, the wave character of the beam in  $\rho$ -directions is lost, permitting us to discuss the problem in terms of geometry, that is to say in terms of rays, or more exactly in terms of annular bundles of rays, each bundle of rays associated with subscript n passing at about a distance  $\rho_n$  from axis z.

Similarly, we might think that the superscript m is associated with an angular  $\varphi$ -discretization in space. Associated with a bundle of rays at distance  $\rho_n$ , we might then introduce a further discretization  $\varphi_m$ . Since m ranges from (-n) to (+n), we would then be faced with (2n+1) bundles of rays for each n-bundle of rays. From rather intuitive and/or heuristic arguments, it has been claimed in Gouesbet et al [371] that this should not be a correct representation and that a wave character must remain associated with the superscript m. This statement may be formally evidenced by considering again the axis location case. This case is a nice "pierre de Rosette" indeed because the formulation of the GLMT may then be expressed in terms of special BSCs  $g_n$  for which the localization problem is solved, or in terms of BSCs  $g_n^{-1}$  and  $g_n^{-1}$ , all the other BSCs  $g_n^m$ ,  $|m| \neq 1$ , being equal to 0 (section VI.1). Furthermore, in this case, we may write (from Rel (VI.3)):

$$g_{n,TM}^1 = g_{n,TM}^{-1} = g_n/2 = g_{n,TM}/2$$
 (VII.21)

$$g_{n,TE}^1 = -g_{n,TE}^{-1} = -i g_n/2 = -i g_{n,TE}/2$$
 (VII.22)

Let us first discuss TM-BSCs involved in the first of these relations. It is known that they are associated with the radial electric field component  $E_r$  expressed in Rel (VII.9) as:

$$E_r = \{ E_0 \cos \varphi \sin \theta \exp(-ikz) \} \mathcal{A}$$
 (VII.23)

Expressing  $\cos \varphi$  in terms of complex exponentials, Rel (VII.23) for  $E_r$  may be rewritten as a two-terms expansion:

$$E_r = E_r^{+1} + E_r^{-1} = \sum_{m=1, -1} E_r^m$$
 (VII.24)

$$E_r^{+1} = \frac{E_0}{2} e^{i\varphi} \sin\theta \exp(-ikz) \mathcal{A}$$
 (VII.25)

$$E_r^{-1} = \frac{E_0}{2} e^{-i\varphi} \sin\theta \exp(-ikz)\mathcal{A}$$
 (VII.26)

in which superscripts m=+1 and m=-1 are associated with exp (i $\varphi$ ) and exp (-i $\varphi$ ) modes, respectively. From Rels (VII.21), (VII.12) and (VII.16), we must therefore have:

$$\tilde{g}_{n,TM}^{\pm 1} = \frac{1}{2}\tilde{g}_n = \frac{1}{2}\tilde{g}_{n,TM} = \frac{1}{2}\hat{f}_{TM}(\mathcal{A}) = \frac{1}{2}\hat{f}(\mathcal{A})$$
 (VII.27)

In other words,  $\tilde{g}_{n,TM}^{+1}$  is obtained from the mode  $E_r^{+1}$  by removing a plane wave contribution  $E_0 \sin \theta \exp(-ikz)$  and the exponential term  $e^{i\varphi}$ , and applying the operator  $\hat{f}$  to the remaining term  $\mathcal{A}/2$ . Similarly,  $\tilde{g}_{n,TM}^{-1}$  is obtained from the mode  $E_r^{-1}$  by removing a plane wave contribution  $E_0 \sin \theta \exp(-ikz)$  and the exponential term  $e^{-i\varphi}$ , and again applying the operator  $\hat{f}$  to the remaining term  $\mathcal{A}/2$ .

The same procedure may be used for TE-BSCs. Expressing  $\sin \varphi$  in terms of complex exponentials, Rel (VII.9) for the radial magnetic component  $H_r$  may be rewritten as a two-terms expansion:

$$H_r = H_r^{+1} + H_r^{-1} = \sum_{m=1, -1} H_r^m$$
 (VII.28)

$$H_r^{+1} = \frac{H_0}{2i} e^{i\varphi} \sin\theta \exp(-ikz)\mathcal{A}$$
 (VII.29)

$$H_r^{-1} = \frac{H_0}{2i} \left( -e^{-i\varphi} \right) \sin \theta \, \exp(-ikz) \mathcal{A} \tag{VII.30}$$

in which superscripts m = +1 and m = -1 are again associated with  $\exp(i\varphi)$  and  $\exp(-i\varphi)$  modes, respectively.

Then Rels (VII.22), (VII.15) and (VII.16), yield:

$$\tilde{g}_{n,TE}^{1} = -\frac{i}{2}\tilde{g}_{n,TE} = -\frac{i}{2}\hat{f}_{TE}(\mathcal{A}) = \frac{1}{2i}\hat{f}(\mathcal{A})$$
 (VII.31)

$$\tilde{g}_{n,TE}^{-1} = \frac{i}{2}\tilde{g}_{n,TE} = +\frac{i}{2}\hat{f}_{TE}(\mathcal{A}) = \frac{-1}{2i}\hat{f}(\mathcal{A})$$
 (VII.32)

In other words,  $\tilde{g}_{n,TE}^{+1}$  is obtained from the mode  $H_r^{+1}$  by removing a plane wave contribution  $H_0 \sin \theta \exp(-ikz)$  and the exponential term  $e^{i\varphi}$ , and applying the operator  $\hat{f}$  to the remaining term  $\mathcal{A}/(2i)$ . Similarly,  $\tilde{g}_{n,TE}^{-1}$  is obtained from the mode  $H_r^{-1}$  by removing a plane wave contribution  $H_0 \sin \theta \exp(-ikz)$  and the exponential term  $e^{-i\varphi}$ , and again applying the operator  $\hat{f}$  to the remaining term  $\mathcal{A}/(-2i)$ . From now on, the operator  $\hat{f}$  is called the localization operator.

As announced before, this new procedure shows that m must not be associated with any discretization but with m-waves  $e^{i\varphi}$  and  $e^{-i\varphi}$  (generally  $e^{im\varphi}$ ), associated with angle  $\varphi$ . Besides, as another support to this conclusion, it is of interest to remark that the circumference at a distance  $\rho_n$  from the axis

is  $2\pi\rho_n = (2n+1)\frac{\lambda}{2}$ , i.e. an integer times the half wave-length, which is a classical (and also a quantum) result for stationary waves. The mental picture which is emerging from these results is as follows. The incident beam is a superposition of annular bundles of rays localized at distances  $\rho_n$  from the axis associated with the subscript n, and for each n-bundle, of (2n+1) stationary waves associated with the superscript m. The principle of localization therefore now induces a particle/wave complementarity.

# VII.4.3 BSCs $g_n^m$ for Arbitrary Location: First Attempt

The previous subsection immediately suggests us a tentative procedure for generalizing the localized approximation to all the BSCs  $g_n^m$  for arbitrary location, namely (i) expand the radial electric and magnetic field components  $E_r$  and  $H_r$  into m-modes  $E_r^m$  and  $H_r^m$  respectively, containing  $\exp(im\varphi)$ , (ii) isolate in these modes the plane wave contributions  $E_0 \sin \theta \exp(-ikz)$ ,  $H_0 \sin \theta \exp(-ikz)$  and the exponential term  $\exp(im\varphi)$  and (iii) apply the localization operator  $\hat{f}$  to the remaining parts of the expressions. This program is now carried out below.

In the case of Gaussian beams at orders L and  $L^-$ , it is conveniently recalled that the radial field components  $E_r$  and  $H_r$  are given by (section IV.2.1):

$$E_r = E_0 \frac{F}{2} \left[ \sum_{jp}^{jp} \Psi_{jp} \exp(ij_+\varphi) + \sum_{jp}^{jp} \Psi_{jp} \exp(ij_-\varphi) \right]$$

$$+ E_0 x_0 G \sum_{jp}^{jp} \Psi_{jp} \exp(ij_0\varphi)$$
(VII.33)

$$H_r = H_0 \frac{F}{2i} \left[ \sum_{jp} \Psi_{jp} \exp(ij_+\varphi) - \sum_{jp} \Psi_{jp} \exp(ij_-\varphi) \right]$$

$$+ H_0 y_0 G \sum_{jp} \Psi_{jp} \exp(ij_0\varphi)$$
(VII.34)

in which:

$$F = \Psi_0^0 \sin \theta \left( 1 - \frac{2Q}{l} \epsilon_L z \right) \exp(-ikz) \exp(ikz_0)$$
 (VII.35)

$$G = \epsilon_L \, \Psi_0^0 \, \frac{2Q}{l} \, \cos\theta \, \exp(-ikz) \, \exp(ikz_0) \tag{VII.36}$$

$$\Psi_0^0 = iQ \exp(-iQ \frac{r^2 \sin^2 \theta}{w_0^2}) \exp(-iQ \frac{x_0^2 + y_0^2}{w_0^2})$$
 (VII.37)

$$\Psi_{jp} = \left(\frac{iQr\sin\theta}{w_0^2}\right)^j \frac{(x_0 - iy_0)^{j-p}(x_0 + iy_0)^p}{(j-p)!p!}$$
(VII.38)

$$\sum_{j=0}^{jp} = \sum_{j=0}^{\infty} \sum_{p=0}^{j}$$
 (VII.39)

$$j_{+} = j + 1 - 2p = j_0 + 1$$
 (VII.40)

$$j_{-} = j - 1 - 2p = j_{0} - 1$$
 (VII.41)

Expanding into m-wave modes according to:

$$\begin{bmatrix} E_r \\ H_r \end{bmatrix} = \sum_{m=-\infty}^{+\infty} \begin{bmatrix} E_r^m \\ H_r^m \end{bmatrix}$$
 (VII.42)

one readily obtains:

$$E_r^m = \{ E_0 \exp(-ikz) \exp(im\varphi) \sin \theta \} \exp(ikz_0) iQ$$

$$\exp\left(-iQ\frac{r^2 \sin^2 \theta}{w_0^2}\right) \exp\left(-iQ\frac{x_0^2 + y_0^2}{w_0^2}\right) \tag{VII.43}$$

$$\left[\frac{1}{2}(1 - \frac{2Q}{l}\epsilon_L z) \left(\sum_{j_+=m}^{jp} \Psi_{jp} + \sum_{j_-=m}^{jp} \Psi_{jp}\right) + x_0\epsilon_L \frac{2Q}{l} \frac{z}{r \sin \theta} \sum_{j_0=m}^{jp} \Psi_{jp}\right]$$

$$H_r^m = \{ H_0 \exp(-ikz) \exp(im\varphi) \sin \theta \} \exp(ikz_0) iQ$$

$$exp\left(-iQ\frac{r^2\sin^2\theta}{w_0^2}\right) \exp\left(-iQ\frac{x_0^2 + y_0^2}{w_0^2}\right)$$
(VII.44)
$$\left[\frac{1}{2i}(1 - \frac{2Q}{l}\epsilon_L z) \left(\sum_{j_+=m}^{jp} \Psi_{jp} - \sum_{j_-=m}^{jp} \Psi_{jp}\right) + y_0\epsilon_L \frac{2Q}{l} \frac{z}{r\sin\theta} \sum_{j_0=m}^{jp} \Psi_{jp}\right]$$

The brace terms  $\{\}$  in Rels (VII.43)-(VII.44) are the ones to dismiss according to our proposal. Then, applying the localization operator  $\hat{f}$  to the rest of the expressions, one finds:

$$\tilde{g}_{n,TM}^{m,old} = \exp(ikz_0) \quad i \, \overline{Q} \, \exp\left[-i\overline{Q} \, (\frac{\rho_n}{w_0})^2\right] \\
\exp\left(-i \, \overline{Q} \frac{x_0^2 + y_0^2}{w_0^2}\right) \quad \frac{1}{2} \quad \left(\sum_{j_+=m}^{jp} \overline{\Psi_{jp}} + \sum_{j_-=m}^{jp} \overline{\Psi_{jp}}\right)$$
(VII.45)

$$\tilde{g}_{n,TE}^{m,old} = \exp(ikz_0)i \,\overline{Q} \,\exp\left[-i\overline{Q} \,(\frac{\rho_n}{w_0})^2\right] \\
\exp\left[-i\,\overline{Q}\frac{x_0^2 + y_0^2}{w_0^2}\right] \,\frac{1}{2i} \,\left(\sum_{j_+=m}^{jp} \overline{\Psi_{jp}} - \sum_{j_-=m}^{jp} \overline{\Psi_{jp}}\right) \tag{VII.46}$$

in which  $\overline{\Psi_{jp}}$  stands for  $\hat{f}(\Psi_{jp})$  that is Rel (VII.38) with Q replaced by  $\overline{Q} = \hat{f}(Q)$  as given by Rel (VII.14), and  $(r\sin\theta)$  replaced by  $\rho_n$ . Superscript 'old' has been introduced for further convenience. It is again observed that the double-valued symbol  $\epsilon_L$  has disappeared, meaning that our procedure does not distinguish between orders L and  $L^-$ . Let us also recall that double summations  $\frac{jp}{L}$  may be replaced by single summations (Appendix D).

To check the coherence of these results against the exact theory, let us consider again the special case of axis location. The condition  $x_0 = y_0 = 0$  readily implies  $\overline{\Psi}_{jp} = 0$  but for  $\overline{\Psi}_{00} = 1$ . From Rels (VII.45)-(VII.46), one then obtains:

$$\tilde{g}_{n,TM}^{m,old} = \tilde{g}_{n,TE}^{m,old} = 0, |m| \neq 1$$

$$\tilde{g}_{n,TM}^{1,old} = \tilde{g}_{n,TE}^{-1,old} = \frac{1}{2} \tilde{g}_{n}$$

$$\tilde{g}_{n,TE}^{1,old} = -\tilde{g}_{n,TE}^{-1,old} = -\frac{i}{2} \tilde{g}_{n}$$
(VII.47)

which relates the approximate BSCs  $\tilde{g}_n^{m,old}$  in the present state of the localized approximation for arbitrary location and the special approximate BSCs  $\tilde{g}_n$  successfully designed for axis location. It was compulsory that Rel (VII.47) holds because such a relation is satisfied for the exact BSCs (see Rel (VI.3)).

Extensive numerical computations in the arbitrary location case have been carried out, comparing the results of the localized approximation of Rels (VII.45)-(VII.46) and so-called rigorous values. Examples of comparisons are given below in Table VII.6 extracted from Gouesbet et al [378]. Note that, although  $z_0 = 10~\mu m$ , we are here still faced with a rather unfavourable case, in so far as  $w_0 \approx \lambda$ .

When |m|=1, the agreement between localized approximation and socalled exact values is very satisfactory. Therefore, we are done as far as coefficients  $g_n^1$  and  $g_n^{-1}$  are concerned. Unfortunately, strong discrepancies are

**Table VII.6.** Comparison between rigorous and approximate values for BSCs  $g_n^m$ , n from 1 to 3.  $w_0 = 0.5 \mu \text{m}$ ,  $\lambda = 0.5 \mu \text{m}$ ,  $z_0 = 10 \mu \text{m}$ ,  $x_0 = y_0 = 2 \mu \text{m}$ .

	Finite series (order $L$ and $L^-$ )	Localized approximation
L	$(0.36247 \ 10^{\circ}, -0.15700 \ 10^{-1})$	**
$g_1^{-1}$		
$L^{-}$	$ \begin{array}{c} (0.36247 \ 10^0, \ -0.1570010^{-1}) \\ (0.98342 \ 10^{-3}, \ 0.91676 \ 10^{-2}) \end{array} $	$(0.36233 \ 10^0, -0.73704 \ 10^-1)$
L	$(0.98342 \ 10^{-3}, \ 0.91676 \ 10^{-2})$	
$g_1^0$	(	(
$L^{-}$	$ \begin{array}{c} (0.00000 \ 10^{0}, \ 0.00000 \ 10^{0}) \\ (0.36247 \ 10^{0}, \ -15700 \ 10^{-1}) \end{array} $	$(0.68724 \ 10^{-2}, -0.15710 \ 10^{-1})$
L	$(0.36247 \ 10^{\circ}, -15700 \ 10^{-1})$	
$egin{array}{c} g_1^1 \ L^- \end{array}$	$(0.26247.10^{0} - 0.157000.10^{-1})$	$(0.36226 \ 10^{0}, \ -0.15710 \ 10^{-1})$
L	$ \frac{(0.36247 \ 10^{0}, \ -0.157000 \ 10^{-1})}{(0.20460 \ 10^{-2}, \ -0.25378 \ 10^{-2})} $	(0.30220 10 , -0.13710 10 )
$g_2^{-2}$	(0.20400 10 , - 0.25576 10 )	
$L^{-}$	$(0.20460\ 10^{-2},\ -0.25378\ 10^{-2})$	$(0.63335 \ 10^{-2}, \ 0.51083 \ 10^{-2})$
L	$ \begin{array}{cccccccccccccccccccccccccccccccccccc$	(**************************************
$g_2^{-1}$		
$L^{-}$	$(0.36234 \ 10^0, -0.15690 \ 10-1)$ $(0.29503 \ 10^{-2}, 0.27503 \ 10^{-1})$	$(0.36210 \ 10^0, -0.15580 \ 10^-1)$
L	$(0.29503 \ 10^{-2}, \ 0.27503 \ 10^{-1})$	
$g_{2}^{0}$	(0.00700.40=20.07700.40=1)	(0.4444.40=1
$L^{-}$	$(0.29503 \ 10^{-2}, \ 0.27503 \ 10^{-1})$ $(0.36221 \ 10^{0}, \ -0.15738 \ 10^{-1})$	$(0.11444 \ 10^{-1}, \ -0.12269 \ 10^{-2})$
L	$(0.36221 \ 10^{\circ}, -0.15738 \ 10^{-1})$	
$\overset{g_2^1}{L^-}$	$(0.36234.10^{0} - 0.15600.10^{-2})$	$(0.36188 \ 10^{0}, \ -0.15802 \ 10^{-1})$
$\frac{L}{L}$	$ \begin{array}{c} (0.36234 \ 10^{0}, \ 0.15690 \ 10^{-2}) \\ (-0.25738 \ 10^{-2}, \ -0.20460 \ 10^{-2}) \end{array} $	(0.30188 10 , -0.13802 10 )
$g_2^2$	(-0.25756 10 , -0.20400 10 )	
$L^{-}$	$(-0.25738 \ 10^{-2}, \ -0.20460 \ 10^{-2})$	$(0.51071 \ 10^{-2}, \ -0.63342 \ 10^{-2})$
L	$ \begin{array}{cccccccccccccccccccccccccccccccccccc$	,
$g_3^{-3}$		
$L^{-}$	$ \begin{array}{cccccccccccccccccccccccccccccccccccc$	$(0.30303 \ 10^{-4}, \ 0.17632 \ 10^{-3})$
$L_{-2}$	$(-0.20438 \ 10-2, \ -0.25343 \ 10^{-2})$	
$g_3^{-2}$	( 0.204444 10=2	(0.00000.10=20.00001.10=2)
$L^-$	$ \frac{(-0.204444 \ 10^{-2}, \ -0.25343 \ 10^{-2})}{(0.36187 \ 10^{0}, \ -0.15507 \ 10^{-1})} $	$(0.89950 \ 10^{-2}, \ 0.69581 \ 10^{-2})$
$g_3^{-1}$	$(0.30167 \ 10^{-}, -0.13307 \ 10^{-2})$	
$U_{L^{-}}^{g_3}$	$(0.36187 \ 10^{0}, -0.15507 \ 10^{-1})$	$(0.36174 \ 10^{0}, \ -0.15465 \ 10^{-1})$
L	$ \begin{array}{c} (0.36187 \ 10^0, \ -0.15507 \ 10^{-1}) \\ (0.58896 \ 10^{-2}, \ 0.54928 \ 10^{-1}) \end{array} $	(0.002.110 , 0.10100 10 )
$g_3^0$	, , , , , , , , , , , , , , , , , , , ,	
$L^{-}$	$(0.49109 \ 10^{-2}, \ 0.45799 \ 10^{-1})$ $(0.36182 \ 10^{0}, \ -0.15796 \ 10^{-1})$	$(0.16002 \ 10^{-1}, \ -0.17144 \ 10^{-2})$
L	$(0.36182 \ 10^{0}, \ -0.15796 \ 10^{-1})$	·
$g_3^1$		
$L^{-}$	$ \begin{array}{cccccccccccccccccccccccccccccccccccc$	$(0.36150 \ 10^0, -0.15764 \ 10^{-1})$
L	$(-0.25345 \ 10^{-2}, \ -0.20434 \ 10^{-2})$	
$g_3^2$	( 0.25255 10-2	(0.71202.10=2 0.00542.10=2)
$L^-$	$ \frac{(-0.25355 \ 10^{-2}, \ -0.20444 \ 10^{-2})}{(0.24840 \ 10^{-5}, \ 0.14433 \ 10^{-4})} $	$(0.71392 \ 10^{-2}, -0.88543 \ 10^{-2})$
$g_3^3$	(0.24040 10 , 0.14433 10 )	
$L^{-}$	$(0.24840 \ 10^{-5}, \ 0.14433 \ 10^{-4})$	$(-0.30300 \ 10^{-4}, \ -0.17626 \ 10^{-3})$

observed when  $|m| \neq 1$ . Another step is therefore required to achieve our goal.

#### VII.4.4 Final Generalization

We are now going to proceed to the final generalization in the context of this book (for more elaborated developments, see the related complement at the end of this chapter). Clues to achieve the goal are as follows. Although the discrepancy between so-called rigorous and approximate values can be dramatic at the present stage when  $|m| \neq 1$ , the first relation in (VII.47) is satisfied, i.e. BSCs  $\tilde{g}_{n,TM}^{m,old}$  and  $\tilde{g}_{n,TE}^{m,old}$ ,  $|m| \neq 1$  tend to 0 when the axis location case is approached, as they should. Furthermore, when symmetries are observed for the exact BSCs  $g_n^m$ , they are also observed for the approximations of Rels (VII.45)-(VII.46), as extensively discussed in Gouesbet *et al* [378]. These facts suggest that the localized approximation in section VII.4.3 is not in deep error. Very likely, normation prefactors are simply lacking. We may therefore tentatively conjecture:

$$\begin{pmatrix} \tilde{g}_{n,TM}^{m} \\ \tilde{g}_{n,TE}^{m} \end{pmatrix} = \begin{pmatrix} Z_{n,TM}^{m} \\ Z_{n,TE}^{m} \end{pmatrix} \begin{pmatrix} \tilde{g}_{n,TM}^{m,old} \\ \tilde{g}_{n,TE}^{m,old} \end{pmatrix}$$
(VII.48)

Then, we may determine the normation prefactors  $Z_n^m$  as empirical coefficients, relying on numerical experiments. Because the normation prefactors are expected to be complex numbers, we set:

$$Z_n^m = R_n^m \Phi_n^m \tag{VII.49}$$

in which subscripts TM and TE have been omitted,  $R_n^m$ 's are real numbers and  $\Phi_n^m$ 's are phase terms reading as:

$$\Phi_n^m = \exp[i\varphi_n^m] \tag{VII.50}$$

It is also conjectured that the normation prefactors  $Z_n^m$  only depend on n and m, i.e.  $Z_n^m = Z(n,m)$ , at least within a good accuracy. The conjecture has been numerically checked in an extensive way in Gouesbet  $et\ al\ 371$  which also provides expressions for the normation prefactors according to:

$$R_{n,TM}^0 = R_{n,TE}^0 = R_n^0 = \frac{2n(n+1)}{(2n+1)}$$
 (VII.51)

$$R_{n,TM}^m = R_{n,TE}^m = R_n^m = \left[\frac{2}{2n+1}\right]^{|m|-1}, |m| \ge 1$$
 (VII.52)

$$\Phi_{n,TM}^{m} = \Phi_{n,TE}^{m} = \Phi_{n}^{m} = i (-i)^{|m|}, \quad \forall m$$
 (VII.53)

For |m| = 1, these expressions yield:

$$Z_{n,TM}^1 = Z_{n,TM}^{-1} = Z_{n,TE}^1 = Z_{n,TE}^{-1} = 1 \tag{VII.54} \label{eq:VII.54}$$

as they should since the 'old' localized approximation worked perfectly well for the BSCs  $g_n^m$ , |m| = 1. Extensive numerical results and discussions in Gouesbet *et al* [371] show that the localized approximation so obtained is very satisfactory.

## VII.4.5 Improved Formulation and Routines

After Gouesbet et al [371], it has been shown that the formulation given in the previous subsection could be improved for the sake of numerical efficiency. The improvements do not involve any physics, but only mathematical manipulations. Therefore, we shall be content in providing the obtained expressions as established in Ren et al [379]. We have:

$$\begin{pmatrix} \tilde{g}_{n,TM}^{m} \\ \tilde{g}_{n,TE}^{m} \end{pmatrix} = \frac{1}{2(1+2iz_{0}^{+})} \exp\left[\frac{iz_{0}^{+}}{s^{2}} - \frac{x_{0}^{+2} + y_{0}^{+2}}{1+2iz_{0}^{+}}\right]$$
(VII.55)
$$\exp\left[-\frac{(n+1/2)^{2}s^{2}}{1+2iz_{0}^{+}}\right] R_{n}^{m}(-i)^{|m|} \begin{bmatrix} iF_{n,TM}^{m} \\ F_{n,TE}^{m} \end{bmatrix}$$

in which  $x_0^+, y_0^+, z_0^+$  are dimensionless  $x_0, y_0, z_0$  (Rel (V.85)), s is the beam shape factor,  $R_n^m$  are given by Rels (VII.51)-(VII.52) and the  $F_n^m$ 's read as:

$$\begin{bmatrix} F_{n,TM}^{0} \\ F_{n,TE}^{0} \end{bmatrix} = \begin{bmatrix} 2x_{0}^{+} \\ 2iy_{0}^{+} \end{bmatrix} \sum_{j=0}^{\infty} a^{2j+1} \frac{X_{-}^{j} X_{+}^{j}}{j!(j+1)!}$$
(VII.56)

$$\begin{bmatrix} F_{n,TM}^{m} \\ F_{n,TE}^{m} \end{bmatrix} = a^{m-1} \frac{X_{-}^{m-1}}{(m-1)!} + \sum_{j=m}^{\infty} a^{2j-m+1} \frac{X_{-}^{j} X_{+}^{j-m}}{j!(j-m)!} \begin{bmatrix} \frac{X_{+}}{j-m+1} + \frac{X_{-}}{j+1} \\ \frac{X_{+}}{j-m+1} - \frac{X_{-}^{j}}{j+1} \end{bmatrix}, m > 0$$
(VII.57)

$$\begin{bmatrix} F_{n,TM}^{-|m|} \\ -F_{n,TE}^{-|m|} \end{bmatrix} = a^{|m|-1} \frac{X_{+}^{|m|-1}}{(|m|-1)!} + \sum_{j=|m|}^{\infty} a^{2j-|m|+1} \frac{X_{-}^{j-|m|} X_{+}^{j}}{j!(j-|m|)!} \begin{bmatrix} \frac{X_{-}}{j-|m|+1} + \frac{X_{+}}{j+1} \\ \frac{X_{-}}{j-|m|+1} - \frac{X_{+}}{j+1} \end{bmatrix}, m < 0$$
(VII.58)

in which:

$$a = \frac{(n+1/2)s}{1+2iz_0^+}$$
 (VII.59)

$$X_{-} = x_{0}^{+} - iy_{0}^{+} \tag{VII.60}$$

$$X_{+} = x_{0}^{+} + iy_{0}^{+} \tag{VII.61}$$

These expressions are implemented in the routine GNMF given in the website connected to this book. Let us also note that, although the above algorithm is very efficient, it is possible to be still more efficient [157].

## VII.4.6 Examples of Results

We now present exemplifying numerical results for the BSCs  $g_n^m$  computed by four different methods:

- (i) approach by a double quadrature, GNM, section IV.3,
- (ii) approach by a triple quadrature, GNMG4R, section IV.3,
- (iii) finite series (programs GNMSF), sections V.4.1 and V.4.2,
- (iv) localized approximation (program GNMF).

All the programs are written in FORTRAN and run on a Sun station 4/60 (Sparcstation). The Gauss-Legendre quadrature method is used because it is easily available from numerical recipes. More efficient integration codes could however be used. We consider a beam with wavelength  $\lambda=0.5145~\mu\mathrm{m}$ , and a waist radius  $w_0=10\mu m$ .

Results are given in Tables VII.7 and VII.8. We use  $x_0 = 5 \,\mu m$  and  $y_0 = z_0 = 0$ . The number of integration points for  $\varphi$  is 100 while the number of integration points in  $\theta$  is of 100 for n = 1, 200 for n = 5, 300 for n = 10, and in kr of 500 points by interval of 200. Table VII.9 presents the computation times corresponding to Tables VII.7 and VII.8. The computational advantage of the localized approximation and of the finite series with respect to quadratures is obvious. As previously mentioned, the fastest method is the localized approximation. Other comparisons may be found in the quoted literature, all of them confirming this statement. The computation time comparisons between localized approximation and finite series may be found to be not impressive, but it is significant. Because the advantage of the localized approximation with respect to the finite series increases when n increases, the reader might correctly infer that the comparisons would become much more impressive if computation times were compared for the computation of series such as those required for scattering diagrams.

# VII.5 Complement on the Localized Approximation

The bulk of the chapter introduced the localized approximation in a heuristic way, and a validation by comparing localized approximation values and other values obtained from so-called rigorous methods. This is certainly the best way to introduce the localized approximation to a newcomer and, furthermore, it corresponds indeed to the chronological development of the story. Let us recall briefly the beginning of this story before proceeding further. The

**Table VII.7.** Comparison between BSCs  $g_n^m$  computed by double and triple quadratures

Method	triple quadratures	double quadratures	
code name	GNMF2	GNMF1	
m=0	$(2.2 \ 10^{-18}, \ 6.377 \ 10^{-3})$	<u>-</u>	
$n=1,  m=0 \\ m=1$	$(3.894 \ 10^{-1}, \ 4.3 \ 10^{-17})$	$(3.875 \ 10^{-1}, \ 4.2 \ 10^{-18})$	
m=0	$(7.2 \ 10^{-18}, \ 9.552 \ 10^{-2})$	_	
m=1	$(3.889 \ 10^{-1}, \ 4.8 \ 10^{-17})$	_	
n=5, m=2	$(4.7 \ 10^{-18}, -1.592 \ 10^{-3})$	_	
m=5	$(4.559 \ 10^{-12}, \ 2.4 \ 10^{-20})$	_	
m=0	$(5.9 \ 10^{-17}, \ 3.486 \ 10^{-1})$	_	
n=10, m=1	$(3.876 \ 10^{-1}, \ 9.3 \ 10^{-17})$	$(3.747 \ 10^{-1}, -2.3 \ 10^{-17})$	
m=5	$(4.536 \ 10^{-12}, \ 2.0 \ 10^{-21})$	_	

**Table VII.8.** Comparison between BSCs  $g_n^m$  computed by finite series and by using the localized approximation

Method	finite series	localized approximation	
code name	GNMSF	GNML	
n=1, $m=0$	$(0, 6.376 \ 10^{-3})$	$(0, 6.377 \ 10^{-3})$	
m=1, m=1	$(3.894 \ 10^{-1}, 0)$	$(3.894 \ 10^{-1}, 0)$	
m=0	$(0, 9.549 \ 10^{-2})$	$(0, 9.552 \ 10^{-2})$	
m=1	$(3.889 \ 10^{-1}, \ 0)$	$(3.889 \ 10^{-1}, \ 0)$	
n=5, m=2	$(0, -1.592 \ 10^{-3})$	$(0, -1.592 \ 10^{-3})$	
m=5	$(4.550 \ 10^{-12}, \ 0)$	$(4.559 \ 10^{-12}, \ 0)$	
m=0	$(0, 3.485 \ 10^{-1})$	$(0, 3.486 \ 10^{-1})$	
n=10, m=1	$(3.876 \ 10^{-1}, \ 0)$	$(3.876 \ 10^{-1}, \ 0)$	
m=5	$(4.527 \ 10^{-12}, \ 0)$	$(4.536 \ 10^{-12}, \ 0)$	

**Table VII.9.** Computation time in seconds for the BSCs by four different methods.

		localized interpretation	finite series	quadratures	
				F1	F2
		GNMF	GNMSF	GNMF1	GNMF2
n=1,	m=0			2.7	-
	m=1	_	-	3.0	3131
n=5,	m=0	0.1	0.1	3	-
	m=1	0.1	0.1	3	-
	m=2	0.1	0.1	3	-
	m=5	0.1	0.1	3	-
n=10,	m=0	0.3	0.5	6.7	-
	m=1	0.3	0.5	7.1	6487
	m=5	0.3	0.5	6.7	-

localized approximation was introduced in 1986 by Gréhan et al 78, betting on the validity of a generalization of the principle of localization of Van de Hulst, in an on-axis case. Validations were provided by comparing scattering diagrams obtained from the on-axis localized GLMT and those obtained using a Rayleigh-Gans approximation for Gaussian illumination, by invoking comparisons with other theoretical results (from Tsai and Pogorzelski 62, and from Yeh et al [67], and by discussing an experimental scattering diagram obtained from a spherical particle optically levitated 57. In 1987, evaluations of beam shape coefficients by quadratures were available and favorable comparisons between quadrature values (so-called exact values) and localized values could be published 81. Similar results are reported in 82, with furthermore a complementary interpretation of optical levitation experiments in forward direction relying on diffraction theory. The on-axis localized approximation was at this time developed enough to allow systematic computations in the framework of the localized on-axis GLMT [83], [84]. In parallel, finite series became available for the on-axis case [87] and for the off-axis case [367]. In Gouesbet et al [87], beam shape coefficients for the on-axis case (Gaussian beams) could then be evaluated by using three methods (quadratures, finite series, localized approximation). The three methods (two of them were so-called rigorous methods) are compared and discussed. This article was the first one in which we introduced finite series. Comparisons between the results obtained permitted a new confirmation of the validity of the localized approximation, with a degree of accuracy that had not been reached up before. The previous articles are dated 1988, the year when the pivot article 2 and his companion article 89 appeared. But the localized approximation was not yet ready to handle arbitrary location of the scatterer in a Gaussian beam (and a fortiori in an arbitrary beam). Notwithstanding an article physically discussing the concept of ray localization in Gaussian beams [372], a first attempt to design a localized approximation to the computation of the general beam shape coefficients  $g_{n,X}^m$ , X = TM, TE, appeared in 1989 [378], completed one year later by publishing a localized approximation allowing one to evaluate all beam shape coefficients  $g_{n,X}^m$  [371]. A faster algorithm to implement the localized approximation has been afterward introduced by Ren et al 379. An alternative compact formulation of the localized approximation, optimal for numerical computations, in terms of either Bessel functions or modified Bessel functions, is introduced by Lock [157]. The localization process (localized approximation or integral localized approximation) has also been applied for other kinds of beams, namely laser sheets [292], [294], [135], top-hat beams [296], [297], and doughnut beams [135]. The localized approximation for laser sheets has been used for the evaluation of a laser-sheet based optical technique [293].

Up to now, the localized approximation had been heuristically and/or empirically introduced, with various kinds of validations to assess its quality, but no rigorous justification for it was available. In an appendix to an article devoted to higher-order rainbows and to the computer implementation of the

GLMT 127, Lock, in 1993, proposed a rigorous justification of the localized approximation for an on-axis Gaussian beam, by using a stationary-phase argument, analogous to the one used by Van de Hulst to derive its localization principle, associating a geometrical light ray with the small group of partial waves for which the phase is stationary. However, this technique failed in the case of off-axis illumination, for a reason which has not been satisfactorily clarified since then. Nevertheless, a rigorous justification, relying on the use of Davis beams, and Taylor series, has been afterward uncovered, for both on-axis and off-axis Gaussian beams [79], [80]. These articles also introduced a declension of Davis beams into various types (mathematically conservative version, L-type radial fields, Barton symmetrized version of the Davis fields), the terminology of localized beam model, a replacement of the localized approximation by a modified localized approximation (very close however to the original localized approximation), and introduced the concept of standard beams which received more developments thereafter. Indeed, Gouesbet 311, discussing higher-order descriptions of Gaussian beams, considered the standard beams, as well as the localized beams generated by the localized approximation, and by the modified localized approximation. These three beam descriptions (standard, localized and modified localized approximations) are also discussed by Gouesbet 313 dealing with an exact description of arbitrary shaped beams for use in light scattering theories. Improved standard beams with application to reverse radiation pressure are discussed by Polaert et al [314]. A complementary justification of the localized approximation to on-axis and off-axis Gaussian beams is available from Doicu and Wriedt [377].

All the works above were essentially dealing with the case of Gaussian beams in spherical coordinates. Next, concerning circular cylindrical coordinates, in connection with the GLMT for infinitely long circular cylinders, see [209], [210], [211]. For elliptical cylindrical coordinates, in connection with the GLMT for infinitely long elliptical cylinders, see [231], [232], [233], [235]. Let us recall that the design of these localized approximations (localized beam models) for cylinders (circular or elliptical) heavily relies on the theory of distributions.

Up to now, we have been mostly dealing with Gaussian beams. However, let us recall that a localized approximation has been efficiently used for other kinds of beams, namely laser sheets, top-hat beams and doughnut beams, hence the conjecture that the localized approximation could be actually valid for any kind of beams. Indeed, a most important result has been afterward obtained, namely that the localized approximation is valid for spheres illuminated by arbitrary shaped beams (or, let us say, in spherical coordinates) [380], although the quality of the approximation may depend on the beam under consideration. This article introduced another slight modification of the modified localized approximation which is actually a minor correction.

A similar procedure also allowed one to assess the validity of the localized approximations previously developed in circular cylindrical and in elliptical cylindrical coordinates to the case of arbitrary shaped beams [381], [236]. Again, for these cylindrical cases (circular or elliptical), the use of the theory of distributions is close to compulsory. Furthermore, when developing his GLMT for circular cylinders [215], [216], Lock introduced his own localized approximation for this case. It is not yet known whether this localized approximation identifies with the one developed in Rouen but, in any case, in the worst case, both of them should certainly generate again quite decent localized beam models.

# VII.6 Complement on the Evaluation of Beam Shape Coefficients

As we have seen, for a given GLMT (a given shape or configuration), many variants are still possible, depending on the kind of beam illuminating the scatterer. The issue of beam description is an essential ingredient of any GLMT and, in any GLMT, it has been found to be the most difficult subtopic to deal with, the one which always required the most significant efforts. However, not only is the examination of this issue quite necessary for any GLMT, but it is also an issue which can be considered and useful in its own right, independently of any GLMT, each time people have to deal with the description of laser beams, beyond the classical approach of Kogelnik, or of Kogelnik and Li [300], [301], [302], as discussed in [77]. This complement provides additional information and insights concerning the issue of beam descriptions.

Basically, a beam description correctly formatted to produce a GLMT takes the form of expansions of fields over an appropriate basis of functions. The expansion coefficients have been named beam shape coefficients and having an adequate description of the illuminating beam is equivalent to knowing the values of the beam shape coefficients. As we now know, beam shape coefficients can be evaluated by using quadratures, finite series, localized approximations, or by a hybrid method called the integral localized approximation.

But other techniques may be used. Let us for instance consider the GLMT for spheroids for which we need a beam description in spheroidal coordinates. Han and Wu [262], [263] examined the beam shape coefficients for a spheroidal particle illuminated by Gaussian beams. A main result of much interest is that the beam shape coefficients of the Gaussian beam in spheroidal coordinates can be computed in terms of beam shape coefficients in spheroidal coordinates. Beam shape coefficients for arbitrary shaped beams in spheroidal coordinates are also discussed by Han [382]. Xu et al [274] claimed that the localization principle is inapplicable to the case of spheroidal coordinates. What is actually inapplicable is the use of the first "classical" version of the

localized approximation. But there is no specific reason, as far as we can see, why a specific localized approximation could not be designed in spheroidal coordinates. Let us furthermore mention that the possibility of expressing spheroidal beam shape coefficients versus spherical beam shape coefficients provides at least one way, although a bit indirect, to obtain a spheroidal localized approximation versus the spherical localized approximation. The design of a genuine spheroidal localized approximation would however possibly provide closed forms fast-running expressions.

Furthermore, addition theorems may be used to evaluate beam shape coefficients. For instance, an interesting application of a (translational) addition theorem for spherical vector wave functions is to provide relationships between on-axis and off-axis beam shape coefficients, more specifically to express off-axis coefficients versus on-axis coefficients [377], although these on-axis and off-axis coefficients can also be independently evaluated, even in a very economical way, when the localized approximation is used. Han et al [383] provided an approach for expansions of incident arbitrary shaped beams, both in spherical and spheroidal coordinates, using addition theorems for spherical vector wave functions under coordinate rotations. Also, relations between spheroidal and spherical vector wave functions are used. In an article devoted to the expansion of electromagnetic fields of a shaped beam in terms of cylindrical vector wave functions, Zhang et al [384] dealt with beam shape coefficients for the GLMT for cylinders, by using the addition theorem for spherical vector wave functions under coordinate rotations and relations between spherical vector wave functions and cylindrical ones. Soon after, Zhang and Han [385] examined a translational addition theorem for spherical wave functions using relations between cylindrical and spherical vector wave functions. They expressed a translational addition theorem for spherical vector wave functions in an integral form, providing a theoretical procedure for the calculation of beam shape coefficients in GLMT. From these results, the beam shape coefficients in cylindrical or spheroidal coordinates can also be obtained. Relations between cylindrical and spherical vector wave functions are discussed by Han et al [386]. They also discussed the expansion and scattering of cylindrical waves in spherical coordinates using the expansion of cylindrical vector wave functions in terms of spherical ones. This work is typical of a theme aiming to solve the general problem of establishing bridges between descriptions in different coordinate systems.

A last issue to be now discussed again, and refined, concerns the use of terminologies like "rigorous values", "rigorous solutions", "exact values", "exact solutions", and so on, concerning beam shape coefficients, or more generally any GLMT under discussion. The origin of the problem is that we only exceptionally possess beam descriptions which exactly satisfy Maxwell's equations. In other words, the ones of Nieminen et al [387], [388], laser beams in their standard descriptions, are not radiation fields, but only approximations to radiation fields. Then, typically, beam shape coefficients evaluated for such beams will not be constant coefficients, as they should if the original

beam under expansion exactly satisfied Maxwell's equations. Let us recall the existence of artifacts produced in such cases when using quadratures. Under such circumstances, it is (and it has been, starting with some of our original works) an abuse of language to tell that the values of the beam shape coefficients obtained by quadratures provided rigorous or exact values. Any appearance of words like "rigorous" and "exact" should be therefore carefully examined in order to evaluate its significance, such as, to give another example, by Neves et al [389], [390], [391], [392].

Several cases (actually two) may happen, that we are now going to summarize. In the first case, we are really facing an abuse of language like when using quadratures to evaluate beam shape coefficients of a beam which does not satisfy Maxwell's equations. Although this process may provide (usually it did) quite decent values to handle a GLMT, it is basically flawed in utmost rigor. In the second case, there is indeed a sense in which obtained values are rigorous or exact, namely the beam shape coefficients obtained are constant, defining beams which exactly satisfy Maxwell's equations, although the original beams under study did not exactly satisfy Maxwell's equations. In these cases, we have to be well aware of the fact that the process used to evaluate beam shape coefficients actually generates a remodelling of the beam, from a non-Maxwellian structure to a Maxwellian structure. This happens with finite series or plane wave spectra, leading to finite series models or plane wave spectrum models of the beam. A fundamental question to be investigated is then to know whether the beam model obtained possesses properties close enough to the ones which were intended, an issue particularly relevant when we want to deal with very tightly focused beams. This also happens with the localized approximations, leading to localized beam models. But these models have been extensively studied and it has been observed that, at least for Gaussian beams, they anticipate the behavior of higher-order Davis beams.

## VIII

# Applications, and Miscellaneous Issues

Some allusions or brief discussions concerning applications of GLMTs have already been provided (and will not be necessarily repeated here). This chapter, to be viewed as, and written as, a complement, is devoted to a more systematic and exhaustive exposition of such applications. Complementary miscellaneous issues will also be discussed.

#### VIII.0.1 Measurement Techniques

The field of optical particle sizing, and more generally, of optical particle characterization of particles in flows constituted the original motivation for the development of GLMTs. The relevance of GLMTs to this field is confirmed in various textbooks such as by Gouesbet and Gréhan [51], [393], Xu [394], Albrecht et al [395], Doicu et al [396], and in review articles such as by Barth and Sun 397 reviewing the issue of particle size analysis, by Bachalo 398 dealing with experimental methods in multiphase flows, by Black et al [399] reviewing laser-based techniques for particle size measurements, including a discussion of industrial applications, and also of the Gaussian nature of the laser beams used, without forgetting a discussion of GLMT, or a discussion of top-hat beam techniques, by Jones 400, telling us that light scattering has proved to be one of the most powerful techniques for probing the properties of particulate systems, or by Durst 401 who concentrated on the many optical techniques developed for particulate systems and fluid mechanics. Another relevant article is by Ren et al [402]. Several measurement techniques are actually concerned, but the most significant ones are likely to be phase-Doppler techniques.

#### Phase-Doppler instruments

Phase-Doppler Instruments (PDI, or Phase-Doppler Anemometers, PDA) originally allowed one to simultaneously measure velocities and sizes of

individual spherical particles in flows. They result from an extension of Laser Doppler Velocimetry (LDV), introduced by Yeh and Cummins [403], described in many places such as by Drain [404] or by Durst et al [405]. The basic idea of the extension from LDV to PDA is due to Durst and Zaré [406]. A review on experimental methods in multiphase flows takes a bit of time discussing phase-Doppler instruments [398], to be complemented by a more restricted specific review devoted to the phase Doppler method [407]. Another account of phase Doppler configurations, including a discussion on ambiguity trajectory effects, is available from Buchhave and von Benzon [408]. Some calculations in this article are carried out by using GLMT. A history of the development of the phase-Doppler technique is available from Hirleman [409]. A review of the development and characteristics of planar PDA (a particular variant of the original standard set-up) is given by Durst et al [410]. A theoretical model for the method of phase-Doppler sizing is discussed by Zhang Song et al [411].

A (hopefully) pedagogic basic presentation of phase-Doppler instruments is available from Gouesbet and Gréhan [92], here summarized as follows. A control volume is produced by the intersection of two laser beams (originating from the same laser). This control volume contains a set of (ideally) parallel interference fringes. When a particle crosses these fringes, it will produce a signal modulated at a certain frequency depending on the fringe spacing and on the transverse velocity of the particle (i.e. perpendicularly to the fringe system). Then, measuring the modulation frequency using one detector and knowing the value of the fringe spacing, we have a measurement of the transverse velocity component. This is the velocimetry part of the instrument. Next, let us add a second detector. Each detector will receive a modulated signal but, due to the different locations of the detectors, one signal is delayed with respect to the other. The phase difference (usually simply called the phase) between the two signals allows one to measure the diameter of the particle, assumed to be spherical. This is the sizing part of the instrument. The set-up configuration so described corresponds to what is often called the standard instrument.

In earlier works, theories predicting the relationship  $\phi(d)$  between the phase  $\phi$  and the diameter d assumed uniform illumination of the particle, and a dominant scattering mode (reflection or refraction) in the collecting direction. These assumptions lead to linear functions  $\phi(d)$ , easy to interpret (within  $2\pi$  phase ambiguities), which furthermore do not depend on the amount of light illumination. This was however too simple and the story became more complicated after 1988 [412] because of the discovery of the Trajectory Ambiguity Effect, TAE, (also named trajectory ambiguity defect, Gaussian beam effect, Gaussian beam defect and other variants).

In phase-Doppler instruments, the transverse characteristic dimension of the illuminating (Gaussian) beam is finite, of the order of the beam waist radius  $w_0$ . If the size of the scatterer is not small with respect to  $w_0$ , then the aforementioned assumption of uniform illumination fails, and extra-effects have to be forecast. Indeed, it then happens that the phase (difference)  $\phi$  becomes dependent on the location of the scatterer within the control volume: this is the TAE. The existence of the TAE was first recognized by Bachalo and Sankar 412, relying on a geometric optics approach.

With the TAE, it was a dogma which crashed down and the announcement was poorly received. Nevertheless, eventually, the existence of TAE was confirmed in the rigorous electromagnetic framework of GLMT by Gréhan et al 3. Computations were performed for a commercial phase Doppler system and various schemes for elimination of the TAE were examined. It was put forward that the errors due to particle trajectories could be eliminated satisfactorily by employing an additional receiving unit, which allows one to detect the asymmetry of the scattered light pattern due to displacement of the particle trajectory from the centre of the measuring volume. A preliminary experimental evaluation of this extended technique is presented and discussed. GLMT is thereafter used again to examine trajectory ambiguities in phase-Doppler systems, for a near-forward and a near-backward geometries 4. Remedies to the disease are discussed, and the extended technique previously introduced is revisited. TAE is discussed by Durst et al [410], with many GLMT simulations used to illustrate TAE and other issues. A very comprehensive article dealing with the implications of the Gaussian intensity distribution of laser beams on the performance of the phase Doppler technique, particularly with sizing uncertainties, is available from Hardalupas and Liu [413]. Lehmann and Schombacher [414] discussed the features of a combined FFT and Hilbert transform for phase Doppler signal processing, including validation strategies to reduce the influence of maltriggered bursts and Gaussian beam effects on measurement results. Also, a device using superimposed noninterfering probes to extend the capabilities of phase Doppler anemometry, relevant to the issue of trajectory effects, is proposed by Onofri  $et \ al \ 415$ .

Although the TAE is a defect, it has been turned to an useful effect when a technique named the dual burst technique has been introduced by Onofri et al 416. In this technique, the set-up is designed (by reducing the beam waist diameter when compared with typical values of the standard set-up) in such a way that two Doppler bursts generated by the same particle crossing the control volume are emitted toward the detectors, one associated with reflection, and the other with refraction, each of these bursts probing different properties. Indeed, only the refracted light is influenced by the material properties of the particle. The phase of the refracted light from a particle depends on the optical set-up, the particle size and the particle refractive index. The phase of the reflected light however depends only on the optical set-up and on the particle size, but does not depend on the particle refractive index. From the reflected burst, the particle diameter can be deduced. Then, knowing the diameter and the optical parameters of the phase-Doppler set-up, the particle refractive index can be determined from the phase of the refracted burst. Furthermore, the intensity ratio of the two bursts can be used for absorption measurements. Simulations based on GLMT and experimental tests using monodispersed droplets of different refractive indices and absorption coefficients have validated this technique. The dual-burst technique is also used by Onofri et al [417] for simultaneous velocity, size, and concentration in suspension measurements of spherical droplets and cylindrical jets. Furthermore, three ways to eliminate particle trajectory effects on the concentration measurements of spherical particles are proposed.

Phase-Doppler instruments were originally designed for spherical particles. However, relying on the GLMT for multilayered spheres 173, the application of phase-Doppler anemometry to multilayered spheres is discussed by Onofri et al [418]. In particular, its specification to phase-Doppler anemometry for the case of water-coated carbon spheres has been considered by using focused laser beams, therefore extending the principle of the dual burst technique. Information on the core and outer particle diameters are shown to be retrievable by carefully analyzing the temporal structure of individual phase-Doppler signals. Also, the influence of refractive index profiles inside droplets, induced by temperature and pressure stresses, on PDA phase-diameter relationships, was investigated. The measurement of cylindrical particles with phase Doppler anemometry is considered by Mignon et al [419]. Although the formalism of the GLMT for cylinders was already well developed, it was not yet computationally implemented, so that this study by Mignon et al relied on geometrical optics. A first application of GLMT for cylinders, however restricted to the use of  $O(s^2)$  Gaussian beams, is available from Gauchet et al 420. GLMT for non-spherical particles with applications to phase-Doppler anemometry is discussed by Doicu et al 421, although the correctness of the used terminology of GLMT may be problematic, in so far as there is no GLMT able to deal with arbitrary shapes of particles. Nevertheless many GLMT ingredients are used in the article, and the applications to PDA concerned spheroidal particles. The response of PDA systems to nonspherical droplets is investigated by Damaschke et al [422]. A discussion concerning optical techniques for the characterization of nonspherical and nonhomogeneous particles is available from Damaschke et al [423]. Size measurements of moving glass fibers using phase Doppler anemometry with theoretical modelling for a tilted cylinder interacting with focused laser beams are discussed by Mignon et al [424]. The feasibility to build an interferometric optical instrument for in-situ measurement of fiber diameter has been demonstrated theoretically and the results have been validated experimentally. On-line sizing of small diameter glass fibers by interferometric phase-Doppler sizing is discussed by Onofri et al 425.

One of the difficulties in using phase-Doppler instruments may be the limitation of the optical access to the system under study, with an illuminating unit and a receiving unit spreading more or less over  $180^{\circ}$ , requiring configurations which are not always feasible under industrial and/or hostile conditions. Therefore, there must be an interest devoted to other optical configurations with a backward collection. As a consequence of such

requirements, Bultynck et al [426] examined the use of a miniature monoblock backward phase-Doppler unit, relying on numerical situations carried out by using the GLMT, a concept validated by experimental tests. A similar commitment is achieved by Blondel et al who dealt with compact monoblock configurations too [427]. Optical particle sizing in backscatter is examined by Damaschke et al [156], with theoretical calculations carried out by using FLMT, plus a discussion on trajectory ambiguity effects. Later on, Wu et al [428] dealt with the sizing of irregular particles using a near backscattered laser Doppler system.

The issue of phase errors in phase-Doppler anemometry, and in particular of TAE, has also been examined by Albrecht et al 429, 430 in a two-part article. As a theoretical tool, they used a method of extended geometrical optics which is based on geometrical optics by including the amplitude and the phase distribution in the laser beam. Phase errors caused by Gaussianbeam intensity distribution and the curvature of the wave fronts beyond the beam waist can be calculated. The influence of the particle trajectories on measured phase and mass concentration is simulated for both reflective and refractive modes of operation. The same issue is treated again by Albrecht et al 152, using both the Fourier LMT (FLMT) and the extended geometrical optics. Yokoi et al [431] provided an estimation of particle trajectory effects and discussed their reduction using polarization, both theoretically (relying on geometrical optics and on GLMT) and experimentally. They investigated a method for reducing the trajectory effect using the separation of reflected and refracted rays on the basis of polarization properties. Later on, the same authors proposed an unidirectional phase-Doppler method for sizing moving spherical particles on the basis of the phase difference between two polarized Doppler beat signals in a single scattering direction [432]. They again performed an analysis based both on geometrical optics and GLMT, and carried out experiments. Complementary studies concerning trajectorydependent scattering errors are also available from Strakey et al [433], [434].

Qiu and Hsu [435] introduced a new PDA-like concept to improve the accuracy of sizing large particles in two-phase flows. This method uses a photodetector array to measure directly the spatial frequency of the light intensity scattered from a spherical particle in the measurement volume. The effect of both the reflected and refracted rays are considered. GLMT-simulations are used. Qiu and Jia [436] introduced an optimized optical orientation angle by taking two scattering mechanisms into consideration, providing high accuracy and avoiding the measurement-volume effect (trajectory ambiguity effect and a slit effect) in sizing large particles (as large as  $1200~\mu m$ ). The performance of the method was simulated by using the GLMT and validated by experiments. The effect of refractive index in optical particle sizing using a PDA-like system with a spatial frequency method is examined by Qiu and Jia [437]. GLMT was again used for simulations. Qiu [438] discussed the elimination of high-order scattering effects in optical microbubble sizing, with a model which relaxes the assumption of a single-scattering mechanism used in

a conventional (standard) PDA-system. Simulations relied on GLMT. Next, the impact of high order refraction on optical microbubble sizing in multiphase flows, by using phase Doppler anemometry, is further investigated, both theoretically (with GLMT) and experimentally, by Qiu and Hsu 439. As a result, an optimization method for accurately sizing air bubbles in water is suggested. The measurement-volume effect (including both the trajectory ambiguity effect and a slit effect) is effectively eliminated using a four-detector PDA system.

Other works are as follows. Von Benzon and Buchhave 440 were concerned with phase-Doppler measurements of very small particles, essentially using LMT but using also GLMT for verification of LMT results. Sankar et al 441 dealt with coherent scattering by multiple particles in phase Doppler interferometry. In this article, like in other articles by the same team, it is stated that, with the geometrical optics, the Gaussian beam illumination of the incident laser beam can be accounted for more efficiently than with the GLMT. It is certainly true that main features of PDA can be examined with geometrical optics. But, for many well known reasons and limitations of geometrical optics (rainbow, glory, extinction paradox, MDRs...) a rigorous theory, when available, is in our mind to be preferred. The invoked lack of efficiency of the GLMT is a subjective statement. It may refer to the mathematical complexity of the theory, but at least one of us finds geometrical optics more complicated than GLMT and, in any case, boring. It may refer to computer programming difficulties but, as soon as well tested computer programs are available, such difficulties vanish in the blue. For a comparison between geometrical optics and wave theory, see Ungut et al [442].

Schaub et al 443 produced a theoretical analysis of the effects of particle trajectory and structural resonances on the performance of a phase-Doppler analyzer. The phase-Doppler model is based on the so-called arbitrary beam theory (actually equivalent to GLMT). Particle trajectory effects are examined. Gupta and Avedisian 444 used phase-Doppler anemometry to investigate the role of combustion on droplet transport in pressure atomized spray flames, taking care of the TAE. Willman et al 445 examined the possibility of phase-Doppler sizing with off-axis angles in Alexander's darkband. They found that an Alexander's darkband configuration is extremely insensitive to Gaussian beam defects. They used a geometrical optics computer program which is however validated by GLMT-computations. Saumweber et al [446] dealt with simultaneous droplet size and gas-phase turbulence measurements in a spray flow using phase-Doppler interferometry. Dahl and Wriedt 447 dealt with the simulation of PDA using the multiple multipole method. Jiang 448 used phase maps to optimize phase Doppler particle-sizing systems. Schaub  $et \ al \ 449$  dealt with the development of a generalized theoretical model for the response of a phase/Doppler measurement system to arbitrarily oriented fibers illuminated by Gaussian beams. Schaub et al [450] discussed a design of a phase/Doppler light-scattering system for measurement of smalldiameter glass fibers during manufacturing. Yu and Rasmuson 451 discussed the projected area of measurement volume in phase-Doppler anemometry and application for velocity bias correction and particle concentration estimation. Wigley et al [452] achieved an experimental analysis of the response of a phase Doppler anemometer to a partially atomized spray, in particular discussing the issues of Gaussian beam effects and sphericity checks. Widman et al [453] are concerned with the identification of burst splitting events in phase Doppler interferometry measurements. Like trajectory-dependent errors due to the Gaussian intensity profile of the laser beam, a burst splitting event, in which noisy environments results in a single droplet being counted as multiple droplets, can spoil the accuracy of recorded data. Widman et al [454] dealt with the improvement of phase Doppler volume flux measurements in low data rate applications. This is a significant issue in PDA because accurate volume flux measurements are more difficult to obtain than size or velocity measurements. Widmann [455] dealt with phase Doppler interferometry measurements in water sprays produced by residential fire sprinklers.

Bergenblock et al [456] dealt with the experimental estimation of particle flow fluctuations in dense unsteady two-phase flow using phase Doppler anemometry, with a discussion of trajectory, slit, burst splitting, perturbation of fringes effects. Hespel et al [457] provided a geometrical optics- and GLMT-based numerical study of the use of glare spots in phase Doppler anemometry. In this system, two large laser beams are used, and the images of the particle formed by the reflected and refracted lights are separated in space. Each detector generates a signal composed of two separate parts, one due to reflection and the other to refraction. The configuration is designed in such a way as to avoid the sensitivity of the instrument to the wave front curvature of the laser beam. The GLMT-based approach incorporates GLMT as an ingredient but, more generally, is constituted by an electromagnetic model allowing one to calculate images. This introduces us to the theme of imaging to which we are going to turn presently.

But, before that, let us just mention the existence of an alternative to PDA, named the dual-cylindrical wave laser technique, discussed by Naqwi et al [291], by Naqwi and Durst [319], and GLMT-analyzed by Gréhan et al [293].

#### Imaging

Imaging is a much interesting field in which the relevance of GLMTs may be significant: how images are formed? Which kind of information can be retrieved from the images, and how? This issue has been attacked, in a GLMT framework, by Ren et al [458] dealing with the measurements of particles by imaging methods. A basic theoretical and simulation scheme is established as follows (i) the light scattering and propagation from the particle to the input plane of a lens is computed by using a light scattering theory (e.g. LMT or GLMT), in a general situation where the incident beam is not necessarily aligned with the beam axis (ii) the propagation of the light from the input

plane to the output plane of the lens (assumed to be a perfect phase lens) is described by a lens transform, introducing only a phase shift and (iii) the propagation of the light from the output plane of the lens to the image plane is computed using a Huygens-Fresnel integral. Many exemplifying results are provided and discussed, including the case of stereoscopic geometries as used in Particle Image Velocimetry (PIV, more to come on this technique). An effective experimental set-up implementing theoretical features previously simulated, and leading to satisfactory results, is discussed. A further study of the same scheme is available from Girasole et al [459], with two exemplifying cases (i) interferometric sizing at large off-axis angles and (ii) imaging in near forward directions, relevant to Shadow Doppler Velocimetry (SDV).

SDV is a technique, based on coherent near-forward off-axis imaging of particles, allowing one to measure the velocity and size of non-spherical and optically non-homogeneous particles, also providing shape information, e.g. Hardalupas et al [460] Maeda et al [461], or Morikita and Taylor [462]. A theoretical evaluation of a shadow Doppler velocimeter, relying on a near forward off-axis imaging of particles, is achieved by Ren et al [463]. In this case, the spherical particle is illuminated by two continuous laser beams and the imaging process previously discussed [458] (with only one beam) has to be (slightly) extended. Independently of SDV, Zinin et al [464] dealt with Fourier optics analysis of spherical particles image formation in reflection acoustic microscopy.

For imaging techniques relevant to PIV, we start with Moreno et al [321] who discussed particle positioning from charge-coupled device (CCD) images by GLMT and carried out comparisons with experiments. In this study, real-time CCD cameras are used to extract 3D position and velocity information by direct analysis of the diffraction patterns of seeding particles in imaging velocimetry. The particle is assumed to be illuminated by Gaussian light beams, light sheets, or a plane light wave, and aberration effects are included. The particular interest of the light sheet is that it corresponds to the usual kind of illumination in conventional PIV. Micrometer-sized particle diffraction images have been quantitatively (and favorably) compared with experimental data. The same topic (particle positioning from CCD images, experiments and comparison with the GLMT) is considered by Guerrero etal 322 and Guerrero-Viramontes 465. See also Funes-Gallanzi et al 466 dealing with the same topic too, but using LMT rather than GLMT. They observed however that the experimental results using classical LMT treatment proved insufficient to provide high accuracy 3D particle positioning so that the algorithm used had to be extended to use a GLMT approach (as reported elsewhere, see above). Relevant to the topic of positioning is also a work by Guerrero et al 467 discussing the case of a spherical wave front including a comparison to experimental data. Scattering light from a spherical particle located on-axis to an electromagnetic spherical wave is numerically predicted using GLMT. Comparisons are made with LMT, and with experimental in-line Fraunhofer holograms of spherical particles, showing good agreement. Another study relevant to PIV is by Ilic *et al* [323] who carried out GLMT-based simulations of laser sheet scattering by microparticles for the case of numerous random spatial distributions of scattering particles.

#### Rainbow and rainbow refractometry

GLMT may be used to study the properties of the rainbow in the case of nonplane-wave illumination. Already cited relevant articles are by Lock 127, Wu et al [175], Adler et al [240], Méès et al [212], Guo and Wu [226], Adler et al [227], Méès et al [346], Han et al [264], Wu and Li [230] and Bakic et al 154. Also, rainbow scattering by a coated sphere is discussed by Lock et al 468. A further article is by Han et al 469 reporting on the study of the behavior of interferences between geometrical rays and surface waves. Such interferences are studied in a GLMT framework, supplemented with a Deby series analysis. Scattering diagrams in the rainbow region and associated FFT spectra (exhibiting Airy frequency, ripple structure, and surface waves, interferences...) are calculated and discussed. A complementary experimental study shows very good agreement between calculated and recorded scattering diagrams and spectra. It is concluded that it is possible to measure the contributions of surface waves associated with rainbow FFT spectra. A proposal is made, according to which the contribution of surface waves in rainbow FFT spectra could allow one to quantify very small variations of the surface of a liquid jet. As a matter of fact, at that time, Han et al 470 already succeeded to characterize initial disturbances (and their exponential growth) in liquid jet by rainbow sizing.

Concerning rainbow refractometry, the use of GLMT is usually not required, or not useful, due to the fact that the size of the illuminating beam is large enough so that LMT is sufficient. Nevertheless, van Beeck and Riethmuller [471], discussing the rainbow phenomena applied to the measurement of droplet size and velocity and to the detection of nonsphericity, used GLMT to emphasize the fact that the optical interference structures of the rainbow can be influenced by the Gaussian intensity distribution of the laser beam that illuminates the droplet under study. They concluded that Gaussian illumination influences the rainbow spectrum considerably and has to be taken into account when identifying peaks in the spectrum of the rainbow. Also, van Beeck and Riethmuller 363, discussing rainbow interferometry with wire diffraction for simultaneous measurement of droplet temperature, size and velocity, used GLMT to simulate a photomultiplier signal. Wilms and Weigand 472 dealt with composition measurements of binary mixture droplets by rainbow refractometry, referring to previous works by Han et al [264], and by Saengkaew et al [473]. Another article by Wilms et al [474] dealt with global rainbow refractometry with a selective imaging method, aiming to minimize measurement errors due to non-sphericity.

#### Miscellaneous measurement techniques

Bemer et al [475] dealt with the calculation of the theoretical response of an optical particle counter. Hesselbacher et al 476 considered a droplet sizing method relying on the evaluation of a fringe spacing of scattered light in the forward direction. They carried out an experimental investigation of Gaussian beam effects associated with this method. Glare points and practical use of glare points are discussed by van de Hulst and Wang 477. Li et al 478 discussed Fizeau digital interferometry with a diffraction-generated spherical wave for testing focusing optics. In this study, they dealt with the diffraction from a spherical particle with a size of several wavelengths or more, using the diffraction theory to describe the far-field distribution of the diffracted light, a theory also discussed in connection with GLMT validations 44. Doornbos et al 479 found that flow cytometric measurements of light scattering of polystyrene calibration beads revealed remarkable Lissajouslike loops in two-parameter scatter plots. Theoretical simulations relied on the implementation of the GLMT. Another complementary article devoted to the Lissajous-like patterns, still using GLMT, is available from Hoekstra et al [480]. Doornbos et al [481] dealt with elastic light-scattering measurements of single biological cells in an optical trap. They however used small enough particles (one twentieth of the beam diameter) to avoid the use of GLMT. Anders et al [482] introduced a new technique for investigating phase transition processes of optically levitated supercooled droplets consisting of water and sulfuric acid, with theoretical computations relying on GLMT. Concerning phase transition, we also have to cite Trunk et al [483] who investigated a phase transition in a single optically levitated microdroplet by Raman-Mie scattering. Min and Gomez 484 discussed high-resolution size measurement of single spherical particles with a fast Fourier transform of the angular scattering intensity. This technique entails imaging the angular scattering intensity onto a photodiode array and applying a fast Fourier transform to the array output to obtain a frequency and phase corresponding to the number and angular position of the scattering lobes. GLMT is used for theoretical analysis. Wang et al 485 discussed measurements of fluidflow-velocity profiles in turbid media by the use of optical Doppler tomography, indicating that the implementation of GLMT into the analysis should give a more realistic and accurate understanding of the technique. Rambert et al 486 dealt with a laboratory study of fungal spore movement using laser Doppler velocimetry, and pointed out the interest of phase Doppler instruments to cylindrical particles (relevant to GLMT for cylinders), for the study of a number of fungal spores. Ovod et al [487] discussed a modified conventional plane-wave scattering approach to be used for the rapid engineering simulation of the influence of the main instrumental parameters of a laser particle-size analyzer on its response function and other main performance characteristics. The correctness of this modified technique is confirmed experimentally and theoretically by comparison with the exact GLMT. Steiner et al [488] discussed a fast in situ sizing technique for single levitated liquid aerosols, making use of the analysis of fast-Fourier-transformed vertically polarized Mie scattering patterns from single liquid aerosols levitated in a Paul-trap-type electrodynamic balance. Allersma et al [489] dealt with a technique to detect the displacement of micron-sized optically trapped particles, relying on a simple theoretical model capturing essential features, although GLMT could be used instead. Godefroy and Adjouadi [490] dealt with particle sizing, under focused Gaussian beam illumination, in a flow environment, using light scattering patterns.

In the same mood, we may refer to flow cytometry which is a technique for counting, characterizing, and sorting microscopic particles in a flow. The characterization of particles in a cytometer under laser illumination may rely on the use of GLMT, e.g. Neukammer et al [279], Doornbos et al [479]. See also Ost, Neukammer and Rinneberg 491 dealing with cytometry investigations under circumstances where LMT and GLMT essentially agree. More precisely, taking into account for experimental error limits, the data presented did not unambiguously show the influence of a finite beam waist on calculated quantities (integrated differential scattering cross-sections). Sloot et al 492 discussed the scattering matrices of monodisperse biological cells in a flow cytometer and provided evidences that quantitative measurements of the elements of these scattering matrices is possible. Experimental data are interpreted with the aid of GLMT. Soini et al [493] introduced a new design for the optical cuvette and a new optical lay-out for the scanning flow cytometer that permits measurement of the angular dependency of the scattered light from individual moving particles. Other articles relevant to cytometry are by Watson et al [494], Venkatapathi et al [221], and by Venkatapathi and Hirleman 222. The topic of flow cytometry is reviewed by Maltsev 495.

Shen and Riebel [496], motivated by particle size analysis using optical counters or transmission fluctuation spectroscopy, investigated the extinction by a large spherical particle located in a narrow Gaussian beam. They present experimental results on the extinction by an absorbent or transparent spherical particle passing through a Gaussian beam. Theoretical predictions are carried out using geometrical optics. They found that the theoretical model agrees approximately with the experimental results except for the near-waist location of the transparent particle. Castagner and Jones 497 discussed a double Gaussian beam method for the determination of particle size, direction and velocity, in which the particle size is measured using the light scattered from Gaussian laser beams. A well-known problem for such measurements, based on scattered intensities, results from the non-uniform profile of the illuminating beam. In the present work however, the uncertainties in illumination due to the beam shape are avoided by determination of the direction and velocity. Particles are assumed to be small compared with the width of the incident beam, so that LMT-calculations are valid. But there would not be any serious difficulty to extend the technique to the case of larger particles and/or of more focused beams and to analyze the system with the aid of GLMT. Castagner *et al* [498] dealt with particle sizing using a fast polar nephelometer, using LMT, but planning to implement GLMT to increase the correlation between experimental data and theoretical prediction.

Castanet et al [499] devoted themselves to the evaluation of temperature gradients within combusting droplets in linear stream using two colors laserinduced fluorescence. At a certain step, a temperature field is reconstructed, involving the use of GLMT (or of a geometrical optics model). More specifically, a light scattering approach is required for the calculation of the internal excitation field. One of the advantages of the GLMT approach is that the calculation is possible even if the beam's axis intersection point is geometrically located outside of the droplet under study. Let us remember here that GLMT can indeed provide excitation fields inside particles and therefore may be helpful to the study of many phenomena, another example being the two-photon fluorescence study, already mentioned, by Méès et al [352], the study of nonlinear effects generating the disruption of droplets [500], 501, or stimulated Raman scattering in cavities 502. Related articles are by Maqua et al 503, 504. Stimulated Raman scattering is further discussed by Zhang et al 505, dealing with the pumping of stimulated Raman scattering by stimulated Brillouin scattering within a single liquid droplet. Also, Yakovlev and Luk'yanchuk 506 proposed a novel microscopic arrangement that allows highly multiplexed nanoscopic imaging. A microsphere may focus light radiation into a small (100 nm)<sup>3</sup> volume. By arranging such microspheres in a close-packed 2D-array, parallel multiplexing can be achieved both for light excitation and signal collection. The authors anticipated that the proposed system can be used for a large variety of optical spectroscopy techniques, in particular concerning enhancement in the efficiency of multiphoton processes.

Wiggins et al [507] discussed the case of a collection of dielectric particles pumped by a laser radiation field. They then may form a strong density grating on the scale of the radiation wavelength, and coherently scatter the incident radiation. Depending on the size of the particles, such a configuration may be relevant to nonlinear optics, optical particle characterization and optical particle discrimination. The authors outlined the theoretical framework and provided the first observations from experiments using a standingwave gradient force trap. Onofri 508 introduced a system based on three interfering beams in laser Doppler velocimetry for particle position and microflow velocity profile measurements, with a GLMT analysis. Onofri et al 509 discussed the critical angle refractometry and sizing technique, and its extension to characterize the size distribution and the mean refractive index of clouds of bubbles. Rigorous simulations are carried out using GLMT. The investigation of a measurement technique to estimate concentration and size of inclusions in droplets is available from Riefler et al [510]. The proposed technique is experimentally studied in an extensive way. This is a case where an implementation of a GLMT with one inclusion 128 (and the development of a GLMT with many inclusions) would be likely welcome. Georgescu et al [511] examined the design of a system to measure light scattering from individual cells excited by an acoustic wave, with tests carried out on live cells. FFT of the scattered light signal was used to extract information about the highly-damped resonant frequencies of the cells, and the detected frequencies are consistent with theoretical predictions. You et al [512] introduced a new micro-bulk defect measurement method in semiconductive materials, which scales the defects by analyzing scattering, based on GLMT. The optical response of a single spherical particle in a tightly focused light beam, relevant to the use of a spatial modulation spectroscopy technique, is discussed by Lermé et al 150. These authors however used an angular spectrum approach, apparently motivated by the erroneous fact that GLMT would be limited to rather weakly convergent light beams (although generalized Mie equations are also provided). Sigel and Erbe 513 dealt with ellipsometric light scattering (an experimental technique allowing one to characterize interfaces of spherical colloidal particles embedded in a medium) which is shown to selectively extract the coherent scattering contribution representing the average properties of a particle ensemble. Illumination by a Gaussian beam implies a loss of coherence which is discussed in the article. The Gaussian beam profile used for the experiments is presented in the framework of GLMT. Smith and Berger 514 discussed a microscopic system that has been constructed to simultaneously acquire traditional Raman spectra and also angle-resolved elastic scattering patterns, using a single focused laser spot. The elastic scattering signal was analyzed using GLMT, representing what the authors believe (and we believe they are right) to be the first experimental validation of the theory prediction of angular backscatter from single spheres. This obviously does not mean the absence of previous experimental validations of the GLMT.

# VIII.0.2 Internal Fields and Morphology-Dependent-Resonances

In most cases, optical particle characterization techniques (laser Doppler velocimetry, phase Doppler anemometry, imaging...) rely on the analysis of scattered fields. It is a kind of inverse problems: you have the tracks of the dragon and you would like to know how the dragon looks like [515]. We are now going to enter the entrails of the dragon, that is to say to deal with internal fields. Obviously, scattered fields and internal fields are not physically independent (remember the boundary conditions at the surface of the scatterer), but it is convenient to pretend that they are independent for the sake of convenience to the exposition. The most interesting topic when dealing with internal fields is likely to be the one of morphology-dependent-resonances (MDRs), or whispering-gallery-modes (WGMs). Recall however that both terminologies are not necessarily equivalent [247].

Let us consider a spherical microcavity and discuss the behavior of rays circulating below its surface, and trapped due to the limit angle of refraction.

When these rays possess closed orbits, with a constructive phase relationship, they build up resonances. Because they depend on the shape of the particle (not necessarily spherical), and on its refractive index, these resonances are called morphology-dependent-resonances (MDRs). They may also be called whispering-gallery-modes (WGMs) in reference to a similar phenomenon encountered in acoustics, which may be experienced under the dome of St. Paul's Cathedral in London, or in the temple of Heaven in Beijing. Whatever the terminology used, the ray picture used above allows one to understand that MDRs generate high intensity fields below the surface of the scatterers, high enough to possibly facilitate the generation of quantum and of non-linear effects, including lasing.

Focal point positioning effects at resonance, associated with the study of internal fields in a spherical particle illuminated by a tightly focused laser beam, are discussed by Barton et al [140]. Cantrell studied a theory relevant to the understanding of pumped stimulated Brillouin scattering with resonances [516], [517]. Lai et al [518] examined the effect of perturbations on the widths of narrow MDRs in Mie scattering. Lai et al [519], dealing with nonlinear elastic scattering of light from a microdroplet, also discussed MDRs perturbations. Eversole et al [520] discussed input/output resonance correlation in laser-induced emission from microdroplets. The phenomenon of morphology-dependent stimulated Raman scattering (MDSRS) is outlined by Aker et al [521]. Trunk et al [483] observed a phase transition from the liquid to the solid state of ammonium sulfate inside a microdroplet by means of MDRs and Raman scattering.

An important issue is that a MDR can be excited, even though the light is not directly incident on the particle. This somewhat counter-intuitive result is explained by Van de Hulst by invoking the localization principle [17], or can be understood under the name of tunneling 522. Partitioning of energy between different modes is determined by using the GLMT. The large enhancement in the excitation rate of MDRs by an off-axis Gaussian beam focused somewhat beyond the edge of a dielectric spherical particle is discussed by Lock, using GLMT 157, to be complemented by Lock 523 dealing with the excitation efficiency of a MDR by a focused Gaussian beam, both for a spherical particle and for a cylindrical particle. Relevant to this issue is also an article by Serpengüzel et al 524 dealing with the excitation of resonances of microspheres on an optical fiber. For the first time, to the knowledge of the authors of this article, the coupling of light between an OFC (optical fiber coupler) and MDRs of an individual microsphere placed on the OFC surface is reported. An interesting aspect of the coupling is its association with off-axis beam excitation. The intensity of various resonance orders is understood using the GLMT associated with the localization principle. Elastic scattering intensities are measured and compared with the results of LMT and GLMT computations. These comparisons show that GLMT is indeed superior to LMT to explain the experimental data. Serpengüzel et al 525 later dealt again with the issue of enhanced coupling to microsphere resonances with optical fibers. In this work, MDRs of polystyrene microspheres were excited by an OFC, with the microsphere being immersed in an index matching oil. The observed MDR-spectra are found to be in good agreement with the GLMT and the localization principle. Furthermore, the scattering efficiency into each MDR is estimated as a function of the impact parameter by means of GLMT. Further related work (concerning microsphere resonators, MDRs of microspheres, focused Gaussian beam excitation in relation with GLMT and the localization principle...) has been published by Serpengüzel and Demir [526].

MDRs in circular cylinders are further discussed by Lock 216. Roll et al 527 presented a caustic model of MDRs based on geometrical optics, which describes the electromagnetic field in cylinders or spheres. As stated by the authors, a limit of the approach concerns the transition of a ray into a sphere, when it is not geometrically incident, in relation to the principle of localization. Aker et al [528], experimentally dealing with MDSRS, could detect nitrate ion concentration as small as  $5.10^{-5}$  M in aerosols. Such a low concentration could be detected by allowing the droplet size to be tuned during an experiment. The authors put forward the fact that it should be possible to detect concentrations a factor of ten lower. Arias-Gonzalez et al [529] dealt with MDRs in the scattering of electromagnetic waves from an object buried beneath a plane or a random rough surface. The topic is relevant to the detection of hidden objects which is an important issue in biology or geophysics. In this article, the interest is more specifically focused on resonances from a cylinder when the cylinder is placed in a dielectric medium that is separated from air by a flat or rough interface. Lock 530 discussed the excitation of MDRs in connection with van de Hulst's localization principle (a principle which, let us recall, is at the origin of the localized approximation). He emphasized the result that, for microparticles whose shape deviates from that of a sphere, partial-wave coupling caused by small surface irregularities leads to the excitation of low-radial-orders MDRs. Pastel and Struthers 531 measured evaporation rates of laser-trapped droplets by use of fluorescent MDRs. Leung et al [532] discussed MDRs in dielectric spheres with many tiny inclusions. They found that MDRs in the sphere may split into multiplets because of the loss of spherical symmetry and manifest themselves as broadened spectral lines in the scattering cross-section. Such features could be put in correspondence with some of the Hamiltonian features observed in the annulard billiard as discussed in [247], and references therein.

A comprehensive review on the theory of eigenmodes in a dielectric sphere, with a particular attention paid to WGMs/MDRs is given by Oraevsky [533]. Next, under certain circumstances, absorption cross sections of particles may have to be integrated over frequency, for instance when dealing with laser pulses, or over droplet size, an integration task which can be made difficult due to the existence of MDRs which can contribute significantly even when their linewidths are extremely narrow. This issue is discussed by Hill [534]. The existence of MDRs can be used to use microspheres as compact optical

filtering elements, as demonstrated by Bilici et al 535 who analyzed this concept using the localization principle and the GLMT. A somewhat subsequent complementary study is available from Isci et al [536]. Normal modes and quality factors of spherical dielectric resonators are studied by Yadav and Singh 537. Liang et al 193 discussed resonances in the case of spherical Bragg "onion" resonators. Rao and Gupta 538 considered a system of two eccentric spheres, wherein an inclusion sphere is embedded in a larger sphere with a different refractive index, and discussed broken azimuthal degeneracy. They used a well known code due to Ngo et al with minor modifications, for plane wave illumination. This is a configuration where the GLMT for a sphere with an eccentrically located spherical inclusion [128] would be of much interest. The significance of MDRs in optical tweezing is pointed out by Fontes et al [539]. Basic properties of dielectric WGM-resonators that are important for applications in optics and photonics are reviewed by Matsko and Ilchenko 540. The issue of deformed cavities, and the induced modifications of MDRs, is discussed by Han et al [269]. Also, Qiu et al [541] dealt with mode frequency shifts and Q-factor changes in 2D microflower cavity and its deformed cavity. Resonances are also discussed by Kiraz et al [542] in the framework of a study devoted to the volume stabilization of single, dye-doped water microdroplets with femtoliter resolution, including GLMT computations for a tightly focused Gaussian beam. See also Kiraz et al [543] dealing with a large spectral tuning of a water-glycerol microdroplet by a focused laser, a study involving the use of a localized GLMT for calculating the absorption of the laser by the droplet, and laser-induced heating. Mojarad et al 544 considered the interaction between metal nanoparticles and a high-numerical-aperture incident beam. A particular interest of these nanoparticles is that they are able to sustain an electromagnetic resonance while being much smaller than the incident wavelength. The interaction is described using a GLMT. Modifications of the cross sections and the nearfield enhancement for gold and silver nanospheres illuminated by the tightly focused beam are discussed. Xu et al 545 discussed second order parametric processes in nonlinear silica microspheres, a topic connected with the possibility of using high-quality factor WGMs in microspheres to generate strong second order nonlinear responses. The proposed nonlinear microsphere can also lead to symmetry-enforced quantum entanglement. In this context, a Gaussian beam may be expressed as a ket  $|\Phi\rangle$  which may be expanded as a superposition of basic kets representing spherical waves.

# VIII.0.3 Mechanical Effects

A very important field of applications of GLMT-approaches concerns the evaluation of radiation pressure forces and torques, something which was not actually expected when we only had applications to optical sizing in mind, a long time ago. Such radiation mechanical effects are relevant to the trapping, manipulation, deformation... of particles in optical traps, optical tweezers,

optical stretchers ... A history of single aerosol particle levitation (electrostatic, magnetic, acoustic, aerodynamic forces, and others, including optical forces) is provided by Davis [546]. An early work concerned a discussion of forward far-field pattern of a laser beam scattered by a water-suspended homogeneous sphere trapped by a focused laser beam, available from Park and Lee [547], with a theoretical analysis relying on the GLMT-like scattering theory of Kim and Lee [68], [69], more or less in the same spirit that other similar experiments used (see later) to validate GLMT results, available from Gréhan and Gouesbet [57], Gréhan et al [78], [548], and Guilloteau et al [58].

In Rouen, after the above articles with publication dates ranging from 1980 to 1992, a further interest, theoretically oriented, for the applications of mechanical effects, is testified since 1994 when, relying on previously published GLMT-formulations such that in 1988 [88], [2], [89], radiation pressure forces exerted on a particle arbitrarily located in a Gaussian beam were calculated by Ren et al [549], with a particular attention paid to the structure of the resonances. Beam shape coefficients are computed using the localized approximation. Emphasis is also stressed on the differences between plane waves and Gaussian waves. Afterward, Ren et al dealt with the prediction of reverse radiation pressure by GLMT 315. The existence of reverse radiation pressure is important for optical trapping processes because it allows particles to be trapped in a single extremely focused beam without having to take gravity into account. GLMT predictions for different descriptions of the incident beam are compared with electrostriction predictions when the particle size is smaller than the wavelength and with geometrical optics predictions when the particle size is larger than the wavelength. The evaluation of the beam shape coefficients is achieved by using the localized approximation and standard beams. Reverse radiation pressure has also been considered by Polaert et al 314 using improved standard beams, under severe focusing conditions  $(w_0 = \lambda/2)$ . Forces and torques exerted on a multilayered spherical particle by a focused Gaussian beam are discussed by Polaert et al 550, with a particular attention paid to the comparison between torque resonances and absorption resonances. Linear and circular polarizations are considered. Several kinds of multilayered spheres are compared. Theoretical predictions of radiation pressure forces exerted on a spheroid by an arbitrary shaped beam are carried out by Xu et al [275]. Among other results, this article numerically simulates the behavior of an optical stretcher allowing one to deform red blood cells. This work has been complemented by a GLMT-analysis of torques by Xu et al [276].

In collaboration with Bernard Pouligny and collaborators, GLMT-like situations and calculations have been discussed for stressing phospholipid membranes using mechanical effects of light [551], trapping and levitating a dielectric sphere with off-centred Gaussian beams, and for dynamometrical applications [552], [553], [554]. In [551], experiments involved giant phospholipid vesicles, focused laser beams, and latex-microparticles. Mechanical effects of light can then be used to tweeze and distort membranes, or to hold

and move solid particles in contact with membranes. Various phenomena can be explored: sphere-membrane adhesion, particle endocytosis, Brownian motion and interactions between solid particles bound to membranes. In the two-part article by Angelova and Pouligny [552], and by Martinot-Lagarde et al [553], the basic problem of measuring the forces exerted by a Gaussian laser beam illuminating a micrometre-sized transparent dielectric sphere is addressed. In the first-part, the authors experimentally used a levitation configuration with vertical parallel beams, investigated the example of polystyrene latex spheres in water, and experimentally measured radiation forces. In the second-part, the experimental results are compared with GLMT-computations. Previous comparisons available from the prior literature were restricted to particles located on beam axis, or to particle large enough for the ray optics approximation to hold. In the present case, comparisons are made under general conditions, requiring the use of off-axis-GLMT. It is found that GLMT-results quantitatively fit the experimental results. In the same filiation, the adhesion of latex sphere to giant phospholipid vesicles (statics and dynamics) is studied by Dietrich et al [555]. In this work, latex beads are manipulated using a long-working-distance optical trap. Measured stiffness values of the optical trap were in fairly good agreement (within 20%) with those computed using GLMT. Furthermore, an optical dynamometric study is carried out by Dimova et al [556] in which micron-sized latex spheres are used to probe the phase state and the viscoelastic properties of bilayers vesicle membrane. In this study, one or two particles were manipulated and stuck to a (giant) vesicle by means of an optical trap. Radiation pressure for the beam geometry used was computed using GLMT.

We now consider a series of articles by Gauthier and collaborators. Gauthier and Ashman [557] dealt with simulated dynamic behavior of single and multiple spheres in the trap region of focused laser beams. More specifically, an enhanced propagation method (or enhanced ray optics theoretical approach) is used to calculate the forces and torques present on each sphere of a system of particles located in the vicinity of focused laser-trapping beams. When a particle configuration is given, the next particle configuration, a small increment of time later, can be determined by applying the laws of classical mechanics using the forces and torques just calculated. Repetition of the process enables the full dynamic behavior of the system to be determined. Gauthier et al [558] experimentally confirmed optical-trapping properties of cylindrical objects, evaluated by using a sophisticated model (enhanced ray optics approach) to predict the trapping and the manipulation properties of elongated cylindrical objects in the focal region of a high-intensity laser beam. Gauthier et al [559] theoretically (again with the enhanced ray-optics approach) and experimentally explored the optical processes involved in laser trapping and optical manipulation, as a means of activating a micrometer-size gear structure. Gauthier 560 investigated the optical levitation and trapping of a micro-optic inclined end-surface cylindrical spinner. Enhanced ray optics is used again for simulations. Afterward, Gauthier [561] dealt with the laser-trapping properties of dual-component spheres consisting of a cocentered outer transparent dielectric spherical shell and an internal solid sphere (still with the enhanced ray optics model). We also mention the study of the self-centering of a ball lens by laser trapping due to Gauthier et al [562] and the computation of the optical trapping force using a numerical grid technique (FDTD: Finite Difference Time Domain) by Gauthier [563]. Some of these works could be completed by comparisons with GLMT-approaches, for instance the aforementioned dual-component spheres are multilayered spheres for which GLMT-approaches can be readily used, e.g. [550].

GLMT computations are carried out by Anders et al 482 to calculate radiation pressure forces, in connection with the design of a new technique to investigate phase transition processes of optically levitated droplets. Wohland et al 564 theoretically determined the influence of polarization on forces exerted by optical tweezers, relying on a combination of ray and wave optics. Cai et al 565 carried out optical levitation measurements with intensity-modulated light beams. More specifically, they pointed out that the illumination of an optically levitated particle with an intensity-modulated transverse beam induces a transverse vibration of a particle in an optical trap. This phenomenon may be used to measure trapping forces. Omori et al 566 discussed the observation of a single-beam gradient-force optical trap for dielectric particles in air. Nemoto and Togo 567 dealt with the axial force acting on a dielectric sphere in a focused laser beam. They relied on ray optics, with a comparison versus GLMT results. Comparisons between theoretical and experimental results are satisfactory, although a matching scaling factor is required. Trunk et al [483] used optical levitation of three-component droplets to study a phase transition. Omori and Suzuki 568 dealt with the collection of UO<sub>2</sub> particles floating in air using radiation pressure of a laser light, for removal and confinement of UO<sub>2</sub> particles being transported by air current or dispersed in a cell box. They performed a GLMT-based analysis of radiation forces. Pastel et al [569] dealt with laser trapping of microscopic particles for undergraduate experiments. Laser trapping is used by Pastel and Struthers 531 to measure evaporation rates. Hoekstra et al 570 used an extended discrete dipole approximation (DDA) to evaluate radiation forces on each dipole of the DDA-model, and obtained the total radiation pressure on a particle by summation of the individual forces. The theory is tested on spherical particles, and compared with LMT (the accuracy is found to be within a few percent). Such a work could possibly be extended to a GLMTconfiguration.

A numerical modelling of optical trapping for spheroidal and cylindrical particles is developed by Nieminen *et al* [571]. They used the T-matrix method with the beam shape coefficients evaluated by using a localized approximation. This work is completed by Nieminen *et al* [572] dealing with the calculation and optical measurement of laser trapping forces on non-spherical particles. The authors insist on the fact that a major problem is the representation of the beam (as we know), due to the fact that usual representations of

Gaussian beams do not exactly satisfy Maxwell's equations. They used the T-matrix method with a decomposition of the trapping beam into a plane wave spectrum (consisting of 97 components). Multipole expansion of strongly focused laser beams is investigated by Nieminen et al [387]. T-matrix method and GLMT are discussed. Bayoudh, Nieminen et al [573] dealt with the use of optical torques to manipulate the orientation of biological cells, with nonspherical shape, using plane-polarized Gaussian beam optical tweezers, and similar theoretical tools. Bishop, Nieminen et al [574] considered the optical application and measurement of torque on microparticles of isotropic nonabsorbing material, dealing with the use of optical torques to controllably rotate or align microscopic particles. The physics of optical tweezers is thoroughly reviewed by Nieminen et al [575]. A computational toolbox for optical tweezers is furthermore provided by Nieminen et al [576].

Resnick discussed the development of a compact optical tweezer package for use on a microscope to be flown on the International Space Station as part of a series of experiments in colloid cristallization 577. Rohrbach and Stelzer [578] calculated trapping forces of dielectric particles in arbitrary fields. In these computations, they determined separately two "classical" components of the optical force, namely the gradient force and the scattering force. This is a welcomed opportunity to remark that these components, although they may be viewed as physically appealing, do not occur (do not exist) in GLMT which provides a more fundamental unified description of optical forces and torques. An interesting prospect would be to derive the two components as approximations arising from the unified description. In any case, the authors dealt with a comparison of the "two-component approach" with GLMT (Barton's version). Rohrback and Stelzer 579 presented a theory together with simulation results describing three-dimensional position detection of a sphere located in a highly focused beam by back-focal plane interferometry. Calculations are carried by using Fourier theory and angular momentum representation. Trapping forces, force constants, and potential depths for dielectric spheres in the presence of spherical aberrations are predicted by Rohrback and Stelzer [580], using a two-component approach that determines the gradient and the scattering force separately. They claimed that, for the first time to their knowledge, it was possible to consider focus distorsion (caused by spherical aberrations or aperture filters) in forces calculations. To the best of our knowledge, the claim is correct. Rohrback et al [581] introduced an improved type of scanning probe microscope system able to measure soft interactions between an optically trapped probe and local environment. They measured trap stiffnesses which are found to coincide well with the calculated stiffnesses obtained from electromagnetic theory.

Harada and Asakura [582] dealt with photon correlation spectroscopy, a quasi-elastic light scattering technique to measure sizes and number-densities of small particles in suspension, or even in flows like soots in flames, illuminated by laser beams [583]. They studied the effects of laser radiation pressure which might disturb measurements carried out by this technique.

Computations of radiation pressure scattering efficiencies are carried out with a plane wave computer program, with the implementation of some modifications due to the Gaussian nature of the laser profile. A related work by Harada and Asakura [584] dealt with the dynamics and dynamic light-scattering properties of Brownian particles under laser radiation pressure. Theoretical calculations relied on the use of the GLMT. Radiation forces on a dielectric sphere in the Rayleigh scattering regime, under Gaussian laser beam illumination, have been studied by Harada and Asakura [585]. Correctness of the derived expressions and validity of the size range of the Rayleigh approximation for the radiation forces as a sum of the scattering force and the gradient force are investigated by a graphical comparison of the calculated forces in longitudinal and transverse components with those obtained from GLMT.

Roth et al [586] dealt with the determination of size, evaporation rate and freezing of water droplets using light scattering and radiation pressure. During the experiments, oscillations of the droplet position along the axes of the laser beam are observed, which are caused by fluctuations of the radiation pressure. This behavior is examined using GLMT. Roll et al [587] discussed an optical trap sedimentation cell, for the sizing of microparticles. This (new) technique is based upon the analysis of the dynamical behavior of the investigated (levitated) particle during a transient interruption of the supporting laser beam. In 1997, Grier [588] provided a review on optical tweezers in colloid and interface science. He stated that despite more than a decade of intense activity, the agreement between theories of optical trapping and experimental force measurements has been considered generally unsatisfactory, a statement which was about correct in 1997 (see however 552, 553), but which is certainly not valid any more nowadays, e.g. [589]. Note that the difficulty is not in the fact of having or not a correct theory (we indeed have one, GLMT) but in the fact of having a correct description of laser beams used. Dufresne and Grier 590 introduced optical tweezer arrays and optical substrates created with diffractive optics. To illustrate the concept, they implemented a 4x4 square array of optical tweezers, called the hexadeca tweezer. Gahagan and Swartzlander 591, experimentally and theoretically (using ray optics) investigated the trapping of low-index microparticles in an optical vortex. Gensch et al [592] dealt with optical trapping combined with transmission microscopy, confocal and nonconfocal fluorescence scanning microscopy, and confocal and noncofocal time-resolved fluorescence spectroscopy, to study latex particles and block copolymer micelles. Shima et al [593] dealt with the forces of a single-beam gradient-force optical trap on dielectric spheroidal particles in the geometric-optics regime. Gittes and Schmidt 594 provided an interference model for back-focal-plane displacement detection in optical tweezers. Although the model is simple, he captured the physical mechanisms of lateral trapping and detection for small particles.

Song et al [595] theoretically analyzed the forces acting on a "Mie particle" by surface plasmon-coupled evanescent fields. GLMT-like ingredients are used

for the theoretical analysis. Concerning plasmon, let us also cite Miao and Lin 596 dealing with trapping and manipulation of biological particles through a plasmonic platform, and stating that, in this context, rigorous calculations of optical forces can be carried out using the GLMT. A significant result is that force components are increased by one or two orders of magnitude at metal boundaries with respect to the case of dielectric boundaries. Next, Benabid etal 597 used optical radiation forces to achieve the guidance of dry micronsized dielectric particles, originally levitated in air, in hollow core photonic crystal fiber. They used a numerical model based on ray optics. Malagnino etal 598 dealt with measurements of trapping efficiency and stiffness in optical tweezers. They reported on an experimental study concerning the radial forces of an optical tweezer acting on spherical polystyrene particles diluted in water solution. A parametric study of the transverse trapping forces was made versus sizes and laser powers for two different objective lenses. Measured forces compared favorably with GLMT-results. Wiggins et al 507 dealt with a discussion of a standing-wave gradient trap, a configuration allowing one to optically confining, for a time long enough, a large number of particles. Afanas'ev et al [599] examined the spatial redistribution of microparticles in a suspension on exposure to an interference laser field, under the effect of optical forces, and theoretically analyzed the influence of the characteristics of the particles and of the characteristics of the field. Associated experiments are carried out.

Nahmias and Odde 589 dealt with radiation forces for laser optical trapping (using a strongly convergent beam) and laser optical guidance (using a weakly convergent beam), and established that GLMT is able to accurately predict experimental results for both schemes (trapping and guidance) without any assumption regarding the size of the particle relative to the wavelength of the radiation. Numerous very satisfactory comparisons between theory and experiments (concerning escape forces, force profiles, radial forces, axial forces) are provided. Also, the authors pointed out one of the advantages of GLMT with respect to ray optics, namely that GLMT can predict the presence of resonances, signifying the creation of electric and magnetic multipoles in the particle. This is a significant advantage indeed because resonance effects cause fluctuations in the trapping forces as a function of the wavelength and particle size. Given the positive assessment of the validity of GLMT for both strongly and weakly convergent beams, the authors concluded that they were in situation to conduct a general analysis of radiation forces for engineering design purpose and that, to use GLMT more effectively in practice, it would be helpful to create dimensionless combinations that can be used to correlate and simplify results. The production of dimensionless parameters is indeed afterward reported by Nahmias et al [600]. They then obtained a set of two simple correlations for the practical design of radiation-force-based systems. Furthermore, in this article, more GLMT simulations (for optical trap stiffness, detector response of an optical trap "back-focal-plane", optical levitation force profile, axial profile in laser guidance) are compared favorably with experiments. It is noticed that both Rayleigh theory and ray theory fail to predict the maximal trap stiffness, whereas the GLMT succeeds. More generally, several comparisons between ray optics, GLMT and experiments prove the superiority of GLMT with respect to ray optics. The authors also addressed the question of the practical usefulness of GLMT due to the fact that it is computationnally demanding. Our reply is that, with the increase of quality of algorithms and more important with the increase in speed of computers, we do not consider any more that GLMT (nowadays, and a fortiori in the future) is computationnally demanding. But, anyway, Nahmias et al pointed out that they have been able to present GLMT predictions as simple graphical representations using dimensionless parameters, so that forces can be estimated directly without the need for extensive computations for a particular set-up.

Zemanek et al [601] provided a simplified description of optical forces acting on a nanoparticle in the Gaussian standing wave, in which GLMT is used to analyze a Gaussian standing wave trap and a single beam trap as a function of particle size, refractive index, and beam waist size. Differences between the electrostatic approximation and GLMT are studied. GLMT is further used by Zemanek et al 602 to compare submicron-sized particle optical trapping in a single focused beam and a standing wave. Jakl et al, including Zemanek 603 discussed the behavior of an optically trapped probe approaching a dielectric interface. On-axis GLMT is used for calculations. The agreement between the predicted and measured behaviors of the trapped sphere while the beam waist approached the surface was very good in terms of location and size of discrete jumps of the trapped sphere between neighboring stable trapping positions. Also, Zemanek et al 604 calculated optical forces acting on Rayleigh particle placed into interference field. The interference field is made out from three interfering laser beams arranged in one plane, forming an optical trap. Furst 605 reviewed the theory and practice of using optical traps in complex fluids. Such optical traps offer the ability to probe nano- and microscopic interactions, structures, and responses that govern the rheology of complex fluids. Applications of laser tweezers in complex fluid rheology are further reviewed by the same author 606. It is shown that optical micromanipulation has expanded to enable control of tens to hundreds of particles in small ensembles using techniques such as holographic tweezers. Mazzoli et al 607 discussed the theory of trapping forces in optical tweezers, starting from a Debye-type integral representation valid for a focused laser beam, and deriving an explicit partial-wave representation for the force exerted on a dielectric sphere of arbitrary radius, position, and refractive index. In their introduction, they however state that theoretical treatments based on nearparaxial approximations (with cited references pointing to GLMT) are not valid descriptions of optical tweezers. It is true that theoretical treatments based on near-paraxial approximations are not valid description of optical tweezers, using tightly focused beams, but recall that GLMT is not limited to near-paraxial approximations. Mund and Zellner 608 dealt with the optical levitation of single microspheres at temperatures down to 180 K, allowing one to examine processes of atmospheric interest with the combination of optical levitation and Raman spectroscopy. The operation of the levitation technique is reviewed on the basis of GLMT. Rubinov  $et\ al\ 609$  devoted themselves to the interaction of interference laser field with an ensemble of particles in liquid, leading to a spatial redistribution of microparticles in a suspension, and to the occurrence of regular crystal-like structures of particles. Buosciolo  $et\ al\ 610$  examined a calibration method for position detector for simultaneous measurements of force constants and local viscosity in optical tweezers.

We are now going to discuss an extensive theoretical study for the calculation of the radiation trapping force for laser tweezers by use of the GLMT, available from a two-part article by Lock [611], [612]. These papers show that GLMT can efficiently deal with the case of beams focused by a high numerical aperture objective, with successful tests against experiments. Part I focused on the issue of beam description, more specifically on the exposition of a localized beam model (related to the so-called localized approximation) to describe an on-axis tightly focused laser beam with spherical aberration, allowing the evaluation of localized beam shape coefficients. Two issues have here to be emphasized. The first one concerns the consideration of spherical aberration. In some simple optical levitation experiments like those by Gréhan and Gouesbet 57, Gréhan et al 548, Guilloteau et al 58 which have been used for experimental validations of the GLMT, in which a vertical laser beam is focused in air, and used both for the levitation of the particle, and as the scattering source, the issue of aberration is not very important. It is conversely important in some more complicated levitation trapping setups. The second issue concerns the possibility of modelling tightly focused laser beams. Both issues are considered by Lock, in his Part I-article. Lock indeed examined an extension of the localized model to a beam tightly focused and truncated by a high-numerical-aperture lens, aberrated by its transmission through the wall of a sample cell, and incident upon a spherical particle (whose center is on the beam axis). This is typically the kind of beam used in laser tweezer experiments. It implies a symmetry breaking so that, for the on-axis case, instead of dealing with a single set  $\{g_n\}$  of special beam shape coefficients, it is required to deal with two sets  $\{g_n\}$  and  $\{h_n\}$ . A localized beam model is found to be appropriate to deal with tightly focused beams. Once an adequate beam description is obtained in Part I, Part II can deal with the study of the efficiency of trapping an on-axis spherical particle for a particle size ranging from the Rayleigh limit to the ray optics limit. The radiation trapping force is calculated for two different beam profiles and compared with experimental data. One of the beam profiles is theoretically simple but experimentally unrealistic. The other is theoretically more complicated but is a more realistic model of the experimental beam. Concerning the unrealistic beam (a freely propagating focused Gaussian beam), for the studied parameters, the calculated Gaussian beam GLMT trapping efficiency is approximately a factor of 2-3 below the experimental efficiency. Similar results are (surprisingly) obtained for the realistic beam. These facts, and the possible origins of the observed discrepancies between theory and experiments, are discussed. Later on, with the same spirit and in the same filiation, Lock et al [613] studied the scattering of a tightly focused beam by an optically trapped particle, examining near-forward scattering, both theoretically and experimentally. A discussion of beam shape coefficients of tightly focused beams is provided. Experimental results confirm theoretical predictions and provide further evidence that Mie theory, augmented by a realistic model for the beam shape coefficients, is capable of accurately predicting both the trapping and scattering properties of tightly focused, as well as paraxial, beams.

The topic of optical trapping is reviewed by Neuman and Block 614. Advances in the development of optical trapping apparatus, including instrument design considerations, position detection schemes and calibration techniques, are discussed. The authors remarked that the optical force has traditionnally been decomposed into two components (i) a scattering force in the direction of propagation and (ii) a gradient force in the direction of the spatial light gradient. They stated that this decomposition is merely a convenient and intuitive means of discussing the overall optical force, but stressed that both components arise from the very same underlying physics. Indeed, let us recall, GLMT provided an unified description of the optical forces, all associated with momentum exchanges. They mention that trapping forces and efficiencies predicted by GLMT-approaches are found to be in reasonable agreement with experimental values (with citations of Nahmias and Odde, and of Wright et al). They also mention good agreement between theory and experiments, concerning computed forces and trapping efficiencies, referring to Rohrback and Stelzer, and the exploration of the effects of spherical aberration, again by Rohrbach and Stelzer. Later on, Neuman et al 615 dealt with the measurement of the effective focal shift in an optical trap. The focus (of an oil-immersion microscope objective, used for the optical trap) is shifted because of the refractive-index mismatch between the cover glass and the aqueous sample of the set-up. The analysis of the experiments involved the use of an ingredient of the GLMT, namely the focused laser beam was modeled with beam shape coefficients derived from the localized approximation to an on-axis Davis first-order beam. Neuman et al 616 furthermore reviewed single-molecule micromanipulation techniques, with an emphasis on optical and magnetic tweezers.

Soifer et al [338] provided another review devoted to optical microparticle manipulation. GLMT is discussed in relation with experiments by Malagnino et al [598], and expressions derived by Harada and Asakura [585]. Rockstuhl and Herzig [241] used a rigorous diffraction theory, to calculate the force on elliptical shaped dielectric cylinders in three different regimes. Later on [617], they also dealt with the calculation of the torque exerted on dielectric elliptical cylinders by highly focused laser beams, with a decomposition of the illuminating beam into 41 plane waves. Experimental observations of light-scattering diagrams from single living cells and beads suspended in an optical

trap were recorded by Watson et al 494. Experimental results concerning light scattering from beads, aiming to the validation of the experimental set-up, were compared with GLMT predictions, leading to fairly good agreements. Zhang et al [324] dealt with optophoresis which is a non-invasive cell analysis technique that is based on the interaction of live cells with optical gradient fields and provided interesting results, such as detecting significant differences between the behavior of normal skin cells and melanoma cells, which indicate a potential biological interest of optophoresis for cellular analysis and cancer diagnostic applications. GLMT is used to provide a better understanding of the behavior of a cell when it passes through a laser gradient. The laser beam is approximated by an elliptical Gaussian intensity shape (laser sheet) with semimajor axis and semiminor axis equal to 24 and to 5.5  $\mu$ m respectively. GLMT is also used to calculate optical forces on a cell. In a work by Fontes et al [539] in which a double tweezers set-up is used to perform ultrasensitive force spectroscopy and observe the forces due to light scattering on a single isolated particle, the influence of MDRs, which can change the force values by more than 30-50%, is pointed out. A Gaussian-shaped beam partial wave decomposition theory (translate: GLMT) was able to explain experimental results for the force magnitude and mode coupling as a function of the perturbing laser wavelength. Also, good agreement was obtained between calculated and experimental positions of the resonance peaks. In a complementary article from the same team, Neves et al 391 proposed an analytical solution for optical trapping force on a spherical dielectric particle for an arbitrary positioned focused beam in a generalized Lorenz-Mie diffraction theory. Theoretical predictions agree well with experimental results. Jaising and Helleso 618 theoretically studied radiation forces on, and guiding velocities experienced by, a "Mie particle" in the evanescent field of an optical waveguide using a GLMT (Barton's version). They stated that the order of magnitude of the calculated guiding velocities agrees with the observed guiding velocities reported so far. Moine and Stout 619 dealt with optical forces in arbitrary beams by use of the vector addition theorem and rotation matrices. They discussed the partial wave decomposition of focused laser beams, and specifically deal with some simple models based on Davis-type corrections to Gaussian-type focused beams.

Chang and Lee [620] dealt with first-order calculations of radiation forces for rotating spheres illuminated by circular polarized Gaussian beams. The beam is actually a focused Hermite-Gaussian mode beam, and the formulas of radiation force used include terms due to the sphere rotation. Chang et al [621] provided theoretical calculations of optical forces exerted on a dielectric sphere in the evanescent field generated with a totally-reflected focused Gaussian beam. The issue of optical force on a sphere caused by an evanescent field is further discussed by Chang et al [622], with the consideration of multiple scattering effects between the sphere experiencing the optical forces and a prism substrate. Later on, Chang et al [623] provided a model for optical

tweezers upon cells in the ray optics regime. The cell is modeled as a spherically symmetric multilayer sphere.

Size and refractive index of microparticles in a two beam optical trapping system are measured, relying on a ray optics model, by Flynn et al 624 The accuracy of applying the ray optics model to the analysis of their system was justified by comparison with GLMT. In the case studied, the ray optics model is found to be a reasonable approximation to GLMT. Han et al 625 carried out GLMT-computations of radiation trapping forces acting on a two-layered spherical particle in a Gaussian beam. Kotlyar and Nalimov 626, 627 dealt with analytical expressions for, and the calculation of, radiation forces exerted on a dielectric cylinder illuminated by a cylindrical Gaussian beam. Kraikivski et al 628 considered the implementation of both short- and longworking distance optical trappings into a commercial microscope. Merenda et al 629 considered escape trajectories of single-beam optically trapped micro-particles in a transverse fluid flow, and studied the transverse and axial equilibrium positions of dielectric micro-spheres trapped in a single-beam gradient optical trap and exposed to an increasing fluid flow transverse to the trapping beam axis. The theoretical model used is a hybrid model combining rigorous vectorial electromagnetic field considerations and ray optics ingredients. Observed oscillatory behaviors however, likely to be the consequence of resonances, could not be predicted by the model, not refined enough to take account of the existence of MDRs. Simpson and Hanna [630] carried out numerical calculations of interparticle forces related to holographic assembly, using the localized approximation to represent incident Gaussian beams. The same authors also dealt with the optical trapping of spheroidal particles in Gaussian beams, modelled by using a fifth order Davis beam [631]. Buajarern et al 632 characterized multiphase organic/inorganic/aqueous aerosol droplets, using optical tweezers, relying on brightfield microscopy, and on (spontaneous and stimulated) Raman scattering. They have to discuss the spectroscopy of deformed and layered droplets, or the influence of a thin shell on the spacing between adjacent TM and TE resonant modes. Chaumet et al 633 theoretically studied the possibility of transferring a particle held in a classical far-field optical tweezer to a near-field trap, called an apertureless probe. They rely on a vectorial nonparaxial representation of the Gaussian laser beam in the waist region. An angular spectrum representation of Gaussian beams is used. Gerlach et al 634 dealt with WGMs and, using radiation pressure, induced mode splitting in a spherical microcavity with an elastic shell. Theoretical calculations are carried out using GLMT. Grzegorczyk and Kong 635 provided an analytical expression of the force due to multiple TM plane-wave incidences (in particular a Gaussian beam) on an infinite lossless dielectric circular cylinder of arbitrary size. Mao et al [366] dealt with the calculation of axial optical forces exerted on medium-sized particles in optical traps, using both a ray optics model and GLMT, invoking an improved localized approximation for beam shape coefficients. By comparing the numerical results of these two approaches, the applicability of the GLMT to particles of arbitrary size and the limit of the ray optics model in the region of small particles are analyzed. Results from GLMT are found to be closer to the experimental data than ray optics predictions. The authors concluded that the validity of the GLMT to describe the optical forces on arbitrary sized particles is proved. They also pointed out on an advantage of GLMT with respect to ray optics approaches, that GLMT can predict resonance effects. Furthermore, the authors demonstrated the feasibility of femtosecond laser tweezers. Neves et al [392] dealt with axial optical trapping efficiency through a dielectric interface, using both an angular spectrum representation and GLMT. Yan and Yao 636 discussed transverse forces of focused Gaussian beams on ellipsoidal particles. Viana et al [637] dealt with the possibility of absolute calibration of optical tweezers. They noticed that the laser beam may be represented by an attempted improvement of the paraxial Gaussian  $TEM_{00}$  model, including fifth-order corrections in powers of the ratio between wavelength and beam waist (i.e. by a fifth-order Davis beam), but that such an approximation does not correctly represent the field near a focus of a high numerical aperture objective. Although this may be so, it is an issue which concerns the beam description, but not at all the GLMT which, let us say it again, is an arbitrary beam theory. Kartashov et al 638 dealt with the measurements of the force parameters of a gradient-force optical trap for dielectric microobjects. This work combines theoretical analytical calculations in relation with experiments on filiform objects (cotton filaments). Ma et al 639 dealt with laser-guidance based detection of cells with singlegene modifications. They demonstrated an impressive result, namely that a laser guidance-based speed-measurement method can precisely distinguish cells that differ by only one gene. The authors of the article discussed ray optics and GLMT. They stated that GLMT is the most complicated one (a matter of taste: at least one of the authors of this book is comfortable with wave theory, but bored by ray optics), but it can be used to explore several phenomena that ray optics cannot, and eventually decided to use GLMT to estimate guidance forces. Hu et al 640 discussed the use of an antireflection coating for improved optical trapping. GLMT is put forward as an efficient theory to deal with the theoretical aspects of the issue. Li et al [641] studied optical forces on interacting plasmonic nanoparticles in a focused Gaussian beam, using a GLMT-approach. For plasmons, see also Cole et al 642.

We would like to end this section by mentioning two fantastic and fascinating applications of GLMT-like theories for optical trapping and manipulation. The first one concerns a new concept of earth-based satellites, as discussed in a NASA report, explicitly referring to GLMT, due to La Pointe [643]. A shepherd satellite is proposed, based on the use of electromagnetic radiation forces to position and hold a large number of small, specialized spacecrafts in a precise array. The concept derives from well-known optical scattering and gradient force techniques which have been used to trap and manipulate microscopic objects using laser radiation. Although the presumed physical dimensions of the satellites will exclude the use of optical wavelengths, it is

proposed that a technique similar to laser optical trapping can be used at millimeter or microwave frequencies more appropriate to larger object sizes. A somewhat similar idea is pointed out by Nahmias and Odde [589] who noted that forces on the order of several newtons are achievable using gigawatts of power. Microwave beams of this size can be used for space applications such as tractor beams, eliminating the need for direct contact and dangerous space walks. Space solar power technology offers power of this magnitude in the foreseable future.

The second application originates from a dream of Labeyrie who would like to photograph exo-planet details, such as possibly mountains, forests, oceans, deserts... many light years away from Earth. This would be achieved using hypertelescopes (made out from small telescopes) ranging over hundreds of kilometers across, with elementary telescopes positioned and held using radiation forces produced by a laser operating in space, e.g. [644]. The relevance of GLMT-like approaches to such a project is known to us via a personal communication.

### VIII.0.4 Multiple Scattering

We have up to now dealt with single scattering, but another important issue is the one of multiple scattering. There has been a long-lasting tradition to study multiple scattering in Rouen, either using four-flux models (see Maheu et al [645], Maheu and Gouesbet [646], Tonon et al [647], Rozé et al [648], [649]), or Monte-Carlo techniques (see [650], [651], [652]), under c.w. plane wave illumination.

Rozé et al [653], [654] dealt with the more complex situation of Monte-Carlo simulations to simulate the interaction between ultra short pulses and a dense scattering medium. In this study, time-dependent scattering characteristics of particles are taken into account, as well as scatterer to scatterer propagation delays. For particles small enough, a centre to centre model is accurate enough and simulations of propagation through a monodisperse slab show the predominance of ballistic photons in a thin time window. For larger particles, multiple scattering is always predominant and scrambles the transmitted signal. Calba et al 655 dealt with the same topic but specialized the simulations to the case of large particles. Single scattering processes (phase function) are pre-computed in a LMT-framework or using Debye series. Later on, Calba et al 656 could compare simulations carried out in the same spirit as above (exhibiting the temporal separation between ballistic light and scattered light) and experimental results, showing a good agreement. The early scattered light contains information on particle size, opening the way to particle sizing in strongly scattering media. With Ovod [657], we come to the much interesting problem of multiple scattering from an ensemble of spheres in a laser beam, a problem which involves the consideration of a GLMT (Barton's version to be specific), the evaluation of beam shape coefficients and the use of a localized approximation.

In the multiple scattering context, it may also be of interest to mention the works of Xu concerning the electromagnetic scattering by an aggregate of spheres [658], [659], [660], and taking the point of view that light incident on a given particle after having been scattered by other particles represents a type of arbitrary beam incident on the given particle which is appropriate for a GLMT analysis. Also, relevant Monte-Carlo simulations are carried out by Berrocal et al [661].

### VIII.0.5 Miscellaneous Topics

In this section, we gather various ingredients which are not sufficiently developed to furnish enough material for an independent section but which, however, are of interest for this chapter.

#### Earlier validations for GLMT

If you believe to Maxwell's equations, then GLMT should be correct. Nevertheless, it is always useful to provide validations, not only to possibly detect computational mistakes but also to check computer programs. In 1980, two years before the first archival article on GLMT, an optical levitation technique of a single particle to study quasi-elastic scattering of light was reported by Gréhan and Gouesbet [57] and a scattering diagram was recorded in the forward direction between typically 15° and 40°. It was impossible to match this experimental diagram with a calculated scattering diagram obtained using the classical LMT. It was expected, at this time, that the discrepancy between theory and experiments was due to the fact that LMT should not be applied to the actual experimental circumstances in which the diameter of the levitated spherical particle was of the same order of magnitude of the laser beam diameter (used simultaneously as the source for levitation and the source for scattering). Indeed, later on, this experimental scattering diagram was satisfactorily reproduced by calculations carried out in a GLMT framework [78]. More extensive experimental validations of GLMT were afterward published by Gréhan et al 548 and Guilloteau et al 58, using both an onebeam and a two-beams set-up (in which the source for levitation is different from the source for scattering). It was concluded that good and most often extremely good agreement between theory and experiments provide a new experimental validation of the GLMT. Conversely, experimental data could not be properly reproduced within the restricted framework of the classical LMT. Significant differences between LMT and GLMT were reported even when the particle diameter is approximately one third of the local beam diameter. Similar experiments have been reported by Misconi et al [662].

Other earlier validations were of a theoretical nature. Chevaillier *et al* [44] dealt with a comparison of diffraction theory and GLMT for a sphere located on the axis of a laser beam. The diffraction theory (near forward

scattering) used was an extension of usual diffraction theory to waves of nonuniform intensity distribution. Beam shape coefficients for GLMT were evaluated using a localized approximation. This work has been completed by another similar work published by Gréhan et al [663]. It was concluded from these studies that a new validation of GLMT was obtained. See also the related work by Chevaillier et al [664]. Another relevant article is by Lock and Hovenac [665] dealing with the diffraction of a Gaussian beam by a spherical obstacle, in which the Kirchhoff integral for diffraction in the near-forward direction is derived from an exact GLMT-approach. Of course, many other validations of GLMT have been obtained, and reported in this book, although they did not originate any more from the ancient times. For example, let us recall the works by Angelova and Pouligny [552], Martinot-Lagarde et al [553], or Nahmias and Odde [589].

#### Debye series

A very useful complementary tool to discuss fields, specifically scattered and internal fields, providing many physical insights, is the use of Debye series. Relying on a previous work by Hovenac and Lock [666], Gouesbet provided a Debye series formulation for the GLMT stricto sensu [667]. Let us recall that a Debye series analysis of scattering of a plane wave by a spherical Bragg grating is available from Lock [196]. Also, Li et al provided Debye series for light scattering by a multilayered sphere, including the case of Gaussian beams [200], [201] or for normally incident plane-wave scattering by an infinite multilayered cylinder [197], without forgetting Wu and Li [230] dealing with Debye series for a multilayered cylinder in an off-axis Gaussian beam.

#### Interactions with atoms

Van Enk and Kimble [668] calculated exact 3D solutions of Maxwell's equations corresponding to strongly focused light beams, and studied their interaction with a single atom in free space. A complementary work is by van Enk and Kimble [669] dealing with the same topic, but putting the results obtained in the context of quantum information processing with single atoms. According to these authors, one question that arises is whether strong focusing has an undesired side effect, namely, that the scattered light contains information about the state of the qubit. The fear would be that the laser intensity would have to be turned down so much, that the absence of a photon from the laser beam becomes in principle detectable. In these works, an ingredient of GLMT (not GLMT itself since the atom is very small compared with the dimensions of the beam) is relevant, namely the problem of description of a strongly focused beam.

#### Extinction paradox

The extinction paradox is studied by Lai et al [670] by applying a partial-wave analysis to a 2D-light beam interaction with a long transverse cylinder without absorption. We recall that the extinction paradox refers to the extinction efficiency becoming twice as much as the value associated with the geometrical interaction between the particle and the incoming wave, in the limit of zero wavelength (or of infinite diameter in the case of spherical particles). The interpretation of extinction in Gaussian-beam scattering was previously discussed by Lock [671], in the framework of an on-axis GLMT.

#### **Symmetries**

There exist symmetry relations in GLMT as studied by Ren et al [312]. It happens that symmetry relations in the description of the electromagnetic beams are converted into symmetry relations satisfied by the beam shape coefficients, and also by other quantities computed by the GLMT, such as scattered electromagnetic fields or cross sections. The symmetry relations may then be used to simplify some analytical work and to check the formulas and the associated numerical results such as those encountered in developing a localized approximation. Being aware of them may also speed up numerical calculations by the elimination of useless repetitive calculations, e.g. see Lock 157. Some of these relations had been earlier obtained in the case of Gaussian beams [379], [127]. Ren et al [312] however established symmetry relations for a large class of electromagnetic beams including Gaussian beams and laser sheets. The symmetry issue is also discussed by Berg et al 672 dealing with reflection symmetry of internal fields in a sphere and its consequences on scattering, using a microphysical approach. A connection between the internal wave, and the scattered wave in the far-field, induced by symmetry considerations, is discussed.

## IX Conclusion

The aim of the present book has been to provide a background in GLMT, allowing presumably a rather easy access to archival literature in journals and conference proceedings.

When the writing of this book started in 1989 (twenty years ago!), taking the opportunity of a summer vacation in the romantic atmosphere of Weissensee, near the king castles of Ludwig der Zweite, in south of Germany, many fundamentals now incorporated in the book were not yet available and, may be more important, no applications of GLMT were produced. The completion of the book required many more years and, during this time, many new fundamental problems have been solved and applications developed much. We therefore had to recurrently up-to-date the contents until it has eventually become necessary to freeze it. The freezing has been made in 2008, one hundred years after the pioneering article of Gustav Mie.

Therefore, clearly, this book is not fully completed in so far as the situation still evolves, i.e. to some extent the story of GLMTs is just beginning. But much of the message (at least the basic message) is now in the hands of the reader, ready to produce new blossoms, in particular a long, endless, and ramified caravan of new fundamental developments and of new applications. This blossoming process is expected to become an asymptotic process requiring the effort of many researchers and engineers, but, very likely, the asymptote itself is certainly located far beyond our Riemanian horizon.

One of the referees of one of our articles stated that he was genuinely convinced that GLMT should be a wave of the future in light scattering. Let us hope so and let us then observe the propagation of this wave at a speed which, unfortunately, cannot exceed the speed of light. For this propagation, the main burden is now charged on the shoulders of the readers, although they could now prefer to take a rest for a while. Actually, this is exactly what the authors want to do: resting a bit.

232 IX Conclusion

The bibliography is presented in two parts. The first part (B1) concerns articles explicitly quoted in the bulk of the book, essentially focusing on journal articles which are of easy access. The second part (B2) concerns articles of less easy access (i.e. from conference proceedings) but which may contain useful information and, more important, many examples of applications.

## Appendix A

## Evaluation of Quadratures, Rels (III.130) and (III.131)

The aim of this Appendix is to evaluate quadratures (III.130)-(III.131) which are rewritten as:

$$I_1 = \int_0^\pi (\tau_n^k \tau_m^k + k^2 \pi_n^k \pi_m^k) \sin \theta \ d\theta \tag{A.1}$$

$$I_2 = \int_0^\pi (\pi_m^k \tau_n^k + \pi_n^k \tau_m^k) \sin \theta \ d\theta \tag{A.2}$$

From the definition of generalized Legendre functions  $\tau_n^k$ ,  $\pi_n^k$  (Rels (III.51)), integrals  $I_1$  and  $I_2$  may be expressed in terms of associated Legendre functions as follows:

$$I_1 = \int_0^{\pi} \left(\frac{dP_n^k}{d\theta} \frac{dP_m^k}{d\theta}\right) \sin\theta \ d\theta + \int_0^{\pi} k^2 \frac{P_n^k}{\sin\theta} \frac{P_m^k}{\sin\theta} \sin\theta \ d\theta \tag{A.3}$$

$$I_2 = \int_{\theta=0}^{\pi} (P_m^k dP_n^k + P_n^k dP_m^k)$$
 (A.4)

A direct integration readily gives  $I_2$ :

$$I_2 = P_m^k(-1)P_n^k(-1) - P_m^k(1)P_n^k(1)$$
(A.5)

But associated Legendre functions satisfy the following relation ([130], t1, p. 87):

$$P_n^k(\pm 1) = 0, \qquad k \neq 0$$
 (A.6)

leading to:

$$I_2 = 0, k \neq 0 (A.7)$$

For  $I_1$ , let us first split the r.h.s of (A.3):

$$I_1 = I_1^1 + I_1^2 = \int_0^\pi \left(\frac{dP_n^k}{d\theta} \frac{dP_m^k}{d\theta}\right) \sin\theta d\theta + \int_0^\pi k^2 \frac{P_n^k}{\sin\theta} \frac{P_m^k}{\sin\theta} \sin\theta d\theta \quad (A.8)$$

We then integrate  $I_1^1$  partially and use the associated Legendre equation (II.68):

$$\frac{d}{d(\cos\theta)}\sin^2\theta \frac{dP_n^k(\cos\theta)}{d(\cos\theta)} + \left[n(n+1) - \frac{k^2}{\sin^2\theta}\right]P_n^k(\cos\theta) = 0 \tag{A.9}$$

to obtain:

$$I_1^1 = m(m+1) \int_0^{\pi} P_n^k(\cos \theta) P_m^k(\cos \theta) \sin \theta \ d\theta$$

$$-k^2 \int_0^{\pi} \frac{P_n^k(\cos \theta)}{\sin \theta} \frac{P_m^k(\cos \theta)}{\sin \theta} \sin \theta d\theta$$
(A.10)

leading to:

$$I_1 = m(m+1) \int_0^{\pi} P_n^k(\cos \theta) P_m^k(\cos \theta) \sin \theta \ d\theta \tag{A.11}$$

(A.11) is a standard integral (130), t1, p.105):

$$\int_{0}^{\pi} P_{n}^{k}(\cos \theta) P_{m}^{k}(\cos \theta) \sin \theta \ d\theta = \frac{2}{2n+1} \frac{(n+k)!}{(n-k)!} \delta_{nm}$$
 (A.12)

Hence we obtain:

$$I_1 = \frac{2m(m+1)}{(2m+1)} \frac{(m+k)!}{(m-k)!} \delta_{nm}$$
(A.13)

## Appendix B

## Evaluation of Quadradures, Rels (III.151) and (III.152)

The aim of this Appendix is to evaluate quadratures (III.151)-(III.152) which are rewritten as:

$$I_3 = \int_0^\pi (\tau_n^k \tau_m^k + k^2 \pi_n^k \pi_m^k) \cos \theta \sin \theta d\theta$$
 (B.1)

$$I_4 = \int_0^{\pi} (\tau_n^k \pi_m^k + \tau_m^k \pi_n^k) \cos \theta \sin \theta d\theta$$
 (B.2)

For  $I_4$ , we use the definitions of  $\tau_n^k, \pi_n^k$  (Rels (III.51), (III.52)) and obtain:

$$I_4 = -\int_0^\pi P_n^k \frac{dP_m^k}{d\cos\theta} \cos\theta \sin\theta \, d\theta - \int_0^\pi P_m^k \frac{dP_n^k}{d\cos\theta} \cos\theta \, \sin\theta \, d\theta \quad (B.3)$$

Integrating partially the first integral in (B.3) and rearranging with (A.6), we find that  $I_4$  is exactly the standard integral (A.12):

$$I_4 = \frac{2}{2n+1} \frac{(n+k)!}{(n-k)!} \delta_{nm}$$
 (B.4)

For  $I_3$ , using again the definition of the generalized Legendre functions  $\tau_n^k$  and  $\pi_n^k$ , it becomes:

$$I_3 = \int_0^{\pi} k^2 P_n^k \frac{P_m^k}{\sin \theta} \cos \theta \ d\theta + \int_0^{\pi} \frac{dP_n^k}{d\theta} \frac{dP_m^k}{d\theta} \cos \theta \ \sin \theta \ d\theta = I_3^1 + I_3^2 \quad (B.5)$$

We integrate partially  $I_3^2$  and rearrange to obtain a new expression for  $I_3$ . Then we use the associated Legendre equation (A.9) under the form:

$$\frac{1}{\sin\theta} \frac{d}{d\theta} \sin\theta \frac{dP_m^k}{d\theta} + m(m+1)P_m^k = \frac{k^2 P_m^k}{\sin^2\theta}$$
 (B.6)

leading to:

$$I_3 = m(m+1) \int_0^{\pi} P_n^k P_m^k \sin \theta \cos \theta d\theta - \int_0^{\pi} P_n^k \left[ \sin^2 \theta \frac{dP_m^k}{d \cos \theta} \right] \sin \theta d\theta$$
 (B.7)

Then we need the following relations between the associated Legendre functions ([130], t1, p.101-102):

$$\sin^2\theta \, \frac{dP_m^k}{d\cos\theta} = -k\cos\theta P_m^k - \sin\theta P_m^{k+1} \tag{B.8}$$

$$\sin \theta P_m^{k+1} = (m-k)\cos \theta P_m^k - (m+k)P_{m-1}^k$$
 (B.9)

We note that, in Robin, there is a misprint to correct for Rel (B.9). We obtain:

$$I_{3} = m(m+2) \int_{0}^{\pi} P_{n}^{k} P_{m}^{k} \cos \theta \sin \theta d\theta - (m+k) \int_{0}^{\pi} P_{n}^{k} P_{m-1}^{k} \sin \theta d\theta$$
 (B.10)

The second integral in the r.h.s. is again the standard integral (A.12). For the first integral, we integrate partially and rearrange. We use (B.8), then (B.9), to make again appearing the standard form, leading to:

$$\frac{n+k}{2+n+m} \frac{2}{2m+1} \frac{(m+k)!}{(m-k)!} \delta_{m,n-1} + \frac{m+k}{2+n+m} \frac{2}{2n+1} \frac{(n+k)!}{(n-k)!} \delta_{n,m-1}$$
(B.11)

We consequently obtain:

$$I_{3} = m(m+2) \left[ \frac{n+k}{2+n+m} \frac{2}{2m+1} \frac{(m+k)!}{(m-k)!} \delta_{m,n-1} + \frac{m+k}{2+n+m} \frac{2}{2n+1} \frac{(n+k)!}{(n-k)!} \delta_{n,m-1} \right] - \frac{2(m+k)}{2n+1} \frac{(n+k)!}{(n-k)!} \delta_{n,m-1}$$
(B.12)

which may be rearranged to a more symmetrical form:

$$I_{3} = \frac{2(n-1)(n+1)}{(2n-1)(2n+1)} \frac{(n+k)!}{(n-1-k)!} \delta_{m,n-1}$$

$$+ \frac{2(m-1)(m+1)}{(2m-1)(2m+1)} \frac{(m+k)!}{(m-1-k)!} \delta_{n,m-1}$$
(B.13)

## Appendix C

## Evaluation of Quadratures, Rels (III.169) and (III.170)

The aim of this Appendix is to evaluate quadratures (III.169)-(III.170):

$$I_5 = \int_0^{\pi} (\tau_n^{|p|} \tau_m^{|p+1|} + p(p+1) \pi_n^{|p|} \pi_m^{|p+1|}) \sin^2 \theta \ d\theta$$
 (C.1)

$$I_6 = \int_0^{\pi} (p\tau_m^{|p+1|} \pi_n^{|p|} + (p+1)\tau_n^{|p|} \pi_m^{|p+1|}) \sin^2 \theta \ d\theta$$
 (C.2)

For  $I_5$ , we first consider the case when  $p \geq 0$ .

$$I_5(p \ge 0) = \int_0^{\pi} (\tau_n^p \tau_m^{p+1} + p(p+1)\pi_n^p \pi_m^{p+1}) \sin^2 \theta \ d\theta$$
 (C.3)

We replace  $\tau_n^k, \pi_m^k$  by their definitions (III.51)-(III.52) and integrate partially the first integral. Then, we use twice Rel (C.4) and also once Rel (C.5) below (15, p. 402):

$$(2l+1)\sin\theta \frac{dP_{l-1}^{m}}{d\theta} = l(l-m+1)P_{l+1}^{m} - (l+1)(l+m)P_{l-1}^{m}$$
 (C.4)

$$(2l+1)\cos\theta P_l^m = (l+m)P_{l-1}^m + (l-m+1)P_{l+1}^m$$
 (C.5)

to obtain:

$$I_{5}(p \ge 0) = \int_{0}^{\pi} P_{n}^{p} \{p(p+1)P_{m}^{p+1} + \frac{m(m-p)(m+1)(m+2)}{(2m+1)(2m+3)} [P_{m}^{p+1} - P_{m+2}^{p+1}] \text{ (C.6)}$$

$$+ \frac{mp(m-p)}{(2m+1)(2m+3)} [(m+1)P_{m}^{p+1} + (m+2)P_{m+2}^{p+1}]$$

$$+ \frac{m(m-1)(m+1)(m+p+1)}{(2m-1)(2m+1)} [P_{m}^{p+1} - P_{m-2}^{p+1}]$$

$$- \frac{p(m+1)(m+p+1)}{(2m-1)(2m+1)} [mP_{m}^{p+1} + (m-1)P_{m-2}^{p+1}] \} d\theta$$

This equation is rearranged in order to take advantage of the following relation (130, t1, p. 101):

$$(2l+1)\sin\theta P_l^m = P_{l-1}^{m+1} - P_{l+1}^{m+1}$$
 (C.7)

In the term {} of (C.6) we manage to produce only terms of the kind of the one in the r.h.s. of (C.7). Having done that, we observe that the integral in (C.6) only contains integrals in the standard form (A.12). Therefore, we have:

$$I_5(p \ge 0) = \frac{2}{(2m+1)(2n+1)} \frac{(m+p+1)!}{(m-1-p)!} [(n-1)(n+1)\delta_{n,m+1} \quad (C.8)$$
$$-(m-1)(m+1)\delta_{m,n+1}]$$

The case p < 0 may be reduced to the case  $p \ge 0$  by changes in the subscript labels:

$$\left. \begin{array}{l} p \to -(p+1) \\ n \to m \\ m \to n \end{array} \right\} \tag{C.9}$$

leading to:

$$I_5(p<0) = \frac{2}{(2m+1)(2n+1)} \frac{(n-p)!}{(n+p)!} [(m-1)(m+1)\delta_{m,n+1} \quad (C.10)$$
$$-(n-1)(n+1)\delta_{n,m+1}]$$

For  $I_6$ , we first consider the case p > 0:

$$I_6(p>0) = \int_0^{\pi} (p\pi_n^p \tau_m^{p+1} + (p+1)\tau_n^p \pi_m^{p+1}) \sin^2 \theta \ d\theta$$
 (C.11)

We replace  $\pi_n^k, \tau_m^k$  by their expressions in terms of  $P_n^k$  and we integrate partially the second integral to obtain:

$$I_6(p>0) = -\int_0^{\pi} P_n^p [\sin \theta \frac{dP_m^{p+1}}{d\theta} + (p+1)\cos \theta P_m^{p+1}] d\theta$$
 (C.12)

By using Rels (C.4) and (C.5), (C.12) becomes:

$$I_6(p>0) = \frac{(p-m)(m+p+1)}{2m+1} \int_0^{\pi} P_n^p [P_{m+1}^{p+1} - P_{m-1}^{p+1}] d\theta$$
 (C.13)

The integral in (C.13) is reduced to the standard form (A.12) by using (C.7):

$$I_6(p>0) = (m-p)(m+p+1) \int_0^{\pi} P_n^p P_m^p \sin\theta d\theta$$
 (C.14)

leading to:

$$I_6(p>0) = \frac{2}{2m+1} \frac{(m+p+1)!}{(m-p-1)!} \delta_{nm}$$
 (C.15)

The case p = 0 is readily treated independently. We find that the result takes the same form as (C.15) which is therefore valid for  $p \ge 0$ . With the same change of subscripts (C.9) as for  $I_5$ , the case p < 0 is reduced to the case  $p \ge 0$ .

We finally obtain:

$$I_{6} = \begin{cases} \frac{2}{2n+1} \frac{(n+p+1)!}{(n-p-1)!} \delta_{nm} & p \ge 0\\ \frac{-2}{2n+1} \frac{(n-p)!}{(n+p)!} \delta_{nm} & p < 0 \end{cases}$$
 (C.16)

## Appendix D

## To Reduce the Double Summations of Chapter IV to Single Summations

The following relations are to be used to reduce double summations  $\sum_{i=1}^{n} f(x_i)$  to single summations  $f(x_i)$ .

$$\sum_{j_{+}=2q}^{jp} A_{jp} = \sum_{j=q-1}^{\infty} A_{2j+1,j+1-q} \qquad q > 0$$
 (D.1)

$$\sum_{j_{+}=2q}^{jp} A_{jp} = \sum_{j=|q|}^{\infty} A_{2j+1,j+1-q} \qquad q \le 0 \quad (D.2)$$

$$\sum_{j_{-}=2q}^{jp} A_{jp} = \sum_{j=q}^{\infty} A_{2j+1,j-q} \qquad q \ge 0$$
 (D.3)

$$\sum_{j_{-}=2q}^{jp} A_{jp} = \sum_{j=|q|-1}^{\infty} A_{2j+1,j-q} \qquad q < 0$$
 (D.4)

$$\sum_{j_{+}=2q+1}^{jp} A_{jp} = \sum_{j=|q|}^{\infty} A_{2j,j-q} \qquad \forall q \qquad (D.5)$$

$$\sum_{j=2q+1}^{jp} A_{jp} = \sum_{j=q+1}^{\infty} A_{2j,j-q-1} \qquad q \ge 0$$
 (D.6)

$$\sum_{j=2q+1}^{jp} A_{jp} = \sum_{j=|q|-1}^{\infty} A_{2j,j-q-1} \qquad q < 0 \quad (D.7)$$

$$\sum_{j_0=2q}^{jp} A_{jp} = \sum_{j=|q|}^{\infty} A_{2j,j-q} \qquad \forall q \qquad (D.8)$$

$$\sum_{j_0=2q+1}^{j_p} A_{jp} = \sum_{j=q}^{\infty} A_{2j+1,j-q} \qquad q \ge 0 \quad (D.9)$$

$$\sum_{j_0=2q+1}^{j_p} A_{jp} = \sum_{j=|q|-1}^{\infty} A_{2j+1,j-q} \qquad q < 0 \quad (D.10)$$

As an example, the demonstration is only provided for the first of them. One has (from (IV.82) and (IV.88)):

$$\bar{A} = \sum_{\substack{j_+ = 2q \\ q > 0}}^{jp} A_{jp} = \sum_{\substack{j=0 \\ j+1-2p=2q > 0}}^{\infty} \sum_{p=0}^{j} A_{jp}$$
 (D.11)

The condition (j + 1 - 2p = 2q) implies that j is greater than 0 and odd and may therefore be written as (j = 2l + 1), l = 0, 1..., leading to:

$$\bar{A} = \underbrace{\sum_{l=0}^{\infty} \sum_{p=0}^{2l+1} A_{2l+1,p}}_{p=l+1-q}$$
(D.12)

Because q is given, the condition (p = l + 1 - q) implies that p is determined for a given l. Therefore, double summations are unnecessary. Now, this condition also reads as (l = p + q - 1), showing that the smallest value of l for p = 0 is (q - 1) in the first summation. Consequently, (A.12) becomes:

$$\bar{A} = \sum_{l=q-1}^{\infty} A_{2l+1,l+1-q} \qquad q > 0$$
 (D.13)

which identifies with (A.1).

The set (A.1)-(A.10) may be rewritten under another form which, although not used in this book, can be worthwhile as in Gouesbet and Lock [80]. This set gathers the cases when  $j_+$ ,  $j_0$ ,  $j_-$  are odd and even, and reads as:

$$\sum_{j_{+}=m}^{jp} A_{jp} = \sum_{j=0}^{\infty} A_{m-1+2j,j} \qquad m > 0$$
 (D.14)

$$\sum_{j_{-}=m}^{jp} A_{jp} = \sum_{j=0}^{\infty} A_{m+1+2j,j} \qquad m > 0$$
 (D.15)

$$\sum_{j_0=m}^{jp} A_{jp} = \sum_{j=0}^{\infty} A_{m+2j,j} \qquad m > 0 \qquad (D.16)$$

$$\sum_{j_{+}=0}^{jp} A_{jp} = \sum_{j=0}^{\infty} A_{2j+1,j+1}$$
(D.17)

$$\sum_{j=0}^{jp} A_{jp} = \sum_{j=0}^{\infty} A_{2j+1,j}$$
 (D.18)

$$\sum_{j_0=0}^{jp} A_{jp} = \sum_{j=0}^{\infty} A_{2j,j}$$
 (D.19)

$$\sum_{j_{+}=m}^{jp} A_{jp} = \sum_{j=0}^{\infty} A_{|m|+1+2j,|m|+1+j} \qquad m < 0$$
 (D.20)

$$\sum_{j_{-}=m}^{jp} A_{jp} = \sum_{j=0}^{\infty} A_{|m|-1+2j,|m|-1+j} \qquad m < 0$$
 (D.21)

$$\sum_{j_0=m}^{jp} A_{jp} = \sum_{j=0}^{\infty} A_{|m|+2j,|m|+j} \qquad m < 0$$
 (D.22)

## Appendix E

# Useful Relations to Derive the BSCs of Chapter IV

The following relations are required to derive the expressions of the BSCs in terms of finite series:

$$\sum_{m=0}^{\infty} \sum_{n=2m+2q}^{\infty} e = \sum_{n=0}^{\infty} \sum_{m=0}^{\frac{1}{2}(n-2q)} \epsilon(n; 0, 2, ..., 2q - 2)$$
 (E.1)

$$\sum_{m=0}^{\infty} \sum_{n=2q+2m+1}^{\infty} o \sum_{n=1}^{\infty} \sum_{m=0}^{\frac{1}{2}(n-2q-1)} \epsilon(n; 1, 3, ..., 2q-1)$$
 (E.2)

As an example, the demonstration is provided for the first of them, with q=1, i.e.:

$$\sum_{m=0}^{\infty} \sum_{n=2m+2}^{\infty} e = \sum_{n=0}^{\infty} e^{\sum_{m=0}^{\frac{n}{2}-1}} \epsilon(n;0)$$
 (E.3)

The double summation in the l.h.s. may be visualized by using an index table:

which may be directly translated to another equivalent index table:

$$\begin{array}{c|c} n & m \\ \hline 0 & \text{no subscript } m \\ 2 & 0 \\ 4 & 0, 1 \\ 6 & 0, 1, 2 \\ \dots \end{array} \tag{E.5}$$

which may be directly converted to the r.h.s. of (B.3). General demonstrations of Rels (B.1) and (B.2) proceed quite similarly.

# Appendix F Computer Programs

This appendix refers to the computer programs contained in the website connected to this book. The list of computer programs, with some comments, is given below. On the website each code is in a directory where are:

- an excecutable version of the code, under Windows,
- the code sources (DELPHI and FORTRAN)
- a notice on how to use with some examples

Originally, codes have been developed on a PC using Lahey 77, and then Lahey 90 compilers. Also, the codes have been tested on various workstations (Sun Sparkstation, HP, Stardent,...). Nevertheless, some difficulties due to the use of specific compilers could possibly still happen. In such a case, please, inform us. However, to be more easy to use, the versions available at the website have been developed with a DELPHI interface while the computations are carried out by a FORTRAN dll.

### (i) Supermidi.

Supermidi [673], [674], [675] is a computer program for classical LMT based on Lentz algorithm [676]. This algorithm deals with the computations of Bessel functions by using a continuous fraction representation. In 1979, Supermidi could deal with very large particles, up to size parameters typically equal to 10<sup>3</sup>, and with complex refractive index having imaginary parts as high as 10<sup>5</sup>, thus corresponding to the case of perfectly conducting scatter centers. The Lentz algorithm has not been implemented in the GLMT-programs presented below in order to speed up computations, but this could be done if required for specific applications.

(ii) Computer programs for finite series (Chapter V) are also available from the website. Two routines, named GNMTM and GNMTE, to compute the beam shape coefficients  $g_{n,TM}^m$  and  $g_{n,TE}^m$  respectively, are provided. Each one contains ten subroutines handling separately the ten different expressions

depending on n and m. These subroutines are named G1234 if  $m \neq 0$ , in which: 1 is E or 0 if n is even or odd respectively; 2 is E or 0 if m is even or odd respectively; 3 is P or N if m is positive or negative respectively; 4 is TM or TE for BSCs  $g_{n,TM}^m$  and  $g_{n,TE}^m$ , respectively. If m=0, the subroutines are named G104, with the same conventions are above for 1 and 4. Programs are provided with many comments. Exemplifying results obtained with the programs are also available from the website.

(iii) The program GNMF computes the beam shape coefficients  $g_{n,X}^m$  by using the localized approximation in the improved formulation of section VII.4.5. The code is organized as follows. The left part of the window is devoted to input parameters i.e.: the wavelength, the beam waist radius, the location  $X_0$ ,  $Y_0$  and  $Z_0$  and the number of terms to be computed. When the computations are finished, it is possible to directly vizualize the behaviour of the  $g_n^m$  coefficient by selecting the TE or TM by using the radiobox and m value by moving the scrollbar. Figures F.1 and F.2 exemplify such behaviours. Figure F.1 plots the behaviour of  $g_{n,TM}^1$  versus n (1 < n < 300) for a plane wave while figure F.2 plots the behaviour of  $g_{n,TM}^0$  versus n (1 < n < 300) at location  $X_0 = 3\mu m$ ,  $Y_0 = 1.5$  and  $Z_0 = 5\mu m$  in a Gaussian beam ( $w_0 = 10\mu m$  and  $\lambda = 0.5145\mu m$ ).

We now deal with a series of more elaborated computer programs, dealing with full GLMT-computations. The routines are specified for Gaussian beams and the BSCs are evaluated by using the localized approximation. Arbitrary location is considered. Instead of the basic localized approximation, the user may implement other techniques, such as finite series, quadratures, or whatsoever. This would be a fairly trivial task. Also, if the reader wants to study other kinds of beams than Gaussian ones, the only essential task to carry out is to modify the subroutines devoted to the computation of the BSCs. There exist also routines for specific applications of GLMTs, for instance devoted to phase-Doppler systems. Such routines are not included in this book which is aiming to a presentation of the basic GLMT (accompanied by complements), not to the details of all meanders which may be generated by these theories. We then now consider four programs dealing with the GLMT stricto sensu.

(iv) DIAGAUS given below is devoted to the computation of scattering diagrams for a scatterer arbitrarily located in a Gaussian beam. The geometry of the problem is defined in Fig III-1. All geometrical inputs are defined with respect to the particle coordinate system, which is the standard case used in developing the theory. The observation point is located at a distance R from the particle center.

The scattering angle  $\theta$  is in the range  $(\theta_{min}, \theta_{min} + n\theta_{pas})$ . It must be noted that intensity values at  $\theta = 0^{\circ}$  cannot be numerically evaluated, although they are well defined indeed, because the Legendre functions  $\pi_n^0$  (cos  $\theta$ ) tend to infinity when  $\theta \to 0^{\circ}$  (or  $\theta \to 180^{\circ}$ ). The values of cos  $\theta$  in the routine

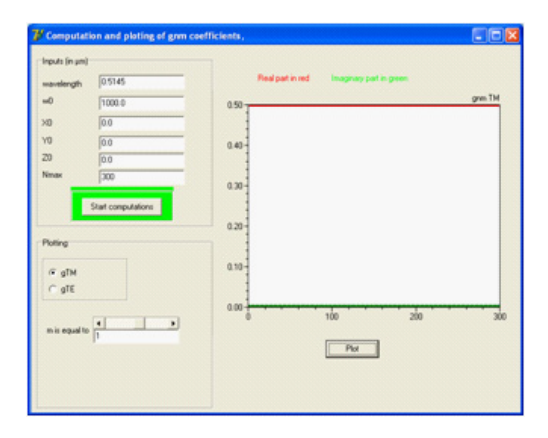


**Fig. F.1.** The interface to compute and display the Beam Shape Coefficient in the Localized Approximation. Example of result for  $g_{n,TM}^1$  for a plane wave.

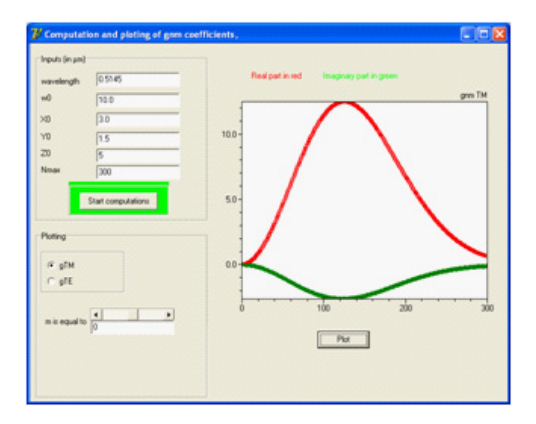


**Fig. F.2.** Example of result for  $g_{n,TM}^0$  and an off-center, off-axis location in a Gaussian beam.

are bounded to remain located in the interval [-0.99999, 0.99999]. The far field computation can be carried out for two complementary configurations: 3D or 2D computations.

• Computation of 3D scattering diagrams: Figures F.3, F.4 and F.5 display some 3D views. The screen is organized in three parts: the input data (wavelength, beam waist, position X, Y, Z, the complex refractive index of the particle, external refractive index, and particle diameter as well as the number of computation points in  $\theta$  and  $\varphi$  directions and the visualization distance), a representation of the scattering geometry where by convention the converging part of the beam is in pink while the diverging part is in green, a representation of the scattered light where the color (red or blue) codes the polarisation of the scattered light. By

clicking left with the mouse in any part of the figure and moving it, it is possible to observe the scattering diagrams from different locations. Such 3D views are displayed in figures F.3.F.5

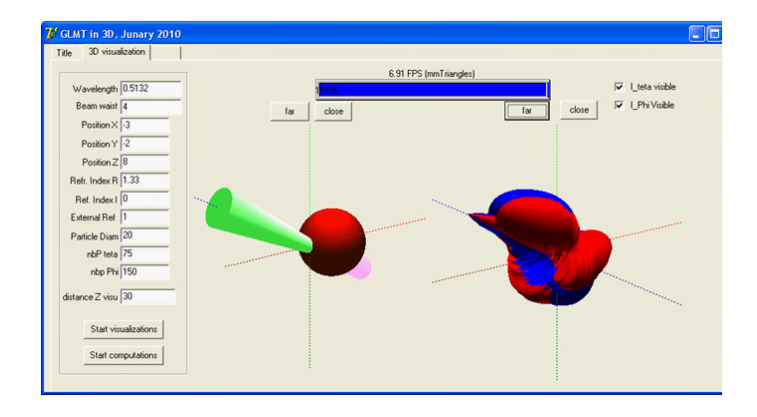


Fig. F.3. Example of a 3D diagram.

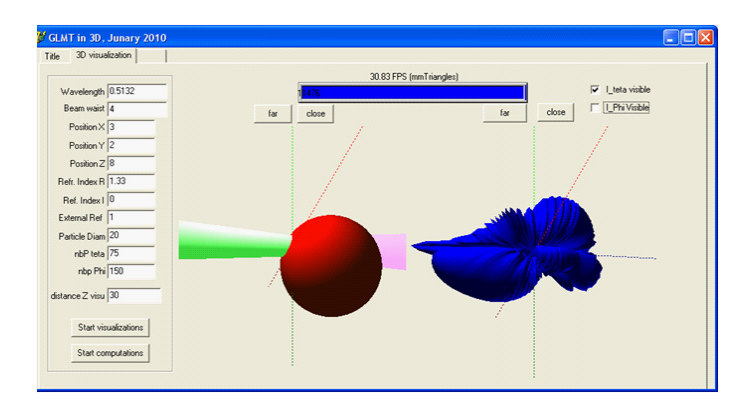


Fig. F.4. Example of a 3D diagram.

- Computation of 2D scattering diagrams. Examples of 2D diagrams are displayed in figures F.6-F.8
- (v) NFORWARD computes properties of the near-forward scattering, taking into account the interference between the incident beam and the scattered light. Examples of forward diagrams, including the interferences between the Gaussian beam and the scattered light are displayed in figures F.94F.111

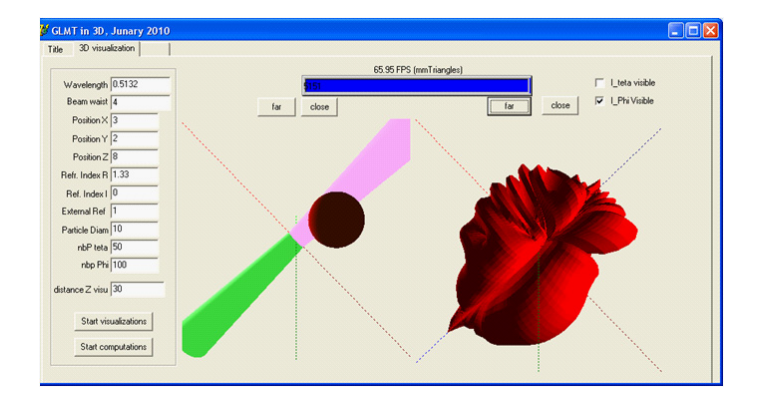


Fig. F.5. Example of input and output screens for 3D computation.

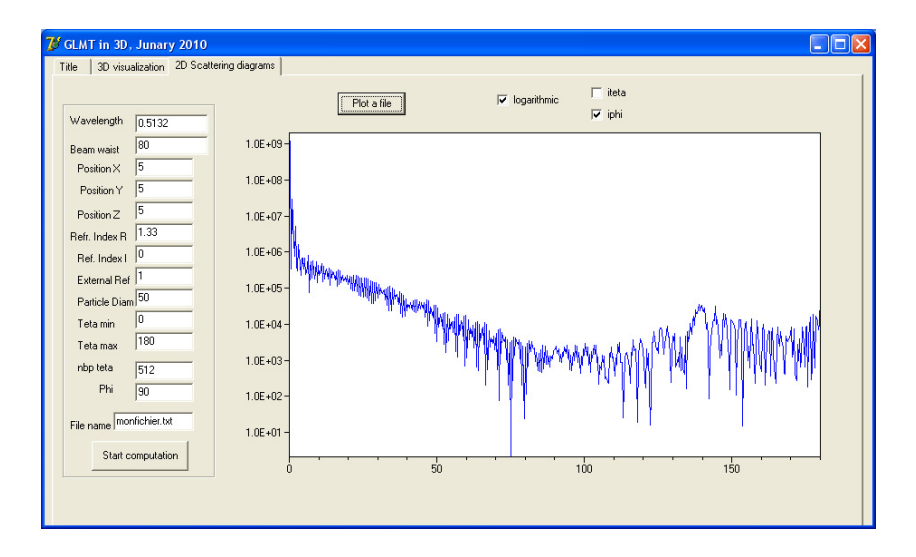


Fig. F.6. Example of a 2D diagram

(vi) Next, CROSS\_SEC computes the cross-sections of extinction, scattering, and absorption, for a spherical particle arbitrarily located in a Gaussian beam. Figure F.12 is an example of input and output.

(vii) The program PRESSION computes the radiation pressure versus the particle location in the Gaussian beam or the particle diameter.

Figure F.13 displays the screen for computations of the pressure versus the particle location. The screen is organized in two parts: input parameters and result vizualization. The input parameters are: beam waist radius, incident wavelength, particle refractive index, laser power, light velocity, particle density, surrounding medium density and particle radius. Then the user must

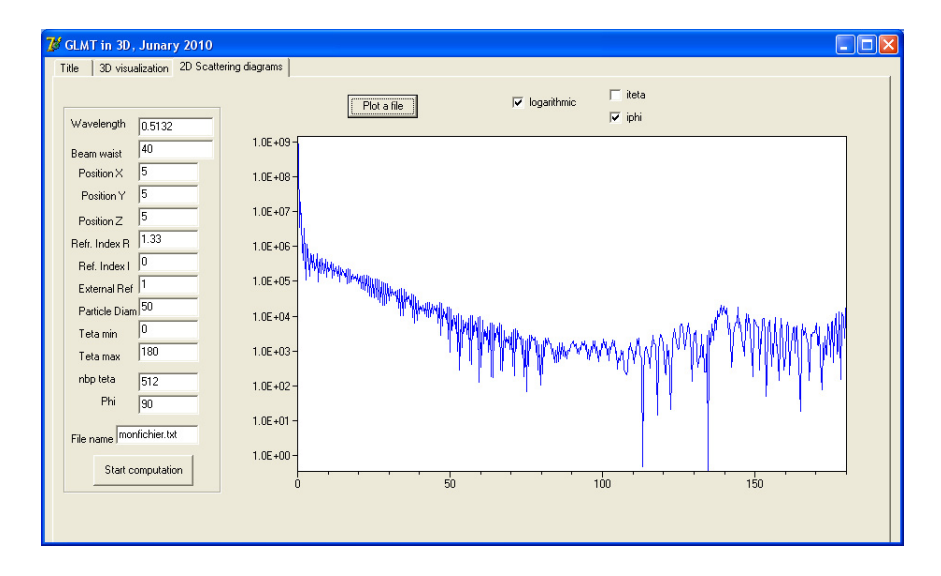


Fig. F.7. Example of a 2D diagram

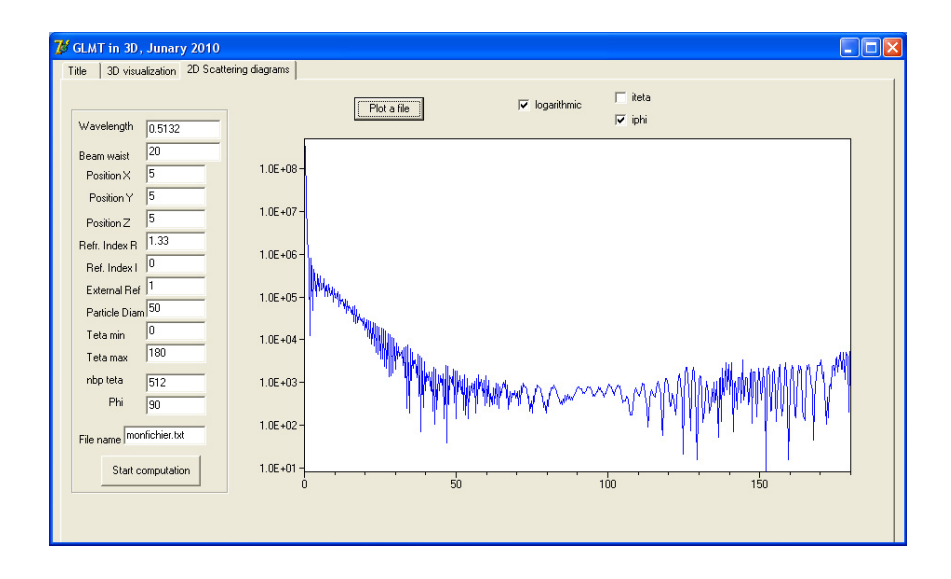
select if the study will be along the X,Y or Z direction. If the X-direction is selected, the user will specify the  $Y_0,Z_0$  positions, the range of  $X_0$  to study as well as the step in  $X_0$ . The user will also give a name for the results file. The extension (.txt) will be automatically added by the software. For this option, the result file is made of 11 columns. The first column is the ordinate along the axis under study. The columns 2 to 4 correspond to the radiation pressure cross-sections  $C_{pr,x}$ ,  $C_{pr,y}$ , and  $C_{pr,z}$ . The columns 5, 6, and 7 are the force components  $F_x$ ,  $F_y$ , and  $F_z$ , corresponding to the laser power defined by the user in the input parameters. The column 8 is the force towards the beam axis, as a combination of the forces  $F_x$  and  $F_y$ . The column 9 corresponds to the laser power to be used to exactly balance the particle weight, for this particle location. The columns 10 and 11 give the force components  $F_x$  and  $F_y$  for the laser power given in column 9.

The relation between the force components and the radiation pressure cross-sections is given by ([17], p. 14):

$$F_i = \frac{I_0 C_{pr,i}}{c} \tag{F.1}$$

where c is the velocity of light in the surrounding medium, and i stands for x, y, or z. Furthermore, for a Gaussian beam, the relation between the total intensity and the intensity on the axis is given by:

$$I_{0,axis} = \frac{2 I_{0,total}}{\pi w_0^2}$$
 (F.2)



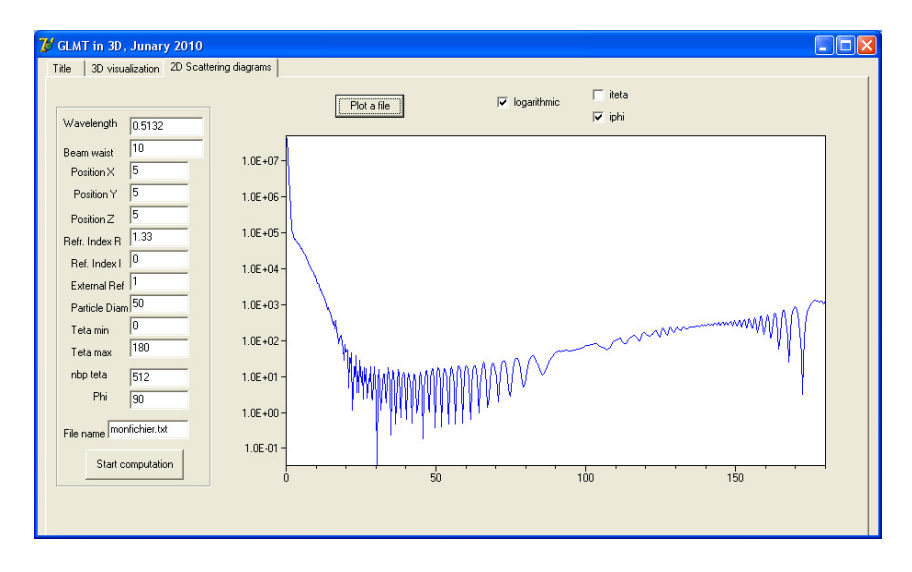


Fig. F.8. Examples of far field scattering diagrams computed for the same particle. The parameter is the beam waist size.

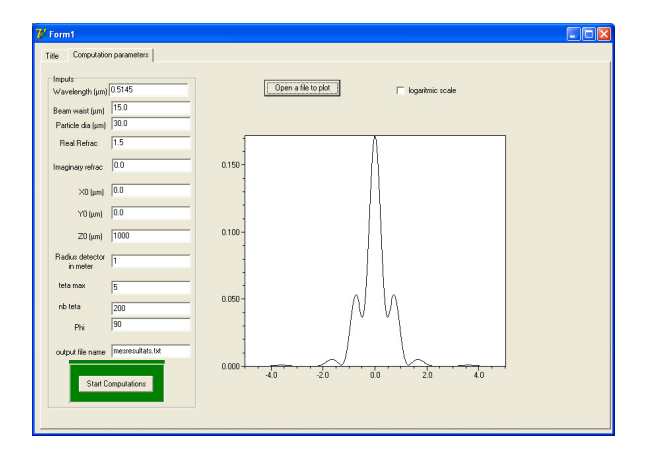


Fig. F.9. Interaction between a Gaussian beam and the light scattered in forward direction: linear scale, axis particle location.

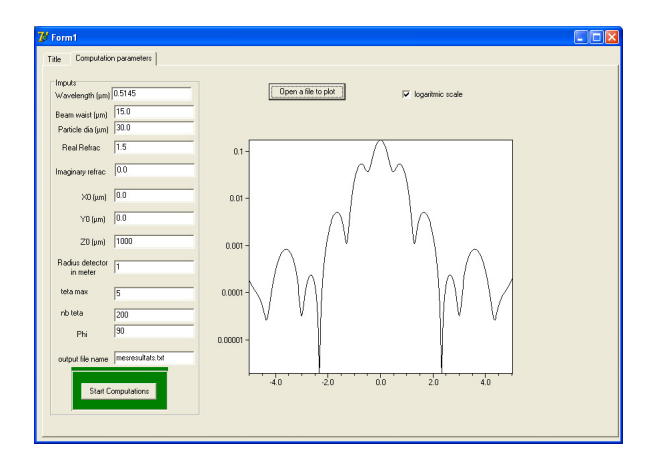


Fig. F.10. Interaction between a Gaussian beam and the light scattered in forward direction: logarithmic scale, axis particle location.

Then the relation between the radiation pressure cross-sections and the forces used in the program is:

$$F_{i} = \frac{2 I_{0,total} C_{pr,i}}{\pi w_{0}^{2} c}$$
 (F.3)

When the computations are finished, the results can be plotted. A radiobox permits to select the quantities to be plotted: cross-sections, forces, combined forces or laser power.

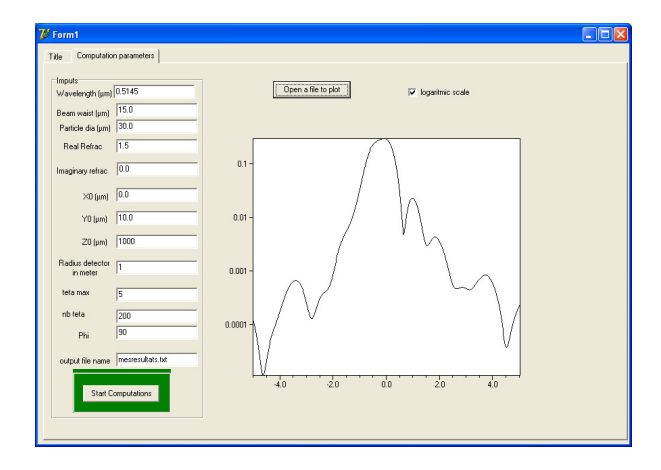


Fig. F.11. Interaction between a Gaussian beam and the light scattered in forward direction: logarithmic scale, off-axis particle location.

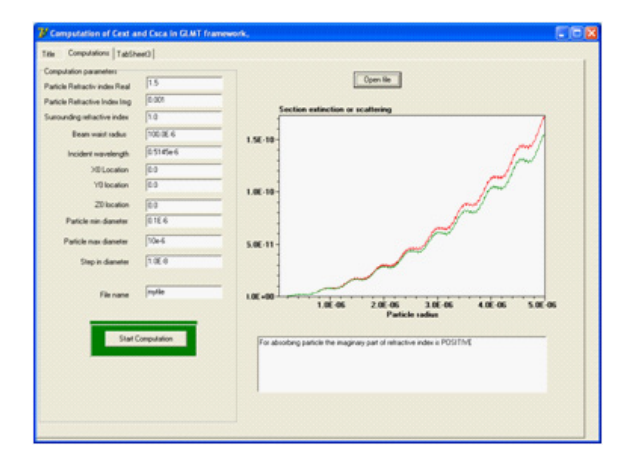


Fig. F.12. Example of input and output for scattering cross-section.

Figure  $\boxed{\textbf{F.14}}$  displays the screen for computations of the pressure versus the particle location. The screen is organized in two parts: input parameters and result vizualization. The input parameters are : beam waist radius, incident wavelength, surrounding refractive index, particle refractive index, laser power, light velocity, particle density, surrounding medium density, gravity constant and the  $X_0, Y_0$  and  $Z_0$  particle location. The range of particle radius as well as the radius step will also be given by the user. Therefore, the program asks for an output file name. The two output files then take, as before, names reading as  $.\mathbf{par}$  and  $.\mathbf{dat}$ . The first file with the .par extension contains the input parameters, while the second one with the .dat extention

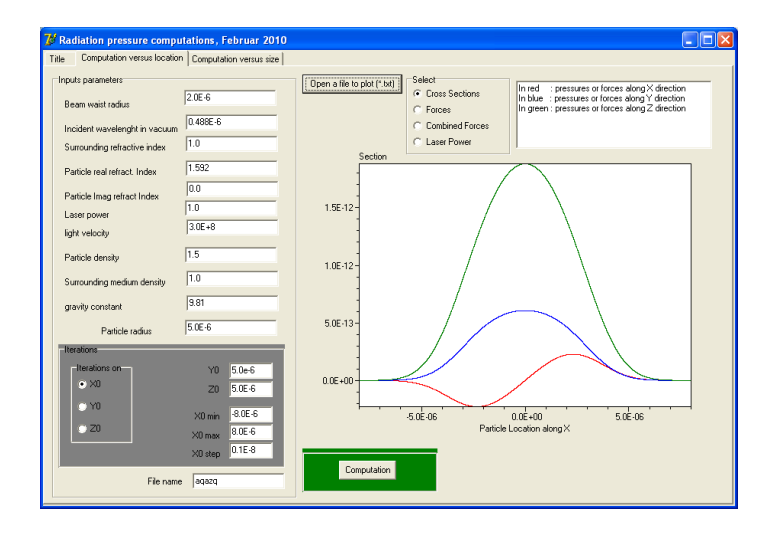


Fig. F.13. Example of a screen when computing the pressure versus the particle location.

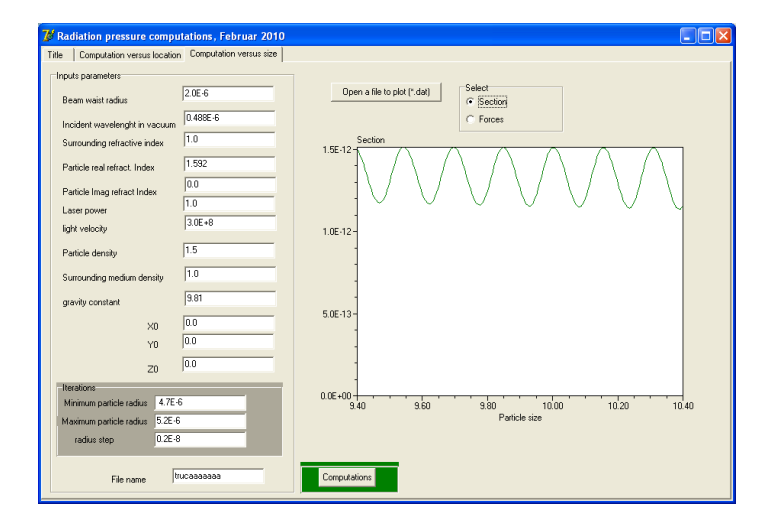


Fig. F.14. Example of a screen when computing the pressure versus the particle diameter.

contains the results, under the form of 7 columns. The first column is the particle diameter, the columns 2, 3 and 4 correspond to  $C_{pr,x}$ ,  $C_{pr,y}$  and  $C_{pr,z}$ , and the last columns 5, 6, and 7 correspond to the force components  $F_x$ ,  $F_y$  and  $F_z$ .

We also provide:

(viii) a commented subroutine to compute the scattering coefficients  $a_n$  and  $b_n$ .

Finally, the website contains some examples of movies showing the development of the interaction between ultra-short pulses and some scatterers (homogeneous and coated spheres).

## References

- [1] Gouesbet, G., Gréhan, G.: Sur la généralisation de la théorie de Lorenz-Mie. Journal of Optics 13(2), 97–103 (1982)
- [2] Gouesbet, G., Maheu, B., Gréhan, G.: Light scattering from a sphere arbitrarily located in a Gaussian beam, using a Bromwich formulation. Journal of the Optical Society of America A 5(9), 1427–1443 (1988)
- [3] Gréhan, G., Gouesbet, G., Naqwi, A., Durst, F.: Particle trajectory effects in phase-Doppler systems: computations and experiments. Particle and Particle Systems Characterization 10, 332–338 (1993)
- [4] Gréhan, G., Gouesbet, G., Naqwi, A., Durst, F.: Trajectory ambiguities in phase-Doppler systems: study of a near-forward and a near-backward geometry. Particle and Particle Systems Characterization 11, 133–144 (1994)
- [5] Sagan, C., Polak, J.B.: Anisotropic nonconservative scattering and the clouds of Venus. J. of Geophys. Res. 72(2), 469–477 (1967)
- [6] Hansen, J.E., Hovenier, J.W.: Interpretation of the polarization of Venus. J. Atm. Sci. 31, 1137–1160 (1974)
- [7] Reynolds, L., Johnson, C., Ishimaru, A.: Diffuse reflectance of a finite blood medium: applications to the modelling of fiber optics catheters. Appl. Opt. 15(9), 2059–2067 (1976)
- [8] Groenhuis, R.A.J., Ten Bosch, J.J., Ferwerda, H.A.: Scattering and absorption of turbid materials determined from reflection measurements. Appl. Opt. 22(16), 2456–2462, 2463–2467 (1983)
- [9] Langerholc, J.: Beam broadening in dense scattering media. Appl. Opt. 21(9), 1593-1598 (1982)
- [10] Ryde, J.W.: The scattering of light by turbid media: Part 1. Proc. Roy. Soc. A131, 451–464 (1931)
- [11] Ryde, J.W., Cooper, B.S.: The scattering of light by turbid media: Part 2. Proc. Roy. Soc. A131, 464–475 (1931)
- [12] Kubelka, P., Munk, F.: Ein Beitrag zur Optik der Farbenstriche. Zeit. für Tech. Phys. 11A, 593–601 (1931)
- [13] Steele, F.A.: The optical characteristics of paper. Paper Trade J., 37–42 (1935)
- [14] Kastler, A.: La diffusion de la lumière par les milieux troubles, Herman et Cie (1952)
- [15] Stratton, J.A.: Electromagnetic theory. McGraw-Hill Book Company, New York (1941/1961)

[16] Born, M., Wolf, E.: Principles of optics, 3rd edn. Pergamon Press, Oxford (1965)

- [17] van de Hulst, H.C.: Light scattering by small particles. Wiley, New York (1957)
- [18] van de Hulst, H.C.: Multiple light scattering, vol. 1 & 2. Academic Press, London (1980)
- [19] Kerker, M.: The scattering of light and other electromagnetic radiation. Academic Press, London (1969)
- [20] Deirmendjian, D.: Electromagnetic scattering on spherical polydispersions. Elsevier, Amsterdam (1969)
- [21] Bayvel, L.P., Jones, A.R.: Electromagnetic scattering and its applications. Applied Science Publishers (1981)
- [22] Bohren, C.F., Huffman, D.: Absorption and scattering of light by small particles. John Wiley, New York (1983)
- [23] Kerker, M.: The scattering of light and other electromagnetic radiation. Academic Press, New York (1969)
- [24] Chandrasekhar, S.: Radiative transfer. Oxford University Press, Oxford (1950)
- [25] Kortüm, G.: Reflectance spectroscopy. Springer, Heidelberg (1969)
- [26] Mie, G.: Beiträge zur Optik trüben Medien speziell kolloidaler Metalösungen. Ann. der Phys. 25, 377–452 (1908)
- [27] Lorenz, L.: Lysbevaegelsen i og uden for en af plane Lysbølger belyst Kulge. Vidensk. Selk. Skr. 6, 1–62 (1890)
- [28] Lorenz, L.: Sur la lumière réfléchie et réfractée par une sphère transparente, Lib. Lehmann et Stage, Oeuvres scientifiques de L. Lorenz, revues et annotées par H. Valentiner (1898)
- [29] Logan, N.A.: Survey of some early studies of the scattering of plane waves by a sphere. Proceedings of the IEEE, 773–785 (1965); Kerker, M. (ed.): Reprinted in selected papers on light scattering, part one. SPIE, vol. 951, pp. 3–15 (1988)
- [30] Kragh, H.: Ludvig Lorenz and the nineteenth century optical theory. The work of a great Danish scientist. Appl. Opt. 30(33), 4688–4695 (1991)
- [31] Kragh, H.: Ludvig V. Lorenz: his contributions to optical theory and light scattering by spheres. In: Hirleman, D. (ed.) Proceedings of the 2nd International Symposium on Optical Particle Sizing, pp. 1–6. Arizona State University (1990)
- [32] Logan, N.A.: Survey of some early studies of the scattering of plane waves by a sphere. In: Hirleman, D. (ed.) Proceedings of the 2nd International Symposium on Optical Particle Sizing, pp. 7–15. Arizona State University (1990)
- [33] Debye, P.: Der Lichtdruck auf Kugeln von beliebigem Material. Ann. der Phys. 4(30), 57–136 (1909)
- [34] Duhem, P.: La théorie physique, son objet, sa structure. English version: the aim and structure of physical theory. Librairie philosophique J. Vrin (1997)
- [35] Quine, W.V.: La poursuite de la vérité. French translation of "Pursuit of Truth". Editions du Seuil, Paris (1993)
- [36] Quine, W.V.: Le mot et la chose. French translation of "Word and Object". Flammarion (1977)
- [37] Quine, W.V.: On empirically equivalent systems of the world. Erkenntnis 9, 313–328 (1975)

[38] Gouesbet, G.: From theories by Lorenz and Mie to ontological underdetermination of theories by experiment. In: Wriedt, T., Hergert, W. (eds.) Mie theory 1908-2008 (to be published by Springer)

- [39] Gouesbet, G.: Phénoménes de diffusion et de thermodiffusion des espéces neutres dans un plasma d'argon et d'hélium. Rouen University, State thesis (1977)
- [40] Gouesbet, G., Trinité, M.: Anémométrie Doppler-laser haute puissance dans un jet de plasma. Letters in Heat and Mass Transfer 4, 141–148 (1977)
- [41] Gouesbet, G., Trinité, M.: Anémométrie laser-Doppler interférentielle dans une torche á plasma haute-fréquence. Journal of Physics E: Scientific Instruments 10, 1009–1016 (1977)
- [42] Gouesbet, G.: A review on measurements of particle velocities and diameters by laser techniques, with special emphasis on thermal plasmas. Plasma Chemistry and Plasma Processing 5(2), 91–117 (1985)
- [43] Gouesbet, G.: Optical sizing, with emphasis on simultaneous measurements of velocities and sizes of particles embedded in flows. In: Soloukhin, R.I., Afgan, N.H. (eds.) Measurement techniques in heat and mass transfer, pp. 27–50. Springer, Heidelberg (1985)
- [44] Chevaillier, J.-P., Fabre, J., Gréhan, G., Gouesbet, G.: Comparison of diffraction theory and generalized Lorenz-Mie theory for a sphere located on the axis of a laser beam. Applied Optics 29(9), 1293–1298 (1990)
- [45] Gouesbet, G., Berlemont, A., Picart, A.: On the dispersion of discrete particles by continuous turbulent motions. Extensive discussion of the Tchen's theory, using a two-parameter family of Lagrangian correlation functions. Phys. of Fluids 27(4), 827–837 (1984)
- [46] Picart, A., Berlemont, A., Gouesbet, G.: Modelling and predicting turbulence fields and the dispersion of discrete particles transported by turbulent flows. Int. J. Multiphase Flows 12(2), 237–261 (1986)
- [47] Desjonquères, P., Gouesbet, G., Berlemont, A., Picart, A.: Dispersion of discrete particles by continuous turbulent motions. New results and discussions. Physics of Fluids 29(7), 2147–2151 (1986)
- [48] Berlemont, A., Desjonquères, P., Gouesbet, G.: Particle Lagragian simulation in turbulent flows. Int. J. Multiphase Flows 16(1), 19–34 (1990)
- [49] Berlemont, A., Granchet, M.S., Gouesbet, G.: On the Lagrangian simulation of turbulence influence on droplet evaporation. Int. J. Heat Mass Transfer 34(11), 2805–2812 (1991)
- [50] Berlemont, A., Granchet, M.S., Gouesbet, G.: Heat and mass transfer coupling between vaporizing droplets and turbulence using a Lagrangian approach. Int. J. Heat and Mass Transfer 38(16), 3023–3034 (1995)
- [51] Gouesbet, G., Gréhan, G. (eds.): Proceedings of the International Symposium: Optical Particle Sizing, Theory and Practice, held in Rouen, May 12-15, 1987. Plenum Publishing Corporation (1988)
- [52] Hirleman, D. (ed.): Proceedings of the 2nd International Congress on Optical Particle Sizing. Arizona State University (1990)
- [53] Maeda, M.: Optical Particle Sizing: Theory and Practice. In: Proceedings of the third symposium held in Yokohama (1993)
- [54] Durst, F., Domnick, J.: 4th International Congress Optical Particle Sizing, Proceedings of PARTEC 1995, Nürnberg, Germany, March 21-23 (1995)
- [55] Ashkin, A.: Atomic-beam deflection by resonance-radiation pressure. Phys. Rev. Lett. 24, 1321–1324 (1970)

[56] Roosen, G., Imbert, C.: Optical levitation by means of two horizontal laser beams: a theoretical and experimental study. Phys. Lett. 59A(1), 6–8 (1976)

- [57] Gréhan, G., Gouesbet, G.: Optical levitation of a single particle to study the theory of the quasi-elastic scattering of light. Applied Optics 19(15), 2485– 2487 (1980)
- [58] Guilloteau, F., Gréhan, G., Gouesbet, G.: Optical levitation experiments to assess the validity of the generalized Lorenz-Mie theory. Applied Optics 31(15), 2942–2951 (1992)
- [59] Chew, H., Kerker, M., Cooke, D.D.: Light scattering in converging beams. Opt. Lett. 1, 138–140 (1977)
- [60] Chew, H., Kerker, M., Cooke, D.D.: Electromagnetic scattering by a dielectric sphere in a diverging radiation field. Phys. Rev. A. 16, 320–323 (1977)
- [61] Morita, N., Tanaka, T., Yamasaki, T., Nakanishi, Y.: Scattering of a beam wave by a spherical object. IEEE Trans. Ant. Prop. AP16(6), 724–727 (1968)
- [62] Tsai, W.C., Pogorzelski, R.J.: Eigenfunction solution of the scattering of beam radiation fields by spherical objects. Journal of the Optical Society of America A 65, 1457–1463 (1975)
- [63] Tam, W.G.: Off beam axis scattering by spherical particles. Appl. Opt. 16(8), 2016–2018 (1977)
- [64] Tam, W.G., Corriveau, R.: Scattering of electromagnetic beams by spherical objects. J. Opt. Soc. Am. 68(6), 763–767 (1978)
- [65] Casperson, L.W., Yeh, C.: Rayleigh-Debye scattering with focused laser beams. Appl. Opt. 17(10), 1637–1643 (1978)
- [66] Colak, S., Yeh, C., Casperson, L.W.: Scattering of focused beams by tenuous particles. Applied Optics 18, 294–302 (1979)
- [67] Yeh, C.W., Colak, S., Barber, P.W.: Scattering of sharply focused beam by arbitrarily shaped dielectric particles: an exact solution. Applied Optics 21, 4426–4433 (1982)
- [68] Kim, J.S., Lee, S.S.: Radiation pressure on a dielectric sphere in a Gaussian laser beam. Optica Acta 29, 801–806 (1982)
- [69] Kim, J.S., Lee, S.S.: Scattering of laser beam and the optical potential well for a homogeneous sphere. Journal of the Optical Society of America 73, 303–312 (1983)
- [70] Barton, J.P., Alexander, D.R., Schaub, S.A.: Internal and near-surface electromagnetic fields for a spherical particle irradiated by a focused laser beam. Journal of Applied Physics 64(4), 1632–1639 (1988)
- [71] Gréhan, G.: Nouveaux progrès en théorie de Lorenz-Mie. Application à la mesure de diamètre de particules dans des écoulements. PhD thesis, Rouen University (1980)
- [72] Gouesbet, G., Gréhan, G.: Report TTI/GG/80/06/IV, Laboratoire de Thermodynamique. Technical report, University of Rouen (1980)
- [73] Gouesbet, G., Gréhan, G.: Advances in quasi-elastic scattering of light with emphasis on simultaneous measurements of velocities and sizes of particles embedded in flows. In: AIAA 16th Thermophysics Conference. Palo-Alto, California, Paper 81-1124, June 23-25 (1981)
- [74] Gouesbet, G.: Partial wave expansions and properties of axisymmetric light beams. Applied Optics 35(9), 1543–1555 (1996)
- [75] Davis, L.W.: Theory of electromagnetic beams. Physical Review 19, 1177– 1179 (1979)

[76] Gouesbet, G., Gréhan, G., Maheu, B.: Scattering of a Gaussian beam by a Mie scatter center, using a Bromwich formulation. Journal of Optics (Paris) 16(2), 83–93 (1985); Republished in Kerker, M. (ed.): selected papers on light scattering. SPIE Milestone series, vol. 951, pp. 83–93 (1988)

- [77] Gouesbet, G., Maheu, B., Gréhan, G.: The order of approximation in a theory of the scattering of a Gaussian beam by a Mie scatter center. Journal of Optics (Paris) 16(5), 239–247 (1985); Republished in Kerker, M. (ed.): selected papers on light scattering. SPIE Milestone series, vol. 951 (1988)
- [78] Gréhan, G., Maheu, B., Gouesbet, G.: Scattering of laser beams by Mie scatter centers: numerical results using a localized approximation. Applied Optics 25(19), 3539–3548 (1986)
- [79] Lock, J.A., Gouesbet, G.: Rigorous justification of the localized approximation to the beam shape coefficients in generalized Lorenz-Mie. I.On-axis beams. Journal of the Optical Society of America A 11(9), 2503–2515 (1994)
- [80] Gouesbet, G., Lock, J.A.: Rigorous justification of the localized approximation to the beam shape coefficients in generalized Lorenz-Mie theory. II.Off-axis beams. Journal of the Optical Society of America A 11(9), 2516–2525 (1994)
- [81] Maheu, B., Gréhan, G., Gouesbet, G.: Generalized Lorenz-Mie theory: first exact values and comparisons with the localized approximation. Applied Optics 26(1), 23–26 (1987)
- [82] Maheu, B., Gréhan, G., Gouesbet, G.: Laser beam scattering by individual spherical particles: theoretical progress and applications to optical sizing. Journal of Particle Characterization 4, 141–146 (1987)
- [83] Maheu, B., Gréhan, G., Gouesbet, G.: Diffusion de la lumière par une sphère dans le cas d'un faisceau d'extension finie -1. Théorie de Lorenz-Mie généralisée, les coefficients  $g_n$  et leur calcul numérique. Journal of Aerosol Science 19(1), 47–53 (1988)
- [84] Gréhan, G., Maheu, B., Gouesbet, G.: Diffusion de la lumière par une sphère dans le cas d'un faisceau d'extension finie -2. Théorie de Lorenz-Mie généralisée: application à la granulométrie optique. Journal of Aerosol Science 19(1), 55–64 (1988)
- [85] Corbin, F., Gréhan, G., Gouesbet, G.: Interaction between a sphere and a Gaussian beam: computations on a micro-computer. Journal of Particle and Particle Systems Characterization 5(3), 103–108 (1988)
- [86] Wriedt, T.: Mie theory 1908, on the mobile phone 2008. Journal of Quantitative Spectroscopy and Radiative Transfer 109, 1543–1548 (2008)
- [87] Gouesbet, G., Gréhan, G., Maheu, B.: Computations of the  $g_n$  coefficients in the generalized Lorenz-Mie theory using three different methods. Applied Optics 27(23), 4874–4883 (1988)
- [88] Gouesbet, G., Maheu, B., Gréhan, G.: Scattering of a Gaussian beam by a sphere using a Bromwich formulation: case of an arbitrary location. Journal of Particle and Particle Characterization 5, 1–8 (1988)
- [89] Maheu, B., Gouesbet, G., Gréhan, G.: A concise presentation of the generalized Lorenz-Mie theory for arbitrary location of the scatterer in an arbitrary incident profile. Journal of Optics (Paris) 19(2), 59–67 (1988)
- [90] Gouesbet, G., Gréhan, G., Maheu, B.: Generalized Lorenz-Mie theory and applications to optical sizing. In: Chigier, N. (ed.) Combustion measurements, pp. 339–384. Hemisphere Publishing Corporation (1991)

[91] Gouesbet, G.: Generalized Lorenz-Mie theory and applications. Particle and Particle Systems Characterization 11, 22–34 (1994)

- [92] Gouesbet, G., Gréhan, G.: Generalized Lorenz-Mie theories, from past to future. Atomization and Sprays 10(3-5), 277–333 (2000)
- [93] Gouesbet, G.: Quasi-elastic light scattering and applications to optical sizing. In: Combustion-flow Diagnostics, pp. 291–304. Kluwer Academic Publishers, Dordrecht (1992)
- [94] Gouesbet, G., Maheu, B., Gréhan, G.: Particle diagnosis in multiphase media. Pure and Applied Chemistry 64(11), 1865–1869 (1992)
- [95] Horvath, H. (ed.): Light scattering: Mie and more, in Journal of Quantitative Spectroscopy and Radiative Transfer (2009)
- [96] Mischenko, M.I., Travis, L.D.: Gustav Mie and the evolving discipline of electromagnetic scattering by particles. Bulletin of the American Meteorological Society (2009) (in press)
- [97] Hough, J.H. (ed.): 11th conference on electromagnetic and light scattering by nonspherical particles, in Journal of Quantitative Spectroscopy and Radiative Transfer (2009)
- [98] Lock, J.A., Gouesbet, G.: Generalized Lorenz-Mie theory and applications. Journal of Quantitative Spectroscopy and Radiative Transfer 110, 800–807 (2009) (Invited Review Paper)
- [99] Gouesbet, G.: Generalized Lorenz-Mie theories, the third decade: a perspective. Journal of Quantitative Spectroscopy and Radiative Transfer 110, 1223–1238 (2009)
- [100] Wriedt, T.: A review of elastic light scattering theories. Particle and Particle Systems Characterization 15, 67–74 (1998)
- [101] Wriedt, T., Hellmers, J.: New scattering information portal for the lightscattering community. Journal of Quantitative Spectroscopy and Radiative Transfer 109(8), 1536–1542 (2008)
- [102] Gouesbet, G.: Expansions in free space of arbitrary quantum wavepackets, quantum laser beams, and Gaussian quantum (on-axis and off-axis) laser beam in terms of free spherical waves. Particle and Particle Systems Characterization 22, 38–44 (2005)
- [103] Gouesbet, G., Lock, J.A.: Quantum arbitrary shaped beam revisited. Optics Communications 273, 296–305 (2007)
- [104] Gouesbet, G.: Asymptotic quantum elastic generalized Lorenz-Mie theory. Optics Communications 266, 704–709 (2006)
- [105] Gouesbet, G.: Asymptotically quantum inelastic generalized Lorenz-Mie theory. Optics Communications 278, 215–220 (2007)
- [106] Gouesbet, G.: Cross-sections in Lorenz-Mie theory and quantum scattering: formal analogies. Optics Communications 231, 9–15 (2004)
- [107] Gouesbet, G.: A transparent macroscopic sphere is cross-sectionnally equivalent to a superposition of two quantum-like radial potentials. Optics Communications 266, 710–715 (2006)
- [108] Gouesbet, G.: Electromagnetic scattering by an absorbing macroscopic sphere is cross-sectionnally equivalent to a superposition of two effective quantum processes. Journal of Optics A: Pure and Applied Optics 9, 369–375 (2007)
- [109] Gouesbet, G.: On the optical theorem and non plane wave scattering in quantum mechanics. Journal of Mathematical Physics 50, Article 112302, 1–5 (2009)

[110] Petit, R.: Ondes électromagnétiques en radio-électricité et en optique, Masson, Paris (1989)

- [111] Dettwiller, L.: Qu'est-ce que l'optique géométrique? Fondements et applications, Dunod (1990)
- [112] Petit, R.: L'outil mathématique, Masson (1987)
- [113] Gouesbet, G., Gréhan, G.: Corrections for Mie theory given in 'the scattering of light and other electromagnetic radiation': comments. Applied Optics 23(24), 4462–4464 (1984)
- [114] Poincelot, P.: Précis d'électromagnétisme théorique, Masson (1965)
- [115] Winogradski, J.: Les méthodes tensorielles de la physique. 1. Calcul tensoriel dans un continuum amorphe; 2. Calcul tensoriel dans un continuum structuré. Masson (1979/1987)
- [116] Morse, P.M., Feshbach, H.: Methods of Theoretical Physics. McGraw-Hill, New York (1953)
- [117] Gouesbet, G., Gréhan, G.: Interaction between shaped beams and an infinite cylinder, including a discussion of Gaussian beams. Particle and Particle Systems Characterization 11, 299–308 (1994)
- [118] Gouesbet, G., Gréhan, G.: Interaction between a Gaussian beam and an infinite cylinder with the use of non-sigma-separable potentials. Journal of the Optical Society of America A 11(12), 3261–3273 (1994)
- [119] Gouesbet, G.: Interaction between Gaussian beams and infinite cylinders, by using the theory of distributions. Journal of Optics (Paris) 26(5), 225–239 (1995)
- [120] Gouesbet, G.: Scattering of a first-order Gaussian beam by an infinite cylinder with arbitrary location and arbitrary orientation. Particle and Particle Systems Characterization 12, 242–256 (1995)
- [121] Gouesbet, G.: The separability theorem revisited with applications to light scattering theory. Journal of Optics (Paris) 26(3), 123–135 (1995)
- [122] Schwartz, L.: Méthodes mathématiques pour les sciences physiques. Hermann (1965)
- [123] Roddier, F.: Distributions et transformations de Fourier. McGraw-Hill, New York (1978)
- [124] Lenglart, E., Gouesbet, G.: The separability "theorem" in terms of distributions with discussion of electromagnetic scattering theory. Journal of Mathematical Physics 37(9), 4705–4710 (1996)
- [125] Bromwich, T.J.: Electromagnetic waves. Phil. Mag. 38, 143–164 (1919)
- [126] Borgnis, F.E.: Elektromagnetische Eigenschwingungen dielektrischer Raüme. Ann. der Phys. 35, 359–384 (1939)
- [127] Lock, J.A.: Contribution of high-order rainbows to the scattering of a Gaussian laser beam by a spherical particle. Journal of the Optical Society of America A 10(4), 693–706 (1993)
- [128] Gouesbet, G., Gréhan, G.: Generalized Lorenz-Mie theory for a sphere with an eccentrically located spherical inclusion. Journal of Modern Optics 47(5), 821–837 (2000)
- [129] Gouesbet, G., Gréhan, G.: Generalized Lorenz-Mie theory for assemblies of spheres and aggregates. Journal of Optics A: Pure and Applied Optics 1, 706-712 (1999)
- [130] Robin, L.: Fonctions sphériques de Legendre et fonctions sphéroïdales, vol. 1, 2, 3. Gauthiers-Villars (1957)

[131] Arfken, G.: Mathematical methods for physicists. Academic Press, London (1976)

- [132] Wang, Z.X., Guo, D.R.: Special functions. World Scientific, Singapore (1989)
- [133] Watson, G.N.: A treatise of the theory of Bessel functions, 2nd edn. Cambridge at the University Press, Cambridge (1962)
- [134] Gouesbet, G., Letellier, C., Ren, K.F., Gréhan, G.: Discussion of two quadrature methods of evaluating beam shape coefficients in generalized Lorenz-Mie theory. Applied Optics 35(9), 1537–1542 (1996)
- [135] Ren, K.F., Gouesbet, G., Gréhan, G.: Integral localized approximation in generalized Lorenz-Mie theory. Applied Optics 37(19), 4218–4225 (1998)
- [136] Courant, D., Hilbert, D.: Methods of mathematical physics, vol. 1. Interscience Publishers Ins., Hoboken (1966)
- [137] Barton, J.P., Alexander, D.R., Schaub, S.A.: Theoretical determination of net radiation force and torque for a spherical particle illuminated by a focused laser beam. Journal of Applied Physics 66(10), 4594–4602 (1989)
- [138] Barton, J.P., Ma, W., Schaub, S.A., Alexander, D.R.: Theoretical determination of the electromagnetic fields for a laser beam incident upon two adjacent spherical particles of arbitrary arrangement. In: Hirleman, D. (ed.) Proceedings of the 2nd International Symposium on Optical Particle Sizing, pp. 50–53. Arizona State University (1990)
- [139] Barton, J.P., Alexander, D.R.: Electromagnetic fields for an irregular shaped, near-spherical particle illuminated by a focused laser beam. J. Appl. Phys. 69, 7973 (1991)
- [140] Barton, J.P., Alexander, D.R., Schaub, S.A.: Internal fields of a spherical particle illuminated by a tightly focused laser beam: focal point positioning effects at resonance. Journal of Applied Physics 65(8), 2900–2906 (1989)
- [141] Lock, J.A.: Partial-wave expansions of angular spectra of plane waves. Journal of the Optical Society of America A 23(11), 2803–2809 (2006)
- [142] Goodman, J.W.: Introduction to Fourier optics. McGraw-Hill, New York (1968)
- [143] Khaled, E.E.M., Hill, S.C., Barber, P.W.: Scattered and internal intensity of a sphere illuminated with a Gaussian beam. IEEE Transactions on antennas and propagation 41(3), 295–303 (1993)
- [144] Khaled, E.E.M., Hill, S.C., Barber, P.W.: Internal electric energy in a spherical particle illuminated with a plane wave or off-axis Gaussian beam. Applied Optics 33(3), 524–532 (1994)
- [145] Khaled, E.E.M., Hill, S.C., Barber, P.W., Chowdhury, D.Q.: Near-resonance excitation of dielectric spheres with plane waves and off-axis Gaussian beams. Applied Optics 31(9), 1166–1169 (1992)
- [146] Ratowsky, R.P., Yang, L., Deri, R.J., Kallman, J.S., Trott, G.: Ball lens reflections by direct solution of Maxwell's equations. Optics Letters 20(20), 2048–2050 (1995)
- [147] Ratowsky, R.P., Yang, L., Deri, R.J., Chang, K.W., Kallman, J.S., Trott, G.: Laser diode to single-mode fiber ball lens coupling efficiency: full-wave calculation and measurements. Applied Optics 36(15), 3435–3438 (1997)
- [148] Doicu, A., Wriedt, T.: Plane wave spectrum of electromagnetic beams. Optics Communications 136, 114–124 (1997)
- [149] Li, P., Shi, K.B., Liu, Z.W.: Optical scattering spectroscopy by using tightly focused supercontinuum. Optics Express 13(22), 9039–9044 (2005)

[150] Lerme, J., Bachelier, G., Billaud, P., Broyer, B.M., Cottancin, E., Marhaba, S., Pellarin, M.: Optical response of a single spherical particle in a tightly focused light beam: application to the spatial modulation spectroscopy technique. Journal of the Optical Society of America A 25(2), 493–514 (2008)

- [151] Albrecht, H.E., Bech, H., Damaschke, N., Feleke, M.: Berechnung der Streuintensität eines beliebig im Laserstrahl positionierten Teilchens mit Hilfe der zweidimensionalen Fouriertransformation. Optik 100(3), 118–124 (1995)
- [152] Albrecht, H.E., Borys, M., Damaschke, N., Tropea, C.: The imaging properties of scattering particles in laser beams. Measurement Science and Technology 10(6), 564–574 (1999)
- [153] Bech, H., Leder, A.: Particle sizing by time-resolved Mie calculations a numerical study. Optik 117, 40–47 (2006)
- [154] Bakic, S., Heinisch, C., Damaschke, N., Tschudi, T., Tropea, C.: Time integrated detection of femtosecond laser pulses scattered by small droplets. Applied Optics 47(4), 523–530 (2008)
- [155] Borys, M., Schelinsky, B., Albrecht, H.E., Krambeer, H.: Light scattering analysis with methods of geometrical optics for a particle arbitrarily positioned in a laser beam. Optik 108(3), 137–150 (1998)
- [156] Damaschke, N., Nobach, H., Semidetnov, N., Tropea, C.: Optical particle sizing in backscattered. Applied Optics 41(27), 5713–5727 (2002)
- [157] Lock, J.A.: Improved Gaussian beam-scattering algorithm. Applied Optics 34(3), 559–570 (1995)
- [158] Moore, N.J., Alonso, M.A.: Closed form formula for Mie scattering of nonparaxial analogues of Gaussian beams. Optics Express 16(8), 5926–5933 (2008)
- [159] Alexander, D.R., Armstrong, J.G.: Explosive vaporization of aerosol drops under irradiation by a  $CO_2$  laser beam. Appl. Opt. 26, 533–538 (1987)
- [160] Schaub, S.A., Alexander, D.R., Barton, J.P., Emanuel, M.A.: Laser beam interaction with methanol droplets: effects of relative beam diameter. Appl. Opt. 28(9), 1666–1669 (1989)
- [161] Slimani, F., Gréhan, G., Gouesbet, G., Allano, D.: Near-field Lorenz-Mie theory and its application to microholography. Applied Optics 23(22), 4140– 4148 (1984)
- [162] Brillouin, L.: The scattering cross-sections of spheres for electromagnetic scattering. J. Appl. Phys. 20, 1110–1125 (1949)
- [163] Lock, J.A., Hodges, J.T., Gouesbet, G.: Failure of the optical theorem for Gaussian-beam scattering by a spherical particle. Journal of the Optical Society of America A 12(12), 2708–2715 (1995)
- [164] Gouesbet, G., Letellier, C., Gréhan, G., Hodges, J.T.: Generalized optical theorem for on-axis Gaussian beams. Optics Communications 125, 137–157 (1996)
- [165] Berg, M.J., Sorensen, C.M., Chakrabarti, A.: Extinction and the optical theorem. Part I. Single particles. Journal of the Optical Society of America A 25(7), 1504–1513 (2008)
- [166] Berg, M.J., Sorensen, C.M., Chakrabarti, A.: Extinction and the optical theorem. Part II. Multiple particles. Journal of Optical Society of America A 25(7), 1514–1520 (2008)
- [167] Ashkin, A.: Acceleration and trapping of particles by radiation pressure. Phys. Rev. Lett. 24, 156–159 (1970)

[168] Ashkin, A., Dziedzic, J.M.: Optical levitation in high vacuum. Applied Physics Letters 28(6), 333–335 (1976)

- [169] Roosen, G.: A theoretical and experimental study of the stable equilibrium position of spheres levitated by two horizontal laser beams. Optics Communications 21(1), 189–436 (1977)
- [170] Roosen, G., de Saint Louvent, F., Slansky, S.: Etude de la pression de radiation excercée sur une sphère creuse transparente par un faisceau cylindrique. Opt. Commun. 24(1), 116–120 (1978)
- [171] Ren, K.F., Gréhan, G., Gouesbet, G.: Radiation pressure forces exerted on a particle arbitrarily located in a Gaussian beam by using the generalized Lorenz-Mie theory, and associated resonance effects. Opt. Communications. 108, 343–354 (1994)
- [172] Hodges, J.T., Gréhan, G., Gouesbet, G., Presser, C.: Forward scattering of a Gaussian beam by a nonabsorbing sphere. Applied Optics 34(12), 2133–2143 (1995)
- [173] Onofri, F., Gréhan, G., Gouesbet, G.: Electromagnetic scattering from a multilayered sphere located in an arbitrary beam. Applied Optics 34(30), 7113–7124 (1995)
- [174] Wu, Z.S., Wang, Y.P.: Electromagnetic scattering for multilayered sphere: recursive algorithm. Radio Science 26, 1393–1401 (1991)
- [175] Wu, Z.S., Guo, L.X., Ren, K.F., Gouesbet, G., Gréhan, G.: Improved algorithms for electromagnetic scattering of plane waves and shaped beams by multilayered spheres. Applied Optics 36(21), 5188–5198 (1997)
- [176] Wu, P., Han, Y.P., Liu, D.F.: Computation of Gaussian beam scattering for larger particle. Acta Physica Sinica 54(6), 2676–2679 (2005)
- [177] Rysakov, V.M., Ston, M.: Light scattering by a "soft" layered sphere: analysis by the method of spectral expansion in Kotel'nikov-Shannon choice functions. Optics and Spectroscopy 88(4), 602–607 (2000)
- [178] Rysakow, W., Ston, M.: The light scattering by core-mantled sphere. Journal of Quantitative Spectroscopy and Radiative Transfer 69(1), 121–129 (2001)
- [179] Sakurai, H., Kozaki, S.: Scattering of a Gaussian beam by a radially inhomogeneous dielectric sphere. Journal of Electromagnetic Waves and Applications 15(12), 1673–1693 (2001)
- [180] Sakurai, H., Kozaki, S.: Scattering of a Gaussian beam by stepped index Luneberg lens. International Journal of Infrared and Millimeter Waves 22(11), 1653–1668 (2001)
- [181] Sakurai, H., Urabe, F., Kozaki, S.: Beam scattering of the Luneberg lens by a complex source point. International Journal of Electronics 90(3), 193–200 (2003)
- [182] Lock, J.A.: Scattering of an electromagnetic plane wave by a Luneberg lens.
  I. Ray theory. Journal of the Optical Society of America A 25(12) (2008)
- [183] Lock, J.A.: Scattering of an electromagnetic plane wave by a Luneberg lens. II. Wave theory. Journal of the Optical Society of America A 25(12) (2008)
- [184] Lock, J.A.: Scattering of an electromagnetic plane wave by a Luneberg lens. III. Finely stratified lens model. Journal of the optical Society of America A 25(12) (2008)
- [185] Smith, D.D., Fuller, K.A.: Photonic bandgaps in Mie scattering by concentrically stratified spheres. Journal of the Optical Society of America B 19(10), 2449–2455 (2002)

[186] Deumie, C., Voarino, P., Amra, C.: Overcoated microspheres for specific optical powders. Applied Optics 41(16), 3299–3305 (2002)

- [187] Stout, B., Andraud, C., Stout, S., Lafait, J.: Absorption in multiple scattering systems of coated spheres. Journal of the Optical Society of America A 20(6), 1050–1059 (2003)
- [188] Yang, W.: Improved recursive algorithm for light scattering by a multilayered sphere. Applied Optics 42(9), 1710–1720 (2003)
- [189] Du, H.: Mie-scattering calculation. Applied Optics 43(9), 1951–1956 (2004)
- [190] Voarino, P., Deumie, C., Amra, C.: Optical properties calculated for multidielectric quarter-wave coatings on microspheres. Optics Express 12(19), 4476–4482 (2004)
- [191] Voarino, P., Zerrad, M., Deumie, C., Amra, C.: Multidielectric quarter-wave coatings on microspheres: a study in colorometric space. Applied Optics 45(7), 1469–1477 (2006)
- [192] Chen, H., Wu, Z.S., Yang, R.K., Bai, L.: Gaussian beam scattering from arbitrarily shaped objects with rough surfaces. Waves in Random Media 14(3), 277–286 (2004)
- [193] Liang, W., Xu, Y., Huang, Y.Y., Yariv, A., Fleming, J.G., Lin, S.Y.: Mie scattering analysis of spherical Bragg "onion" resonators. Optics Express 12(4), 657–669 (2004)
- [194] Combis, P., Robiche, J.: Electromagnetic computational method for the scattering of an axisymmetric laser beam by an inhomogeneous body of revolution. Journal of the Optical Society of America A 22(9), 1850–1865 (2005)
- [195] Voshchinnikov, N.V., Il'in, V.B., Henning, T.: Modelling the optical properties of composite and porous interstellar grains. Astronomy and Astrophysics 429(2), 371–381 (2005)
- [196] Lock, J.A.: Debye series analysis of scattering of a plane wave by a spherical Bragg grating. Applied Optics 44(26), 5594–5603 (2005)
- [197] Li, R.X., Han, X.E., Jiang, H.F., Ren, K.F.: Debye series of normally incident plane-wave scattering by an infinite multilayered cylinder. Applied Optics 45(24), 6255–6262 (2006)
- [198] Burlak, G., Grimalsky, V.: High quality electromagnetic oscillations in inhomogeneous coated microspheres. Optics Communications 263(2), 342–349 (2006)
- [199] Dartois, E.: Spectroscopic evidence of grain ice mantle growth in YSOs. Part I. CO ice modeling and limiting cases. Astronomy and Astrophysics 445(3), 959–970 (2006)
- [200] Li, R.X., Han, X.E., Jiang, H.F., Ren, K.F.: Debye series for light scattering by a multilayered sphere. Applied Optics 45(6), 1260–1270 (2006)
- [201] Li, R.X., Han, X.E., Shi, L.J., Ren, K.F., Jiang, H.F.: Debye series for Gaussian beam scattering by a multilayered sphere. Applied Optics 46(21), 4804–4812 (2007)
- [202] Sun, X.M., Han, Y.P., Wang, H.H.: Near-infrared light scattering by ice-water mixed clouds. Progress in Electromagnetics Research-Pier 61, 133–142 (2006)
- [203] Sun, X.M., Han, Y.P., Shi, X.W.: Monte Carlo simulation of backscattering by a melting layer of precipitation. Acta Physica Sinica 56(4), 2098–2105 (2007)
- [204] Sun, X.M., Wang, H.H., Han, Y.P., Shi, X.W.: A new melting particle model and its application to scattering of radiowaves by a melting layer of precipitation. International Journal of Infrared and Millimeter Waves 28(11), 993–1001 (2007)

[205] Li, H.Y., Wu, Z.S.: Electromagnetic scattering by multi-layered spheres in a 2D Gaussian beam. Acta Physica Sinica 57(2), 833–838 (2008)

- [206] Gouesbet, G.: Theory of distributions and its application to beam parametrization in light scattering. Particle and Particle Systems Characterization 16, 147–159 (1999)
- [207] Gouesbet, G.: Scattering of higher-order Gaussian beams by an infinite cylinder. Journal of Optics 28, 45–65 (1997)
- [208] Gouesbet, G.: Interaction between an infinite cylinder and an arbitrary shaped beam. Applied Optics 36(18), 4292–4304 (1997)
- [209] Ren, K.F., Gréhan, G., Gouesbet, G.: Scattering of a Gaussian beam by an infinite cylinder in the framework of a GLMT, formulation and numerical results. Journal of the Optical Society of America A 14(11), 3014–3025 (1997)
- [210] Gouesbet, G., Gréhan, G., Ren, K.F.: Rigorous justification of the cylindrical localized approximation to speed up computations in the generalized Lorenz-Mie theory for cylinders. Journal of the Optical Society of America A 15(2), 511–523 (1998)
- [211] Gouesbet, G., Ren, K.F., Mees, L., Gréhan, G.: Cylindrical localized approximation to speed up computations for Gaussian beams in the generalized Lorenz-Mie theory for cylinders, with arbitrary location and orientation of the scatterer. Applied Optics 38(12), 2647–2665 (1999)
- [212] Mees, L., Ren, K.F., Gréhan, G., Gouesbet, G.: Scattering of a Gaussian beam by an infinite cylinder with arbitrary location and arbitrary orientation: numerical results. Applied Optics 38(9), 1867–1876 (1999)
- [213] Yokota, M., Takenaka, T., Fukumitsu, O.: Scattering of Hermite-Gaussian beam mode by parallel dielectric circular cylinders. Journal of the Optical Society of America A 3(4), 580–586 (1986)
- [214] Erez, E., Leviatan, Y.: Analysis of beam scattering using clusters of filamentary sources located in complex space. Journal of electromagnetic waves and applications 10(5), 629–641 (1996)
- [215] Lock, J.A.: Scattering of a diagonally incident focused Gaussian beam by an infinitely long homogeneous circular cylinder. Journal of the Optical Society of America A 14(3), 640–652 (1997)
- [216] Lock, J.A.: Morphology-dependent resonances of an infinitely long circular cylinder illuminated by a diagonally incident plane wave or a focused Gaussian beam. Journal of the Optical Society of America A 14(3), 653–661 (1997)
- [217] Barton, J.P.: Internal and near-surface electromagnetic fields for an infinite cylinder illuminated by an arbitrary focused beam. Journal of the Optical Society of America A 16(1), 160–166 (1999)
- [218] Lock, J.A., Adler, C.L., Hovenac, E.A.: Exterior caustics produced in scattering of a diagonally incident plane wave by a circular cylinder: semiclassical scattering theory analysis. Journal of the Optical Society of America A 17(10), 1846–1856 (2000)
- [219] Marston, P.L., Zhang, Y.B., Thiessen, D.B.: Observation of the enhanced backscattering of light by the end of a tilted dielectric cylinder owing to the caustic merging transition. Applied Optics 42(3), 412–417 (2003)
- [220] Mroczka, J., Wysoczanski, D.: Plane-wave and Gaussian-beam scattering on an infinite cylinder. Optical Engineering 39(3), 763–770 (2000)
- [221] Venkatapathi, M., Gregori, G., Ragheb, K., Robinson, J.P., Hirleman, E.D.: Measurement and analysis of angle-resolved scatter from small particles in a cylindrical microchannel. Applied Optics 45(10), 2222–2231 (2006)

[222] Venkatapathi, M., Hirleman, E.D.: Effect of beam size parameters on internal fields in an infinite cylinder irradiated by an elliptical Gaussian beam. Journal of the Optical Society of America A 24(10), 3366–3370 (2007)

- [223] Van den Bulcke, S., Zhang, L., Franchois, A., Geffrin, J.M., Stiens, J.: Plane wave and Gaussian beam scattering by long dielectric cylinders: 2.5D simulations versus measurements. International Journal of Infrared and Millimeter Waves 29(11), 1038–1047 (2008)
- [224] Zhang, H.Y., Han, Y.P.: Scattering of shaped beam by an infinite cylinder of arbitrary orientation. Journal of the Optical Society of America B 25(2), 131–135 (2008)
- [225] Resnick, A., Hopfer, U.: Mechanical stimulation of primary cilia. Frontiers in bioscience 13, 1665–1680 (2008)
- [226] Guo, L.X., Wu, Z.S.: Rainbow scattering by an inhomogeneous cylinder with an off-axis Gaussian beam incidence at normal. International Journal of Infrared and Millimeter Waves 21(11), 1879–1886 (2000)
- [227] Adler, C.L., Lock, J.A., Nash, J.K., Saunders, K.W.: Experimental observation of rainbow scattering by a coated cylinder: twin primary rainbows and thin-film interference. Applied Optics 40(9), 1548–1558 (2001)
- [228] Jiang, H.F., Han, X.E., Li, R.X.: Improved algorithm for electromagnetic scattering of plane waves by a radially stratified tilted cylinder and its application. Optics Communications 266(1), 13–18 (2006)
- [229] Novitsky, A.V.: Matrix approach for light scattering by bianisotropic cylindrical particles. Journal of Physics Condensed Matter 19(8), Art 086213 (2007)
- [230] Wu, Z.S., Li, H.Y.: Debye series of scattering by a multi-layered cylinder in an off-axis 2D Gaussian beam. Chinese Physics Letters 25(5), 1672–1675 (2008)
- [231] Gouesbet, G., Mees, L., Gréhan, G.: Partial-wave description of shaped beams in elliptical-cylinder coordinates. Journal of the Optical Society of America A 15(12), 3028–3038 (1998)
- [232] Gouesbet, G., Mees, L., Gréhan, G.: Partial wave expansions of higher-order Gaussian beams in elliptical cylindrical coordinates. Journal of Optics A: Pure and Applied Optics 1, 121–132 (1999)
- [233] Gouesbet, G., Mees, L., Gréhan, G., Ren, K.F.: Description of arbitrary shaped beams in elliptical cylinder coordinates by using a plane wave spectrum approach. Optics Communications 161, 63–78 (1999)
- [234] Gouesbet, G., Mees, L.: Generalized Lorenz-Mie theory for infinitely long elliptical cylinders. Journal of the Optical Society of America A 16(6), 1333– 1341 (1999)
- [235] Gouesbet, G., Mees, L., Gréhan, G., Ren, K.F.: Localized approximation for Gaussian beams in elliptical cylinder coordinates. Applied Optics 39(6), 1008–1025 (2000)
- [236] Gouesbet, G., Mees, L.: Validity of the elliptical cylinder localized approximation for arbitrary shaped beams in generalized Lorenz-Mie theory for elliptical cylinders. Journal of the Optical Society of America A 16(12), 2946–2958 (1999)
- [237] Gouesbet, G., Mees, L., Gréhan, G., Ren, K.F.: The structure of generalized Lorenz-Mie theory for elliptical infinite cylinders. Particle and Particle Systems Characterization 16, 3–10 (1999)

[238] Gouesbet, G., Mees, L., Gréhan, G.: Introduction to the use of distributions for light scattering in elliptical cylinder coordinates. In: Scattering of shaped light beam and applications, pp. 1–39. Research Signpost (2000)

- [239] Gouesbet, G., Mees, L.: Generalized Lorenz-Mie theory for infinitely long cylinders with elliptical cross-sections. Erratum. Journal of the Optical Society of America A 22(3), 574–575 (2005)
- [240] Adler, C.L., Lock, J.A., Stone, B.R.: Rainbow scattering by a cylinder with a nearly elliptical cross section. Applied Optics 37(9), 1540–1550 (1998)
- [241] Rockstuhl, C., Herzig, H.P.: Rigorous diffraction theory applied to the analysis of the optical force on elliptical nano- and micro-cylinders. Journal of Optics A 6(10), 921–931 (2004)
- [242] Gouesbet, G., Rozé, C., Meunier-Guttin-Cluzel, S.: Instabilities by local heating below an interface, a review. Journal of Nonequilibrium Thermodynamics, special issue 25, 337–379 (2000)
- [243] Gouesbet, G., Meunier-Guttin-Cluzel, S., Ménard, O.: Global reconstruction of equations of motion from data series, and validation techniques, a review. In: Chaos and its reconstruction, pp. 1–160. Novascience Publishers, New York (2003)
- [244] Han, G.X., Han, Y.P., Liu, J.Y., Zhang, Y.: Scattering of an eccentric sphere arbitrarily located in a shaped beam. Journal of the Optical Society of America B 25(12), 2064–2072 (2008)
- [245] Gouesbet, G., Meunier-Guttin-Cluzel, S., Gréhan, G.: Generalized Lorenz-Mie theory for a sphere with an eccentrically located spherical inclusion, and optical chaos. Particle and Particle Systems Characterization 18, 190–195 (2001)
- [246] Gouesbet, G., Meunier-Guttin-Cluzel, S., Gréhan, G.: Periodic orbits in Hamiltonian chaos of the annular billiard. Physical Review E 65, Art 016212, 1–18 (2001)
- [247] Gouesbet, G., Meunier-Guttin-Cluzel, S., Gréhan, G.: Morphology-dependent resonances and/or whispering gallery modes for a two-dimensional dielectric cavity with an eccentrically located spherical inclusion, a Hamiltonian point of view with Hamiltonian (optical) chaos. Optics Communications 201, 223–242 (2002)
- [248] Hentschel, M., Richter, K.: Quantum chaos in optical systems: the annular billiard. Physical Review E 66(5), Art 056207 (2002)
- [249] de Carvalho, R.E., Souza, F.C., Leonel, E.D.: Fermi acceleration of the annular billiard. Physical Review E 73(6), Art 066229 (2006)
- [250] Chattaraj, P.K., Maiti, B., Sengupta, S.: Quantum analogue of the Kolmogorov-Arnold-Moser transition in different quantum anharmonic oscillators. International Journal of Quantum Chemistry 100(3), 254–276 (2004)
- [251] Chattaraj, P.K., Sengupta, S., Giri, S.: Quantum-classical correspondence of a field induced KAM-type transition: A QTM approach. Journal of Chemical Sciences 120(1), 33–37 (2008)
- [252] Gouesbet, G.: Hidden worlds in quantum kingdom (in preparation)
- [253] Barton, J.P., Ma, W., Schaub, S.A., Alexander, D.R.: Electromagnetic field for a beam incident on two adjacent spherical particles. Applied Optics 30(33), 4706–4715 (1991)
- [254] Bai, L., Wu, Z.S., Zhang, M., Ren, K.F., Gréhan, G.: Scattering of cluster spheres located on axis by a Gaussian beam in millimeter waves. International Journal of Infrared and Millimeter Waves 25(8), 1221–1230 (2004)

[255] Bai, L., Wu, Z.S., Chen, H., Guo, L.X.: Scattering of fundamental Gaussian beam from on-axis cluster spheres. Acta Physica Sinica 54(5), 2025–2029 (2005)

- [256] Lecler, S., Takakura, Y., Meyrueis, P.: Interpretation of light scattering by a bisphere in the electrodynamic regime based on apertures interference and cavity resonance. Journal of Optics A: Pure and Applied Optics 9(10), 802– 810 (2007)
- [257] Xu, Y.L., Gustafson, B.A.S.: Comparison between multisphere light-scattering calculations: rigorous solution and discrete-dipole approximation. Astrophysical Journal 513(2), 894–909 (1999)
- [258] Xu, Y.-L., Gustafson, B.A.S.: Comparison between multisphere light-scattering calculations: rigorous solution and discrete dipole approximation. Erratum. The Astrophysical Journal 522, 1206–1208 (1999)
- [259] Khlebtsov, N.G., Dykman, L.A., Krasnov, Y.M., Mel'nikov, A.G.: Light absorption by the clusters of colloidal gold and silver particles formed during slow and fast aggregation. Colloid Journal 62(6), 765–779 (2000)
- [260] Barton, J.P.: Internal and near-surface electromagnetic fields for a spheroidal particle with arbitrary illumination. Applied Optics 34, 5542–5551 (1995)
- [261] Barton, J.P.: Internal, near-surface, and scattered electromagnetic fields for a layered spheroid with arbitrary illumination. Applied Optics 40(21), 3598– 3607 (2001)
- [262] Han, Y.P., Wu, Z.S.: The expansion coefficients of a spheroidal particle illuminated by Gaussian beam. IEEE Transactions on Antennas and Propagation 49(4), 615–620 (2001)
- [263] Han, Y.P., Wu, Z.S.: Scattering of a spheroidal particle illuminated by a Gaussian beam. Applied Optics 40(15), 2501–2509 (2001)
- [264] Han, Y.P., Mees, L., Ren, K.F., Gouesbet, G., Wu, S.Z., Gréhan, G.: Scattering of light by spheroids: the far field case. Optics Communications 210, 1–9 (2002)
- [265] Han, Y.P., Wu, Z.S.: Absorption and scattering by an oblate particle. Journal of Optics A: Pure and Applied Optics 4(1), 74–77 (2002)
- [266] Han, Y.P., Gréhan, G., Gouesbet, G.: Generalized Lorenz-Mie theory for a spheroidal particle with off-axis Gaussian beam illumination. Applied Optics 42(33), 6621–6629 (2003)
- [267] Han, Y.P., Mees, L., Ren, K.F., Gréhan, G., Wu, Z.S., Gouesbet, G.: Far scattered field from a spheroid under a femtosecond pulsed illumination in a generalized Lorenz-Mie theory framework. Optics Communications 231, 71– 77 (2004)
- [268] Zhang, H.Y., Han, Y.P.: Scattering by a confocal multilayered spheroidal particle illuminated by an axial Gaussian beam. IEEE Transactions on Antennas and Propagation 53(4), 1514–1518 (2005)
- [269] Han, Y.P., Mees, L., Gouesbet, G., Wu, Z.S., Gréhan, G.: Resonant spectra of a deformed spherical microcavity. Journal of the Optical Society of America B 23(7), 1390–1397 (2006)
- [270] Han, Y., Zhang, H., Sun, X.: Scattering of shaped beam by an arbitrarily oriented spheroid having layers with non-confocal boundaries. Applied Physics B 84(3), 485–492 (2006)
- [271] Xu, F., Ren, K.F., Cai, X.S.: Extension of geometrical-optics approximation to on-axis Gaussian beam scattering. I. By a spherical particle. Applied Optics 45(20), 4990–4999 (2006)

[272] Xu, F., Ren, K.F., Cai, X.S., Shen, J.Q.: Extension of geometrical-optics approximation to on-axis Gaussian beam scattering. II. By a spheroidal particle with end-on incidence. Applied Optics 45(20), 5000–5009 (2006)

- [273] Xu, F., Ren, K.F., Gouesbet, G., Gréhan, G., Cai, X.: Generalized Lorenz-Mie theory for an arbitrarily oriented, located and shaped beam scattering by a homogeneous spheroid. Journal of the Optical Society of America A 24(1), 119–131 (2007)
- [274] Xu, F., Ren, K.F., Cai, X.S.: Expansion of an arbitrarily oriented, located, and shaped beam in spheroidal coordinates. Journal of the Optical Society of America A 24(1), 109–118 (2007)
- [275] Xu, F., Ren, K.F., Gouesbet, G., Cai, X., Gréhan, G.: Theoretical prediction of radiation pressure force exerted on a spheroid by an arbitrarily shaped beam. Physical Review E 75, Art 026613, 1–14 (2007)
- [276] Xu, F., Lock, J.A., Gouesbet, G., Tropea, C.: Radiation torque exerted on a spheroid: analytical solution. Physical Review A 78, Art 013843, 1–17 (2008)
- [277] Barton, J.P.: Electromagnetic-field calculations for irregularly shaped, axisymmetric layered particles with focused illumination. Applied Optics 35(3), 532–541 (1996)
- [278] Kushta, T.M., Yasumoto, K., Kiseliov, V.K.: Extinction and scattering of a guided beam in a hollow dielectric waveguide. Journal of the Optical Society of America A 18(7), 1690–1695 (2001)
- [279] Neukammer, J., Gohlke, C., Hope, A., Wessel, T., Rinneberg, H.: Angular distribution of light scattered by single biological cells and oriented particle agglomerates. Applied Optics 42(31), 6388–6397 (2003)
- [280] Kant, R.: Generalized Lorenz-Mie scattering theory for focused radiation and finite solids of revolution: case i: symmetrically polarized beams. Journal of Modern Optics 52(15), 2067–2092 (2005)
- [281] Wang, Y.H., Guo, L.X., Wu, Q.: Electromagnetic scattering from two parallel 2D targets arbitrarily located in a Gaussian beam. Chinese Physics 15(8), 1755–1765 (2006)
- [282] Wang, Y.H., Guo, L.X., Wu, Z.S.: Electromagnetic scattering of Gaussian beam by two-dimensional targets. Radio Science 42(4), Art RS4012 (2007)
- [283] Wang, Y.H., Guo, L.X., Wu, Z.S.: Electromagnetic scattering of plane wave/Gaussian beam by parallel cylinders. Acta Physica Sinica 56(1), 186– 194 (2007)
- [284] Guo, L.X., Wang, Y.H., Wu, Z.S.: Application of the equivalence principle and the reciprocity theorem to electromagnetic scattering from two adjacent spherical objects. Acta Physica Sinica 55(11), 5815–5823 (2006)
- [285] Moneda, A.P., Chrissoulidis, D.P.: Dyadic Green's function of a cluster of spheres. Journal of the Optical Society of America A 24(11), 3437–3443 (2007)
- [286] Kasparian, J., Boutou, V., Wolf, J.P., Pan, Y.L., Chang, R.K.: Angular distribution of non-linear optical emission from spheroidal microparticles. Applied Physics B 91(1), 167–171 (2008)
- [287] Gréhan, G., Gouesbet, G., Naqwi, A., Durst, F.: Evaluation of a phase Doppler system using generalized Lorenz-Mie theory. In: Int. Conf. on Multiphase Flows 1991, Tsukuba, Japan, pp. 291–296 (1991)
- [288] Gréhan, G., Gouesbet, G., Naqwi, A., Durst, F.: On elimination of the trajectory effects in phase Doppler systems. In: 5 th European Symposium on Particle Characterization (PARTEC 1992), Nürnberg, March 24-26, pp. 309– 318 (1992)

[289] Gouesbet, G., Berlemont, A., Gréhan, G., Desjonquères, P.: On modelling and measurement problems in the study of turbulent two-phase flows with particles. In: Sommerfeld, M. (ed.) Proceedings of the Sixth Workshop on Two-phase Flow Predictions, Erlangen,invited lecture, 1992. Proceedings: Forschungszentrum Jülich GmbH, bilateral seminar of the international bureau, vol. 14, pp. 365–387 (1993)

- [290] Naqwi, A., Ziema, M., Gréhan, G., Gouesbet, G.: Influence of the Gaussian profile effect on the accuracy of phase-Doppler anemometer. In: Sixth Workshop on Two-phase Flow Predictions, Erlangen, March 23-26, Proceedings:Forschungszentrum Julich GmbH, bilateral seminar of the international bureau, vol. 14, pp. 332–338 (1993)
- [291] Naqwi, A.A., Liu, X.-Z., Durst, F.: Evaluation of the dual-cylindrical wave laser technique for sizing of liquid droplets. Particle and Particle Systems Characterization 9, 44–51 (1992)
- [292] Ren, K.F., Gréhan, G., Gouesbet, G.: Laser sheet scattering by spherical particles. Particle and Particle Systems Characterization 10, 146–151 (1993)
- [293] Gréhan, G., Ren, K.F., Gouesbet, G., Naqwi, A., Durst, F.: Evaluation of a particle sizing technique based on laser sheets. Particle and Particle Systems Characterization 11, 101–106 (1994)
- [294] Ren, K.F., Gréhan, G., Gouesbet, G.: Evaluation of laser beam sheet beam shape coefficients in generalized Lorenz-Mie theory by using a localized approximation. Journal of the Optical Society of America A 11(7), 2072–2079 (1994)
- [295] Ren, K.F., Gréhan, G., Gouesbet, G.: Electromagnetic field expression of a laser sheet and the order of approximation. J. Optics (PARIS) 25(4), 165–176 (1994)
- [296] Corbin, F., Gréhan, G., Gouesbet, G.: Top-hat beam technique: improvements and application to bubble measurements. Particle and Particle Systems Characterization 8, 222–228 (1991)
- [297] Gouesbet, G., Lock, J.A., Gréhan, G.: Partial wave representations of laser beams for use in light scattering calculations. Applied Optics 34(12), 2133– 2143 (1995)
- [298] Gouesbet, G., Maheu, B., Gréhan, G.: Scattering of a Gaussian beam by a sphere using a Bromwich formulation: case of an arbitrary location. In: the International Symposium: Optical Particle Sizing: Theory and Practice, May 12-15, Plenum Publishing Company, New York (1987)
- [299] Lax, M., Louisell, W.H., Mc Knight, L.: From Maxwell to paraxial optics. Phy. Rev. A 11(4), 1365–1370 (1975)
- [300] Kogelnik, H., Li, T.: Laser beams and resonators. Proceedings of the IEEE 54, 1312–1329 (1965)
- [301] Kogelnik, H.: On the propagation of Gaussian beams of light through lenslike media including those with a loss or gain variation. Applied Optics 4(12), 1562–1569 (1965)
- [302] Kogelnik, H., Li, T.: Laser beams and resonators. Applied Optics 5(10), 1550– 1556 (1966)
- [303] Laures, P.: Geometrical approach to Gaussian beam propagation. Appl. Opt 6(4), 747-755 (1967)
- [304] Agrawal, G.P., Pattanayak, D.N.: Gaussian beam propagation beyond the paraxial approximation. J. Opt. Soc. Amer. 69(4), 575–578 (1979)

[305] Couture, M., Belanger, P.A.: From Gaussian beam to complex-source-point spherical wave. Phys. Rev. A 24(1), 355–359 (1981)

- [306] Agrawal, G.P., Lax, M.: Free-space wave propagation beyond the paraxial approximation. Physical Review A 27(3), 1693–1695 (1983)
- [307] Takenaka, T., Fukumitsu, Y.: Propagation of light beams beyond the paraxial approximation. J. Opt. Soc. Am. A 2(6), 826–829 (1985)
- [308] Gouesbet, G., Gréhan, G., Maheu, B.: The order of approximation in a theory of the scattering of a Gaussian beam by a Mie scatter center. J. Optics (PARIS) 16(5), 239–247 (1985); Republished in Kerker, M. (ed.): selected papers on light scattering Part-I. SPIE Milestoneseries, vol. 951, pp. 352–360 (1988)
- [309] Barton, J.P., Alexander, D.R.: Fifth-order corrected electromagnetic field components for fundamental Gaussian beams. Journal of Applied Physics 66(7), 2800–2802 (1989)
- [310] Schaub, S.A., Barton, J.P., Alexander, D.R.: Simplified scattering coefficient expression for a spherical particle located on the propagation axis of a fifthorder Gaussian beam. Appl. Phys. Lett 55, 2709–2711 (1989)
- [311] Gouesbet, G.: Higher-order descriptions of Gaussian beams. Journal of Optics (Paris) 27(1), 35–50 (1996)
- [312] Ren, K.F., Gréhan, G., Gouesbet, G.: Symmetry relations in generalized Lorenz-Mie theory. Journal of the Optical Society of America A 11(6), 1812– 1817 (1994)
- [313] Gouesbet, G.: Exact description of arbitrary shaped beams for use in light scattering theories. Journal of the Optical Society of America A 13(12), 2434– 2440 (1996)
- [314] Polaert, H., Gréhan, G., Gouesbet, G.: Improved standard beams with applications to reverse radiation pressure. Applied Optics 37(12), 2435–2440 (1998)
- [315] Ren, K.F., Gréhan, G., Gouesbet, G.: Prediction of reverse radiation pressure by generalized Lorenz-Mie theory. Applied Optics 35(15), 2702–2710 (1996)
- [316] Barton, J.P.: Electromagnetic-field calculations for a sphere illuminated by a higher-order Gaussian beam. I. Internal and near-field effects. Applied Optics 36(6), 1303–1311 (1997)
- [317] Barton, J.P.: Electromagnetic field calculations for a sphere illuminated by a higher-order Gaussian beam. II. Far-field scattering. Applied Optics 37(15), 3339–3344 (1998)
- [318] Evers, T., Dahl, H., Wriedt, T.: Extension of the program 3D MMP with a fifth order Gaussian beam. Electronics letters 32(15), 1356–1357 (1996)
- [319] Naqwi, A.A., Durst, F.: Analysis of laser light-scattering interferometric devices for in-line diagnostics of moving particles. Applied Optics 32(21), 4003–4018 (1993)
- [320] Ren, K.F., Gréhan, G., Gouesbet, G.: Electromagnetic field expression of a laser sheet and the order of approximation. Journal of Optics (Paris) 25(4), 165–176 (1994)
- [321] Moreno, D., Santoyo, F.M., Guerrero, J.A., Funes-Gallanzi, M.: Particle positioning from charge-coupled device images by the generalized Lorenz-Mie theory and comparison with experiment. Applied Optics 39(28), 5117–5124 (2000)

[322] Guerrero, J.A., Santoyo, F.M., Moreno, D., Funes-Gallanzi, M., Fernandez-Orosco, S.: Particle positioning from CCD images: experiments and comparison with the generalized Lorenz-Mie theory. Measurement Science and Technology 11(5), 568–575 (2000)

- [323] Ilic, J., Cantrak, D., Sreckovic, M.: Laser sheet scattering and the cameras' positions in particle image velocimetry. Acta Physica Sinica 112(5), 1113– 1118 (2007)
- [324] Zhang, H.C., Tu, E., Hagen, N.D., Schnabel, C.A., Paliotti, M.J., Hoo, W.S., Nguyen, P.M., Kohrumel, J.R., Butler, W.F., Chachisvillis, M., Marchand, P.J.: Time-of-flight optophoresis analysis of live whole cells in microfluidic channels. Biomedical Microdevices 6(1), 11–21 (2004)
- [325] Allano, D., Gouesbet, G., Gréhan, G., Lisiecki, D.: Droplet sizing using a tophat laser beam technique. Journal of Physics D: Applied Physics 17, 43–58 (1984)
- [326] Gréhan, G., Gouesbet, G.: Simultaneous measurements of velocities and sizes of particles in flows using a combined system incorporating a top-hat beam technique. Applied Optics 25(19), 3527–3538 (1986)
- [327] Pogorzelski, R.J.: Provision of exact form for the forward scattering of a Gaussian beam by a nonabsorbing sphere: comment. Applied Optics 34(36), 8474 (1995)
- [328] Lock, J.A., Hodges, J.T.: Far-field scattering of an axisymmetric laser beam of arbitrary profile by an on-axis spherical particle. Applied Optics 35(21), 4283–4290 (1996)
- [329] Lock, J.A., Hodges, J.T.: Far-field scattering of a non-Gaussian off-axis axisymmetric laser beam by a spherical particle. Applied Optics 35(33), 6605–6616 (1996)
- [330] Gouesbet, G.: Measurements of beam shape coefficients in generalized Lorenz-Mie theory and the density-matrix approach. I: measurements. Particle and Particle Systems Characterization 14, 12–20 (1997)
- [331] Gouesbet, G.: Measurements of beam shape coefficients in generalized Lorenz-Mie theory and the density-matrix approach. II. the density-matrix approach. Particle and Particle Systems Characterization 14, 88–92 (1997)
- [332] Polaert, H., Gouesbet, G., Gréhan, G.: Measurements of beam shape coefficients in the generalized Lorenz-Mie theory for the on-axis case: numerical simulations. Applied Optics 37(21), 5005–5013 (1998)
- [333] Polaert, H., Gouesbet, G., Gréhan, G.: Laboratory determination of beam shape coefficients for use in generalized Lorenz-Mie theory. Applied Optics 40(10), 1699–1706 (2001)
- [334] Guttierez-Vega, J.C., Iturbe-Castillo, M.D., Ramirez, G.A., Tepichin, E., Rodriguez-Dagnino, R.M., Chavez-Cerda, S., New, G.H.C.: Experimental demonstration of optical Mathieu beams. Optics Communications 195(1-4), 35–40 (2001)
- [335] Bouchal, Z.: Nondiffracting optical beams: physical properties, experiments, and applications. Czechoslovak Journal of Physics 53(7), 537–578 (2003)
- [336] Wu, X., Wang, Y., Takiguchi, Y., Kan, H.F., Lu, Z.K.: Analysis of beam properties in the neighbourhood of a double-heterostructure laser source. Journal of Modern Optics 50(8), 1225–1235 (2003)
- [337] Chen, C.H., Tai, P.T., Hsieh, W.F.: Bottle beam from a bare laser for single-beam trapping. Applied Optics 43(32), 6001–6006 (2004)

[338] Soifer, V.A., Kotlyar, V.V., Khonina, S.N.: Optical microparticle manipulation: Advances and new possibilities created by diffractive optics. Physics of Particles and Nuclei 35(6), 733–766 (2004)

- [339] Marston, P.L.: Scattering of a Bessel beam by a sphere. J. Acoust. Soc. Am. 121(2), 753–758 (2007)
- [340] Yin, J.P., Gao, W.J., Zhu, Y.F.: Generation of dark hollow beams and their applications. Progress in Optics 45, 119–204 (2003)
- [341] Tryka, S.: Spherical object in radiation field from Gaussian source. Optics Express 13(16), 5925–5938 (2005)
- [342] van De Nes, A.S., Torok, P.: Rigorous analysis of spheres in Gauss-Laguerre beams. Optics Express 15(20), 13360–13374 (2007)
- [343] Quinten, M., Pack, A., Wannemacher, R.: Scattering and extinction of evanescent waves by small particles. Applied Physics B 68(1), 87–92 (1999)
- [344] Gouesbet, G., Gréhan, G.: Generic formulation of a generalized Lorenz-Mie theory for a particle illuminated by laser pulses. Particle and Particle Systems Characterization 17(5-6), 213–224 (2000)
- [345] Gouesbet, G., Mees, L., Gréhan, G.: Generic formulation of a generalized Lorenz-Mie theory for pulsed laser illumination. In: Adrian, D., Durst, H., Maeda, W. (eds.) Laser techniques for fluid mechanics, pp. 175–188. Springer, Heidelberg (2002)
- [346] Mees, L., Gréhan, G., Gouesbet, G.: Time-resolved scattering diagrams for a sphere illuminated by plane wave and focused short pulses. Optics Communications 194(1-3), 59–65 (2001)
- [347] Mees, L., Gouesbet, G., Gréhan, G.: Scattering of laser pulses (plane wave and focused Gaussian beams) by spheres. Applied Optics 40(15), 2546–2550 (2001)
- [348] Mees, L., Gouesbet, G., Gréhan, G.: Interaction between femtosecond pulses and a spherical microcavity: internal fields. Optics Communications 199, 33– 38 (2001)
- [349] Mees, L., Gouesbet, G., Gréhan, G.: Numerical predictions of microcavity internal fields created by femtosecond pulses, with emphasis on whispering gallery modes. Journal of Optics A: Pure and Applied Optics 4, 8150–8153 (2002)
- [350] Brunel, M., Mees, L., Gouesbet, G., Gréhan, G.: Cerenkov-based radiation from superluminal excitation in microdroplets by ultra-short pulses. Optics Letters 26(20), 1621–1623 (2001)
- [351] Mees, L., Ren, K.F., Gouesbet, G., Gréhan, G.: Transient internal and near-scattered fields from a multilayered sphere illuminated by a pulsed laser. In: Proceedings of the 17th International Symposium on Applications of Laser Techniques to Fluid Mechanics, Lisbon, July 8-11 (2002)
- [352] Mees, L., Wolf, J.P., Gouesbet, G., Gréhan, G.: Two-photon absorption and fluorescence in a spherical micro-cavity illuminated by using two laser pulses: numerical simulations. Optics Communications 208, 371–375 (2002)
- [353] Brevik, I., Kluge, R.: Oscillations of a water droplet illuminated by a linearly polarized laser pulse. Journal of the Optical Society of America B 16(6), 976–985 (1999)
- [354] Favre, C., Boutou, V., Hill, S.C., Zimmer, W., Krenz, M., Lambrecht, H., Yu, J., Chang, R.K., Woeste, L., Wolf, J.P.: White-light nanosource with directional emission. Physical Review Letters 89(3), Art 035002 (2002)
- [355] Lindinger, A., Hagen, J., Socacio, L.D., Bernhardt, T.M., Woste, L., Duft, D., Leisner, T.: Time-resolved explosion dynamics of H<sub>2</sub>O droplets induced by femtosecond laser pulses. Applied Optics 43(27), 5263–5269 (2004)

[356] Bech, H., Leder, A.: Particle sizing by ultrashort laser pulses - numerical simulation. Optik 115(5), 205–217 (2004)

- [357] Mejean, G., Kasparian, J., Yu, J., Frey, S., Salmon, E., Wolf, J.P.: Remote detection and identification of biological aerosols using a femtosecond terawatt lidar system. Applied Physics B 78(5), 535–537 (2004)
- [358] Mejean, G.: Propagation of femtosecond terawatt laser in atmosphere and applications. Annales de Physique 30(6), 1–154 (2005)
- [359] Kasparian, J., Wolf, J.P.: Physics and applications of atmospheric nonlinear optics and filamentation. Optics Express 16(1), 466–493 (2008)
- [360] Courvoisier, F., Bonacina, L., Boutou, V., Guyon, L., Bonnet, C., Thuillier, B., Extermann, J., Roth, M., Rabitz, H., Wolf, J.P.: Identification of biological microparticles using ultrafast depletion spectroscopy. Faraday Discussions 137, 37–49 (2008)
- [361] Jones, A.R.: Some calculations on the scattering efficiencies of a sphere illuminated by an optical pulse. Journal of Physics D 40(23), 7306–7312 (2007)
- [362] Lee, C.J., van der Slot, P.J.M., Boller, K.J.: Using ultra-short pulses to determine particle size and density distribution. Optics Express 15(19), 12483–12497 (2007)
- [363] van Beeck, J.P.A.J., Riethmuller, M.L.: Rainbow interferometry with wire diffraction for simultaneous measurement of droplet temperature, size and velocity. Particle and Particle Systems Characterization 14, 186–192 (1997)
- [364] Saengkaew, S., Charinpanitkul, T., Vanisri, H., Tanthapanichakoon, W., Biscos, Y., Garcia, N., Lavergne, G., Méès, L., Gouesbet, G., Gréhan, G.: Rainbow refractometry on particles with radial refractive index gradients. Experiments in Fluids 43, 595–601 (2007)
- [365] Saengkaew, S., Charinpanikul, T., Laurent, C., Biscos, Y., Lavergne, G., Gouesbet, G., Gréhan, G.: Processing of individual rainbow signals to study droplet evaporation. Experiments in Fluids 48, 111–119 (2010)
- [366] Mao, F.L., Xing, Q.R., Wang, K., Lang, L.Y., Chai, L., Wang, Q.Y.: Calculation of axial optical forces exerted on medium-sized particles by optical trap. Optics and Laser Technology 39(1), 34–39 (2007)
- [367] Gouesbet, G., Gréhan, G., Maheu, B.: Expressions to compute the coefficients gnm in the generalized Lorenz-Mie theory, using finite series. Journal of Optics (Paris) 19(1), 35–48 (1988)
- [368] Gouesbet, G., Gréhan, G., Maheu, B.: Expressions to compute the coefficients  $g_n^m$  in the generalized Lorenz-Mie theory using finite series. J. Optics (PARIS) 19(1), 35–48 (1988)
- [369] Abramowitz, M., Stegun, I.: Handbook of mathematical functions with formulas, graphs, and mathematical tables. Dover Publications Inc., New York (1964)
- [370] Ferguson, D.C., Currie, I.G.: Theoretical evaluation of LDA techniques for two-phase flow measurements. Presented at the third International Symposium on applications of laser anemometry to fluid mechanics. Actually, although the paper was available at the conference, it has not been included in the paperback proceedings due to a delay problem. We therefore invite the normal reader to consider this reference as a private communication. The hearty reader might be lucky enough to succeed in getting somewhere, somehow, a copy of it (July 1986)

[371] Gouesbet, G., Gréhan, G., Maheu, B.: Localized interpretation to compute all the coefficients  $g_n^m$  in the generalized Lorenz-Mie theory. J. Opt. Soc. Amer. A 7(6), 998–1007 (1990)

- [372] Maheu, B., Gréhan, G., Gouesbet, G.: Ray localization in Gaussian beams. Optics Communications 70(4), 259–262 (1989)
- [373] Danos, M., Maximon, L.C.: Multipole matrix elements of the translation operator. J. of Mathematical Physics 16(5), 766–778 (1965)
- [374] Liang, C., Lo, Y.T.: Scattering by two spheres. Radio Science 2(12), 1481– 1495 (1967)
- [375] Ronchi, J.: An addition theorem for spherical wave functions. Lettere al nuovo cimento 35(11), 353–357 (1982)
- [376] Dalmas, J., Deleuil, R.: Etablissement d'une formule de récurrence pour l'addition des fonctions d'onde scalaires sphéroïdales intervenant dans l'étude de la diffusion multiple des ellipsoïdes de révolution. Optica Acta 30(12), 1697–1705 (1983)
- [377] Doicu, A., Wriedt, T.: Computation of the beam-shape-coefficients in the generalized Lorenz-Mie theory by using the translational addition theorem for spherical vector wave functions. Applied Optics 36(13), 2971–2978 (1997)
- [378] Gouesbet, G., Gréhan, G., Maheu, B.: On the generalized Lorenz-Mie theory: first attempt to design a localized approximation to the computation of the coefficients  $g_n^m$ . Journal of Optics (Paris) 20(1), 31–43 (1989)
- [379] Ren, K.F., Gréhan, G., Gouesbet, G.: Localized approximation of generalized Lorenz-Mie theory. Faster algorithm for computation of the beam shape coefficients  $g_n^m$ . Particle and Particle Systems Characterization 9(2), 144–150 (1992)
- [380] Gouesbet, G.: Validity of the localized approximation for arbitrary shaped beams in generalized Lorenz-Mie theory for spheres. Journal of the Optical Society of America A 16(7), 1641–1650 (1999)
- [381] Gouesbet, G.: Validity of the cylindrical localized approximation for arbitrary shaped beams in generalized Lorenz-Mie theory for circular cylinders. Journal of Modern Optics 46(8), 1185–1200 (1999)
- [382] Han, Y.P.: An approach to expand the beam coefficients for arbitrarily shaped beam. Acta Physica Sinica 54(11), 5139–5143 (2005)
- [383] Han, Y.P., Zhang, H.Y., Han, G.X.: The expansion coefficients of arbitrary shaped beam in oblique illumination. Optics Express 15(2), 735–746 (2007)
- [384] Zhang, H.Y., Han, Y.P., Han, G.X.: Expansion of the electromagnetic fields of a shaped beam in terms of cylindrical vector wave functions. Journal of the Optical Society of America B 24(6), 1383–1391 (2007)
- [385] Zhang, H.Y., Han, Y.P.: Addition theorem for the spherical vector wave functions and its application to the beam shape coefficients. Journal of the Optical Society of America B 25(2), 255–260 (2008)
- [386] Han, G.X., Han, Y.P., Zhang, H.Y.: Relations between cylindrical and spherical vector wavefunctions. Journal of Optics A: Pure and Applied Optics 10(1), Art 015006 (2008)
- [387] Nieminen, T.A., Rubinsztein-Dunlop, H., Heckenberg, N.R.: Multipole expansion of strongly focussed laser beams. Journal of Quantitative Spectroscopy and Radiative Transfer 79, 1005–1017 (2003)

[388] Nieminen, T.A., Rubinsztein-Dunlop, H., Heckenberg, N.R.: Calculation of the T-matrix: general considerations and applications of the point-matching method. Journal of Quantitative Spectroscopy and Radiative Transfer 79, 1019–1029 (2003)

- [389] Neves, A.A.R., Fontes, A., Padilha, L.A., Rodriguez, E., Cruz, C.H.D., Barbosa, L.C., Cesar, C.L.: Exact partial wave expansion of optical beams with respect to an arbitrary origin. Optics Letters 31(16), 2477–2479 (2006)
- [390] Neves, A.A.R., Padilha, L.A., Fontes, A., Rodriguez, E., Cruz, C.H.B., Barbosa, L.C., Cesar, C.L.: Analytical results for a Bessel function times Legendre polynomials class integrals. Journal of Physics A 39(18), L293–L296 (2006)
- [391] Neves, A.A.R., Fontes, A., Pozzo, L.D.Y., de Thomas, A.A., Chillce, E., Ro-driguez, E., Barbosa, L.C., Cesar, C.L.: Electromagnetic forces for an arbitrary optical trapping of a spherical dielectric. Optics Express 14(26), 13101–13106 (2006)
- [392] Neves, A.A.R., Fontes, A., Cesar, C.L., Camposeo, A., Cingolani, R., Pisignano, D.: Axial optical trapping efficiency through a dielectric interface. Physical Review E 76(6), Art 061917 (2007)
- [393] Gouesbet, G., Gréhan, G. (eds.): Scattering of shaped light beam and applications. Research Signpost, India (2000)
- [394] Xu, R.: Particle characterization: light scattering methods. Kluwer Academic, Dordrecht (2000)
- [395] Albrecht, H.E., Borys, M., Damaschke, N., Tropea, C.: Laser Doppler and phase Doppler measurement. Springer, Heidelberg (2003)
- [396] Doicu, A., Wriedt, T., Eremin, Y.A.: Light scattering by systems of particles. Springer, Heidelberg (2006)
- [397] Barth, H.G., Sun, S.-T.: Particle size analysis. Anal. Chem. 61, 143R–152R (1989)
- [398] Bachalo, W.D.: Experimental methods in multiphase flows. International Journal of Multiphase Flows 20, 261–295 (1994)
- [399] Black, D.L., McQuay, M.Q., Bonin, M.P.: Laser-based techniques for particlesize measurement: a review of sizing methods and their industrial applications. Prog. Energy Combust. Sci. 22, 267–306 (1996)
- [400] Jones, A.R.: Light scattering for particle characterization. Progress in Energy and Combustion Science 25(1), 1–53 (1999)
- [401] Durst, F.: Experimental and numerical techniques in fluids. Journal of Pressure Vessel Technology Transactions of the ASME 130(1), Art 011304 (2008)
- [402] Ren, K.F., Gouesbet, G., Gréhan, G., Yiping, W.: Generalized Lorenz-Mie theory and its application in particle sizing. Chinese Journal of Radioscience 9(2), 7–12 (1994) (in chinese)
- [403] Yeh, Y., Cummins, H.: Localized fluid flow measurements with a He-Ne laser spectrometer. Applied Physics Letters 4, 176–178 (1964)
- [404] Drain, L.E.: The laser Doppler technique. Wiley, Chichester (1980)
- [405] Durst, F., Melling, A., Whitelaw, J.H.: Principles and practice of laser-Doppler anemometry. Academic Press, London (1981)
- [406] Durst, F., Zaré, M.: Laser Doppler measurements in two-phase flows. In: Proceedings LDA-Symposium, Copenhagen, Denmark, pp. 403–429 (1975)
- [407] Bachalo, W.D.: The phase Doppler method: analysis, performance evaluations, and applications. Particle and Particle Systems Characterization 11, 73–83 (1994)

[408] Buchhave, P., von Benzon, H.H.: Exploring PDA configurations. Particle and Particle Systems Characterization 13, 68–78 (1996)

- [409] Hirleman, E.D.: History of development of the phase-Doppler particle-sizing velocimeter. Particle and Particle Systems Characterization 13(2), 59–67 (1996)
- [410] Durst, F., Brenn, G., Xu, T.H.: A review of the development and characteristics of planar phase-Doppler anemometry. Measurement Science and Technology 8, 1203–1221 (1997)
- [411] Zhang, S., Ren, K.F., Shen, X., Gréhan, G., Gouesbet, G.: A theoretical model for the method of phase-Doppler particle sizing in two-phase flows. Journal of Experimental Mechanics 15(1), 43–50 (2000)
- [412] Bachalo, W.D., Sankar, S.V.: Analysis of the light scattering interferometry for spheres larger than the light wavelength, paper 1.8. In: Proceedings of the 4th international symposium on applications of laser anemometry to fluid mechanics, Lisbon, Portugal (1988)
- [413] Hardalupas, Y., Liu, C.H.: Implications of the Gaussian intensity distribution of laser beams on the performance of the phase Doppler technique: sizing uncertainties. Prog. Energy Combust Sci. 23, 41–63 (1997)
- [414] Lehmann, P., Schombacher, E.H.: Features of a combined FFT and Hilbert transform for phase Doppler signal processing. Meas. Sci. Technol. 8, 409–421 (1997)
- [415] Onofri, F., Lenoble, A., Radev, S.: Superimposed noninterfering probes to extend the capabilities of phase Doppler anemometry. Applied Optics 41(18), 3590–3600 (2002)
- [416] Onofri, F., Girasole, T., Gréhan, G., Gouesbet, G., Brenn, G., Domnick, J., Xu, T.H., Tropea, C.: Phase-Doppler anemometry with the dual burst technique for measurement of refractive index and absorption coefficient simultaneously with size and velocity. Particle and Particle Systems Characterization 13, 112–124 (1996)
- [417] Onofri, F., Bergougnoux, L., Firpo, J.L., Misguich-Ripault, J.: Size, velocity, and concentration in suspension measurements of spherical droplets and cylindrical jets. Applied Optics 38(21), 4681–4690 (1999)
- [418] Onofri, F., Blondel, D., Gréhan, G., Gouesbet, G.: On the optical diagnosis and sizing of spherical coated and multilayered particles with phase-Doppler anemometry. Particle and Particle Systems Characterization 13, 104–111 (1996)
- [419] Mignon, H., Gréhan, G., Gouesbet, G., Xu, T.H., Tropea, C.: Measurement of cylindrical particles with phase-Doppler anemometry. Applied Optics 35(25), 5180–5190 (1996)
- [420] Gauchet, N., Girasole, T., Ren, K.F., Gréhan, G., Gouesbet, G.: Application of generalized Lorenz-Mie theory for cylinders to cylindrical particle characterization by phase-Doppler anemometry. Optical Diagnostics in Engineering 2(1), 1–10 (1997)
- [421] Doicu, A., Schabel, S., Ebert, F.: Generalized Lorenz-Mie theory for nonspherical particles with applications to phase-Doppler anemometry. Particle and Particle Systems Characterization 13, 79–88 (1996)
- [422] Damaschke, N., Gouesbet, G., Gréhan, G., Mignon, H., Tropea, C.: Response of phase Doppler anemometer systems to non-spherical droplets. Applied Optics 37(10), 1752–1761 (1998)

[423] Damaschke, N., Gouesbet, G., Gréhan, G., Tropea, C.: Optical techniques for the characterization of non-spherical and non-homogeneous particles, editorial paper for a special issue of "Measurement Science and Technology. Measurement Science and Technology 9, 137–140 (1998)

- [424] Mignon, H., Schaub, S.A., Naqwi, A.A., Fandrey, C.W., Berkner, L.S.: An interferometric optical technique for in-situ measurement of fiber diameter. Particle and Particle Systems Characterization 16(3), 128–134 (1999)
- [425] Onofri, F., Lenoble, A., Radev, S., Bultynck, H., Guering, P.H., Marsault, N.: Interferometric sizing of single-axis birefringent glass fibers. Particle and Particle Systems Characterization 20(3), 171–182 (2003)
- [426] Bultynck, H., Gouesbet, G., Gréhan, G.: A miniature monoblock backward phase-Doppler unit. Measurement Science and Technology 9, 161–170 (1998)
- [427] Blondel, D., Bultynck, H., Gouesbet, G., Gréhan, G.: Phase Doppler measurements with compact monoblock configurations. Part. Part. Syst. Charact. 18, 79–90 (2001)
- [428] Wu, X.C., Gréhan, G., Cen, K., Ren, K.F., Wang, Q.H., Luo, Z.Y., Fang, M.X.: Sizing of irregular particles using a near backscattered laser Doppler system. Applied Optics 46(36), 8600–8608 (2007)
- [429] Albrecht, H.E., Borys, M., Wenzel, M., Wriedt, T.H.: Influence of the measurement volume on the phase error in phase Doppler anemometry. Part 1: reflective mode operation. Particle and Particle Systems Characterization 11, 339–344 (1994)
- [430] Albrecht, H.E., Borys, M., Wenzel, M.: Influence of the measurement volume on the phase error in phase Doppler anemometry, Part 2: analysis by extension of geometrical optics to the laser beam; refractive mode operation. Particle and Particle Systems Characterization 13, 18–26 (1996)
- [431] Yokoi, N., Aizu, Y., Mishina, H.: Estimation of particle trajectory effects and their reduction using polarization in phase-Doppler particle measurements. Optical Engineering 38(11), 1869–1882 (1999)
- [432] Yokoi, N., Aizu, Y., Mishina, H.: Unidirectional phase-Doppler method for particle size measurements. Applied Optics 40(7), 1049–1064 (2001)
- [433] Strakey, P.A., Talley, D.G., Sankar, S.V., Bachalo, W.D.: Phase-Doppler interferometry with probe-to-droplet size ratios less than unity. I. Trajectory errors. Applied Optics 39(22), 3875–3886 (2000)
- [434] Strakey, P.A., Talley, D.G., Sankar, S.V., Bachalo, W.D.: Phase-Doppler interferometry with probe-to-droplet size ratios. II. Application of the technique. Applied Optics 39(22), 3887–3893 (2000)
- [435] Qiu, H., Hsu, C.-T.: Minimum deviation of spatial frequency in large-particle sizing. Applied Optics 37(28), 6787–6794 (1998)
- [436] Qiu, H.H., Jia, W.C.: High-resolution optical particle sizing in an optimized orientation. Optical Engineering 38(12), 2104–2113 (1999)
- [437] Qiu, H.H., Jia, W.: Effect of refractive index in optical particle sizing by using spatial frequency method. Optics Communications 178(1-3), 199–210 (2000)
- [438] Qiu, H.H.: Eliminating high-order scattering effects in optical microbubble sizing. Journal of the Optical Society of America A 20(4), 690–697 (2003)
- [439] Qiu, H.H., Hsu, C.T.: The impact of high order refraction on optical microbubble sizing in multiphase flows. Experiments in Fluids 36(1), 100–107 (2004)
- [440] von Benzon, H.-H., Buchhave, P.: The phase-Doppler method applied to very small particles. Particle and Particle Systems Characterization 11, 55–62 (1994)

[441] Sankar, S.V., Ibrahim, K.M., Bachalo, W.D.: Coherent scattering by multiple particles in phase Doppler interferometry. Particle and Particle Systems Characterization 11, 35–42 (1994)

- [442] Ungut, A., Gréhan, G., Gouesbet, G.: Comparisons between geometrical optics and Lorenz-Mie theory for transparent particles in forward directions. Applied Optics 20(17), 2911–2918 (1981)
- [443] Schaub, S.A., Alexander, D.R., Barton, J.P.: Theoretical analysis of the effects of particle trajectory and structural resonances on the performance of a phase-Doppler particle analyzer. Applied Optics 33(3), 473–483 (1994)
- [444] Gupta, A.K., Avedisian, C.T.: Role of combustion on droplet transport in pressure-atomized spray flames. Journal of propulsion and power 12(3), 543– 553 (1996)
- [445] Willmann, M., Glahn, A., Wittig, S.: Phase-Doppler particle sizing with offaxis angles in Alexander's darkband. Particle and Particle Systems Characterization 14, 122–128 (1997)
- [446] Saumweber, C., Friedman, J.A., Renksizbulut, M.: Simultaneous droplet size and gas-phase turbulence measurements in a spray flow using phase-Doppler interferometry. Particle and Particle Systems Characterization 14, 233–242 (1997)
- [447] Dahl, H., Wriedt, T.: The simulation of phase-Doppler anemometry by the multiple multipole method. Particle and Particle Systems Characterization 14, 181–185 (1997)
- [448] Jiang, Z.: Phase maps based on the Lorenz-Mie theory to optimize phase Doppler particle-sizing systems. Applied Optics 36(6), 1367–1375 (1997)
- [449] Schaub, S.A., Lock, J.A., Naqwi, A.A.: Development of a generalized theoretical model for the response of a phase/Doppler measurement system to arbitrarily oriented fibers illuminated by Gaussian beams. Applied Optics 37(33), 7842–7855 (1998)
- [450] Schaub, S.A., Naqwi, A.A., Harding, F.L.: Design of a phase/Doppler light-scattering system for measurement of small-diameter glass fibers during fiber-glass manufacturing. Applied Optics 37(3), 573–585 (1998)
- [451] Yu, Z., Rasmuson, A.C.: Projected area of measurement volume in phase-Doppler anemometry and application for velocity bias correction and particle concentration estimation. Experiments in Fluids 27(2), 189–198 (1999)
- [452] Wigley, G., Heath, J., Pitcher, G., Whybrew, A.: Experimental analysis of the response of a Laser/Phase Doppler Anemometer system to a partially atomized spray. Particle and Particle Systems Characterization 18(4), 169– 178 (2001)
- [453] Widmann, J.F., Presser, C., Leigh, S.D.: Identifying burst splitting events in phase Doppler interferometry measurements. Atomization and Sprays 11(6), 711–733 (2001)
- [454] Widmann, J.F., Presser, C., Leigh, S.D.: Improving phase Doppler volume flux measurements in low data rate applications. Measurement Science and Technology 12(8), 1180–1190 (2001)
- [455] Widmann, J.F.: Phase Doppler interferometry measurements in water sprays produced by residential fire sprinklers. Fire Safety Journal 36(6), 545–567 (2001)

[456] Bergenblock, T., Onofri, F., Leckner, B., Tadrist, L.: Experimental estimation of particle flow fluctuations in dense unsteady two-phase flow using phase Doppler anemometry. International Journal of Multiphase Flow 33(8), 849– 872 (2007)

- [457] Hespel, C., Ren, K.F., Gréhan, G., Onofri, F.: Numerical study of glare spot phase Doppler anemometry. Optics Communications 281(6), 1375–1383 (2008)
- [458] Ren, K.F., Lebrun, D., Ozkul, C., Kleitz, A., Gouesbet, G., Gréhan, G.: On the measurements of particles by imaging methods: theoretical and experimental aspects. Particle and Particle Systems Characterization 13, 156–164 (1996)
- [459] Girasole, T., Ren, K.F., Lebrun, D., Gouesbet, G., Gréhan, G.: Particle imaging sizing: GLMT simulations. Journal of Visualization (Visualization Society of Japan) 3(2), 195–202 (2000)
- [460] Hardalupas, Y., Hishida, K., Maeda, M., Morikita, H., Taylor, A.M.K.P., Whitelaw, J.: Shadow Doppler technique for sizing particles of arbitrary shape. Applied Optics 33, 8417–8426 (1994)
- [461] Maeda, M., Morikita, M., Prassas, I., Taylor, A.M.K.P., Whitelaw, J.: Shadow Doppler velocimetry for simultaneous size and velocity measurements of irregular particles in confined reacting flows. Particle and Particle Systems Characterization 14, 79–87 (1997)
- [462] Morikita, H., Taylor, A.M.K.P.: Application of shadow Doppler velocimetry to paint spray: potential and limitations in sizing optically inhomogeneous droplets. Measurement Science and Technology 9, 221–231 (1998)
- [463] Ren, K.F., Girasole, T., Taylor, A.K.M.P., Gouesbet, G., Gréhan, G.: Theoretical evaluation of a shadow Doppler velocimeter. Optics Communications 220, 269–280 (2003)
- [464] Zinin, P., Weise, W., Lobkis, O., Kolosev, O., Boseck, S.: Fourier optics analysis of spherical particles image formation in reflection acoustic microscopy. Optik 98(2), 45–60 (1994)
- [465] Guerrero-Viramontes, J.A., Moreno-Hernandez, D., Mendoza-Santoyo, F., Funes-Gallanzi, M.: 3D particle positioning from CCD images using the generalized Lorenz-Mie theory and Huygens-Fresnel theories. Measurement Science and Technology 17(8), 2328–2334 (2006)
- [466] Funes-Gallanzi, M., Guerrero, J.A., Moreno, D., Barrientos, B., Santoyo, F.M., Torales, G.G.: Non-spherical seeding 3D positioning from CCD images using Lorenz-Mie theory. Measurement Science and Technology 15(11), 2333–2340 (2004)
- [467] Guerrero, J.A., Santoyo, F.M., Moreno, D., Funes-Gallanzi, M.: The case of a spherical wave front for the generalized Lorenz-Mie theory including a comparison to experimental data. Optics Communications 203(3-6), 175–182 (2002)
- [468] Lock, J.A., Jamison, J.M., Lin, C.-Y.: Rainbow scattering by a coated sphere. Applied Optics 33(21), 4677-4690 (1994)
- [469] Han, X., Ren, K.F., Mees, L., Gouesbet, G., Gréhan, G.: Surface waves/geometrical rays interferences: numerical and experimental behaviour at rainbow angles. Optics Communications 195, 49–54 (2001)
- [470] Han, X., Ren, K.F., Wu, Z., Corbin, F., Gouesbet, G., Gréhan, G.: Characterization of initial disturbances in liquid jet by rainbow sizing. Applied Optics 37(36), 8498–8503 (1998)

[471] van Beeck, J.P.A.J., Riethmuller, M.L.: Rainbow phenomena applied to the measurement of droplet size and velocity and to the detection of nonsphericity. Applied Optics 35(13), 2259–2266 (1996)

- [472] Wilms, J., Weigand, B.: Composition measurements of binary mixture droplets by rainbow refractometry. Applied Optics 46(11), 2109–2118 (2007)
- [473] Saengkaew, S., Charinpanitkul, T., Vanisri, H., Tanthapanichakoon, W., Méès, L., Gouesbet, G., Gréhan, G.: Rainbow refractometry: on the validity domain of Airy's and Nussenzweig's theories. Optics Communications 259, 7–13 (2006)
- [474] Wilms, J., Gréhan, G., Lavergne, G.: Global rainbow refractometry with a selective imaging method. Particle and Particle Systems Characterization 25(1), 39–48 (2008)
- [475] Bemer, D., Fabries, J.F., Renoux, A.: Calculation of the theoretical response of an optical particle counter and its practical usefulness. Journal of Aerosol Science 21(5), 689–700 (1990)
- [476] Hesselbacher, K.H., Anders, K., Frohn, A.: Experimental investigation of Gaussian beam effects on the accuracy of a droplet sizing method. Applied Optics 30(33), 4930–4935 (1991)
- [477] van de Hulst, H.C., Wang, R.T.: Glare points. Applied Optics 30(33), 4755–4763 (1991)
- [478] Li, L., Szapiel, S., Delisle, C.: Fizeau digital interferometry with a diffractiongenerated spherical wave for testing focusing optics. Applied Optics 31(7), 866–875 (1992)
- [479] Doornbos, R.M.P., Hoekstra, A.G., Deurloo, K.E.I., De Grooth, B.G., Sloot, P.M.A., Greve, J.: Lissajous-like patterns in scatter plots of calibration beads. Cytometry 16, 236–242 (1994)
- [480] Hoekstra, A.G., Doornbos, R.M.P., Deurloo, K.E.I., Noordmans, H.J., De Grooth, B.G., Sloot, P.M.A.: Another face of Lorenz-Mie scattering: monodisperse distributions of spheres produce Lissajous-like patterns. Applied Optics 33(3), 494–500 (1994)
- [481] Doornbos, R.M.P., Schaeffer, M., Hoekstra, A.G., Sloot, P.M.A., De Grooth, B.G., Greve, J.: Elastic light-scattering measurements of single biological cells in an optical trap. Applied Optics 35(4), 729–734 (1996)
- [482] Anders, K., Roth, N., Frohn, A.: New technique for investigating phase transition processes of optically levitated droplets consisting of water and sulfuric acid. Journal of geophysical research 101(D14), 19,223–19,229 (1996)
- [483] Trunk, M., Lübben, J.F., Popp, J., Schrader, B., Kiefer, W.: Investigation of a phase transition in a single optically levitated microdroplet by Raman-Mie scattering. Applied Optics 36(15), 3305–3309 (1997)
- [484] Min, S.L., Gomez, A.: High-resolution size measurement of single spherical particles with a fast Fourier transform of the angular scattering intensity. Applied Optics 35(24), 4919–4926 (1996)
- [485] Wang, X.-J., Milner, T.E., Chen, Z., Nelson, J.S.: Measurement of fluid-flow-velocity profile in turbid media by the use of optical Doppler tomography. Applied Optics 36(1), 144–149 (1997)
- [486] Rambert, A., Huber, L., Gougat, P.: Laboratory study of fungal spore movement using laser Doppler velocimetry. Agricultural and forest meteorology 92, 43–53 (1998)

[487] Ovod, V.I., Stintz, M., Heidenberg, E.: Modified conventional plane-wave scattering approach to estimate performance characteristics of laser particlesize analysers. Journal of Modern Optics 45(2), 299–314 (1998)

- [488] Steiner, B., Berge, B., Gausmann, R., Rohmann, J., Ruhl, E.: Fast in situ sizing technique for single levitated liquid aerosols. Applied Optics 38(9), 1523–1529 (1999)
- [489] Allersma, M.W., Gittes, F., de Castro, M.J., Stewart, R.J., Schmidt, C.F.: Two-dimensional tracking of ncd motility by back focal plane interferometry. Biophysical Journal 74, 1074–1085 (1998)
- [490] Godefroy, C., Adjouadi, M.: Particle sizing in a flow environment using light scattering patterns. Particle and Particle Systems Characterization 17(2), 47–55 (2000)
- [491] Ost, V., Neukammer, J., Rinneberg, H.: Flow cytometric differentiation of erythrocytes and leukocytes in dilute whole blood by light scattering. Cytometry 32, 191–197 (1998)
- [492] Sloot, P.M.A., Hoekstra, A.G., van der Liet, H., Figdor, C.G.: Scattering matrix elements of biological particles measured in a flow through system: theory and practice. Applied Optics 28(10), 1752–1762 (1989)
- [493] Soini, J.T., Chernyshev, A.V., Hänninen, P.E., Soini, E., Maltsev, V.P.: A new design of the flow cuvette and optical set-up for the scanning flow cytometer. Cytometry 31, 78–84 (1998)
- [494] Watson, D., Hagen, N., Diver, J., Marchand, P., Chachisvilis, M.: Elastic light scattering from single cells: Orientational dynamics in optical trap. Biophysical Journal 87(2), 1298–1306 (2004)
- [495] Maltsev, V.P.: Scanning flow cytometry for individual particle analysis. Review of Scientific Instruments 71(1), 243–255 (2000)
- [496] Shen, J.Q., Riebel, U.: Extinction by a large spherical particle located in a narrow Gaussian beam. Particle and Particle Systems Characterization 18(5-6), 254–261 (2002)
- [497] Castagner, J.L., Jones, A.R.: A double Gaussian beam method for the determination of particle size, direction and velocity. Particle and Particle Systems Characterization 21(1), 5–14 (2004)
- [498] Castagner, J.L., Bigio, I.J.: Particle sizing with a fast polar nephelometer. Applied Optics 46(4), 527–532 (2007)
- [499] Castanet, G., Delconte, A., Lemoine, F., Mees, L., Gréhan, G.: Evaluation of temperature gradients within combusting droplets in linear stream using two colors laser-induced fluorescence. Experiments in Fluids 39(2), 431–440 (2005)
- [500] Schaub, S.A., Alexander, D.R., Barton, J.P., Emanuel, M.A.: Focused laser beam interactions with methanol droplets: effects of relative beam diameter. Applied Optics 28(9), 1666–1669 (1989)
- [501] Alexander, D.R., Barton, J.P., Schaub, S.A., Holtmeier, G.M.: Nonlinear interaction of KrF laser radiation with small water droplets. Applied Optics 30(12), 1455–1460 (1991)
- [502] Matsko, A.B., Savchenkov, A.A., Letargat, R.J., Ilchenko, V.S., Maleki, L.: On cavity modification of stimulated Raman scattering. Journal of Optics B 5(3), 272–278 (2003)
- [503] Maqua, C., Castanet, G., Lemoine, F., Doué, N., Lavergne, G.: Temperature measurements of binary droplets using three-color laser-induced fluorescence. Experiments in Fluids 40, 786–797 (2006)

[504] Maqua, C., Depredurand, V., Castanet, G., Wolff, M., Lemoine, F.: Composition measurement of bicomponent droplets using laser-induced fluorescence of acetone. Experiments in Fluids 43(6), 979–992 (2007)

- [505] Zhang, J.-Z., Chen, G., Chang, R.K.: Pumping of stimulated Raman scattering by stimulated Brillouin scattering within a single liquid droplet: input laser linewidth effects. Journal of the Optical Society of America B 7(1), 108–115 (1990)
- [506] Yakovlev, V.V., Luk'yanchuk, B.: Multiplexed nanoscopic imaging. Laser Physics 14(8), 1065–1071 (2004)
- [507] Wiggins, S.M., Robb, G.R.M., McNeil, B.W.J., Jaroszynski, D.A., Jones, D.R., Jamison, S.P.: Collective Rayleigh scattering from dielectric particles. Measurement Science and Technology 13(3), 263–269 (2002)
- [508] Onofri, F.: Three interfering beams in laser Doppler velocimetry for particle position and microflow velocity profile measurements. Applied Optics 45(14), 3317–3324 (2006)
- [509] Onofri, F., Krysiek, M., Mroczka, J.: Critical angle refractometry and sizing of bubble clouds. Optics Letters 32(14), 2070–2072 (2007)
- [510] Riefler, N., Schuh, R., Wriedt, T.: Investigation of a measurement technique to estimate concentration and size of inclusions in droplets. Measurement Science and Technology 18(7), 2209–2218 (2007)
- [511] Georgescu, R., Khismatullin, D., Holt, R.G., Castagner, J.L., Aámar, O.: Design of a system to measure light scattering from individual cells excited by an acoustic wave. Optics Express 16(6), 3496–3503 (2008)
- [512] You, Z., Li, Y.P., Chen, J.: Measurement of novel micro bulk defects in semiconductive materials based on Mie scatter. Indian Journal of Pure and Applied Physics 45(4), 372–376 (2007)
- [513] Sigel, R., Erbe, A.: Effects of sample polydispersity and beam profile on ellipsometric light scattering. Applied Optics 47(12), 2161–2170 (2008)
- [514] Smith, Z.J., Berger, A.J.: Integrated Raman- and angular-scattering microscopy. Optics Letters 33(7), 714–716 (2008)
- [515] Bohren, G.F., Huffman, D.R.: Absorption and scattering of light by small particles. J. Wiley and sons, Chichester (1983)
- [516] Cantrell, C.D.: Theory of nonlinear optics in dielectric spheres. II. Coupled-partial-wave theory of resonant, resonantly pumped stimulated Brillouin scattering. Journal of Optical Society America B 8(10), 2158–2180 (1991)
- [517] Cantrell, C.D.: Theory of nonlinear optics in dielectric spheres. III. Partial-wave-index dependence of the gain for stimulated Brillouin scattering. Journal of Optical Society America B 8(10), 2181–2189 (1991)
- [518] Lai, H.M., Lam, C.C., Leung, P.T., Young, K.: Effect of perturbations on the widths of narrow morphology-dependent resonances in Mie scattering. Journal of the Optical Society of America B 8(9), 1962–1973 (1991)
- [519] Lai, H.M., Leung, P.T., Ng, C.K., Young, K.: Nonlinear elastic scattering of light from a microdroplet: role of electrostrictively generated acoustic vibrations. Journal of the Optical Society of America B 10(5), 924–932 (1993)
- [520] Eversole, J.D., Lin, H.B., Campillo, A.J.: Input/output resonance correlation in laser-induced emission from microdroplets. Journal of Optical Society America B 12(2), 287–296 (1995)
- [521] Aker, P.M., Moortgat, P.A., Zhang, J.-X.: Morphology-dependent stimulated Raman scattering imaging. I. Theoretical aspects. Journal of Chemical Physics 105(17), 7268–7275 (1996)

[522] Nussenzveig, H.M.: Diffraction effects in semiclassical scattering. Cambridge University Press, Cambridge (1992)

- [523] Lock, J.A.: Excitation efficiency of a morphology-dependent resonance by a focused Gaussian beam. Journal of the Optical Society of America A 15(12), 2986–2994 (1998)
- [524] Serpengüzel, A., Arnold, S., Griffel, G.: Excitation of resonances of microspheres on an optical fiber. Optics Letters 20(7), 654–656 (1995)
- [525] Serpengüzel, A., Arnold, S., Griffel, G., Lock, J.A.: Enhanced coupling to microsphere resonances with optical fibers. Journal of the Optical Society of America 14(4), 790–795 (1997)
- [526] Serpengüzel, A., Demir, A.: Silicon microspheres for near-IR communication applications. Semiconductor Science and Technology, Art 064009 23(6) (2008)
- [527] Roll, G., Kaiser, T., Lange, S., Schweiger, G.: Ray interpretation of multipole fields in spherical dielectric cavities. Journal of the Optical Society of America A 15(11), 2879–2891 (1998)
- [528] Aker, P.M., Zhang, J.X., Nichols, W.: Nitrate ion detection in aerosols using morphology-dependent stimulated Raman scattering. Journal of Chemical Physics 110(4), 2202–2207 (1999)
- [529] Arias-Gonzalez, J.R., Nieto-Vesperinas, M., Madrazo, A.: Morphology-dependent resonances in the scattering of electromagnetic waves from an object buried beneath a plane or a random rough surface. Journal of the Optical Society of America A 16(12), 2928–2934 (1999)
- [530] Lock, J.A.: Excitation of morphology-dependent resonances and van de Hulst's localization principle. Optics Letters 24(7), 427–429 (1999)
- [531] Pastel, R., Struthers, A.: Measuring evaporation rates of laser-trapped droplets by use of fluorescent morphology-dependent resonances. Applied Optics 40(15), 2510–2514 (2001)
- [532] Leung, P.T., Ng, S.W., Pang, K.M., Lee, K.M.: Morphology-dependent resonances in dielectric spheres with many tiny inclusion. Optics Letters 27(20), 1749–1751 (2002)
- [533] Oraevsky, A.N.: Whispering-gallery waves. Quantum electronics 32(5), 377–400 (2002)
- [534] Hill, S.C.: Method for integrating the absorption cross sections of spheres over wavelength or diameter. Applied Optics 42(21), 4381–4388 (2003)
- [535] Bilici, T., Isci, S., Kurt, A., Serpengüzel, A.: GaInNAs microspheres for wavelength division multiplexing. In: IEE Proceedings-Optoelectronics, vol. 150(1), pp. 89–91 (2003)
- [536] Isci, S., Bilici, T., Kurt, A., Serpengüzel, A.: Morphology-dependent resonances of optical microsphere resonators for the realization of passive wavelength-division multiplexing components. Optical Engineering 43(5), 1051–1055 (2004)
- [537] Yadav, R.A., Singh, I.D.: Normal modes and quality factors of spherical dielectric resonators: I-shielded dielectric sphere. Pramana-Journal of Physics 62(6), 1255–1271 (2004)
- [538] Rao, V.S.C.M., Gupta, S.D.: Broken azimuthal degeneracy with whispering gallery modes of microspheres. Journal of Optics A: Pure and Applied Optics 7(7), 279–285 (2005)

[539] Fontes, A., Neves, A.A.R., Moreira, W.L., de Thomaz, A.A., Barbosa, L.C., Cesar, C.L., de Paula, A.M.: Double optical tweezers for ultrasensitive force spectroscopy in microsphere Mie scattering. Applied Physics Letters, Art 221109 87(22) (2005)

- [540] Matsko, A.B., Ilchenko, V.S.: Optical resonators with whispering-gallery modes. Part I: basics. IEEE Journal of Selected Topics in Quantum Electronics 12(1), 3–14 (2006)
- [541] Qiu, S.L., Cai, J.X., Li, Y.P., Han, Z.F.: Mode frequency shifts and Q-factor changes in 2D microflower cavity and its deformed cavity. Optics Communications 277(2), 406–410 (2007)
- [542] Kiraz, A., Kurt, A., Dundar, M.A., Yuce, M.Y., Demirel, A.L.: Volume stabilization of single, dye-doped water microdroplets with femtoliter resolution. Journal of the Optical Society of America B 24(8), 1824–1828 (2007)
- [543] Kiraz, A., Karadag, Y., Muradoglu: Large spectral tuning of a water-glycerol microdroplet by a focused laser: characterization and modeling. Physical Chemistry Chemical Physics 10, 1–9 (2008)
- [544] Mojarad, N.M., Sandoghdar, V., Agio, M.: Plasmon spectra of nanospheres under a tightly focused beam. Journal of the Optical Society of America B 25(4), 651–658 (2008)
- [545] Xu, Y., Han, M., Wang, A.B., Liu, Z.W., Heflin, J.R.: Second order parametric processes in nonlinear silica microspheres. Physical Review Letters 100(16), Art 163905 (2008)
- [546] Davis, E.J.: A history of single aerosol particle levitation. Aerosol Science and Technology 26, 212–254 (1997)
- [547] Park, S.O., Lee, S.S.: Forward far-field pattern of a laser beam scattered by a water-suspended homogeneous sphere trapped by a focused laser beam. Journal of the Optical Society of America A 4(3), 417–422 (1987)
- [548] Gréhan, G., Guilloteau, F., Gouesbet, G.: Generalized Lorenz-Mie theory validations: the off-axis case. Particle and Particle Systems Characterization, special issue for Prof. Leschonskii 60th anniversary 7(4), 248–249 (1990)
- [549] Ren, K.F., Gréhan, G., Gouesbet, G.: Radiation pressure forces exerted on a particle arbitrarily located in a Gaussian beam by using the generalized Lorenz-Mie theory, and associated resonance effects. Optics Communications 108, 343–354 (1994)
- [550] Polaert, H., Gréhan, G., Gouesbet, G.: Forces and torques exerted on a multilayered spherical particle by a focused Gaussian beam. Optics Communications 155, 169–179 (1998)
- [551] Angelova, M.I., Pouligny, B., Martinot-Lagarde, G., Gréhan, G., Gouesbet, G.: Stressing phospholipid membranes using mechanical effects of light. Prog. Coll. and Polymer Sci. 97, 293–297 (1994)
- [552] Angelova, M.I., Pouligny, B.: Trapping and levitation of a dielectric sphere with off-centred Gaussian beams. I. Experimental. Pure and Applied Optics 2, 261–276 (1993)
- [553] Martinot-Lagarde, G., Pouligny, B., Angelova, M.I., Gréhan, G., Gouesbet, G.: Trapping and levitation of a dielectric sphere with off-centred Gaussian beams. II. GLMT-analysis. Pure and Applied Optics 4, 571–585 (1995)
- [554] Martinot-Lagarde, G., Angelova, M.I., Pouligny, B., Gréhan, G., Gouesbet, G.: Laser trappings of micron particles and dynamometrical applications. Annales de Physique 20(2), 127–128 (1995)

[555] Dietrich, C., Angelova, M., Pouligny, B.: Adhesion of latex spheres to giant phospholipid vesicles: statics and dynamics. J. Phys. II, France, 1651–1682 (1997)

- [556] Dimova, R., Pouligny, B., Dietrich, C.: Pretransitional effects in dimyristoylphosphatidylcholine vesicle membranes: optical dynamometry study. Biophysical Journal 79(1), 340–356 (2000)
- [557] Gauthier, R.C., Ashman, M.: Simulated dynamic behavior of single and multiple spheres in the trap region of focused laser beams. Applied Optics 37(27), 6421–6431 (1998)
- [558] Gauthier, R.C., Ashman, M., Grover, C.P.: Experimental confirmation of the optical-trapping properties of cylindrical objects. Applied Optics 38(22), 4861–4869 (1999)
- [559] Gauthier, R.C., Tait, R.N., Mende, H., Pawlowicz, C.: Optical selection, manipulation, trapping, and activation of a microgear structure for applications in micro-optical-electromechanical systems. Applied Optics 40(6), 930–937 (2001)
- [560] Gauthier, R.C.: Optical levitation and trapping of a micro-optic inclined end-surface cylindrical spinner. Applied Optics 40(12), 1961–1973 (2001)
- [561] Gauthier, R.C.: Laser-trapping properties of dual-component spheres. Applied Optics 41(33), 7135–7144 (2002)
- [562] Gauthier, R.C., Friesen, M., Gerrard, T., Hassouneh, W., Koziorowski, P., Moore, D., Oprea, I., Uttamalingam, S.: Self-centering of a ball lens by laser trapping: fiber ball-fiber coupling analysis. Applied Optics 42(9), 1610–1619 (2003)
- [563] Gauthier, R.C.: Computation of the optical trapping force using an FDTD based technique. Optics Express 13(10), 3707–3718 (2005)
- [564] Wohland, T., Rosin, A., Stelzer, E.H.K.: Theoretical determination of the influence of the polarization on forces exerted by optical tweezers. Optik 102(4), 181–190 (1995)
- [565] Cai, W., Li, F., Sun, S., Wang, Y.: Optical levitation measurements with intensity-modulated light beams. Applied Optics 36(30), 7860–7863 (1997)
- [566] Omori, R., Kobayashi, T., Suzuki, A.: Observation of a single-beam gradient-force optical trap for dielectric particles in air. Optics Letters 22(11), 816–818 (1997)
- [567] Nemoto, S., Togo, H.: Axial force acting on a dielectric sphere in a focused laser beam. Applied Optics 37(27), 6386–6394 (1998)
- [568] Omori, R., Suzuki, A.: Uranium dioxide particles collection using radiation pressure of a laser light in air. Journal of Nuclear Science and Technology 35(11), 830–832 (1998)
- [569] Pastel, R., Struthers, A., Ringle, R., Rogers, J., Rohde, C., Geiser, P.: Laser trapping of microscopic particles for undergraduate experiments. American Journal of Physics 68(11), 993–1001 (2000)
- [570] Hoekstra, A.G., Frijlink, M., Waters, L.B.F.M., Sloot, P.M.A.: Radiation forces in the discrete-dipole approximation. Journal of the Optical Society of America A 18(8), 1944–1953 (2001)
- [571] Nieminen, T.A., Rubinsztein-Dunlop, H., Heckenberg, N.R., Bishop, A.I.: Numerical modelling of optical trapping. Computer Physics Communications 142(1-3), 468–471 (2001)
- [572] Nieminen, T.A., Rubinsztein-Dunlop, H., Heckenberg, N.R.: Calculation and optical measurement of laser trap forces on non-spherical particles. Journal of Quantitative Spectroscopy and Radiative Transfer 70(4-6), 627-637 (2001)

[573] Bayoudh, S., Nieminen, T.A., Heckenberg, N.R., Rubinsztein-Dunlop, H.: Orientation of biological cells using plane-polarized Gaussian beam optical tweezers. Journal of Modern Optics 50(10), 1581–1590 (2003)

- [574] Bishop, A.I., Nieminen, T.A., Heckenberg, N.R., Rubinsztein-Dunlop, H.: Optical application and measurement of torque on microparticles of isotropic nonabsorbing material. Physical Review A 68(3), Art 033802 (2003)
- [575] Nieminen, T.A., Knoner, G., Heckenberg, N.R., Rubinsztein-Dunlop, H.: Physics of optical tweezers. Laser Manipulation of Cells and Tissues 82, 207–236 (2007)
- [576] Nieminen, T.A., Loke, V.L.Y., Stilgoe, A.B., Knoner, G., Branczyk, A.M., Heckenberg, N.R., Rubinsztein-Dunlop, H.: Optical tweezers computational toolbox. Journal of Optics A: Pure and Applied Optics 9(8), S196–S203 (2007)
- [577] Resnick, A.: Design and construction of a space-borne optical tweezer apparatus. Review of Scientific Instruments 72(11), 4059–4065 (2001)
- [578] Rohrbach, A., Stelzer, E.H.K.: Optical trapping of dielectric particles in arbitrary fields. Journal of the Optical Society of America A 18(4), 839–853 (2001)
- [579] Rohrbach, A., Stelzer, E.H.K.: Three-dimensional position detection of optically trapped dielectric particles. Journal of Applied Physics 91(8), 5474–5488 (2002)
- [580] Rohrbach, A., Stelzer, E.H.K.: Trapping forces, force constants, and potential depths for dielectric spheres in the presence of spherical aberrations. Applied Optics 41(13), 2494–2507 (2002)
- [581] Rohrbach, A., Tischer, C., Neumayer, D., Florin, E.L., Stelzer, E.H.K.: Trapping and tracking a local probe with a photonic force microscope. Review of Scientific Instruments 75(6), 2197–2210 (2004)
- [582] Harada, Y., Asakura, T.: Effects of the laser radiation pressure in photon correlation spectrocopy. Optics Communications 107, 161–169 (1994)
- [583] Lhuissier, N., Gouesbet, G., Weill, M.E.: Extensive measurements on soot particles in laminar premixed flames by quasi-elastic light scattering spectroscopy. Combustion science and technology 67, 17–36 (1989)
- [584] Harada, Y., Asakura, T.: Dynamics and dynamic light-scattering properties of Brownian particles under laser radiation pressure. Pure Appl. Opt. 7, 1001– 1012 (1998)
- [585] Harada, Y., Asakura, T.: Radiation forces on a dielectric sphere in the Rayleigh scattering regime. Optics Communications 124, 529–541 (1996)
- [586] Roth, N., Anders, K., Frohn, A.: Determination of size, evaporation rate and freezing of water droplets using light scattering and radiation pressure. Particle and Particle Systems Characterization 11, 207–211 (1994)
- [587] Roll, G., Kaiser, T., Schweiger, G.: Optical trap sedimentation cell A new technique for the sizing of microparticles. Journal of Aerosol Science 27(1), 105–117 (1996)
- [588] Grier, D.G.: Optical tweezers in colloid and interface science. Current Opinion in Colloid and Interface Science 2(3), 264–270 (1997)
- [589] Nahmias, Y.K., Odde, D.J.: Analysis of radiation forces in laser trapping and laser-guided direct writing applications. IEEE Journal of Quantum electronics 38(2), 131–141 (2002)
- [590] Dufresne, E.R., Grier, D.G.: Optical tweezer arrays and optical substrates created with diffractive optics. Review of scientific instruments 69(5), 1974– 1977 (1998)

[591] Gahagan, K.T., Swartzlander Jr., G.A.: Trapping of low-index microparticles in an optical vortex. Journal of the Optical Society of America B 15(2), 524– 534 (1998)

- [592] Gensch, T., Hofkens, J., van Stam, J., Faes, H., Creutz, S., Tsuda, K., Jérôme, R., Masuhara, H., De Schryver, F.C.: Transmission and confocal fluorescence microscopy and time-resolved fluorescence spectroscopy combined with a laser trap: investigation of optically trap block copolymer micelles. J. Phys. Chem. B 102, 8440–8541 (1998)
- [593] Shima, K., Omori, R., Suzuki, A.: Forces of a single-beam gradient-force optical trap on dielectric spheroidal particles in the geometric-optics regime. Jpn. J. Appl. Phys. 37, 6012–6015 (1998)
- [594] Gittes, F., Schmidt, C.F.: Interference model for back-focal-plane displacement detection in optical tweezers. Optics Letters 23(1), 7–9 (1998)
- [595] Song, Y.G., Han, B.M., Chang, S.: Force of surface plasmon-coupled evanescent fields on Mie particles. Optics Communications 198(1-3), 7–19 (2001)
- [596] Miao, X.Y., Lin, L.Y.: Trapping and manipulation of biological particles through a plasmonic platform. IEEE Journal of Selected Topics in Quantum Electronics 13(6), 1655–1662 (2007)
- [597] Benabid, F., Knight, J.C., Russell, P.S.: Particle levitation and guidance in hollow-core photonic crystal fiber. Optics Express 10(21), 1195–1203 (2002)
- [598] Malagnino, N., Pesce, G., Sasso, A., Arimondo, E.: Measurements of trapping efficiency and stiffness in optical tweezers. Optical Communications 214(1-6), 15–24 (2002)
- [599] Afanas'ev, A.A., Katarkevich, V.M., Rubinov, A.N., Efendiev, T.S.: Modulation of particle concentrations in the interference laser radiation field. Journal of Applied Spectroscopy 69(5), 782–787 (2002)
- [600] Nahmias, Y.K., Gao, B.Z., Odde, D.J.: Dimensionless parameters for the design of optical traps and laser guidance systems. Applied Optics 43(20), 3999–4006 (2004)
- [601] Zemanek, P., Jonas, A., Liska, M.: Simplified description of optical forces acting on a nanoparticle in the Gaussian standing wave. Journal of the Optical Society of America A 19(5), 1025–1034 (2002)
- [602] Zemanek, P., Jonas, A., Jakl, P., Jezek, J., Sery, M., Liska, M.: Theoretical comparison of optical traps created by standing wave and single beam. Optics Communications 220(4-6), 401–412 (2003)
- [603] Jakl, P., Sery, M., Jozek, J., Jonas, A., Liska, M., Zemanek, P.: Behaviour of an optically trapped probe approaching a dielectric interface. Journal of Modern Physics 50(10), 1615–1625 (2003)
- [604] Zemanek, P., Karasek, V., Sasso, A.: Optical forces acting on a Rayleigh particle placed into interference field. Optics Communications 240(4-6), 401– 415 (2004)
- [605] Furst, E.M.: Interactions, structure, and microscopic response: complex fluid rheology using laser tweezers. Soft Materials 1(2), 167–185 (2003)
- [606] Furst, E.M.: Applications of laser tweezers in complex fluid rheology. Current Opinion in Colloid and Interface Science 10(1-2), 79–86 (2005)
- [607] Mazolli, A., Neto, P.A.M., Nussenzveig, H.M.: Theory of trapping forces in optical tweezers. Proceedings of the Royal Society of London, Series A 459(2040), 3021–3041 (2003)
- [608] Mund, C., Zellner, R.: Optical levitation of single microdroplets at temperatures down to 180 K. Chemphyschem 4(6), 630–638 (2003)

[609] Rubinov, A.N., Katarkevich, V.M., Afanas'ev, A.A., Efendiev, T.S.H.: Interaction of interference laser field with an ensemble of particles in liquid. Optics Communications 224(1-3), 97–106 (2003)

- [610] Buosciolo, A., Pesce, G., Sasso, A.: New calibration method for position detector for simultaneous measurements of force constants and local viscosity in optical tweezers. Optics Communications 230(4-6), 357–368 (2004)
- [611] Lock, J.A.: Calculation of the radiation trap force for laser tweezers by use of generalized Lorenz-Mie theory. I. Localized model description of an onaxis tightly focused laser beam with spherical aberration. Applied Optics 43, 2532–2544 (2004)
- [612] Lock, J.A.: Calculation of the radiation trapping force for laser tweezers by use of generalized Lorenz-Mie theory. II. On-axis trapping force. Applied Optics 43(12), 2545–2554 (2004)
- [613] Lock, J.A., Wrbanek, S.Y., Weiland, K.E.: Scattering of a tightly focused beam by an optically trapped particle. Applied Optics 45(15), 3634–3645 (2006)
- [614] Neuman, K.C., Block, S.M.: Optical trapping. Review of Scientific Instruments 75(9), 2787–2809 (2004)
- [615] Neuman, K.C., Abbondanzieri, E.A., Block, S.M.: Measurement of the effective local shift in an optical trap. Optics Letters 30(11), 1318–1320 (2005)
- [616] Neuman, K.C., Lionnet, T., Allemand, J.F.: Single-molecule micromanipulation techniques. Annual Review of Materials Research 37, 33–67 (2007)
- [617] Rockstuhl, C., Herzig, H.P.: Calculation of the torque on dielectric elliptical cylinders. Journal of the Optical Society of America A 22(1), 109–116 (2005)
- [618] Jaising, H.Y., Helleso, O.G.: Radiation forces on a Mie particle in the evanescent field of an optical waveguide. Optics Communications 264(4-6), 373–383 (2005)
- [619] Moine, O., Stout, B.: Optical force calculations in arbitrary beams by use of the vector addition theorem. Journal of the Optical Society of America B 22(8), 1620–1631 (2005)
- [620] Chang, S., Lee, S.S.: First-order calculations of radiation force for rotating sphere illuminated by circularly polarized Gaussian beam. Japanese Journal of Applied Physics 33, 2552–2558 (1994)
- [621] Chang, S., Jo, J.H., Lee, S.S.: Theoretical calculations of optical force exerted on a dielectric sphere in the evanescent field generated with a totally-reflected focused Gaussian beam. Optics Communications 108, 133–143 (1994)
- [622] Chang, S., Kim, J.T., Jo, J.H., Lee, S.S.: Optical force on a sphere caused by the evanescent field of a Gaussian beam, effects of multiple scattering. Optics Communications 139, 252–261 (1997)
- [623] Chang, Y.R., Hsu, L., Chi, S.: Optical trapping of a spherically symmetric sphere in the ray-optics regime: a model for optical tweezers upon cells. Applied Optics 45(16), 3885–3892 (2006)
- [624] Flynn, R.A., Shao, B., Chachisvilis, M., Ozkan, M., Esener, S.C.: Counter-propagating optical trapping system for size and refractive index measurement of microparticles. Biosensors and Bioelectronics 21(7), 1029–1036 (2006)
- [625] Han, Y.P., Du, Y.G., Zhang, H.Y.: Radiation trapping forces acting on a two-layered spherical particle in a Gaussian beam. Acta Physica Sinica 55(9), 4557–4562 (2006)
- [626] Kotlyar, V.V., Nalimov, A.G.: Analytical expression for radiation forces on a dielectric cylinder illuminated by a cylindrical Gaussian beam. Optics Express 14(13), 6316–6321 (2006)

[627] Kotlyar, V.V., Nalimov, A.G.: Calculating the pressure force of the non-paraxial cylindrical Gaussian beam exerted upon a homogeneous circular-shaped cylinder. Journal of Modern Optics 53(13), 1829–1844 (2006)

- [628] Kraikivski, P., Pouligny, B., Dimova, R.: Implementing both short- and long-working-distance optical trappings into a commercial microscope. Review of Scientific Instruments 77(11), Art 113703 (2006)
- [629] Merenda, F., Boer, G., Rohner, J., Delacretaz, G., Salathe, R.P.: Escape trajectories of single-beam optically trapped micro-particles in a transverse fluid flow. Optics Express 14(4), 1685–1699 (2006)
- [630] Simpson, S.H., Hanna, S.: Numerical calculation of interparticle forces arising in association with holographic assembly. Journal of the Optical Society of America A 23(6), 1419–1431 (2006)
- [631] Simpson, S.H., Hanna, S.: Optical trapping of spheroidal particles in Gaussian beams. Journal of the Optical Society of America A 24(2), 430–443 (2007)
- [632] Buajarern, J., Mitchem, L., Reid, J.P.: Characterizing multiphase organic/inorganic/aqueous aerosol droplets. Journal of Physical Chemistry A 111(37), 9054–9061 (2007)
- [633] Chaumet, P.C., Pouligny, B., Dimova, R., Sojic, N.: Optical tweezers in interaction with an apertureless probe. Journal of Applied Physics 102(2), Art 024915 (2007)
- [634] Gerlach, M., Rakovich, Y.P., Donegan, J.F.: Radiation-pressure-induced mode splitting in a spherical microcavity with an elastic shell. Optics Express 15(6), 3597–3606 (2007)
- [635] Grzegorczyk, T.M., Kong, J.A.: Analytical expression of the force due to multiple TM plane-wave incidences on an infinite lossless dielectric circular cylinder of arbitrary size. Journal of the Optical Society of America A 24(3), 644–652 (2007)
- [636] Yan, S.H., Yao, B.L.: Transverse trapping forces of focused Gaussian beam on ellipsoidal particles. Journal of the Optical Society of America B 24(7), 1596–1602 (2007)
- [637] Viana, N.B., Rocha, M.S., Mesquita, O.N., Mazolli, A., Neto, P.A.M., Nussenzveig, H.M.: Towards absolute calibration of optical tweezers. Physical Review E 75(2), Art 021914 (2007)
- [638] Kartashov, I.A., Leibov, E.M., Makarova, D.S., Shishaev, A.V.: Measuring the force parameters of a gradient-force optical trap for dielectric microobjects. Technical Physics 53(4), 504–509 (2008)
- [639] Ma, Z., Burg, K.J.L., Wei, Y.Z., Yuan, X.C., Peng, X., Gao, B.Z.: Laser-guidance based detection of cells with single-gene modification. Applied Physics Letters 92(21), Art 213902 (2008)
- [640] Hu, Y., Nieminen, T.A., Heckenberg, N.R., Rubinsztein-Dunlop, H.: Antireflection coating for improved optical trapping. Journal of Applied Physics 103(9), Art 093119 (2008)
- [641] Li, Z.P., Kall, M., Xu, H.: Optical forces on interacting plasmonic nanoparticles in a focused Gaussian beam. Physical Review B 77(8), Art 085412 (2008)
- [642] Cole, R.M., Baumberg, J.J., Garcia de Abajo, F.J., Mahajan, S., Abdel-salam, M., Bartlett, P.N.: Understanding plasmons in nanoscale voids. Nano Letters 7(7), 2094–2100 (2007)
- [643] La Pointe, M.R.: Formation flying with shepherd satellites. Technical report, Ohio Aerospace Institute, Cleveland, Final report, NASA institute for advanced concepts, grant 07600-072

[644] Gillet, S., Riaud, P., Lardiere, O., Dejongle, J., Schmitt, J., Arnold, L., Bocealetti, A., Horville, D., Labeyrie, A.: Imaging capabilities of hypertelescopes with a pair of micro-lens arrays. Astronomy and Astrophysics 400, 393–396 (2003)

- [645] Maheu, B., Le Toulouzan, J.N., Gouesbet, G.: Four-flux model to solve the scattering transfer equation in terms of Lorenz-Mie parameters. Applied Optics 23(19), 3353–3362 (1984)
- [646] Maheu, B., Gouesbet, G.: Four-flux models to solve the scattering transfer equation. Special cases. Applied Optics 25(7), 1122–1128 (1986)
- [647] Tonon, C., Roze, C., Girasole, T., Dinguirard, M.: Four-flux model for a multilayer, plane absorbing and scattering medium: application to the optical degradation of white paint in a space environment. Applied Optics 40(22), 3718–3725 (2001)
- [648] Rozé, C., Girasole, T., Gréhan, G., Gouesbet, G., Maheu, B.: Average crossing parameter and forward scattering ratio values in four-flux model for multiple scattering media. Optics Communications 194(4-6), 251–263 (2001)
- [649] Rozé, C., Girasole, T., Gréhan, G., Gouesbet, G., Maheu, B.: Corrigendum to average crossing parameter and forward scattering ratio values in four-flux model for multiple scattering media. Optics Communications 203, 445 (2002)
- [650] Maheu, B., Briton, J.P., Gouesbet, G.: Four-flux model and a Monte-Carlo code: comparisons between two simple and complementary tools for multiple scattering calculations. Applied Optics 28(1), 22–24 (1989)
- [651] Gouesbet, G., Maheu, B., Le Toulouzan, J.N.: Simulation of particle multiple scattering and applications to particle diagnosis. In: Carvalho, M.G., Lockwood, F., Taine, J. (eds.) Heat Transfer in Radiating and Combusting Systems, pp. 173–185. Springer, Heidelberg (1991)
- [652] Briton, J.P., Maheu, B., Gréhan, G., Gouesbet, G.: Monte-Carlo simulation of multiple scattering in arbitrary 3D-geometry. Particle and Particle Systems Characterization 9, 52–58 (1992)
- [653] Rozé, C., Girasole, T., Gréhan, G., Gouesbet, G.: Time-resolved propagation of femtosecond pulses in turbid medium. In: Sixth International Congress on Optical Particle Characterization, Brighton, April 2-5 (2001)
- [654] Rozé, C., Girasole, T., Mees, L., Gréhan, G., Hespel, L., Delfour, A.: Interaction between ultra short pulses and a dense scattering medium by Monte-Carlo simulation: consideration of particle size effects. Optics Communications 220(4-6), 237–245 (2003)
- [655] Calba, C., Roze, C., Girasole, T., Mees, L.: Monte-Carlo simulation of the interaction between an ultra-short pulse and a strongly scattering medium: the case of large particles. Optics Communications 265(2), 373–382 (2006)
- [656] Calba, C., Mees, L., Roze, C., Girasole, T.: Ultrashort pulse propagation through a strongly scattering medium: simulation and experiments. Journal of the Optical Society of America A 25(7), 1541–1550 (2008)
- [657] Ovod, V.I.: Modeling of multiple scattering from an ensemble of spheres in a laser beam. Particle and Particle Systems Characterization 16(3), 106–112 (1999)
- [658] Xu, Y.L.: Electromagnetic scattering by an aggregate of spheres. Applied Optics 34, 4573–4588 (1995)
- [659] Xu, Y.L.: Electromagnetic scattering by an aggregate of spheres: errata. Applied Optics 37, 6494 (1998)

[660] Xu, Y.L.: Electromagnetic scattering by an aggregate of spheres: errata. Applied Optics 40, 5508 (2001)

- [661] Berrocal, E., Churmakov, D.Y., Romanov, V.P., Jermy, M.C., Meglinski, I.V.: Crossed source-detector geometry for a novel spray diagnostic: Monte-Carlo simulation and analytical results. Applied Optics 44(13), 2519–2529 (2005)
- [662] Misconi, N.Y., Oliver, J.P., Ratcliff, K.F., Rusk, E.T., Wang, W.-X.: Light scattering by laser levitated particles. Applied Optics 29(15), 2276–2281 (1990)
- [663] Gréhan, G., Gouesbet, G., Guilloteau, F., Chevaillier, J.P.: Comparison of the diffraction theory and the generalized Lorenz-Mie theory for a sphere arbitrarily located into a laser beam. Optics Communications 90, 1–6 (1992)
- [664] Chevaillier, J.P., Fabre, J., Hamelin, P.: Forward scattered light intensities by a sphere located anywhere in a Gaussian beam. Applied Optics 25(7), 1222–1225 (1986)
- [665] Lock, J.A., Hovenac, E.A.: Diffraction of a Gaussian beam by a spherical obstacle. American Journal of Physics 8, 698–707 (1993)
- [666] Hovenac, E.A., Lock, J.A.: Assessing the contribution of surface waves and complex rays to far-field Mie scattering by use of the Debye series. Journal of the Optical Society of America A 9, 781–785 (1992)
- [667] Gouesbet, G.: Debye series formulation for generalized Lorenz-Mie theory with the Bromwich method. Particle and Particle Systems Characterization 20(6), 382–386 (2003)
- [668] van Enk, S.J., Kimble, H.J.: Single atom in free space as a quantum aperture. Physical Review A 61(5), Art 051802 (2000)
- [669] van Enk, S.J., Kimble, H.J.: Strongly focused light beams interacting with single atoms in free space. Physical Review A 63(2), Art 023809 (2001)
- [670] Lai, H.M., Wong, W.Y., Wong, W.H.: Extinction paradox and actual power scattered in light beam scattering: a two-dimensional study. Journal of the Optical Society of America A 21(12), 2324–2333 (2004)
- [671] Lock, J.A.: Interpretation of extinction in Gaussian-beam scattering. Journal of the Optical Society of America A 12(5), 929–938 (1995)
- [672] Berg, M.J., Sorensen, C.M., Chakrabarti, A.: Reflection symmetry of a sphere's internal field and its consequences on scattering: a microphysical approach. Journal of the Optical Society of America A 25(1), 98–107 (2008)
- [673] Gréhan, G., Gouesbet, G.: The new computer program MIDI for Mie scattering theory calculations using the Lentz algorithm. Technical report, UMR CNRS 6614, Internal Report TTI/GG/78/10/30 (1978)
- [674] Gréhan, G., Gouesbet, G.: The computer program SUPERMIDI for Mie theory calculations, without practical size nor refractive index limitations. Technical report, UMR CNRS 6614, Internal Report TTI/GG/79/03/20 (1979)
- [675] Gréhan, G., Gouesbet, G.: Mie theory calculations: new progress, with emphasis on particle sizing. Applied Optics 18(20), 3489–3493 (1979)
- [676] Lentz, W.J.: Generating Bessel functions in Mie scattering calculations using continued fractions. Applied Optics 15(3), 668–671 (1976)

The first bibliography, associated with the bulk of the book, was devoted to journals (archival literature), but for a few exceptions, and could be made rather exhaustive. We now provide a second bibliography devoted to references in proceedings which, usually, are more difficult to reach. Concerning references from the Rouen group, a fair exhaustivity can be claimed. This is obviously more difficult for references outside from the Rouen group. References are sorted out according to relevant topics.

```
Computations of beam shape coefficients and localized approximation : [1], [2], [3], [4], [5], [6]
```

Generalities on particle characterization: [7, 8, 9, 10, 11, 12, 13, 14, 15, 16, 17, 18, 19, 20, 21, 22, 23, 24, 25, 26, 27, 28, 29, 30, 31, 32

Generalities on theories, and on GLMT: [7, 8], [33], [16], [17], [27], [28], [29], [30], [34]

GLMT, theory and experiments: 35, 36, 14, 18, 37, 38, 39

Imaging: 40, 41, 42, 43, 44, 45, 46,

Laser pulses: 47, 48, 49, 50, 51, 52, 45, 53, 54, 55, 56, 57, 32

Laser sheets: [58], [59], [60]

Mechanical effects: 61, 62, 63, 64, 65, 66, 67, 68, 69

Morphology-dependent-resonances: [70], [71], [72]

Optical (Hamiltonian) chaos: [73], [74], [75], [76], [55], [57]

Other GLMTs: [77, [78, [79, [74], [75], [80, [54], [81], [72]

Phase-Doppler technique: **82**, **83**, **84**, **85**, **86**, **87**, **88**, **89**, **90**, **91**, **92**, **93**, **94**, **95**, **96**, **97**, **98**, **99**, **100**, **101**, **102**, **103**, **104**, **105**, **106**, **107**, **108**, **109**, **110**, **111**, **112**, **113**, **114**, **115**, **116** 

Top-hat beams: 117, 118, 119, 120, 121, 122, 123, 19.

## References

- [1] Maheu, B., Gréhan, G., Gouesbet, G.: Diffusion de la lumière par une sphère dans le cas d'un faisceau d'extension finie, partie 1: theorie de Lorenz-Mie généralisée, les coefficients gn et leur calcul numérique. 3èmes Journées d'Etudes sur les Aérosols, Paris. Article publié dans le Journal of Aerosol Science (19, 47–53,1988) (1986)
- [2] Gréhan, G., Maheu, B., Gouesbet, G.: Localized approximation to the generalized Lorenz-Mie theory and its application to optical particle sizing. In: Proceedings of the Fifth International Congress on Applications of Lasers and Electro-Optics. The changing frontiers of flow and particle diagnostics. Arlington, Virginia, USA (1986)
- [3] Gréhan, G., Gouesbet, G., Maheu, B.: Diffusion d'un faisceau laser par une particule sphérique: calcul des coefficients gnm. Actes des 5èmes Journées d'Etudes sur les Aérosols, 13–19 (1988)
- [4] Gouesbet, G., Gréhan, G., Maheu, B.: The localized interpretation to compute the coefficients gn, gn+1, and gn-1, in the framework of the generalized Lorenz-Mie theory. In: Proceedings of Icaleo, Santa-Clara, Californy, USA, pp. 263–273 (1988)

[5] Gréhan, G., Gouesbet, G.: Scattering of a laser beam by one particle: behaviour of gnm's coefficients. In: 3rd International Aerosol Conference, Kyoto, Japan. Published in "Aerosols: science, industry, health and environment", vol. 1, pp. 273–276 (1990)

- [6] Gouesbet, G., Lock, J.A., Gréhan, G.: Do you know what a laser beam is? In: Proceedings of the Seventh Workshop on Two-Phase Flow Predictions, Erlangen (1994)
- [7] Gouesbet, G., Gréhan, G.: Advances in quasi-elastic scattering of light with emphasis on simultaneous measurements of velocities and sizes of particles embedded in flows. In: AIAA 16th Thermophysics Conference, Palo Alto, California, Paper 81-1124 (1981)
- [8] Gouesbet, G., Gréhan, G.: The quasi-elastic scattering of light: a lecture with emphasis on particulates diagnosis. In: Proceedings of NATO Workshop on Soot in Combustion Systems and its Toxic Properties. Le Bischenberg, France, pp. 395–412. Plenum Publishing Company Ltd., New York (1981/1983)
- [9] Kleine, R., Gouesbet, G., Rück, B.: Lokale, optische Messungen von Teilchengeschwindigkeiten, Teilchengrössenverteilungen, und Teilchenkonzentrationen. In: Sensor 1982, Essen, Germany (1982)
- [10] Gouesbet, G.: Optical sizing, with emphasis on simultaneous measurements of velocities and sizes of particles embedded in flows, an invited lecture. In: Proceedings of the 15th International Symposium on Heat and Mass Transfer, Dubrovnik, Yougoslavia (1983)
- [11] Gouesbet, G., Gougeon, P., Gréhan, G., Le Toulouzan, J.N., Lhuissier, N., Maheu, B., Weill, M.E.: Laser optical sizing from 100 angströms- to 1-mm diameter, and from 0 to 10 kg/m3 concentration. In: AIAA 20th Thermophysics Conference, Williamsburg, USA, Paper 85-1083 (1985)
- [12] Gréhan, G., Maheu, B., Gouesbet, G.: Diffusion de la lumière par une sphère dans le cas d'un faisceau d'extension finie, partie 2: théorie de Lorenz-Mie généralisée, applications à la granulométrie optique. 3èmes Journées d'Etudes sur les Aérosols, Paris. Article publié dans le Journal of Aerosol Science (19, 55–64, 1988) (1986)
- [13] Gouesbet, G.: Particules discrètes et défense, conférence plénière d'introduction à la journée "Aérosols et Défense", tenue dans le cadre des 4èmes Journées d'Etudes sur les Aérosols (GAMS-COFERA), Centre d'Etudes du Bouchet, Vert-le-Petit, France. Actes publiés par le COFERA, 127–144 (1987)
- [14] Maheu, B., Gréhan, G., Gouesbet, G.: Laser beam scattering by individual spherical particles: theoretical progress and applications to optical sizing. In: International Symposium: Optical Particle Sizing, Theory and Practice, Rouen, France. Plenum Publishing Corporation, NewYork (1987/1988)
- [15] Gouesbet, G.: Discussion of two problems appearing in spray optical sizing, and in the prediction of the behaviour of spray droplets in turbulent flows. keynote lecture. In: Proceedings of the Conference on Spray Combustion, Ilass-Europe, Rouen, France (1988)
- [16] Gouesbet, G.: Advanced theory of light scattering. Applications to optical sizing, invited keynote lecture. In: Proceedings of the 6th Symposium of Japan Association of Aerosol Science and Technology, Osaka, pp. 106–108 (1988)

[17] Gouesbet, G.: Recent advances in shaped beam scattering and applications, invited lecture. In: 3rd International Aerosol Conference, Kyoto, Japan. Published in "Aerosols: science, industry, health and environment", vol. 1, pp. 61–66 (1990)

- [18] Gouesbet, G., Gréhan, G., Maheu, B.: Generalized Lorenz-Mie theory and applications to optical sizing. In: Proceedings of the 2nd International Symposium on Optical Particle Sizing: Theory and Practice. Arizona State University, Phoenix (1990)
- [19] Gréhan, G., Le Toulouzan, J.N., Gouesbet, G.: In situ supermicronic aerosol measurement. In: 3rd International Aerosol Conference, Kyoto, Japan. Published in "Aerosols: science, industry, health and environment", vol. 1, pp. 572–575 (1990)
- [20] Hesselbacher, K., Anders, K., Frohn, A.: Experimental investigation of the influence of a Gaussian intensity distribution on the scattering characteristics of droplets. In: Hirleman, D. (ed.) Proceedings of the Second International Symposium on Optical Particle Sizing, pp. 491–500. Arizona State University, Phoenix (1990)
- [21] Sloot, P., Hoekstra, A., van der Liet, H., Figdor, C.: Arbitrarily-shaped particles measured in flow through systems. In: Hirleman, D. (ed.) Proceedings of the Second International Symposium on Optical Particle Sizing, pp. 605–611. Arizona State University, Phoenix (1990)
- [22] Maheu, B., Gréhan, G., Gouesbet, G.: Techniques optiques pour la granulométrie: principes et caractéristiques, conférence invitée. In: Actes de Mesucora (1991)
- [23] Gouesbet, G., Maheu, B., Gréhan, G.: Particle diagnosis in multiphase media. Plenary lecture. In: 7th International Conference, Surface and Colloid Science, Compiègne, France (1991); Proceedings published in the Journal of Pure and Applied Chemistry, vol. 64(11), pp. 1685–1689 (1992)
- [24] Gouesbet, G., Berlemont, A., Desjonquères, P., Gréhan, G.: On modelling and measurement problems in the study of turbulent two-phase flows with particles. Invited lecture. In: Sixth Workshop on Two-Phase Flow Predictions, Erlangen, Germany (1992); Sommerfeld, M. (ed.): Proceedings from Forschungszentrum Jülich GmbH, bilateral seminar of the international bureau, vol. 14, pp. 365–387 (1993)
- [25] Gouesbet, G.: Single and multiple scattering of laser beams and applications. Invited lecture. In: Proceedings of the First International Conference-Workshop on Modelling in Measurement Processes, pp. 30–50. Technical University of Wroclaw, Szklarska-Poreba, Poland (1993)
- [26] Gréhan, G., Ren, K.F., Gouesbet, G., Naqwi, A., Durst, F.: Application of the generalized Lorenz-Mie theory to multiphase flows experimental techniques. In: Proceedings of the Ninth Symposium on Turbulent Shear Flows, Kyoto, Japan. Paper 27-1-1 (1993)
- [27] Gouesbet, G.: Generalized Lorenz-Mie theory and applications. Plenary lecture. In: Proceedings of the Third International Symposium on Optical Particle Sizing, Yokohama, Japan, pp. 393–405 (1993)
- [28] Gouesbet, G.: Recent advances in light scattering theory and optical particle characterization, Invited lecture. In: European Aerosol Conference, Blois, 1994. Published in the Journal of Aerosol Science, 25(Suppl. 1), S.341–S.342 (1994)

[29] Gouesbet, G., Gréhan, G.: Last progress in generalized Lorenz-Mie theory with applications in multiphase flows. In: Serizawa, A., Fukano, T., Bataille, J. (eds.) Proceedings of the 2nd International Conference on Multiphase Flow, Kyoto, Japan. Paper selected for Multiphase Flows 1995, pp. 703–710. Elsevier, Amsterdam (1995)

- [30] Gouesbet, G., Gréhan, G.: Generalized Lorenz-Mie theory: last developments with applications to particle sizing. Invited lecture. In: Xiong, S., Xijin, S. (eds.) Proceedings of the Third International Conference on Fluid Dynamic Measurement and its Applications, Beijing, China, pp. 31–38 (1997)
- [31] Ren, K.F., Gouesbet, G., Gréhan, G.: Interaction lumière laser/particules: applications métrologiques. In: Actes du Colloque du Club de la Société Française d'Optique: "Contrôles et Mesures Optiques pour l'Industrie", Mittelwihr, Alsace, France (1999)
- [32] Gouesbet, G., Gréhan, G., Méès, L.: Light scattering theory and practice: beyond velocity and size measurements. Keynote lecture. In: Proceedings of the 10th International Conference of Liquid Atomization and Spray Systems, Kyoto, Japan (2006)
- [33] Gouesbet, G., Gréhan, G., Maheu, B.: Advances in light scattering theory for use in aerosol characterization. In: Proceedings of the Second International Conference, Berlin, Germany, pp. 730–733 (1986)
- [34] Gouesbet, G., Gréhan, G.: Petite et grande histoire de la GLMT, conférence invitée. In: par Most, J.M., David, L., Penot, F., Brizzi, L.E. (eds.) Actes du 11ème Congrès Francophone de Techniques Laser, Poitiers, France (2008)
- [35] Maheu, B., Gouesbet, G., Gréhan, G.: A theory of Gaussian beam scattering by a sphere. In: Proceedings of 9ème Colloque d'Optique Hertzienne et des Diélectriques, Pise, Italy, pp. 41–45 (1987)
- [36] Gouesbet, G., Maheu, B., Gréhan, G.: Scattering of a Gaussian beam by a sphere using a Bromwich formulation: case of an arbitrary location. In: International Symposium: Optical Particle Sizing, Theory and Practice, Rouen, France. Plenum Publishing Corporation, New York (1987/1988)
- [37] Hoekstra, A., Doornbos, R., Deurloo, K., Noordmans, H., de Grooth, B., Sloot, P.: An unexpected signature of Lorenz-Mie scattering observed in low cytometric experiments. In: Maeda, M. (ed.) Proceedings of the Third International Symposium on Optical Particle Sizing, Yokohama, Japan, pp. 153–157 (1993)
- [38] Hodges, J.T., Gréhan, G., Presser, C., Semerjian, H.G.: Elastic scattering from spheres under non plane-wave illumination. In: Proceedings of the SPIE International Symposium of Los Angeles, California. Session: laser applications in combustion and combustion diagnostics, SPIE Proceedings, vol. 1862(33) (1993)
- [39] Hodges, J.T., Gréhan, G., Presser, C., Gouesbet, G.: Forward scattering of a Gaussian laser beam by a sphere. In: Yule, A.J., Dumouchel, C. (eds.) Proceedings of Iclass 1994, Rouen, France, pp. 506–512. Begell House Inc., NewYork (1994)
- [40] Ren, K.F., Gréhan, G., Gouesbet, G.: Laser imaging of small particles by using the generalized Lorenz-Mie theory. In: Chen, X.-J., Chen, T.-K., Zhou, F.-D. (eds.) Third International Symposium on Multiphase Flow and Heat Transfer, Xi'an, China, pp. 787–794. Xi'an-Jiatong University Press, Begell House Inc., NewYork (1994)

[41] Ren, K.F., Lebrun, D., Ozkül, C., Kleitz, A., Gouesbet, G., Gréhan, G.: On the measurements of particles by imaging methods: theoretical and experimental aspects. In: Proceedings of the Fourth International Symposium on Optical Particle Sizing, Nürnberg, Germany, pp. 97–106 (1995)

- [42] Girasole, T., Ren, K.F., Lebrun, D., Belaid, S., Gouesbet, G., Gréhan, G.: Generalized Lorenz-Mie theory: an application to imaging of off-axis and defocused droplets. In: Proceedings of the International Conference on Optical Technology and Image Processing in Fluid, Thermal and Combustion Flow, Yokohama, Japan (1998)
- [43] Meunier-Guttin-Cluzel, S., Girasole, T., Gouesbet, G., Gréhan, G.: Diffusion de la lumière par des particules complexes: imagerie aux grands angles. In: Actes du 15ème Congrès Français sur les Aérosols, Paris, France, pp. 155–160 (1999)
- [44] Boulnois, G., Ren, K.F., Girasole, T., Gouesbet, G., Taylor, A.K.M.P., Gréhan, G.: Imagerie de cylindres aux petits angles: application au Shadow Doppler Velocimeter. In: Actes du Congrès Fluvisu, Insa de Rouen, France, pp. 65–70 (2001)
- [45] Méès, L., Ren, K.F., Gouesbet, G., Gréhan, G.: Imagerie pulsée femtoseconde d'une particule réfractante unique. In: Actes du Congrès Fluvisu, Insa de Rouen, France, pp. 105–111 (2001)
- [46] Meunier-Guttin-Cluzel, S., Gouesbet, G., Gréhan, G.: Imagerie cohérente de particules complexes: relation entre champ interne et image en champ lointain. In: Actes du Congrès Fluvisu, Insa de Rouen, France, pp. 113–118 (2001)
- [47] Gouesbet, G., Gréhan, G.: Interaction entre des pulses de lumière et des particules. In: Actes du 15ème Congrès Français sur les Aérosols, Paris, France, pp. 99–105 (1999)
- [48] Méès, L., Gréhan, G., Gouesbet, G.: Interaction between a pulsed laser beam and a spherical particle. In: Proceedings of the Asian Particle Technology Conference, Bangkok, Thaîland (2000)
- [49] Méès, L., Gouesbet, G., Gréhan, G.: Diffusion de pulses laser par des particules. In: Actes du Colloque du Club "Contrôles et Mesures Optiques pour l'Industrie" de la Société Française d'Optique, Biarritz, France, pp. 430–435 (2000)
- [50] Gouesbet, G., Méès, L., Gréhan, G.: Generic formulation of a generalized Lorenz-Mie theory for pulsed illumination. In: Tenth International Symposium on Applications of Laser Techniques to Fluid Mechanics, Lisbon, Portugal (2000)
- [51] Méès, L., Gouesbet, G., Gréhan, G.: Lasers pulsés et aérosols. In: Actes du 16ème Congrés Français sur les Aérosols, Paris, France, pp. 35–40 (2000)
- [52] Méès, L., Gréhan, G., Gouesbet, G.: Diffusion d'un pulse court par une particule. In: Actes de l'Ecole Femtoseconde, Saint-Etienne, France. Publications de l'Université de Saint-Etienne (2001)
- [53] Méès, L., Meunier-Guttin-Cluzel, S., Ren, K.F., Gouesbet, G., Gréhan, G.: Interaction entre impulsions laser courtes et particules. In: Actes du 17ème Congrès Français sur les Aérosols, INA, Paris, France, pp. 35–40 (2001)
- [54] Méès, L., Ren, K.F., Gouesbet, G., Gréhan, G.: Transient internal and near-scattered fields from a multilayered sphere illuminated by a pulsed laser. In: Proceedings of the 11th International Symposium on Application of Laser Techniques into Fluid Mechanics, Lisbon, Portugal (2002)

[55] Gouesbet, G., Gréhan, G., Méès, L., Meunier-Guttin-Cluzel, S.: New advances in generalized Lorenz-Mie theory: femtosecond pulses and optical chaos. Plenary lecture. European Aerosol Conference, Madrid, Spain. Journal of Aerosol Science, EAC 2003, S957–S959 (2003)

- [56] Gouesbet, G., Méès, L., Rozé, C., Girasole, T., Gréhan, G.: Diagnostic par laser pulsé femtoseconde en diffusion simple et multiple: application aux diagnostics particulaires. Conférence invitée. In: Gobin, D., Pons, M., Lauria, G., Le Queré, P. (eds.) Congrès de la Société Française des Thermiciens. Actes: Transferts en Milieux Hétérogènes, pp. 13–18 (2004)
- [57] Gouesbet, G., Gréhan, G., Méès, L., Meunier-Guttin-Cluzel, S.: New advances and prospectives on generalized Lorenz-Mie theories: pulsed lasers, optical chaos and quantum mechanical analogies, Invited plenary lecture. In: Proceedings of the Kongress Metrologii, Wroclaw, Poland, pp. 11–15 (2004)
- [58] Ren, K.F., Gréhan, G., Gouesbet, G.: Laser sheet scattering by spherical particles. In: Proceedings of the Sixth International Symposium on Applications of Laser Techniques to Fluid Mechanics, Lisbon, Portugal (1992)
- [59] Mroczka, J., Ren, K.F., Gréhan, G., Gouesbet, G.: Particle sizing by using polarization ratios, on the use of laser sheets. In: Proceedings of the First International Conference-Workshop on Modelling in Measurement Processes. Technical University of Wroclaw, Szklarska-Poreba, Poland (1993)
- [60] Gréhan, G., Ren, K.F., Gouesbet, G., Naqwi, A., Durst, F.: Evaluation of particle sizing technique based on laser sheets. In: Proceedings of the Third International Symposium on Optical Particle Sizing, Yokohama, Japan (1993)
- [61] Ren, K.F., Gréhan, G., Gouesbet, G.: Theorie de Lorenz-Mie généralisée: un outil pour l'étude des barrières laser de protection locale. In: Actes des 8èmes Journées d'Etudes sur les Aérosols, CNAM, Paris, France, pp. 65–70 (1991)
- [62] Shimizu, I., Yamamoto, N., Suzuki, S., Takahara, Y., Agu, M., Gréhan, G., Gouesbet, G.: Elimination and manipulation of small particles suspended in the atmosphere by laser beams. In: Proceedings of the International Symposium: the Future Practice of Contamination Control, London, England (1992)
- [63] Shimizu, I., Ichige, K., Takahara, Y., Gréhan, G., Gouesbet, G.: Size sieving of particles by radiation pressure. In: Proceedings of the Third International Symposium on Optical Particle Sizing, Yokohama, Japan (1993)
- [64] Harada, Y., Asakura, T.: Effects of the laser radiation pressure on optical particle sizing by means of photon correlation spectroscopy. In: Maeda, M. (ed.) Proceedings of the Third International, Symposium on Optical Particle Sizing, Yokohama, Japan, pp. 89–95 (1993)
- [65] Angelova, M.I., Pouligny, B., Martinot-Lagarde, G., Gréhan, G., Gouesbet, G.: Stressing phospholipid membranes using mechanical effects of light. In: Proceedings of the Conference of European Society of Colloids, Bristol, England (1993)
- [66] Ichige, K., Shimizu, I., Ohtake, Y., Gréhan, G., Gouesbet, G.: Contamination control by radiation pressure. In: Proceedings of the 12th ISCC Conference, Yokohama, Japan, pp. 463–465 (1994)
- [67] Martinot-Lagarde, G., Angelova, M.I., Pouligny, B., Gréhan, G., Gouesbet, G.: Laser trapping of micron particles and dynamometrical applications. In: 3ème Colloque sur les Lasers et l'Optique Quantique, Limoges, France (1993); Article publié dans les Annales de Physique, 20(2), 127–128 (1995)

[68] Ren, K.F., Onofri, F., Gouesbet, G., Gréhan, G., Martinot-Lagarde, G., Pouligny, B.: Radiation pressure, a tool for optical measurements of pico-Newton forces? In: Proceedings of the Fourth International Symposium on Optical Particle Sizing, Nürnberg, Germany, pp. 483–491 (1995)

- [69] Polaert, H., Gréhan, G., Gouesbet, G.: Rotation d'une particule sphérique piégée dans un faisceau laser. In: Actes des 12èmes Journées d'Etudes sur les Aérosols, Asfera, Paris, France (1996)
- [70] Ducastel, J., Méès, L., Gréhan, G., Gouesbet, G.: Etude des résonances morphologiquement dépendentes. In: Actes du 18ème Congrès Français sur les Aérosols, Paris, France, pp. 97–102 (2002)
- [71] Ducastel, J., Méès, L., Gréhan, G., Gouesbet, G.: Etude des résonances morphologiquement dépendentes. In: Actes du 21ème Congrès Français sur les Aérosols, Paris, France, pp. 22–28 (2005)
- [72] Han, Y.P., Liu, J.Y., Méès, L., Gouesbet, G., Gréhan, G.: Resonance shift and Q-factors of distortional liquid droplet. In: 5th International Symposium on Measurement Techniques for Multiphase Flows/ 2nd International Workshop on Process Tomography, Macau (2006); In: Cai, X., Huang, Z., Wang, S., Wang, M. (eds.): AIQ Conference Proceedings. Multiphase Flow, the Ultimate Challenge, pp. 509–513 (2007)
- [73] Gouesbet, G., Meunier-Guttin-Cluzel, S., Gréhan, G.: Diffusion de la lumière par des particules complexes: chaos optique hamiltonien et diffusion irrégulière. In: Actes du 15ème Congrès Français sur les Aérosols, Paris, France, pp. 87–97 (1999)
- [74] Gouesbet, G., Meunier-Guttin-Cluzel, S., Gréhan, G.: Scattering of light by a sphere with an eccentrically located spherical inclusion: generalized Lorenz-Mie approach and optical chaos. In: Proceedings of the Asian Particle Technology Conference, Bangkok, Thaîland (2000)
- [75] Gouesbet, G., Meunier-Guttin-Cluzel, S., Gréhan, G.: Generalized Lorenz-Mie theory for a sphere with an eccentrically located spherical inclusion and optical chaos. In: Tenth International Symposium on Applications of Laser Techniques to Fluid Mechanics, Lisbon, Portugal (2000)
- [76] Gouesbet, G., Meunier-Guttin-Cluzel, S., Gréhan, G.: Chaos hamiltonien dans le billard annulaire et hyper-résonances. In: Actes des Rencontres du Non-Linéaire Institut Henri Poincaré, Paris, France, pp. 129–134 (2001)
- [77] Ren, K.F., Gouesbet, G., Gréhan, G.: Scattering of a Gaussian beam by an infinite cylinder: numerical results in GLMT-framework. In: Proceedings of the Eight International Symposium on Applications of Laser Techniques to Fluid Mechanics, Lisbon, Portugal (1996)
- [78] Méès, L., Gouesbet, G., Gréhan, G.: Diffusion d'un faisceau laser par une fibre cylindrique infinie: résultats numériques. In: Actes des 13èmes Journées d'Etudes sur les Aérosols, Paris, France, pp. 77–82 (1997)
- [79] Wysoczanski, D., Mroczka, J., Gréhan, G., Gouesbet, G.: Single light scattering on infinite cylinder: plane wave and Gaussian beam. In: Proceedings of the Partec Conference, Nürnberg, Germany, pp. 665–674 (1998)
- [80] Han, Y.P., Ren, K.F., Méès, L., Gouesbet, G., Gréhan, G.: Diffusion de la lumière par un ellipsoïde: implications en réfractométrie d'arc-en-ciel. In: Actes du 17ème Congrès Français sur les Aérosols, INA, Paris, France, pp. 29–34 (2001)

[81] Ren, K.F., Gréhan, G., Gouesbet, G.: Mesure précise du diamètre de fibre en étirement par échantillonnage du diagramme de diffusion. In: Actes du Quatrième Colloque Francophone de la Société Française d'Optique sur les Méthodes et Techniques Optiques pour l'Industrie, Belfort, pp. 470–475 (2003)

- [82] Gréhan, G., Gouesbet, G., Vannobel, F., Dementon, J.B.: Generalized Lorenz-Mie theory: an application to phase-Doppler technique. In: Proceedings of the Fifth International Symposium on Applications of Laser Anemometry to Fluid Mechanics, Lisbon, Portugal (1990)
- [83] Gréhan, G., Gouesbet, G., Naqwi, A., Durst, F.: Evaluation of phase-doppler system using generalized Lorenz-Mie. In: Proceedings of the International Conference on Multiphase Flows, Tsukuba, Japan (1991)
- [84] Gréhan, G., Gouesbet, G., Naqwi, A., Durst, F.: On elimination of the trajectory effects in phase-Doppler systems. In: Proceedings of the 5th European Symposium on Particle Characterization, Nürnberg, Germany, pp. 309–318 (1992)
- [85] Gréhan, G., Gouesbet, G., Naqwi, A., Durst, F.: Trajectory ambiguities in phase-Doppler systems: use of polarizers and additional detectors to suppress the effect. In: Proceedings of the Sixth International Symposium on Applications of Laser Techniques to Fluid Mechanics, Lisbon, Portugal (1992)
- [86] von Benzon, H., Buchhave, P.: The phase-Doppler method applied to very small particles. In: Maeda, M. (ed.) Proceedings of the Third International Symposium on Optical Particle Sizing, Yokohama, Japan, pp. 261–267 (1993)
- [87] Haugen, P., von Benzon, H.: Phase-Doppler measurement of the diameter of large particles, considerations for optimization. In: Maeda, M. (ed.) Proceedings of the Third International Symposium on Optical Particle Sizing, Yokohama, Japan, pp. 301–306 (1993)
- [88] Naqwi, A., Ziema, M., Gréhan, G., Gouesbet, G.: Influence of the Gaussian profile effect on the accuracy of phase-Doppler anemometer. In: Sixth Workshop on Two-Phase Flow Predictions, Erlangen, Germany (1992); Sommerfeld, M. (ed.): Proceedings from the Forschungszentrum Jülich GmbH, bilateral seminar of the international bureau, vol. 14, pp. 412–420 (1993)
- [89] Domnick, J., Dorfner, V., Durst, F., Yamashita, M.: Performance evaluation of different phase-Doppler systems. In: Maeda, M. (ed.) Proceedings of the Third International Symposium on Optical Particle Sizing, Yokohama, Japan, pp. 425–433 (1993)
- [90] Manasse, U., Wriedt, T., Bauckhage, K.: Reconstruction of real size distributions hidden in phase-Doppler anemometry results obtained from droplets of inhomogeneous liquids. In: Maeda, M. (ed.) Proceedings of the Third International Symposium on Optical Particle Sizing, Yokohama, Japan, pp. 293–299 (1993)
- [91] Naqwi, A.: Innovative phase-Doppler systems and their applications. In: Maeda, M. (ed.) Proceedings of the Third International Symposium on Optical Particle Sizing, Yokohama, Japan, pp. 245–260 (1993)
- [92] Nonn, T., Dagan, Z.: Analysis of particle mixtures exhibiting different scattering modes by phase discrimination. In: Maeda, M. (ed.) Proceedings of the Third International Symposium on Optical Particle Sizing, Yokohama, Japan, pp. 269–273 (1993)

[93] Nonn, T., Dagan, Z.: Characterizing bubble growth using phase-Doppler technique. In: Maeda, M. (ed.) Proceedings of the Third International Symposium on Optical Particle Sizing, Yokohama, Japan, pp. 449–452 (1993)

- [94] Sankar, S., Ibrahim, K., Buermann, D., Fidrich, M., Bachalo, W.: An integrated phase-Doppler/rainbow refractometer system for simultaneous measurement of droplet size, velocity, and refractive index. In: Maeda, M. (ed.) Proceedings of the Third International Symposium on Optical Particle Sizing, Yokohama, Japan, pp. 275–284 (1993)
- [95] Yosoya, H., Oboka, T.: PDA measurement and LHF analysis of Diesel type sprays. In: Maeda, M. (ed.) Proceedings of the Third International Symposium on Optical Particle Sizing, Yokohama, Japan, pp. 495–502 (1993)
- [96] Mignon, H., Onofri, F., Gréhan, G., Gouesbet, G., Tropea, C.: Mesure de particules non sphériques par phase-Doppler: cas des cylindres et des particules irrégulières. In: Actes du 4ème Congrès Francophone de Vélocimétrie Laser, pp. 1–4. Poitiers-Futuroscope, France (1994)
- [97] Onofri, F., Gréhan, G., Gouesbet, G., Xu, T.H., Brenn, G., Tropea, C.: Phase-Doppler anemometry with dual-burst technique for particle refractive index measurements. In: Proceedings of the Seventh International Symposium on Applications of Laser Techniques to Fluid Mechanics, Lisbon, Portugal, pp. 21.4.1–21.4.8 (1994)
- [98] Gréhan, G., Onofri, F., Girasole, T., Gouesbet, G., Durst, F., Tropea, C.: Measurement of bubbles by phase-Doppler technique and trajectory ambiguity. In: Proceedings of the Seventh International Symposium on Applications of Laser Techniques to Fluid Mechanics, Lisbon, Portugal, 18.2.1–18.2.8; republished in selected papers book. Adrian, Durao, Durst, Heitor, Maeda, Whitelaw (eds.): Developments in Laser Techniques and Applications to Fluid Mechanics, pp. 290–302. Springer, Heidelberg (1994)
- [99] Gouesbet, G., Gréhan, G.: Gaussian beam errors in phase-Doppler anemometry and their elimination. Invited plenary lecture. In: Proceedings of the Seventh International Symposium on Applications of Laser Techniques to Fluid Mechanics, Lisbon, Portugal, pp. 1.2.1–1.2.9; Republished in selected papers book. Adrian, Durao, Durst, Heitor, Maeda, Whitelaw (eds.): Developments in Laser Techniques and Applications to Fluid Mechanics, pp. 243–259. Springer, Heidelberg (1994)
- [100] Onofri, F., Gréhan, G., Gouesbet, G., Xu, T.H., Tropea, C.: Mesure de particules non sphériques par phase-Doppler: cas des cylindres et des particules irrégulières. In: Actes du 4ème Congrès Francophone de Vélocimétrie Laser, paper 1–4, Poitiers-Futuroscope (1994)
- [101] Tropea, C., Xu, T., Gréhan, G., Onofri, F., Haugen, P.: Dual-mode phase-Doppler anemometry. In: Proceedings of the Seventh International Symposium on Applications of Laser Techniques to Fluid Mechanics, paper 18-13, Lisbon, Portugal (1994)
- [102] Aizu, Y., Washiyama, H., Mishina, H.: Consideration of Gaussian beam defect in design of PDA-systems. In: Durst, F., Domnick, J. (eds.) Proceedings of the Fourth International Symposium on Optical Particle Sizing, Nürnberg, Germany, pp. 141–150 (1995)
- [103] Onofri, F., Mignon, H., Gouesbet, G., Gréhan, G.: On the extension of phase-Doppler anemometry to the sizing of spherical multilayered and cylindrical particles. In: Proceedings of the Fourth International Congress on Optical Particle Sizing, Nürnberg, Germany, pp. 275–284 (1995)

[104] Blondel, D., Onofri, F., Gréhan, G., Garo, A., Gouesbet, G.: Détection de particules sphériques inhomogènes par anémométrie phase-Doppler: particules à coeur. In: Actes des 11èmes Journées d'Etudes sur les Aérosols, Paris, France, pp. 104–111 (1995)

- [105] Doicu, A., Schabel, S., Ebert, F.: Generalized Lorenz-Mie theory for spherical and non-spherical particles with applications to phase-Doppler anemometry. In: Durst, F., Domnick, J. (eds.) Proceedings of the Fourth International Symposium on Optical Particle Sizing, Nürnberg, Germany, pp. 119–128 (1995)
- [106] Brenn, G., Domnick, J., Tropea, C., Xu, T.H., Onofri, F., Gréhan, G., Gouesbet, G.: The dual-burst technique and its application to optically nonhomogeneous particles. In: Proceedings of the Fourth International Symposium on Optical Particle Sizing, Nürnberg, Germany, pp. 397–406 (1995)
- [107] Buchhave, P., von Benzon, H.: Exploring PDA-configurations. In: Durst, F., Domnick, J. (eds.) Proceedings of the Fourth International Symposium on Optical Particle Sizing, Nürnberg, Germany, pp. 1–20 (1995)
- [108] Gouesbet, G., Gréhan, G.: The calculation of properties of phase-Doppler signals. Invited contribution to the seminar on the 20th anniversary of phase-Doppler anemometry. In: Proceedings published by the Lehrstuhl für Strömungsmechanik, Universität Erlangen-Nürnberg, Erlangen, Germany (1995)
- [109] Mignon, H., Gréhan, G., Gouesbet, G., Xu, T.H., Tropea, C.: Measurement of cylindrical particles using phase-Doppler anemometers. In: Wriedt, T., Quinten, M., Bauckhage, K. (eds.) Proceedings of the 1st Workshop on Electromagnetic and Light Scattering Theory and Applications, Bremen, Germany, Distributed by University-Buchhandlung, pp. 39–43 (1996)
- [110] Gréhan, G., Onofri, F., Gouesbet, G.: Anémométrie phase-Doppler en milieux multiphasiques: vers de nouvelles possibilités. La Houille Blanche 1/2, 98–104 (1996)
- [111] Blondel, D., Girasole, T., Gréhan, G., Gouesbet, G.: Application de l'anémométrie phase-Doppler à des milieux d'accès optique difficile. In: Actes des 12èmes Journées d'Etudes sur les Aérosols, Asfera, Paris, France (1996)
- [112] Gauchet, N., Gréhan, G., Gouesbet, G.: Mesures de particules cylindriques par anémométrie phase-Doppler. In: Actes des 12èmes Journées d'Etude sur les Aérosols, Asfera, Paris, France (1996)
- [113] Mignon, H., Gréhan, G., Damaschke, N., Tropea, C., Gouesbet, G.: Influence de la forme de particules sur une mesure APD: cas des particules ellipsoïdes allongées et aplaties. In: Proceedings du 5ème Congrès Francophone de Vélocimétrie Laser, Rouen, France (1996)
- [114] Bultynck, H., Onofri, F., Gréhan, G., Gouesbet, G.: Sonde phase-Doppler miniature: applications aux diagnostics en milieux hostiles. In: Proceedings du 5ème Congrés Francophone de Vélocimétrie Laser, Rouen, France (1996)
- [115] Onofri, F., Bultynck, H., Gréhan, G.: Mélange de jets de gouttes: mesure par phase-Doppler. In: Actes du 4éme Congrès Francophone de Vélocimétrie Laser, Rouen, France (1996)
- [116] Blondel, D., Gréhan, G., Gouesbet, G.: In situ phase-Doppler measurements in three-phase flows. In: Proceedings of the Third International Conference on Multiphase Flows, Lyon, France (1998)

[117] Allano, D., Gouesbet, G., Gréhan, G., Lisiecki, D.: Comparative measurements of calibrated droplets using Gabor holography and corrected top-hat laser beam sizing with discussion of simultaneous velocimetry. In: Proceedings of the International Symposium on Applications of Laser-Doppler Anemometry to Fluid Mechanics, Lisbon, Portugal (1982)

- [118] Gouesbet, G., Gréhan, G., Kleine, R.: Simultaneous optical measurement of velocity and size of individual particles in flows. In: Proceedings of the Second International Symposium on Applications of Laser Anemometry to FLuid Mechanics, Lisbon, Portugal (1984)
- [119] Gréhan, G., Kleine, R., Gouesbet, G.: Combined measurements of velocity and size of supermicronic particles in flows using a top-hat laser beam technique. In: Proceedings of the Conferences on Particle Size Analysis, organized by the Particle Size Group of the Analytical Division of the Royal Society of Chemistry. University of Bradford, England (1985)
- [120] Gréhan, G., Gouesbet, G.: Mesure de la taille et de la vitesse de particules supermicroniques entraînées par un fluide, à l'aide d'un faisceau "créneau". In: Actes des Secondes Journées d'Etudes sur les Aérosols (GAMS-COFERA), Paris, France (1985)
- [121] Gréhan, G., Gouesbet, G., Kleine, R., Renz, V., Wilhelmi, I.: Corrected laser beam techniques for simultaneous velocimetry and sizing of particles in flows and applications. In: Proceedings of the Third International Symposium on Applications of Laser Anemometry to Fluid Mechanics, Lisbon, Portugal (1986)
- [122] Gréhan, G., Gouesbet, G., Kleine, R.: Simultaneous measurements of sizes and velocities of aerosol particles using a top-hat laser beam technique. In: Proceedings of the Second International Aerosol Conference, Berlin, Germany, pp. 774–775 (1986)
- [123] Corbin, F., Gréhan, G., Gouesbet, G.: Top-hat beam technique: improvements and application to bubble measurements. In: Proceedings of the 2nd International Sympoisum on Optical Particle Sizing: Theory and Practice. Arizona State University, Phoenix (1990)